Nicotinic Acetylcholine Receptors and Their Interaction with $A\beta_{1-42}$

by

Nicola Crawford B.Sc., M.Sc

A thesis submitted for the degree of Doctor of Philosophy
at the University of Edinburgh

November 2005

Division of Neuroscience
School of Biomedical and Clinical Laboratory Sciences
College of Medicine and Veterinary Medicine
University of Edinburgh
Supervisor: Dr Keith Finlayson

Declaration of ownership

This submission is the result of my own endeavour. All help and advice, other than received from tutors, has been acknowledged. All primary and secondary sources of information have been properly attributed. Should this statement prove to be untrue, I recognise the right and duty of the Board of Examiners to recommend what action should be taken in line with the University's regulations on assessment contained in the postgraduate study handbook.

Signature

Date

Abstract

Alzheimer's Disease (AD) is a progressive, age-related disease that is positively characterised by the post-mortem presence of neurofibrillary tangles and amyloid plaques. At present ~ 5 % of those aged over 65 years are diagnosed with AD, with this figure increasing to ~ 20 % for those aged over 75 years. It is nearly 100 years since AD was first characterised in 1907, however the exact cause has yet to be determined with the cholinergic and beta-amyloid (Aβ) hypotheses remaining central to the aetiology. The cholingergic hypothesis suggests that loss of the cholinergic pathways precedes that of any other neurotransmitter making it a primary target in AD and predating the amyloid hypothesis which itself postulates that deposition of Aβ is primarily responsible for the neurodegeneration in AD. Until recently, these two hypotheses have been almost exclusively studied in separation. However, recent studies suggest that the two major CNS cholinergic nicotinic acetylcholine receptor subtypes $\alpha_4\beta_2$ and α_7 may interact directly with Aβ and therefore, a multidisciplinary approach has been used to evaluate the reported interaction.

Radioligand binding was used to characterise the $\alpha_4\beta_2$ nAChR ([^{3}H]-epibatidine and [^{3}H]-cytisine) and α_7 nAChR ([^{3}H]-methyllycaconitine ([^{3}H]-MLA) and [^{3}H]-αBungarotoxin ([^{3}H]-αBgTx)) in rat and mouse brain tissue and in SH-EP1 cell lines overexpressing human forms of the $\alpha_4\beta_2$ or α_7 nAChRs. No species difference in ligand affinities were observed for the $\alpha_4\beta_2$ nAChR. In contrast, nicotinic agonists exhibited significantly higher affinity (~100 fold) for human α_7 nAChRs compared to their rat counterparts with no change in antagonist affinity. Interestingly, evaluation of [^{3}H]-MLA and [^{3}H]-αBgTx binding indicated the latter ligand bound to a restricted number of sites on the α_7 nAChR. Furthermore, neither human nor rat $A\beta_{1\text{-}42}$ inhibited [^{3}H]-cytisine or [^{3}H]-MLA binding to nAChRs. In parallel to behavioural studies, these binding assays were also employed to assess nAChR pharmacology in transgenic α_7 knockout mice. With no alteration in $\alpha_4\beta_2$ nAChR pharmacology, the deficit in sustained attention exhibited by these α_7-KO mice is probably due to loss of the α_7 nAChR.

Finally, a series of studies was performed to examine the functional interaction between $A\beta_{1\text{-}42}$ and nAChRs. (-)Nicotine evoked changes in calcium flux or membrane potential in SH-EP1-h$\alpha_4\beta_2$ cells were not inhibited by soluble or insoluble human $A\beta_{1\text{-}42}$. Even whole cell patch clamp analysis of single cells showed no direct interaction between the $\alpha_4\beta_2$ nAChR and $A\beta_{1\text{-}42}$. The examination of the functional interaction between α_7 nAChRs and $A\beta_{1\text{-}42}$ using whole cell patch clamp or fluorescence based assays was compromised by a lack of consistent expression of functional human α_7 nAChRs in the SH-EP1 cell line. In addition, neither human $\alpha_4\beta_2$ nor α_7 nAChRs co-immunoprecipitated with human $A\beta_{1\text{-}42}$.

In conclusion, using a systematic multidisciplinary approach incorporating functional and non-functional assays the following major observations were made (1) species differences in α_7 but not $\alpha_4\beta_2$ nAChR pharmacology, (2) the two α_7 nAChR antagonists MLA and αBgTx differ in their ability to bind the α_7 homopentamer, (3) removal of the α_7 nAChR does not alter $\alpha_4\beta_2$ nAChR pharmacology in transgenic mice (4) neither soluble or insoluble $A\beta_{1\text{-}42}$ interacted in pharmacological, functional, or biochemical assays with the rodent or human $\alpha_4\beta_2$ or α_7 nAChRs.

Table of Contents

Discussion – Functional Characterisation of nAChRs

List of Figures

List of Tables

Acknowledgements

I would like to thank my supervisor, Dr. Keith Finlayson for all his help and guidance throughout my Ph.D. In addition, I would like to thank Professor John S. Kelly for taking a chance on a Kiwi and encouraging me to study for a Ph.D. in Edinburgh. I believe that I have benefited immensely from my time at the University of Edinburgh and I am indebted to him for all his support.

I would also like to thank Fujisawa Pharmaceuticals Co. (now Astellas Pharma Inc.) for their generous financial support for this project the over the last three years.

I must make particular mention of Dr. Joseph Hodgkiss and Mrs Joyce McLuckie for the amazing support, teaching, and chats and to Dr. Lorraine Kerr for all the biochemistry help. Thanks must also be given to Mr Darren Downing for being a great friend and providing constant computer support and beer, and to Mrs Margaret Rennex for dealing with all the bureaucracy and sourcing equipment from all over the world.

Special mention must go to David and Elizabeth Fairbairn for their incredible support. Thank you for generously taking in a homeless Kiwi and providing constant encouragement when things got tough.

Thank you to my parents (Robin and Bronwen) for constantly encouraging me to follow my dreams and continuing to support me in countless ways despite being half a world away! Thank you also to my siblings, Deborah, Kim, and Anthony for your hilarious emails that have made me laugh and cry throughout the past few years.

Finally I must say thank you to Dr. Andrew Baxter. Thank you for being there for me, for listening, for the loan of your computer (!) and for all the things you did and I never noticed.

To my parents, Robin and Bronwen

my grandparents, William Reynold and Frances

and my siblings, Deborah, Kim, and Anthony

Arohanui

1.1 Alzheimer's Disease

Alzheimer's Disease (AD) was first characterised by Alois Alzheimer in 1907 and it is estimated that there are more than 25 million suffers worldwide (Wimo *et al.*, 2003). With the growing tendency towards an aging demographic, it appears likely that these figures will rise in the near future. At present approximately 5 % of those aged over 65 years are diagnosed with AD, with this figure increasing to approximately 20 % for those aged over 75 years. Consequently, AD is a serious problem for healthcare authorities worldwide (Sloane *et al.*, 2002; Leung *et al.*, 2003; Sadik *et al.*, 2003).

1.1.1 Familial and Sporadic Alzheimer's Disease

Alzheimer's disease is routinely divided into two distinct types based upon age of onset. Familial AD (FAD, or early onset AD) is classified on the basis of age, with onset generally being less than 65 years of age and with family history being a distinct risk factor (Hirst *et al.*, 1994). In contrast, the vast majority are late-onset cases (over 65 years of age at time of onset) and are classified as sporadic AD (Ling *et al.*, 2003). With the exception of the earlier onset (and for some patients a shorter disease duration), FAD is pathologically indistinguishable from sporadic or non-FAD.

FAD is transmitted as an autosomal-dominant trait with at least 3 recognised genetic loci (Bertram *et al.*, 2004). The first gene mutation identified was at position 717 on the amyloid precursor protein (APP), occurring as a consequence of a substitution of a valine for an isoleucine (Goate *et al.*, 1991). Further mutations within the APP gene have also been reported including but not limited to $APP717_{val\text{-}gly}$, $APP717_{val\text{-}phe}$, and the $APP_{670/671}$ (APP_{swe}) mutations, with the latter identified in a Swedish family which resulted in a double mutation at residues 670 and 671 of the APP gene (Chartier-Harlin *et al.*, 1991; Mullan *et al.*, 1992).

Despite the number of mutations identified in APP, these account for only 5 – 10 % of FAD pedigrees (Strittmatter *et al.*, 1996; Lendon *et al.*, 1997). The more common FAD mutations are linked to the presenilins (PS), transmembrane proteins primarily localised to the endoplasmic reticulum of cells throughout the body with Schellenberg and colleagues (1992) finding many early onset pedigrees mapped to chromosome 14. The causative genes, PS1 and PS2, were subsequently cloned and the PS1 gene is now known to have in excess of 45 individual mutations while at least 2 mutations have been identified for PS2 (Levy-Lahad *et al.*, 1995; Schellenberg, 1995; Cruts *et al.*, 1996; Dewji, 2005). A fourth gene locus, the ε4 allele of apolipoprotein E (ApoE), has also been identified as having a causal link in AD (Strittmatter *et al.*, 1996; Poirier, 2005). Apolipoprotein E has 3

naturally occurring alleles, ε2, ε3, and ε4 which differ from each other by a single codon (Strittmatter *et al.*, 1996). Interestingly, the ε4 allele is substantially overexpressed in AD patients when compared to control subjects and as such is associated with an increased risk of both familial and sporadic AD (Strittmatter *et al.*, 1996; Farrer *et al.*, 1997; Horsburgh *et al.*, 2000).

1.1.2 Clinical Characteristics of Alzheimer's Disease

Alzheimer's Disease is characterised by an irreversible, progressive neurodegeneration of the central nervous system (CNS), that is associated with a gradual decline in cognitive function (Selkoe, 1990; Teplow, 1998). Clinically, AD is difficult to truly define as patients in the early stages of the disease often present with only slight problematic memory loss, (usually manifesting as an inability to recall recent events or encode some (but not all) new memories), but have otherwise normal neurological function (Rossor *et al.*, 1996; Backman *et al.*, 2004). Typically, over a period of months sufferers continue to lose short-term (working) memory and then gradually episodic (memory for past and personally experienced events) and semantic memory (knowledge for the meaning of words and how to apply them) (Tulving *et al.*, 1990; Rossor *et al.*, 1996).

In the late stages of AD, multiple cognitive and behavioural symptoms are observed including sudden involuntary jerking movements as well as orientation and language difficulties (Romanelli *et al.*, 1990; Morris *et al.*, 1991; Rossor *et al.*, 1996). The average lifespan from time of AD diagnosis is 7 – 10 years making it a long process for both the patient and their family (Australian Alzheimers Association, 2000).

Clinical heterogeneity is a common feature of neurological disease in general and as such, a positive AD diagnosis can only be determined at autopsy (Dickson, 1997a). Neurodegeneration and synaptic loss, activation of microglia and astrocytes, and increased levels of inflammatory mediators are all observed in the AD brain (Akiyama *et al.*, 2000a,b). In addition, AD patients have an increased incidence of cerebro-vasculature disease, possibly related to the deposition of amyloid protein on the vasculature walls (Ray *et al.*, 1998). However, the AD brain has two distinguishing pathological features; neurofibrillary tangles and neuritic (senile) plaques (Katzman, 1986; Dickson, 1997a), which are discussed in more detail below.

1.1.3 Histopathological Characterisation of Alzheimer's Disease

1.1.3.1 Neurofibrillary Tangles

Neurofibrillary tangles (NFTs) are composed primarily of microtubule associated protein (MAP) tau and constitute intracellular deposits within the cell bodies of neurons and/or glia (Iqbal *et al.*, 2005). Tau, MAP1, and MAP2, the major microtubule associated proteins in the normal mature neuron, promote the assembly and stability of microtubules (Weingarten *et al.*, 1975; Lindwall *et al.*, 1984; Iqbal *et al.*, 2005). Microtubules themselves are essential for axonal transport and consequently neuronal activity (Iqbal *et al.*, 2005). In the human brain, there are six known isoforms of tau, generated from a single gene by alternative mRNA splicing (Goedert *et al.*, 1989). These isoforms differ by the presence or absence of a 29 or 58 amino acid (aa) insert in the amino terminal and by the presence or absence of a 31 aa repeat that is encoded by exon 10 in the carboxy terminus (Himmler *et al.*, 1989; Goedert *et al.*, 2005). The biological activity of tau is regulated by its degree of phosphorylation, with normal tau requiring 2-3 mol of phosphate per mol of protein for optimal activity (Kopke *et al.*, 1993).

Hyperphosphorylation (at ~4-6 mol phosphate per mol of tau protein) depresses its ability to assemble and stabilise microtubules (Lindwall *et al.*, 1984; Alonso *et al.*, 2004). In AD brain tissue, tau is found to be abnormally hyperphosphorylated in two subcellular pools; (1) polymerised into intraneuronal tangles of paired helical filaments (PHFs) mixed with straight filaments or (2) in a non-fibrilised form in the cytosol (Iqbal *et al.*, 1986; Bancher *et al.*, 1989; Kopke *et al.*, 1993). The tau observed in NFTs appears inert until enzymatic degradation takes place allowing promotion of microtubule assembly. In contrast, when examined *in vitro* cytosolic tau sequesters normal tau (in addition to other MAP isoforms) causing inhibition and disassembly of microtubules (Kopke *et al.,* 1993; Alonso *et al.,* 1994, 1996, 1997; Iqbal *et al.,* 1994).

To form the PHFs so frequently observed in AD neurons, tau undergoes a series of seemingly ordered events. In its random coil configuration tau in pretangle neurons becomes progressively truncated at both its amino- and carboxy-terminals (Braak *et al.*, 1994). This is followed by truncation of both termini to a Tau-66 state and further cleavage in the NFTs (Binder *et al.*, 2005). The critical problem with tau is that it may be phosphorylated at over 30 serine/threonine sites in the AD brain (Alonso *et al.*, 1997; Hanger *et al.*, 1998). For example, phosphorylation at ser-262 or thr-231 has been shown to inhibit tau binding to microtubules (Sengupta *et al.*, 1998). Although there is still some debate as to whether NFTs or plaques occur first, the majority of evidence now suggests NFTs occur secondary to

plaque formation (Games *et al.*, 1995; Hsaio *et al.*, 1996; Oddo *et al.*, 2003, 2004; Gotz *et al.*, 2004; Bloom *et al.*, 2005).

1.1.3.2 Amyloid Plaques

The 'neuritic' or 'senile' plaques, which are characteristic of AD, are primarily composed of beta-amyloid (Aβ) protein. Initially identified in the meningeal blood vessels of AD patients, Aβ was found to be the primary component of the plaques observed in AD brain tissue (Glenner *et al.*, 1984; Masters *et al.*, 1985; Kang *et al.*, 1987). Two forms of plaque, diffuse and neuritic, may be present in the AD brain with much debate as to which is the more toxic form (Dickson, 1997b; Dickson *et al.*, 2001). Diffuse plaques are generally composed of shapeless, loosely aggregated Aβ and typically not associated with the dystrophic neurons and neuronal degeneration observed in AD patient brains (Ray *et al.*, 1998). In contrast, the cluster core of neuritic plaques contain extracellular densely aggregated fibrillar Aβ and are generally associated with degeneration and neuronal cell loss (Ray *et al.*, 1998; Velez-Pardo *et al.*, 1998). Much of the recent progress in elucidating AD pathogenesis has centred on the apparent role of amyloid$_{1\text{-}40}$ ($A\beta_{1\text{-}40}$) and $A\beta_{1\text{-}42}$ as the unifying pathological features of all forms of AD, which will be discussed more extensively in Section 1.3.

1.2 The Cholinergic Hypothesis of AD

It has long been accepted that AD is associated with a severe loss of neurons and associated neurotransmitter systems (Perry *et al.*, 1978; Whitehouse *et al.*, 1981, 1982). These neurotransmitter systems include the cholinergic, glutamatergic, and gamma aminobutyric acid (GABA)ergic pathways, effectively encompassing all three of the major neurotransmitter systems in the body (Rossor *et al.*, 1982; Lowe *et al.*, 1990; Francis *et al.*, 1993). Until recently the influence of these neurotransmitter systems on AD aetiology have been (almost exclusively) investigated separately. However, it is the degeneration of the cholinergic system that has historically been shown to be pivotal in AD aetiology and, until recently, was the only target of marketed drug treatments.

The most severe neuronal loss in AD brain tissue occurs in the nucleus basalis of Meynert, an area of the brain that provides the major source of cortical cholinergic innervation (Shute & Lewis, 1967; Mesulam & Van Hoesen, 1976; Wenk *et al.*, 1980; Whitehouse *et al.*, 1981, 1982). Initial biochemical studies conducted using AD brain tissue indicated substantial neocortical deficits in choline acetyltransferase (ChAT) and

acetylcholinesterase (AChE), the enzymes responsible for regulation of the main cholinergic neurotransmitter acetylcholine (ACh) (Davies & Mahoney, 1976; Perry *et al.,* 1977, 1978b; Bowen & Davison, 1980; Whitehouse *et al.,* 1982; Prado *et al.,* 2002). The reduction in these presynaptic ACh markers was found to correlate well with the degree of cognitive impairment observed in AD patients when compared to age-matched control subjects (Perry *et al.,* 1978a,b; Sugaya *et al.,* 1990; Rinne *et al.,* 1991). Loss of these connections is clearly detrimental as the basal and rostral forebrain cholinergic pathways serve important functional roles in memory processes such as attention and working memory, facets which are impaired in AD patients (Perry *et al.*, 1999; Stolerman *et al.*, 2000; Levin *et al.*, 2002; Singer *et al.*, 2004; Young *et al.*, 2004). In addition to the components highlighted above, a loss of high affinity nicotinic acetylcholine receptors (nAChRs e.g. $\alpha_4\beta_2$) is consistently observed in cortical post-mortem brain tissue relative to age-matched controls (Flynn & Mash, 1986; Nordberg & Winblad, 1986; Perry *et al.,* 1990, 1995; Sugaya *et al.*, 1990; Schroder *et al.,* 1991; Sabbagh *et al.,* 2001). This reduction in nAChR number is not only over and above that observed in normal aging, but the apparent loss in receptor number correlates significantly with the level of cognitive impairment in AD patients (Nordberg *et al.,* 1995, 1997).

The predominant high affinity nAChR (> 80 %) in the central nervous system is the $\alpha_4\beta_2$ nAChR yet surprisingly limited research has assessed its role in AD progression (Flores *et al.*, 1992; Paterson *et al.*, 2000; Dani, 2001; Drago *et al.*, 2003). Positron emission tomography studies utilizing (*S*)(-)[^{11}C]nicotine have demonstrated nicotine binding deficits in the temporal and frontal cortices of AD patients *in vivo* while an array of *in vitro* binding and autographical assays utilizing [^{3}H]-epibatidine, [^{3}H]-cytisine, and [^{3}H]-nicotine have been used to determine the number of high affinity nAChR binding sites and their subsequent reduction in AD brain tissue (Nordberg & Winblad, 1986; Whitehouse *et al.,* 1986; Nordberg *et al.,* 1988, 1990, 1995; Perry *et al.,* 1995; Marutle *et al.,* 1999; Sihver *et al.,* 1999). Although the majority of studies have identified a reduction in $\alpha_4\beta_2$ nAChR density, it would appear that this loss is a result of a reduction in α_4 subunit expression only as, somewhat surprisingly, the expression of the β_2 subunit appears to remain intact (Guan *et al.*, 2000).

The recent availability of transgenic animals that model some aspects of AD, has facilitated the largest advances in the understanding of an interaction between nAChRs and Aβ. Mice expressing the APP_{swe} mutation exhibit some degeneration of ChAT-immunoreactive fibres, reduced high affinity choline uptake, decreased cortical nicotinic

ligand binding, as well as a deficit in learning and memory trials (Wong *et al.*, 1999; Apelt *et al.*, 2002; Bednar *et al.*, 2002; Boncristiano *et al.*, 2002; Dineley *et al.*, 2002a; Luth *et al.*, 2003). Furthermore, treatment of APP_{swe} mice with nicotine has been shown to reduce Aβ deposition in the brain and cerebral blood vessels (Nordberg *et al.*, 2002; Hellstrom-Lindahl *et al.*, 2004) and to exacerbate *tau* pathology in the new triple transgenic mice that express mutations in presenilin I, human APP_{swe}, and human *tau* (Oddo *et al.*, 2005). The role of altered AChE in AD aetiology has been further strengthed by observations that glycosylation of AChE (increasing AChE levels) is altered in mice expressing APP_{swe} prior to Aβ plaque deposition and that expression of the human AChE gene in mice already expressing APP_{swe} leads to shortening of the time frame over which Aβ plaques normally develop (Fodero *et al.*, 2002; Rees *et al.*, 2003). Observations from studies utilizing bigenic mice have also endorsed a direct association between the cholinergic system and Aβ in AD. Mice expressing both the APP_{swe} and PSI_{M146L} FAD mutations develop age-related dense and diffuse amyloid plaques in conjunction with a decreased density of cholinergic boutons (Hu *et al.*, 2003). Interestingly, an increase in cholinergic bouton number was observed in mice expressing the APP_{swe} mutation alone, with no change observed in mice expressing only the PSI_{M146L} mutation (Wong *et al.*, 1999; Wengenack *et al.*, 2000). Decreased cholinergic fibre length and small cholinergic neurons are also common in mice expressing the APP_{swe} mutation (Boncristiano *et al.*, 2002; Klingner *et al.*, 2003). Finally, until the NMDA antagonist memantine received market approval, the only registered pharmacological interventions for AD were the AChE inhibitors such as tacrine, donepezil, and galanthamine (Palmer, 2003). These ACh-mimetics, although initially associated with significant side-effects and short plasma half-lives, do not cure the disease but do significantly delay the onset of many AD symptoms (Palmer, 2003). With the other major neurotransmitter systems seemingly unaffected in the early stages of AD, it was this wealth of evidence highlighting a central role for the cholinergic system in AD aetiology, has underlain the so-called "cholinergic hypothesis" of AD.

First postulated nearly 30 years ago, the cholinergic hypothesis suggested that the loss of cholinergic pathways precedes that of other neurotransmitter systems making it central to AD (Bowen *et al.*, 1976; Davies *et al.*, 1976; Perry *et al.*, 1977). The cholinergic neuron degeneration in the basal forebrain and associated loss of cholinergic neurotransmission in the cerebral cortex was thought to contribute significantly to the deterioration in cognitive function observed in AD patients (Bartus *et al.*, 1982).

The endogenous neurotransmitter of the cholinergic system is acetylcholine (ACh) and, in a reaction catalysed by choline acetyltransferase (ChAT), ACh is produced in the presynaptic terminal by the interaction of choline and acetyl-coenzyme A (CoA; Figure 1.1). Following release of ACh into the synaptic cleft, ACh binds to receptors on both the pre- and postsynaptic membranes while the remainder is broken down by AChE to choline and CoA. Choline itself then undergoes reuptake into the presynaptic terminal via a choline transporter protein (Dani, 2001). This endogenous neurotransmitter can act at both muscarinic (metabotropic) and nicotinic (ionotropic) acetylcholine receptors. Because they are not central to this thesis, only a brief overview of muscarinic AChRs will be presented, prior to a more in-depth look as the nicotinic AChR sutype.

1.2.1 The Neuronal AChR Family

The ACh receptor (AChR) gene family is divided into muscarinic and nicotinic AChRs, the latter of which may be subdivided further into nicotinic AChRs that bind or do not bind the snake toxin αBungarotoxin (αBgTx).

1.2.1.1 The Muscarinic AChR

Muscarinic AChRs (mAChRs) are members of the 7 transmembrane-spanning receptor superfamily and are widely distributed throughout the central (CNS) and peripheral (PNS) nervous system (Paterson *et al.*, 2000; Dani, 2001). In addition to having 7 transmembrane domains and conserved regions characteristic of G-protein linked receptors, mAChRs also share conserved tyrosine and threonine residues thought to be critical in forming the agonist binding site (Figure 1.2; Wess, 1993). A total of five different subtypes, (M_1, M_2, M_3, M_4, and M_5), have been cloned from both human and rat tissue (Volpicelli *et al.*, 2004). The first mAChR cDNA was cloned approximately 20 years ago with this achievement closely followed by the cloning of other related receptor subtypes (Kubo *et al.*, 1986; Bonner *et al.*, 1987, 1988; Peralta *et al.*, 1987). The muscarinic receptor subtypes M_1, M_3, and M_5 are coupled to the G_q protein which activates phospholipase C, whilst the M_2 and M_4 receptors couple to the $G_{i/o}$ protein, which results in inhibition of adenylate cyclase (Figure 1.2; Eglen *et al.*, 2001).

A number of studies have implicated muscarinic receptors (in particular M_1) in AD aetiology as they appear to undergo a preferential loss in the brains of AD patients (Flynn *et al.*, 1995; Fisher, 2000; Eglen *et al.*, 2001; Kihara *et al.*, 2004a). However, almost

Figure 1.1

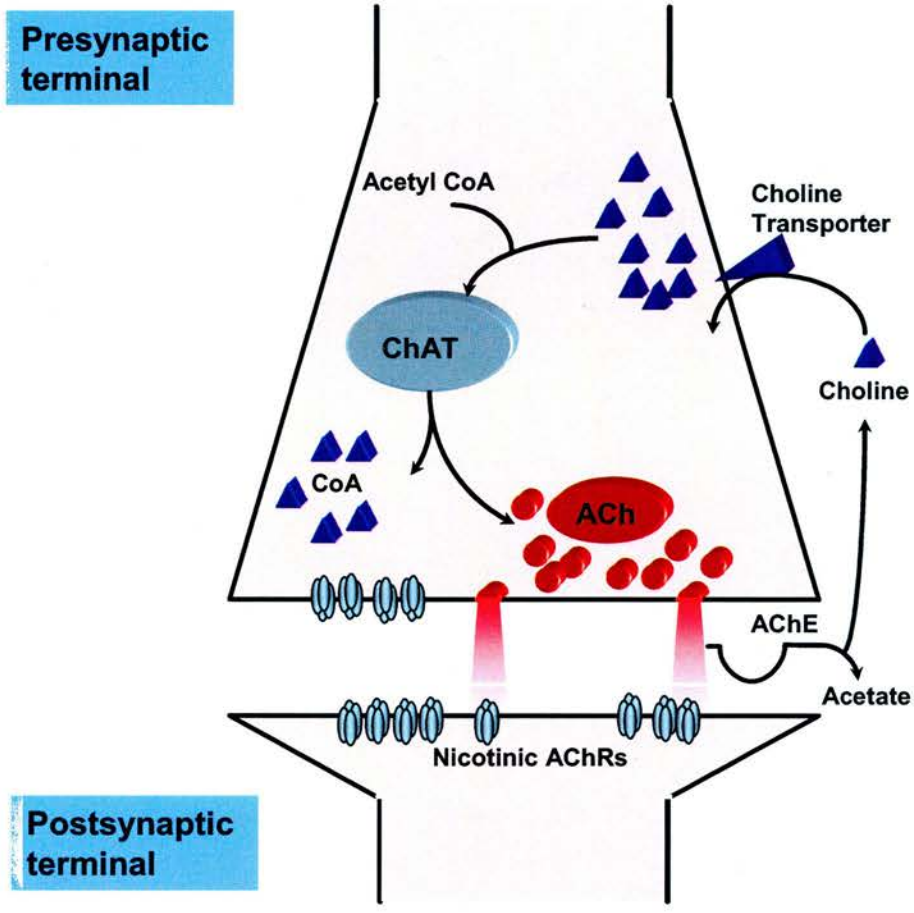

Synthesis of the Endogenous Cholinergic Neurotransmitter Acetylcholine. In a reaction catalysed by choline acetyltransferase (ChAT), acetylcholine (ACh) is produced from the interaction between choline and acetyl coenzyme A (acetyl CoA). On release into the synaptic cleft, ACh can interact with its receptors (AChRs) on either the pre- or postsynaptic membranes. Any excess ACh is degraded by acetylcholinesterase (AChE) to form acetate and choline. Choline itself undergoes reuptake into the synapse via a choline transporter protein.

all muscarinic M_1 agonists that have entered clinical trial have experienced problems due to the lack of specific agonists and antagonists, unacceptable side effects, low efficacy, and poor plasma pharmacokinetics (Eglen *et al.*, 2001). The problems associated with muscarinic ligands in clinical trials and the vast body of experimental evidence on neuronal nicotinic AChRs (nAChRs) means the majority of studies continue to focus on the role of these latter subtypes in AD.

1.2.1.2 Nicotinic AChR Stoichiometry

In contrast to the five mAChRs, there are 12 nAChR genes encoding for the ionotropic nAChRs characterized in humans, rodents, and chickens (Paterson *et al.*, 2000; Drago *et al.*, 2003). The α_2 - α_7, α_9, α_{10} and β_2 - β_4 subunits have been cloned from human tissue with an additional α subunit (α_8) found in avians (Elgoyhen *et al.*, 1994, 2001; Le Novere & Changeux, 1995). The nAChR subunits form either functional heterozygous or homozygous pentameric receptors, with heterozygous receptors generally assembling according to a $2\alpha3\beta$ stoichiometry using a combination of α_2-α_6 and β_2-β_4 subunits (Figure 1.3). However, growing evidence suggests more than one type of α or β subunit may be used in the pentameric structure giving rise to the so-called "triplet" receptor subunit configuration (Ramirez-Latorre *et al.*, 1996; Wang *et al.*, 1996; Boorman *et al.*, 2000; Groot-Kormelink *et al.*, 2001). Indeed, α_5 and α_6 nAChR subunits have been observed to form functional receptors in "triplet" formations with $\alpha_4\beta_2$ (Conroy *et al.*, 1992; Ramirez-Latorre *et al.*, 1996; Wang *et al.*, 1996; Groot-Kormelink *et al.*, 1998, 2001; Boorman *et al.*, 2000, Champtiaux *et al.*, 2003). In contrast, the α_7, α_8, and α_9 nicotinic subunits form homomeric receptors in mammalian tissue (Paterson *et al.*, 2000; Dani, 2001) with the latest addition to the nAChR subunit family (α_{10}) only forming functional receptors when co-expressed with α_9 (Elgoyhen *et al.*, 2001). The two predominant nAChRs in the CNS are the $\alpha_4\beta_2$ and the α_7 nAChR (Paterson *et al.*, 2000; Dani, 2001). The pharmacology and functional roles of these two receptors is discussed more extensively below.

1.2.1.2A The $\alpha_4\beta_2$ nAChR

The $\alpha_4\beta_2$ nAChR is the predominant nAChR in the CNS, comprising > 80 % of all high affinity nAChR binding sites (Paterson *et al.*, 2000; Dani, 2001; Drago *et al.*, 2003). The gene encoding the human β_2 subunit was cloned almost 15 years ago and exhibits a high degree of homology with the β_2 subunits cloned from rat (97 %) and chick

Figure 1.2

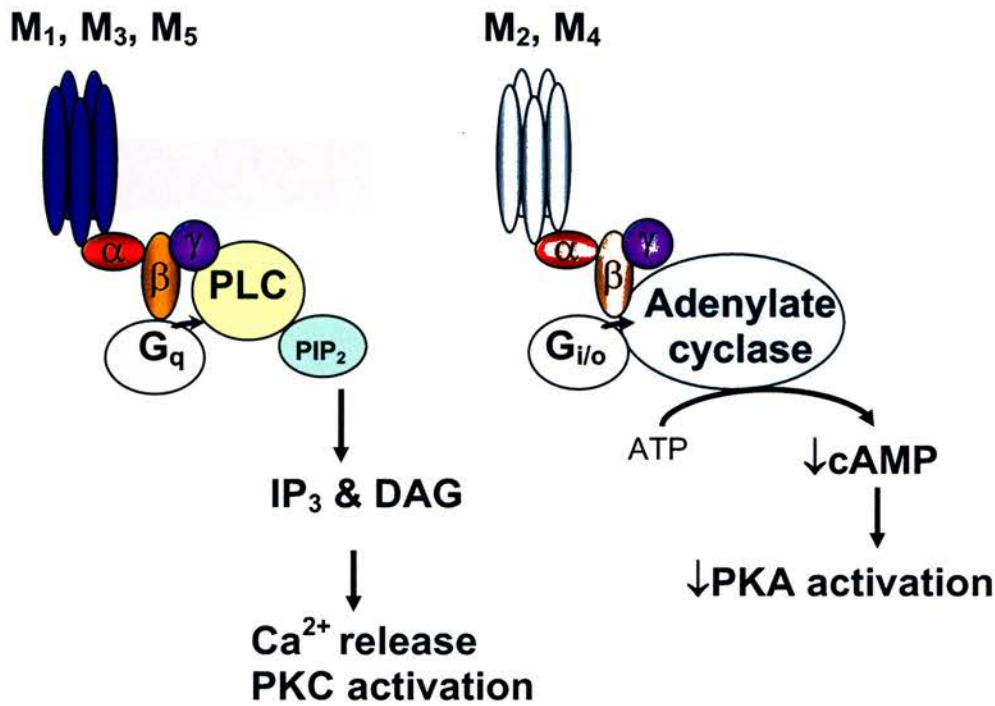

Muscarinic Acetylcholine Receptor G-protein Coupled Signalling Pathways. The stimulatory pathway (depicted on the left) is composed of receptors containing muscarinic subunits M_1, M_3, or M_5. ACh is released from the presynaptic terminal by depolarisation, and travels across the cleft to bind to the mAChR, thereby activating phospholipase-C (PLC) via a G-protein dependent mechanism. Activation of PLC stimulates phosphatidylinositol-4,5-bisphophate (PIP_2) hydrolysis generating the second messengers inositol (1,4,5-trisphosphate (IP_3) and diacylglycerol (DAG) resulting in intracellular calcium release and protein kinase C activation. The inhibitory pathway (depicted on the right) is composed of receptors containing the muscarinic subunits M_2 or M_4. The binding of ACh to the mAChR activates an inhibitory G_i-protein pathway that inhibits phosphorylation of adenylate cyclase. Consequently, the generation of adenosine 3',5'-cyclic monophosphate (cAMP) is reduced as well as protein kinase A (PKA) activation.

Figure 1.3

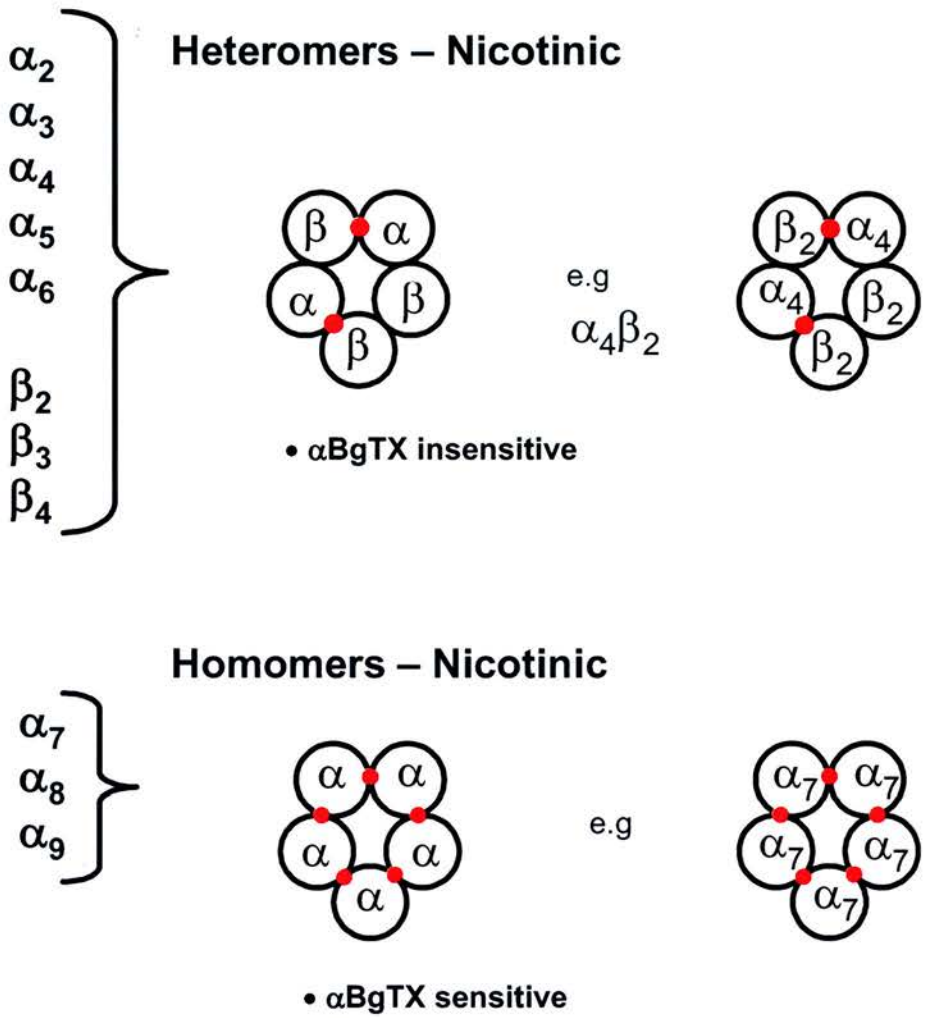

Schematic Representation of the Neuronal Nicotinic Acetylcholine Receptor Stoichiometry. Heterozygous nAChRs generally assemble according to a 2α3β stoichiometry using a combination of α_2-α_6 and β_2-β_4 subunits while α_7, α_8, and α_9 nAChR generally form homomeric nAChRs. However, recent evidence suggests the existance of "triplet" receptors that contain 1 or more different α or β subunits. The red dots depicted in the nicotinic AChR diagrams represent potential agonist binding sites. Figure adapted from (Sharples *et al.*, 2004).

(90 %) (Deneris *et al.*, 1988; Schoepfer *et al.*, 1988; Anand *et al.*, 1990). In contrast, the human α_4 subunit was not cloned until 1995, and only then was it co-expressed in human embryonic kidney cells (HEK 293) with the human β_2 subunit (Monteggia *et al.*, 1995). The human α_4 cDNA again has a high degree of homology to rat (84 %) and chick (76 %), although less than the β_2 subunit, with phosphorylation sites differing between species as a consequence of base changes in the cytoplasmic domain (Goldman *et al.*, 1987; Nef *et al.*, 1988; Monteggia *et al.*, 1995). The $\alpha_4\beta_2$ nAChR is widely expressed in all forebrain regions where it has a primary conformation of 2 identical α and 3 identical β subunits (Paterson *et al.*, 2000; Dani, 2001). However, as discussed above, functional $\alpha_4\beta_2$ receptors comprised of two or more different α and β subunits have been observed (Conroy *et al.*, 1992; Wang *et al.*, 1996; Nelson *et al.*, 2003). Furthermore, the α_4 subunit has itself been shown to exist in two isoforms although incorporation of the β_2 subunit means the two α_4 isoforms are indistinguishable on a pharmacological basis (Connolly *et al.*, 1992).

1.2.1.2B The α_7 nAChR

The other principal nicotinic acetylcholine receptor in the CNS is the homomeric α_7 receptor (Paterson *et al.*, 2000; Dani, 2001). Initially cloned from chick brain, the α_7 nAChR was subsequently cloned from rat and human brain (Couturier *et al.*, 1990; Schoepfer *et al.*, 1990; Seguela *et al.*, 1993; Peng *et al.*, 1994b). Sequence homology is again high between the species with the human α_7 nAChR having a 94 % and 92 % sequence identity to the rat and the chick α_7 nAChRs, respectively (Peng *et al.*, 1994b). Until the cloning of the α_7 nAChR, controversy surrounded its existance, although it is now generally agreed that the α_7 nAChR can be identified on the basis of its pharmacological interaction with αBgTx (Paterson *et al.*, 2000; Dani, 2001). The α_7 nAChR exhibits high calcium permeability, is rapidly desensitised, and it appears early in development (Role *et al.*, 1996; Albuquerque *et al.*, 1998; Agulhon *et al.*, 1999; Adams *et al.*, 2002). Recently, two isoforms of the α_7 nAChR were identified in rat intracardiac neurons, however they differ in their desensitisation properties, and in their sensitivity to αBgTx (Severance *et al.*, 2004). When expressed in *X. Laevis* oocytes, the α_7-2 nAChR was found to reversibly bind αBgTx and slower desensitisation properties when compared to the α_7-1 nAChR (Severance *et al.*, 2004).

Like the α_8 and α_9 subunits, α_7 nAChRs generally form functional homomeric receptors, however a variability in sensitivity to αBgTx and MLA has been demonstrated,

which has led to some evidence suggesting that heteromeric α_7 nAChRs may be found in some cellular systems (Yum *et al.,* 1996; Guo *et al.,* 1998; Yu & Role, 1998a,b). While the majority of studies support a homomeric structure, data from some, but limited, biochemical, pharmacological, and biophysical studies favour a heteromeric structure (Quik *et al.*, 1996; Yu *et al.*, 1998; Girod *et al.*, 1999; Palma *et al.*, 1999; Rakhilin *et al.*, 1999; Drisdel *et al.*, 2000; Ferreira *et al.*, 2001). Therefore, it is probable that the composition of the α_7 nAChR is species and/or region-specific. Indeed, α_7 and β_2 nAChR subunits have been observed to coassemble in rat hippocampal neurons and subsequent studies have shown that these subunits form functional receptors when expressed in Xenopus oocytes (Sudweeks *et al.*, 2000; Khiroug *et al.*, 2002). Moreover, the α_7 subunit has also been observed to form heteromers with the α_8 subunit in chick brain and may combine with other subunits in chick sympathetic neurons (Couturier *et al.*, 1990; Elgoyhen *et al.*, 1994; Gotti *et al.*, 1994).

1.2.2 Structure of nAChR

Despite the wide variety of potential nAChR subtypes conferred by the numerous individual subunits the general receptor structure remains the same for all (Dani, 2001). The neuronal nAChR receptor is a water filled pentamer with each individual subunit having a tetrameric structure (Figure 1.4, *upper*) (Paterson *et al.*, 2000; Dani, 2001). The general receptor structure comprises of a large hydrophilic amino terminus that faces the synaptic cleft and contains the ACh binding site, several glycosylation sites and a 15 residue cysteine loop between amino acids 128-142 (Devillers-Thiery *et al.*, 1993; Corringer *et al.*, 2000; Brejc *et al.*, 2001). Secondly, it has a compact hydrophobic region that may be further subdivided into 3 transmembrane segments (M1, M2, and M3) composed of 19-28 uncharged amino acids, separated from each other by short hydrophilic sections (Drago *et al.*, 2003). The hydrophilic components of the five M2 subunit segments form the wall of the ion channel and allow the flow of the cations, sodium (Na^+), potassium (K^+), and calcium (Ca^{2+}) (Leonard *et al.*, 1988; Akabas *et al.*, 1994; Corringer *et al.*, 2000). The third domain is a hydrophilic cytoplasmic loop (M4) of variable length that contains phosphorylation sites and like the N-terminus, M4 is exposed to the synaptic cleft where it plays a role in ligand binding (Paterson *et al.*, 2000; Dani, 2001). Finally, there is a short hydrophobic carboxyl terminus of approximately 20 aa which is exposed to the cytoplasm and contains further glycosylation sites (Paterson *et al.*, 2000; Dani, 2001), with all neuronal nAChRs possessing adjacent cytseine residues (analogous to cysteines 192 – 193 on the α_1 subunit of the AChR)

(Arias, 2000; Brejc *et al.*, 2001). The known ligand binding sites on the nAChR are illustrated in Figure 1.4 (*lower*) and are discussed in greater detail below.

1.2.2.1 Activation and Conformational Changes of the nAChR

The neuronal nAChR exists in one of four functionally distinct conformations (Paterson *et al.*, 2000; Dani, 2001). When an agonist binds to the receptor it undergoes an allosteric transition from the resting (closed) state, to an active (open) state, in which cations can permeate through the channel (Changeux *et al.*, 1998). In this latter state the channel opens on a micro- to millisecond time scale, binding agonists with low affinity (Galzi *et al.*, 1995). Continued presence of the agonist leads to closure of the channel and receptor desensitisation, with multiple desensitisation states postulated to exist (Changeux *et al.*, 1998). In the desensitized state the closed receptor channel has a refractory period to allow for re-activation and it becomes sensitive to high affinity ligand binding thereby promoting the active receptor conformation once more. Prolonged exposure of nAChRs to agonists is thought (although still controversially) to primarily result in an increase in receptor number, rather than the down regulation which is observed for many other ion channels (Kem, 2000). Of all the nAChRs, the $\alpha_4\beta_2$ and α_7 are thought to be the most sensitive to upregulation (Hsu *et al.*, 1996; Olale *et al.*, 1997) with a number of laboratories demonstrating that chronic nicotine exposure causes upregulation of both receptor subtypes when expressed in *Xenopus* oocytes (Peng *et al.*, 1994a), HEK293 (Gopalakrishnan *et al.*, 1996; Eilers *et al.*, 1997; Molinari *et al.*, 1998), and M10 cell lines (Peng *et al.*, 1994a) as well as an increase in the number of nAChR binding sites in human brain (Benwell *et al.*, 1988; Breese *et al.*, 1997; Court *et al.*, 1998). This effect has also been observed *in vivo* following chronic exposure of both rats and mice to cigarette smoke (Yates *et al.*, 1995; Pietila *et al.*, 1998; Nuutinen *et al.*, 2005). It is thought that the observed increase in receptor number in chronic exposure studies is not from increased receptor trafficking but because the nAChR undergoes a structural conformational change stabilising its expression at the cell surface (Peng *et al.*, 1994a).

1.2.2.2 Ligand Binding Sites on the nAChR

A number of binding domains have been identified within the structure of the neuronal nAChR, that encompasses sites for agonists, antagonists, allosteric modulators, and steroids all of which are illustrated in Figure 1.4 (*lower).*

Figure 1.4

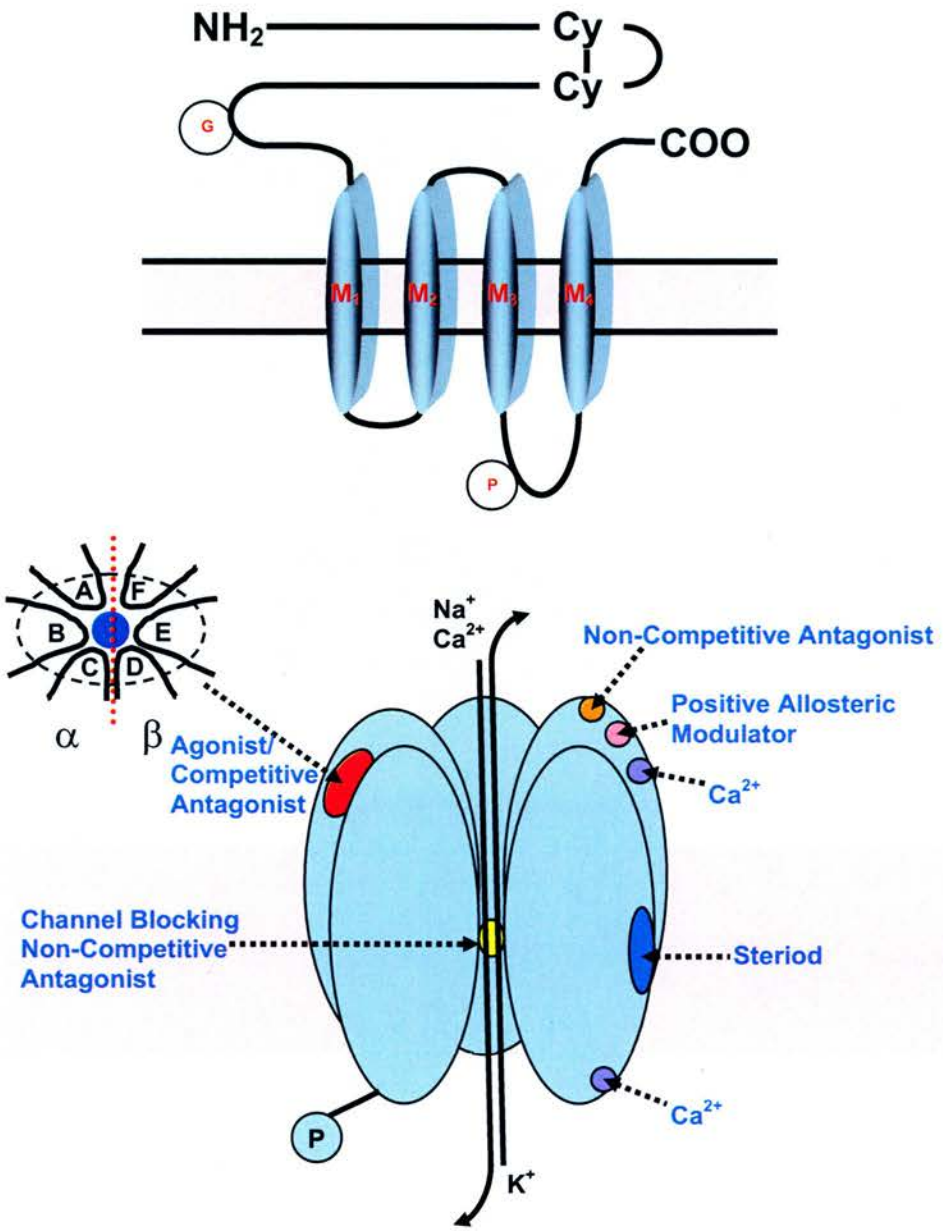

Schematic Representation of Neuronal Acetylcholine Receptor Structure and Ligand Binding Site Locations. The *upper* panel illustrates the proposed subunit structure, comprising of 4 prinicipal domains, adjacent cysteine residues, glycosylation and phosphorylation sites. The *lower* panel illustrates the proposed ligand binding sites on the nAChR with the *inset* on the lower diagram showing the agonist binding pocket loops. Loops A-C are on the α subunit and form the principal component while loops D-F form the complementary component on the adjacent α or β subunit. Figure adapted from Sharples & Wonnacott, 2004).

1.2.2.2A Agonist Binding Site on the nAChR

Until recently, the location of the agonist binding site on the nAChR had remained the subject of much debate (Brejc *et al.*, 2001). A great deal of research had focused binding primarily on techniques such as photoaffinity labeling (Chiara *et al.,* 2003a,b), mutagenesis (Sullivan *et al.*, 2000; Wilson *et al.*, 2001; Yassin *et al.*, 2002), and computer modeling of the nAChR (Sansom *et al.*, 1998) in an attempt to elucidate the location of the agonist binding site. However, in 2001, Brejc and colleagues described a 210aa acetylcholine binding protein (AChBP) that they had isolated from the fresh water snail *Lymnaea stagnalis.* ACh bound to this protein and these authors showed it was analogous to the α subunit of the nAChR. The determination of the AChBP crystalline structure provided confirmation that the agonist binding site lay on the α subunit interface adjacent to the other α and/or β subunits of the nAChR. Both the principal (located on the α subunit) and the complementary components (located on the adjacent α or β subunit) are required for a functional binding site. Indeed, all the nAChR agonist binding sites must be occupied for channel activation to occur (Colquhoun & Sakmann, 1985; Hess *et al.,* 1987; Udgaonkar & Hess 1987a,b; Keleshian *et al.,* 2000; Dajas-Bailador *et al.,* 2003).

In general, and as discussed earlier, the heteromeric nAChR (e.g. $\alpha_4\beta_2$) is composed of 2α and 3β subunits, and therefore it contains 2 agonist binding sites located at the interface between the α subunits and their adjacent β subunit (Alkondon *et al.*, 1993). In contrast, homomeric nAChRs (e.g. α_7) are comprised of 5α subunits giving rise to 5 potential binding sites, located at the interface between all 5 individual α subunits (Corringer *et al.*, 1995; Palma *et al.*, 1996; Wang *et al.*, 1996). Further site-directed mutagenesis studies identified the existence of six loops labeled A-F that participated in the formation of the agonist binding site (Figure 1.4 *lower*; Corringer *et al.,* 2000). The α subunit which harbours the principal component of the binding sites contains loops A, B, and C while the complementary component contains loops D, E, and F (Figure 1.4, *lower*).

1.2.2.2B Antagonist Binding Sites on the nAChR

Competitive antagonists such as *d*-tubocurarine (*d*-TC) interact reversibly with the nAChR, at or in close proximity to the agonist binding site (Figure 1.4; Arias, 2000). On binding to the receptor antagonists stabilise the receptor in the closed conformation, effectively blocking agonist access to the binding site. In contrast, non-competitive antagonists (e.g. mecamylamine) interact at a site distinct from the agonist binding site which is potentially located within or near the entrance of the ion channel (Figure 1.4). In

order for the non-competitive antagonists to interact with their binding site on the nAChR, it must first undergo activation prior to inhibition (Arias, 2000).

1.2.2.2C Allosteric Modulation of the Neuronal AChR

In addition to inhibiting the breakdown of ACh, acetylcholinesterase inhibitors can also function as non-competitive positive allosteric modulators of the neuronal nAChR by enhancing channel opening and consequently ion conductance (Pereira *et al.*, 1993). The competitive allosteric activator site was found to be located on the α subunit of the receptor, however it is again distinct from the agonist binding site (Figure 1.4, *lower*; Pereira *et al.,* 1993; Storch *et al.,* 1995).

Non-competitive negative allosteric modulators such as barbiturates and ethanol inhibit ion channel function without directly affecting ACh binding, with both high and low affinity sites identified (Dodson *et al.*, 1987; Lena *et al.*, 1993; Yost *et al.*, 1993). The high affinity site is believed to bind ligands in the nanomolar range and is located within the ion channel. Once the channel is activated, the negative allosteric modulator can bind to the high affinity site on the channel causing a rapid but reversible channel block (Valenzuela *et al.*, 1994). In contrast the low affinity site is thought to be located between the receptor protein and lipid membrane where the binding of ligands accelerates desensitisation. In addition to positive and negative allosteric modulation, the neuronal nAChR may also undergo modulation by phosphorylation via a number of different kinases that include protein kinases A and C, both of which can cause desensitisation of the receptor (Huganir *et al.*, 1990).

1.2.2.2D Steroid and Dihydropyrridine Binding to the Neuronal AChR

Recent studies have shown that neurosteroids are potential endogenous regulators of nAChR activity (Paradiso *et al.*, 2001; Curtis *et al.*, 2002). Indeed, non-endogenous steriods have been shown to bind to the extracellular hydrophilic domain of the nAChR at a site distinct from the agonist binding site, causing desensitisation of the receptor (Figure 1.4; Bertrand *et al.,* 1991; Inoue & Kuriyama, 1991). Furthermore, a number of dihydropyridine binding sites are also proposed to exist within the ion channel structure, with these thought to accommodate binding sites for L-type Ca^{2+} channel antagonists such as nifedipine and nimodipine (Lopez *et al.*, 1993).

1.3 The Amyloid Hypothesis of Alzheimer's Disease

Following on from the "cholinergic" hypothesis, the amyloid hypothesis of AD emerged in the mid-1980's and postulated that Aβ deposition was responsible for the

neurodegeneration observed in AD brains (Glenner *et al.*, 1984). As a degradation product of amyloid precursor protein (APP) metabolism, a role for Aβ in AD pathogenesis emerged when APP was found to be localised to chromosome 21 (Goldgaber *et al.*, 1987a,b; Kang *et al.*, 1987; Robakis *et al.*, 1987; Tanzi *et al.*, 1987). This was considered significant as those with trisomy 21 (Down's syndrome) evolved AD pathology in later life (Olson *et al.*, 1969). These studies led to the development of transgenic mice overexpressing mutant APP which were shown to have highly elevated Aβ levels, and extensive plaque deposition in the same regions as those observed in human AD patients (Sturchler-Pierrat *et al.*, 2000).

To thoroughly understand the complex role that Aβ plays in AD, its processing from the amyloid precursor protein must first be described.

1.3.1 Amyloid Precursor Protein

Amyloid precursor protein (APP), a normal constituent of the human brain and blood vessels, is an integral membrane protein with a large extracellular domain, a membrane anchoring domain, and a short intracellular C-terminal tail. Initially cloned and expressed in 1987, APP exists in multiple isoforms generated as a consequence of alternative splicing of APP mRNA with each variant named according to their amino acid (aa) length (e.g. APP_{695}, APP_{770}) (Goldgaber *et al.*, 1987a,b; Kang *et al.*, 1987; Robakis *et al.*, 1987; Tanzi *et al.*, 1987). The longer forms of the amyloid precursor protein are 751 and 770 aa in length and contain a 56 aa domain with homology to the Kunitz family of serine proteases inhibitors (Ponte *et al.*, 1988).

The immature form of APP can undergo several post-translational modifications including *N*- and *O*-glycosylation, and Tyr-sulphation to reach maturity (Hardy *et al.*, 2002). Following these initial modifications, APP is then subject to proteolytic processing by at least 3 individual proteolytic enzymes (α, β, and γ secretases) producing at least two different forms of β-amyloid. The most common peptides are 39-43 aa in length and are composed of a transmembrane domain of 11-15 aa and a 28 aa peptide generated from the extracellular domain of APP (Figure 1.5; Glenner & Wong, 1984; Masters *et al.*, 1985). As described below, these secretases are central to amyloidgenic and non-amyloidgenic processing of APP with the normal regulation of APP metabolism involving a contribution from a number of intracellular second messenger systems. The protein kinase C (PKC) pathway was the first APP-linked signal transduction system described, with increased PKC activity consistently observed in AD brain tissue (Gillespie *et al.*, 1992; Buxbaum *et al.*, 1993; Caporaso *et al.*, 1994). PKC has several calcium-dependent and independent

isoforms, although it is not known which isoform triggers soluble APP ($sAPP_\alpha$) secretion, however PKC is believed to target α-secretase, rather than APP itself (Sinha *et al.*, 1999b). Other studies utilising thapsigargin, an irreversible calcium reuptake inhibitor in the endoplasmic reticulum have implicated a Tyr-kinase dependent pathway, effectively bypassing the PKC pathway, and indicating an alternative target for therapeutic intervention (Buxbaum *et al.*, 1994; Petryniak *et al.*, 1996). Furthermore, downstream messengers such as IP_3-kinase have also been shown to stimulate $sAPP_\alpha$ release (Solano *et al.*, 2000). However, because proteolysis of APP by the α, β, and γ secretases are central to AD pathology, these are described in more detail.

1.3.1.1 α-secretase Processing of APP (The Non-Amyloidogenic Pathway)

The non-amyloidogenic, and putatively non-toxic pathway of APP processing, so-called as full length Aβ is not formed, involves proteolytic cleavage of APP by α-secretase (Figure 1.5). α-secretase cleaves APP in the extracellular domain near the middle of the Aβ sequence at residues Lys16 and Leu17 (Esch *et al.*, 1990; Sisodia, 1992). The soluble ectodomain (sAPPα) is released into the extracellular space while the 83 aa residue C-terminal fragment (C83) remains membrane anchored (Weidemann *et al.*, 1989; Haass *et al.*, 1992a; Sisodia, 1992). C83, a substrate for γ-secretase, undergoes further proteolysis in the transmembrane domain releasing a 3 kDa peptide p3 ($A\beta_{17-43}$) or $A\beta_{17-40}$ while the C-terminal fragment remains membrane bound. The p3 product is a significant component of diffuse amyloid plaques (Gowing *et al.*, 1994). APP cleavage by α-secretase is determined by the distance of the hydrolysed bond from the membrane (12-13 aa) and a local helical conformation rather than by specific residues (Sisodia, 1992). Although it is likely processing events occur in the trans-Golgi network, the exact subcellular localisation of α-secretase remains unclear (Kuentzel *et al.*, 1993).

Members of the disintergin and metalloprotease (ADAM) family, ADAM9, ADAM10, and ADAM17 (also known as tumour necrosis factor alpha converting enzyme, TACE) are believed to constitute α-secretase (Buxbaum *et al.*, 1998; Koike *et al.*, 1999; Lammich *et al.*, 1999). These proteases are implicated in both the constitutive and PKC regulated α-secretase pathways (Buxbaum *et al.*, 1998; Lammich *et al.*, 1999). Indeed it should be noted that while all cells contain a basal level of α-secretase activity, α-secretase proteolysis of APP may also be stimulated by phorbol esters (increasing PKC activity) or by diacylglycerol (DAG) generation after stimulation of muscarinic, glutamatergic, or

Figure 1.5

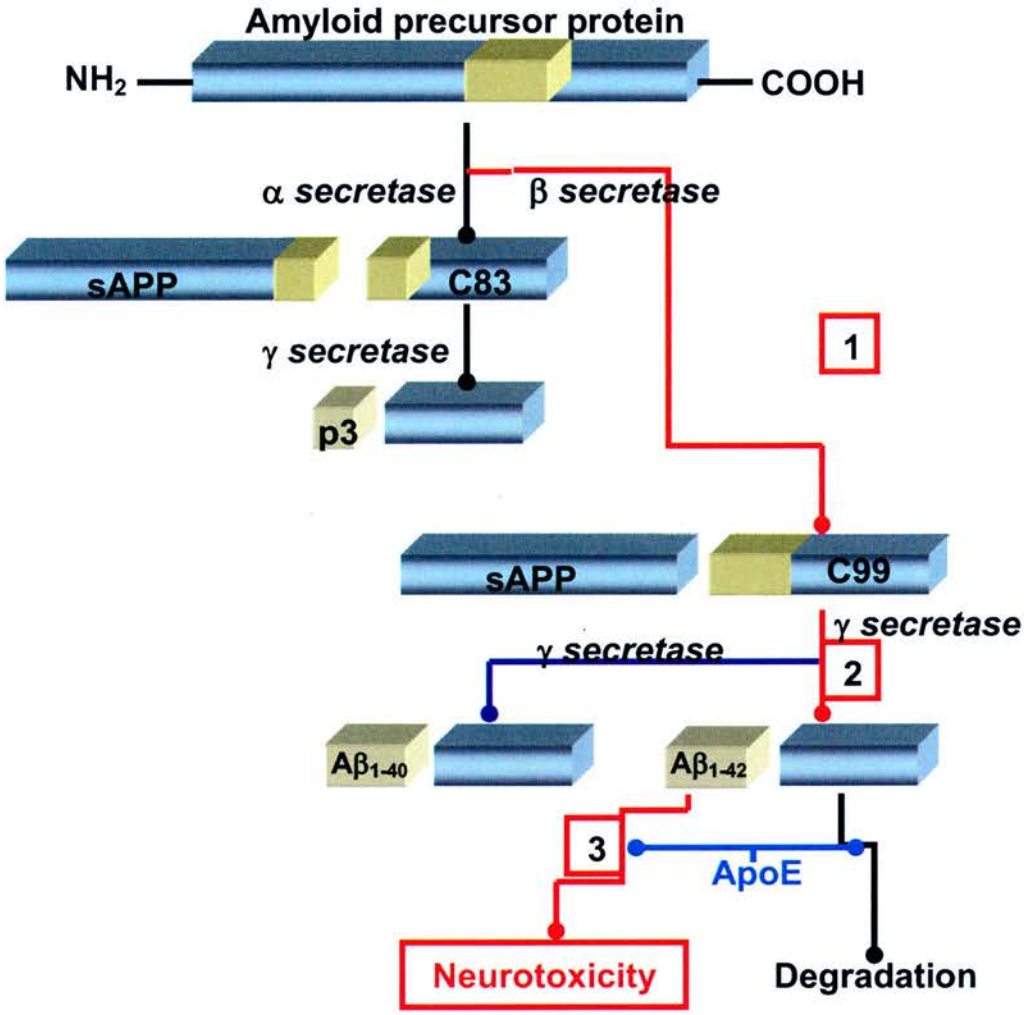

Proteolytic Processing of APP. APP, an integral membrane protein undergoes proteolytic cleavage by at least 3 enzymes to produce $A\beta_{1-40/1-42}$. Cleavage by α-secretase results in an 83 aa C-terminal peptide (C83) and soluble APP (sAPPα). Subsequent C83 cleavage by γ-secretase produces the small 3 kDa peptide p3 and a membrane bound C-terminus. Cleavage by β-secretase results in a 99 aa C-terminal peptide (C99) and soluble APP (sAPPβ). Further proteolytic cleavage of C99 by γ-secretase results in the release of either $A\beta_{1-40}$ or $A\beta_{1-42}$. The postulated neurotoxic pathway is illustrated in red. Numbered points represent where the following mutations are believed to occur: (1) Swedish APP (2) presenilin I & II and APP transmembrane (3) Flemish/Dutch and artic mutations. Apolipoprotein E (ApoE) is believed to exert its influence following the release of $A\beta_{1-42}$.

serotonergic neurons (Buxbaum *et al.*, 1990, 1993; Nitsch *et al.*, 1992; Caporaso *et al.*, 1994; Lee *et al.*, 1995).

1.3.1.2 β-secretase Processing of APP (The Amyloidogenic Pathway)

The amyloidogenic and putatively toxic pathway of APP processing results in the formation of full length Aβ and involves proteolytic cleavage of APP by β-secretase (Figure 1.5; Hardy & Selkoe, 2002). APP undergoes proteolysis at the NH_2-terminus by β-secretase to produce a truncated form of sAPP ($sAPP_\beta$) and a membrane bound 12 kDa C-terminal fragment (C99) that acts as a substrate for γ-secretase. C99 undergoes further heterogeneous proteolysis by γ-secretase in the transmembrane domain releasing a 4 kDa full length Aβ fragment. The majority of the Aβ species produced is a 40 aa peptide ($A\beta_{1\text{-}40}$), while a small proportion is a 42 aa C-terminal variant ($A\beta_{1\text{-}42}$; Esler & Wolfe, 2001). Traditionally it has been thought that this latter form, $A\beta_{1\text{-}42}$, is the toxic component of Aβ plaque formations.

The identification and cloning of the β-secretase enzyme (also known as beta-site APP cleaving enzyme, BACE), has demonstrated that β-secretase consists of a single transmembrane domain that contains two active site motifs and a conserved sequence (Hussain *et al.*, 1999; Sinha *et al.*, 1999a; Vassar *et al.*, 1999; Yan *et al.*, 1999; Lin *et al.*, 2000). Consistent with findings that Aβ is produced by a number of difference cell types, β-secretase mRNA is highly expressed in brain and in a variety of other tissues (Haass *et al.*, 1992a; Haass *et al.*, 1992b; Seubert *et al.*, 1992; Shoji *et al.*, 1992; Busciglio *et al.*, 1993; Vassar *et al.*, 1999; Yan *et al.*, 1999; Lin *et al.*, 2000). Cleavage by β-secretase has generally been considered to occur in the endosomal/lysosomal pathway, although there are reports of the potential involvement of the endoplasmic reticulum and Golgi apparatus (Chyung *et al.*, 1997; Sinha *et al.*, 1999a; Vassar *et al.*, 1999; Yan *et al.*, 1999; Lin *et al.*, 2000).

Targeting the accumulation of Aβ in brain tissue is being actively pursued in the search for a new treatment for AD, however, Aβ plaques may also accumulate in vascular tissue (Castellani *et al.*, 2004). Studies using transgenic mice have already demonstrated some potential side effects of vascular Aβ accumulation including haemorrhage and neuroinflammation (Winkler *et al.*, 2001; Herzig *et al.*, 2004). However, it is interesting to note that the β-secretase homolog BACE2 is found in highly vascularised systemic tissues such as the heart, kidney, placenta (Yan *et al.*, 1999; Farzan *et al.*, 2000), and therefore inhibitors of BACE1 may yet be beneficial in AD.

1.3.1.3 γ-secretase Processing of APP

The third secretase involved in APP proteolysis is γ-secretase and it exhibits some rather unusual characteristics. Firstly, before proteolysis of APP by γ-secretase may take place, the target protein must first be cleaved within its ectodomain (Figure 1.5; Struhl & Adachi, 2000; Esler *et al.*, 2001). Secondly, although proteolytic cleavage of proteins normally takes place under hydrophilic conditions (e.g. in the cytoplasm or extracellular space), due to the need for water, γ-secretase cleaves APP in the hydrophobic lipid bilayer (Struhl *et al.*, 2000; Esler *et al.*, 2001). Finally, cleavage by γ-secretase can produce not one but two different C-terminal peptides, $A\beta_{1-40}$ or $A\beta_{1-42}$, making it the rate-limiting step in APP proteolysis. Of the Aβ species produced, $A\beta_{1-40}$ constitutes approximately 90% of secreted Aβ while the majority of the remaining 10% in non-Alzheimer's Disease brains is composed of $A\beta_{1-42}$ (Mattson, 1997; Mills *et al.*, 1999). As suggested earlier, it is this latter peptide, $A\beta_{1-42}$, that is ultimately thought to be responsible for the insoluble Aβ plaques that accumulate in AD.

Until recently, there was considerable debate over the identity of γ-secretase, with the majority of evidence suggesting that γ-secretase was comprised of the integral membrane proteins presenilin I and presenilin II. However, very recent studies have shown that the complex contains four proteins; presenilin, nicastrin, *aph*-1, and *pen*-2 (for reviews see Steiner, 2004; Tomita & Iwatsubo, 2004). Whilst a full description of the role of these proteins is beyond the scope of this thesis, it is believed that presenilin carries the active site of γ-secretase while the other components are required for assembly, stabilisation, and maturation of the complex (Prokop *et al.*, 2004; Shirotani *et al.*, 2004; De Strooper, 2005).

To date, many pharmaceutical companies are pursuing α-secretase activation and inhibition of β- and γ-secretases in order to identify new therapies that could potentially treat AD (Chang *et al.*, 2004; Cumming *et al.*, 2004; Tomita *et al.*, 2004; Minter *et al.*, 2005).

1.3.2 Controversies Surrounding the Amyloid Hypothesis

Despite extensive research, there is still debate over the role of amyloid in AD, not least because it remains unknown how γ-secretase cleavage results in one predominant form of Aβ species (Pollack *et al.*, 2005). However, the major criticisms and concerns regarding this hypothesis can be generally subdivided into two areas; (1) a lack of plaque and symptom correlation (including the tau and amyloid time debate) and (2) the identity of the neurotoxic Aβ species. Ultimately on-going clinical trials which target the amyloid protein, such as

vaccines (e.g. Elan Pharmaceuticals, Inc.) or β-sheet breakers (Sereno Pharmaceuticals Inc.) will prove or disprove the role of Aβ in AD.

1.3.2.1 Amyloid Plaques and Symptom Correlation

To date, it is still true that diagnosis of AD can only be conclusively defined by the presence of neuritic plaques and neurofibrillary tangles after a post-mortem (Alzheimer, 1907). However, the number of plaques does not correlate well with the degree of impairment seen in patients (Wang *et al.*, 1999), and over 20% of elderly humans with AD-like dementia fail to meet pathological criteria (Lue *et al.*, 1999). In addition, some cognitively normal patients do meet pathological criteria and are referred to in studies as having "preclinical AD" (Lue *et al.*, 1999; Wang *et al.*, 1999). Part of the diagnosis problem probably arises from the way AD is clinically classified. Most humans over 60 years of age will experience some form of dementia, with symptom classification similar for all forms of dementia. Age and genetic variability affect the susceptibility to such diseases, and the degree to which a person is affected; this problem is not confined to humans. For example, although a number of APP-transgenic mice have been generated, the majority of mice fail to show clear-cut neuronal loss (Irizarry *et al.,* 1997a,b). However, a recent biochemical study of human AD brain tissue showed a better correlation between $A\beta_{1-42}$ levels and cognitive decline (Naslund *et al.*, 2000).

The literature discussing plaque and symptom correlation is associated with a large body of publications addressing whether Aβ or tau pathology is the underlying cause of AD, or to be more precise, whether plaques or tangles occur first. The belief tau pathology preceded that of Aβ primarily rested on a pivotal paper by Braak and Braak in 1991. In it they observed that the neurofibrillary degeneration of cell bodies gradually increased with age, and most importantly, they showed that this increase in tangle formation appeared to predate morphologically detectable Aβ plaques (Braak *et al.*, 1991). However, as the so-called "Braak Stage I" neuropathology was based on non-demented elders, it is impossible to know whether the neurofibrillary tangles observed were a result of AD (Hardy *et al.*, 2002). Indeed, other human studies contradict the Braak and Braak study, demonstrating Aβ pathology prior to tangle formation not only in AD patients but in those suffering Down's Syndrome (Mann *et al.*, 1986; Lemere *et al.*, 1996). In addition, a study following the fate of an Australian family with a variant form of FAD, showed that a member of that family who died from unrelated causes prior to the onset of dementia exhibited plaques but no tangles (Smith *et al.*, 2001).

Critically, there is now evidence from studies using double and triple transgenic mice which support the view that Aβ deposition occurs prior to tangle formation. Transgenic mice overexpressing both human APP and human tau produce increased tau-positive tangles when compared to mice expressing tau alone (Lewis *et al.*, 2001; Oddo *et al.*, 2003, 2004; Billings *et al.*, 2005). Importantly, the structure and number of Aβ plaques remained the same suggesting alterations in APP processing occurred prior to changes in tau metabolism. Transgenic mice overexpressing human APP alone experience a time-dependent increase in Aβ deposition and certain neuropathological and behavioural alterations that are comparable to those observed in AD, although they fail to show clear cut neuronal loss (Irizarry *et al.*, 1997a,b; Hsia *et al.*, 1999; Moechars *et al.*, 1999). In contrast, mice expressing both PS1 and human APP experience an acceleration in Aβ pathology (Borchelt *et al.*, 1996, 2002; Scheuner *et al.*, 1996; Citron *et al.*, 1997) and finally, as discussed earlier, inheritance of one or two ε4 alleles of apolipoprotein E (ApoE) is a strong genetic risk factor for AD (Corder *et al.*, 1993; Saunders *et al.*, 1993). When mice overexpressing APP are crossed with mice deficient for apoE, cerebral Aβ deposition is significantly decreased in the offspring supporting the evidence that apoE genotype is likely to influence Aβ metabolism (Bales *et al.*, 1999).

However, care must be taken when interpreting transgenic data. Indeed, the degree of pathology seen in APP-transgenics has been shown to be dependent upon the mouse strain (Hsiao, 1998). For example, mice expressing the Val717-Phe FAD mutation only express Aβ plaques beyond the age of 12 months, however these animals show cognitive impairment from as young as 3 months of age (Moechars *et al.*, 1999).

1.3.2.2 Determining the Neurotoxic Form of Aβ

Which form of Aβ is supposedly neurotoxic and what its relationship to neuronal degeneration continues to remain the subject of much debate. *In vitro*, Aβ spontaneously aggregates into fibrils that appear to be indistinguishable from those found *in vivo* (Selkoe, 1994; Lendon *et al.*, 1997; Lamb *et al.*, 1999). However, in all animals, Aβ is present in multiple conformations including monomers, oligomers, protofibrils, and mature fibrils, and as such it is difficult to define which form causes neurodegeneration (Walsh *et al.*, 1997, 2002a; Teplow *et al.*, 1998; Conway *et al.*, 2000; Bitan *et al.*, 2003). It is over 10 years since Selkoe (1993) reported that Aβ is predominantly found in a fibrillar form in the brains of AD patients, however, recent studies also show that soluble oligomers of Aβ, but not monomers or fibrils, inhibit long term potentiation (LTP; Walsh *et al.*, 2000a). As LTP is

thought to be pivotal in the formation of new memories, it is clear that various conformations of Aβ are likely to modify particular functions in the brain.

To date, the majority of recent AD research has focused on $A\beta_{1-42}$, the longer of the two Aβ species produced as a consequence of γ-secretase cleavage of APP (Ling *et al.*, 2003). Because of its length, $A\beta_{1-42}$ is more likely to form fibrils and once formed, these fibrils are more stable than those of $A\beta_{1-40}$ (Hardy *et al.*, 2002). Indeed, $A\beta_{1-42}$ can aggregate up to 70 times faster in solution than $A\beta_{1-40}$ (Thunecke *et al.*, 1998). $A\beta_{1-42}$ is believed to be a central component of insoluble neuritic plaques, with these plaques being a defining factor of AD neuropathology. However, recent evidence from a number of laboratories indicates that soluble rather than insoluble Aβ may be the more toxic species, although at present $A\beta_{1-42}$ still seems to be crucial in AD neuropathology (Tucker *et al.*, 2002; Walsh *et al.*, 2005). The situation is constantly evolving with additional questions likely to arise from continuing research.

Until recently, a central tenet of the amyloid hypothesis has been that Aβ exerts its neurotoxic effects extracellularly, however, new evidence suggests Aβ may accummulate intraneuronally (Blanchard *et al.*, 2003; Oddo *et al.*, 2003; Billings *et al.*, 2005; Crowther *et al.*, 2005). Although generally ignored, Masters and colleagues (1985) suggested 20 years ago that Aβ plaques form in neurons prior to deposition in the extracellular space. In 2003, Blanchard and colleagues demonstrated a high level of neuronal loss in their aged mouse, bigenic for PS1 and APP mutations. Although the neuronal loss did not correlate with amyloid plaque load, a high level of intraneuronal Aβ was observed indicating a possible involvement of intraneuronal Aβ in neurotoxicity (Blanchard *et al.*, 2003). Oddo and colleagues (2003) simultaneously produced a triple transgenic mouse (PS1, tau, and APP mutations) that showed synaptic dysfunction and intraneuronal amyloid immunoreactivity, prior to plaque or tangle deposition (Oddo *et al.*, 2003; Billings *et al.*, 2005). Furthermore, following expression of the artic $A\beta_{1-42}$ mutation in *Drosphilia melanogaster* intraneuronal Aβ accumulation was observed and it alone was enough to cause neurotoxicity (Crowther *et al.*, 2005). Taken together these recent studies indicate intraneuronal Aβ accumulation may not only precede Aβ plaque and tangle deposition but could underlie the neurotoxic loss observed in AD brain tissue. These findings will have a significant impact on future AD research considering the historical dogma that Aβ was only found extracellularly.

1.4 Interaction Between Aβ and nAChRs in Alzheimer's Disease

The individual roles of nAChRs and Aβ in AD have been well documented and although the cholinergic and amyloid hypotheses have been developed in parallel, both have been treated as almost distinct entities. Indeed, until recently, studies examining the interaction between Aβ and nAChRs were almost exclusively confined to the preservation or loss of cholinergic receptors in AD (Flynn & Mash, 1986; Nordberg & Winblad, 1986; Perry *et al.,* 1990, 1995; Sugaya *et al.,* 1990; Schroder *et al.,* 1991; Sabbagh *et al.,* 2001). For example, while the $\alpha_4\beta_2$ nAChR appears to be the predominant nAChR lost in AD, the α_7 nAChR is in fact quite well preserved, although there is some region-specific loss (Sugaya *et al.*, 1990; Perry *et al.*, 1995; Martin-Ruiz *et al.*, 1999; Guan *et al.*, 2000).

It is only in the last 5 years that evidence was provided to support a direct pharmacological interaction between nAChRs and Aβ in AD pathology. Wang and colleagues (2000a) showed that the α_7 nAChR and $A\beta_{1\text{-}42}$ could be co-immunoprecipitated in samples from human AD brain tissue and in cell lines transfected with the human α_7 nAChR and spiked with Aβ. Furthermore, radioligand binding studies using the α_7 nAChR antagonists [^{3}H]-αBgTx and [^{3}H]-MLA indicated that picomolar concentrations of $A\beta_{1\text{-}42}$ could inhibit binding to the α_7 nAChR (Wang *et al.*, 2000a). These initial findings were closely followed by a second study demonstrating that $A\beta_{1\text{-}42}$ exhibited > 5,000-fold higher affinity for the α_7 nAChR compared with the $\alpha_4\beta_2$ nAChR (Wang *et al.*, 2000b). Subsequent electrophysiological studies have indicated that nanomolar concentrations of Aβ inhibit nicotine-evoked currents in rat hippocampal slices, cultured neurons, and at $\alpha_4\beta_2$ and α_7 nAChRs expressed in *Xenopus laevis* oocytes (Dineley *et al.,* 2001, 2002a; Liu *et al.,* 2001; Pettit *et al.,* 2001; Tozaki *et al.,* 2002; Grassi *et al.,* 2003; Wu *et al.,* 2004). These papers generated considerable interest and there is now an emerging body of research that has shown a direct interaction between Aβ and, in particular, the α_7 nAChR (Kihara *et al.,* 1997, 1998, 2001; Dineley *et al.,* 2001, 2002b; Guan *et al.,* 2001; Liu *et al.,* 2001; Pettit *et al.,* 2001; Tozaki *et al.,* 2002; Fu & Jhamandas, 2003; Grassi *et al.,* 2003; Fodero *et al.,* 2004; Wu *et al.,* 2004; Xiao & Kellar, 2004). In addition, nicotine, a well characterized high affinity nAChR ligand, has been shown to breakdown fresh and preformed Aβ fibrils *in vitro,* slow Aβ fibril formation *in vivo,* as well as exerting neuroprotective properties by inhibiting Aβ-induced neuronal cell death in a range of standard cell and primary neuronal cultures (Hunter *et al.*, 1994; Salomon *et al.*, 1996; Kihara *et al.*, 1997; Zamani *et al.*, 1997; Kihara *et al.*, 1998; Kihara *et al.*, 2001; Shimohama *et al.*, 2001; Ono *et al.*, 2002; Grassi *et*

al., 2003; Martin *et al.*, 2004). Furthermore, a significant reduction in $A\beta_{1-42}$ deposition was observed when mice expressing the APP_{swe} mutation were treated (acutely and chronically) with nicotine (Nordberg *et al.*, 2002; Hellstrom-Lindahl *et al.*, 2004). .

One of the principal obsevations of the cholinergic hypothesis of AD was a general loss in AChE levels, and this was the primary driving force in the development of a number of ACh-mimetics that now include compounds such as tacrine, donepezil and galanthamine, with yet more still under clinical development (Yamada *et al.*, 2002; Palmer, 2003; Francotte *et al.*, 2004). Nevertheless, whilst the overall level of AChE is decreased in AD brain tissue, the concentration of the enzyme is increased around Aβ plaques and in neurofibrillary tangle-bearing neurons early in the Aβ deposition process (Atack *et al.*, 1983; Fishman *et al.*, 1986; Mesulam *et al.*, 1986; Geula *et al.*, 1989). Fodero and colleagues (2004) showed that this increase was mediated via the interaction of $A\beta_{1-42}$ with the α_7 nAChRs. In addition to the role of ACh itself, it is clear that the α_7 nAChR in particular plays an important role in learning and memory perhaps through modification of the MAP kinase pathway (Figure 1.6; Dineley *et al.,* 2001). Indeed, as in humans, deficits in attention and in learning and memory are observed in transgenic mouse models of AD (Tulving *et al.*, 1990; Hsiao *et al.*, 1996; Rossor *et al.*, 1996; Gordon *et al.*, 2001; Savonenko *et al.*, 2005). Importantly, the α_7 nAChR was found to be upregulated in a number of AD transgenic mouse models (Bednar *et al.,* 2002; Dineley *et al.,* 2002a). Furthermore, using the 5-CSR task, our group have shown that α_7 nAChR knockout mice exhibit deficits in sustained attention in comparison to their age-matched wildtype littermates and that the administration of nicotine significantly reversed this effect (Young *et al.*, 2004). However, care must be taken when interpreting data from mouse to human. Indeed, although the α_7 nAChR was found to be upregulated in transgenic models of AD, studies of human AD brain tissue indicate the α_7 nAChR is either lost or unchanged (Sugaya *et al.*, 1990; Martin-Ruiz *et al.*, 1999; Guan *et al.*, 2000).

Although a growing body of evidence now supports a direct interaction between $A\beta_{1-42}$ and nAChRs, controversy exists over the nature of this interaction and indeed the type of nAChR involved. Whilst Wang and colleagues (2000a,b) showed $A\beta_{1-42}$ inhibited [^{125}I]αBgTx binding at picomolar concentrations, other groups have failed to replicate this results despite the use of $A\beta_{1-42}$ concentrations ranging from femtomolar to nanomolar (de Fiebre *et al.*, 2005). Furthermore, although some functional studies suggest $A\beta_{1-42}$ is able to directly activate α_7 nAChRs this finding remains controversial with some studies showing

Figure 1.6

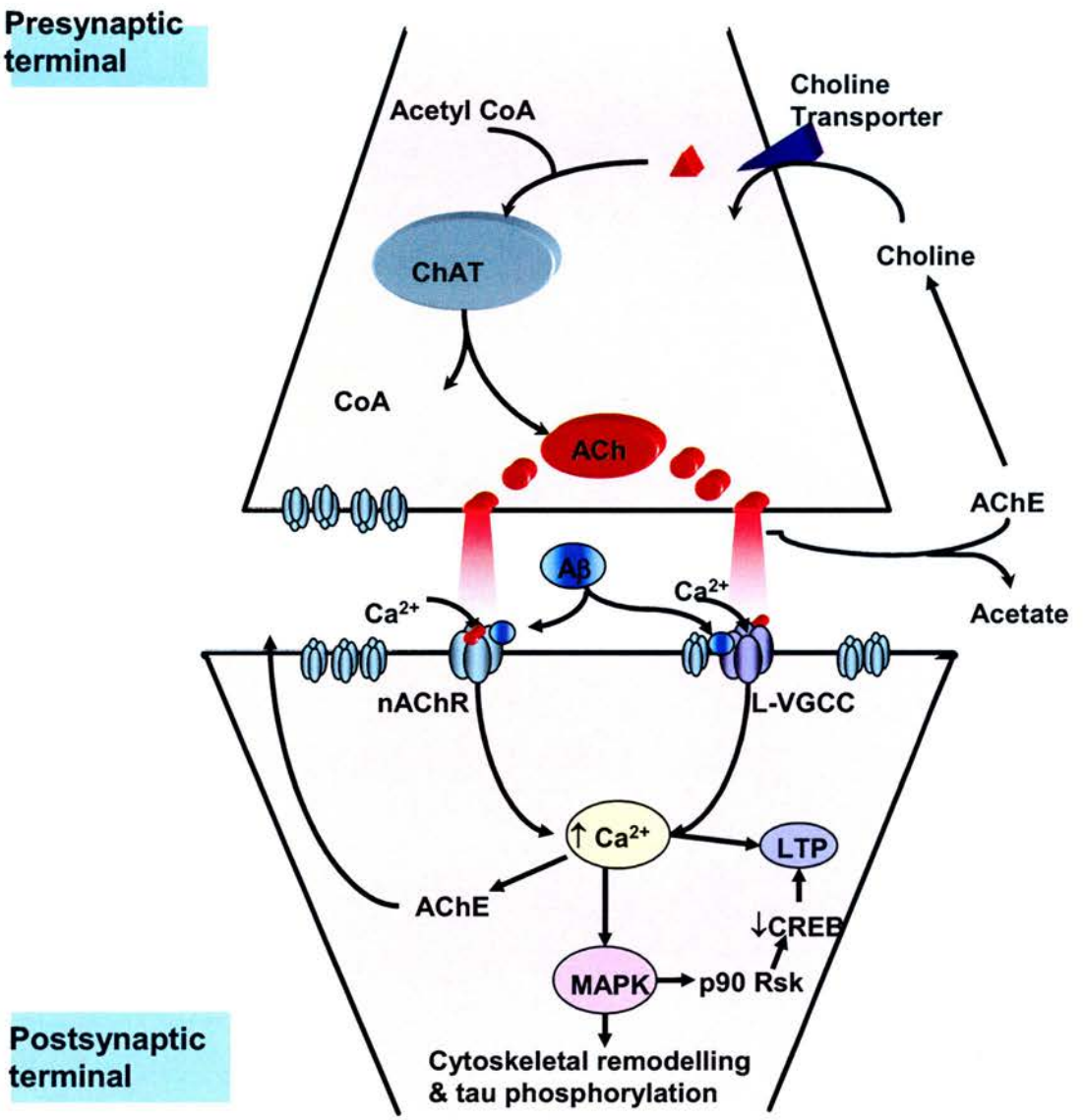

Effect of ACh and β-amyloid on the α_7 nAChR. Aβ is thought to alter calcium (Ca^{2+}) concentrations by binding directly to α_7 nAChRs or by interacting directly or indirectly with L-type voltage-gated Ca^{2+} channels (L-VGCC). Raising intraneuronal Ca^{2+} levels could influence long term potentiation (LTP) and thereby learning and memory processes directly or indirectly via the mitogen-activated protein kinase (MAPK) pathway. MAPK stimulates p90 Rsk which renders cAMP response element binding (CREB) protein transciptionally incompetent through phosphorylation of its serine133 residue leading to changes in LTP.

the $\alpha_4\beta_2$ nAChR may be the primary target of Aβ (Guan *et al.*, 2001; Liu *et al.*, 2001; Tozaki *et al.*, 2002; Dineley *et al.*, 2002b; Fu *et al.*, 2003; Grassi *et al.*, 2003). For example, Fu and Jhamandas (2003) demonstrated Aβ was able to evoke a concentration-dependent increase in inward current in rat basal forebrain neurons, however, this effect on single channel and whole cell currents was blocked by the general nicotinic antagonists mecamylamine and dihydro-β-erthroidine but not by α_7-specific antagonist MLA. In contrast, Tozaki and colleagues (2002) found $A\beta_{1\text{-}42}$ and $A\beta_{1\text{-}40}$ significantly inhibited the rat $\alpha_4\beta_2$ nAChR but not the α_7 nAChR when both were expressed in *Xenopus oocytes* (Tozaki *et al.*, 2002).

The possibility of a direct interaction between Aβ and nAChRs enables new pharmaceutical interventions to be developed for AD, and as such, it is important to fully investigate these potential interactions between Aβ and nAChRs. Therefore, in late 2001 following the publication of the Wang papers (2000a,b) I began to examine the interaction between the human $\alpha_4\beta_2$ and α_7 nAChRs and human $A\beta_{1\text{-}42}$. A comprehensive approach was taken incorporating pharmacological, functional, and biochemical techniques. It should be noted that my Ph.D. programme at the University of Edinburgh was sponsored by Fujisawa Pharmaceuticals Ltd. and that this has influenced the design of the radioligand binding assays. In particular these binding assays have been designed to not only assess nAChR pharmacology but so that they might be used in high-throughput screening (e.g. small volume design). Furthermore, this approach influenced the choice of tissue used in these experiments. Ideally, a species comparison of rat and human nAChRs would be carried out using brain tissue from rodents and human autopsy tissue. However, human brain tissue is not only a precious resource but presents many difficulties in terms of health and safety issues (e.g. separate equipment due to potential pathogen contamination). Therefore, I chose to work with a human cell line in which the human $\alpha_4\beta_2$ or α_7 nAChR was over-expressed. As this cell line does not natively express these receptors it has the added advantage of allowing the researcher to fully assess each individual receptor.

It should also be noted that the α_7 nAChR knockout mouse data presented in my thesis represents the initial data from an on-going collaborative study with other members of our Institute (Fujisawa Institute for Neuroscience in Edinburgh now Astellas Centre for Neuroscience in Edinburgh). This project involves cross-breeding the α_7 nAChR-knockout mouse with another mouse in which the human APP_{swe} gene has been over-expressed. Ultimately, this breeding programme will allow us to study the interaction of $A\beta_{1\text{-}42}$ and the α_7 nAChR *in vivo*. At the completion of my thesis only the α_7 nAChR-knockout mouse had been breed to sufficient levels to enable binding studies to be performed.

1.5 Hypothesis and Aims

I hypothesized that $A\beta_{1-42}$ interacts both pharmacologically and functionally with the $\alpha_4\beta_2$ and α_7 nAChRs. As such, the aims of my thesis were as follows:

(1) To establish a number of radioligand binding assays ([^{3}H]-epibatidine, [^{3}H]-cytisine, [^{3}H]-methyllycaconitine, and [^{3}H]-αBungarotoxin) to characterise the pharmacology of the rodent and human $\alpha_4\beta_2$ and α_7 nAChRs.

(2) To use the established radioligand binding assays in a collaborative study with other researchers within our Institute (Fujisawa Institute of Neuroscience in Edinburgh) to assess the pharmacology (affinity and binding density) of $\alpha_4\beta_2$ and α_7 nAChRs in a transgenic mouse model.

(3) To use the established radioligand binding assays to assess the ability of various forms of $A\beta_{1-42}$ to inhibit binding to rat and human $\alpha_4\beta_2$ and α_7 nAChRs.

(4) To establish a functional assay (calcium fluorescence, membrane potential fluorescence, whole cell patch-clamp electrophysiology) to assess the function of the human $\alpha_4\beta_2$ and α_7 nAChRs expressed in a non-native cell line.

(5) To use the established functional assay to determine any functional interaction between $A\beta_{1-42}$ and human $\alpha_4\beta_2$ and/or α_7 nAChRs.

(6) To determine whether $A\beta_{1-42}$ and nAChR subunits α_4 and/or α_7 co-immunoprecipitate.

2.0 MATERIALS AND METHODS

2.1 Experimental Animals

2.1.1 Rats and Non-Transgenic Mice

Unless otherwise stated, the animals used were either male Sprague Dawley rats (250-350 g) or male C57 Black 16/J mice (20-25 g) both supplied by Charles River (U.K.). Prior to tissue removal, animals were given food and water *ad libitum* and maintained on a 12 hour light/12 hour dark cycle. Studies were performed under licence by United Kingdom authorities (Scientific Animal Procedures Act, 1986, http://www.homeoffice.gov.uk), and in accordance with the Guide for the Care and Use of Laboratory Animals as adapted and promulgated by the National Institute of Health.

2.1.2 Transgenic α_7 nAChR Mice

An α_7 nAChR-null breeding pair were supplied by Jackson Laboratories (B6.12957-Chrna7^{tm1}Bay/J; Jackson Laboratories, Bar Harbour, U.S.A.) and backcrossed 11 times onto a C57B16/J background to produce litters of wildtype, heterozygous, and knockout mice. Animals were given food and water *ad libitum* and maintained on a 12 hour light/12 hour dark cycle. As detailed in Section 2.1.1, studies were performed under licence by United Kingdom authorities (Scientific Animal Procedures Act, 1986, http://www.homeoffice.gov.uk), and in accordance with the Guide for the Care and Use of Laboratory Animals as adapted and promulgated by the National Institute of Health.

To confirm the genotype of the α_7 nAChR transgenic mice, animals were tail tipped under halothane/nitrous oxide anaesthesia and tail DNA obtained by proteinase K treatment of tail samples (Promega, Southampton, U.K.). Three primer pairs were used corresponding to both wildtype (forward primer 5'-CCT GGT CCT GCT GTG TAA AAC TGC TTC-3', reverse primer 5'-CTG CTG GGA AAT CCT AGG CAC ACT TGA G-3', producing a 440 base pair (bp) product; and disrupted: (same forward primer as for wildtype, but reverse primer 5'-GAC AAG ACC GCG TTC CAT CC -3', producing a 750 bp product) alleles.

2.2 Maintenance of Cell Lines in Culture

2.2.1 SH-EP1-pCEP4-h$\alpha_4\beta_2$ and SH-EP1-pCEP4-hα_7 Cell Lines

SH-EP1 human epithelial cells containing either the cloned human $\alpha_4\beta_2$ nAChR (SH-EP1-pCEP4-h$\alpha_4\beta_2$; SH-EP-h$\alpha_4\beta_2$) or the cloned human α_7 nAChR, were kindly provided by Dr. R.J. Lukas, and both have been described previously (Pacheco *et al.*, 2001

and Peng *et al.*, 1999, respectively). Both stable cell lines were grown in Dulbecco's modified Eagle's medium (DMEM; Sigma, U.K.) 500 ml supplemented with 10 % of heat inactivated (56°C, 30 min) horse serum (Invitrogen, U.K.) and 5 % ml of foetal bovine serum (Invitrogen, U.K.). In addition, 5 ml of 100 units/ml penicillin / 100 mg/ml of streptomycin (Sigma), 4 ml of 50 mg/ml hygromycin (Sigma), 100 µl of 250 µg/ml amphotericin B (Sigma) and 10 ml of 4 mM glutamate (Sigma). In addition, 3 ml of 100mg/ml zeocin (Sigma) was added to SH-EP1-hα_7 media. The cells were incubated at 37°C in a humidified atmosphere with 95% air/5% CO_2 and passaged once per week when 90 % confluent. Media was changed twice weekly.

2.2.2 GH4C1-hα_7 Stable Cell Line

This cell line was transfected by Dr. K. Finlayson. As a component of the overall α_7 nAChR project, a human α_7 nAChR cDNA (Genbank Accession No. X70297) was cloned from an adult brain cDNA library by Cytomyx (Cambridge, U.K.) and ligated into the pcDNA3.1 expression vector between BamH1 and Not1. GH4C1 cells, a rat pituitary cell line were obtained from the European Collection of Cell Cultures (ECACC, U.K.) and stable cell lines generated following transfection with the human α_7 nAChR cDNA (Cytomyx, U.K.). The stably transfected cells were grown in Hams F-10 medium (500 ml, Sigma, U.K.), supplemented with horse serum (15 % v/v, Invitrogen, U.K.) and foetal bovine serum (2.5 % v/v, Invitrogen, U.K.). In addition, L-glutamine (2 mM, Sigma, U.K.), penicillin (100 units/ml, Sigma, U.K.), streptomycin (100 µg/ml, Sigma, U.K.), and G418 (500 µg/ml, Sigma, U.K.) was added, with the cells subsequently incubated at 37°C in a humidified atmosphere with 95% air/5% CO_2. Cells were passaged once a week while media was changed twice weekly.

2.2.3 Transient Transfection of SH-EP1 Cells with a Human α_7 nAChR cDNA

SH-EP1 null cells (a generous gift from Dr. R. Lukas) were transiently-transfected with the human α_7 nAChR cDNA from Cytomyx (U.K.) as described in Section 2.2.2, with cells studied 24-48 h post-transfection. This work was performed by Dr. K. Finlayson.

2.2.4 CHO-APP Cells

Chinese hamster ovaries (CHO) over-expressing the human amyloid precursor protein (APP) were obtained from the European Collection of Cell Cultures (ECACC,

U.K.). The stably expressing cells were maintained in Ham's F12 media with L-glutamate (500 ml, Invitrogen, U.K.) supplemented with 50 ml foetal bovine serum (Invitrogen, U.K.). 5 ml gentamicin (Invitrogen, U.K.) was added and cells incubated at 37°C in a humidified atmosphere with 95% air/5% CO_2. Cells were passaged once a week while media was changed twice weekly.

2.3 Radioligand Binding Studies

2.3.1 Membrane Preparation

2.3.1.1 Rodent Brain Membrane Preparation

Animals were sacrificed by Home Office Schedule one procedure, the brains were removed, and immediately placed in ice-cold saline (0.9% NaCl, Sigma, U.K.). The whole brain minus the cerebellum (due to the low density of α_7 nAChR, Davies *et al.*, 1999) was used for the P2 synaptosomal membrane preparation. Following dissection, the brain tissue was rolled on filter paper to remove superficial blood vessels, and weighed. At this point, tissues were either pooled (in general 30 mouse brains or 10 rat brains) or treated individually where noted. Brain tissue was homogenised in 15 volumes (15 vol. v/w) of 0.32 M sucrose using a glass/Teflon homogeniser, the homogenate centrifuged at 1,000 g for 10 min (4°C), and the resulting supernatant centrifuged at 17,000 g (20 min, 4°C). The synaptosomal/mitochondrial P_2 pellet was lysed in 30 vol. (v/w) of ice-cold water for 60 min and centrifuged at 50,000 g (10 min, 4°C). The membrane pellet was resuspended in the appropriate assay buffer (see Section 2.3.2.1), centrifuged at 50,000 g for 10 min (4°C), resuspended in 5 vol. (v/w) of the appropriate assay buffer and stored in 1.5 or 6 ml aliquots at -20°C.

On the day of use, frozen membranes were thawed, resuspended in 30 vol. (v/w) of appropriate assay buffer and the suspension centrifuged at 50,000 g for 10 min at 4°C. The final pellet was then resuspended in the appropriate assay buffer and kept on ice prior to use in the binding assay. The protein content of the brain tissue was determined using Molecular Devices BCA protein assay kit (Molecular Devices, UK; Section 2.3.1.3).

For α_7 nAChR transgenic mice experiments, brain membranes were prepared in the same manner as above. However, for the determination of specific [^{3}H]-methyllycaconitine or [^{3}H]-cytisine binding in transgenic mice brains, some brain tissue was initially prepared as individual brains rather than as a pooled group.

2.3.1.2 SH-EP1-hα_7 and SH-EP1-h$\alpha_4\beta_2$ Cell Membrane Preparations

Flasks (175cm^2; Corning® Life Sciences, U.K.) containing confluent (90%) cells were rinsed twice with 10 ml of pre-warmed (37°C) Hanks Balanced Salt Solution (HBSS, Sigma, U.K.), prior to addition of 15 ml of 5 mM Tris buffer (4°C, pH 7.4). The cells were dislodged from the flasks using a cell scraper and the suspension then placed on ice for 2 h to lyse. The lysate was spun at 50,000 g (10 min, 4°C) and the pellet resuspended in a 5x (v/w) of either 50 mM potassium phosphate buffer (pH 7.4; SH-EP1-hα_7) or 15 mM HEPES buffer (pH 7.4; SH-EP1-$\alpha_4\beta_2$) and stored in 1 ml aliquots at –20°C.

2.3.1.3 BCA Protein Assay

Bovine serum albumin (BSA) standards (BCA Protein Assay Kit, Pierce, U.K.) were made up in MLA/Cytsine assay buffer at a concentration of 0.03, 0.06, 0.125, 0.25, 0.5, and 1 mg/ml. In a 96-well flat bottomed clear plate (Corning® Life Sciences, U.K.), 100 µl of appropriate assay buffer was added into wells A1 and B1 which act as blank wells. Standards (10 µl) were added in duplicate in rows A2 – A7 and B2 – B7. Samples (10 µl) were then added to the 96-well plate in triplicate. The BCA reagent was made up to a dilution of 98 % Reagent A + 2 % Reagent B and 200 µl of BCA reagent added to each well. The plate was then covered in foil and incubated for 30 min at 37°C, prior to reading on a Dynex® MRX plate reader at an excitation wavelength of 560 nm.

2.3.2 Binding Experiments

2.3.2.1 Binding Buffers

2.3.2.1A [^{3}H]-Epibatidine Buffer

The [^{3}H]-epibatidine binding buffer consisted of 50 mM Tris-HCl containing 120 mM NaCl, 5 mM KCl, 1 mM $MgCl_2.6H_2O$, and 2.5 mM $CaCl_2.2H_2O$, pH to 7.4 with 5 M Hydrochloric acid (HCl) at room temperature. The [^{3}H]-epibatidine wash buffer consisted of 25 mM Tris HCl (pH 7.4).

2.3.2.1B [^{3}H]-Cytisine Buffer

The assay buffer and wash buffers were identical for the [^{3}H]-cytisine binding experiments. The buffer consisted of 50 mM Trizma® hydrochloride, 120 mM NaCl, 5 mM KCl, 1 mM $MgCl_2$ and 2.5 mM $CaCl_2$, pH to 7.0 with 5 M HCl at room temperature.

2.3.2.1C [^{3}H]-Methyllycaconitine and [^{3}H]-αBungarotoxin Buffers

The [^{3}H]-MLA and [^{3}H]-αBgTx assay buffer was a phosphate buffered saline solution (pH 7.4 with NaOH). One litre of assay buffer was made up using 395 ml of 0.1 M KH_2PO_4, 105 ml of 0.1 M K_2HPO_4 and 500 ml of MilliQ H_2O supplemented with 1 mM EDTA and 0.1 % (w/v) sodium azide. At room temperature this gives the buffer a pH of 7.4.

The [^{3}H]-MLA and [^{3}H]-αBgTx wash buffer consisted of 20 mM Na_2HPO_4, 5 mM KH_2PO_4, 150 mM NaOH, pH to 7.4 with 5 M NaOH.

2.3.2.2 Time Course Experiments

Time course experiments allow determination of when equilibrium of ligands and receptors has been reached, allowing hot saturation and competitive inhibition binding studies to be performed correctly. The time course of binding of the different radioligands was performed using rodent brain, SH-EP1-hα_7 or SH-EP1-h$\alpha_4\beta_2$ membranes at a fixed concentration of radioligand, excess cold inhibitor (non-specific binding (NSB), and membranes. These assays were terminated by filtration through GF/B glass-fibre filters (Whatman, U.K.) which had been presoaked (3 h) in [^{3}H]-epibatidine assay buffer, [^{3}H]-cytisine assay buffer, or 0.3 % polyethylemine ([^{3}H]-MLA and [^{3}H]-αBgTx), using a Brandel cell harvester (SEMAT Technical (UK) Ltd., U.K.), separating bound from free radioligand. Concentrations of radioligand, membranes, and non-specific inhibitor are listed in Table 2.1. Filters were then placed in 6 ml scintillation vials (VWR Scientific Products, U.K.) and 4 ml of Emulsifier Safe™ scintillation fluid added. Vials were left overnight to equilibrate before radioactivity was determined in a Packard 2500TR liquid scintillation counter using automatic quench correction.

2.3.2.3 Hot Saturation Experiments

Radioligand binding levels in a membrane preparation (e.g. tissue or cells) are dependent upon the protein content of the preparation and the specific activity and concentration of the chosen radioligand (Bennett, 1985; Keen, 1995; Foreman, 2002). Parameters measured are total binding, (TB, the amount of binding measured in the absence of an unlabelled competitor) and non-specific binding (NSB, the amount of binding measured in the presence of an excess unlabelled competitor). Specific binding (SB) is then determined by subtracting NSB from TB. By keeping the membrane (receptor) density and inhibitor concentrations fixed and only varying the radioligand concentration, these experiments allow the determination of the equilibriation dissociation constant K_d of the

radioligand and the number of binding sites B_{max} it labels. In brief, radioligands (at concentrations at least 10 (but preferably 100)-fold above and below the estimated K_D, see Table 2.2, pg 37) were incubated with rat brain, SH-EP1-h$\alpha_4\beta_2$, or SH-EP1-hα_7 cell membranes for a minimum of 1 h at 22°C in 6 ml polypropylene tubes (12 x 75 mm, VWR).

Following the incubation period, bound radioligand was separated from free by filtration through GF/B glass-fibre filters using a Brandel harvester and filters treated as described in Section 2.3.2.2. Exact assay conditions for individual radiolabels are detailed in Table 2.2.

2.3.2.4 Competitive Inhibition Binding Experiments

In competitive inhibition studies, the incubation time, membrane concentration, and the radioligand concentration are all kept constant with the concentration of the competing drug varied. As the concentration of the competing drug is increased the amount of bound radioligand decreases, allowing determination of the concentration of the ligand which inhibits 50% of specific radioligand binding (IC_{50}). In brief, the radioligand (at a fixed concentration) was incubated with membranes and increasing concentrations of inhibitor for a set time period. Following the incubation period, bound radioligand was separated as described previously (Section 2.3.2.2). Exact assay conditions for individual radiolabels are detailed in Table 2.2.

2.3.2.4A [^{3}H]-Epibatidine Competitive Inhibition Experiments

[^{3}H]-Epibatidine (NEN DuPont, U.K., 48 Ci/mmol) competitive binding assays were carried out by modification of a method described by Houghtling and colleagues (1995). Epibatidine assay buffer (Section 2.3.2.1A) or test drug was incubated with [^{3}H]-epibatidine (final concentration 15 pM) and either 3 mg of rat brain membranes or 0.03 mg of SH-EP1-h$\alpha_4\beta_2$ cell membranes in a total assay volume of 4 ml for 4 h at 22°C. Non-specific binding was determined in the presence of 300 μM (-)nicotine. To reduce NSB, the glass-fibre filters were pre-soaked in epibatidine assay buffer for 3 hours prior to use. Binding was terminated as described previously (Section 2.3.2.2). Full assay conditions are detailed in Table 2.2. This work was performed by Dr. K. Finlayson.

Table 2.1 Assay Conditions for Time Course Experiments Using [^{3}H]-Epibatidine, [^{3}H]-Cytisine, [^{3}H]-Methyllycaconitine, and [^{3}H]-αBungarotoxin.

Radioligand	Supplier	[Radioligand] (nM)	Rat Brain Membranes (mg)	SH-EP1-h$\alpha_4\beta_2$ Cell Membranes (mg)	SH-EP1-hα_7 Cell Membranes (mg)	Mouse Brain Membranes (mg)	Non-Specific Inhibitor
[^{3}H]-Epibatidine	NEN Dupont NET1102	0.015	3	0.03	-	-	300 μM (-)Nicotine
[^{3}H]-Cytisine	NEN Dupont NET1054	3	0.4	0.115	-	-	10 μM (-)Nicotine
[^{3}H]-MLA	Tocris R1029	2.5	0.4	-	0.15	0.85	10 μm *d*-tubocurarine
[^{3}H]-αBgTx	Amersham Biosciences TRK603	2	-	-	0.60	-	10 μM (-)Nicotine

Radioligands were incubated with the appropriate membrane preparation for up to 2 h ([^{3}H]-cytisine and [^{3}H]-methyllycaconitine), 6 h ([^{3}H]-epibatidine), or 8 h ([^{3}H]-αBungarotoxin) at 22°C (or where stated 4°C or 37°C). At the end of the incubation period, bound radioligand was separated from free by filtration through GF/B glass-fibre filters (pre-soaked for 3 h in 1 % polyethylemine (PEI, [^{3}H]-epibatidine), 0.3 % PEI [^{3}H]-MLA and [^{3}H]-αBgTx), or [^{3}H]-cytisine assay buffer) using a Brandel harvester. Filters were then placed in 6 ml scintillation vials and 4 ml of Emulsifier Safe™ scintillation fluid added. Vials were left overnight to equilibrate before radioactivity was determined in a Packard 2500TR liquid scintillation counter using automatic quench correction. Each TB data point was performed in duplicate (NSB data points in singulate), with a minimum of 3 individual experiments performed. Methods are adapted from Gnadish *et al.,* 1999 ([^{3}H]-epibatidine), Gopalakrishnan *et* al., 1996 ([^{3}H]-cytisine), Davies *et al.*, 1999 ([^{3}H]-MLA) and Lukas *et al.*, 1981 ([^{3}H]-αBgTx).

Table 2.2: Assay Conditions for [^{3}H]-Epibatidine, [^{3}H]-Cytisine, [^{3}H]-Methyllycaconitine, and [^{3}H]-αBungarotoxin Hot Saturation and Competitive Inhibition Experiments

Radioligand	Specific Activity Ci/mmol	[RL]	Rat Brain Membranes (mg)	SH-EP1-hα$_4$β$_2$ Cell Membranes (mg)	SH-EP1-hα$_7$ Cell Membranes (mg)	Incubation Time (h)	Non-Specific Inhibitor
[^{3}H]-Epibatidine	48	0.015 – 470 pM	3	0.03	-	4	300 μM (-)nicotine
[^{3}H]-Cytisine	35.2	0.03 – 72 nM	0.4	0.115	-	1	10 μM (-)nicotine
[^{3}H]-MLA	56.17	0.22 – 36 nM	0.4	-	0.15	1	10 μM *d*-tubocurarine
[^{3}H]-αBgTx	59	0.02 – 18 nM	-	-	0.15	6	10 μM *d*-tubocurarine

Increasing concentrations of radiolabels ([RL]) were incubated with rat brain tissue or SH-EP1 cell membrane preparations for 1 h ([^{3}H]-cytisine and [^{3}H]-methyllycaconitine), 4 h ([^{3}H]-epibatidine), or 6 h ([^{3}H]-αBungarotoxin) at 22°C. At the end of the incubation period, bound radioligand was separated from free by filtration through GF/B glass-fibre filters (pre-soaked for 3 h in 1 % polyethylemine (PEI, [^{3}H]-epibatidine), 0.3 % PEI [^{3}H]-MLA and [^{3}H]-αBgTx), or [^{3}H]-cytisine assay buffer) using a Brandel harvester. Filters were then placed in 6 ml scintillation vials and 4 ml of Emulsifier Safe™ scintillation fluid added. Vials were left overnight before radioactivity was determined in a Packard 2500TR liquid scintillation counter using automatic quench correction. Each data point was performed in duplicate (NSB data points in singulate) with a minimum of 3 individual experiments performed.

2.3.2.4B [^{3}H]-Cytisine Competitive Inhibition Experiments

[^{3}H]-Cytisine (NEN®DuPont, U.K., 35.2 Ci/mmol) competitive binding assays were carried out by modification of a method described by Sabey and colleagues (1998). Cytisine assay buffer or test drug was incubated with [^{3}H]-cytisine (final concentration 3 nM) and either 400 µg of rat brain membranes or 115 µg of SH-EP1-h$\alpha_4\beta_2$ cell membranes in a final assay volume of 250 µl (60 min, 22°C). Non-specific binding was determined in the presence of 10 µM (-)nicotine with binding terminated as described previously (Section 2.3.2.2). To reduce NSB, GF/B glass fibre filters (Whatman) were pre-soaked in cytisine assay buffer. Full assay conditions are detailed in Table 2.2.

2.3.2.4C [^{3}H]-Methyllycaconitine Competitive Inhibition Experiments

The [^{3}H]-Methyllycaconitine (([^{3}H]-MLA), Tocris; 19.8 Ci/mmol) competitive binding assay was carried out by modification of a method described by Davies *et al.,* (1999). Assay buffer or test drug was incubated with [^{3}H]-MLA (final assay concentration of 2 nM) and either 400 µg of rat brain membranes or 150 µg SH-EP1-hα_7 cell membranes in a total assay volume of 250 µl (60 min, 22^{0}C). Non-specific binding was determined in the presence of 1 mM *d*-tubocurarine. Binding was terminated as previously described (Section 2.3.2.2) using GF/B glass fibre filters pre-soaked in 0.3 % v/v poly(ethyleneimine). Full assay conditions are detailed in Table 2.2.

2.3.2.4D [^{3}H]-αBungarotoxin Competitive Inhibition Experiments

The [^{3}H]-αBungarotoxin ([^{3}H]-αBgTx) competitive inhibition experiments were carried out in the same manner as the [^{3}H]-MLA competitive assay using the same assay buffer and only the following a small modification in assay protocol. The specific binding of [^{3}H]-αBgTx (2 nM; NEN®DuPont, U.K., 59 Ci m/mol) was determined by the addition of 10 µM *d*-tubocurarine to assess NSB. Preliminary studies indicated αBgTx is an irreversible ligand at α_7 nAChRs and does not reach equilibrium. As a consequence, all studies were terminated following a 6 h incubation period when specific binding consistently reached 65 % with extended incubation times not producing any further increase in the level of specific binding. It should be noted that because αBgTx is an irreversible ligand, K_D and K_i values calculated for αBgTx are apparent values only and are dependent upon the length of incubation time. Assay conditions are detailed in Table 2.2.

2.3.2.4E Data Analysis

(i) Hot Saturation Studies

Data were fitted using a one-site saturation equation in SigmaPlot 2002, version 8 (SPSS UK Ltd., U.K).

$$y = \frac{B_{max} \cdot x}{K_D + x}$$

where y is the specific binding (total – non-specific; in fmol/mg protein), x is the concentration of free ligand, B_{max} is the maximum number of binding sites (fmol/mg protein), and K_D is the concentration of ligand to reach half maximal binding.

(ii) Competitive Inhibition Studies

Data were fitted using an iterative, non-linear least square curve fitting program SigmaPlot 2002 (version 8, SPSS UK Ltd., U.K.) to a one-site logistic model:

$$y = \text{min} + \frac{\text{max} - \text{min}}{1 + 10^{(x - \log EC50)}}$$

where x is the log concentration of drug, y is the total or specific binding, *min* is the minimum response plateau, *max* is the maximum response plateau, *log* EC_{50} is the log of EC_{50} or IC_{50}.

The following equation was used for assessing any potential two-site binding;

$$y = \left[\text{min} + (\text{max} - \text{min}) \cdot \frac{F_1}{1 + 10^{(x - \log EC501)}} + \frac{1 - F_1}{1 + 10^{(x - \log EC502)}} \right]$$

where x is the log concentration of the inhibitor (cold ligand), y is total or specific binding, *min* is non-specific binding, *max* is maximum binding in the absence of cold ligand, F_1 is the fraction of first class of receptor with the $logEC_{50l}$ being the affinity of the ligand for

this site, and $logEC_{502}$ being the affinity of the ligand for the second site. Units for *max* and *min* are identical as those used for *y*.

When the inhibitor was the unlabelled form of the radioligand, the binding site affinity, (K_D) and the binding site density, (B_{max}) were calculated using the following equations;

$$\textbf{(A)} \qquad K_D = IC_{50} - [[^3H]\text{-radioligand}]$$

$$\textbf{(B)} \qquad B_{max} = \frac{(SB / RL_{SA})}{[\text{protein}]}$$

where IC_{50} is the concentration of the cold unlabelled ligand that inhibits 50 % of the radiolabel binding to the receptor, *SB* is the specific binding (disintergrations per minute, d.p.m.), RL_{SA} is the specific activity of the radiolabel, and *[protein]* is the protein concentration of tissue sample (mg).

For all other unlabelled competing ligands, K_i values were calculated using the Cheng-Prusoff approximation (Cheng & Prusoff, 1973).

$$K_i = \frac{IC_{50}}{1 + ([[^3H]\text{-radioligand}] / K_D}$$

2.3.2.4F Preparation of Soluble and Insoluble $A\beta_{1-42}$

Human (or rat where stated) $A\beta_{1-42}$ (Calbiochem, U.K.) was resuspended in the following manner to make 100 μM stock solutions of soluble amyloid (1) 5 % acetic acid (Sigma) and MilliQ (MQ) H_2O e.g. (Pettit *et al.*, 2001), (2) 100 mM Tris buffer (pH 9.0) containing 50 % dimethyl sulfoxide (DMSO, Sigma) and giving a final pH 8.0 (e.g. Wang *et al.*, 2000 *personal communication*), or (3) 100 mM HEPES (pH 8.5; Sigma, e.g. Dineley *et al.*, 2001). Likewise, human $A\beta_{1-42}$ obtained from Rpeptide (U.S.A.) was resuspended to 100 μM in sterile MQ H_2O.

A solution of aggregated $A\beta_{1-42}$ was made in accordance with the instructions supplied by Calbiochem (U.K.). In brief, 250 μg of $A\beta_{1-42}$ was dissolved to a concentration of 6 mg/ml in sterile MQ H_2O and then diluted to 1 mg/ml in magnesium-free, calcium-free phosphate buffered solution (Invitrogen, U.K.). The stock solution was incubated at 37°C for 48 h and, following the incubation period, the solution was diluted to 100 μM in sterile MQ H_2O.

All 100 μM $A\beta_{1-42}$ stock solutions were aliquoted (100 μM) and used fresh, or frozen following storage at -20°C. On the day of use, $A\beta_{1-42}$ aliquots were diluted in the appropriate assay buffer with all frozen aliquots used within 6 weeks.

2.3.2.4G Radioligands and Unlabelled Compounds

[^{3}H]-Epibatidine (48 Ci/mmol) and [^{3}H]-cytisine (35.2 Ci/mmol) were purchased from NEN®DuPont, (U.K.) with [^{3}H]-αBgTx (59 Ci/mmol) from Amersham Biosciences UK Ltd. Galantamine hydrobromide, [^{3}H]-MLA (56.17 Ci/mmol), methyllycaconitine citrate, physostigmine sulphate, and tacrine hydrochloride were purchased from Tocris (Bristol, U.K.). Acetylcholine, 4-aminopyridine (4-AP), atropine, bicuculline methoiodide, α-bungarotoxin, choline, cytisine, 1,1-dimethyl-4-phenylpiperazinium iodide (DMPP), *d*-tubocurarine, epibatidine, methylcarbamylcholine chloride (MCCC), McN-A-343, mecamylamine, methacholine chloride, (-)nicotine, pilocarpine, RJR2403, scopolamine, and tetraethylammonium (TEA) were from Sigma (U.K). E2020 was supplied by Fujisawa Pharmaceuticals Ltd. (Japan). The stereoisomers of the putatively selective α_7 nAChR agonist (-)AR-R17779 and (+)ARR-17779 (Mullen *et al.*, 2000) were custom synthesised by Tocris Cookson, (U.K.). Stock solutions for all drugs were prepared in distilled H_2O and diluted into the appropriate buffer on the day of the assay. All other standard chemicals were of research grade.

2.4 Thioflavin T Assay For the Assessment of $A\beta_{1-42}$ Aggregation

Human $A\beta_{1-42}$ stock solutions were prepared as detailed in Section 2.3.2.4F. The degree of β-sheet aggregation of the $A\beta_{1-42}$ solutions was then determined using the fluorescent dye, thioflavin T (Sigma, U.K.), which specifically binds to fibrous β-sheet structures (Vassar & Culling, 1959; LeVine, 1993; Yoshiike *et al.*, 2003). For time course experiments, 40 μl of aggregated $A\beta_{1-42}$ stock solution (1 mg/ml; final assay concentration, 40 μM) was added to 20 μl of thioflavin T (final assay concentration 10 μM) and 140 μl of sterile Milli Q water. For all other experiments, 10 μl of $A\beta_{1-42}$ (final assay concentration, 5

μM) was added to 20 μl of thioflavin T (final assay concentration, 10 μM), and 170 μl of appropriate assay buffer ([^{3}H]-MLA, [^{3}H]-cytisine, or electrophysiology buffers). The assay was conducted in a 96-well clear flat-bottomed black plates (Corning® Life Sciences, U.K.), with samples shaken for 10 s prior to each measurement. For time course experiments, measurements were made every 30 min for 48 h whereas for all other experiments, plates were read immediately after the addition of thioflavin T.

The relative degree of β-sheet aggregation was assessed in terms of fluorescence intensity, which was measured at 37°C (time course experiments) or 22°C (all other experiments) using a Flexstation® Microplate Reader (Molecular Devices, U.K.). These temperatures were chosen as 37°C is the Calbiochem recommended temperature to aggregate $A\beta_{1-42}$ while all other experiments were conducted at 22°C to assess their degree of aggregation under normal experimental conditions. Measurements were performed at an excitation wavelength of 444 nm and an emission wavelength of 485 nm, resulting in a maximal detection of bound thioflavin T (Yoshiike *et al.*, 2003). The fluorescence intensity of control samples containing either dye and cells, or dye, cells, and the control vehicle for the $A\beta_{1-42}$ sample of interest were subtracted from that of each $A\beta_{1-42}$ sample to account for background fluorescence. Results are presented in the form of mean ± S.E.M. which is an average of three individual wells.

2.5 Intracellular Calcium and Membrane Potential Experiments

2.5.1 Cell Culture and 96-well Plate Preparation

The SH-EP1-h$\alpha_4\beta_2$ or SH-EP1-hα_7 cells were maintained in culture as described in Section 2.2.1 and 2.2.2, respectively. For both fluorescence based assays, cells were grown in 150 cm^2 cell culture (vent cap/canted neck) flasks (Corning® Life Sciences, U.K.). Two days before the experiment, 100 μl of poly-D-lysine (1 mg/ml, diluted 1:50) was added to each well of a 96-well clear flat-bottomed black plates (Corning® Life Sciences, U.K.) and left overnight in a laminar flow hood. The following day, an appropriate number of flasks containing SH-EP1-h$\alpha_4\beta_2$ or SH-EP1-hα_7 cells were removed from the incubator, the waste media removed using a stripette (Corning® Life Sciences, U.K.) and the cells rinsed twice with pre-warmed (37°C) Hank's balanced salt solution (HBSS; Invitrogen, U.K.). To encourage cell dissociation, 2.5 ml of trypsin-EDTA (0.25 % trypsin, 1 mM EDTA.4Na, Invitrogen, U.K.) was added to the flasks prior to placement in the the incubator. After 5 min, 2.5 ml of the appropriate cell media was then added to neutralise the effects of trypsin and the cell suspension transferred to a 50 ml centrifugation tube (Corning® Life Sciences,

U.K.) prior to centrifugation at 150 g for 5 min. The supernatant was then removed and the cell pellet resuspended in 10 ml of the appropriate cell media, prior to cell counting using a haemocytometer. The cell suspension was diluted again if required to generate a solution of approximately 1 million cells / ml. Any excess poly-D-lysine was removed from the 96-well plate using a sterile yellow pipette tip attached to a vacuum filtration system and 100 µl of cell suspension added to each well (final cell density was 100,000 cells/well). When higher cell densities were required, the initial cell dilution was altered, and then the 96-well plates were returned to the incubator and left overnight at 37°C, prior to use in either the intracellular calcium or membrane potential assays.

2.5.2 Intracellular Calcium ($[Ca^{2+}]_i$) Assay

On the experimental day, the cell plates were removed from the incubator and the supernatant removed. Calcium assay buffer (100 µl HBSS with 2 mM HEPES, pH 6.0; Molecular Devices, U.K.) with an additional 2.5 mM Ca^{2+} added to the plate followed by 100 µl of calcium assay dye (FLIPR® Calcium Assay Kit, Molecular Devices, U.K.) added. The plates were then incubated for 1 h at 37°C to facilitate equilibration. Agonist ligands were made up at 5 x their final concentration in a separate 96-well flat bottomed clear plate (Corning® Life Sciences, U.K.) and were added to the cell plate by the Flexstation® fluorescence plate reader (Molecular Devices, U.K.) robotics system. In studies using antagonists, the ligands (25 µl at 10 x final concentration) were added to the cell plates 50 min into the dye equilibration and preincubated for 10 min. Changes in $[Ca^{2+}]_i$ were measured by a change in fluorescence intensity determined by the Flexstation® plate reader (Molecular Devices, U.K.) with excitation and emission wavelengths set at 485 and 525 nm, respectively.

2.5.3 Membrane Potential Assay

Membrane potential assays were performed using a modification of the $[Ca^{2+}]_i$ assay method. On the experimental day, the cell plates were removed from the incubator and the supernatant removed. Membrane potential assay buffer (100 µl of HBSS with 2 mM HEPES, pH 6.0; Molecular Devices, U.K.) and 100 µl of membrane potential dye (FLIPR® Membrane Potential Assay Kit, Molecular Devices, U.K.) were added and the plates were incubated for 30 min at 25°C to facilitate equilibration. Agonist ligands were made up at 5 x their final required concentration in a separate 96-well flat bottomed clear plate (Corning® Life Sciences, U.K.) and were added to the cell plate by the Flexstation® fluorescence plate

reader (Molecular Devices, U.K.) robotics system. In studies using antagonists, following a 20 min incubation, the ligands (25 µl at 10 x their final required concentration) were added to the cell plates and preincubated for 10 min. Changes in membrane potential were assessed by a change in fluorescence intensity determined by the Flexstation® plate reader (Molecular Devices, U.K.) with excitation and emission wavelengths set at 535 and 560 nm, respectively.

2.6 Whole-Cell Patch-Clamp Recordings

2.6.1 Preparation of SH-EP1-h$\alpha_4\beta_2$ and SH-EP1-hα_7 Cell Lines

The cell lines used in these studies were the SH-EP1 human neuroblastoma cells stably transfected with either human $\alpha_4\beta_2$ nAChRs or human α_7 nAChRs or GH4C1 cells, a clonal rat pituitary cell line also stably expressing the human α_7 nAChR. Cells were maintained as previously described in Sections 2.2.1 - 2.2.3. For whole-cell patch-clamp recordings, cells were plated on 35 mm dishes (Nunc™, U.K.) at a density of 2 x 10^4 cells/ml and examined when 80 - 90 % confluent. Prior to electrophysiological recordings, the cell media was removed, the cells rinsed in the appropriate bath solution, and allowed to equilibrate at room temperature for 30 min.

2.6.2 Preparation of Recording Electrodes

Glass electrodes for whole-cell patch-clamp electrodes were made from borosilicate glass (Intracel, U.K.) with glass dimensions of 1.5 mm O.D. x 1.17 mm I.D. and containing a filament. The glass was mounted onto a Narashige pipette puller (Figure 2.2A) and pulled, with respect to the ramp value of the glass, into a patch electrode. The electrode tips were then fire polished using a heated platinum-iridium wire (Goodfellow Metals, U.K.) to the required 4-6 MΩ resistance.

2.6.3 Whole-Cell Patch Clamp Electrophysiology Recording

To reduce ambient noise and vibration, a major problem associated with electrophysiology, all recordings were conducted in a Faraday cage with the recording equipment mounted on a pressurised air table. Cells were visualised with a Nikon Diaphot inverted microscope with Hoffman modulation contrast (Modulation Optics Inc., USA) with plates mounted on the microscope stage (List L/M-PC patch clamp amplifier, List-Medical, Germany). Borosilicate glass patch electrodes back filled with the appropriate electrode solution were mounted on a head stage (List L/M-PC patch clamp amplifier, List-Medical,

Germany) which was fixed to a micromanipulator (List L/M-PC patch clamp amplifier, List-Medical, Germany). After forming a tight seal (>1 GΩ) on the cell surface suction was applied to convert to conventional whole-cell recording. After breakthrough from the cell-attached configuration to the whole-cell configuration, the cells were clamped at -60 mV by a List L/M-PC patch clamp amplifier (List- Medical). Drugs were applied to cells using an eight inlet barrel micromanifold (see Figure 2.3) with a single outlet tube having a diameter of 200 μm. Drug delivery was controlled electronically using Lee valves and a valve controller. The outlet tube was positioned close to the cell which was continuously superfused with bath solution (1 ml/min into a holding chamber with an approximate volume of 2 ml) via one inlet tube. Switching to other inlet tubes permitted application of multiple drugs or drug concentrations. Suction also occurred at 1 ml/min to allow for circulation of the recording solution in the holding chamber and the maintenance of a constant volume.

Whole-cell patch experiments were performed using a patch clamp amplifier (List L/M-PC, Germany). Currents were low pass filtered at 1 kHz, digitised at 5 kHz using an analogue-to-digital converter (Digitdata 1200A, Axon Instruments, USA) and stored on a personal computer. Access resistance (R_a) and cell capacitance (C_m) were routinely compensated, with R_a determined at the start and end of the experiment and data rejected if it had changed more than 25 % from the initial value of <15 MΩ before compensation. Series resistance (R_e) was routinely compensated at 70 %. Voltage commands were generated with pClamp7 software (Axon Instruments, U.K.).

2.6.3.1 Drug Application Protocols For Electrophysiology

To determine the stability of nAChR responses 10 μM (-)Nicotine was applied for 375 ms every 3 min. Nicotine dose-response curves (0.3 nM – 1 mM) were generated in the presence and absence of 100 μM d-tubocurarine (*d*-TC) applied pseudo-randomly as described above. For studies investigating soluble human $A\beta_{1-42}$, sixteen cells were randomly allocated into 4 groups of four with (-)nicotine (10 μM) again applied every 3 min to produce an inward current (I_{nic}). Following the initial application of nicotine, the perfusing solution was switched from bath solution to one of the following for 6 min before returning to bath solution; soluble human $A\beta_{1-42}$ (100 or 300 nM), Hepes vehicle, 5 % acetic acid vehicle, 50/50 DMSO/Tris vehicle or BS. A delay of ~45 s was observed before the new solution exited the outlet tube.

2.6.3.2 Recording Solutions and Drug Dilutions

Whole-cell patch clamp recordings were made from SH-EP1 cell lines continuously superfused in one of two bath solutions; (1) bath solution one (BS_1) comprised of (mM); 150 NaCl, 2.5 KCl, 2 $CaCl_2$, 1 $MgCl_2$, 10 D-glucose, 0.0005 tetrodotoxin, 10 Hepes, (Liu *et al.*, 2001) or (2) bath solution two (BS_2) comprised of (mM);. 120 NaCl, 3 KCl, 2 $CaCl_2$, 2 $MgCl_2$, 25 D-Glucose, 10 Hepes, (Zhao *et al.*, 2003; Wu *et al.*, 2004). Both solutions were pH balanced to 7.4 with NaOH, and osmolarity maintained between 300 and 310 mOsm

Pipette electrode solutions were matched to the bath solution. BS_1 pipettes were filled with (mM); 100 $CsCH_3SO_3$, 20 CsCl, 2 $MgCl_2$, 2 Mg-ATP, 10 Hepes, 20 phosphocreatine, adjusted to pH 7.2 with CsOH (Liu *et al.*, 2001). In contrast, BS_2 pipettes were filled with a K^+-free electrode solution (mM); 110 Tris phosphate dibasic, 28 Tris base, 11 EGTA, 2 $MgCl_2$, 0.1 $CaCl_2$, 4 Na-ATP, pH 7.3 with Tris base (Zhao *et al.*, 2003).

(-)Nicotine was dissolved and serially diluted in the appropriate bath solution. *d*-Tubocurarine was dissolved in MilliQ water and serially diluted in bath solution. Human $A\beta_{1-42}$ was prepared as previously described in Section 2.3.2.4F (Rpeptide $A\beta_{1-42}$ in sterile water, Calbiochem $A\beta_{1-42}$ dissolved in Hepes, 5 % acetic acid, or 50/50 DMSO/Tris) and serially diluted in the BS_2. The 100 μM $A\beta_{1-42}$ stock aliquots were frozen at -20°C and used fresh or within 6 weeks of reconstitution. On the day of the experiment, $A\beta_{1-42}$ aliquots were dissolved in bath solution to a concentration of either 100 or 300 nM.

2.6.3.3 Data Analysis

All inward current responses are based on measurements of peak current amplitude using pClamp7 software (Axon Instruments, U.K.). Data were exported into SigmaPlot 2002 (version 8, SPSS UK Ltd., U.K.) for graphing and fitted using an iterative, non-linear least square curve fitting program to a one-site logistic model as described in Section 2.3.2.4E.

2.7 Western Blot and Co-Immunoprecipitation Studies of Human $\alpha_4\beta_2$ and α_7 nAChRs and Human $A\beta_{1-42}$

2.7.1 Preparation of SH-EP1-h$\alpha_4\beta_2$ and SH-EP1-hα_7 and CHO-APP Cell Lysates for Western Blot Analysis

SH-EP1 cell lines stably expressing the human $\alpha_4\beta_2$ or α_7 nAChRs were maintained in culture as previously described (Section 2.2.1) with both cell lines plated at a

density of 5 million/10 cm^2 dish (Corning® Life Sciences, U.K.) and left overnight at 37°C. On the following day, each dish was rinsed three times with 2 ml of warm sodium phosphate buffer (NP Buffer; 100 mM NaCl, 25 mM NaH_2PO_4, pH 7.4), a further 5 ml of NP buffer added to each dish, the cells scraped and collected in a 50 ml centrifuge tube. Samples were then spun at 1,000 g for 5 min (22°C) and the supernatant discarded. The pellet was resuspended in NP buffer (200 µl/confluent plate) containing protease inhibitors (Complete protease inhibitor cocktail mini tablet, 1 tablet per 10 ml, Roche Diagnostics, U.K.) and homogenised using a Teflon-glass homogeniser (10 strokes, at 4°C). The resultant solution was then centrifuged (Biofuge Fresco, Heraceus Instruments, U.K.) at 13,000 r.p.m. for 10 min at 4°C, the supernatant discarded and the pellet resuspended in either NP extraction buffer (Extraction Buffer 1 (EB_1): 200 µl/confluent plate; supplemented with protease inhibitors and 1 % Triton X-100) or in sodium chloride extraction buffer (Extraction Buffer 2 (EB_2): 150 mM NaCl, 10 mM HEPES, 0.01 % CHAPS, 0.001 mM PMSF, 10 µg/ml protease inhibitor cocktail (Sigma, U.K.), pH 7.4). The tube was secured on a rotating platform at room temperature (22 – 25°C). After 45 min the tube was centrifuged (Biofuge Fresco, Heraceus Instruments, U.K.) at 13,000 r.p.m. for 10 min and the supernatant fraction containing the solubilised membrane protein retained. Total protein concentration was determined using the BCA protein assay kit (Section, 2.3.1.3; Pierce, UK).

2.7.2 Immunoprecipitation of nAChR

SH-EP1-h$\alpha_4\beta_2$ and SH-EP1-hα_7 cells were maintained in culture as previously described (Section 2.2.1) with both cell lines plated at a density of 5 million/10 cm^2 dish (Corning® Life Sciences, U.K.) and left overnight at 37°C. On the following day, each dish was rinsed three times with 2 ml of warm NP buffer (see Section 2.7.1), a further 5 ml of NP buffer added to each dish, the cells scraped and collected in a 50 ml centrifuge tube. Samples were then spun at 1,000 g for 5 min (22°C) and the supernatant discarded. The pellet was resuspended in NP buffer (200 µl/confluent plate) containing protease inhibitors (Complete protease inhibitor cocktail mini tablet, 1 tablet per 10 ml, Roche Diagnostics, U.K.) and homogenised using a Teflon-glass homogeniser (10 strokes, at 4°C). The tube was secured on a rotating platform at room temperature (22 – 25°C). After 45 min the tube was centrifuged at 13,000 r.p.m. (10 min at 4°C) and the pellet discarded. A small volume of supernatant was kept and labelled as starting material (SM). The remaining supernatant fraction (1 mg) was incubated overnight at 4°C with the appropriate antibody (Table 2.3) in the presence of protein G agarose beads (Sigma, U.K.). Immunoprecipitates were collected

by centrifugation (13,000 r.p.m., 10 s, 4°C) and washed three times in NPT buffer (NP Buffer supplemented with 1 % Triton X-100) before resuspension in SDS-PAGE sample buffer (NuPAGE® sample buffer, Invitrogen, U.K.) containing β-mercaptoethanol (20 µl per sample, Sigma, U.K.). Samples of supernatant were retained after each wash step and labelled (in order) W1, W2, W3 and depleted supernatant (DSn). The immunoprecipitant and sample buffer mix was heated at 95°C for 10 min before undergoing western analysis.

2.7.3 Western Blot Analysis

Lysates (30 µg protein) prepared in EB_1 were diluted in Nupage® LDS sample buffer (Invitrogen, U.K.) containing the reducing agent β-mercaptoethanol (20 µl per sample) and heated at 95°C for 10 min. Likewise, lysates (30 µg protein) prepared in EB_2 were diluted in the same sample buffer but containing the reducing agent DL-Dithreitol (0.1 M) and heated at 95 °C for 10 min. Solubilised protein, regardless of sample buffer utilised, was collected and subjected to SDS-PAGE separation on pre-cast 4-12% acrylamide gels (NuPAGE® Bis-Tris, Invitrogen, U.K.). The Western blot apparatus was supplied by Invitrogen, U.K. (XCell Surelock™ Mini Cell) and was assembled as follows; The comb was gently removed from the pre-cast gel cassette exposing the gels' sample loading wells which were gently rinsed with running buffer (NuPAGE® MES SDS Running Buffer, Invitrogen, U.K.). The tape covering the slot on the back of the gel cassette was also removed. The buffer core was lowered into the lower buffer chamber so that the negative electrode fit the opening in the gold plate on the lower buffer chamber. The gel tension wedge (unlocked) was inserted behind the buffer core and the gel cassette(s) were placed on either side of the core with the "well" side of the cassette facing the buffer core. To hold the gels in place the gel tension wedge was pulled into the locked position. The upper chamber (the void between the two gel cassettes) was filled with ~200 ml of running buffer ensuring complete coverage of the sample wells. Finally, 500 µl of antioxidant (NuPAGE® Antioxidant, Invitrogen, U.K.) was added to the upper chamber. Individual samples and markers (2 µl of MagicMarkers™ Western Protein Standards and 5 µl of Seeblue® Plus2 standard protein markers, Invitrogen, U.K.) were loaded into the sample wells and run for 35- 40 min at a constant 200 V.

At the end of the run, the gel cassettes were removed from the chamber and the two plates separated using a gel knife. Sponge pads (Invitrogen, U.K.), filter paper (BioRad, U.K.) and nitrocellulose transfer membranes (Hybond ECL, Amersham Biosciences, U.K.) were pre-soaked for 10 min in NuPAGE® Transfer buffer (Invitrogen). When polyvinylidene

difluoride (PVDF: Hybond™-P, Amersham Biosciences) transfer membranes were used, the membrane was pre-wet in 100 % methanol and rinsed in deionised water before soaking in Nupage® transfer buffer (Invitrogen, U.K.) for 10 min. Gels, transfer membrane, and blotting pads were arranged in the following order on top of the cathode (-) core of the XCell II™ Blot Module (Invitrogen; for 1 gel); 2 blotting pads, filter paper, gel, transfer membrane, filter paper, 2 blotting pads. After placing the anode (+) core on top of the pads, the blot cassette was placed in the cathode core of the XCell II™ Blot Module (Invitrogen, U.K.), in line with the guide rails, and the gel tension wedge locked in place. The blot module was filled with transfer buffer until the gel/membrane assembly was completely covered. The outer buffer chamber was filled with ~650 ml of deionised water and the gels were transferred at a constant 30 V for 1 h.

At the end of the transfer period the membrane was blocked by phosphate buffered saline (PBS: 137 mM NaCl, 2.7 mM KCl, 10 mM phosphate buffer solution, pH 7.4) containing 5 % skimmed milk powder (BioRad, U.K.) and incubated overnight (4°C) with the appropriate antibody (Table 2.3). After three 5 min washes in PBS containing 0.05 % Tween 20 (Sigma, U.K.) the appropriate secondary horseradish peroxidase conjugated antibody was added in PBS containing 5 % skim milk powder for 1 h at room temperature (Table 2.3). After a further three 5 min washes in PBS containing 0.05 % Tween 20, the horseradish peroxidase, second antibody labelled bands were visualised using an ECL Plus Western Blotting detection kit (Amersham Biosciences).

2.7.4 Co-Immunoprecipitation Analysis of Human nAChRs and Human $A\beta_{1-42}$

SH-EP1 cell lines stably expressing the human $\alpha_4\beta_2$ or α_7 nAChRs were maintained in culture as previously described (Section 2.2.1) with both cell lines plated at a density of 5 million/10 cm^2 dish (Corning® Life Sciences, U.K.) and left overnight at 37°C. On the following day, each dish was rinsed three times with 2 ml of warm sodium phosphate buffer (NP Buffer; 100 mM NaCl, 25 mM NaH_2PO_4, pH 7.4), a further 5 ml of NP buffer added to each dish, the cells scraped and collected in a 50 ml centrifuge tube. Samples were then spun at 1,000 g for 5 min (22°C) and the supernatant discarded. The pellet was resuspended in NP buffer (200 µl/confluent plate) containing 1 µM human $A\beta_{1-42}$ (Rpeptide, U.S.A.) and the tube secured on a rotary mixer (22 – 25°C) to allow for equilibration. After 1 h the tube was centrifuged for 10 min at 13,000 rpm (4°C), the supernatant discarded and the pellet resuspended in NP buffer (200 µl/confluent plate) containing protease inhibitors supplemented with 1 % Triton X-100 (NPT Buffer). The tube was secured again on a

Table 2.3: Antibodies Used for Western Blot and Co-Immunoprecipitation, Immunoprecipitation Experiments

Experiment	IP Antibody	Western Blot Antibody	HRP Secondary Antibody
Immunoprecipitation of nAChR α_4	H-133 rabbit anti-α_4 nAChR (polyclonal) 5 μg/mg protein Santa Cruz Biotechnology, Inc., U.K.	mAb299 rat anti-α_4 nAChR (monoclonal) 1:1,000 Sigma	sc-2006 goat anti-rat IgG 1:1,000 Santa Cruz Biotechnology, Inc., U.K.
Immunoprecipitation of nAChR α_7	sc-5544 rabbit anti-α_7 nAcHR (polyclonal) 1:200 Santa Cruz	M220 mouse anti-α_7 nAChR (monoclonal) 1:1,000 Sigma	anti-mouse IgG 1:10,000 Sigma
	M220 mouse anti-α_7 nAChR (monoclonal) 1:500 Sigma	sc-5544 rabbit anti-α_7 nAChR (polyclonal) 1:200 Santa Cruz	anti-rabbit IgG 1:10,000 Sigma
Immunoprecipitation of $A\beta_{1-42}$	4G8 mouse anti-$A\beta_{1-42}$ (monoclonal) 1:500 Signet Laboratories, U.S.A.	171609 Rabbit anti-$A\beta_{1-42}$ (polyclonal) 1:500 Calbiochem, U.K.	anti-rabbit IgG 1:10,000 Sigma
Co-Immunoprecipitation of α_4 and $A\beta_{1-42}$	4G8 mouse anti-$A\beta_{1-42}$ (monoclonal) 1:500 Signet Laboratories, U.S.A.	mAb299 rat anti-α_4 nAChR (monoclonal) 1:1,000 Sigma	sc-2006 goat anti-rat IgG 1:1,000 Santa Cruz Biotechnology, Inc., U.K.

All antibodies were diluted in PBS with 5 % non-fat milk unless otherwise stated. The goat polyclonal antibody sc-1447 (Santa Cruz) was used at a dilution of 1:100 for α_7 nAChR Western blots with an anti-goat IgG secondary antibody (1:10,000, Sigma).

rotating platform at room temperature (22 – 25°C). After 45 min the tube was centrifuged at 13,000 r.p.m. for 10 min (4°C) and the pellet discarded. A small amount of supernatant was kept and labelled as starting material (SM). The remaining supernatant fraction (1 mg) was incubated overnight (4°C) with the appropriate antibody (Table 2.3) in the presence of protein G agarose beads (Sigma, U.K.). Immunoprecipitates were collected by centrifugation and washed three times in NPT buffer before resuspension in NuPAGE® LDS sample buffer (Invitrogen, U.K.) containing β-mercaptoethanol (20 µl per sample, Sigma). Samples of supernatant were retained after each wash step and labelled (in order) W1, W2, W3 and depleted supernatant (DSn). The immunoprecipitate and sample buffer mix was heated at 95°C for 10 min before undergoing western analysis as described above.

3 PHARMACOLOGICAL CHARACTERISATION OF THE $\alpha_4\beta_2$ AND α_7 nAChRs

3.1 INTRODUCTION

Although a number of recent papers have highlighted a potentially direct interaction between the nAChRs and $A\beta_{1-42}$ (Kihara *et al.*, 1998; Wang *et al.*, 2000a,b; Court *et al.*, 2001; Dineley *et al.*, 2001, 2002a,b; Liu *et al.*, 2001; Pettit *et al.*, 2001; Tozaki *et al.*, 2002; Fu & Jhamandas, 2003; Grassi *et al.*, 2003; Fodero *et al.*, 2004; Wu *et al.*, 2004; Kihara & Shimohama, 2004a,; de Fiebre & de Fiebre, 2005), controversy remains as to the exact nature of these interactions or indeed the subtype(s) of nAChR involved. To date, the majority of these new but still limited studies have focused primarily on the interaction between the α_7 nAChR and $A\beta_{1-42}$ (Wang *et al.*, 2000a,b; Dineley *et al.*, 2001, 2002a,b; Liu *et al.*, 2001; Pettit *et al.*, 2001; Grassi *et al.*, 2003; Fodero *et al.*, 2004) although some have focused on the interaction with the $\alpha_4\beta_2$ nAChR (Kihara *et al.*, 1998; Tozaki *et al.*, 2002; Fu & Jhamandas, 2003; Wu *et al.*, 2004).

The functional characterisation of the α_7 nAChR both *in vitro* and *in vivo* has proven somewhat difficult due to the combined lack of subtype-selective ligands (Kem, 2000) and difficulties with maintaining stable expression of the α_7 nAChR in cultured mammalian cell lines (Cooper & Millar, 1997). Although some studies have demonstrated the presence of α_7 mRNA (Aztiria *et al.*, 2000; Sweileh *et al.*, 2000) or protein (Cooper & Millar, 1997) in a variety of cell types transfected with the α_7 nAChR, only a limited number of these cell lines have sufficient surface expression of this receptor to characterise radioligand binding of the α_7 nAChR-specific antagonist, αBgTx (Cooper & Millar, 1997; Craig *et al.*, 2004). To solve the problem of low or no surface expression of the α_7 nAChR, many researchers have resorted to overexpressing the α_7 nAChR in cell lines that endogenously express other types of nAChRs (Puchacz *et al.*, 1994; Blumenthal *et al.*, 1997) or by generating an α_7/5-hydroxytryptamine-3 ($5HT_3$) receptor chimera that retains α_7 nAChR pharmacology whilst utilising the effective expression of the $5HT_3$ receptor (Cooper & Millar, 1998; Dineley & Patrick, 2000; Craig *et al.*, 2004). The human neuroblastoma cell line SH-SY5Y has been used to successfully over-express the α_7 nAChR (Puchacz *et al.*, 1994; Cooper & Millar, 1997), however this cell line endogenously expresses a range of nAChRs including the α_7 nAChR itself (Cooper & Millar, 1997). In contrast, the SH-EP1 human epithelial cell line which is related to the SH-SY5Y cell line (Peng *et al.*, 1999), has no native nAChRs and can be treated to produce many of the characteristics of neurons (Ross *et al.*, 1983). This cell-line has been used to stably express both the $\alpha_4\beta_2$ (Eaton *et al.*,

2003) and α_7 nAChRs (Peng *et al.*, 1999) and, through an excellent collaboration, Dr. R. J. Lukas (Barrow Neurological Institute, Texas, U.S.A.) has kindly supplied these two stable cell lines.

Historically, characterisation of the α_7 nAChR has been performed using αbungarotoxin (αBgTx), a potent α_7 nAChR antagonist derived from the venom of the snake *Bungarus multicinctus* (Couturier *et al.*, 1990; Schoepfer *et al.*, 1990; Seguela *et al.*, 1993). However, unlike the small molecule methyllycaconitine (MLA), controversy exists around whether a large peptide such as αBgTx can access all 5 potential binding sites on the α_7 nAChR (Conti-Tronconi & Raftery, 1986; Palma *et al.*, 1996; Balass *et al.*, 1997; Rangwala *et al.*, 1997; Arias, 2000). The recent availability of the α_7 nAChR-specific antagonist methyllycaconitine in a tritiated form ([^{3}H]-MLA; Davies *et al.*, 1999) facilitates a more in-depth analysis of the α_7 nAChR, although the number of studies to date remain limited to a few separate studies of α_7 nAChR pharmacology in rat (Davies *et al.*, 1999), mouse (Whiteaker *et al.*, 1999), and insect brain tissues (Lind *et al.*, 2001). Importantly, because of the problems surrounding α_7 nAChR expression in neuronal cell lines discussed above, no systematic cross-species comparison of rodent and human α_7 nAChRs has been performed nor indeed has a systematic analysis of the human α_7 nAChR itself been performed using [^{3}H]-MLA. However, initial [^{3}H]-MLA binding studies in rodent brain tissue have suggested that although the majority of binding sites in rat (Davies *et al.*, 1999) and mouse (Whiteaker *et al.*, 1999) brain are labelled by [^{3}H]-MLA, a small proportion of sites were found to be insensitive to αBgTX.

Prior to assessing whether $A\beta_{1-42}$ interacts with $\alpha_4\beta_2$ and/or α_7 nAChRs, it is important to establish robust information of the pharmacology of both receptor subtypes. As such, two radioligand binding assays were established to examine the pharmacology of the $\alpha_4\beta_2$ nAChR ([^{3}H]-epibatidine and [^{3}H]-cytisine) and the α_7 nAChR ([^{3}H]-MLA and [^{3}H]-αBgTx). The affinity of a core group of nicotinic ligands ((-)nicotine, cytisine, 1,1-dimethyl-4-phenylpiperazinium, *d*-tubocurarine & MLA; Paterson & Nordberg, 2000; Sharples & Wonnacott, 2004) for $\alpha_4\beta_2$ and α_7 nAChRs was determined using [^{3}H]-epibatidine, [^{3}H]-cytisine, and [^{3}H]-MLA binding assays. In addition, the range of compounds examined in the [^{3}H]-MLA assay was expanded to include drugs such as the putative α_7 nAChR-specific agonists AR-R17779 (Levin *et al.*, 1999) and RJR-2403 (Bencherif *et al.*, 1996), acetylcholinesterase inhibitors such as galanthamine (Zwart *et al.*, 2000), and allosteric potentiating ligands such as codeine (Storch *et al.*, 1995). Furthermore,

using the SH-EP1 cell line in which the human α_7 nAChR was overexpressed, the [^{3}H]-MLA and [^{3}H]-αBgTx assays have been directly compared to further investigate the differences in the ability of MLA and αBgTx to bind to the α_7 nAChR, observed in previous studies using rat and mouse brain tissue (Davies *et al.*, 1999; Whiteaker *et al.*, 1999).

Finally, the [^{3}H]-cytisine and [^{3}H]-MLA binding assays were used as part of a collaborative set of studies with the behaviourists in out Fujisawa Institute of Neuroscience in Edinburgh to examine α_7 nAChR knockout mice and their heterozygous and wildtype littermates. Aspects of this work have been incorporated into one published (Young *et al.*, 2004) and one accepted manuscript (Young *et al.*, 2006, *in press*).

3.2 RESULTS

3.3 Characterisation of $\alpha_4\beta_2$ nAChR Pharmacology in Rat Brain and SH-EP1-h$\alpha_4\beta_2$ Cell Membrane Preparations Using [^{3}H]-Epibatidine

Species differences in receptor pharmacology have been observed for a number of ion channels (Price *et al.*, 1996; Hibell *et al.*, 2000). The availability of SH-EP1 cells overexpressing the human $\alpha_4\beta_2$ nAChR allowed the thorough characterisation of the pharmacology of this receptor subtype, prior to examining its interaction with $A\beta_{1-42}$. Membranes were prepared from rat brain tissue (P2 fraction) and the SH-EP1-h$\alpha_4\beta_2$ cell line and $\alpha_4\beta_2$ nAChR pharmacology examined using the high affinity nicotinic agonist [^{3}H]-epibatidine. Epibatidine itself is an alkaloid isolated from skin extracts of the poisonous Ecuadorian frog *epipedorates tricolour* (Daly, 1995).

3.3.1 Time Course of [^{3}H]-Epibatidine Binding in the SH-EP1-h$\alpha_4\beta_2$ Cell Membrane Preparation

To determine when [^{3}H]-epibatidine binding to the $\alpha_4\beta_2$ nAChR was at equilibrium, the radioligand (15 pM) was incubated with membranes prepared from rat brain tissue or from the SH-EP1 cell line over-expressing human $\alpha_4\beta_2$ nAChRs (SH-EP1-h$\alpha_4\beta_2$) and specific binding measured as a function of time (Figure 3.1). When [^{3}H]-epibatidine was incubated with rat brain membranes at 22°C, equilibrium was attained by ~2 h and remained constant for at least 6 h (Figure 3.1A). In contrast, when [^{3}H]-epibatidine was incubated with the SH-EP1-h$\alpha_4\beta_2$ cell membranes, equilibrium was only attained at 4 h and held at a constant level of specific binding for up to 6 h (Figure 3.1B). As a consequence, all subsequent [^{3}H]-epibatidine binding experiments were terminated by vacuum filtration after a 4 h incubation period.

3.3.2 Concentration Dependence of [^{3}H]-Epibatidine Binding in SH-EP1-h$\alpha_4\beta_2$ Cell Membrane Preparations

Radioligand binding levels in a membrane preparation (e.g. tissue or cells) are dependent upon the protein content of the preparation and the specific activity of the chosen radioligand (Bennett, 1985; Keen, 1995; Foreman, 2002). Parameters measured are total binding, (the amount of binding measured in the absence of an unlabelled competitor) and non-specific binding (the amount of binding measured in the presence of an excess unlabelled competitor e.g. in the current experiments non-specific binding was determined

by 300 μM (-)nicotine) with specific binding determined by subtracting the non-specific from the total binding.

To determine the equilibrium dissociation constant (K_D) for [^{3}H]-epibatidine binding sites in rat brain and SH-EP1-h$\alpha_4\beta_2$ cell membranes, hot saturation experiments were performed using increasing concentrations of [^{3}H]-epibatidine (Figure 3.2). These studies showed that [^{3}H]-epibatidine binding was saturable and consistent with a single high affinity binding site in rat brain ($n_H = 0.88 \pm 0.06$, $n = 4$) and SH-EP1-h$\alpha_4\beta_2$ cell membranes ($n_H = 1.00 \pm 0.05$, $n = 4$). From the representative examples of the concentration dependence of [^{3}H]-epibatidine in rat brain and SH-EP1-h$\alpha_4\beta_2$ membrane preparations shown in Figure 3.2, K_D values were calculated to be 26.1 ± 2.5 pM ($n = 4$) and 28.5 ± 5.5 pM ($n = 4$) in the rat and human preparations, respectively. Specific [^{3}H]-epibatidine binding in rat brain membranes accounted for 92.2 ± 0.6 % of total binding sites at a free radiolabel concentration close to the K_D (20 – 30 pM; Figure 3.3A). Similar levels of specific binding were observed in the SH-EP1-h$\alpha_4\beta_2$ cell membranes where specific binding accounted for 91.4 ± 3.1 % of total binding sites (Figure 3.3B).

In all subsequent binding experiments, [^{3}H]-epibatidine binding (15 pM) was performed at 25°C for 4 h.

3.3.3 Inhibition of [^{3}H]-Epibatidine Binding to Rat and Human $\alpha_4\beta_2$ nAChRs by Cholinergic Agonists and Antagonists

A range of standard nAChR ligands were examined for their ability to inhibit [^{3}H]-epibatidine (15 pM) binding to rat brain or SH-EP1-h$\alpha_4\beta_2$ cell membrane preparations. All six nicotinic ligands examined inhibited [^{3}H]-epibatidine (15 pM) binding in both rat brain and SH-EP1-h$\alpha_4\beta_2$ cell membranes in a concentration-dependent manner (Figure 3.4). The rank order of potency for the ligands studied was (±)epibatidine > cytisine > (-)nicotine > 1,1-dimethyl-4-phenylpiperazinium iodide (DMPP) > MLA = *d*-tubocurarine with data from a typical experiment shown in Figure 3.4 and with average K_D/K_i values shown in Table 3.1. Unlabelled (±)epibatidine inhibited [^{3}H]-epibatidine binding in rat brain and SH-EP1-h$\alpha_4\beta_2$ cell membranes with K_{Ds} values equal to 26.9 ± 7.05 pM ($n = 9$) and 42.2 ± 13.2 pM ($n = 4$), respectively. These values are consistent with the K_D values obtained in the hot saturation experiments. The affinity (K_i) of the other compounds examined ranged

Figure 3.1

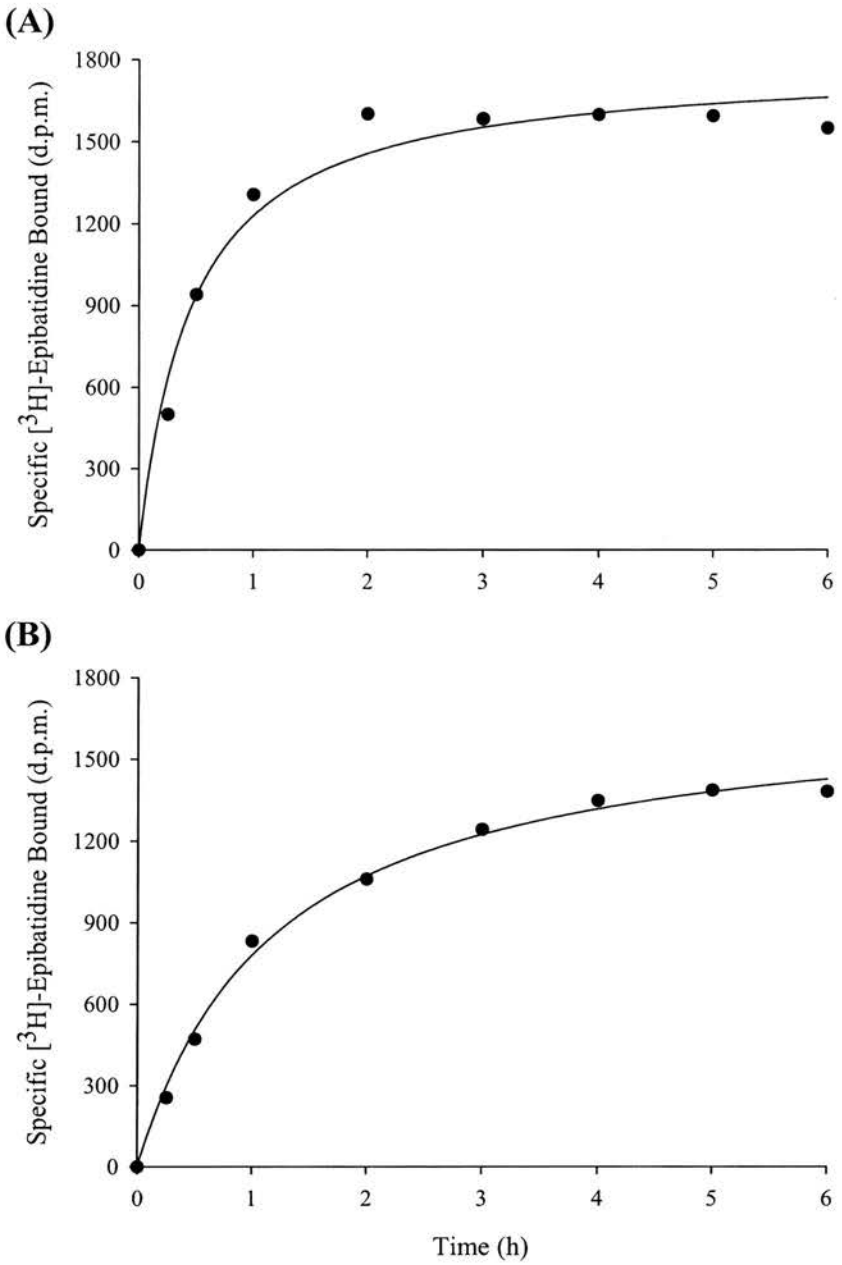

Time Course of Specific [^{3}H]-Epibatidine Binding in (A) Rat Brain and (B) SH-EP1-h$\alpha_4\beta_2$ Membrane Preparations. Membranes (250 µg rat; 80 µg SH-EP1-h$\alpha_4\beta_2$) were incubated (22°C) with [^{3}H]-epibatidine (15 pM) in a total assay volume of 4 ml for up to 6 h. Each total binding was tested in duplicate with its non-specific counterpart (defined by 300 µM (-)nicotine) tested in singulate. Specific binding points were derived by subtracting non-specific binding from total binding with these data representing a typical experiment.

Figure 3.2

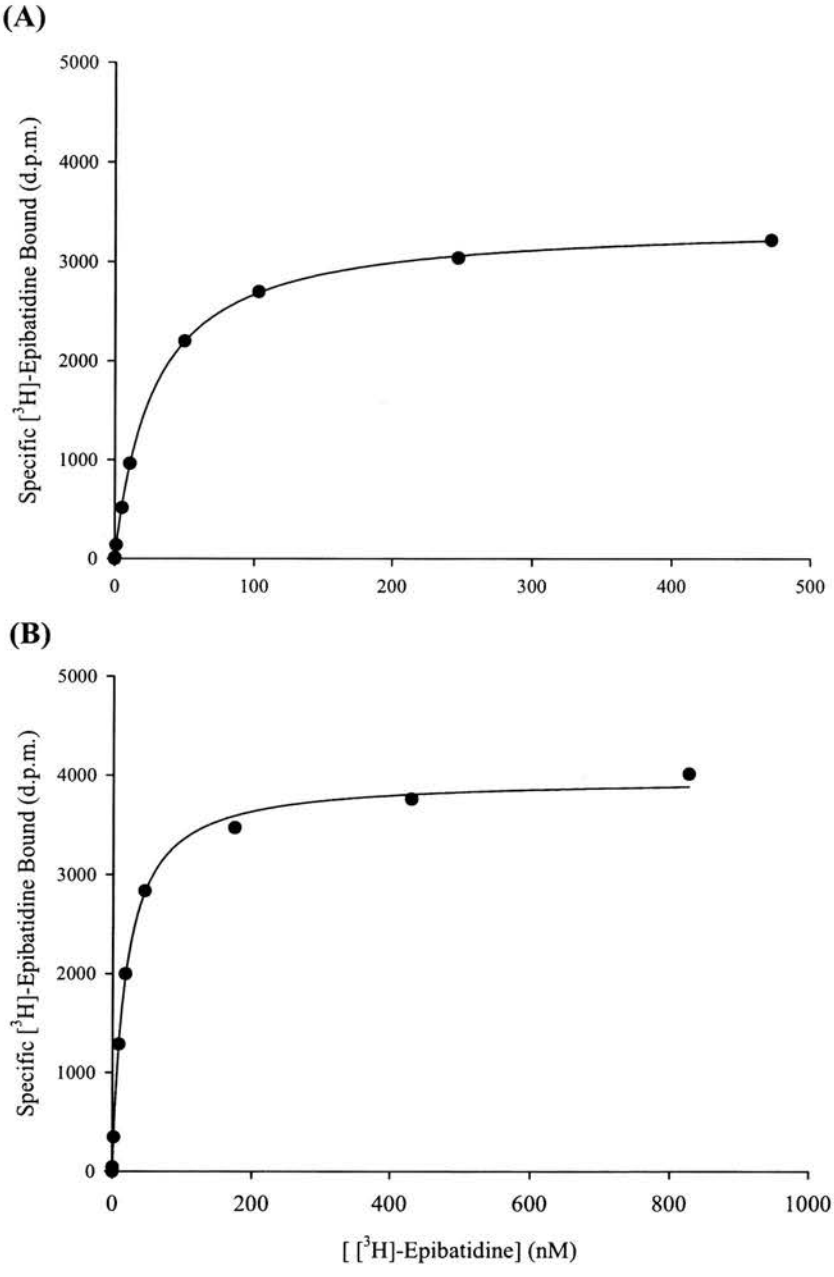

Concentration Dependence of [^{3}H]-Epibatidine Binding in $\alpha_4\beta_2$ nAChR Membrane Preparations. (A) Rat brain (250 μg) or (B) SH-EP1-h$\alpha_4\beta_2$ cell membranes (80 μg) were incubated (22°C) with increasing concentrations of [^{3}H]-epibatidine in a total assay volume of 4 ml for 4 h. Non-specific binding was determined in the presence of 300 μM (-)nicotine. These data are from representative hot saturation studies in rat brain and SH-EP1-h$\alpha_4\beta_2$ cell membranes, respectively.

from nanomolar for cytisine (540 ± 110 pM, $n = 4$ in rat brain; 1710 ± 500 pM, $n = 4$ in SH-EP1-h$\alpha_4\beta_2$ cells) to the micromolar range for MLA (3.27 ± 0.95 μM, $n = 5$ in rat brain; 4.70 ± 1.31 μM, $n = 5$ in SH-EP1-h$\alpha_4\beta_2$ cells) (Figure 3.4, Table 3.1). In general the Hill coefficients (n_H) for both the agonists and antagonists were close to unity in both membrane preparations (Figure 3.4, Table 3.1) and are in agreement with the single site affinity observed in the hot saturation experiments. No significant differences in compound affinity was detected on comparing the results for both species, giving an excellent correlation for the ligand affinities at $\alpha_4\beta_2$ nAChRs in rat brain and in the SH-EP1-h$\alpha_4\beta_2$ cell membranes ($r^2 = 1.00$ with slope = 1.00; Figure 3.5).

Figure 3.3

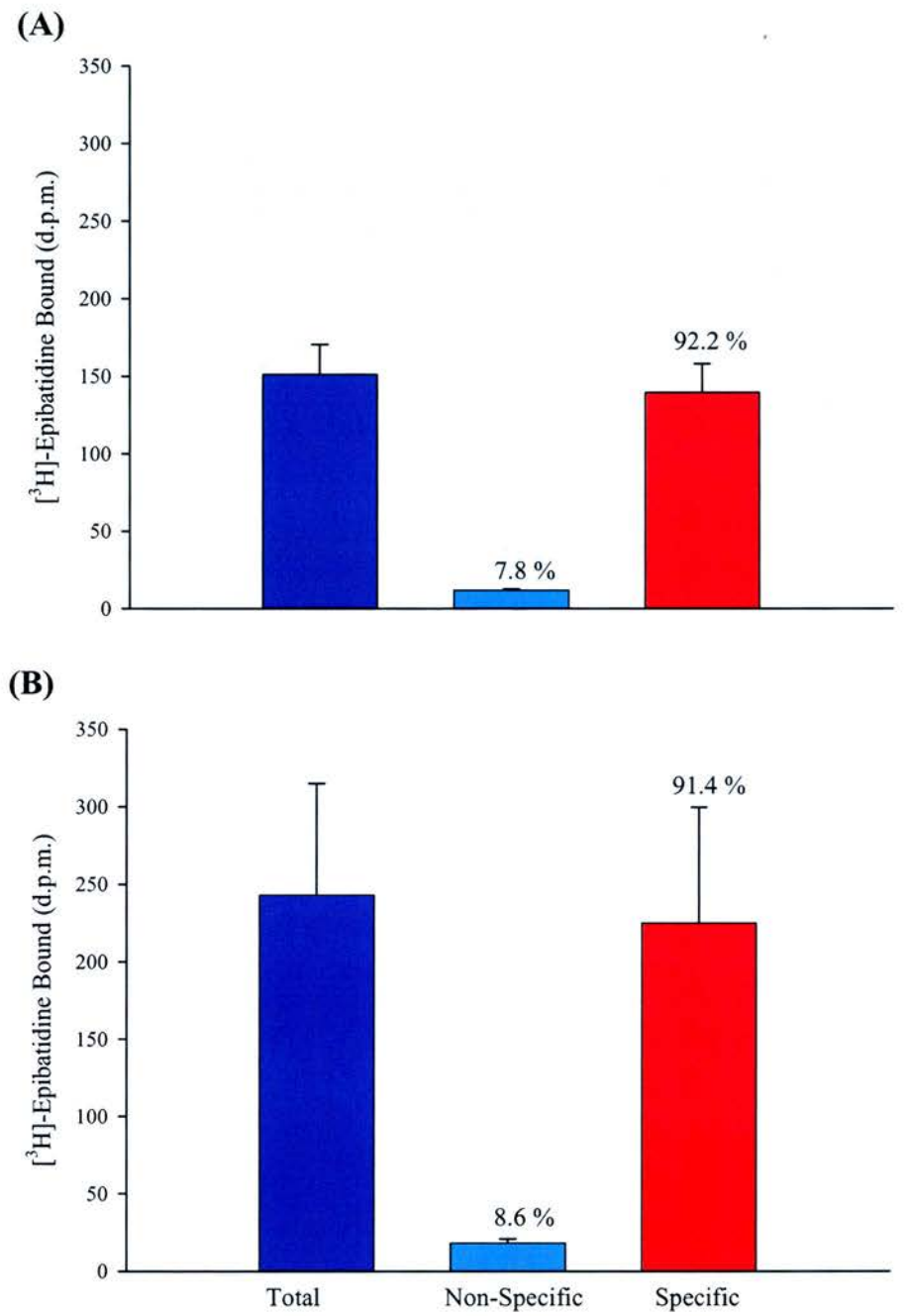

Proportions of [^{3}H]-Epibatidine Binding in Rat Brain or SH-EP1-h$\alpha_4\beta_2$ Cell Membrane Preparations. Membranes ((A) 250 µg, rat or (B) 80 µg, SH-EP1-h$\alpha_4\beta_2$ cells) were incubated with [^{3}H]-epibatidine (15 pM) in a total assay volume of 4 ml for 4 h at 22°C. Non-specific binding was determined in the presence of 300 µM (-)nicotine. These data are from an average of 4 separate hot saturation experiments.

Figure 3.4

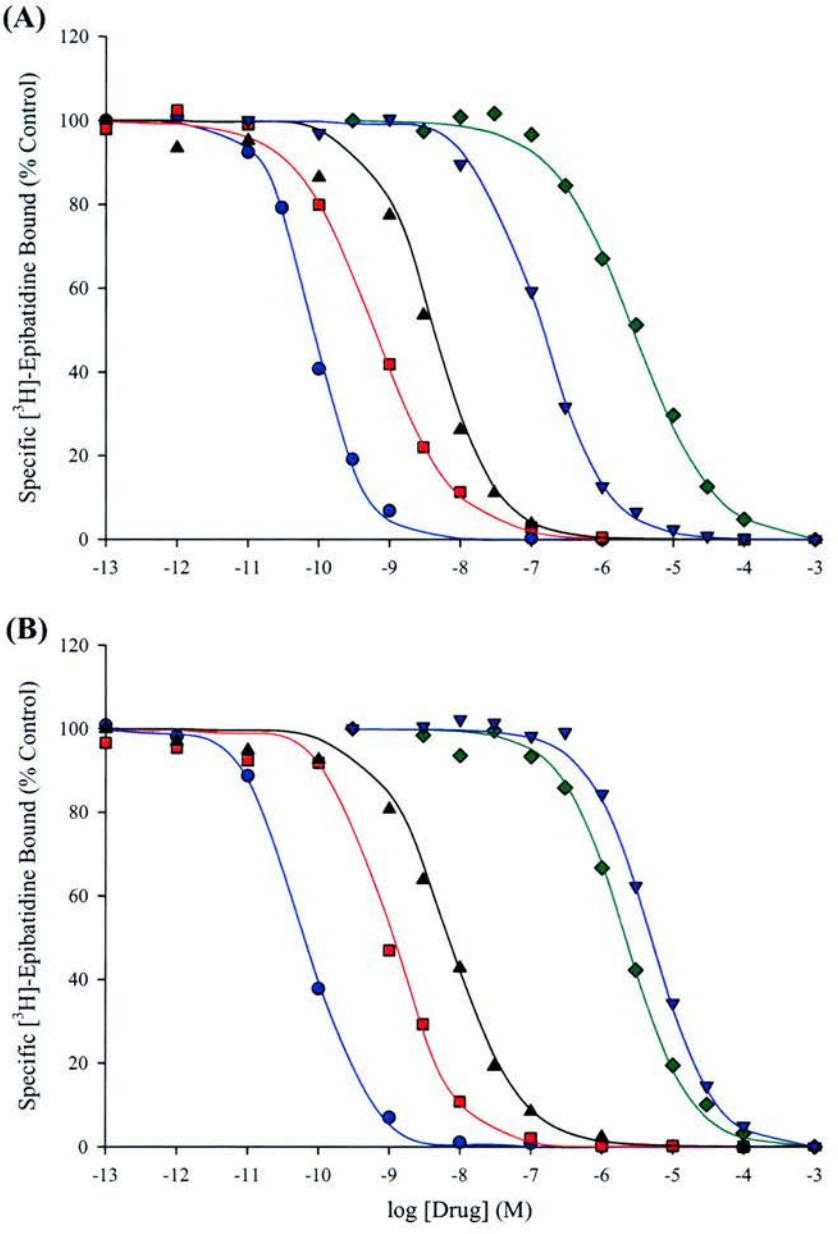

Pharmacology of [^{3}H]-Epibatidine Binding Sites in Rat and Human $\alpha_4\beta_2$ nAChR Membranes. (A) Rat brain (250 µg) or (B) SH-EP1-h$\alpha_4\beta_2$ cell membranes (80 µg) were incubated (22°C) with [^{3}H]-epibatidine (15 pM) in the presence of the nicotinic agonists (±)epibatidine (●) cytisine (■) and (-)nicotine (▲) and the antagonists *d*-tubocurarine (▼) and MLA (◆) in a total assay volume of 4 ml for 4 h. Non-specific binding was determined in the presence of 300 µM (-)nicotine. The data represent a typical experiment with each point performed in duplicate and with mean data obtained from at least 3 individual experiments (Table 3.1).

Table 3.1: The Affinity (K_D/K_i) of Nicotinic Ligands for [^{3}H]-Epibatidine Binding Sites in Rat Brain and SH-EP1-h$\alpha_4\beta_2$ Cell Membranes

Compound	Rat Brain K_i (nM)	n_H	*n*	SH-EP1-h$\alpha_4\beta_2$ K_i (nM)	n_H	*n*	K_i ratio (Rat/Human)
Agonists							
(±)Epibatidine	0.027 ± 0.007	1.01 ± 0.04	9	0.042 ± 0.013	0.95 ± 0.07	4	0.6
Cytisine	0.54 ± 0.11	0.76 ± 0.03	4	1.71 ± 0.50	0.93 ± 0.03	4	0.3
(-)Nicotine	3.73 ± 0.50	1.00 ± 0.04	4	5.31 ± 0.62	0.91 ± 0.05	4	0.7
DMPP	21.3 ± 1.7	0.97 ± 0.04	5	42.9 ± 5.9	0.95 ± 0.03	4	0.5
Antagonists							
MLA	3,270 ± 950	0.71 ± 0.03	5	4,700 ± 1,310	0.85 ± 0.07	5	0.7
***d*-Tubocurarine**	2,830 ± 1,240	0.84 ± 0.12	5	5,450 ± 1,190	0.95 ± 0.03	3	0.5

K_i and Hill slopes (n_H) were determined in the [^{3}H]-epibatidine inhibition studies as described in the methods. Compounds examined were (±)epibatidine, cytisine, (-)nicotine, 1,1-dimethyl-4-phenylpiperazinium iodide (DMPP), methyllycaconitine (MLA) and *d*-tubocurarine. Values are expressed as mean ± S.E.M. (n = 3-9). Statistical analyses were performed using one-way ANOVA with Bonferroni post-hoc testing where $p < 0.05$ was used to indicate a significant difference. No significant difference in ligand affinity between species was observed.

Figure 3.5

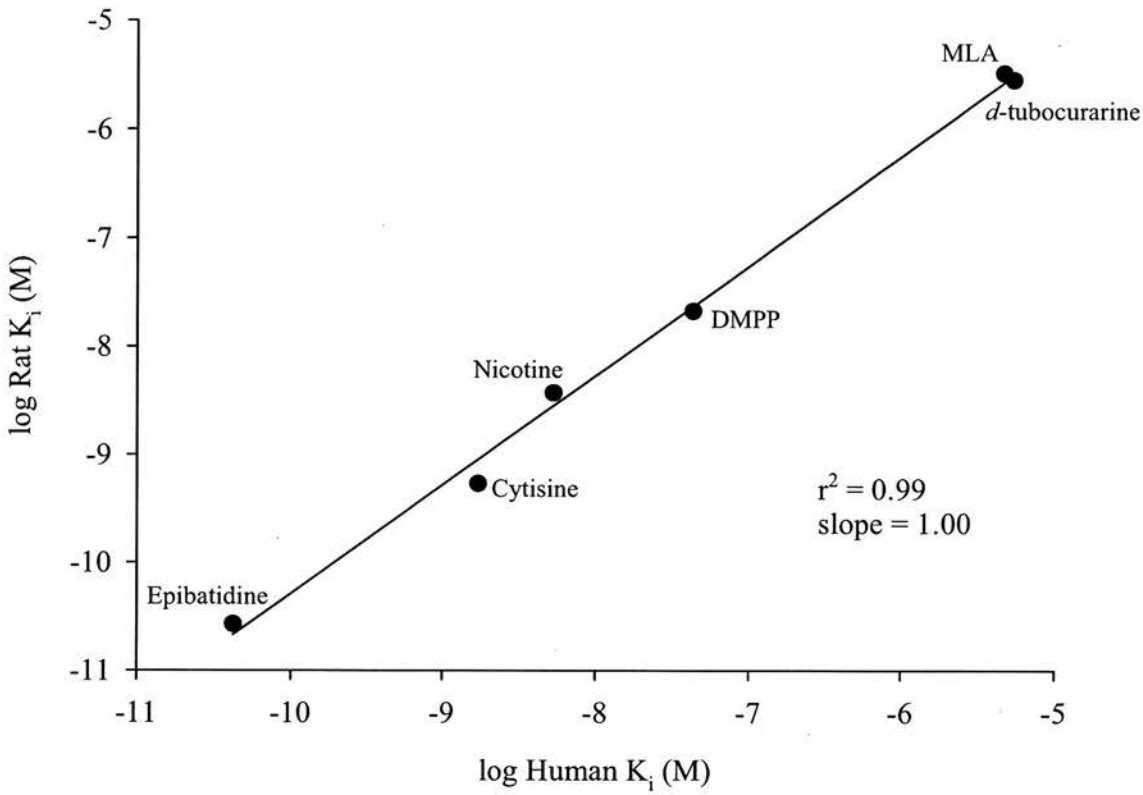

Correlation of the K_i values of Nicotinic Ligands for [^{3}H]-Epibatidine Binding Sites in Rat Brain and SH-EP1-h$\alpha_4\beta_2$ Cell Membranes. The solid line represents a linear regression through the K_i values shown in Table 3.1. The r^2 value (0.99) is close to unity indicating no species differences in compound affinity for rat and human $\alpha_4\beta_2$ nAChRs.

3.4 Pharmacological Characterisation of the $\alpha_4\beta_2$ nAChR in Rat Brain and SH-EP1-h$\alpha_4\beta_2$ Cell Membranes Using [^{3}H]-Cytisine

Historically, radiolabelled versions of the nicotinic agonists epibatidine and cytisine have been used to characterise $\alpha_4\beta_2$ nAChR pharmacology (Pabreza *et al.*, 1991; Gnadisch *et al.*, 1999). The [^{3}H]-epibatidine assay described in Section 3.1 used a large assay volume and a low ligand concentration in an attempt to avoid depletion. However, this assay is not amenable to miniaturisation and cannot be reduced to a 96-well format for high throughput characterisation of $\alpha_4\beta_2$ nAChR pharmacology.

In addition to assessing whether depletion had occurred in the [^{3}H]-epibatidine assay, I was given the opportunity to visit the laboratories of my Ph.D sponsor, the Fujisawa Pharmaceutical Company (now Astellas Pharma Inc.) in Japan, where I was involved in the set up and miniaturisation of high throughput screening assays for the nicotinic receptor programme. Both the [^{3}H]-cytisine and [^{3}H]-MLA (see Section 3.3) binding assays were successfully transferred to 96-well plate format and screening was initiated. Although I personally screened approximately 40,000 compounds, reorganisation of disease areas and project rationalisation led to the discontinuation of this approach. To date, there is still a lack of truly receptor-selective $\alpha_4\beta_2$ and α_7 nAChR agonists and antagonists which would help in clearly elucidating the role of these receptors in a variety of central and peripheral diseases.

In this next section I will present the development of the [^{3}H]-cytisine binding assay for the assessment of rat and human $\alpha_4\beta_2$ nAChR pharmacology.

3.4.1 Time Course of [^{3}H]-Cytisine Binding in Rat and Human $\alpha_4\beta_2$ nAChR Membrane Preparations

The incubation temperature of any assay can affect the time it takes for a ligand-receptor interaction to reach equilibrium. While colder temperatures (e.g. 4°C) may increase the time to attain equilibrium, conversely warmer temperatures (e.g. 37°C) may decrease it (Bennett, 1985).

To determine when [^{3}H]-cytisine binding (3 nM) to rat $\alpha_4\beta_2$ nAChRs reached equilibrium, the binding of this radioligand was examined in rat brain tissue as a function of time (Figure 3.6 & 3.7). Initial time course studies were performed at 4°C as Pabreza and colleagues (1991) had shown that [^{3}H]-cytisine binding in rat brain membranes achieved equilibrium within 60 min. In contrast, my studies showed that when [^{3}H]-cytisine (3 nM) was incubated with rat brain membranes at 4°C, specific binding failed to attain equilibrium

despite using incubation periods of up to 4 h (Figure 3.6). Therefore, I examined [^{3}H]-cytisine (3 nM) binding in rat brain membranes at 25°C and 37°C (Figure 3.7). At both incubation temperatures [^{3}H]-cytisine (3 nM) binding in rat brain $\alpha_4\beta_2$ membranes reached equilibrium within minutes remaining constant for up to 4 h (Figure 3.7).

To facilitate a direct comparison between [^{3}H]-cytisine binding in rat brain tissue with membranes prepared from the SH-EP1 cell line over-expressing the human $\alpha_4\beta_2$ nAChRs (SH-EP1-h$\alpha_4\beta_2$), and with the [^{3}H]-epibatidine binding studies, the time course of [^{3}H]-cytisine binding was examined using the latter membrane preparation. When SH-EP1-h$\alpha_4\beta_2$ cell membranes were incubated with [^{3}H]-cytisine (3 nM) at 25°C, equilibrium was attained by about 10 min, even faster than that observed for rat brain membranes and remained constant for up to 2 h (Figure 3.8).

As a consequence, all subsequent [^{3}H]-cytisine binding experiments using both rat brain and SH-EP1-h$\alpha_4\beta_2$ cell membranes were terminated by vacuum filtration after a 60 min period at 25°C.

3.4.2 Concentration Dependence of [^{3}H]-Cytisine Binding in Rat and Human $\alpha_4\beta_2$ Membrane Preparations

At a free radiolabel concentration close to the expected K_D (2.5 – 4 nM), specific [^{3}H]-cytisine binding in rat brain membranes accounted for 85.2 ± 3.9 % of total binding sites. This value was higher in SH-EP1-h$\alpha_4\beta_2$ cell membranes where specific binding accounted for 95.2 ± 1.3 % of total binding sites (Figure 3.9).

In order to determine K_D and $_{max}$ values for [^{3}H]-cytisine binding sites in rat brain and SH-EP1-h$\alpha_4\beta_2$ cell membrane preparation, hot saturation experiments were conducted with increasing concentrations of the radioligand. Representative examples of the concentration dependence of [^{3}H]-cytisine binding in rat brain and SH-EP1-h$\alpha_4\beta_2$ membrane preparations are shown in Figure 3.10. The affinity (K_D) of [^{3}H]-cytisine was equal to 3.77 ± 0.86 nM (n = 4) and 4.11 ± 1.21 nM (n = 5) in rat brain and SH-EP1-h$\alpha_4\beta_2$ cell membranes, respectively (Figure 3.10, Table 3.2). These studies showed that [^{3}H]-cytisine binding was saturable and consistent with a high affinity binding site in rat brain (n_H = 0.81 ± 0.10, n = 4) and SH-EP1-h$\alpha_4\beta_2$ cell membranes (n_H = 1.32 ± 0.35, n = 5; Table 3.2). The density of [^{3}H]-cytisine binding sites ($_{max}$) in rat membranes was significantly less ($_{max}$ = 0.43 ± 0.15 pmol/mg protein; n = 4) than that found in the SH-EP1-h$\alpha_4\beta_2$ cell membrane preparations ($_{max}$ = 131 ± 35 pmol/mg protein; n = 5; $p < 0.05$ (Table 3.2). However, the $_{max}$ value for rat brain tissue is consistent with those previously reported (Pabreza *et al.,* 1991; Hall *et al.,*

Figure 3.6

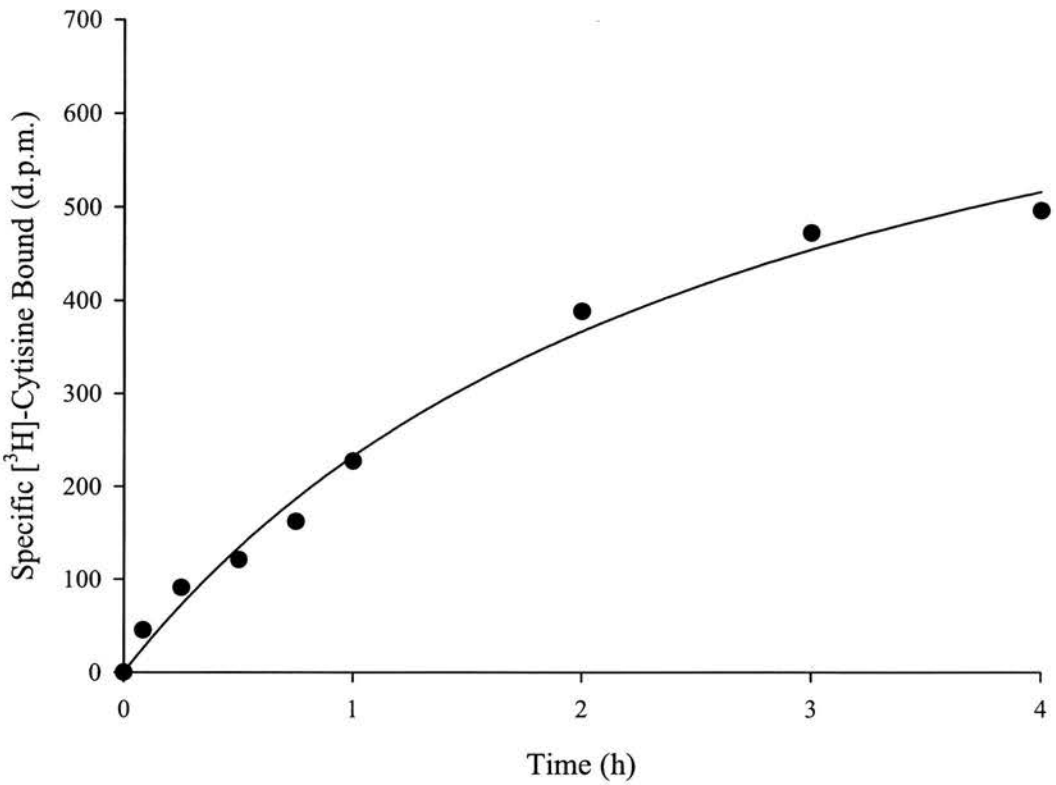

Time Dependence of [^{3}H]-Cytisine Binding in Rat Brain Membrane Preparations at 4°C. Membranes (400 µg) were incubated with [^{3}H]-cytisine (3 nM) in a total assay volume of 250 µl for various times at 4°C. For each time point, total binding was determined in duplicate with their non-specific counterpart (defined by 10 µM (-)nicotine) tested in singlet. Specific binding was calculated by subtracting non-specific binding from total binding, with this figure representing a typical experiment.

Figure 3.7

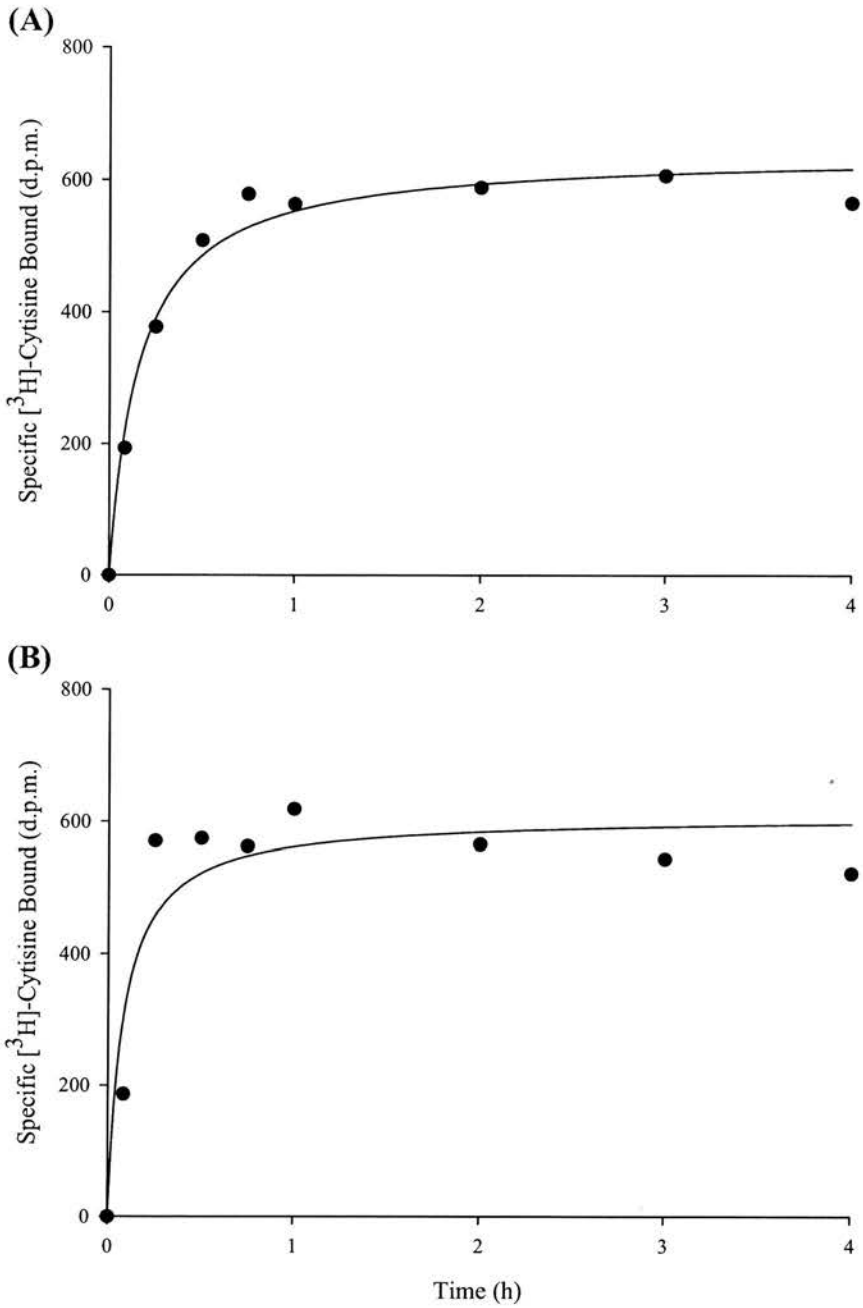

Time Dependence of [^{3}H]-Cytisine Binding in Rat Brain Membrane Preparations at 25°C and 37°C. Membranes (400 µg) were incubated with [^{3}H]-cytisine (3 nM) in a total assay volume of 250 µl for various times at (A) 25°C or (B) 37°C. For each time point, total binding points was determined in duplicate with their non-specific counterpart (defined by 10 µM (-)nicotine) tested in singlet. Specific binding was calculated by subtracting non-specific binding from total binding, with this figure representing a typical experiment.

Figure 3.8

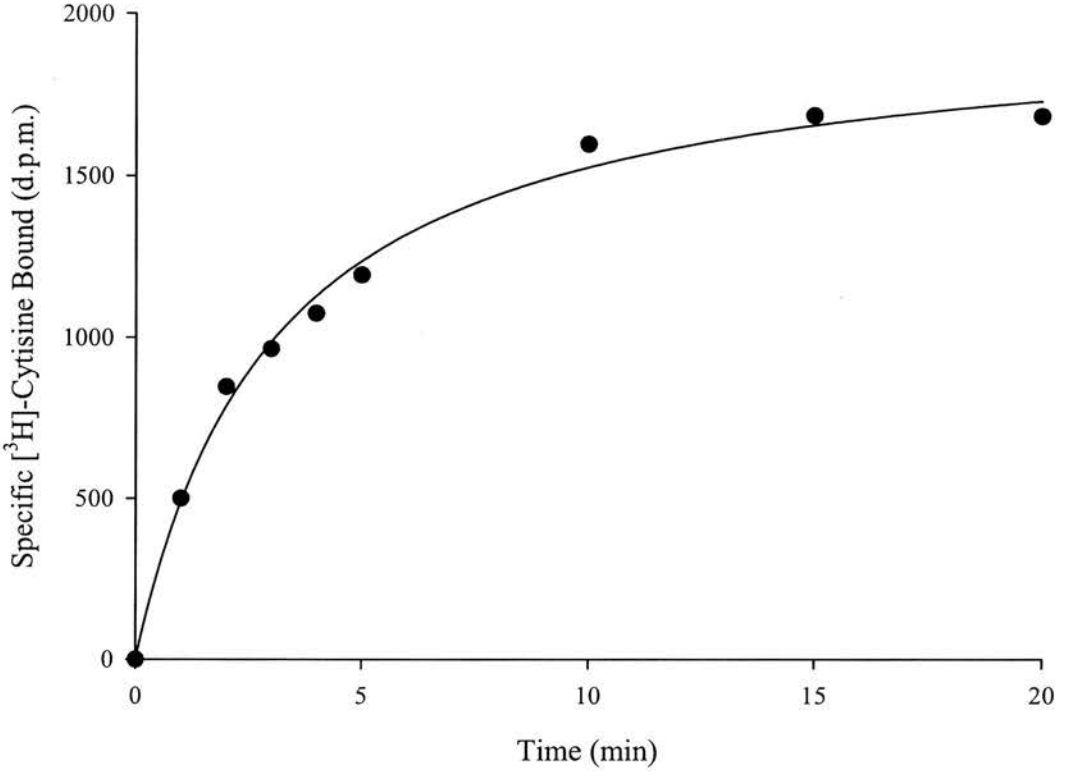

Incubation of [^{3}H]-Cytisine with SH-EP1-h$\alpha_4\beta_2$ Cell Membranes. Membranes (SH-EP1-h$\alpha_4\beta_2$, 115 µg) were incubated with [^{3}H]-cytisine (3 nM) in a total assay volume of 250 µl for various times at 25°C. Bound radioligand was separated from free by filtration through GF/B glass-fibre filters and analysed using liquid scintillation spectrometry. Total binding points were tested in duplicate with their non-specific counterpart (defined by 10 µM (-)nicotine) tested in singulate. Specific binding points were derived by subtracting non-specific binding from total binding with these data representing a typical experiment.

Figure 3.9

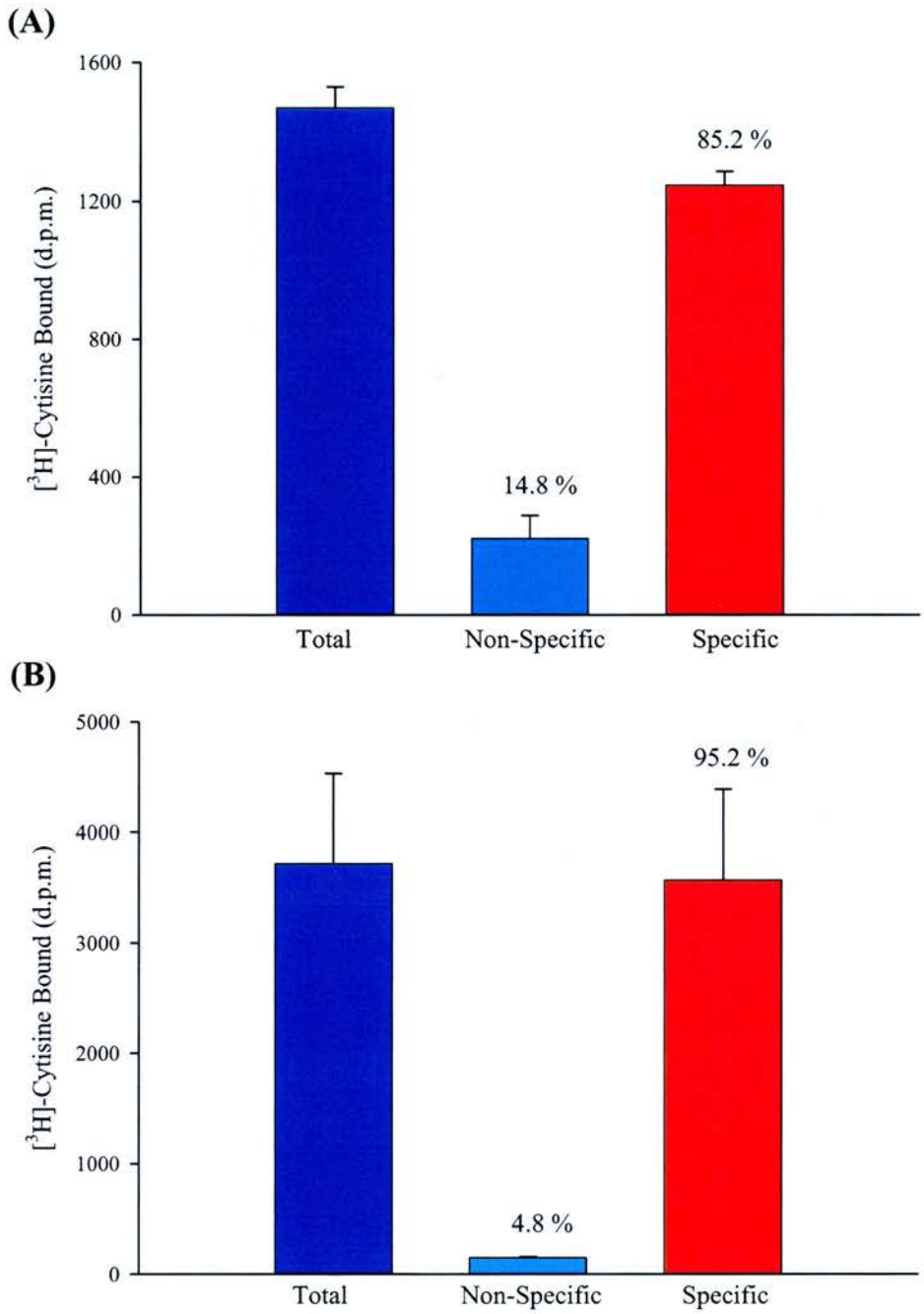

Proportions of [^{3}H]-Cytisine Binding in Membranes Prepared From Rat Brain or SH-EP1-h$\alpha_4\beta_2$ Cell Membrane Preparations. (A) Rat brain (400 µg) or (B) SH-EP1-h$\alpha_4\beta_2$ cell membranes (115 µg) were incubated (22°C) with [^{3}H]-cytisine (3 nM) in a total assay volume of 250 µl for 60 min. These data are from an average of 4-5 individual hot saturation studies.

Figure 3.10

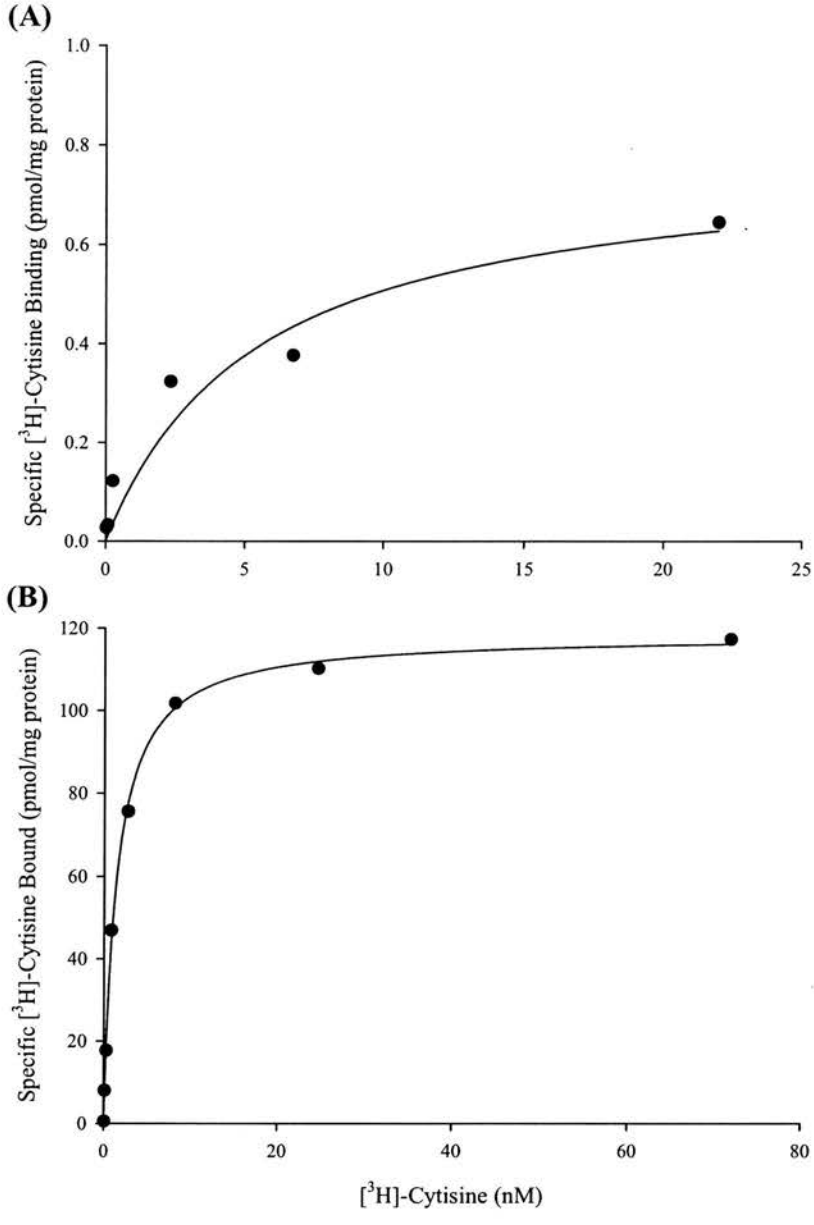

Concentration Dependence of [^{3}H]-Cytisine Binding in $\alpha_4\beta_2$ nAChR Membrane Preparations. (A) Rat brain (400 µg) or (B) SH-EP1-h$\alpha_4\beta_2$ cell membranes (115 µg) were incubated with increasing concentrations of [^{3}H]-cytisine in a total assay volume of 250 µl for 60 min at 25°C. Bound radioligand was separated from free by filtration through GF/B glass-fibre filters and analysed using liquid scintillation spectrometry. Non-specific binding was determined in the presence of 10 µM (-)nicotine. These data are from a representative hot saturation study.

Table 3.2 K_D and B_{max} Values for [^{3}H]-Cytisine Binding Sites in Rat Brain and SH-EP1-h$\alpha_4\beta_2$ Cell Membranes

Species	K_D (nM)	*n*	n_H	B_{max} (pmol/mg protein)
Rat	3.77 ± 0.86	4	0.81 ± 0.10	0.43 ± 0.15*
Human	4.11 ± 1.21	5	1.32 ± 0.35	131 ± 35*

Affinity (K_D), Hillslope (n_H), and binding site densities (B_{max}) determined for [^{3}H]-cytisine binding using hot saturation assays as described in the methods. Values are expressed as mean ± S.E.M., (n = 4-5). Statistical analyses were performed using one-way ANOVA with Bonferroni post-hoc testing where $p < 0.05$ was used to indicate a significant difference. No difference in ligand affinity between species was observed, although there was a considerable difference in receptor density.

1993; Gopalakrishnan *et al.*, 1997). The high density of [^{3}H]-cytisine binding sites in the SH-EP1 stable cell line (~300-fold higher than in rat brain membranes) makes these cells particularly useful for pharmacological studies of the binding properties of ligands, as much less tissue is used when compared to that required in the rodent studies.

For the subsequent competitive inhibition studies, [^{3}H]-cytisine was used at a final concentration of 3 nM, just below the K_D value.

3.4.3 Inhibition of [^{3}H]-Cytisine Binding to Rat and Human $\alpha_4\beta_2$ nAChRs by Cholinergic Agonists and Antagonists

Five cholinergic agonists and antagonists were examined in the [^{3}H]-cytisine binding assay. All the nicotinic ligands examined inhibited [^{3}H]-cytisine (3 nM) binding in both rat brain and SH-EP1-h$\alpha_4\beta_2$ cell membranes in a concentration dependent manner (Figure 3.11). The rank order of potency for the ligands studied in both membrane preparations was cytisine = (-) nicotine > DMPP > MLA > *d*-tubocurarine with data from a typical experiment shown in Figure 3.11 (Table 3.3). Unlabelled cytisine inhibited [^{3}H]-cytisine binding in rat brain and SH-EP1-h$\alpha_4\beta_2$ cell membranes with K_D values equal to 1.18 ± 0.30 nM ($n = 4$) and 3.35 ± 0.43 nM ($n = 3$), respectively (Table 3.3). As predicted, the K_D values for cytisine at rat and human $\alpha_4\beta_2$ nAChRs were similar when determined in hot (K_D) and/or cold saturation experiments (Tables 3.2 & 3.3). The affinity (K_i) of the other compounds tested ranged from low nanomolar for (-)nicotine (3.81 ± 1.91 nM, $n = 3$ in rat brain; 4.40 ± 1.50 nM, $n = 4$ in SH-EP1-h$\alpha_4\beta_2$ cells) to the micromolar range for *d*-tubocurarine (17.2 ± 2.03 μM, $n = 3$ in rat brain; 5.05 ± 1.14 μM, $n = 4$ in SH-EP1-h$\alpha_4\beta_2$ cells) (Figure 3.11, Table 3.3).

Although the range of compounds examined is limited, Figure 3.12 shows a good correlation between the K_i values of the ligands for rat brain and SH-EP1-h$\alpha_4\beta_2$ cell membranes. However, the agonist DMPP (256 ± 47 nM in rat brain vs. 71.5 ± 14.4 nM in SH-EP1-h$\alpha_4\beta_2$ cells; $p < 0.05$) and the antagonist *d*-tubocurarine (17.2 ± 2.0 μM in rat brain vs. 5.04 ± 1.14 μM in SH-EP1-h$\alpha_4\beta_2$ cell membranes; $p < 0.05$), both exhibited marginally higher affinities at the human $\alpha_4\beta_2$ nAChRs. This difference is evident when the K_i ratios are determined for the individual ligands with both DMPP and *d*-TC having a ratio of around 3 (Table 3.3). Although the Hill coefficients for the nicotinic ligands were generally close to unity in both membrane preparations although there was some degree of variability particularly with cytisine which had a $n_H = 1.92 \pm 0.39$ ($n = 5$; Figure 3.11, Table 3.3).

Figure 3.11

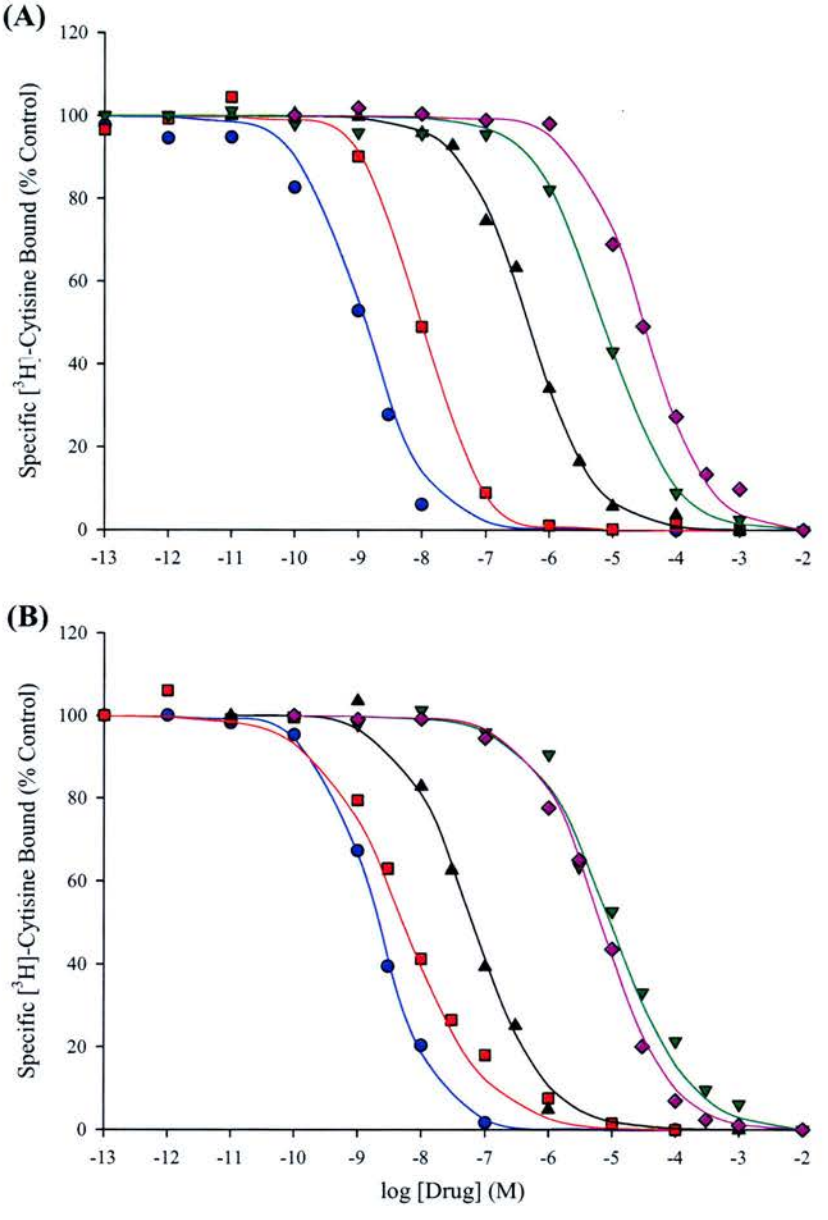

Pharmacology of [^{3}H]-Cytisine Binding Sites in Rat and Human $\alpha_4\beta_2$ nAChR Membranes. (A) Rat brain (400 µg) or (B) SH-EP1-h$\alpha_4\beta_2$ cell membranes (115 µg) were incubated (22°C) with [^{3}H]-cytisine (3 nM) in the presence of the nicotinic agonists cytisine (●), (-)nicotine (■), DMPP (▲), and the antagonists MLA (▼) and *d*-tubocurarine (◆) in a total assay volume of 250 µl for 60 min. Bound radioligand was separated from free by filtration through GF/B glass-fibre filters and measured using liquid scintillation spectrometry. Non-specific binding was determined in the presence of 10 µM (-)nicotine. These data represent a typical experiment with each point performed in duplicate with mean data obtained from at least 3 experiments (Table 3.3).

Figure 3.12

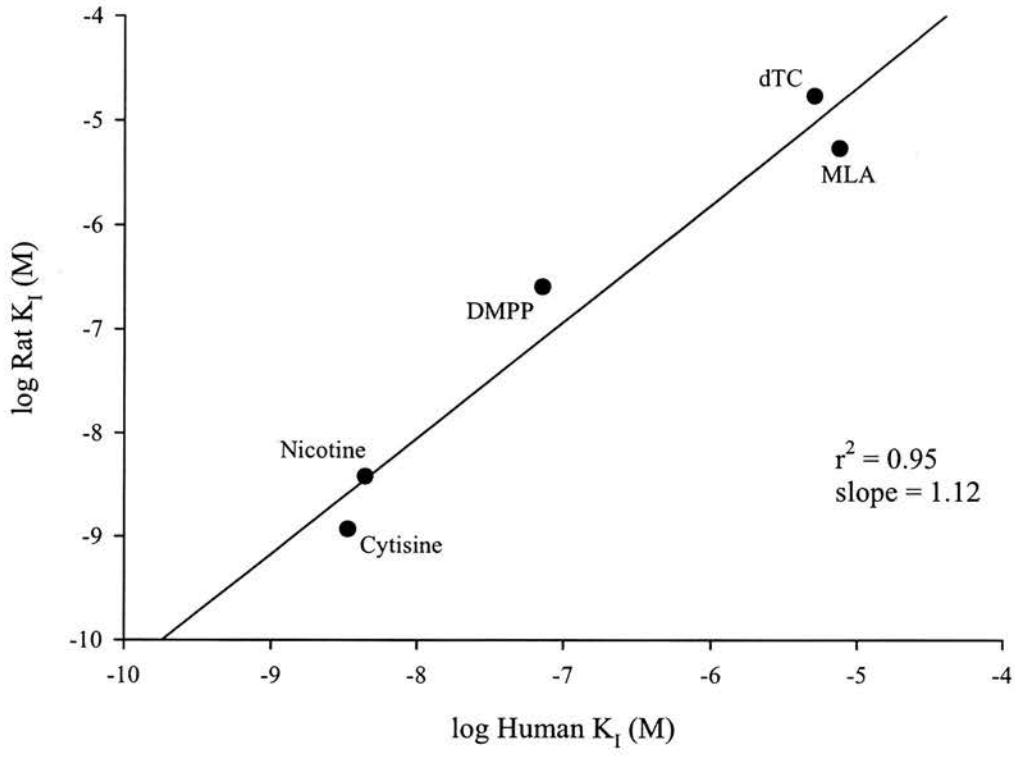

Correlation of the K_i values of Nicotinic Ligands for [^{3}H]-Cytisine Binding Sites in Rat Brain and SH-EP1-h$\alpha_4\beta_2$ Cell Membranes. The solid line represents a linear regression through the nicotinic data represented in Table 3.3. The similarity of both the r^2 value (0.95) and slope (1.12) to unity indicates no species differences in compound affinity for rat and human $\alpha_4\beta_2$ nAChRs.

Table 3.3: The Affinity of Nicotinic Ligands at [^{3}H]-Cytisine Binding Sites in Rat Brain and SH-EP1-h$\alpha_4\beta_2$ Cell Membranes

Compound	Rat Brain K_i (nM)	n_H	*n*	SH-EP1-h$\alpha_4\beta_2$ K_i (nM)	n_H	*n*	K_i ratio (Rat/Human)
Agonist							
Cytisine	1.18 ± 0.30	1.05 ± 0.16	4	3.35 ± 0.43	1.92 ± 0.39	5	0.35
Nicotine	3.81 ± 1.91	0.89 ± 0.27	3	4.40 ± 1.50	0.95 ± 0.19	4	0.9
DMPP	256.1 ± 47.0	0.95 ± 0.07	4	71.54 ± 14.42*	0.76 ± 0.02	4	3.6
Antagonist							
MLA	5,428 ± 2,155	0.89 ± 0.16	3	7,517 ± 1,709	0.68 ± 0.04	4	0.7
***d*-Tubocurarine**	17,206 ± 2,029	0.89 ± 0.02	3	5,045 ± 1,143*	0.91± 0.15	4	2.6

Affinity (K_i) and Hillslopes (n_H) were determined in [^{3}H]-cytisine competitive inhibition studies as described in the methods. Compounds examined were cytisine, (-)nicotine, 1,1-dimethyl-4-phenylpiperazinium iodide (DMPP), methyllycaconitine (MLA) and *d*-tubocurarine. Values are expressed as mean ± S.E.M. (n = 3-5). K_i values obtained in SH-EP1-h$\alpha_4\beta_2$ cells that are statistically different from those obtained in rat brain membranes are indicated by asterisks with $p<0.05$ (*). Statistical analyses were performed using one-way ANOVA and a Bonferroni *post*-hoc test.

As mentioned earlier, due to the picomolar affinity of epibatidine, binding studies unless conducted properly could be subject to depletion. To circumvent this problem we increased the volume of the [^{3}H]-epibatidine binding assay to 4 ml. As Figure 3.13 clearly shows; there is an excellent correlation between the ligand affinities in the [^{3}H]-cytisine and [^{3}H]-epibatidine assays using the human $\alpha_4\beta_2$ nAChR membrane preparation. Although slightly more variable, a similar pattern is also seen for the rat brain tissue (Tables 3.1 and 3.3).

Figure 3.13

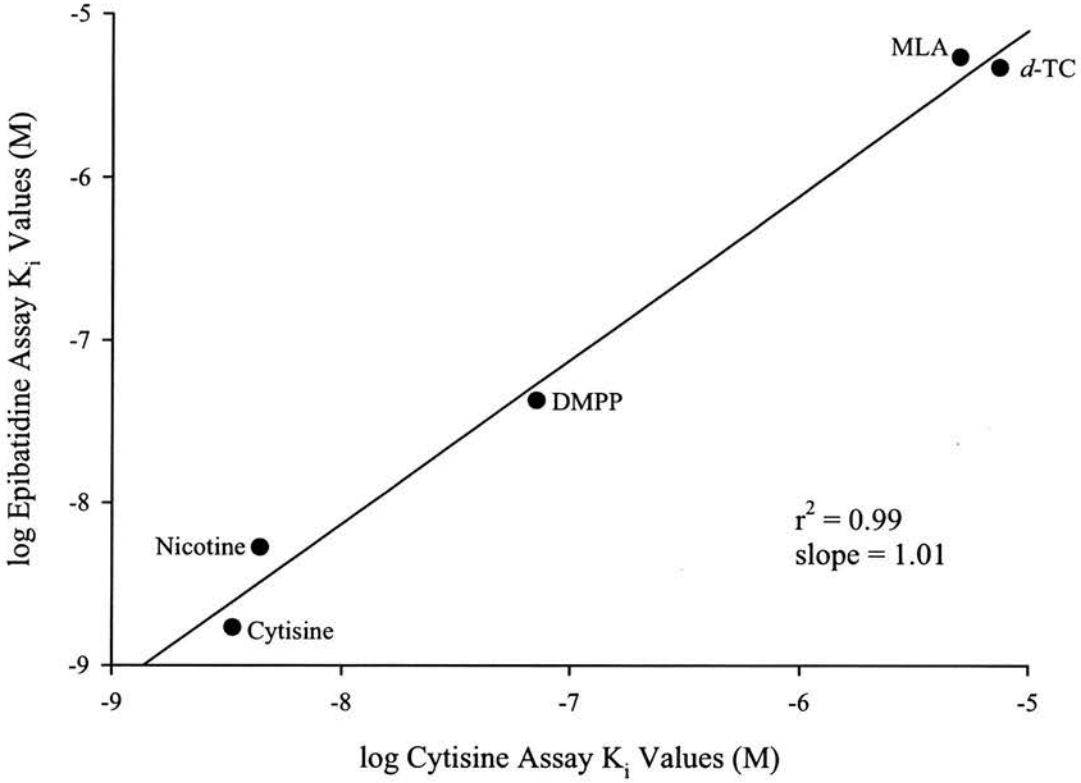

Correlation of the K_i values of Nicotinic Ligands for [^{3}H]-Epibatidine and [^{3}H]-Cytisine Binding Sites in SH-EP1-h$\alpha_4\beta_2$ Cell Membranes. The solid line represents a linear regression for the compound affinities (K_i) represented in Tables 3.1 & 3.3. Both the r^2 value (0.99) and the slope (1.01) are at unity indicating no differences in ligand affinity between the two assays.

3.5 Pharmacological Characterisation of the α_7 nAChR in Rat Brain and SH-EP1-hα_7 Cell Membranes Using [^{3}H]-Methyllycaconitine

As discussed in the introduction, the $\alpha_4\beta_2$ and α_7 nAChRs are the two major nicotinic receptors in the CNS. The α_7 nAChR continues to be investigated as it has potential roles in inflammation (e.g. Wang *et al.*, 2003), schizophrenia (e.g. Guan *et al.*, 1999; De Luca *et al.*, 2004; Deutsch *et al.*, 2005), and AD (e.g. Bednar *et al.*, 2002; O'Neill *et al.*, 2002; Yu *et al.*, 2005). Although there are still no potent and selective α_7 nAChR agonists commonly available in a radiolabelled form, historically the antagonist αBungarotoxin ([^{125}I]-αBgTx) has been used to characterised α_7 nAChR pharmacology (Clarke *et al.*, 1985; Falk *et al.*, 2003). The identification of MLA as a small and potent competitive α_7 nAChR antagonist (unlike the large peptide antagonist αBgTx) therefore potentially circumvented problems such as use of the iodinated compound and access to synaptic receptors and therefore led to the production of [^{3}H]-MLA (Aiyar *et al.*, 1979; Davies *et al.*, 1999; Whiteaker *et al.*, 1999; Lind *et al.*, 2001). However, [^{3}H]-MLA binding studies remain limited to studies analysing the rodent (Davies *et al.*, 1999; Whiteaker *et al.*, 1999) or amphibian α_7 nAChR (Lind *et al.*, 2001). Therefore, a systematic and comprehensive comparison of rat and human α_7 nAChR pharmacology was conducted using the antagonist [^{3}H]-MLA.

3.5.1 Time Course Determination of [^{3}H]-MLA Binding in Rat Brain and SH-EP1-hα_7 Cell Membrane Preparations

To determine when [^{3}H]-MLA binding to the α_7 nAChR attained equilibrium, the antagonist was incubated with membranes prepared from either rat brain tissue or from a human cell line over-expressing the human α_7 nAChR (SH-EP1-hα_7) and specific binding measured over a two hour period. [^{3}H]-MLA binding attained equilibrium within 20 min (at 25°C) in both membrane preparations and held constant for at least 2 h (Figure 3.14). These observations are consistent with the findings of Davies and colleagues (1999) using rat brain membranes and as a consequence, all subsequent experiments were conducted for 60 min at 25°C and terminated by vacuum filtration.

3.5.2 Concentration Dependence of [^{3}H]-MLA Binding in α_7 nAChR membrane preparations

Specific [^{3}H]-MLA binding in rat brain tissue accounted for 70.9 ± 3.4% of total binding sites at a free radiolabel concentration close to the expected K_D (~2 nM; Davies *et al.*,

Figure 3.14

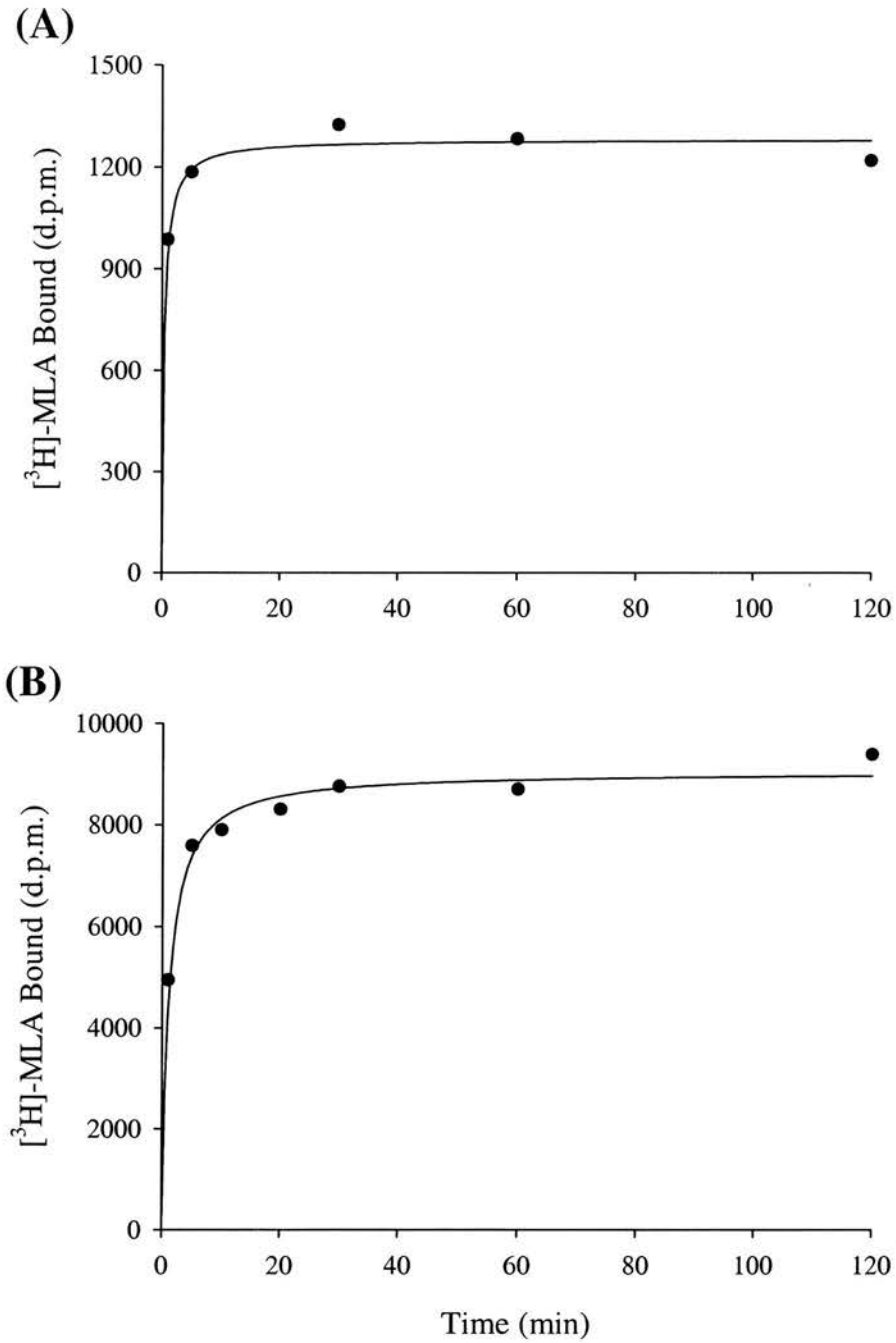

Time Course of Specific [^{3}H]-MLA binding in (A) Rat Brain and (B) SH-EP1-hα_7 Membrane Preparations. Membranes (400 μg rat; 60 μg SH-EP1-hα_7) were incubated (22°C) with [^{3}H]-MLA (2.5 nM) in a total assay volume of 250 μl for up to 2 h. Each total binding was tested in duplicate with its non-specific counterpart (defined by 10 μM *d*-tubocurarine) tested in singulate. Specific binding points were derived by subtracting non-specific binding from total binding with these data representing a typical experiment.

1999). This value was slightly higher in SH-EP1-hα_7 cell membranes where specific binding accounted for 80.3 ± 4.5% of total binding sites (Figure 3.15).

To determine K_D and B_{max} values for [^{3}H]-MLA binding sites in membranes from rat brain and SH-EP1-hα_7 cells, hot saturation experiments were performed with increasing concentrations of [^{3}H]-MLA. Representative examples of the concentration dependence of [^{3}H]-MLA binding to rat and human membrane preparations are shown in Figure 3.16, with affinity (K_D) values of 1.71 ± 0.32 nM (n = 5) and 5.10 ± 0.95 nM (n = 5) in rat brain and SH- EP1-hα_7 cell membranes, respectively shown in Table 3.4. [^{3}H]-MLA binding was saturable and consistent with a single high affinity binding site in both rat brain (n_H = 1.37 ± 0.20, n = 5) and SH-EP1-hα_7 cell membranes (n_H = 1.17 ± 0.05, n = 5; Figure 3.16). Furthermore, saturable binding in the hot saturation studies allowed the measurement of the density of α_7 nAChRs in these membrane preparations, giving B_{max} values of 0.18 ± 0.01 pmol/mg protein (rat; n = 5) and 7.08 ± 0.70 pmol/mg protein (SH-EP1-hα_7; n = 5; Figure 3.16, Table 3.4). The K_D/K_i of MLA was also determined using inhibition studies in which [^{3}H]-MLA (2.5 nM) was incubated with increasing concentrations of unlabelled MLA. In excellent agreement with the K_D values determined in the hot saturation studies, the K_D/K_i values for MLA in the inhibition experiments were 2.74 ± 0.34 (n = 9) and 5.04 ± 0.68 (n = 11) in rat brain and SH-EP1-hα_7 cell membranes, respectively (Figure 3.17). Indeed, the high density of [^{3}H]-MLA binding sites in the stable cell line (~35 times greater than in rat brain tissue) makes these cells particularly useful for pharmacological studies of the binding properties of ligands, as much less tissue is required for studying the human α_7 nAChR.

In all subsequent binding experiments, [^{3}H]-MLA binding (2.5 nM) was performed at 25°C for 60 min unless otherwise stated.

3.5.3 Inhibition of [^{3}H]-MLA Binding to Rat and Human α_7 nAChRs by Cholinergic Agonists and Antagonists

3.5.3.1 Inhibition of [^{3}H]-MLA Binding to Rat Brain and SH-EP1-hα_7 Cell Membranes by Cholinergic Receptor Antagonists

The receptor-selective antagonists MLA (Figure 3.17) and αBgTx both inhibited [^{3}H]-MLA binding in rat brain and SH-EP1-hα_7 cell membranes in a concentration-dependent manner (Figure 3.18). The rank order of potency for the four nicotinic antagonists examined was αBgTx = MLA > *d*-tubocurarine > mecamylamine in both membrane preparations, with representative inhibition curves shown in Figure 3.18 and Table 3.5. The affinity (K_i) of the cholinergic ligands varied from the nanomolar range for

Figure 3.15

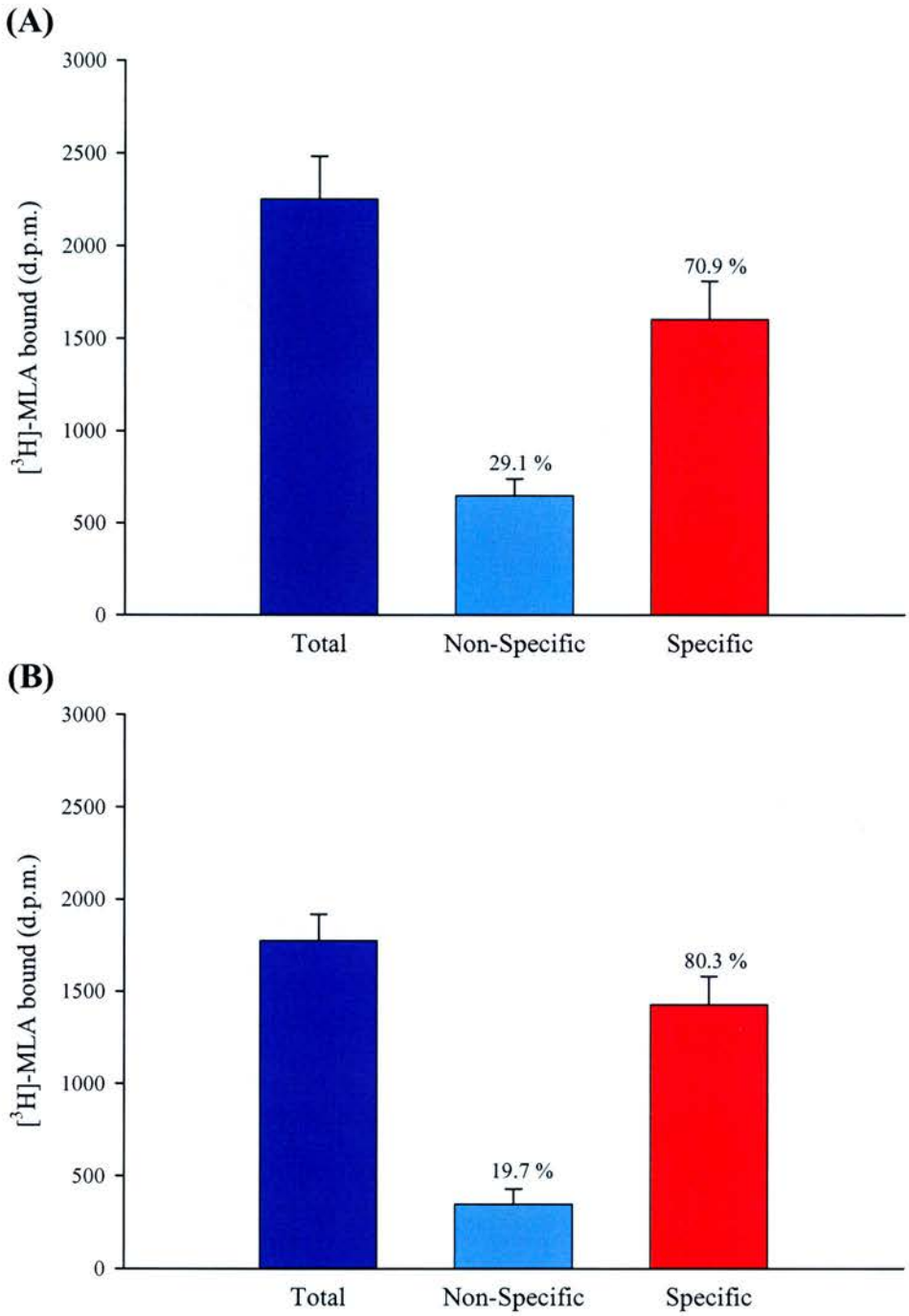

Proportions of [^{3}H]-MLA Binding in Rat Brain or SH-EP1-hα_7 Cell Membrane Preparations. Membranes ((A) 400 µg rat; (B) 60 µg, SH-EP-hα_7) were incubated with [^{3}H]-MLA (2.5 nM) in a total assay volume of 250 µl for 60 min at 22°C. Non-specific binding was determined in the presence of 10 µM *d*-tubocurarine. These data are from an average of 4 separate hot saturation experiments.

Figure 3.16

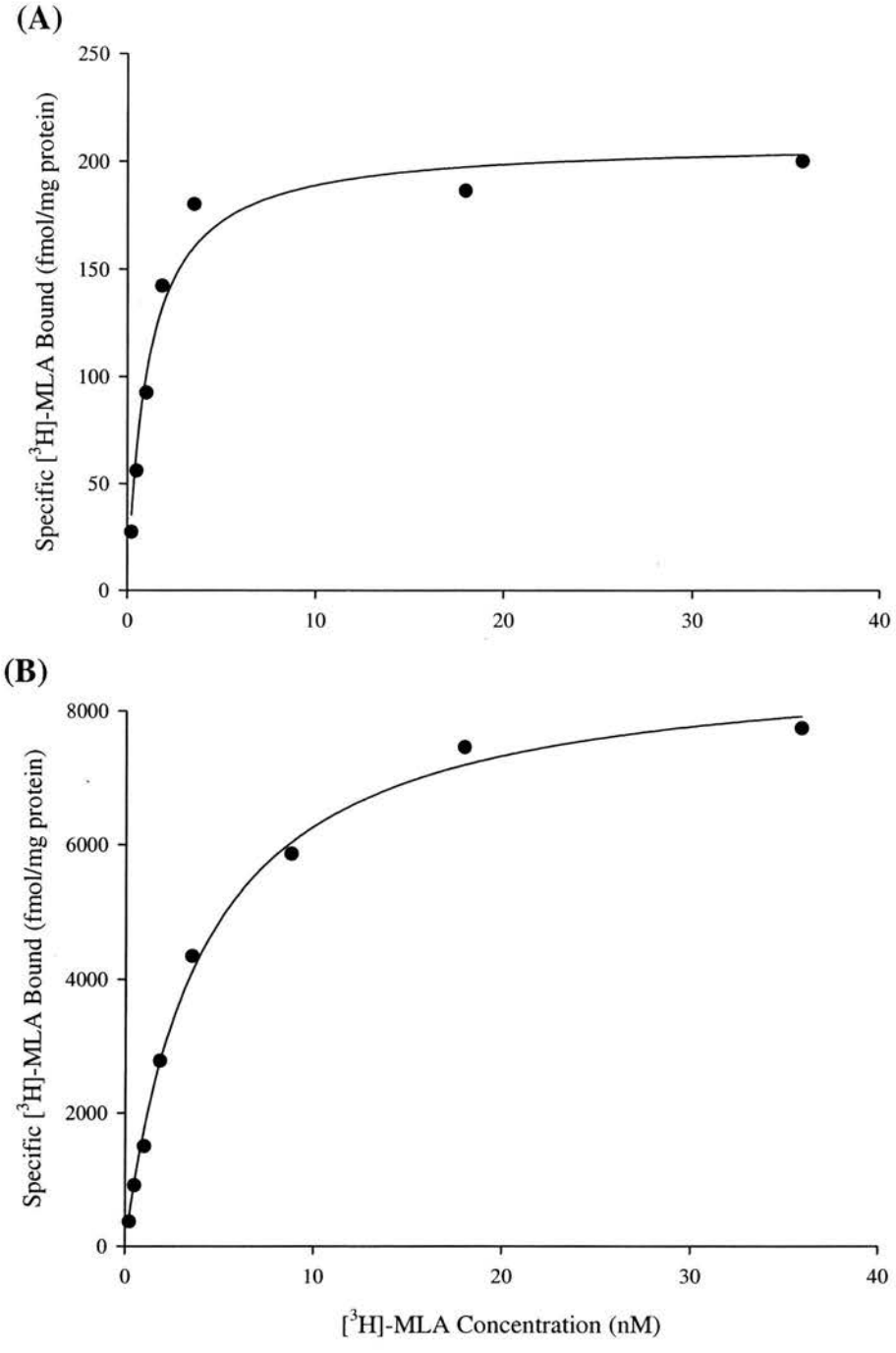

Concentration Dependence of [^{3}H]-MLA Binding in α_7 nAChR Membrane Preparations. (A) Rat brain (400 µg) or (B) SH-EP1-hα_7 cell membranes (60 µg) were incubated with increasing concentrations of [^{3}H]-MLA in a total assay volume of 250µl for 60 min at 22°C. Non-specific binding was determined in the presence of 10 µM *d*-tubocurarine. These data are from representative hot saturation studies in rat brain and SH-EP1-hα_7 cell membranes, respectively.

Table 3.4 **K_D and B_{max} Values Determined for [^{3}H]-MLA Binding Sites in Rat Brain and SH-EP1-hα_7 Cell Membranes**

Species	K_D (nM)	*n*	n_H	B_{max} (pmol/mg protein)
Rat	1.71 ± 0.32	5	1.37 ± 0.20	0.18 ± 0.01
Human	5.01 ± 0.95	5	1.17 ± 0.05	7.08 ± 0.70*

Affinity (K_D), Hill slope (n_H), and B_{max} determined in [^{3}H]-MLA binding studies using hot saturation assays as described in the methods. Values are expressed as mean ± S.E.M., (n = 5). Statistical analyses were performed using one-way ANOVA with Bonferroni post-hoc testing. No difference in ligand affinity between species was observed, although there was a significant difference in receptor density ($p < 0.05$).

Figure 3.17

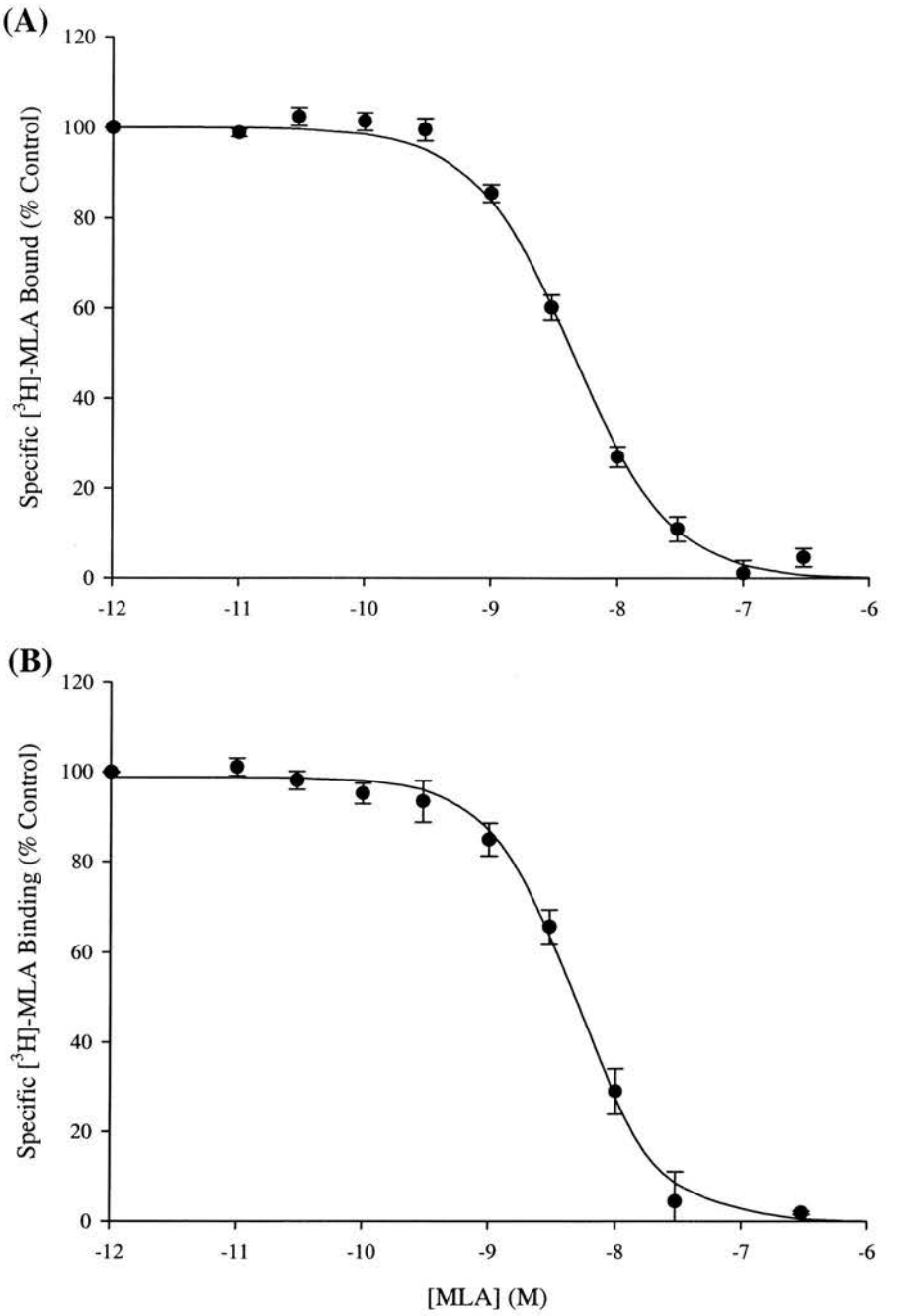

Inhibition of [^{3}H]-MLA Binding by Unlabelled MLA in Rat Brain and SH-EP1-hα_7 Cell Membrane Preparations. (A) Rat brain (400 µg) or (B) SH-EP1-hα_7 cell membranes (60 µg) were incubated with [^{3}H]-MLA (2.5 nM) and increasing concentrations of unlabelled MLA in a total assay volume of 250 µl for 60 min at 25°C. Non-specific binding was determined in the presence of 10 µM *d*-tubocurarine. The data represent the mean ± S.E.M. of (A) n = 9, rat or (B) n = 11, SH-EP1-hα_7 cold saturation experiments.

αBgTx (K_i = 1.40 ± 0.42 nM; n = 4;rat brain) and K_i = 2.40 ± 0.40; n = 8; SH-EP1-hα_7) to the millimolar range for mecamylamine (10.3 mM; n = 2; rat) and 1.2 ± 0.3 mM (n = 3, SH-EP1-hα_7). However, it must be noted that even concentrations of up to 3 μM αBgTx did not produce full inhibition in either rat brain or SH-EP1-hα7 cell membrane preparations. In rat brain tissue 1 μM αBgTx produced a maximal inhibition of 80 %, whilst a higher (3 μM) concentration produced only 40 % inhibition in SH-EP1-hα_7 membranes (Figure 3.18). This intriguing observation has been investigated further and these studies are reported in Section 3.6.

In addition to looking at nicotinic antagonists, the ability of the muscarinic antagonists atropine and scopolamine to inhibit [^{3}H]-MLA binding to rat and human α_7 nAChRs was also examined. Interestingly, both compounds inhibited [^{3}H]-MLA binding with atropine 2-3 fold more potent than scopolamine in both rat and SH-EP1-hα_7 membrane preparations (Table 3.5). Indeed, both compounds were an order of magnitude more potent than mecamylamine. In general, Hill coefficients (n_H) for all the cholinergic antagonists were close to unity in both membrane preparations (Table 3.5).

Although the number of nicotinic antagonists was limited (MLA, αBgTx, *d*-tubocurarine, and mecamylamine), there is excellent correlation between nicotinic antagonist K_i values for rat brain and SH-EP1-hα_7 cell membranes, with an r^2 = 1.00 and a slope of 1.20 (Figure 3.19). Statistical analyses generally showed no significant change in nicotinic antagonist affinity for the two α_7 nAChR membrane preparations. However, the muscarinic antagonists atropine and scopolamine, were more potent at the human α_7 nAChR ($p < 0.05$).

3.5.3.2 Inhibition of [^{3}H]-MLA Binding to Rat Brain and SH-EP1-hα$_7$ Cell Membranes by Cholinergic Receptor Agonists

A range of cholinergic agonists were examined for their ability to inhibit [^{3}H]-MLA binding in rat brain and SH-EP1-hα_7 cell membranes. All 11 agonists examined inhibited [^{3}H]-MLA binding in a concentration-dependent manner with a rank order of potency at rat α_7 nAChRs being; (-)AR-R17779 = (±)epibatidine > DMPP > cytisine > (-)nicotine > methylcarbamylcholine chloride (MCCC) > (+)AR-R17779 > RJR-2403 > acetylcholine > choline > methacholine chloride (Table 3.6). For simplicity, Figure 3.20 shows inhibition curves for four of these compounds. In rat brain tissue, the affinity of the nicotinic ligands varied from the high nanomolar range for (-)AR-R17779 (K_i = 252 ± 51 nM; n = 6) to the millimolar range for methacholine chloride (9.34 ± 0.49 mM; n = 3).

Figure 3.18

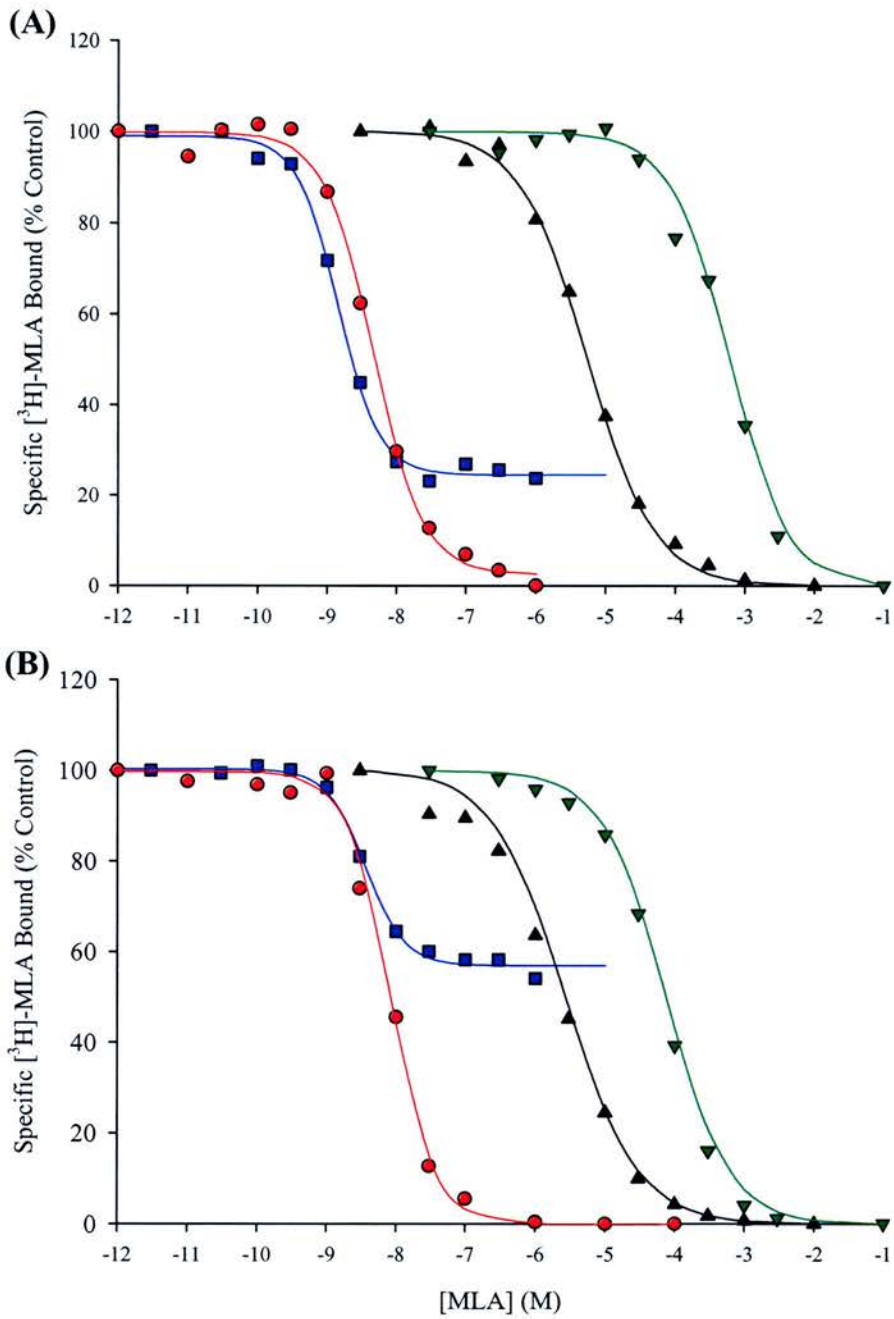

Inhibition of [^{3}H]-MLA Binding by Cholinergic Antagonists. (A) Rat brain (400 µg) or (B) SH-EP1-hα_7 cell membranes (60 µg) were incubated (22°C) with [^{3}H]-MLA (2.5 nM) in the presence of nicotinic antagonists methyllycaconitine (●), αbungarotoxin (■), *d*-tubocurarine (▲), and atropine (▼) in a total assay volume of 250 µl for 60 min. Non-specific binding was determined in the presence of 10 µM *d*-tubocurarine. The data represent a typical experiment with each point performed in duplicate with mean data obtained from at least 3 experiments (Table 3.5).

Table 3.5: The Affinity (K_i) of Cholinergic Antagonists for [^{3}H]-MLA Binding Sites in Rat Brain and SH-EP1-hα_7 Cell Membranes

Compound	Rat Brain K_i (nM)	n_H	*n*	SH-EP1-hα_7 K_i (nM)	n_H	*n*	K_i Ratio Rat/Human
Nicotinic							
αBgTx	1.40 ± 0.42	1.29 ± 0.05	4	2.40 ± 0.40	1.29 ± 0.07	8	0.6
MLA	2.74 ± 0.34	1.11 ± 0.03	9	5.04 ± 0.68	1.11 ± 0.05	11	0.5
***d*-Tubocurarine**	2,757 ± 282	1.03 ± 0.06	4	2,506 ± 369	0.96 ± 0.05	4	1.1
Mecamylamine	10,270,000		2	1,190,000 ± 320,000*	1.49 ± 0.26	3	8.6
Muscarinic							
Atropine	970,865 ± 134,420	1.15 ± 0.12	4	101,213 ± 8,496*	0.97 ± 0.06	4	9.6
Scopolamine	1,949,000 ± 272,000	1.24 ± 0.14	4	339,415 ± 43,537*	1.00 ± 0.04	4	5.7

Affinity (K_i) and Hill slopes (n_H) were determined in the [^{3}H]-MLA inhibition assays as described in the methods. Compounds examined were α-Bungarotoxin (αBgTx; apparent K_i), methyllycaconitine (MLA), *d*-tubocurarine, mecamylamine, atropine, and scopolamine. Values are expressed as mean ± S.E.M., n = 2-11. Statistical analyses were performed using one-way ANOVA with Bonferroni post-hoc testing. K_i values obtained in SH-EP1-hα_7 cells differing from those obtained in rat brain membranes are indicated with an asterisk where $p < 0.05$ (*).

Figure 3.19

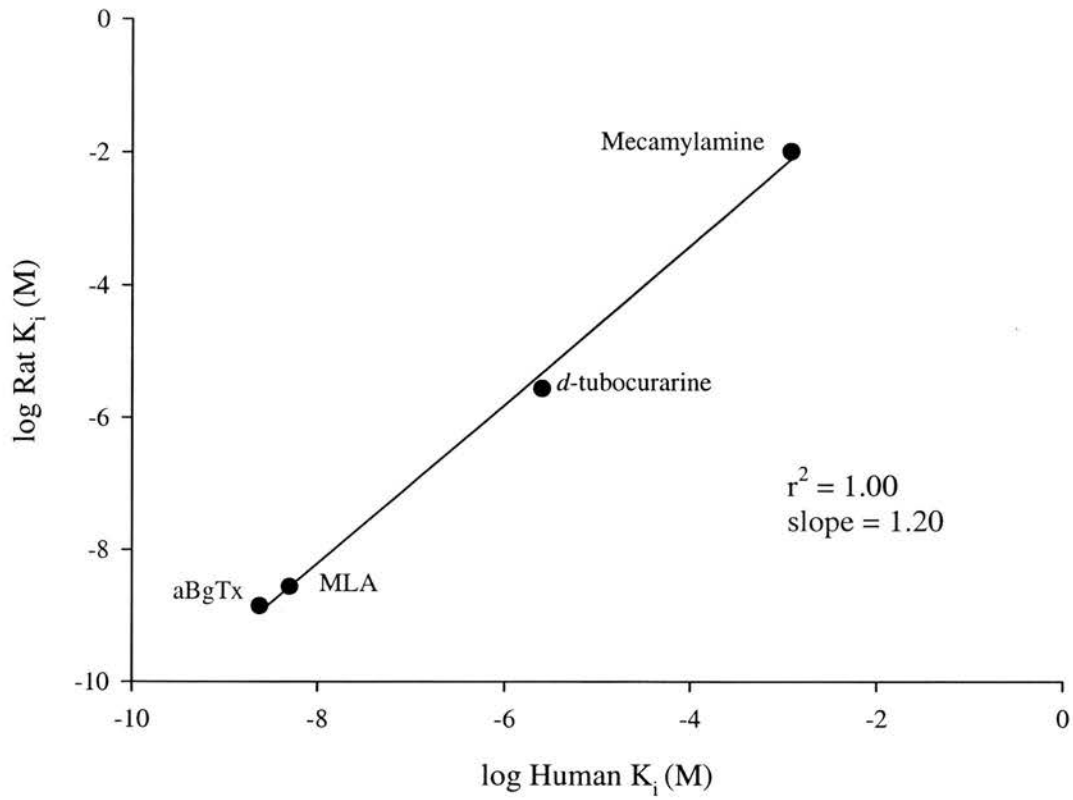

Correlation of the Affinity (K_i) of Nicotinic Antagonists at [^{3}H]-MLA Binding Sites in Rat Brain and SH-EP1-hα_7 Cell Membranes. The ability of the antagonists αbungarotoxin (αBgTx; apparent K_i), methyllycaconitine (MLA), *d*-tubocurarine, and mecamylamine to inhibit [^{3}H]-MLA binding in rat brain and SH-EP1-hα_7 cell membranes. The solid line represents a linear regression through the mean K_i values for the nicotinic antagonists represented in Table 3.5. Both the r^2 value (1.00) and the slope (1.20) are at unity indicating no differences in ligand affinity between the two species.

In SH-EP1 cell membranes expressing the human α_7 nAChR, the rank order of potency for nicotinic agonists in SH-EP1-hα_7 cell membranes was slightly different (±)epibatidine > (-)AR-R17779 > DMPP > (-)nicotine > cytisine > MCCC > acetylcholine > RJR-2403 > (+)AR-R17779 > choline > methacholine chloride (Figure 3.20, Table 3.6). In contrast to the ligand affinities determined for rat brain membranes, the affinity of the nicotinic compounds in SH-EP1-hα_7 cell membranes varied from the low nanomolar range for (±)epibatidine (K_i = 3.35 ± 0.63 nM; n = 8) to the micromolar range for methacholine chloride (K_i = 80.5 ± 11.9 μM; n = 4, Table 3.6).

The nicotinic agonists generally exhibited a much higher affinity (~2 orders of magnitude) for human α_7 nAChRs when compared to those found in rat brain tissue (Table 3.6). Indeed, (±)epibatidine inhibited [^{3}H]-MLA binding to SH-EP1-hα_7 nAChRs with a K_i value of 3.4 ± 0.6 nM (n = 8) whereas, the K_i value in rat brain tissue was more than 100-fold higher (K_i = 372 ± 46 nM, n = 4; $p < 0.005$). Interestingly, although (-)AR-R17779 had a similar potency (K_i = 20.4 ± 8.9 nM; n = 6) to (±)epibatidine in SH-EP1-hα_7 cell membranes, it exhibited only a 10-fold increase in potency in rat brain membranes (K_i = 252 ± 51; n = 6). The observation that (-)nicotine had more than 100-fold higher affinity for the human α_7 nAChRs in SH-EP1 cell line (K_i = 0.3 ± 0.07 μM, n = 6) compared to the rat brain membrane preparation (K_i = 39.8 ± 5.3 μM, n = 7), has major implications in health and disease. As the muscarinic antagonists scopolamine and atropine inhibited [^{3}H]-MLA binding, I also examined two muscarinic agonists McN-A-343 and pilocarpine. Both compounds inhibited [^{3}H]-MLA binding in rat brain and SH-EP1-hα_7 cell membranes with McN-A-343 more potent than a number of nicotinic agonists (Table 3.7).

Agonist Hill coefficients obtained in rat brain tissue were generally greater than unity, perhaps indicative of some form of positive co-operativity (Table 3.6 & 3.7). In contrast, Hill coefficients obtained for agonists at the human α_7 nAChR were equal to or below unity (Table 3.6 & 3.7). These differences in agonist affinity at the α_7 nAChR in different species are illustrated clearly in Figure 3.21, which correlates agonist affinities for rat and human α_7 nAChRs. There is an excellent correlation between agonist affinities determined in the two membrane preparations with r^2 = 0.92 and a slope of 1.09.

Figure 3.20

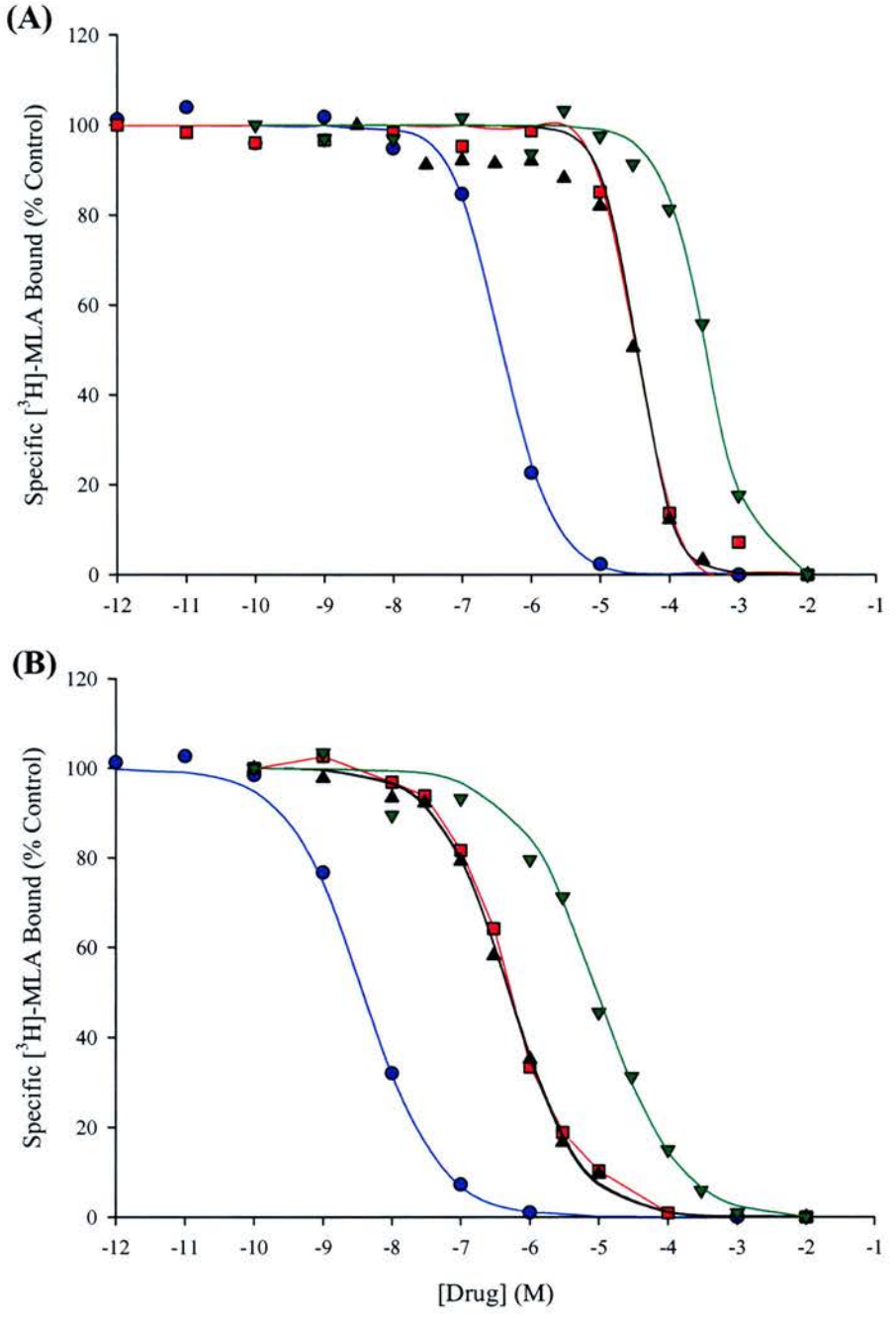

Inhibition of [^{3}H]-MLA Binding by Cholinergic Agonists. (A) Rat brain (400 µg) or (B) SH-EP1-hα_7 cell membranes (60 µg) were incubated (22°C) with [^{3}H]-MLA (2.5 nM) and various concentrations of the nicotinic agonists (-)AR-R17779 (●), (-)nicotine (■), cytisine (▲), and (+)AR-R17779 (▼) in a total assay volume of 250 µl for 60 min. Non-specific binding was determined in the presence of 10 µM *d*-tubocurarine. These data represent a typical experiment with each point performed in duplicate with mean data obtained from at least 3 experiments (Table 3.6).

Table 3.6: The Affinity (K_i) of Nicotinic Agonists at [^{3}H]-MLA Binding Sites in Rat Brain and SH-EP1-hα_7 Cell Membranes

Compound	Rat Brain K_i (nM)	n_H	*n*	SH-EP1-hα_7 K_i (nM)	n_H	*n*	K_i ratio Rat/Human
(-) AR-R17779	252 ± 51	1.54 ± 0.23	6	20.4 ± 8.9*	0.89 ± 0.08	6	13
(±)Epibatidine	372 ± 46	1.25 ± 0.11	4	3.4 ± 0.6*	0.94 ± 0.08	8	111
DMPP	24,690 ± 784	1.33 ± 0.18	5	276 ± 49*	0.74 ± 0.03	5	90
Cytisine	25,000 ± 2,673	1.79 ± 0.07	4	537 ± 60*	0.78 ± 0.04	4	47
(-) Nicotine	39,880 ± 5,346	1.21 ± 0.11	7	311 ± 74*	0.85 ± 0.06	6	128
MCCC	99,705 ± 4,993	1.37 ± 0.15	5	1,721 ± 215*	0.91 ± 0.01	4	58
(+)AR-R17779	236,384 ± 43,443	1.36 ± 0.10	6	7,161 ± 962*	0.89 ± 0.08	7	33
RJR-2403	383,574 ± 44,435	1.28 ± 0.17	4	3,440 ± 479*	0.94 ± 0.02	4	67
Acetylcholine	1,340,000 ± 130,000	1.60 ± 0.09	5	2,180 ± 422*	0.87 ± 0.11	5	615
Choline	1,860,000 ± 400,000	1.27 ± 0.11	4	15,500 ± 0.980*	0.80 ± 0.08	4	120
Methacholine Chloride	9,340,000 ± 490,000	0.94 ± 0.06	3	80,456 ± 11,929*	0.95 ± 0.09	4	116

K_i and Hill slopes (n_H) were determined in [^{3}H]-MLA binding assay as described in the methods. Values are expressed as mean ± S.E.M. (n = 3-8). Statistical comparisons were made using a one-way ANOVA with Bonferroni post-hoc test. K_i values in SH-EP1-hα_7 cell membranes that differ from those obtained in rat brain membranes are indicated with an asterisk (*; $p < 0.05$).

Table 3.7: The Affinity (K_i) of Muscarinic Agonists at [^{3}H]-MLA Binding Sites in Rat Brain and SH-EP1-hα_7 Cell Membranes

Compound	Rat Brain K_i (nM)	n_H	*n*	SH-EP1-hα_7 K_i (nM)	n_H	*n*	K_i Ratio Rat/Human
McN-A-343	53,678 ± 4,150	1.79 ± 0.16	4	805 ± 39*	0.80 ± 0.03	3	67
Pilocarpine	2,630,000 ± 170,000	1.18 ± 0.04	3	444,079 ± 24,858*	1.26 ± 0.07	4	5.9

K_i and Hill slope (n_H) values were determined in the [^{3}H]-MLA binding assay as described in the methods. Values are expressed as mean ± S.E.M. (n = 3-4). Statistical comparisons were made using a one-way ANOVA with Bonferroni post-hoc test. K_i values in SH-EP1-hα_7 cell membranes that differ from those obtained in rat brain membranes are indicated with an asterisk (*; $p < 0.05$).

Figure 3.21

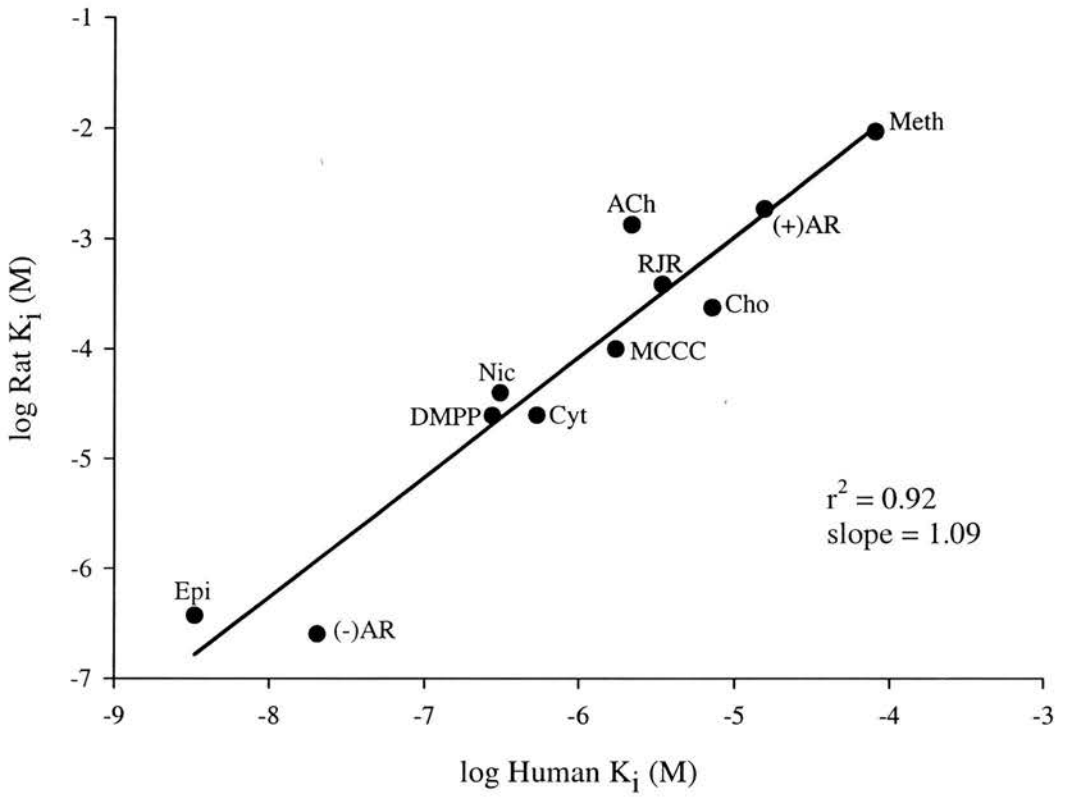

Correlation of the Affinity (K_i) of Nicotinic Agonists at [^{3}H]-MLA Binding Sites in Rat Brain and SH-EP1-hα_7 Cell Membranes. The solid line represents a linear regression through the data represented in Table 3.6 with an $r^2 = 0.92$ and a slope of 1.09. Data points represent (±)epibatidine (Epi), (-)AR-R17779 ((-)AR), 1,1-dimethyl-4-phenylpiperazinium iodide (DMPP), (-)nicotine (Nic), cytisine (Cyt), MCCC (MCCC), acetylcholine (ACh), RJR-2403 (RJR), choline (Cho), (+)AR-R17779 ((+)AR), and methacholine chloride (Meth).

3.5.3.3 Inhibition of [^{3}H]-MLA Binding to Rat Brain and SH-EP1-hα_7 Cell Membranes by Acetylcholinesterase Inhibitors, Allosteric Potentiating Ligands, and General Channel Blockers

It has been known for some time that acetylcholinesterase (AChE) inhibitors such as galanthamine may also interact directly with nAChRs (Pascuzzo *et al.,* 1984; Alkondon *et al.,* 1997; Samochocki *et al.,* 2000; Kihara *et al.,* 2004). The ability of related acetylcholinesterase inhibitors and putative allosteric potentiating ligands to inhibit [^{3}H]-MLA (2.5 nM) binding in rat brain and SH-EP1-hα_7 cell membranes was examined. I also examined non-selective channel blockers that included 4-aminopyridine (4-AP), tetraethylammonium (TEA), and (-)bicuculline.

All eight compounds examined inhibited [^{3}H]-MLA binding in a concentration-dependent manner with four representative compounds shown in Figure 3.22. The rank order of potency for these ligands at α_7 nAChRs in rat brain membranes was; E2020 > bicuculline methiodide = tacrine > physostigmine > codeine > galanthamine > 4-AP > TEA (Table 3.8). The rank order of affinity at human α_7 nAChRs differed slightly from that seen in the rat brain membrane preparation being; bicuculline methiodide > E2020 > tacrine > galanthamine = physostigmine = codeine > 4-AP > TEA (Table 3.8). The affinity of the ligands in the two membrane preparations differed slightly, although not as considerably as seen for the agonists. K_i values for the compounds in rat brain varied from the micromolar range for E2020 (K_i = 44.13 ± 1.72 μM; n = 4) to the high millimolar range for TEA (K_i = 897 ± 106 mM; n = 4), while ligand affinity in the SH-EP1-hα_7 cell membrane preparation were from low micromolar for E2020 (K_i = 11.1 ± 1.4, n = 4) to low millimolar for TEA (K_i = 22.8 ± 2.8 mM, n = 4).

Hill coefficients for ligands examined in rat brain and SH-EP1-hα_7 cell membranes were generally equal to or marginally greater than unity (Table 3.8). Due to the varying ligand pharmaco-profiles a correlation plot has not been drawn, however, statistical analyses using a one-way ANOVA with Bonferroni post-hoc testing indicates the compounds in general examined exhibited lower affinity for binding sites in rat brain membranes than in SH-EP1-hα_7 cell line membranes ($p < 0.001$).

Figure 3.22

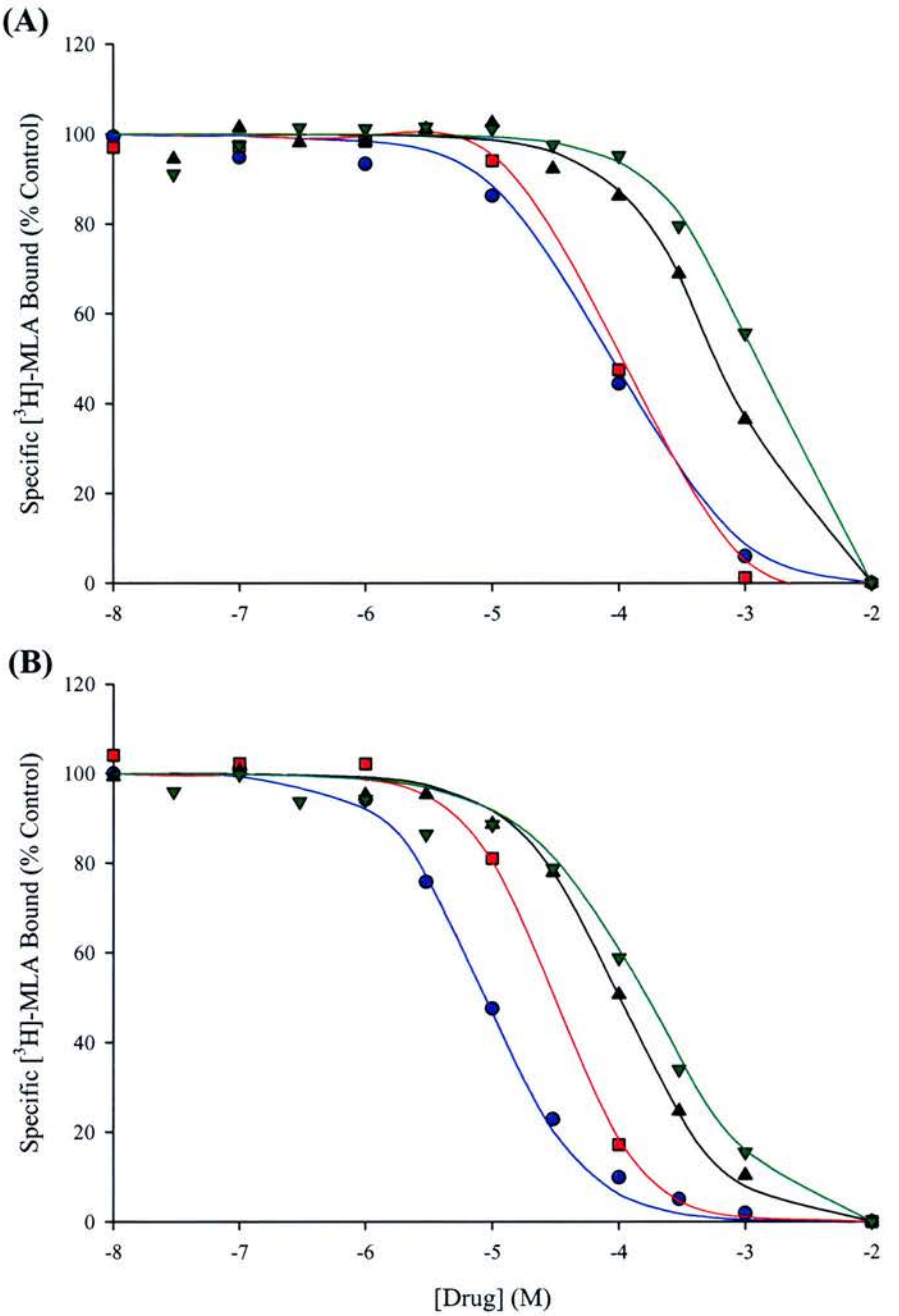

Inhibition of [^{3}H]-MLA Binding by Acetylcholinesterase Inhibitors, Allosteric Potentiating Ligands, or General Channel Blockers in Rat Brain and SH-EP1-hα_7 Cell Membranes. (A) Rat brain (400 µg) or (B) SH-EP1-hα_7 cell membranes (60 µg) were incubated (22°C) with [^{3}H]-MLA (2.5 nM) and compounds including bicuculline (●), tacrine (■), codeine (▼), or galanthamine (▲) in a total assay volume of 250 µl for 60 min. Non-specific binding was determined in the presence of 10 µM *d*-tubocurarine. The data represent a typical experiment with each point performed in duplicate with mean data obtained from at least 3 experiments (Table 3.8).

Table 3.8: K_i Values for Acetylcholinesterase Inhibitors, Allosteric Potentiating Ligands, and General Channel Blockers at [^{3}H]-MLA Binding Sites in Rat Brain and SH-EP1-hα_7 Cell Membranes.

Compound	Rat Brain K_i (μM)	SH-EP1-hα_7 n_H	*n*	K_i (μM)	n_H	*n*	K_i ratio Rat/Human
Acetylcholinesterase Inhibitors							
E2020	44.1 ± 1.7	1.07 ± 0.06	4	11.1 ± 1.4*	1.14 ± 0.07	4	4
Tacrine	65.6 ± 5.45	1.26 ± 0.07	4	29.3 ± 3.8	1.21 ± 0.10	5	2.2
Physostigmine	326 ± 55	1.14 ± 0.09	3	120 ± 19*	1.04 ± 0.08	4	2.7
Galanthamine	300 ± 58	1.24 ± 0.14	4	78.09 ± 8.9*	0.99 ± 0.06	3	3.8
Allosteric Potentiating Ligand							
Codeine	534 ± 92	1.14 ± 0.13	3	128 ± 21*	0.94 ± 0.05	6	4.2
General Channel Blockers							
4-aminopyridine	12.58 ± 2.07	0.98 ± 0.29	5	462 ± 69*	1.05 ± 0.14	4	27.2
(-)Bicuculline	57,649 ± 3,676	1.15 ± 0.07	4	5,749 ± 667*	1.01 ± 0.05	4	10
TEA	896,700 ± 106,100	0.98 ± 0.16	4	22,756 ± 2,814*	0.94 ± 0.07	4	39

K_i and Hill slope (n_H) values determined in the [^{3}H]-MLA binding assay as described in the methods. Values are expressed as mean ± S.E.M. (n = 3-6). Statistical comparisons were made using a one-way ANOVA with Bonferroni post-hoc test. K_i values in SH-EP1-hα_7 cell membranes that differ from those obtained in rat brain membranes are indicated with $p < 0.05$ (*).

3.6 Comparison of [^{3}H]-αBgTx and [^{3}H]-MLA Binding Sites in SH-EP1-hα$_7$ Cell Membranes

Unlike methyllycaconitine, controversy exists as to whether a large peptide such as αBgTx can access all 5 potential binding sites on the α$_7$ nAChR (Conti-Tronconi & Raftery, 1986; Palma *et al.*, 1996; Balass *et al.*, 1997; Rangwala *et al.*, 1997; Arias, 2000). In agreement with the only reasonably comprehensive study on [^{3}H]-MLA binding (Davies *et al.*, 1999), unlabelled αBgTx only produced 80 % inhibition of [^{3}H]-MLA binding sites in rat brain membranes (Section 3.5, Figure 3.18; Figure 3.23). In addition to αBgTx not completely inhibiting MLA binding to rat brain, the Hill coefficient was slightly greater than unity ($n_H = 1.29 \pm 0.05$, $n = 4$), which requires further investigation. To address these issues, more detailed studies of the αBgTx/[^{3}H]-MLA interaction was examined using the SH-EP1-hα$_7$ cell line. As this cell line contains no native nACh receptors and has only been transfected with the human α$_7$ nAChR it should serve as a pure α$_7$ nAChR population with potentially no additional sites (Peng *et al.*, 1999; Sweileh *et al.*, 2000). Despite this pure α$_7$ nAChR population, unlabelled αBgTx only produced 40 % inhibition of [^{3}H]-MLA binding sites in SH-EP1-hα$_7$ cell membranes, even less than that observed in the rat brain membranes (Section 3.5, Figure 3.18; Figure 3.23). The Hill coefficient for αBgTx inhibition at the human α$_7$ nAChR was however, still slightly greater than unity ($n_H = 1.29 \pm 0.07$, $n = 8$).

To determine whether the lack of inhibition of [^{3}H]-MLA binding sites by αBgTx was due to accessibility because of the large size of αBgTx, the assay length was varied to allow the study of the time course of binding, giving αBgTx an extended period of time to penetrate the cells/membranes and gain access to the α$_7$ nAChR. Rat brain and SH-EP1-hα$_7$ cell membranes were incubated in the presence of αBgTx for up to 140 min prior to the termination of the assay (Figure 3.24). Even using a preincubation period of up to 140 min for αBgTx in rat brain and SH-EP1-hα$_7$ cell membranes resulted in no increase in the level of inhibition of [^{3}H]-MLA binding. Data for the latter membranes is shown in Figure 3.24. This was despite a slight increase in the affinity of αBgTx with increasing incubation time (Table 3.9). For comparison these studies were also carried out with MLA and as Table 3.9 shows, the affinity of MLA for SH-EP1-hα$_7$ did not vary with the incubation period.

With no changes in the level of inhibition by αBgTx with time, these differences were investigated further by establishing a [^{3}H]-αBgTx binding assay using the human α$_7$ nAChR cell membranes. The use of [^{3}H]-αBungarotoxin rather than [^{125}I]-αBungarotoxin

Figure 3.23

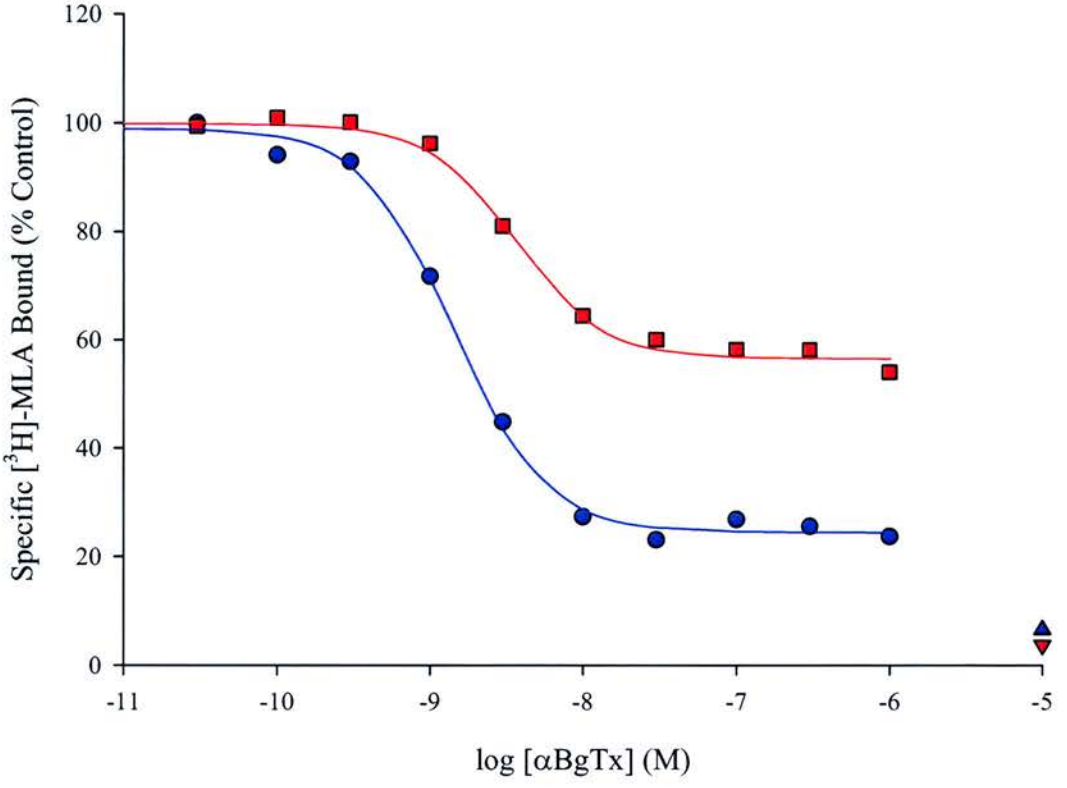

Inhibition of [^{3}H]-MLA Binding Sites in Rat Brain and SH-EP1-hα_7 Cell Membranes by αBgTx. Rat brain (●, 110 µg) or SH-EP1-hα_7 cell membranes (■, 60 µg) were incubated (22°C) with [^{3}H]-MLA (2.5 nM) and various concentrations of unlabelled αBgTx in a total assay volume of 250 µl for 60 min. Non-specific binding was determined in the presence of 10 µM *d*-tubocurarine. Specific binding points were derived by subtracting non-specific binding from total binding with these data representing a typical experiment. Triangles represent non-specific binding levels in the rat brain (▲) and SH-EP1-hα_7 cell membranes (▼).

Figure 3.24

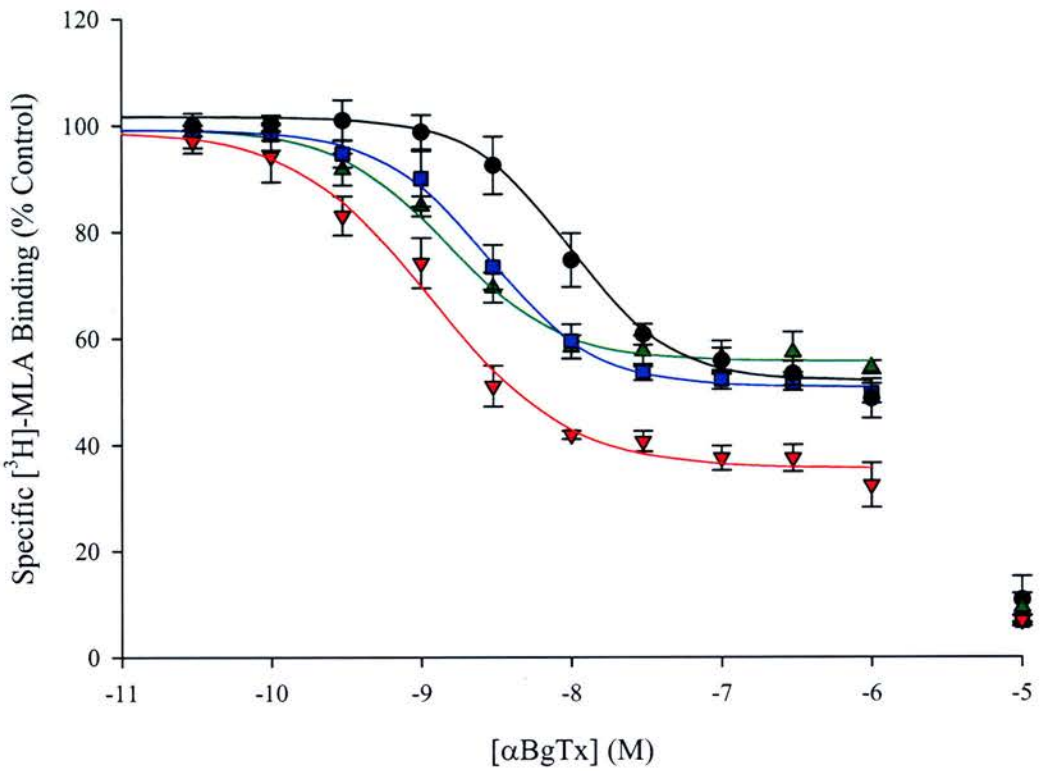

The Effect of Lengthening the Incubation Period on αBgTx Inhibition of [^{3}H]-MLA Binding Sites in SH-EP1-hα$_7$ Cell Membranes. SH-EP1-hα$_7$ cell membranes (60 μg) were incubated with various concentrations of αBgTx for 20 (●), 60 (■), 80 (▲), and 140 (▼) min at 22°C with [^{3}H]-MLA (2.5 nM) in a total assay volume of 250 μl. Non-specific binding was determined in the presence of 10 μM *d*-tubocurarine with these data representing the mean ± S.E.M. of 4 -5 separate experiments.

facilitated a more direct comparison of [^{3}H]-MLA and [^{3}H]-αBgTx binding sites in SH-EP1-hα$_7$ cell membranes, without the inclusion of a large iodine molecule.

3.6.1 Time Course Determination of [^{3}H]-αBungarotoxin Binding in the SH-EP1-hα$_7$ Cell Membrane Preparation

To determine when [^{3}H]-αBungarotoxin ([^{3}H]-αBgTx) binding to the human α$_7$ nAChR attained equilibrium, SH-EP1-hα$_7$ cell membranes were incubated with [^{3}H]-αBgTx (2 nM) and the interaction examined as a function of time (Figure 3.25). Despite incubation (22°C) of [^{3}H]-αBgTx (2 nM) with SH-EP1-hα$_7$ cell membranes for up to 8 h, specific binding failed to reach equilibrium (Figure 3.25).

This is probably the result of αBgTx being an irreversible antagonist (Alkondon & Albuquerque, 1991). To ensure consistency and sufficient specific binding, an incubation period of 6 h was used in all subsequent studies. At this time point, specific binding of [^{3}H]-αBgTx to SH-EP1-hα$_7$ cell membranes was approximately 65% of total binding (Figure 3.25).

3.6.2 Concentration Dependence of [^{3}H]-αBgTx Binding in the SH-EP1-hα$_7$ Cell Membrane Preparation

After a 6 h incubation period, specific [^{3}H]-αBgTx binding in SH-EP1-hα$_7$ membranes accounted for 64.3 ± 1.9 % of total binding sites at a free radiolabel concentration close to the K_D (2.5 – 4 nM), with non-specific binding accounting for 35.7 ± 1.9 % (Figure 3.26A).

To determine K_D (apparent) and B_{max} values for [^{3}H]-αBgTx binding in SH-EP1-hα$_7$ cell membranes, hot saturation experiments were performed using increasing concentrations of radioligand. A representative [^{3}H]-αBgTx saturation curve for SH-EP1-hα$_7$ membrane preparations is shown in Figure 3.26B. These studies demonstrated [^{3}H]-αBgTx binding was saturable and consistent with a single high affinity binding site in SH-EP1-hα$_7$ cell membranes (n_H = 1.14 ± 0.11, n = 4). The apparent affinity of [^{3}H]-αBgTx in SH-EP1-hα$_7$ cell membranes was equal to 2.66 ± 0.73 nM (n = 4; Figure 3.26, Table 3.10). Saturable binding allowed measurement of the density of α$_7$ nAChRs in this membrane preparation giving a B_{max} equal to 2.40 ± 0.70 pmol/mg protein; n = 4; Table 3.10). The density of α$_7$ nAChR binding sites determined using [^{3}H]-αBgTx is approximately 35 % of

Table 3.9 **Effect of Incubation Period on the Affinity of αBgTx for [^{3}H]-MLA Binding Sites in Rat Brain and SH-EP1-hα$_7$ Cell Membranes**

	Rat Brain (αBgTx)		SH-EP1-hα$_7$ Cells (αBgTx)		SH-EP1-hα$_7$ Cells (MLA)	
Time (min)	**K_i (nM)**	**n_H**	**K_i (nM)**	**n_H**	**K_i (nM)**	**n_H**
20	4.32 ± 0.52 (3)	1.32 ± 0.04	8.3 ± 2.5 (5)	1.25 ± 0.02	7.0 ± 0.41 (3)	1.16 ± 0.03
80	0.45 ± 0.02 (3)	1.25 ± 0.07	2.35 ± 0.55 (5)	1.29 ± 0.09	6.7 ± 0.86 (3)	1.21 ± 0.05
140	0.27 ± 0.01 (3)	1.22 ± 0.06	1.28 ± 0.25 (5)	1.20 ± 0.14	7.2 ± 1.35 (3)	1.30 ± 0.05
60	1.40 ± 0.40 (8)	1.29 ± 0.05	2.48 ± 0.54 (3)	1.29 ± 0.07	5.14 ± 0.7 (10)	1.13 ± 0.05

Affinity (apparent K_i) and Hill slopes (n_H) for αBgTx and MLA inhibition of [^{3}H]-MLA binding sites in rat brain and SH-EP1-hα$_7$ cell membranes determined using the [^{3}H]-MLA binding assay as described in the methods. Values are expressed as mean ± S.E.M with sample numbers (n = 3 – 8) given in brackets. Extending the incubation up to 140 min did not result in an increase in the level of inhibition of [^{3}H]-MLA binding sites by αBgTx in rat brain or SH-EP1-hα$_7$ cell membranes.

Figure 3.25

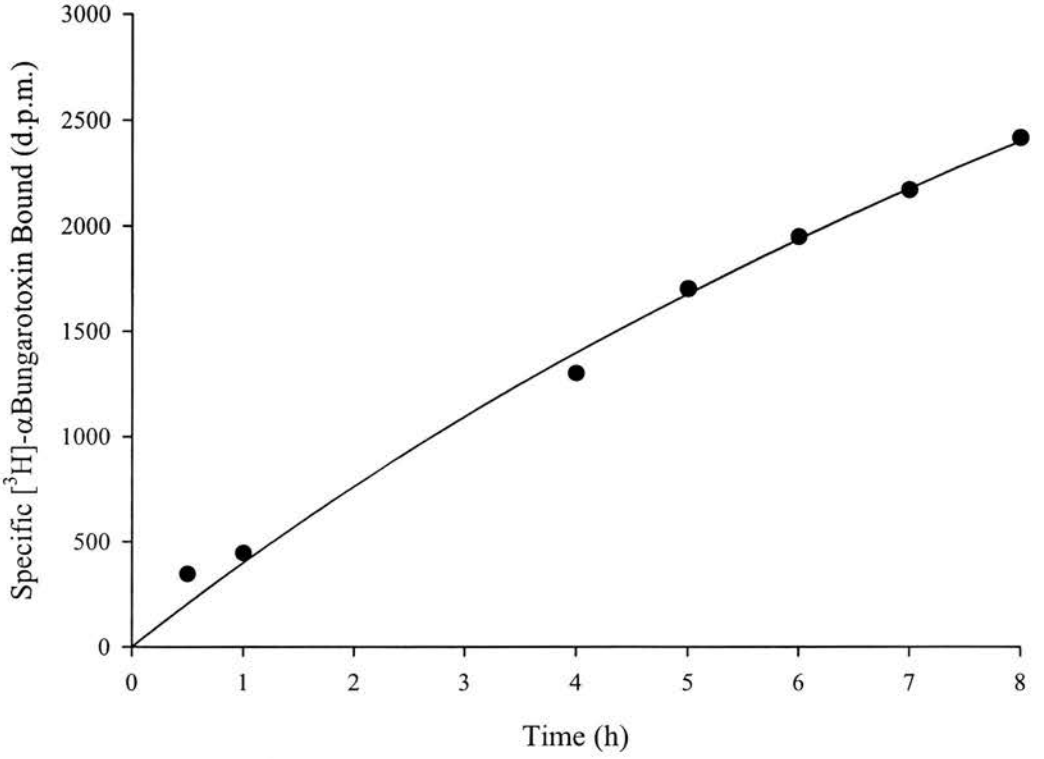

Time Course of Specific [^{3}H]-αBgTx Binding in SH-EP1-hα$_7$ Cell Membranes. SH-EP1-hα$_7$ cell membranes (60 µg) were incubated (22°C) with [^{3}H]-αBgTx (2 nM) in a total assay volume of 250 µl for up to 8 h. Each total binding was tested in duplicate with its non-specific counterpart (defined by 10 µM (-)nicotine) tested in singulate. Specific binding points were derived by subtracting non-specific binding from total binding with these data representing a typical experiment.

Figure 3.26

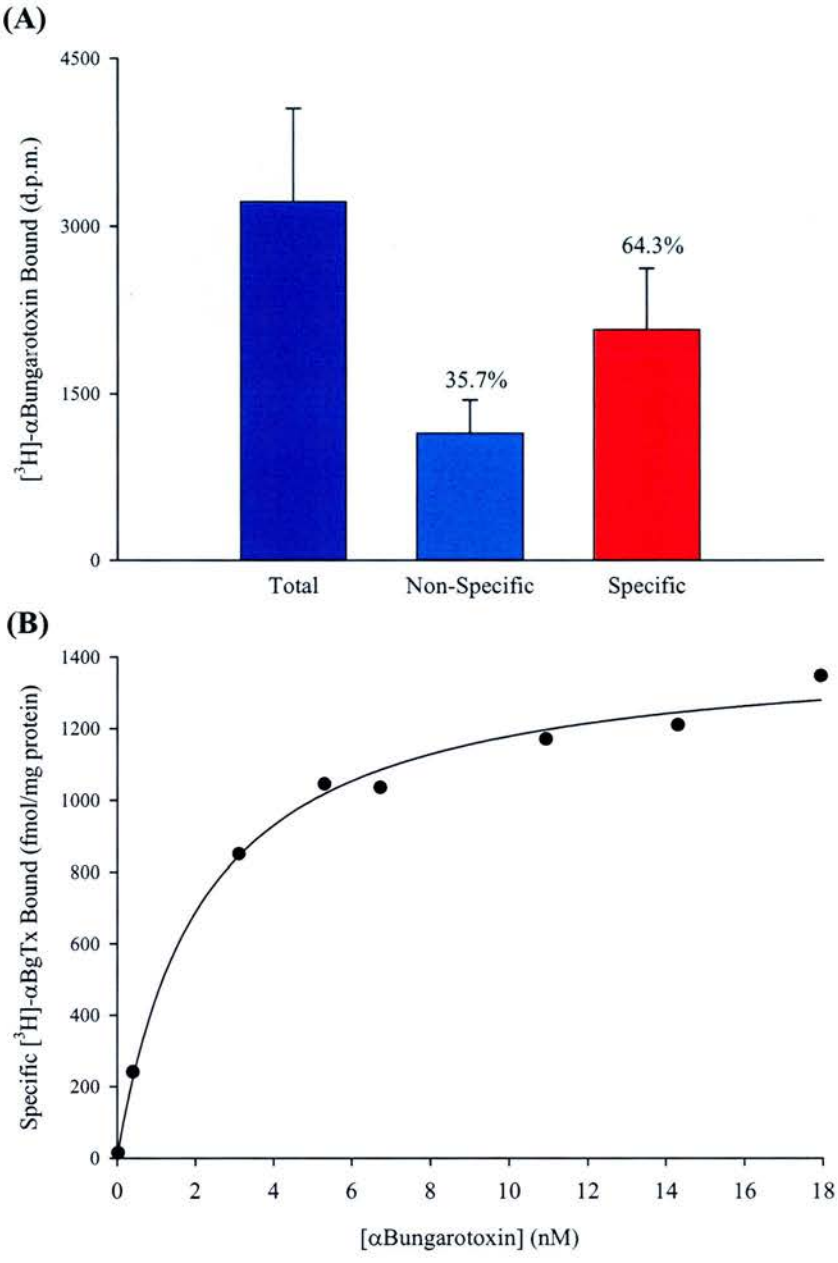

Concentration Dependence of [^{3}H]-αBgTx Binding in SH-EP1-hα$_7$ Cell Membrane Preparations. (A) Proportions of [^{3}H]-αBungarotoxin Binding. (B) Hot Saturation Analysis of [^{3}H]-αBgTx Binding. Membranes (60 µg) were incubated with 2 nM [^{3}H]-αBgTx in a total assay volume of 250 µl for 6 h at 25°C. Non-specific binding was determined in the presence of 10 µM (-)Nicotine. These data represent (A) an average of 4 separate hot saturation experiments or (B) a typical hot saturation experiment.

Table 3.10 Comparison of K_D and B_{max} Generated Using [^{3}H]-αBgTx and [^{3}H]-MLA in SH-EP1-hα$_7$ Cell Membranes

Radiolabel	K_D (nM)	*n*	n_H	B_{max} (pmol/mg protein)
αBgTx	2.66 ± 0.73	4	1.14 ± 0.11	2.40 ± 0.70*
MLA	5.10 ± 0.95	5	1.17 ± 0.05	7.08 ± 0.70*

Apparent affinity (K_D), Hill slope (n_H), and receptor density (B_{max}) values were determined in the [^{3}H]-αBgTx binding assay as described in the methods. Corresponding values for [^{3}H]-MLA are taken from Section 3.5. Values are expressed as mean ± S.E.M., (n = 4-5) with statistical analyses (one-way ANOVA with Bonferroni post-hoc testing) where $p < 0.05$ was used to indicate a significant difference. (*) A significant difference in receptor density was determined.

that determined using [^{3}H]-MLA (B_{max} = 7.08 ± 0.70 pmol/mg protein; n = 5; Section 3.5.2; Table 3.10). This is consistent with the earlier finding showing αBgTx can only inhibit 40 % of [^{3}H]-MLA binding in SH-EP1-hα$_7$ cells (Figure 3.23 & 3.24)

In all subsequent [^{3}H]-αBgTx binding studies (2 nM) were performed at 22°C for 6 h with a limited range of compounds to examine whether this had any effect of human α$_7$ nAChR pharmacology.

3.6.3 Inhibition of [^{3}H]-αBgTx Binding Sites by Cholinergic Ligands in SH-EP1-hα$_7$ Cell Membranes

To characterise [^{3}H]-αBgTx binding sites in SH-EP1-hα$_7$ cell membranes, the ability of the agonists (-)nicotine and cytisine and the antagonists αBgTx and MLA to inhibit [^{3}H]-αBgTx binding in SH-EP1-hα$_7$ cell membranes was examined. (-)Nicotine and cytisine both inhibited [^{3}H]-αBgTx binding in SH-EP1-hα$_7$ cell membranes in a concentration-dependent manner (Figure 3.27A) giving a K_i value for (-)nicotine of 63.6 ± 14.5 nM (n = 3) and a K_i value of 905 ± 115 nM (n = 3) for cytisine. These values are consistent with the K_i values determined using [^{3}H]-MLA as the radioligand (Figure 3.26A, Table 3.11). The Hill coeffients (n_H) for the two agonists were slightly less than unity at 0.82 ± 0.09 (n = 3) for (-)nicotine and 0.70 ± 0.10 (n = 3) for cytisine, again consistent with the Hillslopes observed for all the agonists in the [^{3}H]-MLA binding assay (Table 3.6, pg 91).

Although only partial inhibition of [^{3}H]-MLA binding was achieved by αBgTx (Figure 3.23 & 3.24), both αBgTx and MLA inhibited [^{3}H]-αBgTx binding to SH-EP1-hα$_7$ cell membranes to the same extent in a concentration-dependent manner (Figure 3.27B). There was no change in the affinity of αBgTx or MLA for [^{3}H]-αBgTx when compared to [^{3}H]-MLA binding sites in SH-EP1-hα$_7$ cell membranes (Table 3.11). Hill coefficients for the antagonists in the [^{3}H]-MLA and [^{3}H]-αBgTx binding studies using SH-EP1-hα$_7$ cell membranes were slightly higher than unity (Table 3.11).

Figure 3.27

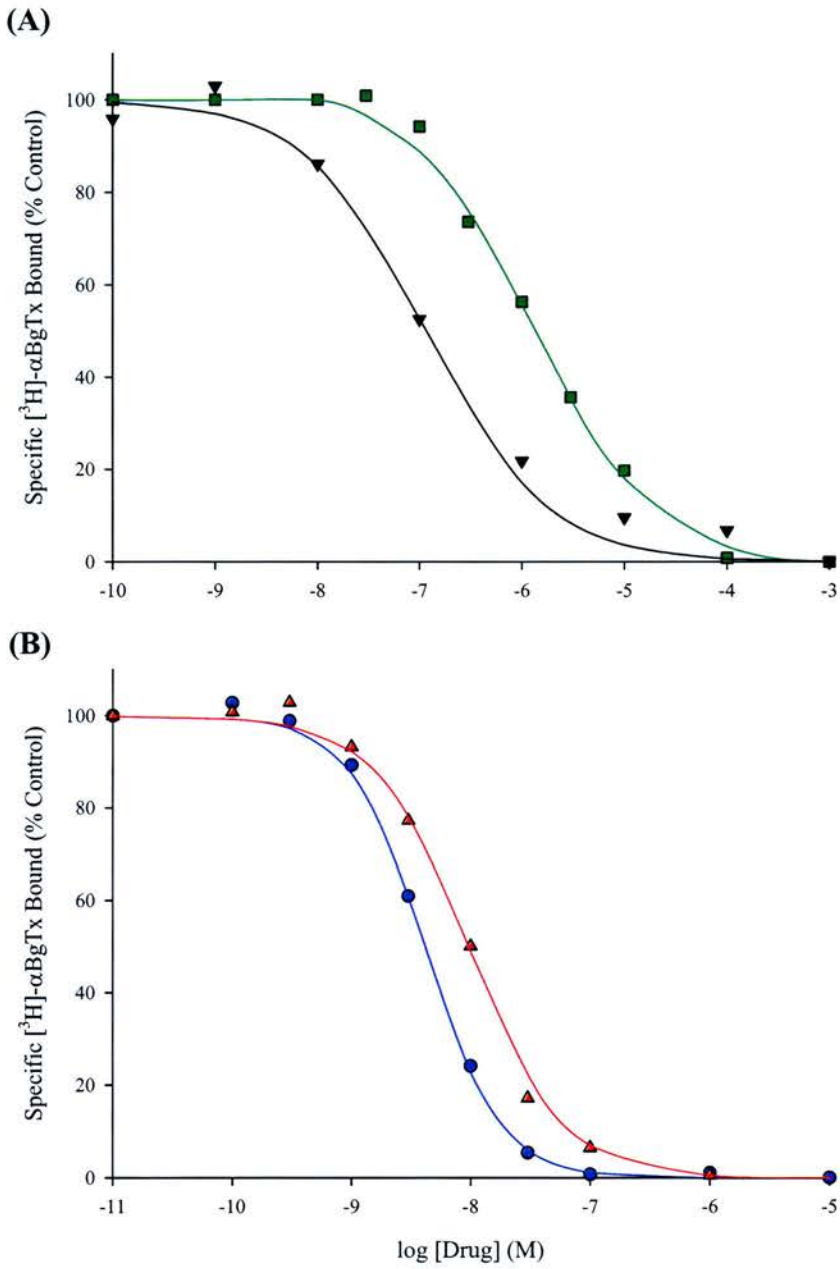

Inhibition of [^{3}H]-αBgTx Binding by Cholinergic Ligands in SH-EP1-hα$_7$ Cell Membranes. SH-EP-hα$_7$ cell membranes (60 µg) were incubated with [^{3}H]-αBgTx (2 nM) and (A) agonists cytisine (■) and (-)nicotine (▼) or (B) antagonists methyllycaconitine (●) and αBungarotoxin (▲) in a total assay volume of 250 µl for 6 h at 25°C. Non-specific binding was determined in the presence of 10 µM (-)nicotine with these data representing a typical experiment.

Table 3.11: Comparison of Agonist and Antagonist Affinity at [^{3}H]-αBgTx and [^{3}H]-MLA Binding Sites in SH-EP1-hα$_7$ Cell Membranes

	[^{3}H]-αBgTx			[^{3}H]-MLA		
Inhibitor	**K_D/K_i (nM)**	**n_H**	***n***	**K_D/K_i (nM)**	**n_H**	***n***
Agonists						
(-)Nicotine	63.6 ± 14.5	0.82 ± 0.09	3	311 ± 74	0.85 ± 0.06	6
Cytisine	905 ± 115	0.70 ± 0.10	3	537 ± 60	0.78 ± 0.04	4
Antagonists						
αBgTx	1.82	1.42	2	2.09 ± 1.09	1.22 ± 0.22	4
MLA	7.37 ± 1.89	1.12 ± 0.09	5	3.68 ± 0.61	1.31 ± 0.15	5

Affinity (K_i) and Hill slopes (n_H) were determined in the [^{3}H]-αBgTx and [^{3}H]-MLA binding assays as described in the methods. Membranes (60 µg) were incubated (22°C) with [^{3}H]-αBgTx (2 nM) in a total assay volume of 250 µl for 6 h. Non-specific binding was determined in the presence of 10 µM (-)nicotine. These data represent an average of 2-6 individual inhibition experiments. No statistical difference in αBgTx and MLA affinity (K_i) was observed between K_i values determined in the two assays. However, significant differences in agonist affinity were observed for [^{3}H]-αBgTx and [^{3}H]-MLA binding sites in SH-EP1-hα$_7$ cell membranes.

3.7 Pharmacological Characterisation of $\alpha_4\beta_2$ and α_7 nAChR Binding Sites in Mouse Brain Membranes Using [^{3}H]-Cytisine and [^{3}H]-MLA

A number of transgenic mouse models are now available to study the effect of knocking in, or out, nAChRs *in vivo* (Orr-Urtreger *et al.*, 1997; Xu *et al.*, 1999a,b; Bansal *et al.*, 2000; Ross *et al.*, 2000; Broide *et al.*, 2001; Champtiaux *et al.*, 2002; Gil *et al.*, 2002; Wang *et al.*, 2002; Whiteaker *et al.*, 2002; Cui *et al.*, 2003; Lester *et al.*, 2003; Orb *et al.*, 2004; Sales *et al.*, 2004). Indeed, as discussed extensively in the introduction, nicotine and nAChRs are thought to play a key role in regulating attention and memory with pivotal roles in AD (e.g. Bednar *et al.*, 2002; O'Neill *et al.*, 2002; Yu *et al.*, 2005) and schizophrenia (e.g. Guan *et al.*, 1999; De Luca *et al.*, 2004; Deutsch *et al.*, 2005). In parallel to my *in vitro* characterisation of nAChRs and their interaction with $A\beta_{1-42}$, our group has also examined the role of these receptors (in particular the α_7 nAChR) *in vivo*, using a range of behaviour models.

The 5-choice serial reaction time task (5-CSRTT) is used to assess sustained attention in rodents and is analogous to the Connors continuous performance test used in humans (Stolerman *et al.*, 2000). Using this task, our group showed for the first time in mice, that nicotine could enhance sustained attention, and moreoever, that when the α_7 nAChR was knocked-out these mice exhibited a deficit in this task (Young *et al.*, 2004). This initial observation has now been extended with a second 5-CSRTT study comparing wildtype, α_7-nAChR heterozygote, and α_7-nAChR knockout mice. Importantly, there is a graduated decrease in the ability of the mice, with the α_7- nAChR heterozygous mice exhibiting reduced attention compared to their wildtype littermates and knockout mice showing a significantly more pronounced deficit in sustained attention. These new observations have been submitted to Psychopharmacology and the manuscript is under review. As transgenic manipulations may produce compensatory changes in nAChR density or changes in receptor pharmacology, in parallel, I examined the nAChR pharmacology of these mice to strengthen the above findings, and as a result I am a co-author on both manuscripts.

The α_7 nAChR-transgenic mice used in these studies were purchased from Jackson Laboratories (B6.12957 – Chrna7^{tm1bay}; Jackson Laboratories, Bar Harbour, U.S.A.) and backcrossed onto a C57B16/J background 11 times to produce litters of wildtype, heterozygous, and knockout mice. Before assessing $\alpha_4\beta_2$ and α_7 nAChR pharmacology and receptor number in the α_7-transgenic mice and due to the limited characterisation (when compared to [^{3}H]-cytisine) of [^{3}H]-MLA binding sites in mouse (Whiteaker *et al.*, 1999),

[^{3}H]-MLA binding sites were initially characterised in brain membranes from non-littermate C57B16/J wildtype mice.

3.7.1.1 Time Course Determination of [^{3}H]-MLA Binding in a Mouse Brain Membrane Preparation

To determine when [^{3}H]-MLA binding to the mouse α_7 nAChR attained equilibrium, the radioligand was incubated with membranes prepared from C57B16/J mice and specific binding measured as a function of time (Figure 3.28). At 25°C [^{3}H]-MLA binding (2 nM) attained equilibrium at 15 min and held constant for at least 2 h, consistent with observations in rat brain and SH-EP1-hα_7 cell membranes (Figure 3.28).

As a consequence, all subsequent [^{3}H]-MLA hot saturation and inhibition studies using mouse brain membranes were terminated by vacuum filtration after a 60 min incubation period at 25°C; for direct comparison with rat and SH-EP-hα_7 studies.

3.7.1.2 Pharmacological Analysis of [^{3}H]-MLA Binding in Mouse Brain Membrane Preparations

Specific [^{3}H]-MLA binding in mouse brain membranes accounted for 49.8 ± 4.6 % of total binding sites at a free radiolabel concentration close to the expected K_D (~1.5 nM; Figure 3.29A).

To determine K_D and B_{max} values for [^{3}H]-MLA binding sites in mouse brain membranes, cold saturation experiments were performed using 2.5 nM [^{3}H]-MLA and increasing concentrations of unlabelled MLA. The affinity of [^{3}H]-MLA (K_D/K_i) was equal to 1.34 ± 0.26 nM (n = 5) in mouse brain membranes with a receptor density (B_{max}) of 0.016 ± 0.003 pmol/mg protein (n = 5), consistent with previously published studies in mouse brain membranes using [^{3}H]-MLA or [^{125}I]-αBgTx (Figure 3.29B; Marks & Collins, 1982; Whiteaker *et al.*, 1999). This receptor and K_D density is also similar to binding variables determined using rat brain membranes in Section 3.5.2 (pg 105). These studies showed [^{3}H]-MLA binding was consistent with a single high affinity binding site in mouse brain membranes with a Hillslope of 0.87 ± 0.04 (n = 5).

3.7.1.3 Inhibition of [^{3}H]-MLA Binding Sites by Cholinergic Ligands in a Mouse Brain Membranes

Three nAChR agonists and two antagonists, all of which were used in earlier studies, were examined for their ability to inhibit [^{3}H]-MLA (2.5 nM) binding in mouse

Figure 3.28

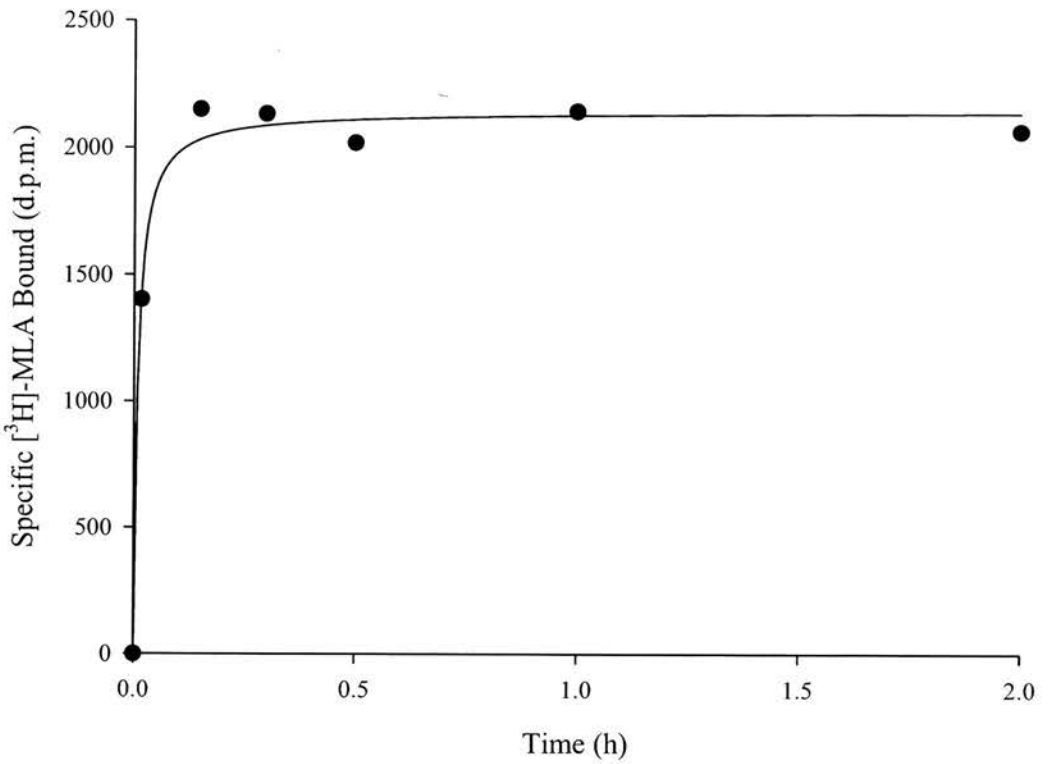

Time Course of Specific [^{3}H]-MLA binding in Mouse Brain Membranes. Membranes (850 μg) were incubated (22°C) with [^{3}H]-MLA (2.5 nM) in a total assay volume of 250 μl for up to 2 h. Total binding was tested in duplicate with its non-specific counterpart (defined by 10 μM *d*-tubocurarine) tested in singulate. Specific binding points were derived by subtracting non-specific binding from total binding with these data representing a typical experiment.

Figure 3.29

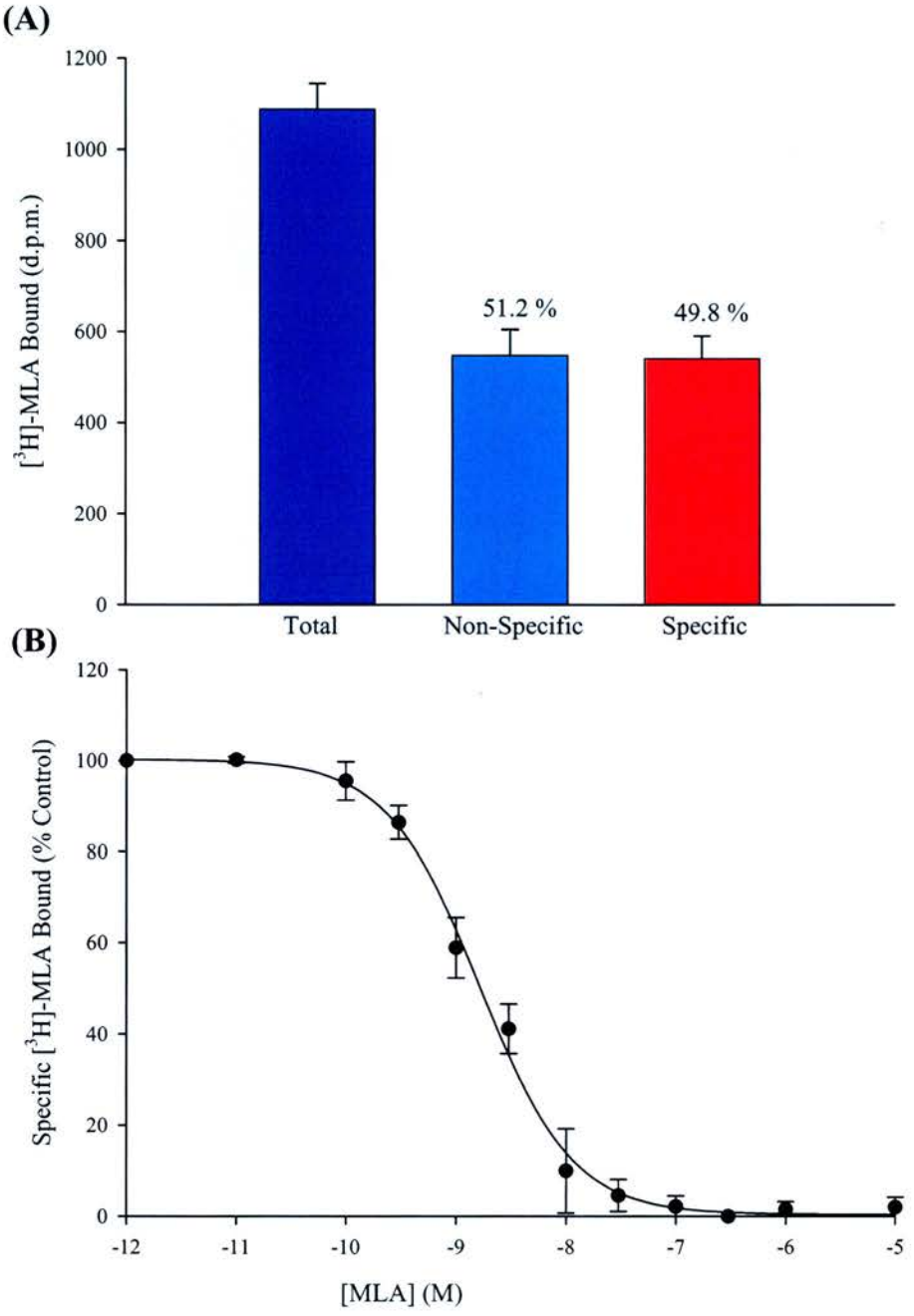

Pharmacological Characterisation of [^{3}H]-MLA Binding Sites in Mouse Brain. (A) Proportions of specific and non-specific [^{3}H]-MLA binding and (B) inhibition of [^{3}H]-MLA binding by unlabelled MLA. Membranes (850 µg) were incubated (22°C) with [^{3}H]-MLA (2.5 nM) in a total assay volume of 250 µl for 60 min. Non-specific binding was determined in the presence of 10 µM *d*-tubocurarine with these data representing an average of 5 individual inhibition experiments.

brain membranes. All five compounds produced a concentration-dependent inhibition of [^{3}H]-MLA binding in mouse brain membranes (Figure 3.30). The rank order of potency for the ligands studied was; MLA > (-)AR-R17779 > *d*-tubocurarine > (-)nicotine > (+)AR-R17779 with data from a typical experiment shown in Figure 3.30 and with mean K_i values presented in Table 3.12. As discussed above, unlabelled MLA inhibited [^{3}H]-MLA binding in mouse brain membranes with a K_D/K_i value equal to 1.34 ± 0.26 nM (n = 5). The affinity (K_i) of the other compounds tested ranged from nanomolar for (-)AR-R17779 (247 ± 23 nM, n = 5) to the high micromolar range for its less active enantiomer (+)AR-R17779 (136 ± 19 μM; n = 6). In general the Hill coefficients for the nicotinic ligands were close to unity although there was a degree of variability. This may be a consequence of the large amount of tissue required due to the low receptor density affecting filtration. Importantly, the affinity of the compounds for mouse [^{3}H]-MLA binding sites was similar to that observed for rat brain membranes (Tables 3.4 & 3.5 in Section 3.5.3, pgs 83 & 87; Table 3.12). Therefore, it would appear that mouse and rat [^{3}H]-MLA binding sites are different from human α_7 nAChR pharmacology, and although antagonist potencies are similar, agonists are clearly more potent (~100-fold) at the human α_7 nAChR.

Having characterised [^{3}H]-MLA binding in wildtype mouse membranes, this and the [^{3}H]-cytisine binding assays were used to characterise $\alpha_4\beta_2$ and α_7 nAChR pharmacology in α_7 nAChR wildtype, heterozygous, and knockout mice. With male mice limited as they were used in behavioural studies, and with female mice used in a previous behavioural study (Paylor *et al.*, 1998), tissue from both sexes of mice were used to see if any pharmacological differences were observed in the radioligand binding assays.

3.7.2 Concentration Dependence of [^{3}H]-MLA Binding in α_7 nAChR-Transgenic Mouse Brain Membrane Preparation

To assess the affinity (K_D) and receptor density (B_{max}) of [^{3}H]-MLA and [^{3}H]-cytisine binding at α_7 and $\alpha_4\beta_2$ nAChRs, respectively, membranes were prepared from littermate male and female α_7-WT, α_7-HT, and α_7-KO mice. Initially, [^{3}H]-MLA binding was assessed in transgenic mouse brain membranes by treating each brain individually. As Figure 3.31 clearly shows, at a radiolabel concentration of 3 nM, specific [^{3}H]-MLA binding accounted for 74.4 ± 2.2 % of total binding sites in male α_7-WT mouse brain membranes (panel A) and 62.9 ± 5.9 % in male α_7-HT membranes (panel B). The amount of specific [^{3}H]-MLA binding in male α_7-WT brain membranes is consistent with that observed in standard C57B16/J mouse brain membranes in the earlier section (Section 3.7.1.2). In

Figure 3.30

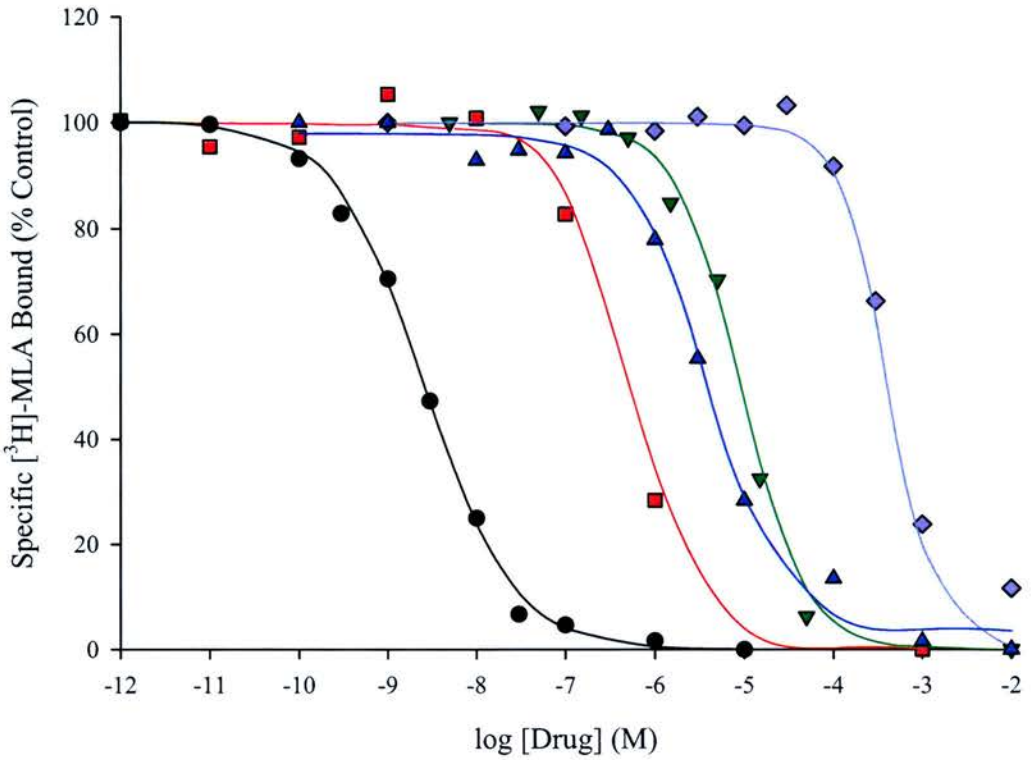

Inhibition of [^{3}H]-MLA Binding by Cholinergic Ligands in Mouse Brain Membranes. Mouse brain membranes (850 µg) were incubated (22°C) with [^{3}H]-MLA (2.5 nM) and the antagonists antagonists methyllycaconitine (●) or *d*-tubocurarine (▲) or with the agonists (-)nicotine (▼), (-)AR-R17779 (■), or (+)AR-R17779 (◆) in a total assay volume of 250 µl for 60 min. Non-specific binding was determined in the presence of 10 µM *d*-tubocurarine with these curves representing a typical experiment.

Table 3.12: The Affinity of Cholinergic Ligands for [^{3}H]-MLA Binding Sites in Mouse Brain Membranes

Compound	K_i (nM)	n_H	*n*
Antagonists			
MLA	1.34 ± 0.26	0.87 ± 0.04	5
***d*-Tubocurarine**	1,811 ± 74	1.48 ± 0.44	3
Agonists			
(-)AR-R17779	247 ± 23	1.41 ± 0.19	5
(-)Nicotine	5,262 ± 829	1.06 ± 0.09	3
(+)AR-R17779	135,504 ± 19,118	1.37 ± 0.12	6

Affinity (K_i) and Hillslopes (n_H) were determined in the [^{3}H]-MLA binding assay as described in the methods. Values are expressed as mean ± S.E.M. of 3-6 individual experiments.

Figure 3.31

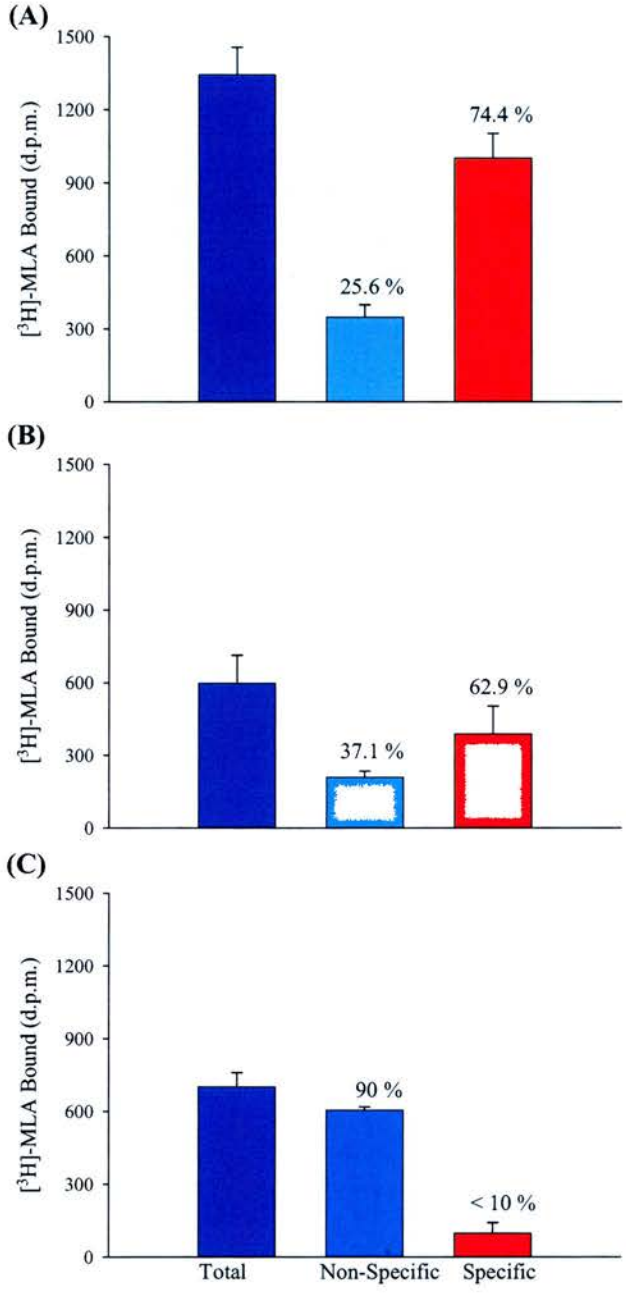

Proportions of [^{3}H]-MLA Binding Sites in Male α_7 nAChR Transgenic Mouse Brain Preparations. Membranes (~850 µg) from individual male (A) α_7-WT (B) α_7-HT or (C) α_7-KO mouse brains were incubated (22°C) with [^{3}H]-MLA (2.5 nM) in a total assay volume of 250 µl for 60 min. Non-specific binding was determined in the presence of 10 µM *d*-tubocurarine and these data represent an average of 4-7 male mouse brains each examined individually.

Figure 3.32

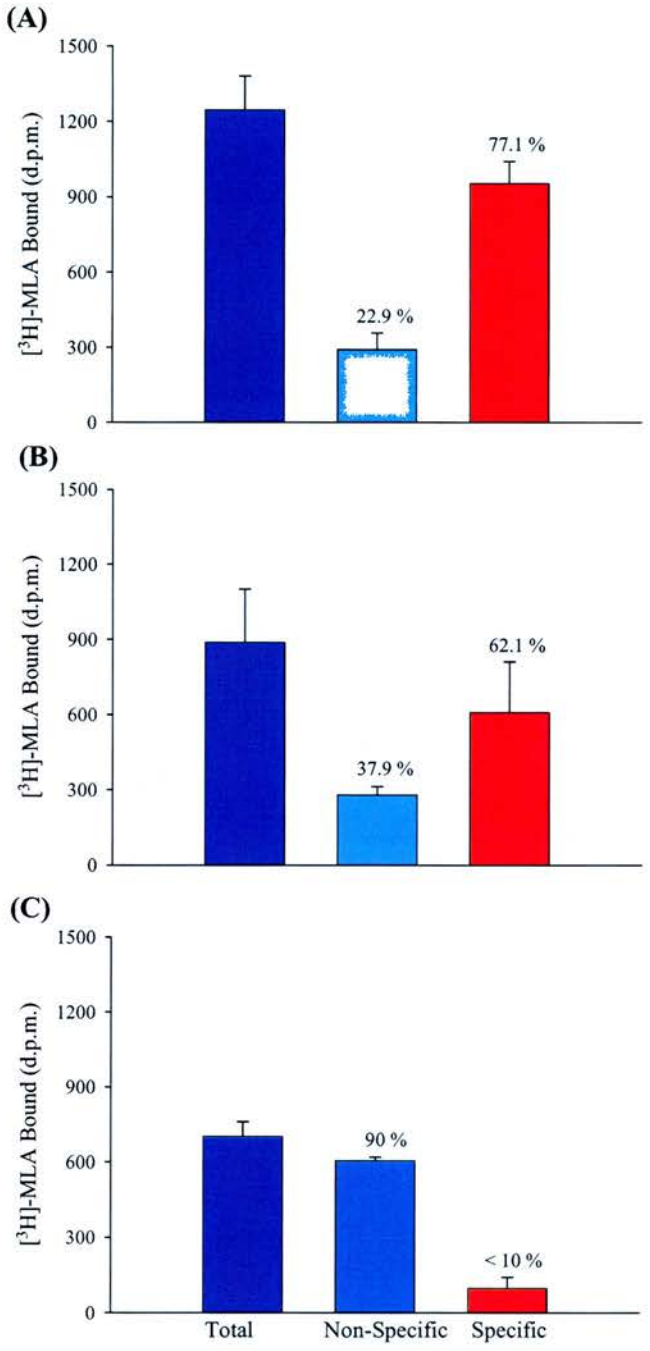

Proportions of [^{3}H]-MLA Binding Sites in Female α_7 nAChR Transgenic Mouse Brain Preparations. Membranes (~850 μg) from individual female (A) α_7-WT (B) α_7-HT or (C) α_7-KO mouse brains were incubated (22°C) with [^{3}H]-MLA (2.5 nM) in a total assay volume of 250 μl for 60 min. Non-specific binding was determined in the presence of 10 μM *d*-tubocurarine and these data represent an average of 4-7 female mice brains, each examined individually.

addition and in excellent agreement with [^{3}H]-MLA binding in male mouse brain membranes, specific binding accounted for 77.1 ± 3.4 % of total binding sites in female α_7-WT mouse brain membranes (Figure 3.32A) and 62.1 ± 9.4 % in female α_7-HT brain membranes (Figure 3.32B). Moreover, and most importantly, male and female α_7-KO mice exhibited no appreciable specific [^{3}H]-MLA binding, consistent with deletion of the α_7 nAChR gene (Figure 3.31C & 3.32C). To confirm these binding data showing loss of α_7 nAChRs, genotyping was also performed in parallel to the binding studies. Wildtype α_7 nAChR mice produced a single 440 b.p. band on the PCR gel (Figure 3.33). In contrast, α_7-HT mice produced two bands (440 b.p. and 750 b.p.) while α_7-KO mice produced a single 750 b.p. band (Figure 3.33), indicating the absence of the α_7 nAChR gene. Because brain tissue from α_7-KO mice exhibited no specific binding and because of the low receptor density, all subsequent experiments comparing α_7-nAChR pharmacology were conducted using male and female α_7-WT and α_7-HT mice using pooled brain membranes.

To determine K_D and B_{max} values for [^{3}H]-MLA binding sites in α_7-WT and α_7-HT mouse brain membranes, hot saturation experiments were performed using increasing concentrations of [^{3}H]-MLA. Representative saturation curves for [^{3}H]-MLA binding in α_7-WT and α_7-HT transgenic mouse brain membranes are presented in Figure 3.34. These studies showed that [^{3}H]-MLA binding was saturable in both membrane preparations. The density of α_7 nAChRs (B_{max}) in male wildtype littermate mouse brain membranes was 66.6 ± 8.0 fmol/mg protein (n = 5). Importantly, this receptor density was reduced by almost exactly 50% in male α_7-HT brain tissue with a B_{max} = 34.2 ± 2.3 (n = 3, p = 0.006). Although there was a significant reduction in receptor density between the preparations, the K_D of [^{3}H]-MLA was not significantly different between wildtype (K_D = 7.41 ± 0.75, n = 5) and α_7-HT mice (K_D = 10.7 ± 2.2, n = 3; Figure 3.34A, Table 3.13).

A similar observation was made when K_D and B_{max} values were measured using female α_7-nAChR transgenic mouse brain membranes. The density of receptors in female wildtype mouse brain membranes was 73.1 ± 3.6 fmol/mg protein (n = 5), consistent with their male counterparts. Again this number was also significantly reduced by just over half in female α_7-HT brains with a B_{max} = 27.0 ± 4.0 (n = 5; $p < 0.001$). Likewise, although there was a significant reduction in receptor density between the female α_7-WT and α_7-HT membrane preparations, the ligand affinity was not significantly different with a K_D value of 7.32 ± 0.58 (n = 5) and 10.5 ± 2.6 (n = 5) in wildtype and heterozygous preparations,

Figure 3.33

α_7 nAChR Trangenic Mouse Genotyping. Confirmation of the genotypes of α_7 nAChR wildtype (WT), heterozygous (HT), and knockout (KO) mice. Wildtype mice exhibit only one allele (at 440 b.p.), knockout mice exhibit a single allele at 750 b.p., whilst heterozygous mice exhibit both alleles.

respectively (Figure 3.34B, Table 3.13). These values were almost identical to the K_D values obtained for male mouse brain membranes. In general, the Hill coefficients (n_H) were close to unity in both male and female α_7-WT and α_7-HT mouse brain membrane preparations (Table 3.13).

3.7.3 Concentration Dependence of [^{3}H]-Cytisine Binding in α_7 nAChR-Transgenic Mouse Brain Membrane Preparation

Although there was no change in the affinity of [^{3}H]-MLA for α_7 nAChRs despite a reduction in receptor density, a genetic alteration in α_7-nAChR gene expression might result in a compensatory change in the density of other cholinergic receptors. If such a change occurred, this could have made interpretation of our behavioural data more problematic (Young *et al.,* 2004; Young *et al.*, 2006, *in press*). Therefore, it was necessary to determine the density and pharmacology of the $\alpha_4\beta_2$ nAChR, the other major nicotinic receptor in rodent brain (Paterson & Nordberg, 2000). To characterise the $\alpha_4\beta_2$ nAChR pharmacology a [^{3}H]-cytisine binding was established and K_D and B_{max} values were determined using pooled membranes prepared from male and female α_7-WT littermates, α_7-HT, and α_7-KO mouse brains. As Figure 3.35 clearly shows, at a radiolabel concentration of 3 nM, specific binding accounted for 89.8 ± 3.9 % (n = 4) of total binding sites in male α_7-WT littermate mouse brain membranes (Figure 3.35A) and 67.6 ± 7.8 % (n = 4) in male α_7-HT mouse brain membranes (Figure 3.35B). Consistent with [^{3}H]-cytisine binding in male mouse brain membranes, specific binding accounted for 79.1 ± 3.1 % (n = 4) of total binding sites in female α_7-WT mouse brain membranes (Figure 3.36A) and 80.9 ± 3.7 % (n = 3) in female α_7-HT mouse brain membranes (Figure 3.36B). The level of specific [^{3}H]-cytisine binding was not significantly reduced in either male (70.6 ± 6.8 %; n = 4) or female (67 %, n = 2) α_7-KO mouse brain membranes when compared to the level of specific binding in their respective WT and HT littermate mouse brain membranes (Figure 3.35C & 3.36C).

To determine K_D and B_{max} values for [^{3}H]-cytisine binding in α_7-WT, α_7-HT, and α_7-KO mouse brain membranes, hot saturation experiments were performed using increasing concentrations of [^{3}H]-cytisine. Representative saturation curves for [^{3}H]- cytisine binding in α_7-WT, α_7-HT and α_7-KO male transgenic mouse brain membranes are shown in Figure 3.37. These studies showed that [^{3}H]-cytisine binding was saturable in all three male mouse membrane preparations, with comparable K_D for [^{3}H]-cytisine binding; K_D = 2.75 ± 0.31 nM (α_7-WT, n = 4), 7.39 ± 1.10 (α_7-HT, n = 4) and 7.45 ± 1.64 (α_7-KO, n = 4) (Figure

Figure 3.34

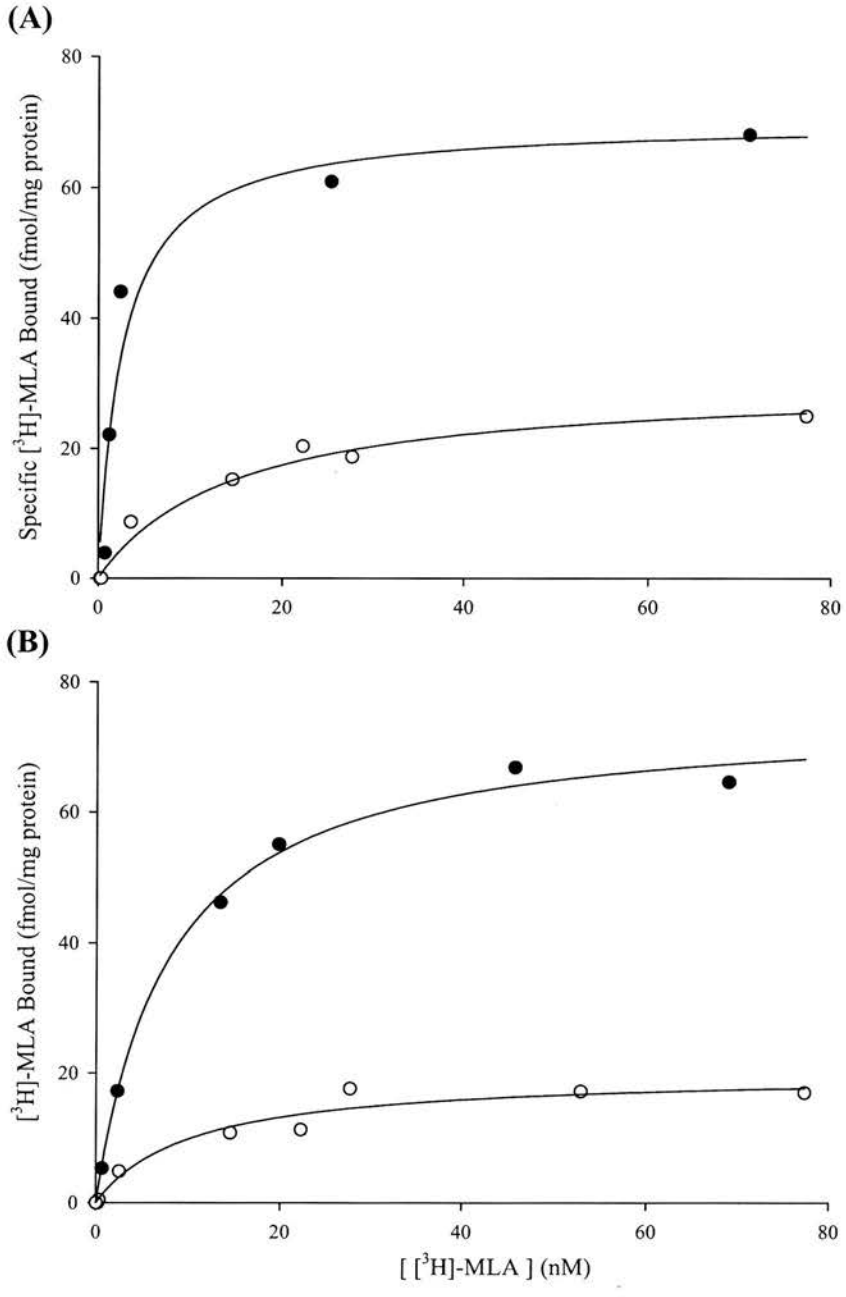

Concentration Dependence of [^{3}H]-MLA Binding in α_7-nAChR Transgenic Mice. Membranes (850 µg) from littermate (A) male WT (•) or HT (○) (B) female WT (•) or HT (○) mice were incubated (22°C) with increasing concentrations of [^{3}H]-MLA in a total assay volume of 250 µl for 60 min. Non-specific binding was determined in the presence of 10 µM *d*-tubocurarine with these data representing an average hot saturation study.

Table 3.13: K_D and B_{max} Values for [^{3}H]-MLA Binding Sites in α_7-Wildtype Littermate and α_7-Heterozygous Mouse Brain Membranes

Transgenic	K_D (nM)	n_H	*n*	B_{max} (fmol/mg protein)
Male				
α7-Wildtype	7.41 ± 0.75	1.00 ± 0.13	5	66.6 ± 8.0*
α7-Heterozygous	10.7 ± 2.2	1.17 ± 0.07	3	34.2 ± 2.3*
Female				
α7-Wildtype	7.32 ± 0.58	1.12 ± 0.09	5	73.1 ± 3.6**
α7 Heterozygous	10.5 ± 2.6	1.19 ± 0.14	5	27.0 ± 4.0**

Affinity (K_D), Hillslopes (n_H), and receptor density (B_{max}) were determined in the [^{3}H]-MLA binding assays as described in the methods. Values are expressed as mean ± S.E.M. (n = 3 - 5) with statistical analyses performed using one-way ANOVA with Bonferroni post-hoc testing. No significant difference in ligand affinity for [^{3}H]-MLA binding sites in α_7-WT and α_7-HT mouse brain membranes was observed, although there was a difference in receptor density with asterisks (*) indicating $p < 0.05$.

Figure 3.35

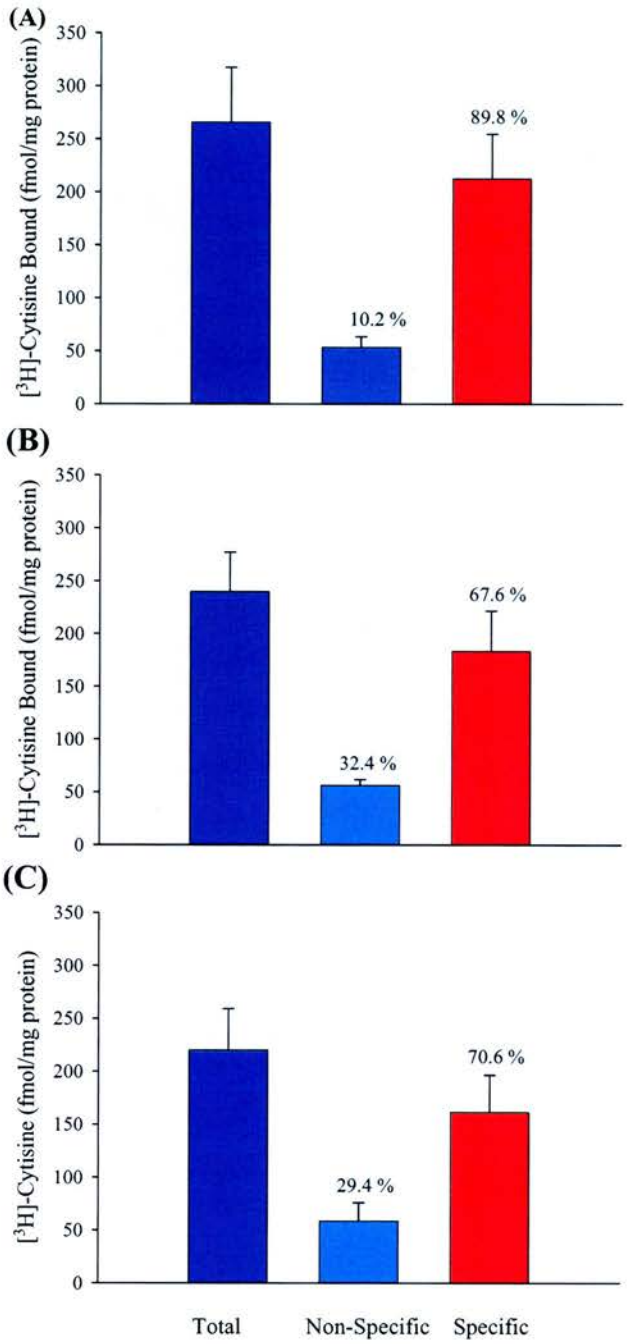

Proportions of [^{3}H]-Cytisine Binding in Male α_7 nAChR Transgenic Mouse Brain Preparations. Membranes (~850 μg) from male (A) α_7-WT (B) α_7-HT or (C) α_7-KO mouse brains were incubated (22°C) with [^{3}H]-cytisine (3 nM) in a total assay volume of 250 μl for 60 min. Non-specific binding was determined in the presence of 10 μM (-)nicotine and these data represent an average of 4 individual male mice brain experiments.

Figure 3.36

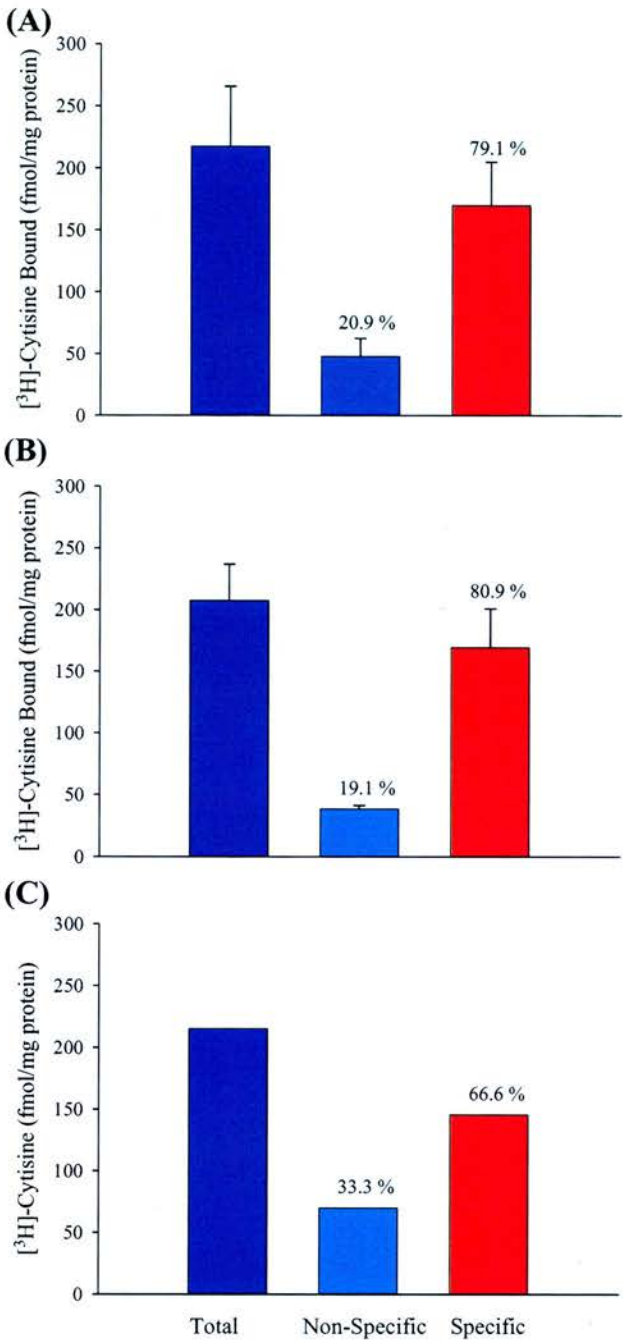

Proportions of [^{3}H]-Cytisine Binding in Female α_7 nAChR Transgenic Mouse Brain Preparations. Membranes (~850 µg) from female (A) α_7-WT (B) α_7-HT or (C) α_7-KO mouse brains were incubated (22°C) with [^{3}H]-cytisine (3 nM) in a total assay volume of 250 µl for 60 min. Non-specific binding was determined in the presence of 10 µM (-)nicotine with these data representing an average of 2-4 individual female mice brain experiments.

3.37, Table 3.14). Receptor densities were also similar across membrane preparations at 269 ± 21 fmol/mg protein for α_7-WT mice, 270 ± 16 for α_7-heterozygotes, and 241 ± 15 for α_7-knockout mice (Figure 3.37, Table 3.14). Indeed, both affinity and receptor density data are consistent with previously published studies of [^{3}H]-cytisine binding sites in roden brain membranes (Pabreza *et al.*, 1991; Anderson & Arneric, 1994; Didier *et al.*, 1995; Davila-Garcia *et al.*, 1999). Although the Hill coefficient for male α_7-WT was close to unity (n_H = 1.05 ± 0.07, n = 4), the Hill coefficients for α_7-HT (1.77 ± 0.20, n =4) and α_7-KO mice (1.54 ± 0.31, n = 4) were slightly above unity, although there was a considerable degree of variability.

Consistent with the observations made for the male α_7-nAChR transgenic mice, the binding affinity (K_D) of [^{3}H]-cytisine was similar in all three female mouse brain preparations; K_D = 5.31 ± 0.79 nM (α_7-WT, n = 4), 7.05 ± 2.27 nM (α_7-HT, n =3), and 4.75 nM (α_7-KO, n = 2) (Figure 3.38, Table 3.14). Again, these K_D values are almost identical to their male counterparts discussed above (Table 3.14). The density (B_{max}) of $\alpha_4\beta_2$ nAChRs in female mouse brains was also reasonably consistent between the three membrane preparations at 254 ± 40 fmol/mg protein for α_7-WT mice (n = 4), 302 ± 42 fmol/mg protein for α_7-heterozygotes (n = 3), and 145 fmol/mg protein for α_7-knockout mice (n = 2; Figure 3.38, Table 3.14). These values are also consistent with the receptor density determined for male mice while the lower value determined for the female α_7-knockout mouse is probably due to the low sample number. In general, Hill coefficients were all above unity; 2.14 ± 0.41 for α_7-WT mice (n = 4), 1.51 ± 0.30 for α_7-heterozygotes (n = 3), and 1.31 for α_7-knockout mice (n = 2; Figure 3.38, Table 3.14).

Figure 3.37

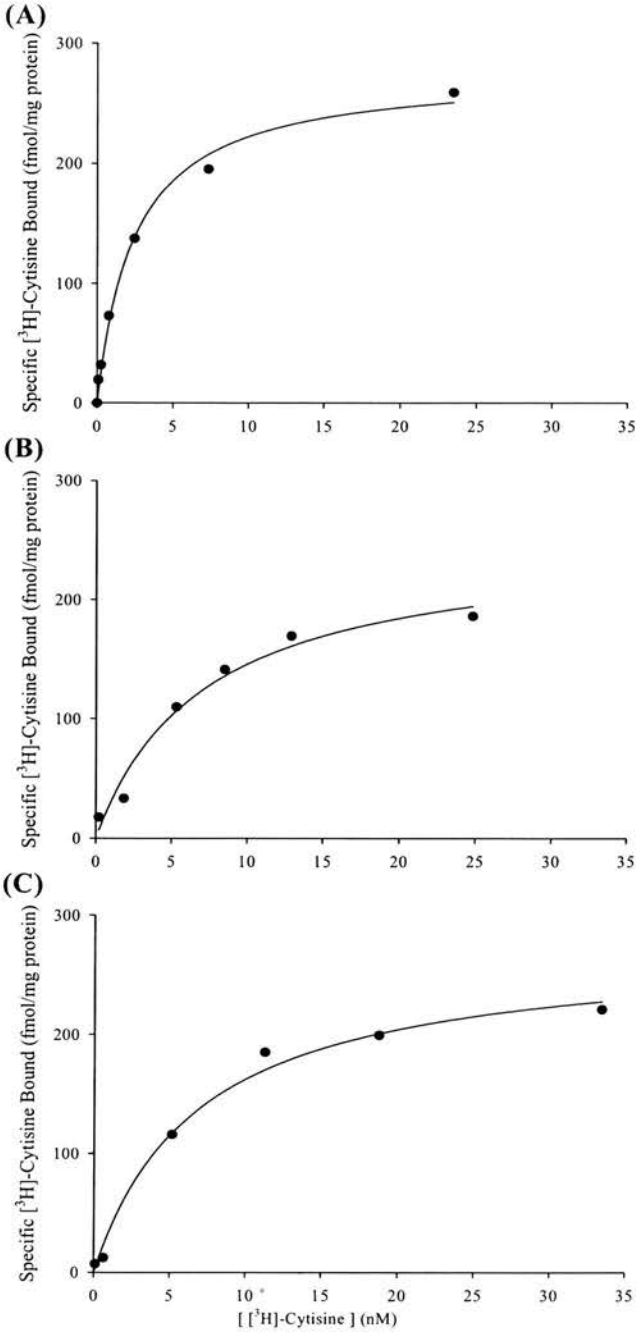

Concentration Dependence of [^{3}H]-Cytisine Binding in Male α_7-nAChR Transgenic Mice. Membranes (850 µg) from littermate male (A) α_7-WT (B) α_7-HT (C) α_7-KO mice were incubated (22°C) with increasing concentrations of [^{3}H]-cytisine in a total assay volume of 250 µl for 60 min. Non-specific binding was determined in the presence of 10 µM (-)nicotine with these data representing an average hot saturation study.

Figure 3.38

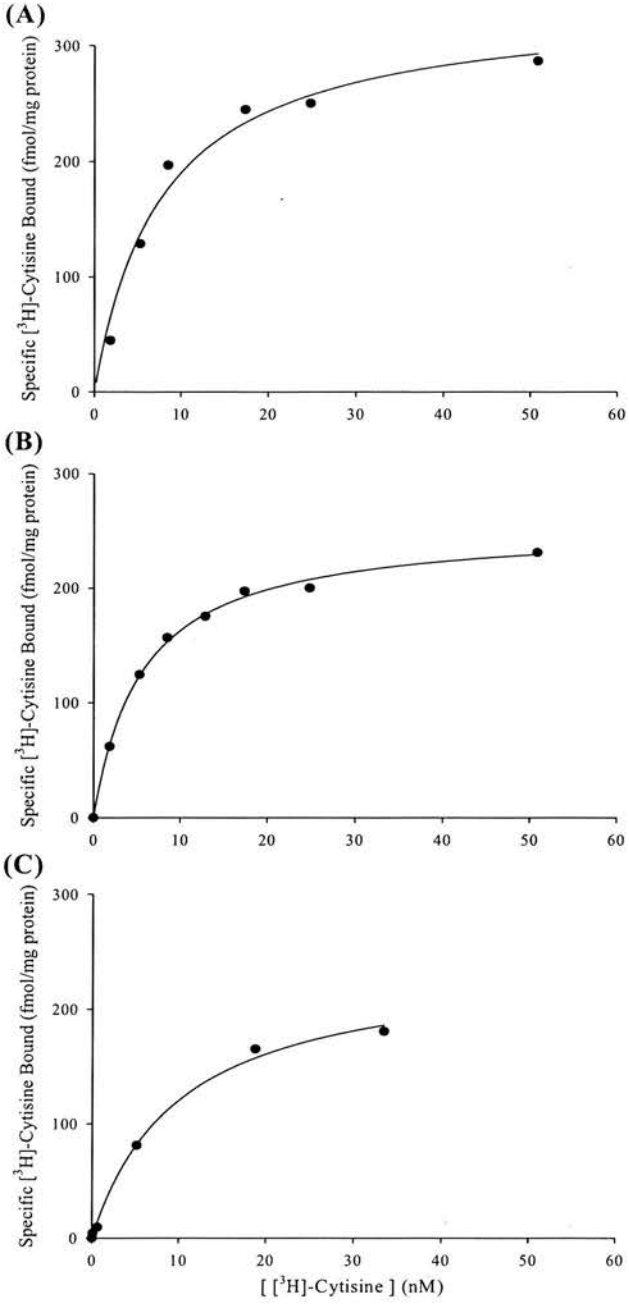

Concentration Dependence of [^{3}H]-Cytisine Binding in Female α_7-nAChR Transgenic Mice. Membranes (850 µg) from littermate female (A) α_7-WT (B) α_7-HT (C) α_7-KO mice were incubated (22°C) with increasing concentrations of [^{3}H]-cytisine in a total assay volume of 250 µl for 60 min. Non-specific binding was determined in the presence of 10 µM (-)nicotine with these data representing an average hot saturation study.

Table 3.14: K_D and B_{max} Values for [^{3}H]-Cytisine Binding Sites in α_7-Wildtype Littermate, α_7-Heterozygous and α_7-Knockout Mouse Brain Membranes

Transgenic	K_D (nM)	n_H	*n*	B_{max} (fmol/mg protein)
Male				
α_7-Wildtype	2.75 ± 0.31	1.05 ± 0.07	4	269 ± 21
α_7-Heterozygous	7.39 ± 1.10	1.77 ± 0.20	4	270 ± 16
α_7-Knockout	7.45 ± 1.64	1.54 ± 0.31	4	241 ± 15
Female				
α_7-Wildtype	5.31 ± 0.79	2.14 ± 0.41	4	254 ± 40
α_7-Heterozygous	7.05 ± 2.27	1.51 ± 0.30	3	302 ± 42
α_7-Knockout	4.75	1.31	2	145

Affinity (K_D), Hillslopes (n_H), and receptor density (B_{max}) were determined in the [^{3}H]-cytisine binding assays as described in the methods. Values are expressed as mean ± S.E.M. (n = 2-4). Statistical analyses were performed using a one-way ANOVA with Bonferroni post-hoc testing. No difference in ligand affinity or $\alpha_4\beta_2$ nAChR density was observed between preparations.

3.8 DISCUSSION

As discussed in the main introduction, although there are two main hypotheses of AD, the cholinergic and the amyloid, both have been treated separately in many respects. During the period of my Ph.D, a number of papers have shown a direct interaction between nAChRs and $A\beta_{1-42}$, however it remains unclear what the basis of this interaction is and indeed which subtypes of nAChRs are actually involved (Wang *et al.*, 2000a,b; Dineley *et al.*, 2001, 2002a; Liu *et al.*, 2001; Pettit *et al.*, 2001; Tozaki *et al.*, 2002; Fu & Jhamandas, 2003; Grassi *et al.*, 2003; Wu *et al.*, 2004; de Fiebre & de Fiebre, 2005). Due to the generosity of Dr. R. J. Lukas who provided the SH-EP1 cell lines stably expressing the human $\alpha_4\beta_2$ and α_7 nAChRs, I have been able to systematically compare human, rat, and mouse nicotinic receptor pharmacology. Two radioligand binding assays were established for both the $\alpha_4\beta_2$ ([^{3}H]-epibatidine and [^{3}H]-cytisine) and α_7 nAChRs ([^{3}H]-MLA and [^{3}H]-αBgTx), and cholinergic receptor pharmacology extensively examined. These assays highlighted species differences in α_7 nAChR pharmacology that were not observed for the $\alpha_4\beta_2$ nAChR as well as showing differences in the properties of the α_7 nAChR ligands [^{3}H]-MLA and [^{3}H]-αBgTx. Moreover, these assays were used to show that various forms of $A\beta_{1-42}$ did not inhibit binding to either nAChR subtype. Finally, these assays were then used in a collaborative set of studies with the behaviourists in our Institute to examine nAChR pharmacology in α_7 nAChR-transgenic mice, which has resulted in one published and one accepted manuscript (Young *et al.*, 2004; 2006 *accepted*). In this discussion for simplicity, I will systematically discuss each of these findings.

3.8.1 Pharmacological Characterisation of [^{3}H]-Epibatidine Binding Sites in Rat Brain and SH-EP1-h$\alpha_4\beta_2$ Cell Membranes

The discovery in the late 1970's that epibatidine was a potent agonist at nAChRs, subsequently led to its radiolabelling with tritium ([^{3}H]-epibatidine) and iodine ([^{125}I]-epibatidine) (Daly *et al.*, 1978; Badio & Daly, 1994). In the current study, [^{3}H]-epibatidine (15 pM) underwent a slow association with the $\alpha_4\beta_2$ nAChR at 22°C in both rat brain and SH-EP1-h$\alpha_4\beta_2$ cell membranes, reaching equilibrium by approximately 2 h. This observation is comparable with earlier studies using human, rat, and mouse membranes (Figure 3.1; Marks *et al.*, 1998; Whiteaker *et al.*, 1998). This time course for epibatidine binding is quicker than some other studies using human $\alpha_4\beta_2$ nAChRs expressed in M10 cells (equilibrium reached within 2 rather than 4 h; e.g. Gnadish *et al.*, 1999) however, as radioligand concentrations and incubation temperatures were identical, this is most likely

due to differences in membranes preparations. All subsequent studies were performed using a 4 h incubation period to allow for a direct comparison between studies using rat brain and human $\alpha_4\beta_2$ nAChRs.

Hot saturation studies indicated that [^{3}H]-epibatidine bound with low picomolar affinity to receptors in rat brain (K_D = 26.1 pM) and to the human $\alpha_4\beta_2$ nAChR stably expressed in SH-EP1 cells (K_D = 28.5 pM; Figure 3.3, pg 61). With the affinity of the ligand in rat brain membranes and the SH-EP1-h$\alpha_4\beta_2$ nAChRs being almost identical, this indicates that under the assay conditions used [^{3}H]-epibatidine bound to $\alpha_4\beta_2$ nAChRs in both membrane preparations, and that there was no species differences in $\alpha_4\beta_2$ receptor pharmacology. Furthermore, Hill slopes were close to unity in both membrane preparations signifying single site binding of the ligand (Figure 3.3, pg 61). It is important to note that although epibatidine also binds to other nicotinic subunits with high affinity (e.g. $\alpha_3\beta_2\alpha_5$ nAChR; Wang *et al.*, 1996), low affinity epibatidine binding sites had, until recently, only been partially characterised. However, Peng and colleagues (2005) have shown that [^{3}H]-epibatidine can be used to characterise the pharmacology of the human α_7 nAChR over-expressed in the SH-EP1 cell line. This cell line is useful as it contains no other nAChR subunits and consequently, these authors demonstrated that [^{3}H]-epibatidine bound with high picomolar affinity (K_D = 640 pM) to the α_7 nAChR and as such, it forms one of the low affinity binding sites for epibatidine. Obviously, this low affinity site would not be detected in the current study due to the non-expression of α_7 nAChRs in the SH-EP1-h$\alpha_4\beta_2$ cell line and because of the radioligand concentration used.

The subnanomolar affinity of [^{3}H]-epibatidine for $\alpha_4\beta_2$ nAChRs in rat brain and SH-EP1-h$\alpha_4\beta_2$ cell membranes means radioligand binding assays utilising this ligand can be fraught with technical difficulties. Indeed, the specific activity of a radioligand, and hence radioligand concentration, can limit accurate estimations of potencies of labelled and unlabelled ligands, particularly when working with tritiated compounds. These difficulties have been described in many studies using both theoretical and practical systems (Goldstein & Barrett, 1987; de Vries *et al.*, 1988; Crawford *et al.*, 1999). In order to obtain an accurate estimate of ligand potencies in any radioligand binding study, it is advisable to use a radioligand concentration that is less than the K_D of the ligand under examination. A variety of K_D/K_i values have been obtained for [^{3}H]-epibatidine in previous studies (Houghtling *et al.*, 1995; Chavez-Noriega *et al.*, 1997; Marks *et al.*, 1998; Sihver *et al.*, 1998; Whiteaker *et al.*, 1998; Gnadisch *et al.*, 1999) and, as such, it has already been noted that some studies may have underestimated the K_D/K_i values for high affinity ligands because of epibatidine's

subnanomolar affinity (Gnadisch *et al.*, 1999). To avoid such problems, Gnadisch and colleagues (1999) increased the incubation time and volume of their [^{3}H]-epibatidine assay, and decreased their radioligand concentration to avoid an underestimation of ligand affinities. Indeed, these conditions were also used in the current studies and, furthermore, whole rat brain tissue was used to compensate for any variations seen in binding characteristics in different brain regions (Gnadisch *et al.*, 1999). Despite these caveats, our K_D value for [^{3}H]-epibatidine of 26.1 pM in rat brain membranes (Figure 3.3) was similar to that obtained by Gnadisch and colleagues (1999; K_D = 8 pM), with both rat and human K_D values also being consistent with those obtained in other studies using rodent and human $\alpha_4\beta_2$ nAChRs (Houghtling *et al.*, 1995; Marks *et al.*, 1998; Sihver *et al.*, 1998). The rank order of potency for ligands competing against [^{3}H]-epibatidine ((±)epibatidine > cytisine > (-)nicotine > DMPP > MLA = *d*-TC) is also consistent with the previous values presented for both rat and human $\alpha_4\beta_2$ nAChRs (Gerzanich *et al.*, 1995; Houghtling *et al.*, 1995; Chavez-Noriega *et al.*, 1997; Marks *et al.*, 1998; Sihver *et al.*, 1998; Whiteaker *et al.*, 1998; Gnadisch *et al.*, 1999).

Interestingly, the non-selective nAChR agonist 1,1-Dimethyl-4-phenylpiperazinium iodide (DMPP) exhibited a small, but significantly higher affinity for $\alpha_4\beta_2$ nAChRs in rat brain membranes (K_i = 21.3 nM) when compared with human $\alpha_4\beta_2$ nAChRs (K_i = 42.9 nM; $p < 0.05$), although Hill slopes were close to unity in both preparations. Unlike the other three agonists examined, when cytisine was used to inhibit [^{3}H]-epibatidine binding in rat brain membranes it yielded a Hill coefficient of less than one, indicating that epibatidine may indeed bind (as discussed above) to more than one binding site, perhaps with similar affinities whereas cytisine can discriminate between then more clearly. Indeed, a biphasic pattern consistent with the presence of two sites has been previously reported for cytisine inhibition of [^{3}H]-epibatidine binding (Marks *et al.*, 1998) whilst in SH-EP1-h$\alpha_4\beta_2$ cell membranes, where only the nAChR present is the $\alpha_4\beta_2$, the cytisine Hill slope is at unity. In agreement with previous studies (Xiao & Kellar, 2004; Sobrio *et al.*, 2005), no differences in affinity were observed for ligands at rat and human $\alpha_4\beta_2$ nAChRs.

3.8.2 Pharmacological Characterisation of [^{3}H]-Cytisine Binding Sites in Rat Brain and SH-EP1-h$\alpha_4\beta_2$ Cell Membranes

Many researchers correct their data sets to minimise or remove the well-documented depletion problems associated with epibatidine binding assays (Houghtling *et*

al., 1995; Chavez-Noriega *et al.*, 1997; Marks *et al.*, 1998; Whiteaker *et al.*, 1998; Gnadisch *et al.*, 1999). In the [^{3}H]-epibatidine binding assay discussed above, the assay volume and incubation time were increased and the concentration of radioligand minimised to mitigate against depletion. However, with the subnanomolar affinity of [^{3}H]-epibatidine for $\alpha_4\beta_2$ nAChRs requiring a large volume assay (4 ml) and low ligand concentration (15 pM) to avoid depletion, this assay was unsuitable for use in a 96-well format for rapid characterisation of $\alpha_4\beta_2$ nAChR pharmacology. Traditionally, radiolabelled versions of both (±)epibatidine and cytisine have been used to characterise $\alpha_4\beta_2$ nAChR pharmacology (Pabreza *et al.*, 1991; Gopalakrishnan *et al.*, 1996; Gnadisch *et al.*, 1999; Eaton *et al.*, 2003). With cytisine reported to bind with low nanomolar, rather than picomolar, affinity to the $\alpha_4\beta_2$ nAChR, it could be usable in a small volume radioligand binding assay avoiding the potential problems of depletion associated with [^{3}H]-epibatidine when utilised incorrectly (Pabreza *et al.*, 1991; Houghtling *et al.*, 1995; Gopalakrishnan *et al.*, 1996; Chavez-Noriega *et al.*, 1997; Gnadisch *et al.*, 1999).

Using rat brain and SH-EP1-h$\alpha_4\beta_2$ cell membranes, initial studies examined the time course of [^{3}H]-cytisine binding (3 nM) in a 250 µl assay volume at 4°C. In contrast to previously published studies in which [^{3}H]-cytisine binding reached equilibrium within 1 h in rat brain (Pabreza *et al.*, 1991) or human $\alpha_4\beta_2$ nAChRs expressed in HEK293 cells (Gopalakrishnan *et al.*, 1996), in the current study, [^{3}H]-cytisine binding did not attain equilibrium at 4°C even when incubated for up to 4 h (Figure 3.6). As a consequence studies were performed at both 25°C and 37°C with the optimal incubation temperature for [^{3}H]-cytisine and rat brain membranes determined to be 25°C with equilibrium reached within 1 h. The reasons for this difference in incubation temperature could relate to tissue/cell or other slight technical differences between these assays, although no systematic examination of the differences was conducted.

Hot saturation studies using increasing concentration of [^{3}H]-cytisine showed that the ligand bound with low nanomolar affinity to receptors in rat brain (K_D = 3.77 nM) and SH-EP1-h$\alpha_4\beta_2$ nAChRs cell membranes (K_D = 4.11 nM) which are consistent with data using rat, mouse, and over-expressed human $\alpha_4\beta_2$ nAChRs (Pabreza *et al.*, 1991; Whiting *et al.*, 1991; Flores *et al.*, 1992; Decker *et al.*, 1995; Didier *et al.*, 1995; Gopalakrishnan *et al.*, 1996). Consistent with the data obtained in the [^{3}H]-epibatidine assay, Hill slopes were close to unity. As such, although cytisine binding to high and low affinity nicotinic sites has been well documented, there is little evidence for such circumstances in the current study. Unsurprisingly, the density of receptors labelled by [^{3}H]-cytisine in rat brain (B_{max} = 0.43

pmol/ mg protein) was considerably lower than that in the SH-EP1 cell line overexpressing the human $\alpha_4\beta_2$ nAChR (B_{max} = 131 pmol/mg protein, $p < 0.05$). However, both B_{max} values were consistent with that already reported by Pabreza and colleagues (1991) for rat (B_{max} = 126 pmol/mg protein) and Eaton and colleagues (2003) using the same cells as chacterised in this study (B_{max} = 140 pmol/ mg protein). The affinity of the other cholinergic compounds for [^{3}H]-cytisine binding sites in rat brain and SH-EP1-h$\alpha_4\beta_2$ cell membranes was also comparable to previously published studies using rat brain (Pabreza *et al.*, 1991) and human $\alpha_4\beta_2$ nAChRs expressed in HEK293 (Gopalakrishnan *et al.*, 1996) or SH-EP1 cells (Eaton *et al.*, 2003) and to that obtained with the [^{3}H]-epibatidine assay (rank order of potency = cytisine > (-)nicotine > DMPP > MLA > *d*-tubocurarine). With the exception of *d*-TC and DMPP, the data sets were remarkably consistent in both species (Table 3.3, pg 76). DMPP exhibited a slightly higher affinity for human $\alpha_4\beta_2$ nAChRs (K_i = 71.5 nM) when compared to rat brain membranes (K_i = 256 nM). Furthermore, a species difference in affinity was also observed for *d*-tubocurarine (K_i = 5.0 μM at human $\alpha_4\beta_2$ nAChRs compared to 17.2 μM at rat $\alpha_4\beta_2$ nAChRs). As discussed above, this difference in affinity is likely to be due to multiple receptor stoichiometries in rat brain membranes, and perhaps the presence of one or more lower affinity binding sites.

Analysis of [^{3}H]-cytisine binding in rat brain and SH-EP1-h$\alpha_4\beta_2$ cell membranes has revealed that cytisine is indeed a potent agonist at $\alpha_4\beta_2$ nAChRs. Furthermore, the similar ligand affinities in the [^{3}H]-cytisine and [^{3}H]-epibatidine assays confirm not only the absence of ligand depletion in the latter assay but also that no species differences exist for rat and human $\alpha_4\beta_2$ nAChRs. Finally, the successful miniaturisation of the [^{3}H]-cytisine binding led to its being successfully used in a small volume assay format for high-throughput screening.

3.8.3 Pharmacological Characterisation of [^{3}H]-MLA Binding Sites in Rat Brain and SH-EP1-hα_7 Cell Membranes

As discussed in Section 3.5 (pg 79), the α_7 nAChR is currently being intensively investigated, with potential roles in inflammation (Wang *et al.*, 2003), schizophrenia (Guan *et al.*, 1999; De Luca *et al.*, 2004; Deutsch *et al.*, 2005), and Alzheimer's disease (Bednar *et al.*, 2002; O'Neill *et al.*, 2002; Yu *et al.*, 2005). A radioligand binding assay using [^{3}H]-MLA, a potent and putatively selective antagonist of the α_7 nAChR, has been previously used to characterise the pharmacology of this receptor in rodent brain and insect tissues (Macallan *et al.*, 1988; Ward *et al.*, 1990; Davies *et al.*, 1999; Whiteaker *et al.*, 1999; Lind *et*

al., 2001). The current study has extended these observations in rodent brain membranes by using [^{3}H]-MLA to comprehensively characterise α_7 nAChR pharmacology in rat brain, mouse brain, and in a SH-EP1 cell line over-expressing the human α_7 nAChR.

In agreement with Davies and colleagues (1999) and consistent with the known properties and selectivity of MLA, [^{3}H]-MLA bound to rat brain membranes with an affinity and pharmacological profile characteristic of α_7-subunit containing nAChRs (Macallan *et al.*, 1988; Ward *et al.*, 1990; Alkondon *et al.*, 1992; Drasdo *et al.*, 1992; Wonnacott *et al.*, 1993; Palma *et al.*, 1996; Tian *et al.*, 1997). Furthermore, [^{3}H]-MLA bound to the human α_7 nAChR over-expressed in the SH-EP1 cell line with a profile similar to that observed in the previously mentioned rat brain studies. Indeed, [^{3}H]-MLA binding reached equilibrium rapidly (at 22°C) in both membrane preparations (Figure 3.14, pg 80). Saturation binding studies showed that [^{3}H]-MLA bound with high affinity to a homogenous receptor population in both rat brain (K_D = 1.71 nM) and SH-EP1-hα_7 cell membranes (5.01 nM), consistent with previous studies in rat brain (K_D = 1.8 nM; Davies *et al.*, 1999) and SH-EP1-hα_7 cell membranes (K_D = 1 nM; Peng *et al.*, 1999). The density of binding sites in both rat brain (B_{max} = 0.18 pmol/mg protein) and SH-EP1-hα_7 cell membranes (B_{max} = 7.08 pmol/mg protein) also correlate well with previously published studies of [^{3}H]-MLA, [^{125}I]-MLA, or [^{125}I]-αBgTx binding to α_7 nAChRs in rat brain (Quik *et al.*, 1996; Davies *et al.*, 1999; Mugnaini *et al.*, 2002; Navarro *et al.*, 2002) and SH-EP1-hα_7 cell membranes (Peng *et al.*, 1999, 2005; Schroeder *et al.*, 2003).

Following this initial characterisation, inhibition studies were performed to assess the pharmacological profile of [^{3}H]-MLA binding sites in both membrane preparations. K_i values for the inhibition of [^{3}H]-MLA binding by various cholinergic antagonists (Table 3.5, pg 88) compare well with those in previously published studies (Davies *et al.*, 1999; Peng *et al.*, 2005). No species differences were apparent between rat and human α_7 nAChRs, however, αBgTx did not completely inhibit [^{3}H]-MLA binding sites in rat brain membranes or those binding sites in SH-EP1-hα_7 cell membranes. This observation has been observed in rat (Davies *et al.*, 1999) and mouse (Whiteaker *et al.*, 1999) brain membranes, however, this is the first reported observation of αBgTx's inability to completely inhibit [^{3}H]-MLA binding to the human α_7 nAChR. As a consequence, the inability of αBgTx's to completely inhibit [^{3}H]-MLA binding to the rat and human α_7 nAChR is discussed below (Section 3.10.3.3).

3.8.3.1 Cholinergic Agonists Exhibit Different Affinity for Rat and Human α_7 nAChRs.

Cholinergic agonists generally exhibited a much higher affinity (~2 orders of magnitude) for human α_7 nAChRs than for rat α_7 nAChRs. Although the slight difference in sequence homology (~ 6 %) between the two species could play a role in this observation, the alteration in affinity may, at least in part, be attributed to potential variations in α_7 nAChR stoichiometry in rat and human membrane preparations (Couturier *et al.*, 1990; Seguela *et al.*, 1993; Peng *et al.*, 1994b). A growing body of evidence now suggests that the α_7 nAChR can exist in a combination of homomeric and heteromeric complexes that are dependent upon species and tissue and cellular source (Quik *et al.*, 1996; Yum *et al.*, 1996; Guo *et al.*, 1998; Yu & Role, 1998; Girod *et al.*, 1999; Palma *et al.*, 1999; Rakhilin *et al.*, 1999; Drisdel & Green, 2000; Ferreira *et al.*, 2001; Severance *et al.*, 2004). Although some splice variants of human and chick α_7 nAChRs have now been identified, almost all of these contain premature stop codons and are unable to be functionally expressed in *Xenopus laevis* oocytes (Garcia-Guzman *et al.*, 1995; Gault *et al.*, 1998; Yu & Role, 1998; Villiger *et al.*, 2002; Saragoza *et al.*, 2003). However, α_7 and β_2 subunits have been reported to coassemble and form functional receptors following expression in *Xenopus laevis* oocytes (Zarei *et al.*, 1999; Khiroug *et al.*, 2002). As these subunits are co-expressed throughout the CNS, these findings suggest native heteromeric receptors containing at least one α_7 subunit may yet be identified (Azam *et al.*, 2003). The α_7 nAChR has been traditionally characterised as a fast desensitising receptor which binds αBgTx irreversibly, however, biophysical and pharmacological differences have been reported between native and expressed receptors (Alkondon & Albuquerque, 1993; Shao & Yakel, 2000; Sudweeks & Yakel, 2000). More specifically, the properties of putative α_7 nAChRs in rat hippocampal interneurons do not have identical pharmacological properties to recombinantly expressed rat homomeric α_7-nAChRs (Shao & Yakel, 2000; Sudweeks & Yakel, 2000). While rat α_7 nAChRs in hippocampal interneurons desensitise rapidly and bind αBgTx irreversibly, native α_7 nAChRs desensitise more slowly and have smaller single channel conductances (Alkondon & Albuquerque, 1993; Shao & Yakel, 2000; Sudweeks & Yakel, 2000). A slow desensitisation of the α_7 nAChR has also been observed in denervated mouse muscle (Tsuneki *et al.*, 2003). Moreover, although Cuevas and Berg (1998) detected a rapidly desensitising α_7-nAChR in rat superior cervical ganglionic neurons, a second distinct α_7 nAChR subtype was also detected in the same preparation that, like those in mammalian

autonomic neurons, desensitises slowly and binds αBgTx rapidly and reversibly (Cuevas & Berg, 1998; Cuevas *et al.*, 2000). Whether these differences reflect combination with the β_2 subunit or triplet receptors remains to be determined. It has been shown that the properties of heterologously expressed chick homomeric α_7 nAChRs also do not match those of native chick α_7 nAChRs (Anand *et al.*, 1993; Yu & Role, 1998; Girod *et al.*, 1999). Again, like the human/rat α_7 nAChR, the chick α_7 nAChR can also form heteromeric α_7 AChRs in heterologous expression systems with β_3 (Palma *et al.*, 1999) and α_5/β_2 nAChR subunits (Girod *et al.*, 1999).

Recently two isoforms of the α_7-nAChR (α_7-1 and α_7-2) were identified in rat brain and intracardiac ganglia and these two isoforms do indeed exhibit different biophysical and pharmacological properties (Severance *et al.*, 2004). Isoform α_7-1 desensitises rapidly and is irreversibly blocked by αBgTx while α_7-2 desensitises slowly and binds αBgTx rapidly and reversibly (Severance *et al.*, 2004). Therefore, it is not inconceivable that the potential presence of homomeric and heteromeric α_7 nAChRs and their associated isoforms results in the observed affinity difference in agonist binding affinity between rat and human α_7 nAChRs. In contrast to the lack of species difference observed between rat and human $\alpha_4\beta_2$ nAChRs (Section 3.4), the several-fold higher affinity of α_7 nAChR agonists for human α_7 compared to rat α_7 nAChRs, has considerable large implications for the use of α_7 nAChR agonists in man. Indeed, when developing α_7 nAChR agonists for clinical use, it is important to note that a micromolar affinity determined in rodent brain tissue may have a nanomolar affinity for the human receptor. Aspects of this work have already been presented in published form (Crawford *et al.*, 2004).

3.8.3.2 Modulation of the α_7 nAChR by Acetylcholinesterase Inhibitors, Allosteric Potentiators, and General Channel Blockers

Until recently, acetylcholinesterase (AChE) inhibitors were the only established treatment for Alzheimer's Disease, however, memantine, an NMDA antagonist, has just been approved (Schmitt *et al.*, 2004; Sonkusare *et al.*, 2005). Tacrine (1,2,3,4-tetrahydro-9-aminoacridine) was the first AChE inhibitor approved for the treatment of AD, which was followed by a second generation of AChE inhibitors such as donepezil and galanthamine, both of which are available for the symptomatic treatment of patients with mild to moderate AD (Whitehouse, 1993; Kelly *et al.*, 1997; Scott & Goa, 2000). However, it has been known for some time that AChE inhibitors such as galanthamine may also interact directly with nAChRs (Alkondon *et al.*, 1988; Taylor *et al.*, 1994; van den Beukel *et al.*, 1998; Zwart *et*

al., 2000). Moreover it is almost 30 years since Katz and Miledi (1977) showed physostigmine could act as an agonist of nAChRs. Subsequently, several laboratories have since demonstrated that galanthamine and physostigmine do not act directly but do in fact cause an allosteric potentiation of the intrinsic ACh response, in addition to their effects on AChE (Zwart & Vijverberg, 1997; Sabey *et al.*, 1999; Maelicke *et al.*, 2000).

Allosteric modulation of receptors is a common mechanism of altering neurotransmission, with probably the most famous example being the benzodiazepine-positive modulation (potentiation) of $GABA_A$ receptor activity which facilitates the opening of the integral receptor chloride channel (MacDonald & Twyman, 1992). On nicotinic receptors, allosteric modulators act at binding sites on the nAChR distinct from those of competitive agonists and antagonists and as such are classed as non-competitive agonists (Figure 1.4, pg 15). Although allosteric potentiators such as galanthamine, physostigmine, and codeine have been shown to bind with low efficacy at nAChRs, the exact subtype of nAChR through which they may exert the majority of their action remains unknown (Storch *et al.*, 1995; Samochocki *et al.*, 2000). Indeed, although Samochocki and colleagues (2000) have reported that galanthamine bound to the $\alpha_4\beta_2$ nAChR, other AChE inhibitors such as tacrine and donazepil failed to do so. With the purported involvement of the α_7 nAChR in AD aetiology, the AChE inhibitors galanthamine, physostigmine, donepezil (E2020; Aricept®), and tacrine and the allosteric modulator codeine (Storch *et al.*, 1995) were examined for their ability to inhibit [^{3}H]-MLA binding sites in both rat brain and SH-EP1-hα_7 cell membranes. In contrast to Samochocki and colleagues (2000) observations for AChE inhibitors at the $\alpha_4\beta_2$ nAChR, all the compounds examined exhibited moderate-to-low affinities for α_7 nAChRs in both membrane preparations. Every compound examined produced a complete concentration dependent inhibition of [^{3}H]-MLA binding in both membrane preparations. In the current studies there were a number of significant differences in affinity between rat and human α_7 nAChRs (Table 3.8, pg 97). For E2020, tacrine, physostigmine, galanthamine, and codeine, there was a 2-4 fold increase in affinity for the human α_7 nAChR. Moreover, this is the first study to show that these compounds can directly inhibit [^{3}H]-MLA binding indicating that there must be some overlap between the allosteric and the agonist/antagonist binding sites on the α_7 nAChR.

The α_7 nAChR is also thought to modulate several other neurotransmitter systems including the GABAergic (Alkondon *et al.*, 2000; Buhler & Dunwiddie, 2002; Kawai *et al.*, 2002) and glutamatergic (Guo *et al.*, 1998; Guo *et al.*, 2005) systems and, therefore, the non-selective ion channel blockers (-)bicuculline, 4-aminopyridine (4-AP), and

tetraethylammonium (TEA) were examined for their ability to inhibit [^{3}H]-MLA binding sites in rat brain and SH-EP1-hα_7 cell membranes. Alpha7 nAChRs are widely expressed on GABAergic interneurons and appear to be involved in GABAergic synaptic activity (Alkondon *et al.*, 2000; Adams *et al.*, 2001; Buhler & Dunwiddie, 2002; Kawai *et al.*, 2002; Hajos *et al.*, 2005). (-)Bicuculline, a potent antagonist of $GABA_A$ receptors, inhibited [^{3}H]-MLA binding sites in rat brain and SH-EP1-hα_7 cell membranes with micromolar affinity with this compound again being 10-fold more potent at the human α_7 nAChR (Table 3.8, pg 97). In agreement with our observation, Demuro and colleagues (2001) showed (-)bicuculline competitively inhibited ACh responses at rat α_7 nAChRs expressed in *Xenopus laevis* occytes while non-competitively inhibiting ACh responses at $\alpha_4\beta_2$ nAChRs. The co-expression of α_7 nAChRs and GABA receptors on GABAergic interneurons and the observed involvement of the α_7 nAChR in GABAergic synaptic transmission indicate examination of compound cross-reactivity is vital when characterising selective agonists for these two receptors. The non-selective channel blockers 4-AP and TEA exhibited millimolar affinity for [^{3}H]-MLA binding sites in rat brain and SH-EP1-hα_7 cell membranes. Interestingly, these compounds, like the range of agonists and allosteric modulators showed significant differences in affinity between α_7 nAChRs expressed in rat brain and SH-EP1-hα_7 cell membranes. These observations highlight the importance of examining drug affinities in more than one species when examining new compounds for potential therapeutic benefit. Indeed, it should be noted that many *in vitro* electrophysiological studies of learning and memory routinely include (-)bicuculline and TEA at this type of concentration and therefore, interpretation of results from these type of studies should take into account that these compounds may be blocking multiple channels.

3.8.3.3 The Inability of αBgTx to Fully Inhibit [^{3}H]-MLA Binding Sites in Rat Brain and SH-EP1-hα_7 Cell Membranes

In agreement with studies performed by Wonnacott and colleagues (Davies *et al.*, 1999; Whiteaker *et al.*, 1999) in rodent brain membranes, our data confirmed that αBgTx was only able to inhibit up to ~ 80 % of [^{3}H]-MLA binding sites in rat brain membranes. If different isoforms of α_7 or heteromeric α_7 nAChR stoichiometries were responsible for the incomplete inhibition of [^{3}H]-MLA binding sites, it is possible to postulate that, by using a homogenous population of α_7 nAChRs, such as those expressed in the SH-EP1-hα_7 cell line which are devoid of other nicotinic receptors (Peng *et al.*, 1994b; Severance *et al.*, 2004), you would expect to see complete inhibition of [^{3}H]-MLA binding. Surprisingly, the reverse

was observed with αBgTx only capable of inhibiting about 40 % of [^{3}H]-MLA binding sites in the SH-EP1-hα_7 cell membranes (Figure 3.23, pg 99). This suggests that although multiple isoforms of the α_7 nAChR or heteromeric receptor stoichiometries may exist, these differences are not the reason why αBgTx fails to fully inhibit [^{3}H]-MLA binding sites in either rat brain or SH-EP1-hα_7 cell membranes. Much debate and subsequent controversy has centred around whether a peptide as large as αBgTx (Mwt = ~ 8 kDa) can access all 5 putative binding sites on the α_7 nAChR (Conti-Tronconi & Raftery, 1986; Palma *et al.*, 1996; Balass *et al.*, 1997; Rangwala *et al.*, 1997; Arias, 2000). In contrast, the norditerpenoid alkaloid, methyllycaconitine (MLA; Aiyar *et al.*, 1979), is a much smaller compound (Mwt = 874) that should be capable of simultaneously binding to all 5 putative binding sites on the α_7 nAChR. To investigate whether αBgTx's inability to completely inhibit [^{3}H]-MLA binding sites is potentially due to its size and whether it is capable of accessing all 5 putative binding sites on the α_7 nAChR two approaches were used. Firstly, the effect of increasing [^{3}H]-MLA binding assay incubation time with αBgTx and secondly, a [^{3}H]-αBgTx binding assay was established and compared directly with the [^{3}H]-MLA assay. If [^{3}H]-MLA binds to more sites than [^{3}H]-αBgTx (putatively 5), it should be completely inhibited by unlabelled MLA but only partially by the larger αBgTx as shown in Figure 3.26B (pg 104). Again for this hypothesis to be true, [^{3}H]-αBgTx should only label a fraction (compared to [^{3}H]-MLA) of the available binding sites on the α_7 nAChR, with these sites being completely inhibited by both unlabelled MLA and αBgTx. Most importantly, the α_7 nAChR binding site density (B_{max}) should therefore be lower when measured using [^{3}H]-αBgTx than when measured using [^{3}H]-MLA. The use of [^{3}H]-αBgTx rather than [^{125}I]-αBgTx allowed the closest possible comparison of binding properties with the smallest labelled compound available.

No change in αBgTx affinity (K_i) or level of inhibition of [^{3}H]-MLA binding sites was observed despite extending the incubation period of the assay up to 140 min, indicating that increased time to allow for penetration of αBgTx did not alter the result. Whilst establishing a [^{3}H]-αBgTx binding assay, I showed that the time course of [^{3}H]-αBgTx (2 nM) binding to SH-EP1-hα_7 cell membranes did not reach equilibrium, despite incubation of the ligand with membranes for up to 8 h. This observation in a binding assay indicates that αBgTx is an irreversible antagonist in a binding assay and, as such, binding was terminated at 6 h when specific binding was consistently ≥ 65 % (Figure 3.25, pg 103). These findings are consistent with the literature showing that αBgTx is an irreversible antagonist (Lukas *et*

al., 1981; Walker *et al.*, 1981). In competitive inhibition studies αBgTx completely inhibited [^{3}H]-αBgTx binding sites in SH-EP1-hα$_7$ cell membranes but only inhibited a maximum of 40 % of [^{3}H]-MLA binding sites in the same membrane preparation. In contrast, MLA fully inhibited both [^{3}H]-αBgTx and [^{3}H]-MLA binding sites in SH-EP1-hα$_7$ cell membranes as did the other nicotinic agonists (cytisine and (-)nicotine) examined. This result is consistent with the above hypothesis that αBgTx and MLA compete for the same binding site.

To determine if [^{3}H]-αBgTx and [^{3}H]-MLA label different densities of binding sites, hot saturation studies were performed using SH-EP1-hα$_7$ cell membranes and the radioligands [^{3}H]-αBgTx and [^{3}H]-MLA. Saturation binding data showed [^{3}H]-αBgTx bound to SH-EP1-hα$_7$ cell membranes with high affinity (K_D = 2.66 nM) with this value correlating well with those from previously published studies on Torpedo californica and rat brain (Lukas *et al.*, 1981; Walker *et al.*, 1981). Although the apparent affinity of αBgTx for α$_7$ nAChRs measured either by hot saturation (K_D = 2.66 nM) or by inhibition studies of [^{3}H]-MLA binding sites in SH-EP1-hα$_7$ cell membranes (K_i = 2.40 nM) was identical, the density of binding sites labelled by [^{3}H]-αBgTx was significantly lower (2.4 pmol/mg protein) than those labelled by [^{3}H]-MLA (7.1 pmol/mg protein; $p < 0.05$).

The significantly lower (65 %) receptor density measured using [^{3}H]-αBgTx indicates that the size of αBgTx appears to prevent it from binding to all the available binding sites on the α$_7$ nAChR. The level of reduction in B_{max} value (65 %) is consistent with αBgTx only inhibiting 40 % of [^{3}H]-MLA binding (Figure 3.18, pg 87). Therefore, these studies indicate that αBgTx is probably only capable of binding to 2 sites on the α$_7$ nAChR pentamer. However, as the agonists cytisine and (-)nicotine fully inhibit [^{3}H]-αBgTx binding, αBgTx must also cover the agonist binding site as it exhibits identical affinity for both [^{3}H]-MLA and [^{3}H]-αBgTx binding sites. Further studies could address whether allosteric modulators or compounds effecting other sites on the α$_7$ nAChR would inhibit [^{3}H]-αBgTx binding.

With the pharmacological characterisation of both [^{3}H]-MLA and [^{3}H]-cytisine binding sites complete, these assays were used to examine the interaction with $A\beta_{1-42}$ prior to characterising the α$_7$ ([^{3}H]-MLA) and α$_4$β$_2$ ([^{3}H]-cytisine) nAChRs in α$_7$ nAChR mutant mice.

3.8.4 Characterisation of α_7 and $\alpha_4\beta_2$ nAChR Pharmacology in α_7 nAChR Transgenic Mice

Nicotine, the predominant psychoactive compound in tobacco smoke and a non-selective nAChR agonist, is able to enhance attention and improve symptomology in diseases such as Alzheimer's, Parkinson's, attention deficit hyperactivity disorder, and schizophrenia (Levin & Simon, 1998; White & Levin, 1999; O'Neill *et al.*, 2002; Shytle *et al.*, 2002; Yang *et al.*, 2002). However, the paucity of truly receptor selective nicotinic ligands has led to the use of a number of nicotinic receptor transgenic mouse models to try and elucidate the exact role of the individual subtypes of nAChR in various diseases (Hsiao, 1998; Gordon *et al.*, 2001; Drago *et al.*, 2003; Savonenko *et al.*, 2005). The α_7 nAChR knockout (null) mouse was developed by Orr-Urtreger and colleagues in 1997; with this mouse lacking αBgTx binding sites and the hippocampal fast nicotinic currents associated with the α_7 nAChR. Furthermore, these mice are generally considered to exhibit normal physiology and behaviour with only two notable exceptions. Firstly, α_7 nAChR knockout mice do not breed well in comparison to their wildtype littermates (Orr-Urtreger *et al.*, 1997; Paylor *et al.*, 1998), with a recent study demonstrating that although female knockouts can achieve pregnancy, litter sizes are significantly smaller than their wildtype littermates, whereas male knockouts have minimal fertility problems (Morley & Rodriguez-Sierra, 2004). In breeding the α_7 knockout mice for behavioural studies discussed below, we encountered the same problem (unpublished observations) and consequently, heterozygous females were predominantly used for breeding. Secondly, in behavioural studies α_7 nAChR knockout mice exhibit mostly normal behavioural although they appear to exhibit anxiety in certain behavioural test when compared to their wildtype controls (Paylor *et al.*, 1998). Finally, α_7 nAChR knockout mice have recently been shown to suffer from some learning difficulties (Keller *et al.*, 2005) which support our data using the 5-CSR task (Young *et al.*, 2004), in which α_7 nAChR knockout mice exhibit deficits in sustained attention when compared to their age-matched littermantes.

For these studies α_7 nAChR knockout mice were bred in our Institute by backcrossing a breeding pair 11 times onto a C57Bl/6 background. The genotype of the transgenic mice (wildtype (WT), heterozygous (HT), or knockout (KO)) was confirmed prior to behavioural studies of [^{3}H]-MLA binding sites. The pharmacological characterisation in brain membranes from non-littermate wildtype (C57Bl/6) mice before examined both α_7 and $\alpha_4\beta_2$ nAChRs binding sites in the α_7-transgenic mice.

Consistent with the data presented earlier in this chapter using using rat brain membranes (Figure 3.14, pg 79) and in agreement with the only other published study, [^{3}H]-MLA (2.5 nM) underwent a fast association with the α_7 nAChR in mouse brain membranes, reaching equilibrium within 15 min (Whiteaker *et al.*, 1999). Futhermore, the K_D (1.32 nM) and B_{max} values (16 fmol/mg protein) for [^{3}H]-MLA in mouse brain are also consistent with previously published data using either [^{125}I]-αBgTx or [^{3}H]-MLA (Marks & Collins, 1982; Whiteaker *et al.*, 1999). Analysis of the affinity of other cholinergic ligands for [^{3}H]-MLA binding sites in mouse brain tissue yielded a rank order of potency of MLA > (-)AR-R17779 > *d*-tubocurarine > (-)nicotine > (+)AR-R17779. The K_i values obtained were comparable to those obtained from rat brain membranes (Tables 3.6 (pg 92), 3.7 (pg 93), 3.13 (pg 122)) and the Hill coefficients were in general slightly greater than unity perhaps indicative of positive co-operativity, however there was some variability, the cause of which is unknown.

As discussed above, only a limited number of studies have assessed the behaviour of mutant α_7 nAChR mice in a variety of tasks, however, no others have systematically addressed whether there are differences in nAChR pharmacology (Orr-Urtreger *et al.*, 1997; Paylor *et al.*, 1998; Franceschini *et al.*, 2002; Morley & Rodriguez-Sierra, 2004; Keller *et al.*, 2005). By definition, a heterozygous α_7 nAChR mouse has only one allele coding for the α_7 nAChR gene whilst a wildtype mouse possesses a pair of α_7 nAChR alleles. Needless to say, α_7 nAChR KO mice possess neither allele. An initial study assessing the density of [^{3}H]-MLA binding sites in individual α_7 transgenic mouse brain membranes confirmed the absence of α_7 nAChRs in KO mice (Young *et al.*, 2004). This initial observation has now been extended with a second 5-CSR study comparing wildtype, α_7-nAChR heterozygote, and α_7-nAChR knockout mice (currently accepted for publication in *European J Psychopharmacology*). As transgenic manipulations may produce compensatory changes in nAChR density or changes in receptor pharmacology, in parallel, the nicotinic receptor pharmacology of these mice was investigated to enhance the above findings, and I am a co-author on both manuscripts.

Although no change in [^{3}H]-MLA affinity was observed between male WT (K_D = 7.4 nM) and HT mice (K_D = 10.7 nM), or between female WT (K_D = 7.3 nM) and HT mice (K_D = 10.5 nM), the receptor density was significantly altered. Indeed, this is the first study to confirm that the [^{3}H]-MLA binding site density in HT mice (B_{max} = 34 and 27 fmol/mg protein in male and female HT mice, respectively) is almost exactly half of that measured in WT mouse membranes (B_{max} = 66 and 73 fmol/mg protein in male and female mice, respectively). These values are consistent with those determined in rat brain and SH-EP1-

hα_7 cell membranes (Section 3.5.2) and with previously published studies using the α_7 nAChR knockout mice (Orr-Urtreger *et al.*, 1997). Furthermore, Hill coefficients were close to unity indicating that [^{3}H]-MLA binds to a single population of receptors in both WT and HT mouse brain membranes, consistent with observations in rat and SH-EP1-hα_7 cell membranes (Section 3.5.2).

Any genetic manipulation in α_7 nAChR gene expression may result in a compensatory change in other cholinergic receptors. As such it was necessary to examine the density and pharmacology of the $\alpha_4\beta_2$ nAChR, the other major nicotinic receptor in rodent brain (Paterson & Nordberg, 2000). When compared to their littermate controls, there was no alteration in the affinity (K_D) of [^{3}H]-cytisine on comparing WT and KO mouse brain membrane preparations. Furthermore, no alteration in [^{3}H]-cytisine binding density was observed between mice (Table 3.14, pg 128). These findings are in agreement with Orr-Utreger and colleagues (1997) who showed α_7 KO mice lack MLA binding sites but still have $\alpha_4\beta_2$ nAChRs when measured using [^{3}H]-cytisine. Interestingly, and in agreement with the current [^{3}H]-MLA binding data (Table 3.13, pg 122), no gender specific differences in [^{3}H]-cytisine binding sites were observed (Table 3.14, pg 128). Hill slopes were close to unity, indicating single-site affinity for [^{3}H]-cytisine. As such it must be concluded that $\alpha_4\beta_2$ nAChRs do not appear to undergo up- or down-regulation to compensate for the loss of [^{3}H]-MLA binding sites in α_7 nAChR KO mouse brain.

3.9 CONCLUSIONS

In order to pharmacologically characterise human and rodent $\alpha_4\beta_2$ and α_7 nAChRs, I successfully established and characterised 4 separate radioligand binding assays using [^{3}H]-epibatidine ($\alpha_4\beta_2$), [^{3}H]-cytisine ($\alpha_4\beta_2$), [^{3}H]-MLA (α_7), and [^{3}H]-αBgTx (α_7). Using these assays I showed that [^{3}H]-cytisine may be successfully substituted for [^{3}H]-epibatidine in order to characterise $\alpha_4\beta_2$ nAChRS in a small volume radioligand binding assay and that no species differences exist. Furthermore, I have utilised the [^{3}H]-MLA and [^{3}H]-αBgTx assays to show that αBgTx and MLA bind to different proportions of the 5 available competitive antagonist sites on the homomeric α_7 nAChR. Finally α_7 nAChR KO mice bred in-house were shown to lack α_7 nAChRs using both the [^{3}H]-MLA binding assay and genotyping. In addition, I have shown that removal of the α_7 nAChR does not result in any compensatory up or down regulation of $\alpha_4\beta_2$ nAChRs. To this end, one behavioural paper has already been published showing removal of the α_7 nAChR results in a deficit in sustained attention in the 5-CSR task (Young *et al.*, 2004) whilst a second paper has also been accepted for publication (*Eur J Psychopharmacology*). This latter paper compares the ability of α_7 nAChR KO mice with their heterozygous and wildtype littermates in the 5-CSR task, showing both KO and heterozygous mice exhibit deficits in sustained attention compared to their wildtype littermates.

4 PHARMACOLOGICAL INTERACTION BETWEEN $A\beta_{1-42}$ AND nAChRs

4.1 INTRODUCTION

Although a growing body of evidence now supports a direct interaction between $A\beta_{1-42}$ and nAChRs, controversy exists over the exact nature of this interaction, the subtype of nAChR involved and indeed, which the form of $A\beta_{1-42}$ is neurotoxic.

In 2000, Wang and colleagues published a paper indicating that picomolar concentrations of $A\beta_{1-42}$ could inhibit the binding of α_7 nAChR antagonists [^{125}I]-αBgTx and [^{3}H]-MLA to the α_7 nAChR (Wang *et al.*, 2000a). These initial findings were closely followed by a second paper indicating that $A\beta_{1-42}$ exhibited >5000-fold higher affinity for the α_7 nAChR compared to the $\alpha_4\beta_2$ nAChR (Wang *et al.*, 2000b). However, these finding have not been replicated by other groups despite the use of $A\beta_{1-42}$ concentrations ranging from femtomolar to nanomolar (de Fiebre & de Fiebre, 2005).

Further complicating the study of any potential interaction between $A\beta_{1}$-42 and nAChRs, is a debate as to which form of $A\beta_{1-42}$ is supposedly neurotoxic. Aβ is present in all animals in multiple conformations including monomers, oligomers, protofibrils, and mature fibrils and as such, it is difficult to define which form causes neurodegeneration (Walsh *et al.*, 1997; Teplow, 1998; Conway *et al.*, 2000; Bitan *et al.*, 2003).

Consequently, in order to examine any potential pharmacological interaction between $A\beta_{1-42}$ and nAChR, the solubility $A\beta_{1-42}$ in a number of different vehicles was first assessed using a thioflavin T aggregation assay. Thioflavin T is a fluorescent dye that specifically binds to β-sheet fibrous structures (Vassar & Culling, 1959; LeVine, 1993; Yoshiike *et al.*, 2003). . Following the assessment of $A\beta_{1-42}$ solubility and by establishing radioligand binding assays (Chapter 3) the ability of $A\beta_{1-42}$ to inhibit [^{3}H]-cytisine and [^{3}H]-MLA binding to $\alpha_4\beta_2$ and α_7 nAChRs, respectively, was studied.

4.2 Human $A\beta_{1-42}$ Has No Direct Effect on Binding to the Human $\alpha_4\beta_2$ and α_7 AChRs

Recent studies provide pharmacological evidence for and against a direct interaction of $A\beta_{1-42}$ with the $\alpha_4\beta_2$ nAChR (Kihara *et al.*, 1998; Wang *et al.*, 2000b; Tozaki *et al.*, 2002; Fu & Jhamandas, 2003; Wu *et al.*, 2004) and the α_7 nAChR (Wang *et al.*, 2000a,b; Dineley *et al.*, 2001, 2002a; Liu *et al.*, 2001; Pettit *et al.*, 2001; Nagele *et al.*, 2002; Grassi *et al.*, 2003; Wu *et al.*, 2004; de Fiebre & de Fiebre, 2005). However, only three of these papers have presented binding data (Wang *et al.*, 2000a,b; de Fiebre & de Fiebre, 2005). In addition, whilst variations exist within these papers in terms of the form, source and species of $A\beta_{1-42}$ used, these former studies acted as a forerunner to a large body of research investigating a direct link between nAChRs and $A\beta_{1-42}$ (for reviews see Kem, 2000; Court *et al.*, 2001; O'Neill *et al.*, 2001; Kihara & Shimohama, 2004a). To address whether there was any such direct interaction between various forms of $A\beta_{1-42}$, the putatively neurotoxic peptide, and nAChRs, $\alpha_4\beta_2$ nAChRs (using [^{3}H]-cytisine) and α_7 nAChRs (using [^{3}H]-MLA) that were characterised in Sections 3.4 and 3.5, respectively, were used. Prior to assessing the action of $A\beta_{1-42}$ at these nAChR subtypes, thioflavin T studies were performed to determine the fibrillation state of $A\beta_{1-42}$ in the various assay buffers and protocols to be used.

4.2.1 Determination of the Aggregation State of Human $A\beta_{1-42}$

Although Aβ is predominantly found in a fibrillar form in the brains of AD patients, recent studies also show that soluble oligomers of Aβ and not monomers or fibrils inhibit long term potentiation and cause neurodegeneration (Selkoe, 1994; Kihara *et al.*, 1997; Walsh *et al.*, 1997, 2002a; Teplow, 1998; Conway *et al.*, 2000; O'Neill *et al.*, 2002; Bitan *et al.*, 2003). Methodologically, Aβ may be resuspended in a range of vehicles to achieve different states of solubility including an aggregated form (Wang *et al.*, 2000a,b; Liu *et al.*, 2001; Pettit *et al.*, 2001). The level of solubility/aggregation of $A\beta_{1-42}$ in a number of different vehicles can be assessed using a Thioflavin T fluorescence based assay (Yoshiike *et al.*, 2003). Thioflavin T (ThT) is a yellow dye that specifically binds to β-sheet structures such as amyloid fibrils (LeVine, 1993; Yoshiike *et al.*, 2003).

4.2.1.1 Time Course of Human $A\beta_{1-42}$ Aggregation

Calbiochem provide human $A\beta_{1-42}$ in a lyophilised form and to induce aggregation they suggest their human $A\beta_{1-42}$ is resuspensed in 1/3 magnesium and potassium-free PBS (PBS), and 2/3 sterile water, prior to incubating the solution at 37°C for 48 h. Using this dilutant, the time course of human $A\beta_{1-42}$ aggregation was assessed by incubating the human $A\beta_{1-42}$ (100 μM final assay concentration) with ThT (10 μM) in a 96-well plate. Fluorometric measurements were carried out every 30 min for 48 h at 37°C using a Flexstation fluorescence plate reader. Human $A\beta_{1-42}$ showed signs of aggregation almost immediately after the incubation was initiated (Figure 4.1). The level of fluorescence and presumably aggregation declined slightly before reaching a plateau that held constant for approximately 32 h.

4.2.1.2 Fluorometric Analysis of $A\beta_{1-42}$ Aggregation in Different Assay Buffers

The controversy surrounding the pharmacologically relevant form (soluble/insoluble) of Aβ makes it important to determine what effect the assay buffer has on the form of $A\beta_{1-42}$ utilised before assessing its interaction with $\alpha_4\beta_2$ and α_7 nAChRs. Aβ was resuspended in 4 different vehicles supposedly producing soluble or aggregated forms of $A\beta_{1-42}$. These samples were then diluted in 3 different assay buffers ([^{3}H]-MLA (α_7 nAChRs), [^{3}H]-cytisine ($\alpha_4\beta_2$ nAChRs) or electrophysiology buffer (α_7 and $\alpha_4\beta_2$ nAChRs, see Chapter 4), and the state of solubility/aggregation assessed using the ThT assay.

The first protocol used was that recommended by Calbiochem® (Product No: PP69) to induce aggregation. As discussed previously, human $A\beta_{1-42}$ (250 μg) was resuspended in a mixture of magnesium and potassium-free PBS and sterile water and then incubated at 37°C for 48 h. Following this incubation period, the human $A\beta_{1-42}$ was serially diluted in either of the two radioligand binding assay buffers or in the electrophysiology buffer at concentrations ranging from 100 pM to 1 μM (Figure 4.1). Levels of aggregation in these experiments were significantly lower than those observed in the time course study, probably reflecting the lower concentration of $A\beta_{1-42}$ (≤ 1 μM) examined (Figure 4.1 & 4.2).

The highest levels of thioflavin T fluorescence were detected in $A\beta_{1-42}$ samples at a concentration > 100 nM $A\beta_{1-42}$, regardless of the assay buffer used (Figure 4.2). Indeed, when compared to control samples, significant aggregation was detected in $A\beta_{1-42}$ samples at concentrations of ≥100 nM when $A\beta_{-42}$ was serially diluted in [^{3}H]-MLA or [^{3}H]-cytisine

Figure 4.1

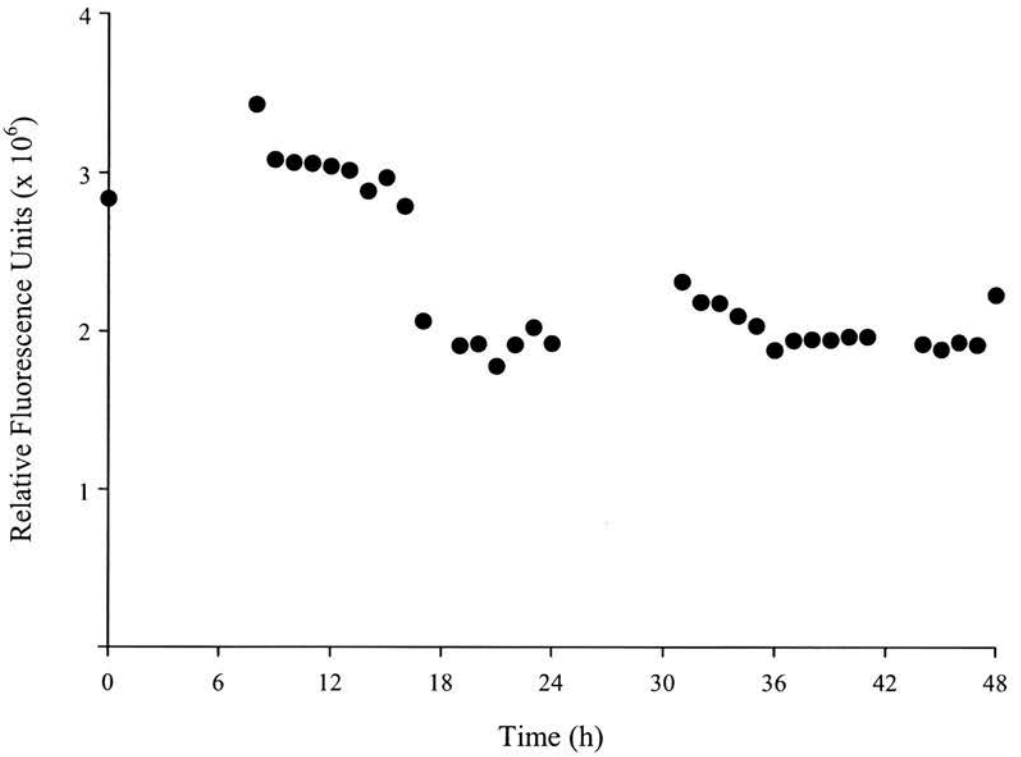

Time Course of Human β-Amyloid$_{1-42}$ Aggregation. β-Amyloid$_{1-42}$ was dissolved in magnesium and potassium-free PBS to a final concentration of 100 μM as recommended by Calbiochem® U.K. The state of aggregation of the peptide was then assessed by dilution in sterile water to a final assay concentration of 1 μM and addition of thioflavin T (10 μM final assay concentration), in a total assay volume of 200 μl. Fluorometric measurements were carried out in triplicate every 30 min for 48 h at 37°C using a Flexstation® Microplate Reader (Molecular Devices, U.K.) with excitation and emission wavelengths set to 444 nm and 485 nm, respectively. Between readings the plate was kept covered at 37°C in a CO_2 (5 %) incubator with the data shown representive of a typical experiment.

radioligand binding assay buffers ($p < 0.05$; Figure 4.2 A&B). Likewise, significant aggregation was not detected at $A\beta_{1-42}$ concentrations < 100 nM in samples serially diluted in electrophysiology buffer (Figure 4.2C). Furthermore, β-sheet aggregation was not detected in any of the diluted $A\beta_{1-42}$ samples at concentration of ≤ 10 nM, regardless of assay buffer (Figure 4.2).

4.2.1.3 Assessment of the Solubility/Aggregation State of Human $A\beta_{1-42}$ Dissolved in 5% Acetic Acid Solution

In the following experiments, a soluble Aβ solution is defined as one in which insignificant or no β-sheet aggregation is detected whilst "control" fluorescence refers to fluorescence measured in a 1 μM sample of pre-aggregated human $A\beta_{1-42}$ and serially diluted in the radioligand binding or electrophysiology buffers as described in Section 3.9.1.2. Calbiochem® recommend resuspending the human $A\beta_{1-42}$ in a 5 % acetic acid solution to generate a soluble form of $A\beta_{1-42}$. β-$Amyloid_{1-42}$ (100 μM) was resuspended in a 5 % acetic acid solution prior to serial dilution in radioligand binding assay and electrophysiological buffers, and assessed for β-sheet aggregation. Surprisingly, aggregation was detected at an $A\beta_{1-42}$ concentration of 1 μM in all the assay buffers examined (Figure 4.3). Levels of fluorescence were highest at 1 μM $A\beta_{1-42}$ in the [^{3}H]-MLA assay buffer (~17 x 10^3 r.f.u., Figure 4.3A) however, β-sheet aggregation was also detected at this concentration in both the [^{3}H]-cytisine assay (~6 x 10^3 r.f.u., Figure 3.30B) and electrophysiological buffers (~11 x 10^3 r.f.u., Figure 4.3C). At all other concentrations examined (0.1 – 100 nM), $A\beta_{1-42}$ in 5 % acetic acid showed little sign of fibril formation in any of the three assay buffers tested (Figure 4.3). Indeed, the amount of fluorescence measured did not reach 10 % of the control fluorescence (Figure 4.3).

4.2.1.4 Assessment of the Solubility/Aggregation State of Human $A\beta_{1-42}$ Dissolved in DMSO/Tris Solution

Wang and colleagues published the two pivotal papers showing that human $A\beta_{1-42}$ binds with picomolar affinity to the α_7 nAChR (Wang *et al.,* 2000a,b). In these papers human $A\beta_{1-42}$ was resuspended in a 50/50 mixture of DMSO and Tris HCl at pH 8.0 to form a soluble $A\beta_{1-42}$ solution (*personal communication*). Therefore, this method was used and human $A\beta_{1-42}$ was resuspended in the Wang DMSO/Tris solution and its degree of solubility/aggregation measured using the ThT assay.

Figure 4.2

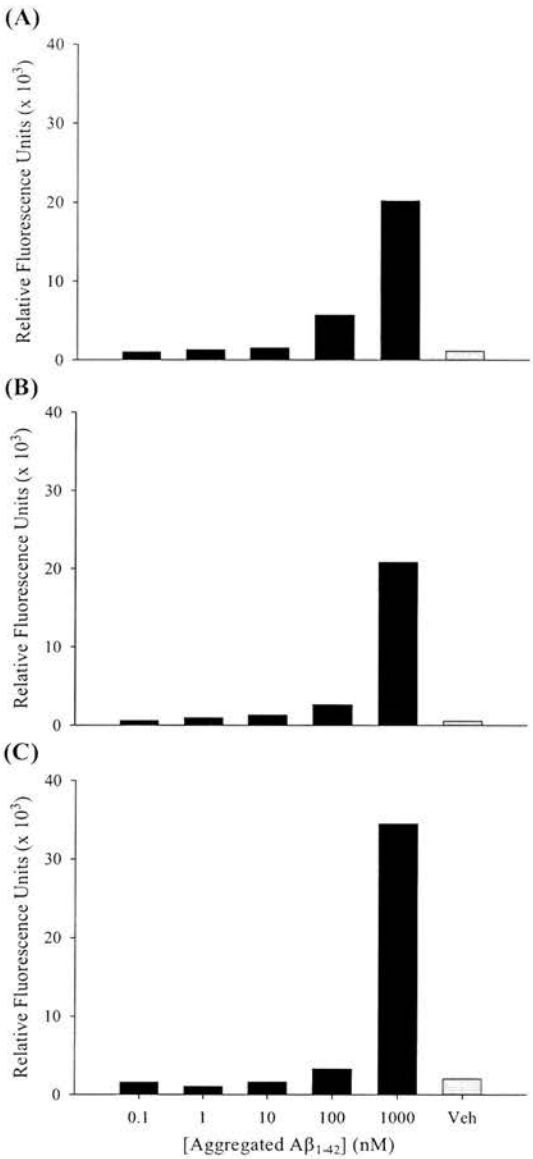

Effect of Dilution in Different Assay Buffers on Pre-Aggregated $A\beta_{1-42}$. Human $A\beta_{1-42}$ (1 mg/ml) was aggregated in a magnesium-free, potassium-free sterile water solution for 48 h at 37°C. Following this incubation, $A\beta_{1-42}$ was serially diluted in (A) [^{3}H]-MLA (α_7 nAChR), (B) [^{3}H]-cytisine ($\alpha_4\beta_2$ nAChR) or (C) electrophysiology assay buffers and aggregation assessed using the β-sheet specific dye Thioflavin T (10 μM). The degree of β-sheet aggregation was assessed by the relative amount of fluorescence intensity. Readings were made at 37°C using the Flexstation® fluorescence plate reader (excitation & emission wavelengths of 444 nm & 485 nm, respectively). When compared to control samples (ThT dye and buffer only), significant levels of β-sheet aggregation were detected in all the human $A\beta_{1-42}$ samples at amyloid concentrations of >100 nM, with the highest levels observed in samples diluted in electrophysiology buffer. Each data point was performed in triplicate.

Figure 4.3

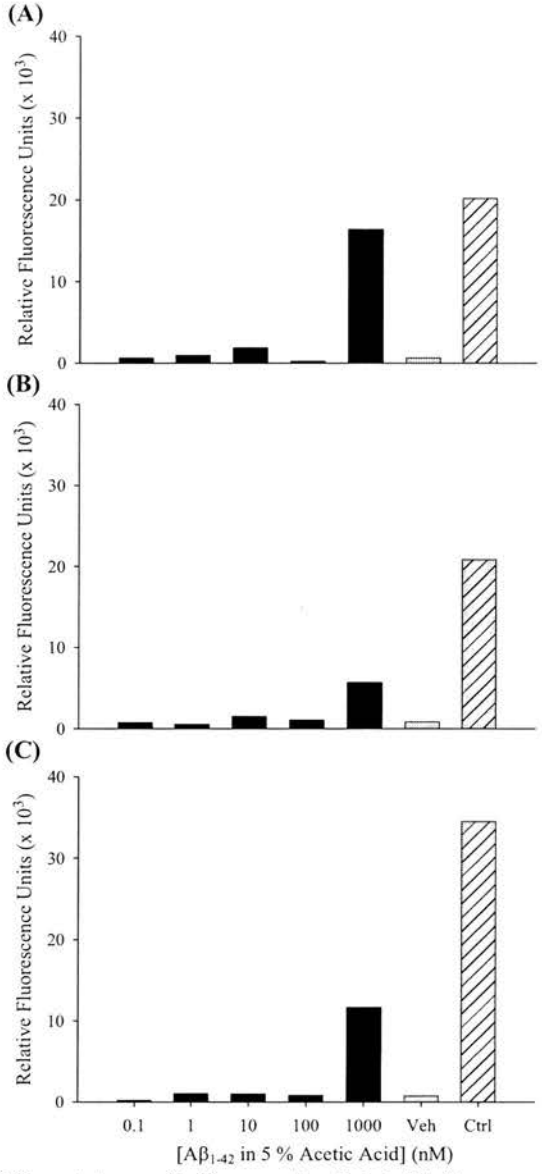

Effect of Dilution in Different Assay Buffers on the Solubility/Aggregation of $A\beta_{1-42}$ Solublised in 5 % Acetic Acid. Human $A\beta_{1-42}$ (100 μM) was solubilised in a 5 % acetic acid solution. Following this incubation, $A\beta_{1-42}$ was serially diluted in (A) [^{3}H]-MLA (α_7 nAChR), (B) [^{3}H]-cytisine ($\alpha_4\beta_2$ nAChR) or (C) electrophysiology assay buffers and assessed for aggregation using the β-sheet specific dye Thioflavin T (10 μM). The degree of β-sheet aggregation was assessed by the relative amount of fluorescence intensity. Readings were made at 37°C using the Flexstation® fluorescence plate reader (excitation and emission wavelengths of 444 nm and 485 nm, respectively). When compared to control samples (ThT dye and buffer only), significant levels of β-sheet aggregation were detected in all 1 μM human $A\beta_{1-42}$ samples. Each data point was performed in triplicate.

When assessed in terms of fluorescence intensity, a high level of β-sheet aggregation were present in the 1 μM human $A\beta_{1-42}$ samples in all three assay buffers examined (Figure 4.4). High levels of fluorescence intensity (indicating β-sheet aggregation) were also observed in the 100 nM $A\beta_{1-42}$ samples diluted in [^{3}H]-cytisine assay buffer (Figure 4.4B). Although the levels of aggregation in the 1 μM $A\beta_{1-42}$ samples dissolved in [^{3}H]-MLA and electrophysiology assay buffers exceeded that measured in their pre-aggregated controls (Figure 4.4 A & C), the 1 μM human $A\beta_{1-42}$ sample dissolved in [^{3}H]-cytisine assay buffer was not significantly different from its pre-aggregated control (Figure 4.4B). At all the other human $A\beta_{1-42}$ concentrations, the degree of aggregation was less than 6 % of their respective aggregated control (Figure 4.4).

4.2.1.5 Assessment of the Solubility/Aggregation State of Rpeptide $A\beta_{1-42}$

Until recently, $A\beta_{1-42}$ was only available as a lyophilized trifluoroacetate salt that required resuspension in a vehicle such as acetic acid or DMSO to generate a soluble Aβ solution. However, β-amyloid$_{1-42}$ prepared in 1,1,1,3,3,3-hexafluoro-2-propanol (HFIP) is now available from Rpeptide as an acetate salt. This has the advantage that the peptide may be resuspended in sterile water with negligible levels of acetic acid present in the final sample. As such, human $A\beta_{1-42}$ was purchased from Rpeptide and resuspended to 1 mg/ml according to their instructions prior to serial dilution in either radioligand or electrophysiology assay buffers.

Very high levels of fluorescence intensity were observed for all 1 μM $A\beta_{1-42}$ solutions regardless of the assay buffer used for dilution (Figure 4.5). Furthermore, at an $A\beta_{1-42}$ concentration of 100 nM, the fluorescence intensity was ~33 % of that observed in the control pre-aggregated samples (Figure 4.5). At concentrations of ≤ 10 nM, β-sheet aggregation was less than 5 % of the value observed in the control samples (Figure 4.5).

In summary, and with the exception of $A\beta_{1-42}$ (100 nM) solublised in DMSO/Tris HCl and diluted in [^{3}H]-cytisine assay buffer but including pre-aggregated controls, all $A\beta_{1-42}$ samples at concentrations of ≤ 100 nM exhibited negligible or no β-sheet aggregation in comparison to their equivalent pre-aggregated control. In contrast, all supposedly soluble and insoluble 1 μM $A\beta_{1-42}$ samples exhibited a significant degrees of β-sheet aggregation.

Figure 4.4

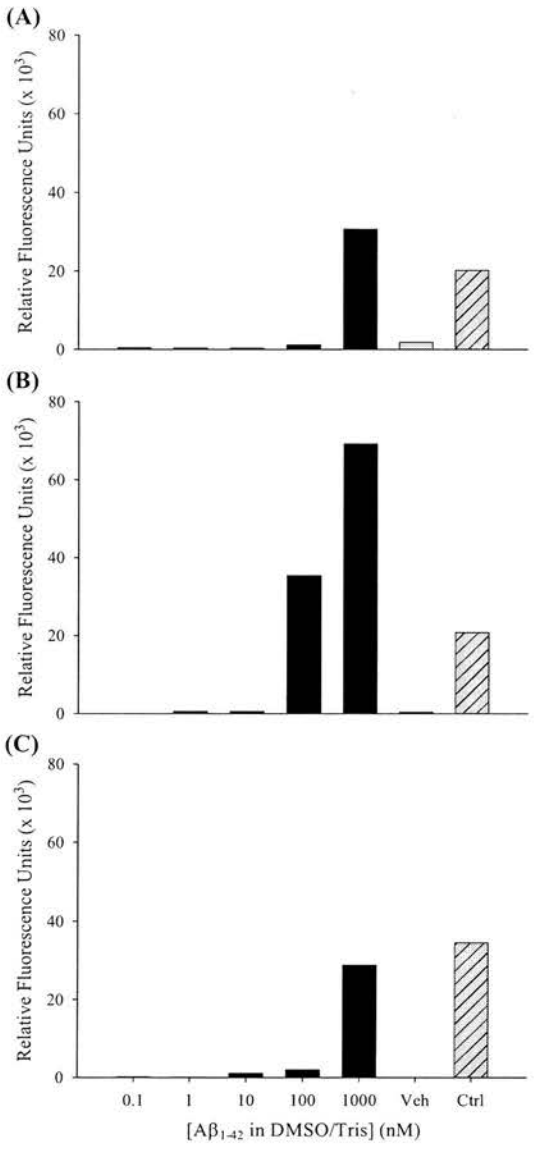

Effect of Dilution in Different Assay Buffers on the Solubility/Aggregation of $A\beta_{1-42}$ Solublised in 50/50 DMSO/Tris HCl. Human $A\beta_{1-42}$ (100 μM) was solubilised in a 50/50 mixture of DMSO/Tris (pH 8.5). Following this incubation, $A\beta_{1-42}$ was serially diluted in (A) [^{3}H]-MLA (α_7 nAChR), (B) [^{3}H]-cytisine ($\alpha_4\beta_2$ nAChR) or (C) electrophysiology assay buffers and assessed for aggregation using the β-sheet specific dye Thioflavin T (10 μM). The degree of β-sheet aggregation was assessed by the relative amount of fluorescence intensity. Readings were made at 37°C using the Flexstation® fluorescence plate reader (excitation and emission wavelengths of 444 nm and 485 nm, respectively). When compared to control samples (ThT dye and buffer only), significant levels of β-sheet aggregation were detected in all 1 μM human $A\beta_{1-42}$ samples, and at 100 nM when diluted in [^{3}H]-cytisine assay buffer. Each data point was performed in triplicate.

Figure 4.5

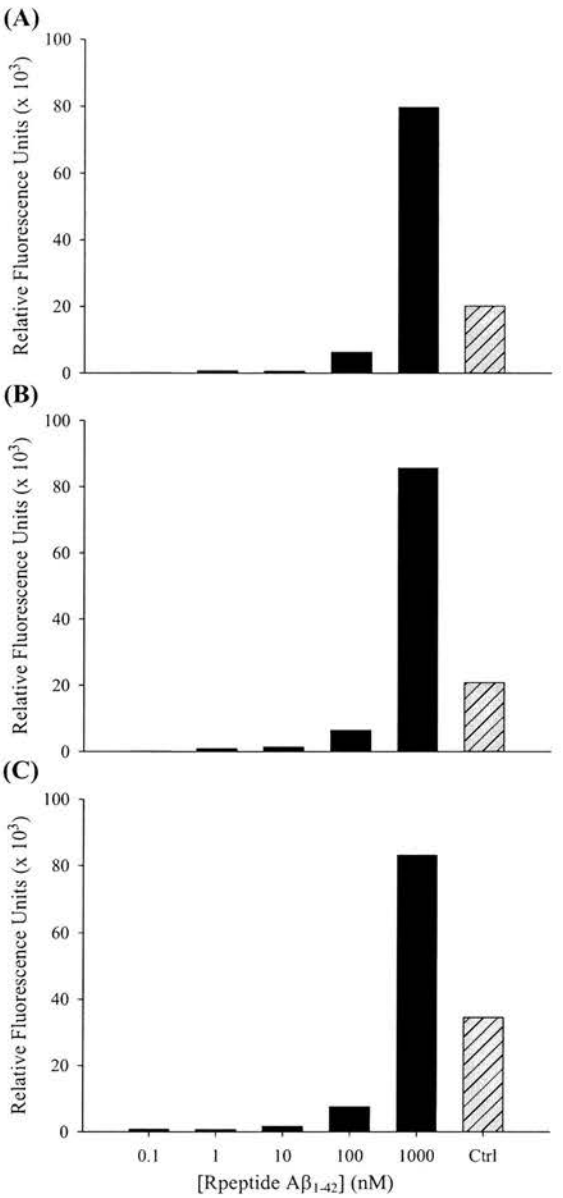

Effect of Dilution in Different Assay Buffer on the Solubility/Aggregation of Rpeptide $A\beta_{1-42}$. Human $A\beta_{1-42}$ (100 μM, Rpeptide) was solubilised in sterile water. Following this incubation, $A\beta_{1-42}$ was serially diluted in (A) [^{3}H]-MLA (α_7 nAChR), (B) [^{3}H]-cytisine ($\alpha_4\beta_2$ nAChR) or (C) electrophysiology assay buffers and assessed for aggregation using the β-sheet specific dye Thioflavin T (10 μM). The degree of β-sheet aggregation was assessed by the relative amount of fluorescence intensity. Readings were made at 37°C using the Flexstation® fluorescence plate reader (excitation and emission wavelengths of 444 nm and 485 nm, respectively). When compared to control samples (ThT dye and buffer only), significant levels of β-sheet aggregation were detected in all 1 μM human $A\beta_{1-42}$ samples. Each data point was performed in triplicate.

4.3 Human and Rat $A\beta_{1-42}$ Do Not Inhibit [^{3}H]-Cytisine or [^{3}H]-MLA Binding Sites in SH-EP1-h$\alpha_4\beta_2$ and SH-EP1-hα_7 Cell Membranes

Human $A\beta_{1-42}$ was purchased from Calbiochem and dissolved in a number of different vehicles to form putatively soluble (5 % acetic acid, 50/50 DMSO/Tris HCl, pH 8.0) or insoluble (magnesium and potassium-free PBS) solutions. The insoluble (aggregated) suspension was prepared 48 h in advance to induce aggregation as previously discussed. Following an initial resuspension, concentrated human $A\beta_{1-42}$ solutions were then serially diluted in either [^{3}H]-cytisine ($\alpha_4\beta_2$ nAChRs) or [^{3}H]-MLA (α_7 nAChRs) assay buffers. Due to Rpeptide $A\beta_{1-42}$ not being available when these initial experiments were performed, its ability to inhibit [^{3}H]-cytisine or [^{3}H]-MLA binding to SH-EP1-h$\alpha_4\beta_2$ or SH-EP1-hα_7 cell membranes, respectively, has not been assessed.

Regardless of the vehicle used for resuspension or the assay buffer used, human $A\beta_{1-42}$ (100 pM – 10 μM) did not inhibit either [^{3}H]-cytisine or [^{3}H]-MLA binding sites in membranes prepared from SH-EP1-h$\alpha_4\beta_2$ or SH-EP1-hα_7 cell membranes, respectively (Figures 4.6). The ability of rat $A\beta_{1-42}$ to inhibit [^{3}H]-MLA binding sites was also examined in rat and mouse brain membranes (Figure 4.7). In agreement with the observations for the human α_7 nAChR in the SH-EP1 cell membrane preparations, and again regardless of vehicle, rat $A\beta_{1-42}$ failed to inhibit [^{3}H]-MLA binding sites in either rat or mouse brain membranes. In contrast to Wang and colleagues (2000a), increasing the number of pre-assay washes of either the rodent brain or SH-EP1 cell membranes from three to five did not reveal any human or rat $A\beta_{1-42}$ inhibition of [^{3}H]-cytisine or [^{3}H]-MLA binding sites in rodent brain, SH-EP1-h$\alpha_4\beta_2$ or SH-EP1-hα_7 cell membranes (*data not shown*).

Figure 4.6

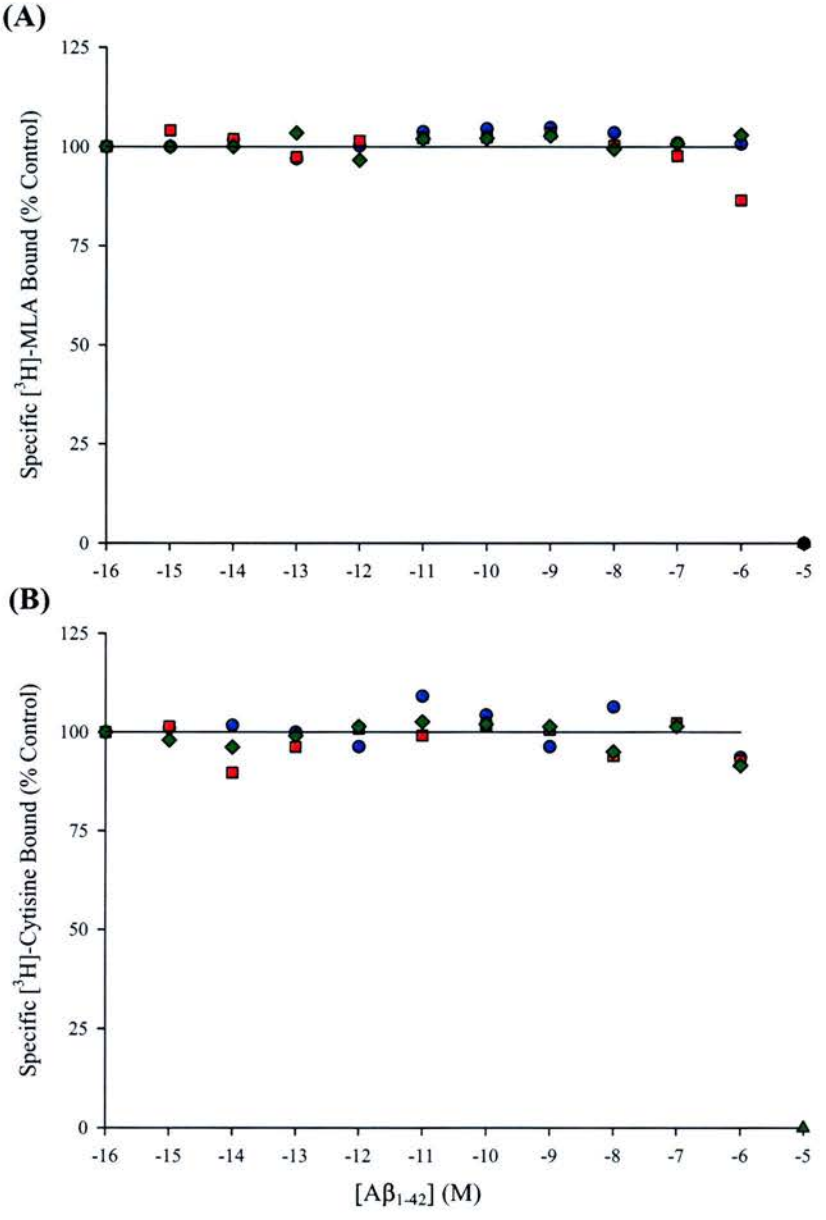

Human $A\beta_{1-42}$ Does Not Inhibit [^{3}H]-Cytisine or [^{3}H]-MLA Binding to Human $\alpha_4\beta_2$ or α_7 nAChRs. Human $A\beta_{1-42}$ was incubated (22°C) with (A) [^{3}H]-cytisine (3 nM) and SH-EP1-h$\alpha_4\beta_2$ membranes (115 µg) or (B) [^{3}H]-MLA and SH-EP1-hα_7 membranes (150 µg) in a total assay volume of 250 µl for 60 min. No human $A\beta_{1-42}$-induced inhibition of [^{3}H]-cytisine or [^{3}H]-MLA binding sites was observed. Symbols represent human $A\beta_{1-42}$ dissolved in 5% acetic acid (●), 50/50 DMSO/Tris HCl (■), or Aggregated in Mg^{2+} and K^+-free PBS (◆); ▲ represent their respective NSB. Non-specific binding was determined in the presence of 10 µM *d*-tubocurarine or 1 mM (-)nicotine with these data representing a typical experiment.

Figure 4.7

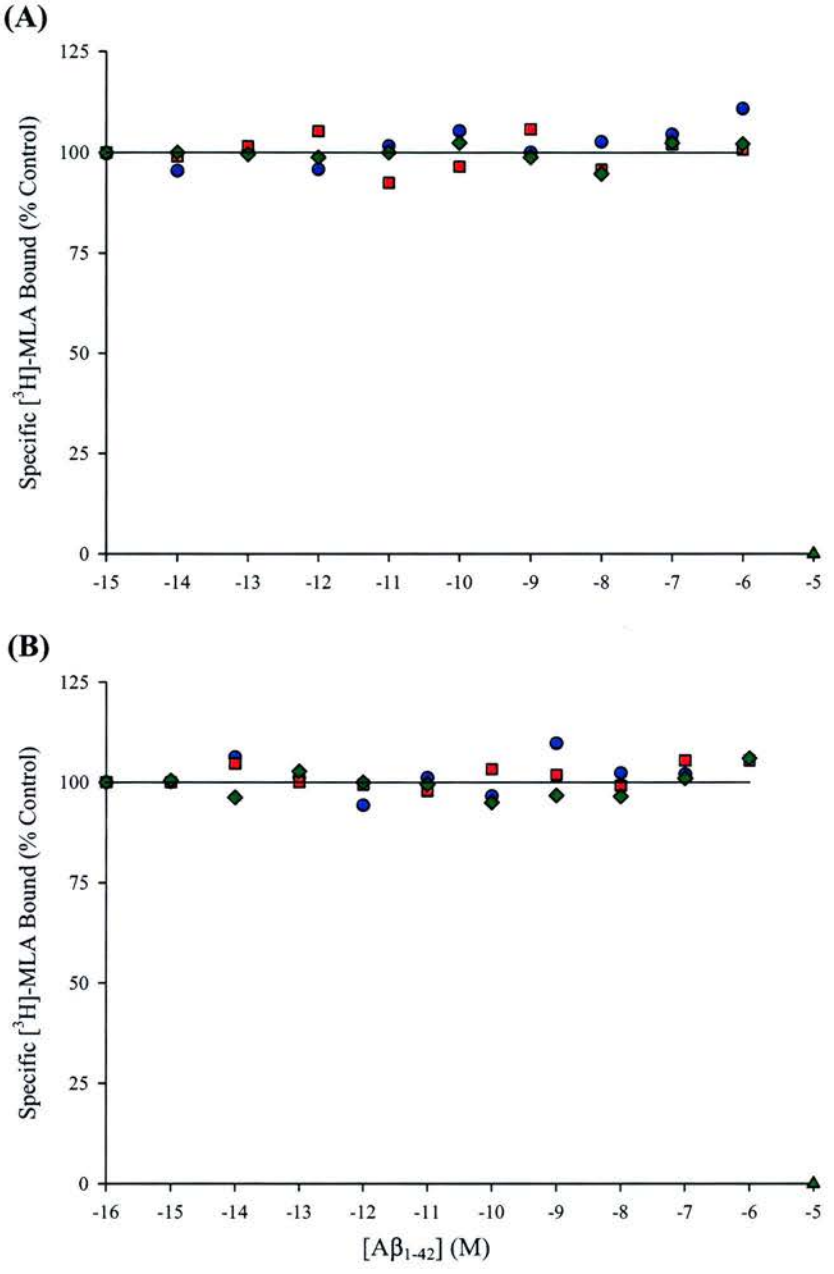

Rat $A\beta_{1-42}$ Does Not Inhibit [^{3}H]-MLA Binding to Rat or Mouse α_7 nAChRs. Rat $A\beta_{1-42}$ was incubated (22°C) with [^{3}H]-MLA (2.5 nM) and (A) rat brain (400 µg) or (B) mouse brain membranes (850 µg) in a total assay volume of 250 µl for 60 min. No rat $A\beta_{1-42}$-induced inhibition of [^{3}H]-MLA binding sites was observed. Symbols represent human $A\beta_{1-42}$ dissolved in 5% acetic acid (●), 50/50 DMSO/Tris HCl (■), or Aggregated in Mg^{2+} and K^+-free PBS (◆); ▲ represent their respective NSB. Non-specific binding was determined in the presence of 10 µM *d*-tubocurarine with these data representing a typical experiment.

4.4 DISCUSSION

As mentioned earlier, a number of recent studies have looked at the effects of $A\beta_{1-42}$ on functional responses at α_7 and $\alpha_4\beta_2$ nAChRs (Dineley *et al.,* 2001, 2002a; Liu *et al.,* 2001; Pettit *et al.,* 2001; Tozaki *et al.,* 2002; Eaton *et al.,* 2003; Fu & Jhamandas, 2003; Wu *et al.,* 2004), with only a limited number assessing binding (Wang *et al.,* 2000a,b; de Fiebre & de Fiebre, 2005). Despite extensive pharmacological characterisation of both the [^{3}H]-cytisine and [^{3}H]-MLA binding assays, these studies provided no direct pharmacological evidence that human $A\beta_{1-42}$ could inhibit radioligand binding to human $\alpha_4\beta_2$ or α_7 nAChRs, or indeed to rat or mouse membranes. The preparation of $A\beta_{1-42}$ to promote the solubility (in 5 % acetic acid or 50/50 DMSO/Tris HCl, pH 8.0) or insolubility (aggregated in Mg^{2+}-free, K^+-free PBS and MQ H_2O for 48 h) of the peptide had no effect on these results, with no form of amyloid directly inhibiting binding at concentrations of up to 10 μM. These findings are in direct contrast to those of Wang and colleagues (2000a,b) who showed human $A\beta_{1-42}$ (prepared in 50/50 DMSO/Tris) selectively inhibited [^{3}H]-MLA and [^{125}]-αBgTx binding to human α_7 nAChRs expressed in SK-N-MC cell membranes. However, our finding is in agreement with de Fiebre and de Fiebre (2005) who reported that rat $A\beta_{1-42}$ did not inhibit [^{125}I]-αBgTx binding to mouse α_7 nAChRs.

Interestingly, neither de Fiebre and de Fiebre (2005) nor Wang *et al.*, (2000a,b) discussed the state of $A\beta_{1-42}$ aggregation in their respective studies. By examining the potential putative conformation of $A\beta_{1-42}$ in all the vehicles used in the current study and those presented in Chapter 4, the Thioflavin T studies revealed that regardless of vehicle or assay buffer used, amyloid conformation was dependent on its concentration. All 1 μM samples of $A\beta_{1-42}$ yielded positive signs of aggregation in the Thioflavin T assay (Section 3.7.1, pg 108). Surprisingly, using the 50/50 DMSO/Tris HCl vehicle, favoured by Wang and colleagues (2000a,b), $A\beta_{1-42}$ diluted in the [^{3}H]-cytisine assay buffer exhibited signs of aggregation at a concentration of 100 μM. Furthermore, even in protocols designed to cause $A\beta_{1-42}$ aggregation, the peptide only exhibited signs of aggregation concentrations in excess of 1 μM. At all other concentrations (0.1 nM – 1 μM) examined in the three assay buffers ([^{3}H]-cytisine, [^{3}H]-MLA, and electrophysiology), human $A\beta_{1-42}$ failed to show signs of aggregation. These findings highlight the difficulty of working with solutions of β-amyloid and the necessity to try and determine whether you have soluble or aggregated $A\beta_{1-42}$ before including the peptide in any study.

Wang and colleagues (2000a) reported that multiple washings of SK-N-MC cells were required to remove soluble factors such as the endoplasmic reticulum amyloid binding protein, and thereby uncover high affinity [^{3}H]-MLA binding sites for $A\beta_{1-42}$. Even after

incorporating this 5-step washing protocol, we could provide no evidence that $A\beta_{1-42}$ inhibited [^{3}H]-MLA binding. De Fiebre and de Fiebre (2005) suggest that this extensive washing of membranes may have uncovered non-α_7 nAChR binding sites for [^{3}H]-MLA and $A\beta_{1-42}$. Furthermore, it is unlikely that the choice of radiolabel plays a role in the negative response observed by de Fiebre and de Fiebre (2005) ([^{125}I]-αBgTx) and ourselves ([^{3}H]-MLA) as Wang and colleagues (2000a,b) utilised both [^{125}I]-αBgTx and [^{3}H]-MLA with identical positive results. Therefore, the major differences between the various assays appear to be technique, vehicle and tissue of choice. However, little detail is given on the exact assay conditions (incubation times, filtrations systems, plates, etc) under which these experiments were performed (Wang *et al.,* 2000a,b; de Fiebre & de Fiebre, 2005).

Both Wang and colleagues (2000a,b, personal communication) and I dissolved human $A\beta_{1-42}$ in a 50/50 mixture of DMSO and Tris HCl at pH 8.0 but with different results. Again, de Fiebre and de Fiebre (2005) used rat $A\beta_{1-42}$ dissolved in either distilled water (and then incubated to promote aggregation) or in HEPES buffer to promote solubility and failed to show $A\beta_{1-42}$-induced inhibition of [^{125}I]-αBgTx binding sites. The other major difference in experimental protocol between Wang and colleagues (2000a,b) and the current studies lie in the choice of cell line for α_7 nAChR expression (Figure 3.32, pg 116). Wang and colleagues (2000a,b) utilised the SK-N-MC cell line to over-express the human α_7 nAChR while we used the SH-EP1 cell line. In contrast, both de Fiebre and de Fiebre (2005) and ourselves used mouse brain homogenates while we also used rat brain homogenates (Figure 3.34, pg 119). Alpha7 nAChRs are notoriously difficult to stably express in cell systems (Cooper & Millar, 1997; Peng *et al.*, 1999; Schroeder *et al.*, 2003; Craig *et al.*, 2004; Williams *et al.*, 2005) and although it is possible that there is a difference in receptor conformation of the α_7 nAChR in the SK-N-MC cell line in comparision to the SH-EP1-hα_7 cells, Biedler and colleagues (1979) did show that these cells were derived from the same original source. However, this would not explain the lack of $A\beta_{1-42}$ inhibition of [^{125}I]-αBgTx binding sites in rat brain homogenates in the current studies and in the mouse brain homogenates used by de Fiebre and de Fiebre (2005).

In addition to [^{3}H]-MLA binding, we showed for the first time that human $A\beta_{1-42}$ did not inhibit [^{3}H]-cytisine binding sites in the SH-EP1-h$\alpha_4\beta_2$ cell line. Although, Wang *et al.*, (2000b) investigated the effects of amyloid on [^{3}H]-cytisine binding sites in rat brain membranes, they did not observe any inhibition.

4.5 CONCLUSIONS

In order to examine any potential pharmacological interaction between $A\beta_{1-42}$ and the nAChRs $\alpha_4\beta_2$ and α_7, I have established the solubility of $A\beta_{1-42}$ in a variety of different vehicles. Furthermore, I have presented evidence that soluble and insoluble forms of human $A\beta_{1-42}$ do not inhibit [^{3}H]-MLA binding to the human α_7 nAChR nor do they inhibit [^{3}H]-cytisine binding to the human $\alpha_4\beta_2$ nAChR. This latter data has been published in two book chapters (Crawford *et al.,* 2004; Finlayson *et al.,* 2005).

5.0 FUNCTIONAL ANALYSIS OF $\alpha_4\beta_2$ AND α_7 nAChRs

5.1 INTRODUCTION

A number of recent studies have examined the functional interaction between $A\beta_{1-42}$ and nAChRs (Kihara *et al.*, 1998; Dineley *et al.*, 2001; Kihara *et al.*, 2001; Liu *et al.*, 2001; Pettit *et al.*, 2001; Tozaki *et al.*, 2002; Dineley *et al.*, 2002a; Fu & Jhamandas, 2003; Grassi *et al.*, 2003; Fodero *et al.*, 2004; Wu *et al.*, 2004). The majority of these studies have focused on the functional interaction between $A\beta_{1-42}$ and the α_7 nAChR (Dineley *et al.*, 2001; Liu *et al.*, 2001; Pettit *et al.*, 2001; Dineley *et al.*, 2002a; Grassi *et al.*, 2003; Fodero *et al.*, 2004). However, the interaction of $A\beta_{1-42}$ with nAChRs is not exclusive to the α_7 nAChR with several studies examining the role of the $\alpha_4\beta_2$ nAChR (Kihara *et al.*, 1998; Tozaki *et al.*, 2002; Fu & Jhamandas, 2003; Fodero *et al.*, 2004; Wu *et al.*, 2004; Lamb *et al.*, 2005). All of the above studies have utilised electrophysiology and have been performed using both native (e.g. the rat hippocampal slice) and expressed nAChRs (e.g. in nAChR-null cell lines or in Xenopus oocytes). As well as the complexity of comparing different preparations of $A\beta_{1-42}$, these studies are further complicated by the number of vehicles in which $A\beta_{1-42}$ has been prepared. For examples, Liu and colleagues (2001) used rat $A\beta_{1-42}$ resuspended in 5 % acetic acid whilst Dineley and colleagues (2001) used a HEPES buffer.

In AD, the exact neurotoxic form of $A\beta_{1-42}$ remains the subject of much debate. Indeed, in the studies mentioned above, $A\beta_{1-42}$ has been dissolved in a range of vehicles to produce both soluble and insoluble $A\beta_{1-42}$. However, although $A\beta_{1-42}$ itself appears to inhibit responses at both $\alpha_4\beta_2$ and α_7 nAChRs, it is perhaps surprisingly that very few of these studies closely examine the effect of the $A\beta_{1-42}$ vehicles used (Kihara *et al.*, 1998; Dineley *et al.*, 2001; Kihara *et al.*, 2001; Liu *et al.*, 2001; Pettit *et al.*, 2001; Tozaki *et al.*, 2002; Dineley *et al.*, 2002a; Fu & Jhamandas, 2003; Grassi *et al.*, 2003; Fodero *et al.*, 2004; Wu *et al.*, 2004). The vehicles used to dissolve $A\beta$ were as diverse as 5 % acetic acid (Liu *et al.*, 2001), 50/50 DMSO/Tris (Wang *et al.*, 2000a, Wang *et al.*, 2000b, personal communication), HEPES buffer (Dineley *et al.*, 2001), and sterile water (Wu *et al.*, 2004).

The maintenance of stable functional expression of nAChRs, in particular the α_7 subtype, also presents a considerable challenge (Cooper & Millar, 1997). In contrast to the $\alpha_4\beta_2$ nAChR, which can be easily over-expressed in cell lines (Gopalakrishnan *et al.*, 1996), only limited reports of successful α_7 nAChR expression exist (Puchacz et al., 1994; Quik et al., 1996; Peng et al., 1999; Zhao et al., 2003), with a number of papers highlighting problems in maintaining stable expression in mammalian cell lines (Cooper & Millar, 1997;

Peng *et al.*, 1999; Sweileh *et al.*, 2000). A considerable amount of research has focused on increasing surface expression by altering cell culture conditions (Molinari *et al.*, 1998; Schroeder *et al.*, 2003), generating α_7-5HT$_3$ chimera's (Eisele et al., 1993; Craig et al., 2004), or by using site-directed mutagenesis studies (Dineley & Patrick, 2000). Indeed, a non-densensitising mutant has also been used *in vitro* and *in vivo* (Orr-Urtreger *et al.*, 2000; Broide *et al.*, 2001; Gil *et al.*, 2002; Dineley *et al.*, 2002a). As discussed in Chapter 3, SH-EP1 cell lines over-expressing the $\alpha_4\beta_2$ and α_7 nAChRs were used for the examination of the functional interaction with human A$\beta_{1\text{-}42}$. SH-EP1 cells contain no native nAChRs, however there are reports of successful expression of the human $\alpha_4\beta_2$ (SH-EP1-h$\alpha_4\beta_2$) and human α_7 (SH-EP1-hα_7) nAChRs (Peng *et al.*, 1999; Eaton *et al.*, 2003; Schroeder *et al.*, 2003; Wu *et al.*, 2004). To comprehensively examine whether human A$\beta_{1\text{-}42}$ has any direct or indirect effect on the $\alpha_4\beta_2$ and α_7 nAChR subtypes, A$\beta_{1\text{-}42}$ was dissolved in several different vehicles to produce both soluble and insoluble forms of A$\beta_{1\text{-}42}$. A number of approaches were taken and include the ability of human A$\beta_{1\text{-}42}$ to effect changes in intracellular calcium or membrane potential, assessed using fluorescence-based assays. Both these assays have been used to assess the functionality of nAChRs with the membrane potential recently shown to be potentially more sensitive than the calcium assay (Fitch *et al.*, 2003). These assays use calcium-sensitive or membrane potential-sensitive fluorescent dyes to assess changes in intracellular calcium and ionic flux, respectively. Whole cell current recording was used to characterise the pharmacology and re-confirm functional expression of $\alpha_4\beta_2$ and α_7 nAChRs in the SH-EP1 stable cell line.

Finally, a recent study has shown A$\beta_{1\text{-}42}$ to co-localise with the α_7 nAChR in tissue from human AD patients (Wang *et al.*, 2000a). Furthermore, it has been demonstrated that amyloid plaque accumulation is accelerated in transgenic mice co-expressing the mutant human presenilin I and amyloid precursor proteins and that the α_7 nAChR is simultaneously upregulated in these animals (Dineley *et al.*, 2002b). Following on from these initial studies, a more direct role for the α_7 nAChR in A$\beta_{1\text{-}42}$ accummulation has been demonstrated (Nagele *et al.*, 2002; Wang *et al.*, 2002). Nagele and colleagues (2002) demonstrated a substantial intracellular accumulation of A$\beta_{1\text{-}42}$ in neurons expressing relatively high levels of α_7 nAChRs. Furthermore, they demonstrated that the rate and extent of A$\beta_{1\text{-}42}$ in these cerebellar neurons was directly proportional to the level of α_7 nAChR protein expression. Wang and colleagues (2002) extended these finding using the neuroblastoma cells expressing high levels of α_7 nAChR, showing rapid internalisation and intracellular

accumulation of $A\beta_{1-42}$ in these cells *in vitro*. As a consequence, I incubated SH-EP1 cells over-expressing either the human $\alpha_4\beta_2$ or α_7 nAChRs with human $A\beta_{1-42}$ and preformed co-immunoprecipitation experiments to examine co-localisation of these human nAChR subtypes with human $A\beta_{1-42}$.

5.2 RESULTS

5.2 Characterisation of Calcium and Membrane Potential Responses in Human $\alpha_4\beta_2$ and α_7 nAChRs

Functional assays for ion channels include classical electrophysiology (Velicelebi *et al.*, 1999; Fucile *et al.*, 2002; Palma *et al.*, 2002; Fayuk & Yakel, 2005), radioisotopic ion flux (Lukas & Cullen, 1988; Bertrand *et al.*, 1997), and fluorescence assays using ion- or voltage-sensitive dyes (Manning & Sontheimer, 1999; Chavez-Noriega *et al.*, 2000; Fitch *et al.*, 2003). In order to detect any functional interaction between the human nAChR subtypes $\alpha_4\beta_2$ and α_7, simple population cell-based assays were performed prior to undertaking data rich but labour-intensive, and complex whole cell patch clamp electrophysiology studies (see Section 5.3). The following two sections describe the characterisation of calcium flux and membrane potential assays in SH-EP1-h$\alpha_4\beta_2$ and SH-EP1-hα_7 cell lines.

5.2.1 Characterisation of Intracellular Calcium ($[Ca^{2+}]_i$) Responses in SH-EP1-h$\alpha_4\beta_2$ Cells.

5.2.1.1 Effect of Cell Density on (-)Nicotine Evoked $[Ca^{2+}]_i$ Responses in SH-EP1-h$\alpha_4\beta_2$ Cells

The calcium flux assay is a cell based fluorescence assay in which changes in intracellular calcium are detected by loading cells with a calcium-sensitive fluorescent dye. The signal is then detected using a standard 510-570 nm emission filter on a fluorescent plate reader such as the FLEXstation® (Molecular Devices (MD), U.K.).

To determine whether exposure to (-)nicotine could elicit $[Ca^{2+}]_i$ response in SH-EP1-h$\alpha_4\beta_2$ cells, different cell densities were plated (50,000, 75,000, and 100,000 cells per well) and incubated overnight. (-)Nicotine produced a concentration-dependent increase with a half-maximal concentration (EC_{50}) of 11.3 nM (50,000 cells), 12.2 nM (75,000 cells) and 12.0 nM (100,000 cells) giving an overall EC_{50} of 11.8 ± 0.4 nM with a Hillslope (n_H) of 1.44 ± 0.4 (n = 3; Figure 5.1). Although the EC_{50} of (-)nicotine was similar at all 3 cell densities, the maximum fluorescence was density-dependent. At a maximal concentration (1 μM) (-)nicotine produced 35.1 ± 0.6 (x 10^3) relative fluorescence units (r.f.u.) when plated at a density of 50,000 cells per well, 53.8 ± 1.1 (x 10^3) r.f.u. at 75,000 cells per well, and 75.0 ± 0.4 (x 10^3) r.f.u. at 100,000 cells per well (Figure 5.1). When cells were plated at 100,000 cells/well a consistent level of confluency was attained, whilst a further increase in cell density resulted in irregular adherence of SH-EP1-h$\alpha_4\beta_2$ cells, and a greater variation in

signal. As such, all subsequent experiments were performed at a SH-EP1-h$\alpha_4\beta_2$ cell density of 100,000 cells/well.

5.2.1.2 Effect of Additional External Calcium on the $[Ca^{2+}]_i$ Response Size in SH-EP1-h$\alpha_4\beta_2$ Cells

It is well documented that nAChR function is modulated by the external Ca^{2+} concentration (Mulle *et al.*, 1992; Vernino *et al.*, 1992; Chavez-Noriega *et al.*, 2000). Indeed, a potentiation of agonist-induced responses is observed at low calcium concentrations, with less enhancement observed at relatively high calcium concentrations (Mulle *et al.*, 1992; Chavez-Noriega *et al.*, 2000). To determine if the (-)nicotine-induced $[Ca^{2+}]_i$ response in SH-EP1-h$\alpha_4\beta_2$ cells was sensitive to changes in external Ca^{2+}, increasing concentration of calcium were included in the buffer prior to exposure to (-)nicotine (10 nM) addition. The standard calcium assay kit buffer (MD, U.K.) already contains 1.4 mM Ca^{2+}, therefore the addition of 2.5 to 20 mM Ca^{2+} gave a final external Ca^{2+} assay concentration that ranged from 1.4 to 21.4 mM. Even the addition of just 2.5 mM Ca^{2+} resulted in a considerable increase in the (-)nicotine evoked $[Ca^{2+}]_i$ response in SH-EP1-h$\alpha_4\beta_2$ cells (Figure 5.2). As such, in all subsequent experiments 2.5 mM Ca^{2+} was added to the assay buffer giving a final Ca^{2+} concentration of 3.9 mM.

5.2.1.3 Pharmacological Characterisation of $[Ca^{2+}]_i$ Responses in SH-EP1-h$\alpha_4\beta_2$ Cells

Prior to examining the effect of human $A\beta_{1-42}$ on $[Ca^{2+}]_i$ responses in SH-EP1-h$\alpha_4\beta_2$ cells, the pharmacological profile of this receptor subtype was determined. To determine the half-effective concentration (EC_{50}) of agonists in the SH-EP1-h$\alpha_4\beta_2$ cell line, data was collected over a range of agonist concentrations (0.001 – 3 μM) fitted to the maximal response and analysed with the empirical Hill equation. The rank order of potency for the three nicotinic agonists studied was (±)epibatidine > (-) nicotine = cytisine, with normalised data shown in Figure 5.3. The EC_{50} value determined for (±)epibatidine was 1.04 ± 0.11 nM (n_H = 1.63 ± 0.25; n = 3), while the EC_{50} for cytisine was 18.3 ± 7.73 nM; n_H = 0.83 ± 0.4; n =3) and (-)nicotine 22.8 ± 6.9 nM; n_H = 1.43 ± 0.42; n = 3; Figure 5.3). Having established and characterised $\alpha_4\beta_2$ nAChR response to these nicotinic agonists, antagonist pharmacology was assessed using (-)nicotine at a concentration of 10 nM, close to its EC_{50} value. Figure 5.4 shows concentration-dependent inhibition of the (-)nicotine

Figure 5.1

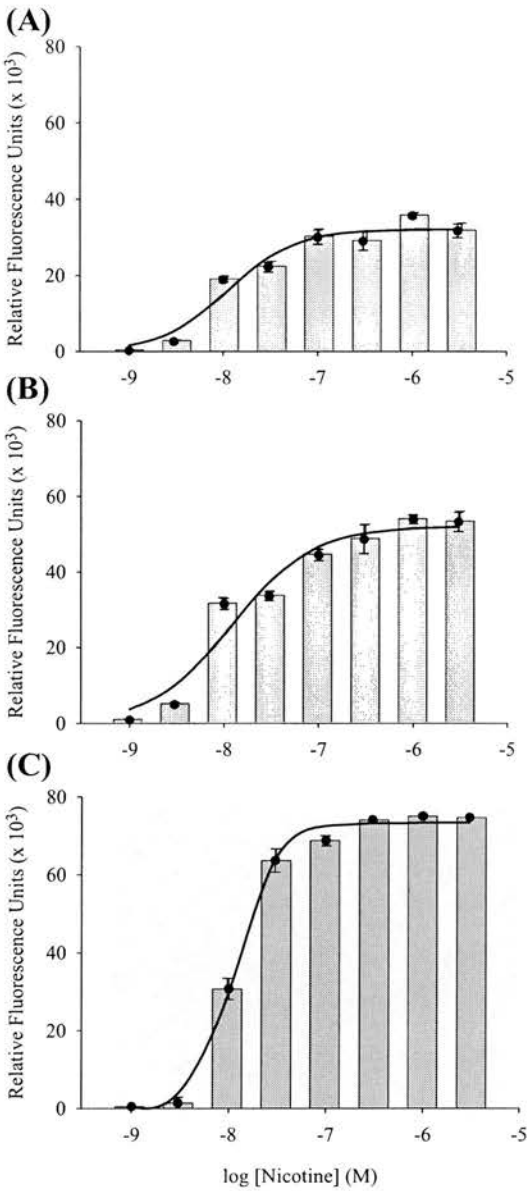

Effect of Cell Density on (-)Nicotine-Evoked $[Ca^{2+}]_i$ Responses in SH-EP1-h$\alpha_4\beta_2$ Cells. Cells were plated at (A) 50,000 (B) 75,000 or (C) 100,000 cells per well in a poly-D-lysine coated 96-well plate and incubated overnight (37°C). Calcium assay buffer and fluorescence dye (MD, UK) were added as detailed in methods. (-)Nicotine concentrations were applied using the robotic microinjection system within the Flexstation fluorescence plate reader (MD, U.K.) and changes in fluorescence analysed. Excitation and emission wavelengths were set to 485 nm and 525 nm, respectively, with these data (maximum response - minimum response) representive of a typical experiment performed in triplicate. Affinity (EC_{50}) was similar at all cell densities, however, maximal fluorescence and confluency of cells was achieved at a cell density of 100,000 cells per well.

Figure 5.2

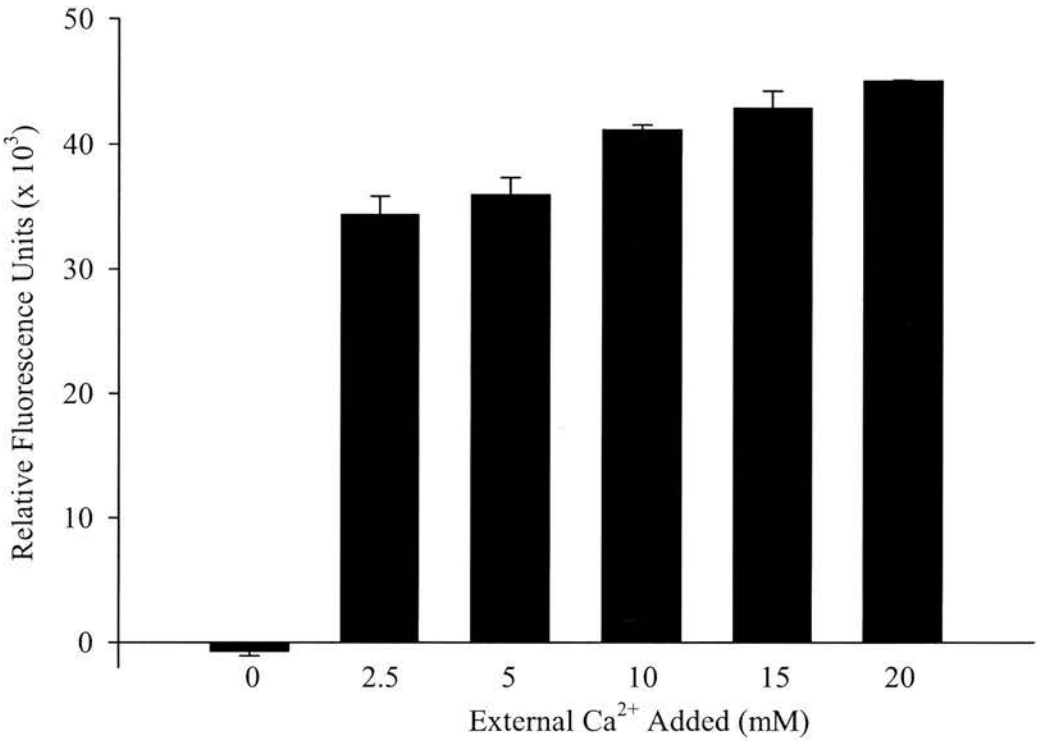

Effect of Adding Additional External Ca^{2+} on the (-)Nicotine Evoked $[Ca^{2+}]_i$ Response in SH-EP1-h$\alpha_4\beta_2$ Cells. Standard calcium assay kit buffer (MD, U.K.) contains 1.4 mM Ca^{2+}, therefore the final assay concentration ranged from 1.4 mM to 21.4 mM. Cells were loaded with a calcium-sensitive dye as described in *Materials and Methods*. (-)Nicotine concentrations were applied using the robotic microinjection system within the Flexstation® (MD, U.K.) and changes in $[Ca^{2+}]_i$ analysed. Excitation and emission wavelengths were set to 485 nm and 525 nm, respectively. These data represent a typical experiment with each data point representing the mean value (maximum response – minimum response) of three experiments.

Figure 5.3

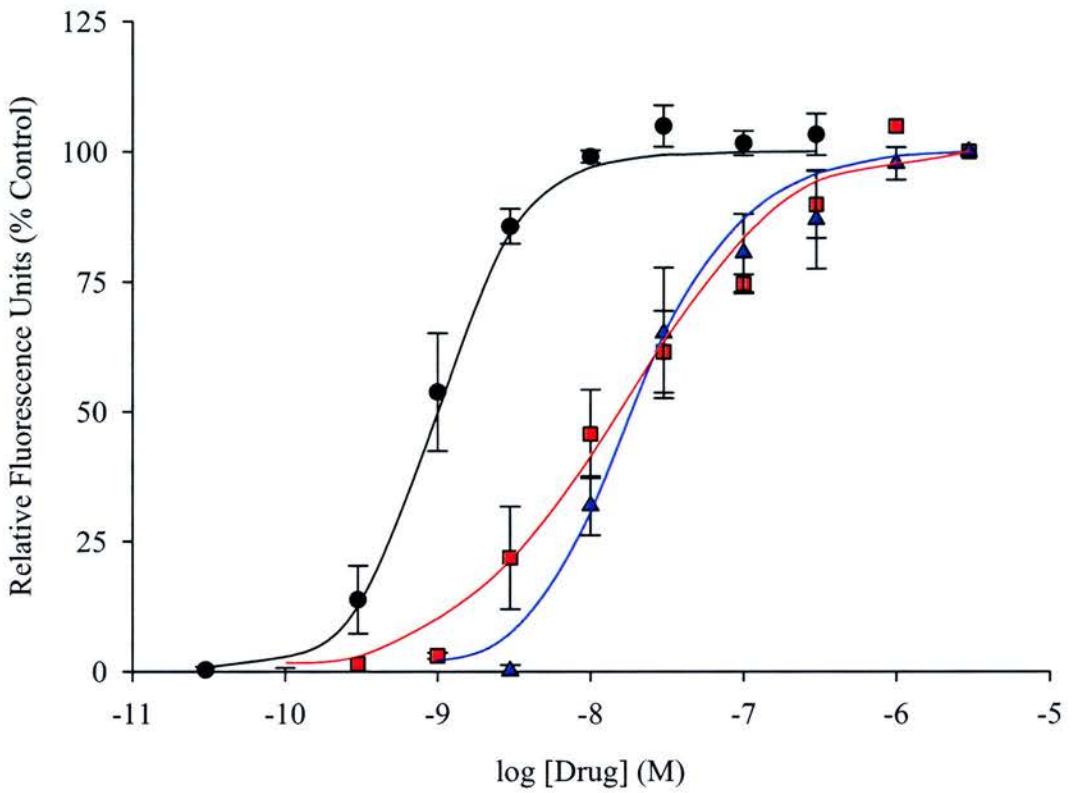

Nicotinic Agonists Produce a Concentration-Dependent Increase in $[Ca^{2+}]_i$ in SH-EP1-h$\alpha_4\beta_2$ Cells. The nAChR agonists (±)epibatidine (●), cytisine (■), and (-)nicotine (▲) evoked a large increase in $[Ca^{2+}]_i$ in a concentration-dependent manner. Calcium assay buffer and fluorescence dye (MD, UK) were added as detailed in methods. Agonist concentrations were applied using the robotic microinjection system within the Flexstation fluorescence plate reader (MD, U.K.) and changes in $[Ca^{2+}]_i$ analysed. Excitation and emission wavelengths were set to 485 nm and 525 nm, respectively, with these data (maximum response - minimum response) representive of a typical experiment performed in triplicate. The rank order of potency for the three nicotinic ligands examined was (±)epibatidine > (-)nicotine = cytisine.

-induced $[Ca^{2+}]_i$ response by the nicotinic antagonists MLA and *d*-tubocurarine in SH-EP1-h$\alpha_4\beta_2$ cells. IC_{50} were 876 ± 66 nM (n_H = 1.61 ± 0.33; n = 3) and 5,315 ± 367 μM (n_H = 1.44 ± 0.62; n = 4) for MLA and *d*-TC, respectively. Antagonists had no effect on $[Ca^{2+}]_i$ response on their own (data not shown).

5.2.1.4 The Effect of Human $A\beta_{1-42}$ on $[Ca^{2+}]_i$ Responses in SH-EP1-h$\alpha_4\beta_2$ Cells

The issue over which form of Aβ is neurotoxic in AD is not resolved (Selkoe, 1993; Tucker *et al.*, 2002; Walsh *et al.*, 2002a) and as previously discussed, $A\beta_{1-42}$ is routinely dissolved in a range of vehicles to produce soluble and insoluble forms of the peptide (Wang *et al.*, 2000a; Wang *et al.*, 2000b; Dineley *et al.*, 2001; Liu *et al.*, 2001; Pettit *et al.*, 2001; Tozaki *et al.*, 2002; Dineley *et al.*, 2002a; Wu *et al.*, 2004). Therefore, the ability of both soluble and insoluble human $A\beta_{1-42}$ to inhibit (-)nicotine-induced $[Ca^{2+}]_i$ responses in SH-EP1-h$\alpha_4\beta_2$ cells was examined. (-)Nicotine was again used at a concentration of 10 nM, consistent with the antagonist studies above.

Human $A\beta_{1-42}$ was dissolved in 100 mM HEPES (pH 8.0) and the effect that this soluble form of $A\beta_{1-42}$ had on (-)nicotine, (±)epibatidine, and cytisine-evoked changes in $[Ca^{2+}]_i$ in SH-EP1-h$\alpha_4\beta_2$ cells was examined (Figure 5.5). On average, $A\beta_{1-42}$ had no effect on agonist-evoked changes in $[Ca^{2+}]_I$ in the SH-EP1-h$\alpha_4\beta_2$ cell line. When $A\beta_{1-42}$ (≤ 10 μM) was dissolved in 5% acetic acid (Figure 5.6A), a 50/50 mixture of DMSO/Tris HCl (Figure 5.6B), or reconstituted as the Rpeptide water soluble acetate salt (Figure 4.6C), no form of soluble human $A\beta_{1-42}$ inhibited the (-)nicotine-evoked changes in $[Ca^{2+}]_i$ in the SH-EP-h$\alpha_4\beta_2$ cell line. Although 10 μM $A\beta_{1-42}$, in the 5% acetic acid and 50/50 DMSO/Tris HCl vehicles appeared to produce significant inhibition (5 % acetic acid) or potentiation (DMSO/Tris) of (-)nicotine-evoked changes in $[Ca^{2+}]_i$ response, respectively, this was clearly due to a vehicle effect as seen in their respective control bars (Figure 5.6).

Having demonstrated that four different forms of soluble $A\beta_{1-42}$ had no effect on agonist-evoked $[Ca^{2+}]_i$ responses in SH-EP1-h$\alpha_4\beta_2$ cells, the ability of aggregated (insoluble) $A\beta_{1-42}$ alone or on (-)nicotine evoked $[Ca^{2+}]_i$ response was assessed. Again, the addition of concentrations of aggregated amyloid that ranged from 100 pM to 10 μM, insoluble $A\beta_{1-42}$ failed to alter $[Ca^{2+}]_i$ in SH-EP1-h$\alpha_4\beta_2$ cells (Figure 5.7).

Figure 5.4

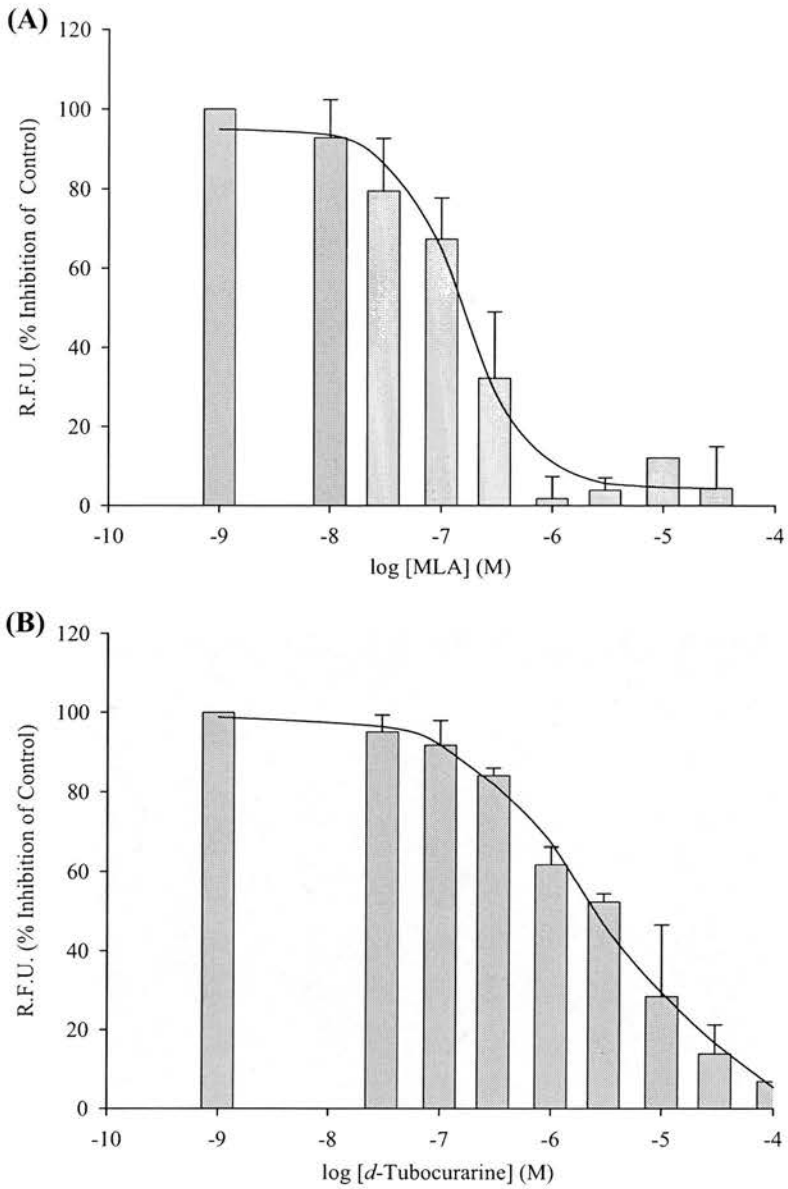

Nicotinic Antagonists Produce a Concentration-Dependent Decrease in the (-)Nicotine-Evoked $[Ca^{2+}]_i$ Response in SH-EP1-h$\alpha_4\beta_2$ Cells. (A) MLA and (B) *d*-tubocurarine were incubated (10 min, 22°C) with calcium assay dye and SH-EP1-h$\alpha_4\beta_2$ cells. (-)Nicotine concentrations were applied using the robotic microinjection system within the Flexstation® and changes in $[Ca^{2+}]_i$ analysed. Excitation and emission wavelengths were set to 485 nm and 525 nm, respectively. Data represent a typical experiment with each data point representing the mean value of three individual wells. The nAChR antagonists MLA and *d*-TC produced a concentration-dependent inhibition of the (-)nicotine (10 nM) evoked $[Ca^{2+}]_i$ response.

Figure 5.5

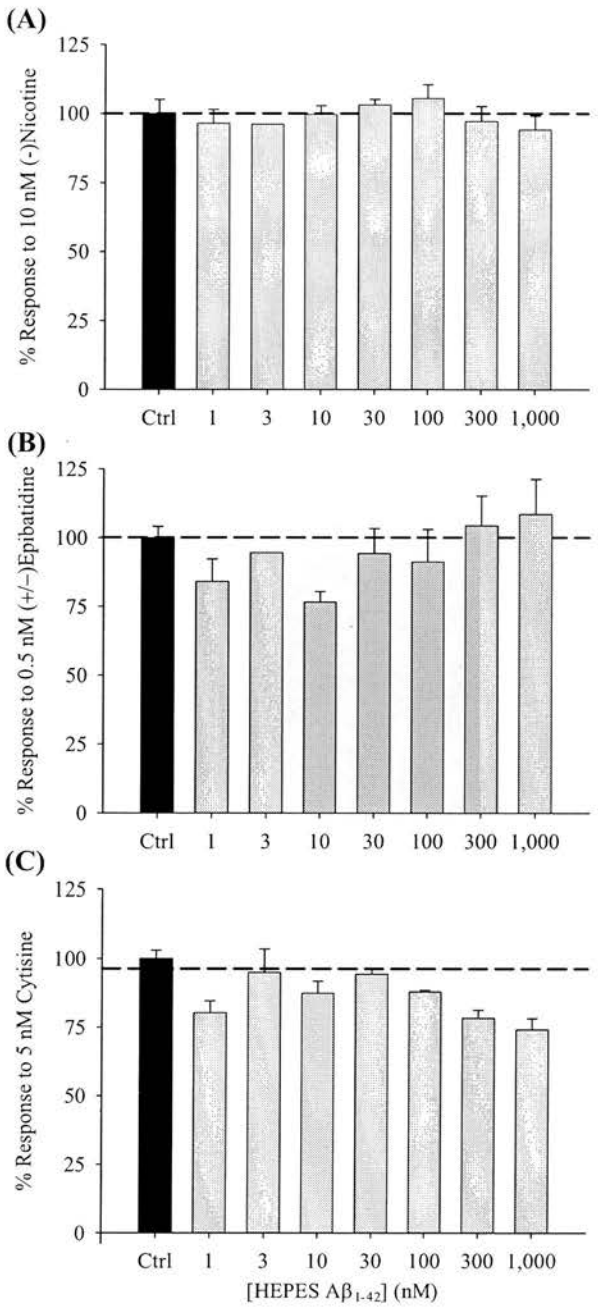

Human $A\beta_{1-42}$ Dissolved in HEPES Did Not Alter (-)Nicotine-Evoked $[Ca^{2+}]_i$ Responses in SH-EP1-h$\alpha_4\beta_2$ Cells. Human $A\beta_{1-42}$ was dissolved in HEPES buffer (pH 8.0) was preincubated for 10 min with SH-EP1-h$\alpha_4\beta_2$ cells and calcium-sensitive dye. (A) 10 nM (-)nicotine, (B) 0.5 nM (±)epibatidine, (C) 5 nM cytisine was applied using the robotic microinjection system within the Flexstation® and changes in $[Ca^{2+}]_i$ analysed. Excitation and emission wavelengths were set to 485 nm and 525 nm, respectively. These data represent a typical experiment with each data point representing the mean value of three individual wells.

Figure 5.6

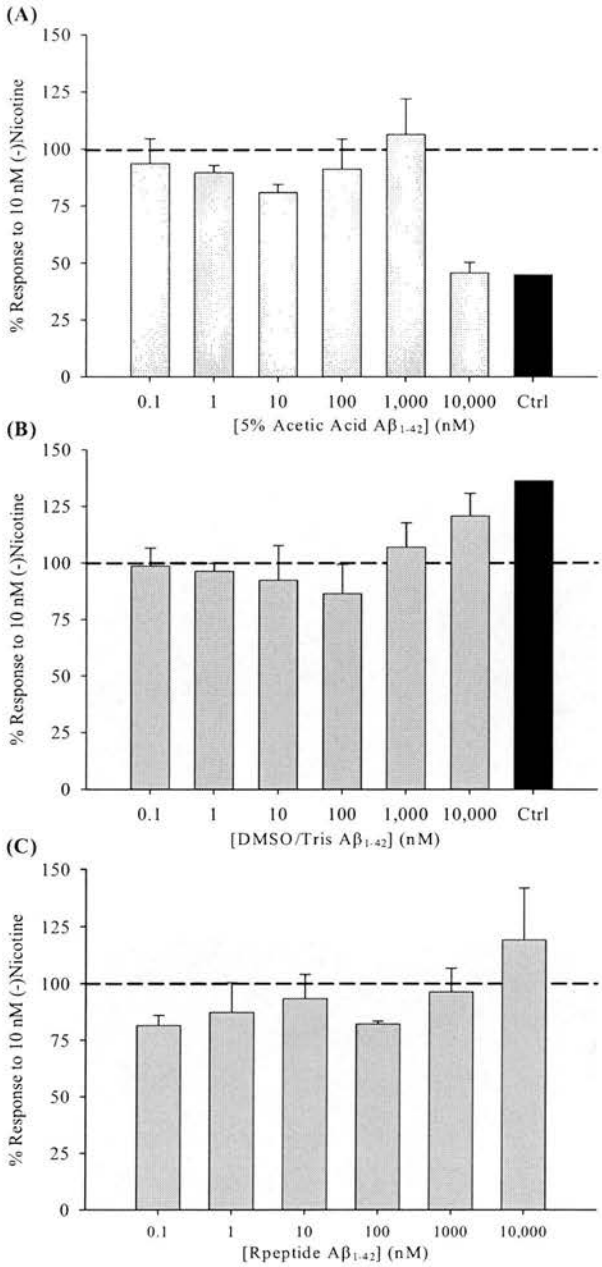

Soluble Human $A\beta_{1-42}$ Does Not Alter (-)Nicotine-Evoked $[Ca^{2+}]_i$ Respones in SH-EP1-h$\alpha_4\beta_2$ Cells. Human $A\beta_{1-42}$ was dissolved in (A) 5 % acetic acid, (B) 50/50 DMSO/Tris HCl mixture, and (C) MQ H_2O and preincubated for 10 min with SH-EP1-h$\alpha_4\beta_2$ cells and the calcium-sensitive dye. (-)Nicotine (10 nM) was applied using the robotic microinjection system within the Flexstation® and changes in $[Ca^{2+}]_i$ analysed. Excitation and emission wavelengths were set to 485 nm and 525 nm, respectively. These data represent a typical experiment with each data point representing the mean value of three individual wells.

Figure 5.7

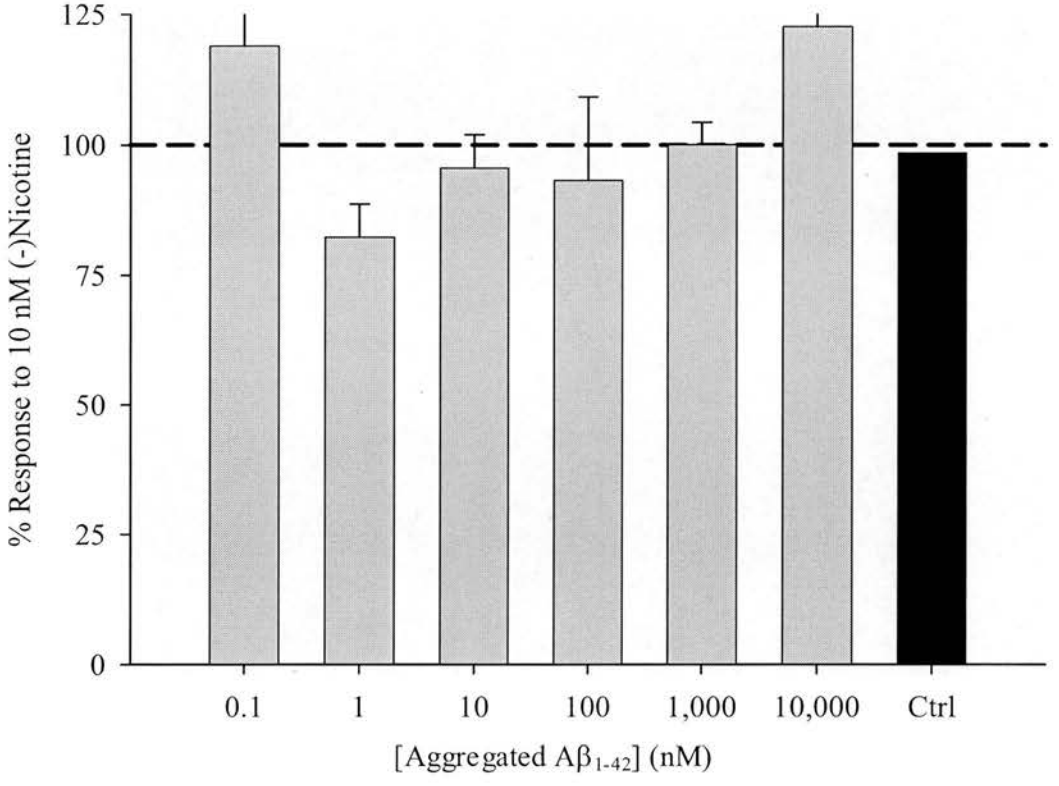

Preaggregated Human $A\beta_{1-42}$ Does Not Alter the (-)Nicotine-Evoked $[Ca^{2+}]_i$ Responses in SH-EP1-h$\alpha_4\beta_2$ Cells. Human $A\beta_{1-42}$ (preaggregated for 48 h) was preincubated for 10 min with SH-EP1-h$\alpha_4\beta_2$ cells and the calcium-sensitive dye. (-)Nicotine (10 nM) was applied using the robotic microinjection system within the Flexstation® and changes in $[Ca^{2+}]_i$ analysed. Excitation and emission wavelengths were set to 485 nm and 525 nm, respectively. These data represent a typical experiment with each data point representing the mean value of three individual wells. Control (Ctrl) data represent calcium assay buffer and dye only.

5.2.2 Establishment of a Membrane Potential Fluorescence Assay for the Characterisation of $\alpha_4\beta_2$ nAChR Pharmacology and its Interaction with Human $A\beta_{1-42}$

Membrane potential assays allow an indirect but relatively rapid and sensitive assessment of ionic flow through ion channels. Ion flow through the channel causes a change in membrane potential which in turn can be detected by a fluorescent dye (Baxter *et al.*, 2002). As with the $[Ca^{2+}]_i$ assay, the membrane potential assay facilitates a functional examination of the effects of agonists and antagonists at ion channels such as the $\alpha_4\beta_2$ nAChR (Baxter *et al.*, 2002). In a recent publication, Fitch and colleagues (2003) showed that the membrane potential assay was more sensitive than the calcium assay in detecting changes in ion flux through rat and human $\alpha_4\beta_2$ nAChRs. Therefore, the membrane potential assay may be more likely to detect changes in ion flux through nAChRs and perhaps identify a more subtle interaction between nAChRs and $A\beta_{1-42}$.

5.2.2.1 Effect of Cell Density on (-)Nicotine-Evoked Alterations in Membrane Potential in SH-EP1-h$\alpha_4\beta_2$ Cells

To determine the optimal cell density to conduct pharmacological studies, SH-EP1-h$\alpha_4\beta_2$ cells were plated at increasing numbers (25,000 to 125,000 cells/well) and incubated (37°C) overnight prior to use in the assay the following day. SH-EP1-h$\alpha_4\beta_2$ cells were incubated with the membrane potential dye (Molecular Devices (MD), U.K.) for 30 min at 22°C, prior to challenge with 10 nM (-)nicotine. (-)Nicotine (10 nM) induced a density dependent increase in fluorescence in SH-EP1-h$\alpha_4\beta_2$ cells, although there was little difference in response size above 50,000 cells/well (Figure 5.8). As described for the $[Ca^{2+}]_i$ assay, when the cells were plated at 100,000 cells/well, there was almost full confluency, therefore and this cell density was used in all subsequent experiments.

5.2.2.2 Effect of Additional Ca^{2+} on (-)Nicotine-Evoked Changes in Membrane Potential in SH-EP1-h$\alpha_4\beta_2$ Cells

For compatability with the $[Ca^{2+}]_i$ assay, the sensitivity of the (-)nicotine-evoked change in membrane potential to an alteration in external Ca^{2+} was examined in SH-EP1-h$\alpha_4\beta_2$ cells. The concentration dependence of the (-)nicotine-evoked change in membrane potential was measured in the presence and absence of an additional 2.5 mM Ca^{2+} in the external solution. In contrast to the $[Ca^{2+}]_i$ assay, the presence of the additional Ca^{2+} decreased the maximal response of SH-EP1-h$\alpha_4\beta_2$ cells across the whole (-)nicotine dose-

Figure 5.8

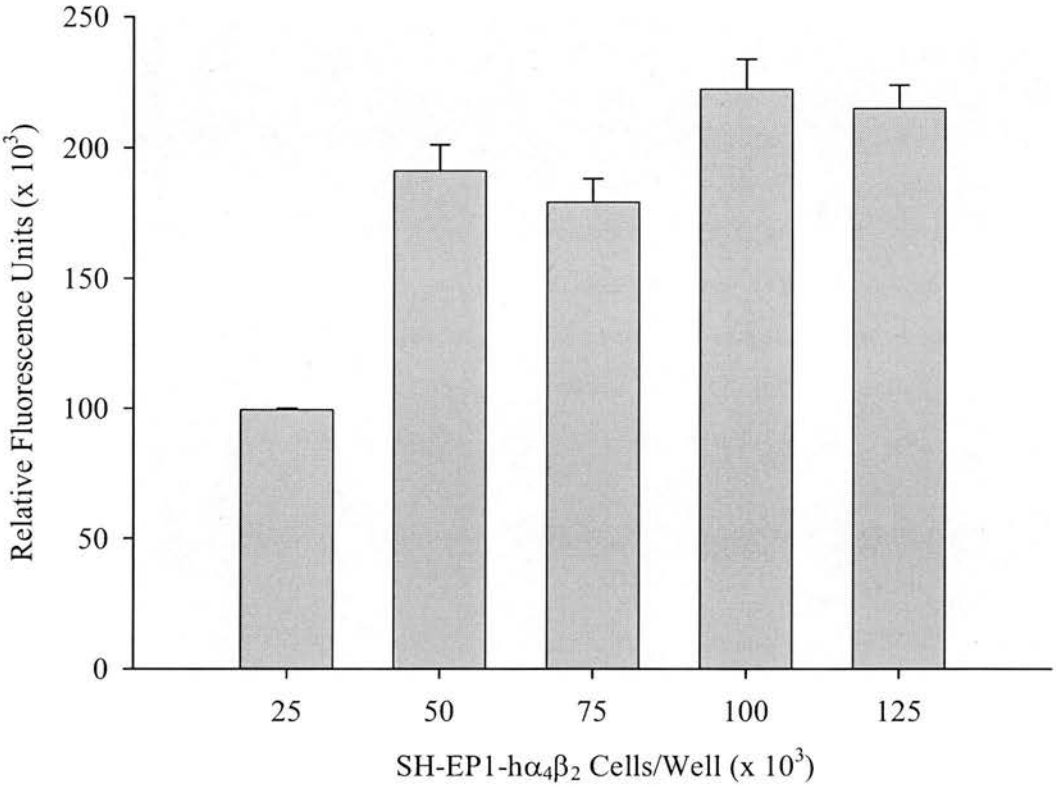

Effect on Cell Density on the (-)Nicotine-Evoked Change in Membrane Potential in SH-EP1-h$\alpha_4\beta_2$ Cells. Cells were plated at increasing densities ranging from 25,000 to 125,000 cells/well in a poly-D-lysine coated 96-well plate and incubated overnight (37°C). Following removal of media, a membrane potential sensitive fluorescence dye (MD, U.K.) was added and the cells equilibrated (22°C) for 30 min. (-)Nicotine (10 nM) was applied using the robotic microinjection system within the Flexstation and changes in membrane potential measured as a change in fluorescence. Excitation and emission wavelengths were set to 535 nm and 560 nm, respectively, with these data representing a typical experiment performed in triplicate. Relative fluorescence units were calculated by subtracting minimum from the maximum response. There was little difference in responses at cell densities above 50,000 cell/well, therefore, as almost full confluency was achieved at 100,000 cells/well, a cell density of 100,000 cells/well was used for all subsequent studies.

response curve (Figure 5.9, grey bars indicate where Ca^{2+} added). Therefore, all subsequent membrane potential experiments were performed in the standard MD assay kit buffer with no additional calcium.

5.2.2.3 Pharmacological Characterisation of Nicotinic Agonists and Antagonists on Membrane Potential Responses in SH-EP1-h$\alpha_4\beta_2$ Cells

Prior to examining the effect of human $A\beta_{1-42}$ on (-)nicotine induced changes in membrane potential in SH-EP1-h$\alpha_4\beta_2$ cells, the pharmacological profile of this nAChR was characterised. To determine the half-effective concentration (EC_{50}) of all the agonists in the SH-EP1-h$\alpha_4\beta_2$ cell line, data was collected over a range of drug concentrations (1 pM – 10 μM), normalised to the maximal drug concentration and fitted with the empirical Hill equation. The rank order of potency for the nicotinic agonist ligands examined was (±)epibatidine > cytisine > nicotine=DMPP with representative data shown in Figure 5.10. The EC_{50} for (-)nicotine was 19.5 ± 6.5 nM with a Hill coefficient of 1.94 ± 0.04 (n = 4; Figure 5.10A). The half-maximal concentrations for the other compounds examined ranged from 0.56 ± 0.11 nM (n_H = 1.23 ± 0.01, n = 3) for (±)epibatidine to 96.9 ± 12.6 nM (n_H = 0.95 ± 0.13, n = 3) for DMPP (Figure 5.10A). Although cytisine gave an EC_{50} value of 3.09 ± 0.83 μM (n = 3), initial studies indicated the Hillslope was less than 1 for cytisine in the SH-EP1-h$\alpha_4\beta_2$ cells. Therefore, the number of cytisine concentrations examined was increased to twenty to try and ascertain whether the cytisine-evoked membrane potential response in human $\alpha_4\beta_2$ nAChRs had more than one component. Using the F-test, cytisine data was better fit with a two-site model rather than a one-site model (Figure 5.10B; $p < 0.05$). EC_{50} vlaues for the high and low affinity sites were 1.03 μM and 3.18 nM, respectively. This is in agreement with previously published data indicating cytisine is a partial agonist at $\alpha_4\beta_2$ nAChRs (Papke & Heinemann, 1994).

In addition, to examine the antagonists I attempted to determine pK_B values for the nicotinic antagonists MLA and *d*-TC at the human $\alpha_4\beta_2$ nAChR expressed in SH-EP1 cells. A full (-)nicotine concentration-response curve was performed in the presence and absence of 3 different antagonist concentrations (30, 100, and 300 nM; Figures 5.11). MLA caused a parallel shift to the right of the (-)nicotine concentration-response curve with no change in maximal response size. The (-)nicotine EC_{50} moved from 11.4 nM (no MLA) to 34.0 nM in the presence of 300 nM MLA. A subsequent Schild analysis generated a slope of -1.40, with the pK_B (pA_2) estimated to be 6.38 (Figure 5.11, inset).

Figure 5.9

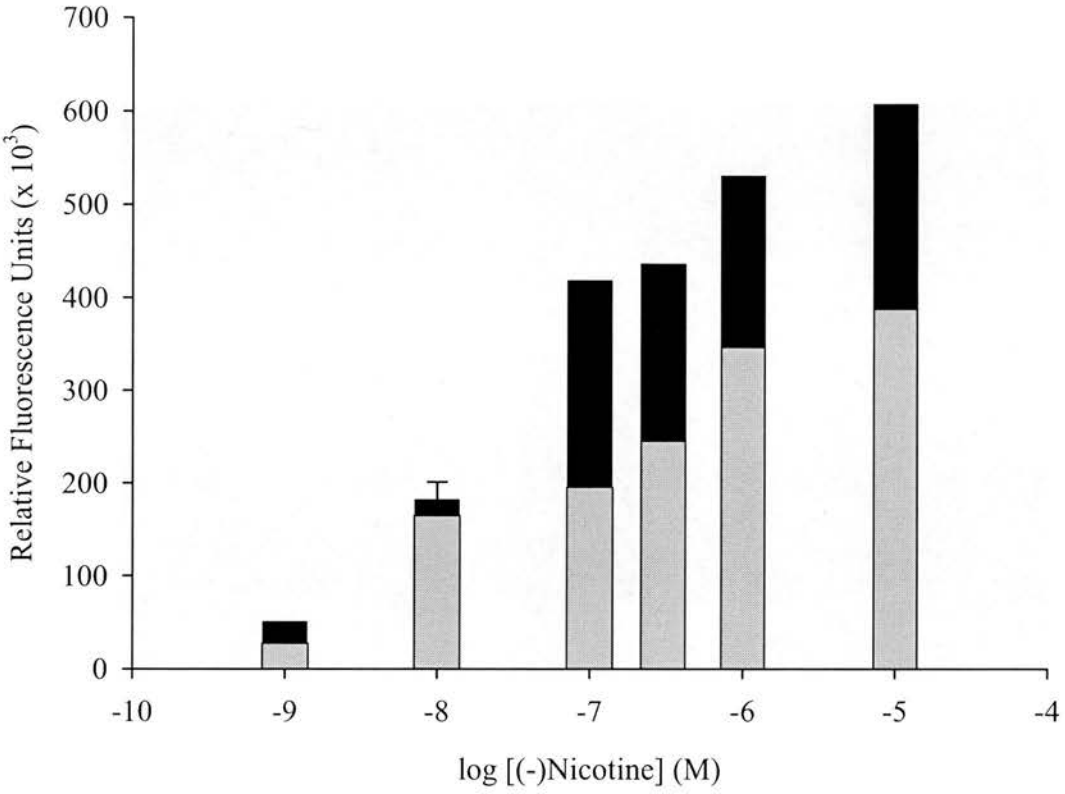

Effect of an Additional 2.5 mM External Ca^{2+} on the (-)Nicotine-Evoked Change in Membrane Potential in SH-EP1-h$\alpha_4\beta_2$ Cells. Standard membrane potential buffer contains 1.26 mM Ca^{2+}, therefore, the final assay concentration of Ca^{2+} was 3.76 mM. Following removal of the media, membrane potential sensitive fluorescence dye (MD, U.K.) was added to the cells and left for for 30 min at 22°C. (-)Nicotine concentrations were applied using the robotic microinjection system within the Flexstation® and changes in membrane potential measured as a change in fluorescence. Excitation and emission wavelengths were set to 535 nm and 560 nm, respectively, with these data representing a typical experiment performed in triplicate. Relative fluorescence units were calculated by subtracting minimum from the maximum response. The addition of an extra 2.5 mM external Ca^{2+} inhibited the (-)nicotine-evoked change in membrane potential in SH-EP1-h$\alpha_4\beta_2$ cells.

Figure 5.10

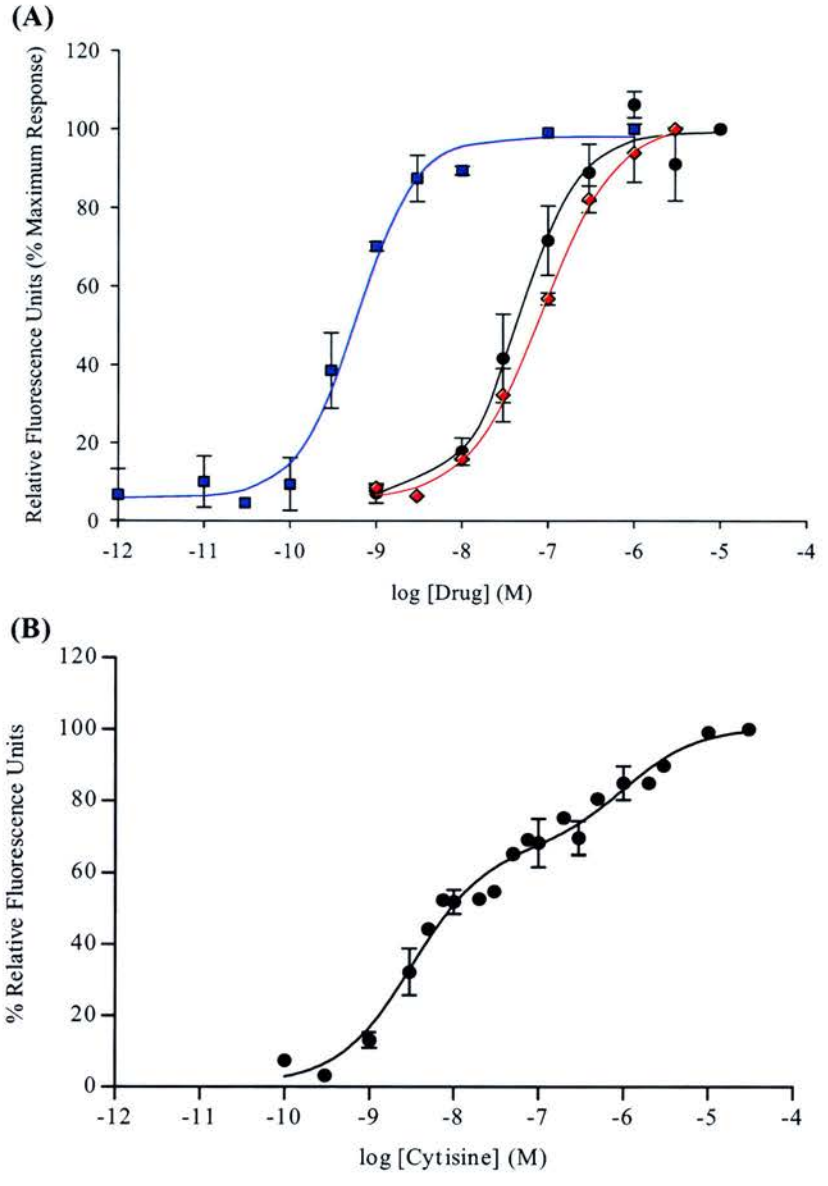

Nicotinic Agonists Produce a Concentration-Dependent Alteration in Membrane Potential in SH-EP1-h$\alpha_4\beta_2$ Cells. The nAChR agonists (A) (±)epibatidine (■), DMPP (●), and (-)nicotine (◆) and (B) cytisine evoked large concentration-dependent increases in fluorescence. Drugs were applied using the robotic microinjection system within the Flexstation® and alterations in membrane potential measured as a change in fluorescence. Excitation and emission wavelengths were set to 535 nm and 560 nm, respectively, with these data representing a typical experiment performed in triplicate. Relative fluorescence units were calculated by subtracting minimum from the maximum response.

Figure 5.11

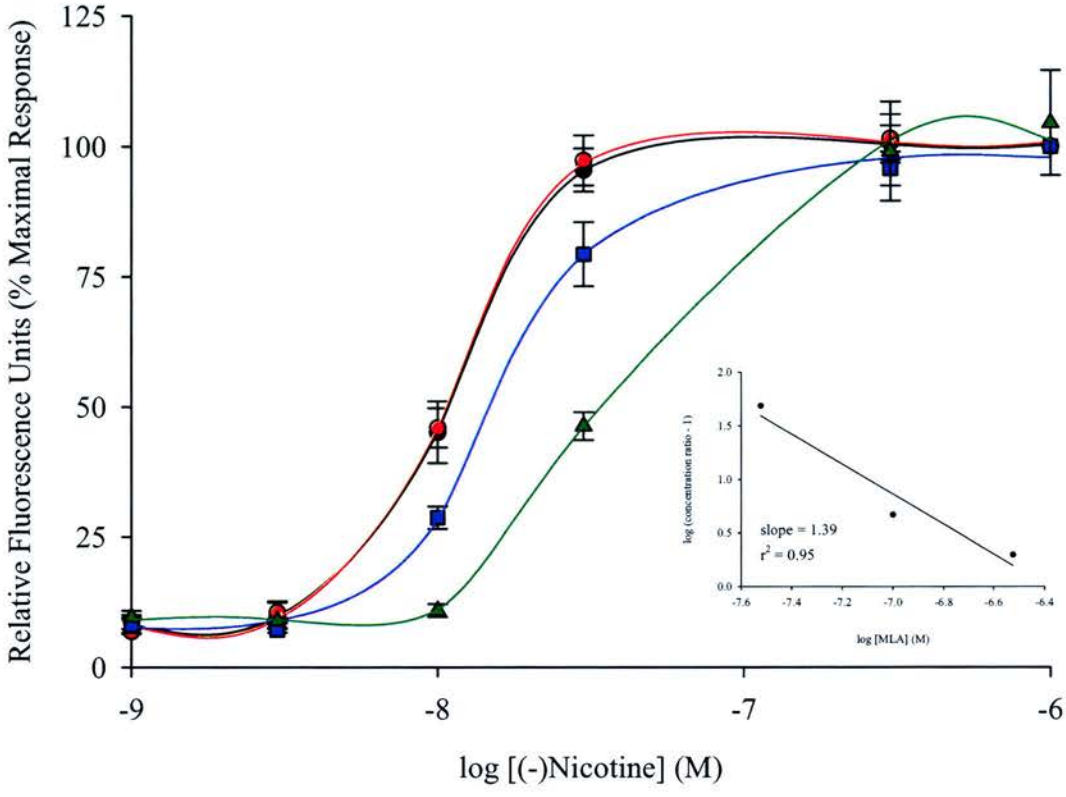

MLA Inhibited the (-)Nicotine-Evoked Changes in Membrane Potential in SH-EP1-h$\alpha_4\beta_2$ Cells in a Competitive Manner. (-)Nicotine concentration-response curves were generated in the absence (●) and presence of 30 nM (●), 100 nM (■) and 300 nM (▲) MLA. MLA was preincubated for 10 min prior to the addition of (-)nicotine which were applied using the robotic microinjection system within the Flexstation®. Changes in membrane potential were measured as changes in fluorescence with excitation and emission wavelengths set to 535 nm and 560 nm, respectively. These data representing a typical experiment performed in triplicate with relative fluorescence units calculated by subtracting the minimum from the maximum response. MLA caused a parallel shift to the right of the (-)nicotine concentration-response curve with no change in maximal response size. *Inset*: Schild analysis of MLA inhibition of (-)nicotine evoked changes in membrane potential in SH-EP1-h$\alpha_4\beta_2$ cells with the pA_2 calculated as 415 nM.

In contrast, solubility issues surrounding high concentrations of *d*-TC (~IC_{50} > 500 μM in membrane potential assay), meant the highest *d*-TC concentration that could be examined was 100 μM. At this concentration, *d*-TC (100 μM) caused a small parallel shift to the right in the (-)nicotine dose-response curve with a subsequent shift in the EC_{50} of (-)nicotine from 27.1 nM to 56.3 nM with no reduction in maximal response (Figure 5.12). Unfortunately, the inability to examine higher concentrations of *d*-TC meant a pK_B value could not be calculated using a Schild plot but can be roughly estimated as ≥ 4.04.

5.2.2.4 Human $A\beta_{1-42}$ Had No Effect on the (-)Nicotine Evoked Change in Membrane Potential in SH-EP1-h$\alpha_4\beta_2$ Cells

The ability of soluble and insoluble human $A\beta_{1-42}$ to modulate membrane potential responses in SH-EP1 cells expressing the human $\alpha_4\beta_2$ nAChRs was assessed. (-)Nicotine was used at a concentration of 10 nM, close to its EC_{50} value and therefore, sufficient to observe both inhibition or potentiation by $A\beta_{1-42}$.

To generate soluble $A\beta_{1-42}$, the peptide was dissolved in 5 % acetic acid, 50/50 DMSO/Tris HCl (pH 8.0), and MQ H_2O (Rpeptide acetate salt). In agreement with the calcium studies, at concentrations up to 10 μM, none of the soluble amyloid preparations had any effect alone (not shown) or on the (-)nicotine evoked change in membrane potential (Figure 5.13). Although it would appear that 10 μM $A\beta_{1-42}$ caused a reduction in membrane potential (Figure 5.13), the equivalent vehicle control produced a similar reduction in response (Figure 5.14). This is consistent with the findings from the calcium assay. Furthermore, studies evaluating the effect of aggregated (insoluble) human $A\beta_{1-42}$ did nothing alone, nor did it inhibit the (-)nicotine evoked change in membrane potential in SH-EP1-h$\alpha_4\beta_2$ cells (Figure 5.15).

5.2.3 Establishment of Calcium Flux and Membrane Potential Assays in the SH-EP1-hα_7 Cell Line

Maintenance of high level, stable expression of human α_7 nAChRs is known to be challenging and appears highly dependent on the cell line used (Cooper & Millar, 1997). The SH-EP1-hα_7 cell line used in these studies is no different with many cells not expressing functional α_7 nAChRs at the cell surface. However, I attempted to established $[Ca^2]_i$ and membranes potential assays in the SH-EP1-hα_7 cell line using the same approach that was successful for the SH-EP1-h$\alpha_4\beta_2$ cell line.

Figure 5.12

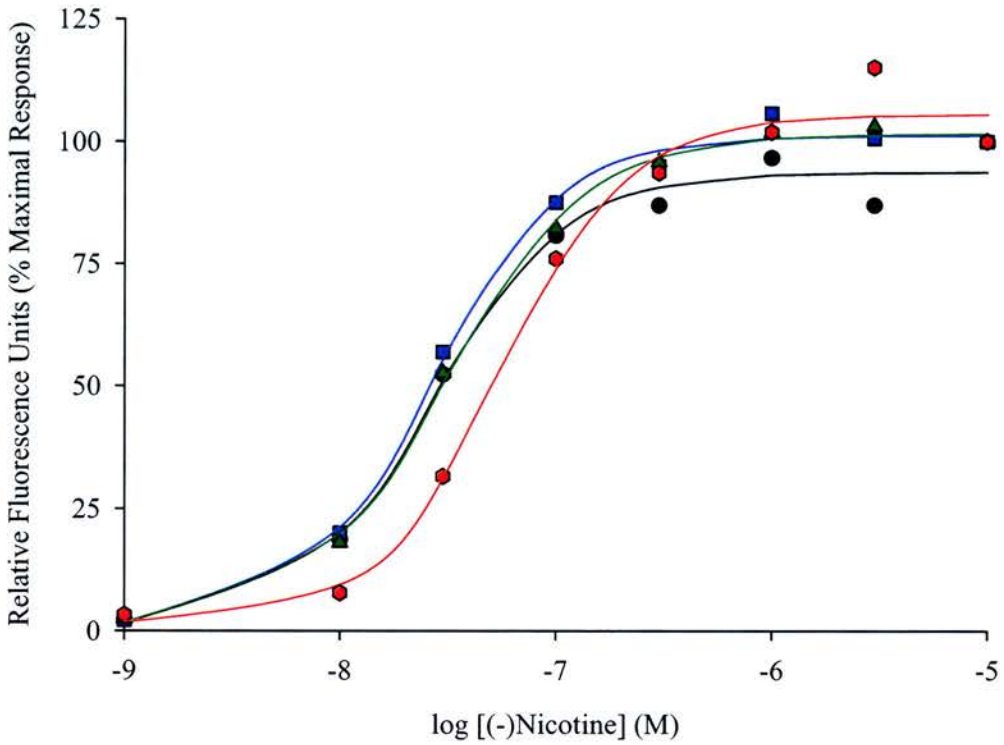

High Concentrations of the Nicotinic Antagonist *d*-TC Inhibited the (-)Nicotine-Evoked Changes in Membrane Potential in SH-EP1-h$\alpha_4\beta_2$ Cells. (-)Nicotine concentration-response curves were generated in the absence (●) and presence of 10 μM (■), 30 μM (▲) and 100 μM (⬢) *d*-TC. The antagonist was preincubated for 10 min prior to the addition of (-)nicotine with the agonist (10 nM) applied using the robotic microinjection system within the Flexstation®. Changes in membrane potential were measured as changes in fluorescence with excitation and emission wavelengths set to 535 nm and 560 nm, respectively. These data representing a typical experiment performed in triplicate with relative fluorescence units calculated by subtracting the minimum from the maximum response.

Figure 5.13

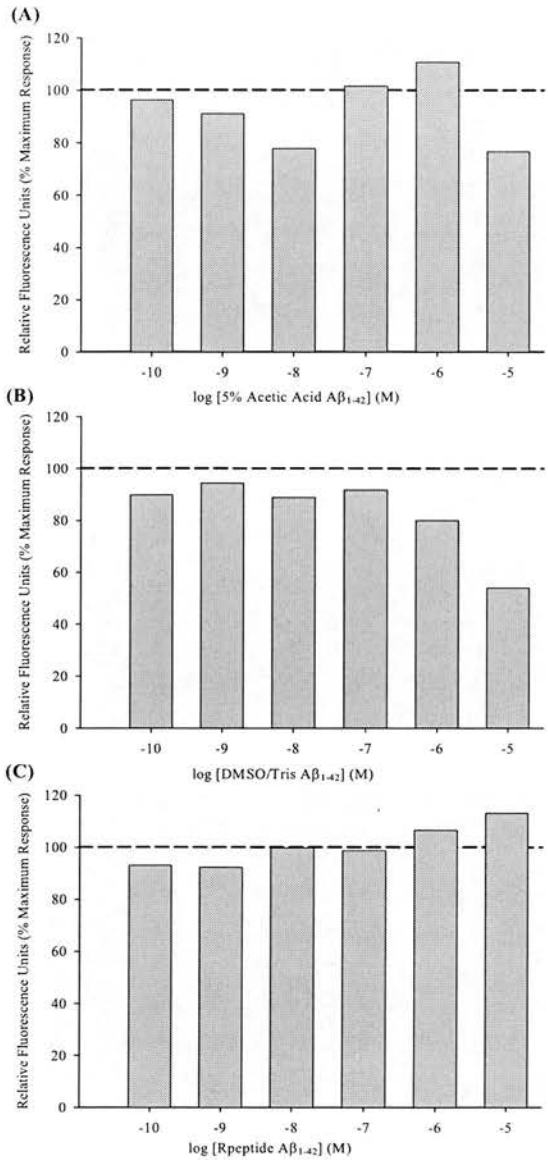

Soluble Human $A\beta_{1-42}$ Does Not Alter the (-)Nicotine Evoked Change in Membrane Potential in SH-EP1-h$\alpha_4\beta_2$ Cells. Human $A\beta_{1-42}$ dissolved in (A) 5 % acetic acid, (B) 50/50 DMSO/Tris HCl (pH 8.0), or MQ H_2O was preincubated for 10 min with SH-EP1-h$\alpha_4\beta_2$ cells and the membrane potential sensitive dye (MD, U.K.). (-)Nicotine (10 nM) was applied using the robotic microinjection system within the Flexstation® and changes in membrane potential measured as alterations in fluorescence. Excitation and emission wavelengths were set to 535 nm and 560 nm, respectively with these data representing a typical experiment performed in triplicate. Relative fluorescence units were calculated by subtracting minimum from the maximum response.

Figure 5.14

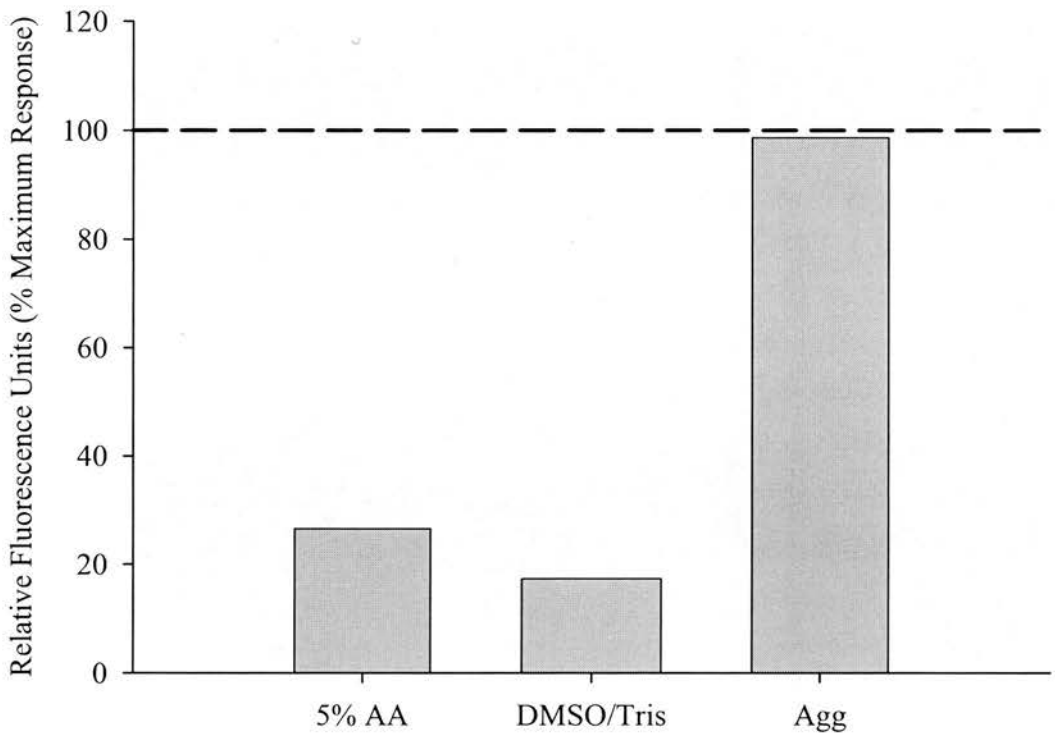

$A\beta_{1-42}$ Vehicles Inhibit the (-)Nicotine Evoked Change in Membrane Potential in SH-EP1-h$\alpha_4\beta_2$ Cells. Human $A\beta_{1-42}$ vehicles 5 % acetic acid (5% AA), 50/50 DMSO/Tris HCl (pH 8.0) (DMSO/Tris), and aggregated (Agg) were preincubated for 10 min with SH-EP1-h$\alpha_4\beta_2$ nAChRs and membrane potential sensitive dye (MD, U.K.). (-)Nicotine (10 nM) was applied using the robotic microinjection system within the Flexstation® and changes in membrane potential were measured as changes in fluorescence. Excitation and emission wavelengths were set to 535 nm and 560 nm, respectively with these data representing a typical experiment performed in triplicate. Relative fluorescence units were calculated by subtracting minimum from the maximum response. Vehicles were examined at concentrations used to dissolve 1 μM $A\beta_{1-42}$.

Figure 5.15

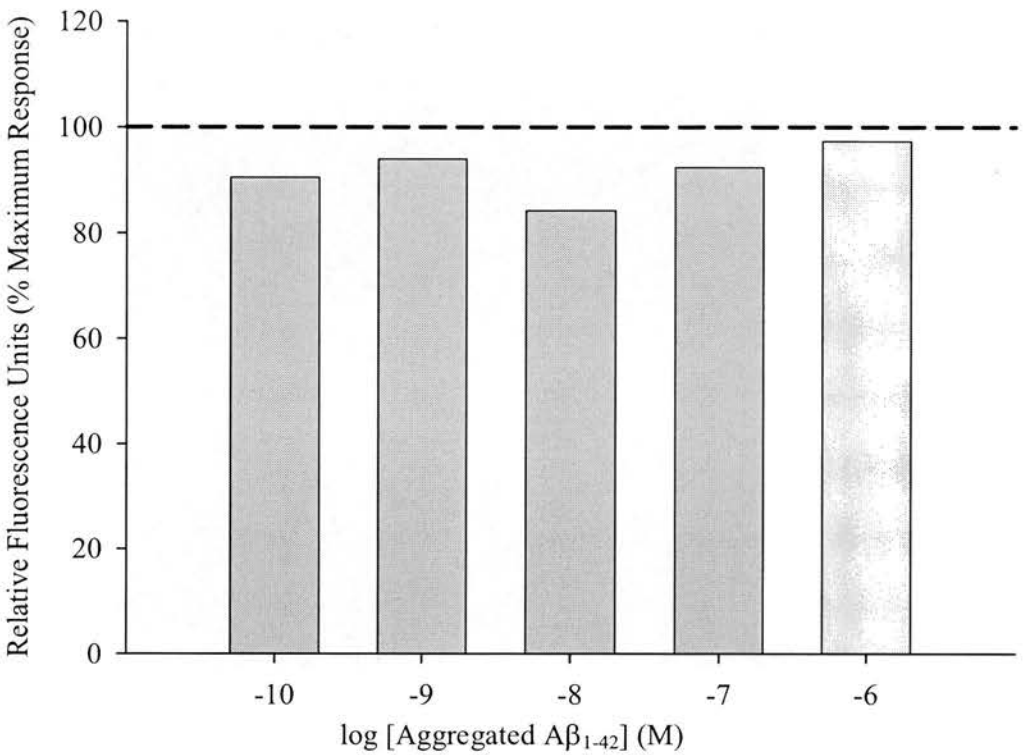

Insoluble Human $A\beta_{1-42}$ Does Not Alter the (-)Nicotine Evoked Change in Membrane Potential in SH-EP1-h$\alpha_4\beta_2$ Cells. Human $A\beta_{1-42}$ was preaggregated for 48 h then preincubated for 10 min with SH-EP1-h$\alpha_4\beta_2$ cells and the membrane potential sensitive dye (MD, U.K.). (-)Nicotine (10 nM) was applied using the robotic microinjection system within the Flexstation® and changes in membrane potential measured as changes in fluorescence. Excitation and emission wavelengths were set to 535 nm and 560 nm, respectively with these data representing a typical experiment performed in triplicate. Relative fluorescence units were calculated by subtracting minimum from the maximum response.

5.2.3.1 (-)Nicotine-Evoked $[Ca^{2+}]_i$ Responses Were Absent in SH-EP1-hα_7 Cells

To determine whether exposure to (-)nicotine could elict a $[Ca^{2+}]_i$ response in SH-EP1-hα_7 cells, a plating density of 100,000 cells/well was used and the cells incubated (37°C) overnight. This was shown to be the optimal density for SH-EP1-h$\alpha_4\beta_2$ cells in the previous section, giving full confluency and large fluorescence responses. (-)Nicotine (0.03 – 30 μM) failed to evoke any change in $[Ca^{2+}]_i$ in the SH-EP1-hα_7 cell line (Figure 5.16A). In an attempt to maintain surface expression of the human α_7 nAChR and therefore increase responses, cells were grown in the presence of MLA (concentration as described by Molinari and colleagues (1998). However, using this treatment, (-)nicotine again failed to evoke a change in $[Ca^{2+}]_i$ response in these cells (Figure 5.16B). In the same set of studies and in contrast to the lack of effect of human α_7 nAChRs, (-)nicotine evoked a large increase in the $[Ca^{2+}]_i$ response in SH-EP1-h$\alpha_4\beta_2$ cells (Figure 5.16C). No change in (-)nicotine evoked $[Ca^{2+}]_i$ response was observed in SH-EP1-host cells (Figure 5.16D).

5.2.3.2 (-)Nicotine Did Not Induce a Change in Membrane Potential in SH-EP1-hα_7 Cells

Fitch and colleagues (2003) showed that membrane potential assays were potentially more sensitive than calcium assays in detecting changes in ion flux through nAChRs. As such, the membrane potential assay may be more likely to detect smaller changes in ion flux through nAChRs, even though no change in $[Ca^{2+}]_i$ was detected.

The ability of (-)nicotine to evoke a change in membrane potential was assessed in SH-EP1-hα_7 cells across a variety of cell densities (Figure 5.17). Although (-)nicotine (50 nM)was examined at a concentration just above the predicted IC_{50} of (-)nicotine at α_7 nAChRs, the ligand failed to evoke a change in membrane potential in SH-EP1-hα_7 cells (Figure 5.17). Indeed, the small responses observed were no different from those observed in SH-EP1-host cells.

The absence of any obvious (-)nicotine-induced change in $[Ca^{2+}]_i$ or membrane potential meant no subsequent gross plate-based fluorescent experiments were performed using the SH-EP1-hα_7 cells.

Figure 5.16

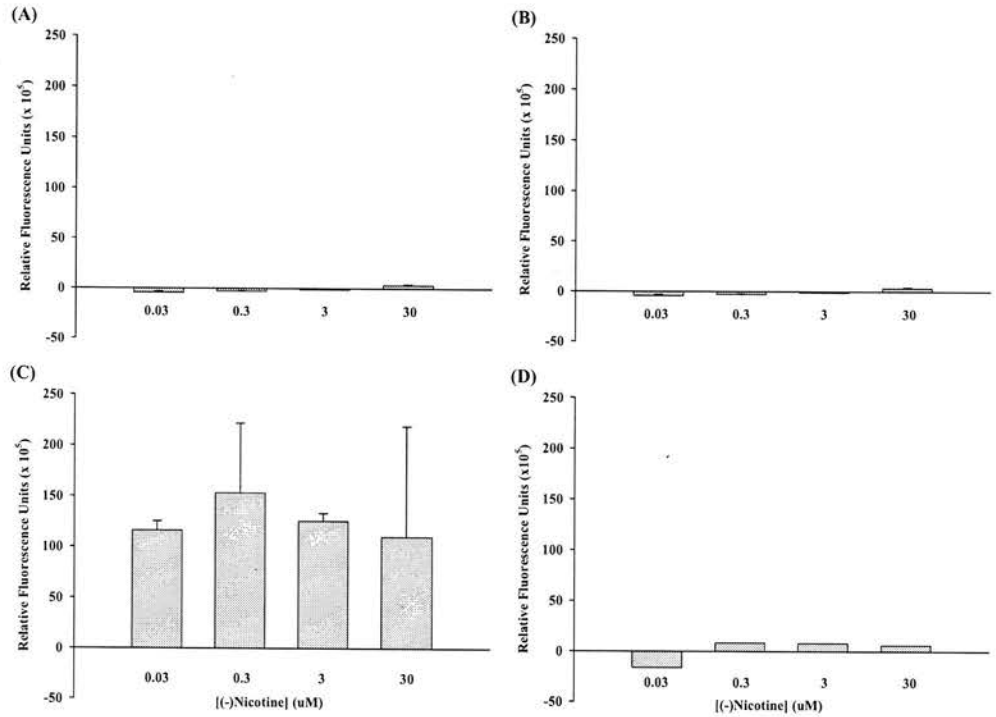

(-)Nicotine Does Not Evoked Changes in $[Ca^{2+}]_i$ in SH-EP1-hα_7 Cells. (A) Non-treated SH-EP1-hα_7 (B) MLA – treated SH-EP1-hα_7 (C) SH-EP1-h$\alpha_4\beta_2$ (D) SH-EP1-Host cells were plated at 100,000 cells/well in a poly-D-lysine coated 96-well plate were incubated overnight at 37°C. Following removal of media, calcium assay buffer and fluorescence dye (Molecular Devices Ltd, UK) were added and the cells equilibrated for 1 h at 37°C. (-)Nicotine concentrations were applied using the robotic microinjection system within the Flexstation fluorescence plate reader (Molecular Devices) and changes in $[Ca^{2+}]_i$ analysed in a Flexstation fluorescence plate reader (Molecular Devices, UK) with excitation and emission wavelengths set to 485 nm and 525 nm, respectively. Data represent a typical experiment performed in triplicate.

Figure 5.17

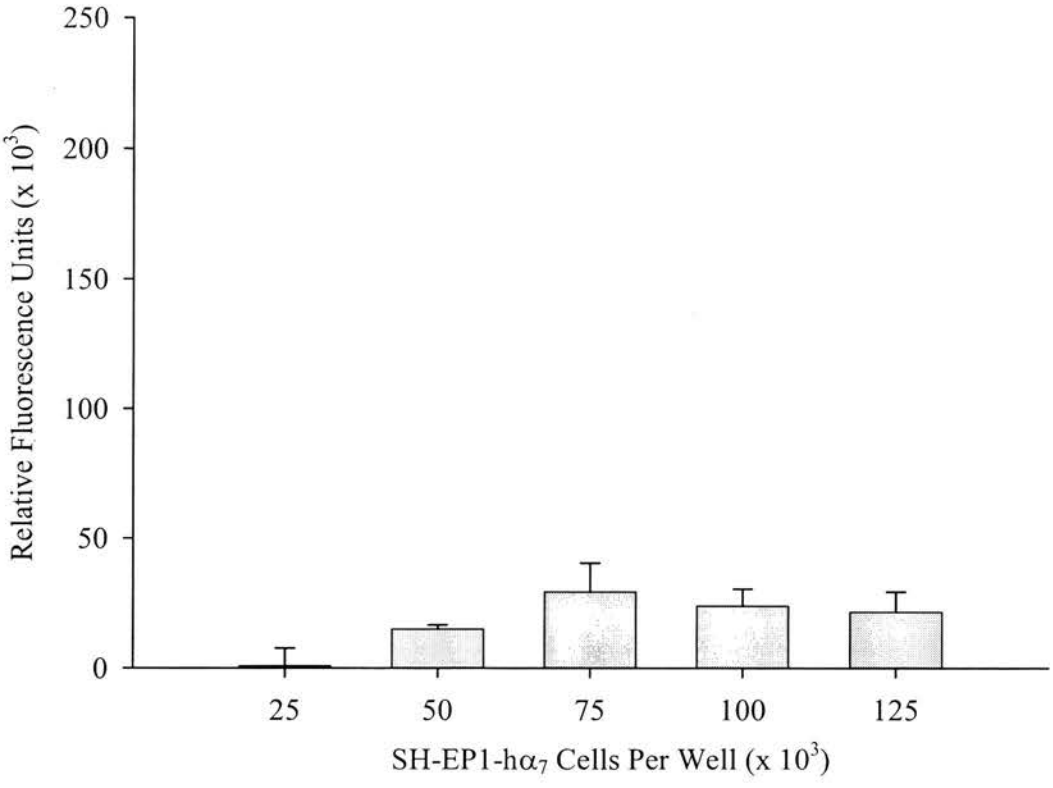

Lack of (-)Nicotine-Evoked Changes in Membrane Potential in SH-EP1-hα$_7$ Cells. SH-EP1-hα$_7$ cells were plated at increasing concentrations from 25,000 to 125,000 cells/well in a poly-D-lysine coated 96-well plate were incubated overnight at 37°C. Following removal of media, membrane potential sensitive fluorescence dye (Molecular Devices Ltd, UK) was added and the cells equilibrated for 30 min at 22°C. (-)Nicotine (50 nM) was applied using the robotic microinjection system within the Flexstation fluorescence plate reader (Molecular Devices) and changes in membrane potential measured as changes in fluorescence, analysed in a Flexstation fluorescence plate reader (Molecular Devices, UK) with excitation and emission wavelengths set to 535 nm and 560 nm, respectively. Data represent a typical experiment performed in triplicate with relative fluorescence units representing maximum response – minimum response.

5.3 Examination of Human $\alpha_4\beta_2$ nAChR Electrophysiology

5.3.1 Nicotine-Induced Currents in $\alpha_4\beta_2$ nAChR expressing SH-EP1 Cells

Whole cell current recording was used to characterise the pharmacology and re-confirm functional expression of $\alpha_4\beta_2$ nAChR in the SH-EP1 stable cell line. Experiments were performed using conventional whole cell recording in the voltage clamp mode at a V_H = -60 mV. Using potassium (K^+) containing electrodes, repeated application of (-)nicotine for 375 ms at intervals of 1 min induced an inward current (I_{Nic}, Figure 5.18A). The (-)nicotine concentration applied (10 μM) was below the predicted EC_{50} value for (-)nicotine in SH-EP1-h$\alpha_4\beta_2$ cells and was used in order to try and minimise receptor desensitisation. The peak I_{Nic} showed "functional rundown", defined as a "loss of peak current amplitude with each repeated application of agonist, with time" (Zhao *et al.*, 2003; Figure 5.18A).

Zhao and colleagues (2003) recently demonstrated that the substitution of Tris base and Tris diphosphate dibasic for KCl in the recording pipette, produced a K^+-free pipette solution (while maintaining comparable concentrations of free Ca^{2+} and ATP), that eliminated functional rundown of I_{Nic} in SH-EP1-hα_7 cells over a 12 – 15 min time interval. Following the introduction of a K^+-free internal solution to our whole cell recordings from SH-EP1-h$\alpha_4\beta_2$ cells, functional rundown was still observed when (-)nicotine was applied every minute (Figure 5.18B). However, in agreement with Zhao and colleagues (2003), the decay time constant (τ) for acute desensitisation increased from 181 ms (n = 2) in the K^+ containing electrode solution, to 322 ± 58 ms (n =3) when responses were recorded in a K^+-free solution. Increasing the (-)nicotine application interval to 3 min slowed but did not abolish functional rundown (Figure 5.18B).

To allow direct comparison with the results published on the SH-EP1-h$\alpha_4\beta_2$ cell line by the Lukas laboratory, all subsequent experiments were performed with (-)nicotine applied at 3 min intervals using identical K^+-free internal and external solutions to those used by Lukas' laboratories (Zhao *et al.*, 2003; Wu *et al.*, 2004).

5.3.2 Characterisation of the Pharmacological Properties of the Human $\alpha_4\beta_2$ nAChR Using Whole Cell Patch Clamp Studies

A number of recent papers have reported a functional interaction between nAChRs and β-amyloid$_{1-42}$ (Aβ_{1-42}), the putatively toxic form of amyloid in Alzheimer's Disease aetiology (Wang *et al.*, 2000a; Wang *et al.*, 2000b; Dineley *et al.*, 2001; Liu *et al.*, 2001; Pettit *et al.*, 2001; Tozaki *et al.*, 2002; Dineley *et al.*, 2002a; Grassi *et al.*, 2003; Wu *et al.*, 2004). Prior to examining the effect of amyloid on the human $\alpha_4\beta_2$ nAChR, the

Figure 5.18

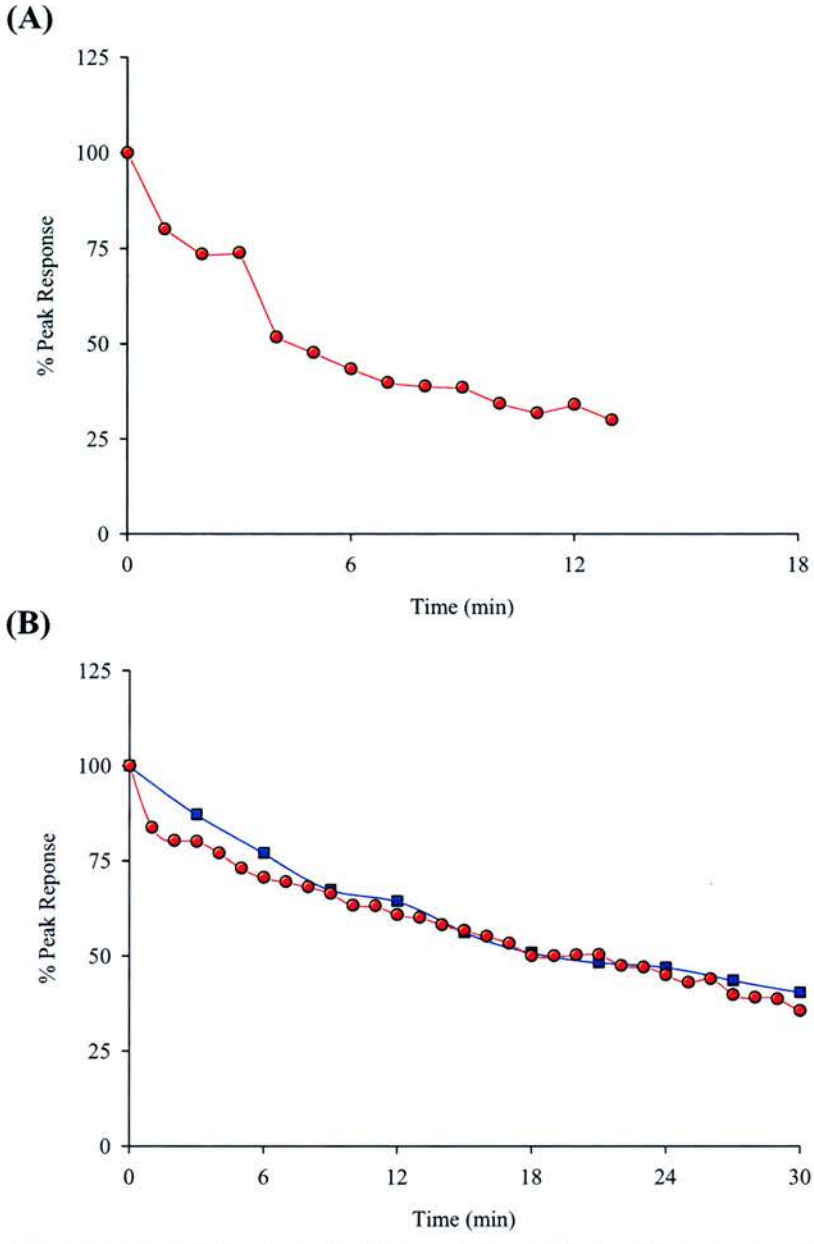

(-)Nicotine-Evoked Current Rundown in Human $\alpha_4\beta_2$ nAChRs Stably Expressed in SH-EP1 Cells. Whole-cell current recording of human $\alpha_4\beta_2$ nAChR responses was measured as described in the *Materials and Methods* using K^+-containing electrodes and K^+-free electrodes at a V_H = -60 mV. Cells were exposed to 10 μM (-)nicotine for 375 ms at 1 min (●) and 3 min (■) intervals. (A) Recordings were made from 2 cells using K^+-containing electrodes with the data points representing the mean response. (B) Recordings were made from 3 cells using K^+-free electrodes with the data points representing the mean current only for reasons of visual clarity.

pharmacological profile of this receptor was characterised using whole-cell voltage-clamp recordings (V_H = -60 mV) of SH-EP1-h$\alpha_4\beta_2$ cells.

Although nominally a stable cell line, peak current amplitude varied greatly between individual cells and ranged from a few picoamperes to > 1 nA, at a (-)nicotine concentration of 10 μM. Despite a maximal current of 3 nA being recorded, the mean current amplitude generated following application of 10 μM (-)nicotine was 724 ± 182 pA at a holding potential of -60 mV (n = 7). Cells were discarded if the initial response was below 100 pA.

In determining the half-effective concentration (EC_{50}) of (-)nicotine in the SH-EP1-h$\alpha_4\beta_2$ cells, data collected over a range of (-)nicotine concentrations (0.3 - 300 μM), was normalised to the maximal agonist response, prior to fitting with the empirical Hill equation. The EC_{50} for (-)nicotine in the SH-EP1-h$\alpha_4\beta_2$ cell line was 22.2 ± 2.2 μM (n = 3) with a Hill coefficient of 1.99 ± 0.55 (n = 3; Figure 5.19A).

To examine inhibition of the human $\alpha_4\beta_2$ nAChR, identical (-)nicotine concentration response-curves were conducted in the presence and absence of the nicotinic antagonist 10 μM *d*-tubocurarine (*d*-TC) with representative traces generated in individual SH-EP1-h$\alpha_4\beta_2$ cells shown in Figure 5.19 (A & B). In agreement with other published studies (Harvey & Luetje, 1996; Palma *et al.*, 1996), *d*-TC inhibited (-)nicotine evoked currents (I_{Nic}) at human $\alpha_4\beta_2$ nAChRs, producing a rightward shift in the concentration-response curve (Figure 5.19C). The EC_{50} value obtained for nicotine in the presence of 10 μM *d*-TC for nicotine was slightly (but not significantly) higher at 31.4 ± 7.8 μM with a Hillslope of 2.27 ± 0.07 (n =3; Figure 5.19C).

Electrophysiological and pharmacological properties presented indicates that the heterologously expressed h$\alpha_4\beta_2$ nAChRs in the SH-EP1 cell line exhibited features characteristic of this receptor subtype, validating the use of this stable cell line as an appropriate model to study human $\alpha_4\beta_2$ nAChRs.

Figure 5.19

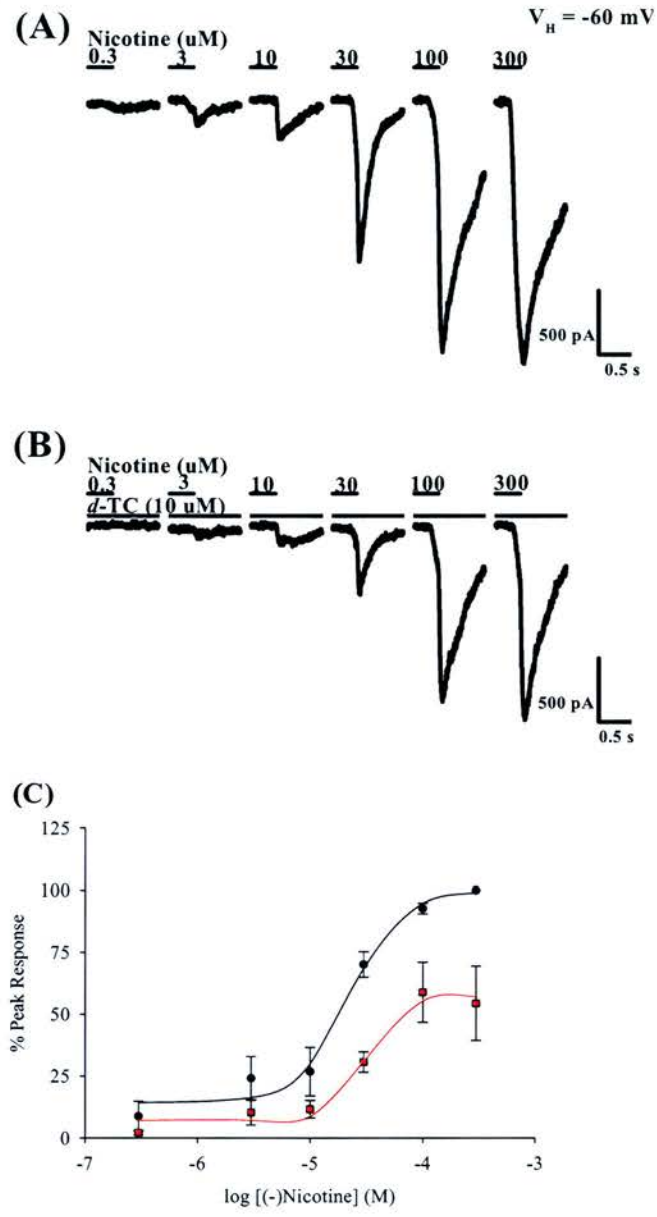

(-)Nicotine Evoked-Currents in SH-EP1-h$\alpha_4\beta_2$ Cells and its Inhibition by the Nicotinic Antagonist *d*-Tubocurarine. Representative traces of a single cell in response to (-)nicotine (A) alone or (B) in the presence of 10 μM *d*-TC. (C) The concentration-response relationship of (-)nicotine with normalised peak current amplitude (ordinate; percentage of response in same cell to 300 μM (-)nicotine as a function of dose (abscissa in molar untils, log scale) of (-)nicotine in the absence (EC_{50} = 22.2 ± 2.2, n_H = 1.99 ± 0.54; *n* = 3) or presence (EC_{50} = 31.4 ± 7.8, n_H = 2.27 ± 0.07; *n* =3) of 10 μM *d*-TC.

5.3.3 Examination of the Effect of Human $A\beta_{1-42}$ on (-)Nicotine Evoked Currents in SH-EP1-h$\alpha_4\beta_2$ cells

Prior to examining the effect of human $A\beta_{1-42}$ on I_{Nic}, initial control studies examined the effect of switching between two separate reservoirs of drug-free bath solution using similar conditions to that described in the previous section with a V_H of -60 mV and cells stimulated with 10 μM (-)nicotine for 375ms at 3 min intervals (total assay time was 66 mins). In brief, immediately following the third (-)nicotine stimulus, the flow from the reservoir was switched to a continuous supply from another reservoir containing either the compound of interest or drug-free bath solution and the cell stimulated a further 10 times with (-)nicotine (10 μM) every 3 min. Directly after the 10^{th} (-)nicotine (10 μM) stimulus the perfusion tube was switched back to the original bath solution and the cell stimulated a further 10 times with the same concentration of (-)nicotine. The entire protocol took 66 minutes.

Figure 5.20A shows a representative trace of I_{Nic} generated in a single SH-EP1-h$\alpha_4\beta_2$ cell exposed to (-)nicotine (10 μM) with a non significant change in peak amplitude observed after the switch to bath solution. Likewise, (-)nicotine-evoked responses generated after the switch back to the original bath solution source, also showed a non-significant decrease in peak amplitude (Figure 5.20B). The normalised peak current average from 3 individual SH-EP1-h$\alpha_4\beta_2$ cells was used as the control measure against which responses in the presence of bath solution or drug were compared. Average I_{Nic} response traces obtained during and after reservoir changes in bath solution are shown in Figure 5.20C.

To determine whether this decrease in I_{Nic} was an artefact of switching reservoirs or a consequence of the rundown described earlier, a direct assessment of the "switchover" effect was performed. Following a single application of (-)nicotine (10 μM), the reservoir either remained the same (no switch) or was switched to another reservoir containing drug-free bath solution (Figure 5.21). Clear functional rundown was observed over the 15 minute experimental interval regardless of whether reservoirs were changed during the experiment.

While conducting our studies investigating the interaction of $A\beta_{1-42}$ and nAChRs, a number of other groups were publishing similar investigation, although the $A\beta_{1-42}$ used was from a range of species, suppliers, and vehicles (Wang *et al.*, 2000a; Wang *et al.*, 2000b; Dineley *et al.*, 2001; Liu *et al.*, 2001; Pettit *et al.*, 2001; Dineley *et al.*, 2002; Tozaki *et al.*, 2002; Grassi *et al.*, 2003; Wu *et al.*, 2004). For example, Liu and colleagues (2001) used $A\beta_{1-42}$ dissolved in 5 % acetic acid whereas Wang and colleagues (2000a,b, personal communication) used $A\beta_{1-42}$ dissolved in a 50/50 mixture of DMSO and Tris HCl, (pH 8.0).

Figure 5.20

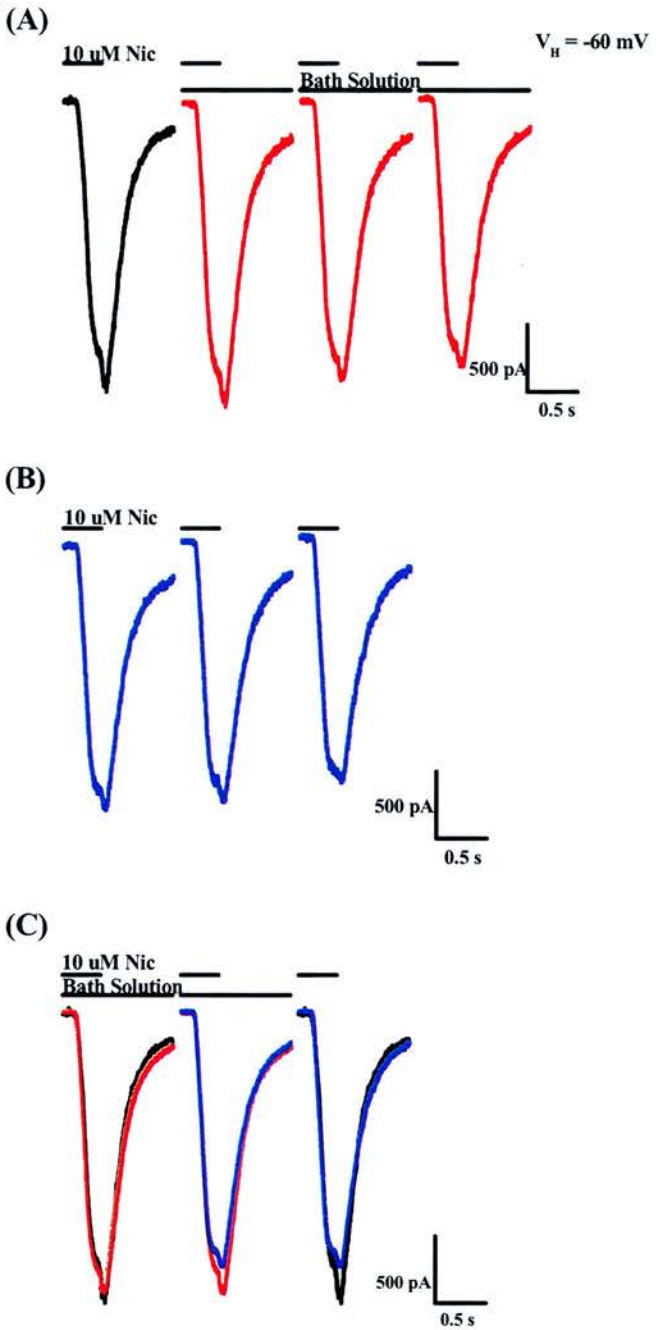

Rundown of (-)Nicotine Induced Currents in SH-EP1-h$\alpha_4\beta_2$ Cells. (A) Application of bath solution from a fresh source induced a significant change in whole cell current induced by (-)nicotine (10 μM). (B) Further characterisation of the washout of (-)nicotine induced currents in the SH-EP1-h$\alpha_4\beta_2$ cell line. (C) Representative overlays of the 3 main currents; control (●), bath solution from fresh source (●) and rundown (●). Traces are from a representative cell.

Figure 5.21

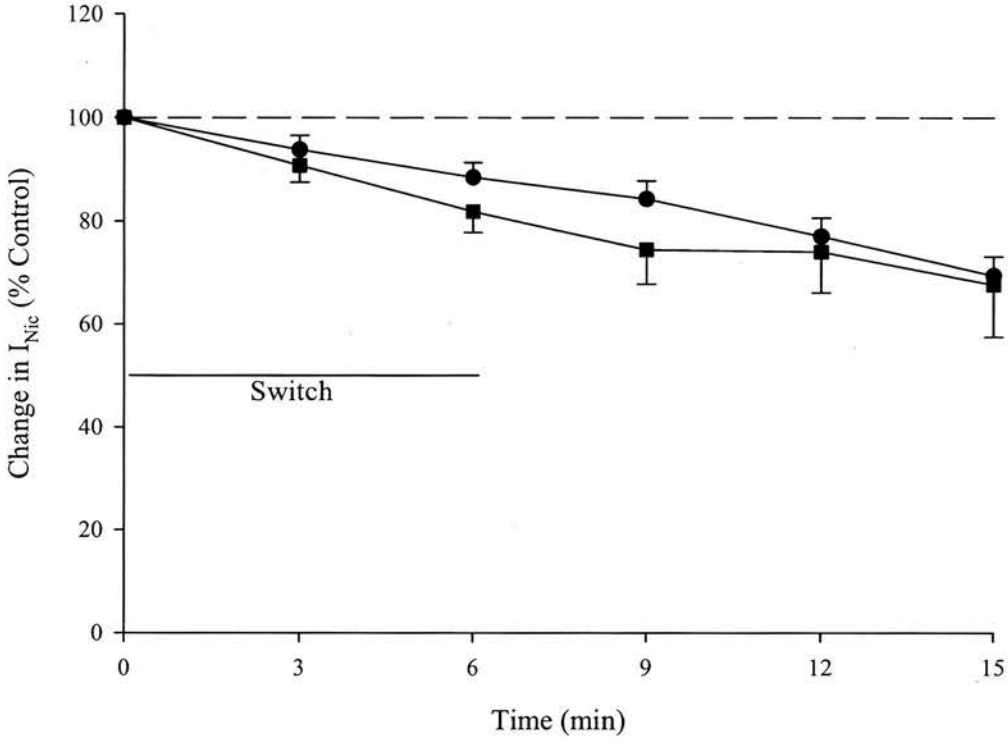

Switchover Does Not Effect Rundown of (-)Nicotine Induced Currents in SH-EP1-h$\alpha_4\beta_2$ Cells. (-)Nicotine (10 μM) was applied every 3 min for 375 ms. Reservoirs supplying bath solution were switched (●) or not switched (■) immediately following the first and third applications. Clear functional rundown of ~30 % was observed over the 15 minute experimental interval (regardless of whether reservoirs were changed during the experiment.

In the next four sections (5.3.3.1 – 5.3.3.4), I will discuss the effect of human $A\beta_{1-42}$ resuspended in HEPES buffer, 5 % acetic acid, DMSO/Tris, and finally in water as a water soluble acetate salt (Rpeptide $A\beta_{1-42}$).

5.3.3.1 Effect of Soluble Human $A\beta_{1-42}$ (Resuspended in 100 mM Hepes Buffer) on (-)Nicotine-Evoked Currents in SH-EP1-h$\alpha_4\beta_2$ Cells

The acute effects of human $A\beta_{1-42}$ on (-)nicotine-evoked current responses in SH-EP1 cells expressing the human $\alpha_4\beta_2$ cells were examined. To avoid peptide aggregation and maintain solubility, human $A\beta_{1-42}$ was resuspended in 100 mM HEPES buffer (pH 7.4) before serial dilution in bath solution. In brief, each cell has its own internal control with responses pre- and post-$A\beta_{1-42}$ treatment allowing for measurement of rundown. Figure 5.22, trace 1 shows the comparison between control response and the average response to 10 μM (-)nicotine in the presence of $A\beta_{1-42}$, while trace 2 compares the average response in the presence of 100 nM $A\beta_{1-42}$ to the average response following drug washout. Finally Figure 5.22, trace three illustrates the rundown present in the cell. To control for any potential vehicle effect, the HEPES buffer was also diluted in bath solution to the equivalent concentration used for the 100 nM $A\beta_{1-42}$ solution.

Initial studies indicated that 100 nM human $A\beta_{1-42}$ significantly inhibited I_{Nic} after 6 minutes of constant perfusion (Figure 5.22A). However, following a 10 min washout period, the current amplitude in response to (-)nicotine was not restored (Figures 5.22C). Somewhat surprisingly, the HEPES buffer control solution produced an inhibition of I_{Nic} in SH-EP1-h$\alpha_4\beta_2$ cells equivalent to that of human $A\beta_{1-42}$ (Figures 5.22 – 5.24). Therefore, these studies indicate the inhibition of I_{Nic} by soluble $A\beta_{1-42}$ (100 nM) in SH-EP1-h$\alpha_4\beta_2$ cells was in fact be due to a vehicle effect with this clearly illustrated in Figure 5.24.

Distinguishing a genuine drug inhibition response from functional rundown was therefore clearly problematic when cells were sustained for such long periods of time (i.e. up to 66 min). A shorter protocol (15 min) was therefore tried as the rundown during this period is considerably less marked. Cells were stimulated once with (-)nicotine (10 μM) before an immediate switch to human $A\beta_{1-42}$, vehicle, or bath solution for 6 min (2 further (-)nicotine applications). Following this 3rd application of (-)nicotine, the cells were

Figure 5.22

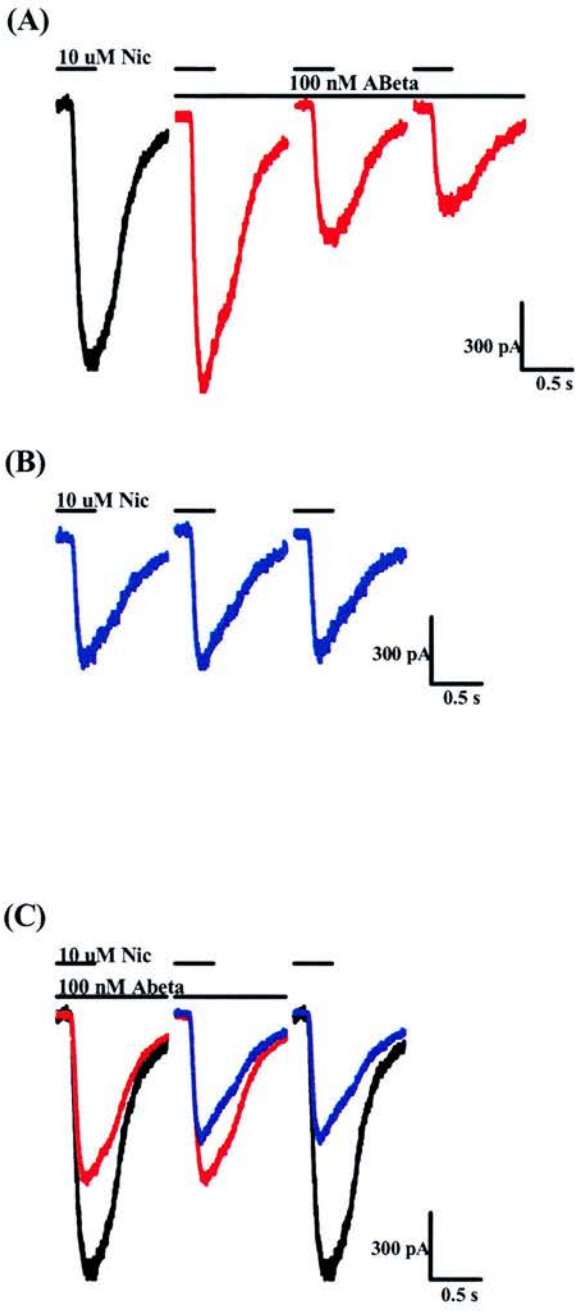

Effect of Soluble Human $A\beta_{1-42}$ (100 nM) Resuspended in HEPES (100 mM) on (-)Nicotine Evoked Currents in SH-EP1-h$\alpha_4\beta_2$ Cells. (A) Application of $A\beta_{1-42}$ produced a significant reduction in the whole cell current induced by (-)nicotine (10 μM) (B) Further characterisation of the current rundown by (-)nicotine application in the SH-EP1-h$\alpha_4\beta_2$ cell line in the absence of $A\beta_{1-42}$. (C) Representative overlays of the 3 main currents; control (●), human $A\beta_{1-42}$ solubilised in HEPES (●) and rundown (●) showing a significant difference between the 3 groups. Traces are from a representative cell.

Figure 5.23

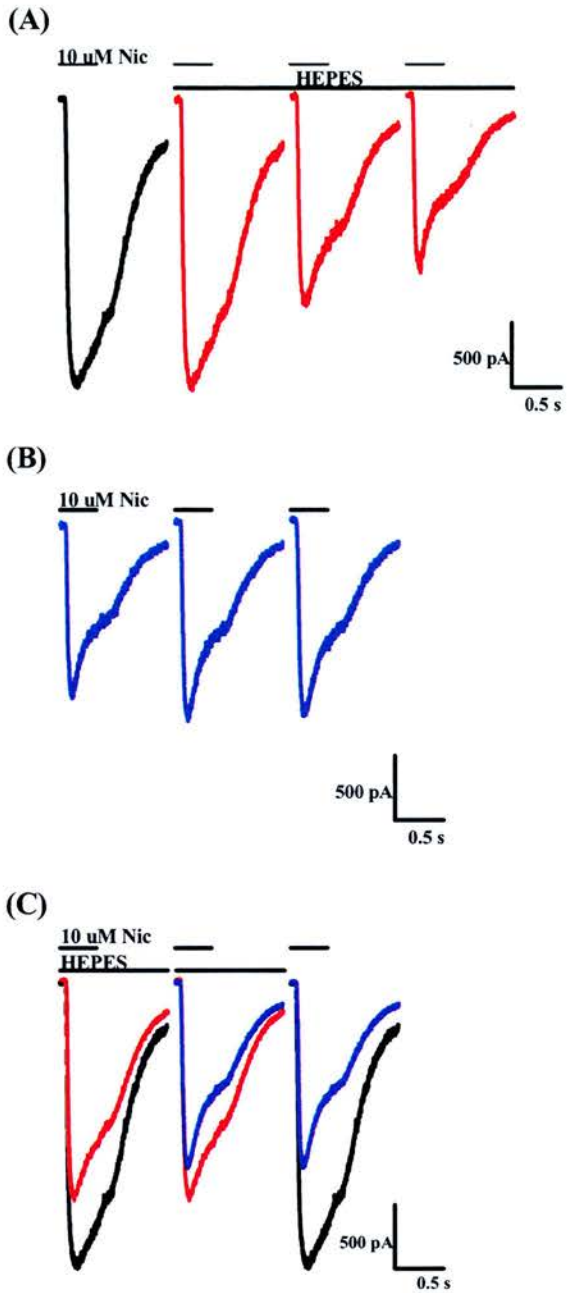

Effect of the $A\beta_{1-42}$ HEPES Vehicle on (-)Nicotine Evoked Currents in SH-EP1-h$\alpha_4\beta_2$ Cells. (A) Application of HEPES (at a concentration used to dissolve 100 nM $A\beta_{-42}$) induced a significant inhibition in the whole cell current induced by (-)nicotine (10 μM) equivalent to that induced by the 100 nM $A\beta_{1-42}$ solution (B) Further characterisation of the rundown of (-)nicotine induced currents in the SH-EP1-h$\alpha_4\beta_2$ cell line. (C) Representative overlays of the 3 main currents; control (●), HEPES vehicle (●) and rundown (●) showing a significant difference between the 3 groups. Traces are from a representative cell.

Figure 5.24

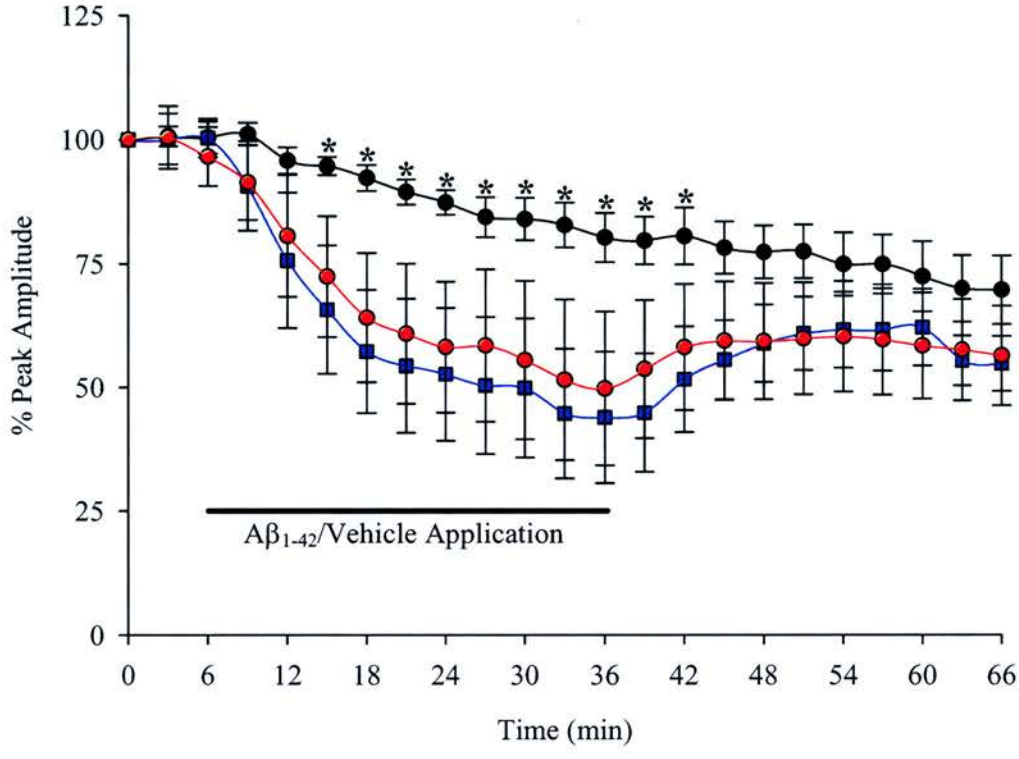

Summary of the Effect of Soluble β-Amyloid$_{1-42}$ (100 nM) Resuspended in HEPES on (-)Nicotine Evoked Currents in SH-EP1-h$\alpha_4\beta_2$ Cells. Whole-cell recording of (-)nicotine-evoked currents in SH-EP1-h $\alpha_4\beta_2$ nAChR cells were measured as described in *Materials and Methods*. (-)nicotine (10 μM) was applied for 375 ms at 3 min intervals. Following the 3rd application of (-)nicotine, the cell was constantly perfused for 30 min with (●) bath solution, (●) 100 nM Aβ_{1-42} originally resuspended in 100 mM Hepes buffer (pH 7.4), or (■) Hepes vehicle control, followed by a washout for a further 30 min. Peak amplitudes were normalised to the initial individual cell response to 10 μM Nic and averaged recordings were made from 3 cells with the data points representing mean ± S.E.M. * indicates significant inhibition of (-)nicotine evoked responses in SH-EP1-h$\alpha_4\beta_2$ cells by human Aβ_{1-42} and vehicle ($p < 0.05$).

returned to a drug-free bath solution. Consequently, this protocol allows for a 6 min constant drug/vehicle perfusion before the 4th application of (-)nicotine and a 3 and 6 min washout period before the 5th and 6th applications, respectively. Figure 5.25A illustrates the 15 min time-frame utilised in the following experiments and panel B-D explain how the data is assessed using this protocol.

As with the longer protocol control experiments were performed using two sources of the same bath solution to facilitate continual perfusion of the cell. Figure 5.26 shows that even using the shorter 15 min protocol, functional rundown of approximately 25% was observed across this time period (Figure 5.26). These responses represent the control data against which all further $A\beta_{1-42}$, antagonist or vehicle responses will be compared.

To demonstrate that I_{Nic} in human $\alpha_4\beta_2$ cells can be antagonised, the effect of the antagonist *d*-TC was examined. At a concentration of 10 μM, *d*-tubocurarine significantly inhibited the (-)nicotine-evoked response in SH-EP1-h$\alpha_4\beta_2$ cells by approximately 30 %, consistent with its dose response curve shown earlier (Figures 5.19 & 5.27).

To determine whether the shorter protocol could identify an effect with β-amyloid$_{1-42}$, the peptide (300 nM) was prepared in HEPES buffer (100 mM, pH 7.4) and serially diluted in bath solution. Representative traces of the effect of 300 nM $A\beta_{1-42}$ and the HEPES buffer vehicle control are shown in Figures 4.28 and 4.29, respectively. Figure 5.28 clearly shows that, following repeated applications of (-)nicotine, internal cell rundown was greater than the response generated by either the vehicle or $A\beta_{1-42}$ in vehicle. Therefore, 300 nM $A\beta_{1-42}$ had no inhibitory effect on the (-)nicotine induced current in SH-EP1-h$\alpha_4\beta_2$ cells (see Figure 5.30 for summary).

Figure 5.25

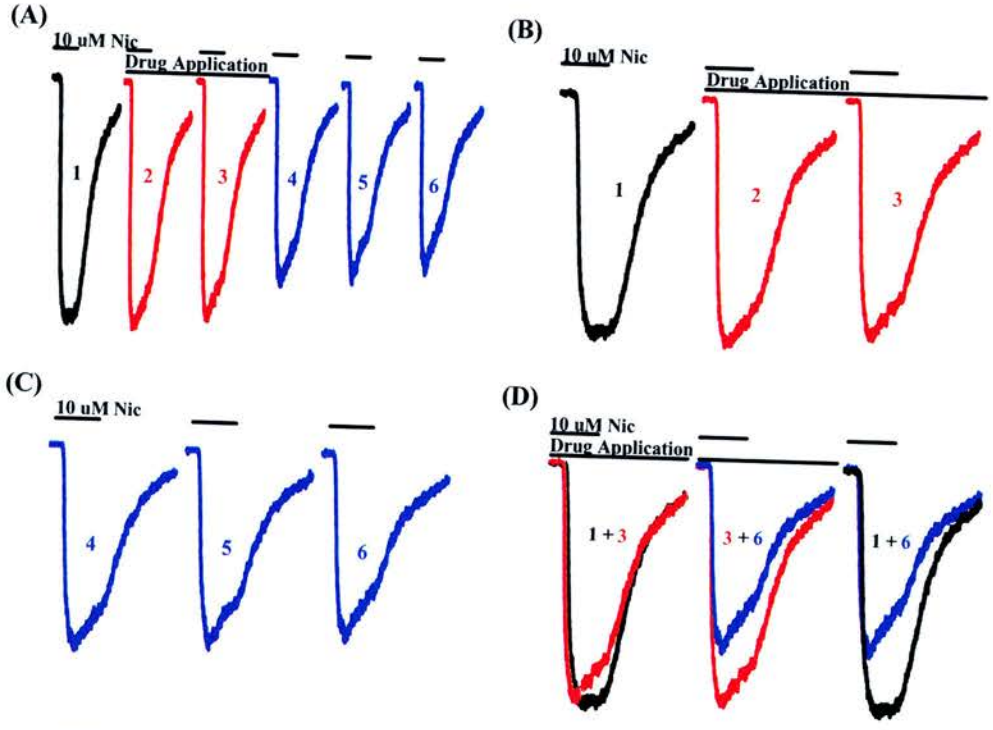

Diagramatic Representation of the 15 min Drug Application Protocol. (A) Immediately following an initial application of (-)nicotine (10 μM for 375 ms), the reservoir source is changed to one supplying drug or drug-free solution and (-)nicotine is applied twice more in this period. The reservoir was then immediately switched back to one supplying bath solution and (-)nicotine applied a further 3 times. (B) –(D) These panels simply illustrate the way in which the results was analysed. (B) This shows the effect of drug/vehicle on the (-)nicotine evoked response (C) This examines what occurs during the washout period (D) This is the composite and attempts to separate any drug effect from that of rundown.

Figure 5.26

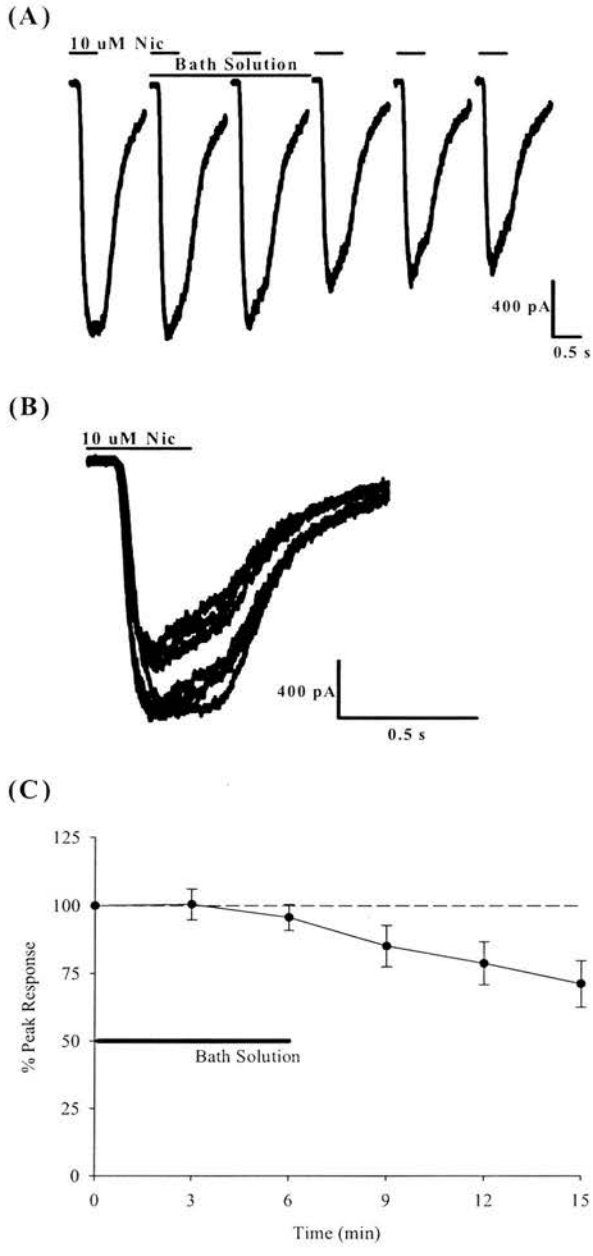

Response of Human $\alpha_4\beta_2$ nAChRs to (-)Nicotine While Under Constant Perfusion with Bath Solution. Whole-cell recording from the human $\alpha_4\beta_2$ nAChR cell line were measured as described in *Materials and Methods* with (-)nicotine (10 μM) applied for 375 ms every 3 min. (A) Representative trace of human $\alpha_4\beta_2$ nAChR responses to 10 μM (-)nicotine in a single cell. (B) Representative overlaid trace of the same cell shows clear functional rundown over the time course of the experiment. (C) Peak currents were normalised to the peak response produced by the first application of 10 μM (-)nicotine with recordings collected from 3 individual cells and the data represent mean± S.E.M.

Figure 5.27

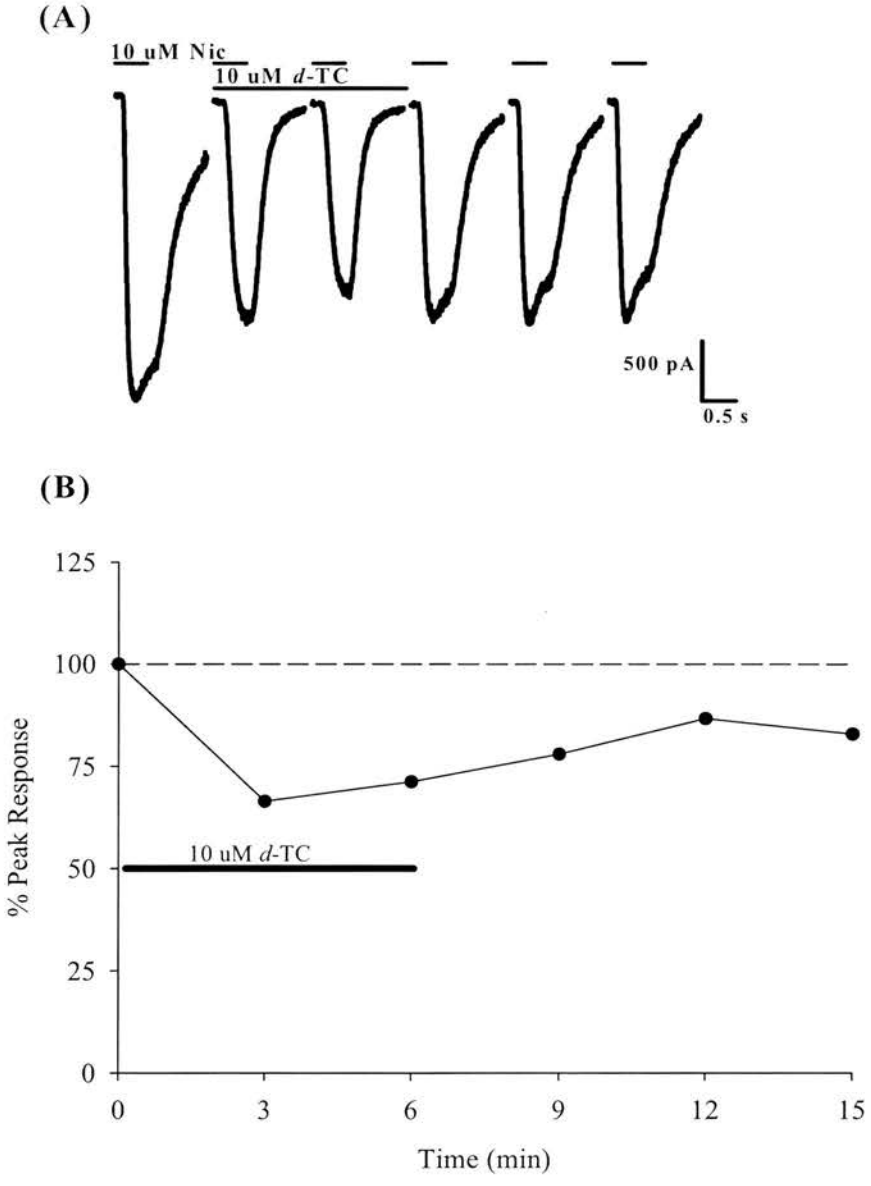

A Short Application of *d*-Tubocurarine Inhibited (-)Nicotine Evoked Currents in SH-EP1-h$\alpha_4\beta_2$ Cells. (-)Nicotine (10 μM) was applied for 375 ms at 3 min intervals. Immediately following the first application of (-)nicotine, bath perfusion reservoir was switched to one supplying 10 μM *d*-TC. Following 2 further applications of (-)nicotine (total *d*-TC application time was 6 min), the *d*-TC perfusion reservoir was switched back to one containing bath solution and a further 3 applications of (-)nicotine were applied (A) Representative trace of human $\alpha_4\beta_2$ nAChR responses to (-)nicotine (10 μM) in the presence and absence of 10 μM d-TC in a single cell (B) Peak currents were normalised to the peak response produced by the first application of 10 μM (-)nicotine with recordings collected from 2 individual cells and the data represented as the mean.

Figure 5.28

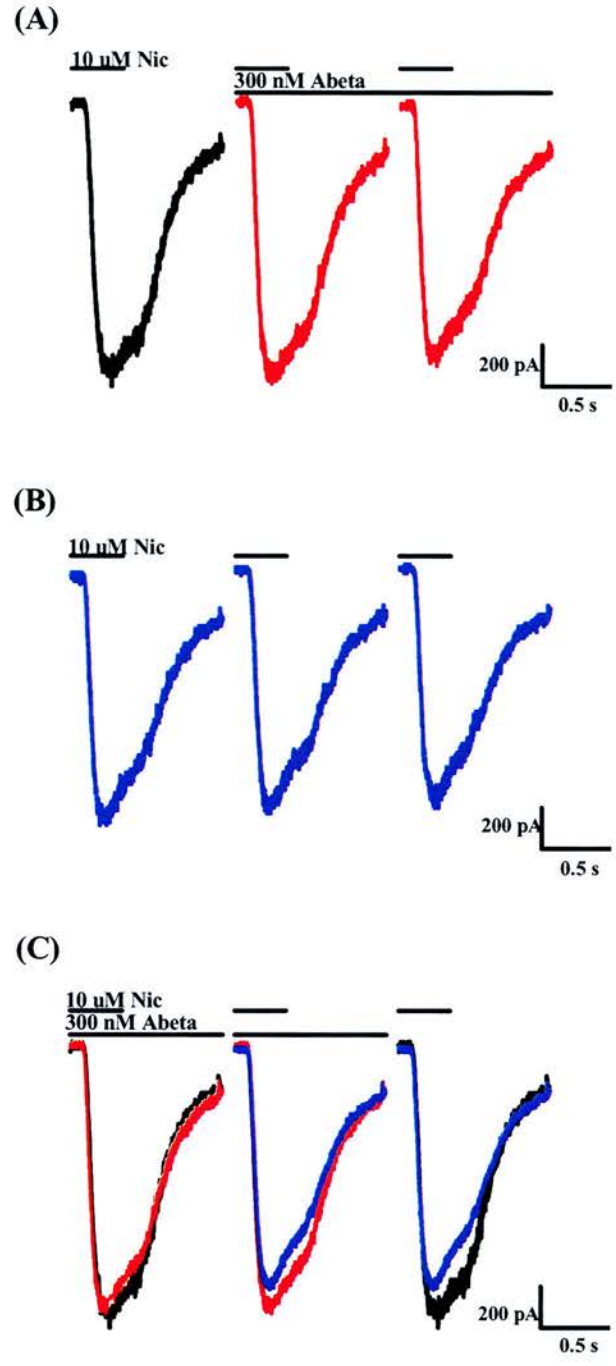

Effect of Soluble Human $A\beta_{1-42}$ (300 nM) Resuspended in HEPES (100 mM) on (-)Nicotine Evoked Currents in SH-EP1-h$\alpha_4\beta_2$ Cells. (A) Application of human $A\beta_{1-42}$ produced a significant reduction in the whole cell current induced by (-)nicotine (10 μM) (B) Further characterisation of the current rundown by (-)nicotine application in the SH-EP1-h$\alpha_4\beta_2$ cell line. (C) Representative overlays of the 3 main currents; control (●), human $A\beta_{1-42}$ solubilised in HEPES (●) and rundown (●) showing a significant difference between the 3 groups. Traces are from a representative cell.

Figure 5.29

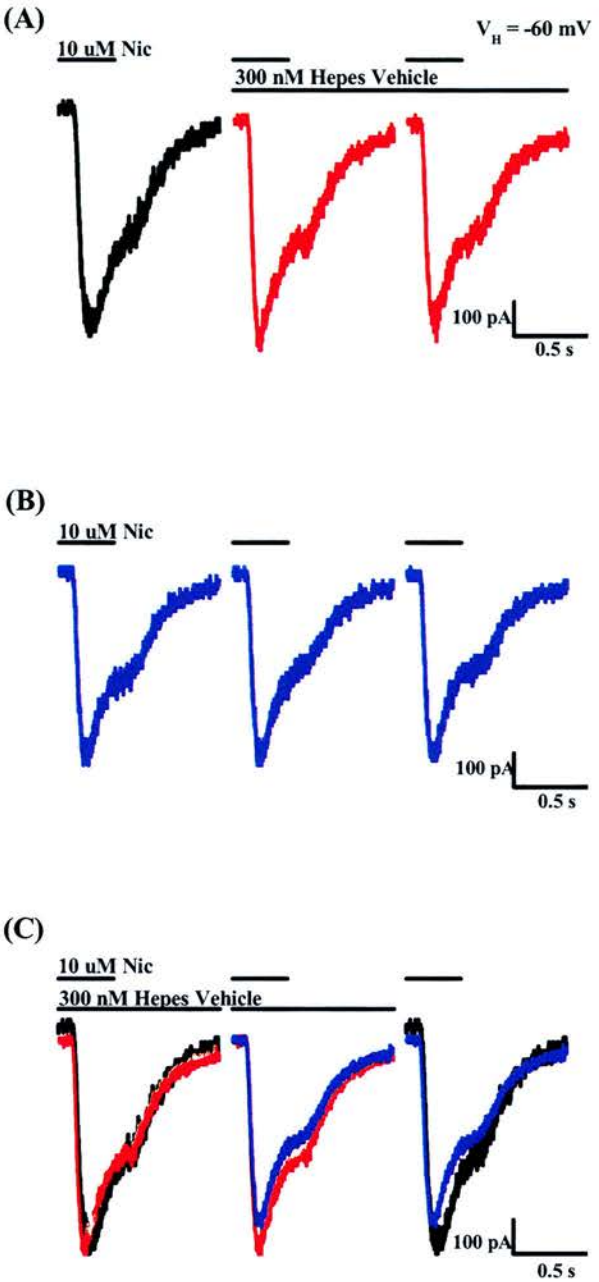

Effect of $A\beta_{1-42}$ (300 nM) HEPES Vehicle on (-)Nicotine Evoked Currents in SH-EP1-h$\alpha_4\beta_2$ Cells. Application of HEPES (at a concentration used to dissolve 300 nM $A\beta_{-42}$) induced a significant inhibition in the whole cell current induced by (-)nicotine (10 μM) equivalent to that induced by the 100 nM $A\beta_{1-42}$ solution (B) Further characterisation of the rundown of (-)nicotine induced currents in the SH-EP1-h$\alpha_4\beta_2$ cell line. (C) Representative overlays of the 3 main currents; control (●), HEPES vehicle (●) and rundown (●) showing a significant difference between the 3 groups. Traces are from a representative cell.

Figure 5.30

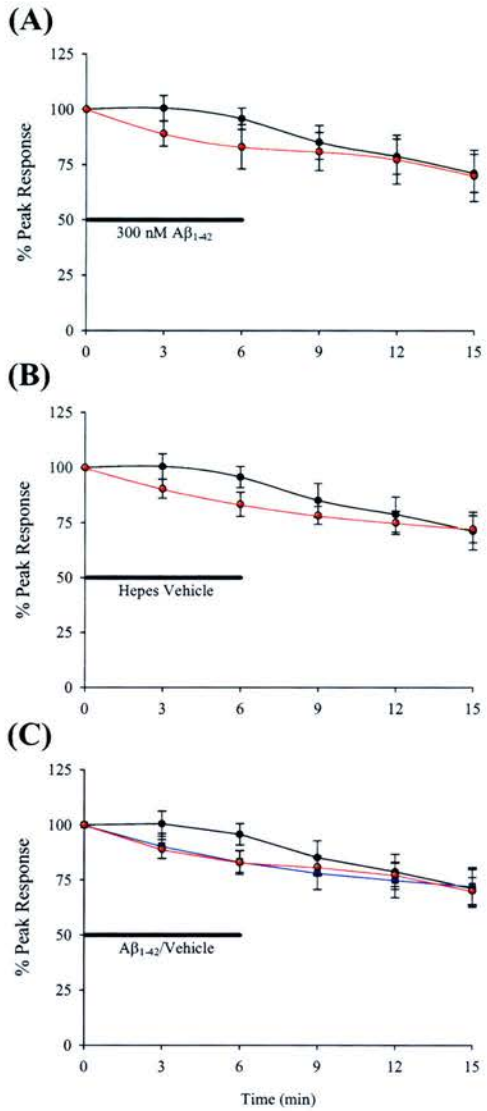

Lack of Inhibition of I_{Nic} in SH-EP1-h$\alpha_4\beta_2$ Cells by Soluble Human Aβ_{1-42} (300 nM) Prepared in HEPES Vehicle. (-)Nicotine (10 μM) was applied for 375 ms at 3 min intervals. Immediately following the initial 10 μM application of (-)nicotine at time zero, bath solution perfusion was changed to one supplying a continuous perfusate of either Aβ_{1-42} solubilised in HEPES buffer (●) or HEPES buffer at an equivalent concentration (●). After 2 further applications of (-)nicotine, the Aβ_{1-42}/Vehicle perfusate was stopped (total application time was 6 min) and the bath solution perfusion reinstated. Peak amplitude response for (A) 100 nM Aβ_{1-42} prepared in HEPES buffer or (B) HEPES buffer vehicle was normalised to the peak response produced by the initial application of (-)Nicotine. (C) Summary of normalised peak recordings for I_{Nic} in the presence and absence of 100 nM Aβ_{1-42} or HEPES buffer vehicle. Recordings were collected from 3 cells and data represent the mean ± S.E.M.

5.3.3.2 Effect of $A\beta_{1-42}$ Solubilised in 5% Acetic Acid on (-)Nicotine Evoked Currents in SH-EP1-h$\alpha_4\beta_2$ Cells

As with all human $A\beta_{1-42}$ studies, each SH-EP1-h$\alpha_4\beta_2$ cell examined has its own internal control with responses pre- and post-human $A\beta_{1-42}$ treatment allowing for measurement of rundown and was subsequently analysed as described in Figure 5.25. To control for any potential vehicle effect, a 5 % acetic solution was also diluted in bath solution to the equivalent concentration used for the 100 nM $A\beta_{1-42}$ solution.

Representative traces of 100 nM $A\beta_{1-42}$ dissolved in 5% acetic acid and its equivalent concentration vehicle control are shown in Figures 5.31 and 5.32, respectively. Again, with the effect of drug (Figure 5.31) and vehicle (Figure 5.32) being almost identical, these figures clearly illustrate that the inhibition of I_{Nic} by $A\beta_{1-42}$ is due to a vehicle response. The mean data for 3 cells is summarised in Figure 5.33 and clearly shows the overlap between vehicle and drug lines.

5.3.3.3 Effect of $A\beta_{1-42}$ Dissolved in 50/50 DMSO/Tris Buffer (-)Nicotine Evoked Currents in SH-EP1-h$\alpha_4\beta_2$ Cells

To produce non-fibrillar, soluble human $A\beta_{1-42}$, Wang and colleagues (2000a & b, personal communication) dissolved the peptide in a 50/50 mixture of DMSO and Tris HCl, (pH 8.0). Representative traces from a single cell, showing (-)nicotine evoked responses in the presence and absence of human $A\beta_{1-42}$ is shown in Figure 5.34. After a 3 min constant perfusion, $A\beta_{1-42}$ significantly inhibited I_{Nic} by almost 30 % ($n = 3$; $p < 0.05$; Figure 5.34). However, when the equivalent concentration of DMSO/Tris buffer was examined, it too was found to inhibit I_{Nic} in SH-EP1-h$\alpha_4\beta_2$ cells by an equivalent extent ($n = 3$; $p < 0.05$; Figure 5.35). The overall data is summarised in Figure 4.36, with human $A\beta_{1-42}$ and the DMSO/Tris HCl having a similar effect on the (-)nicotine evoked current in SH-EP1-h$\alpha_4\beta_2$ cells. Therefore, human $A\beta_{1-42}$ (100 nM) dissolved in 50/50 DMSO/Tris HCl had no inhibitory effect on I_{Nic} in SH-EP1-h$\alpha_4\beta_2$ cells.

Figure 5.31

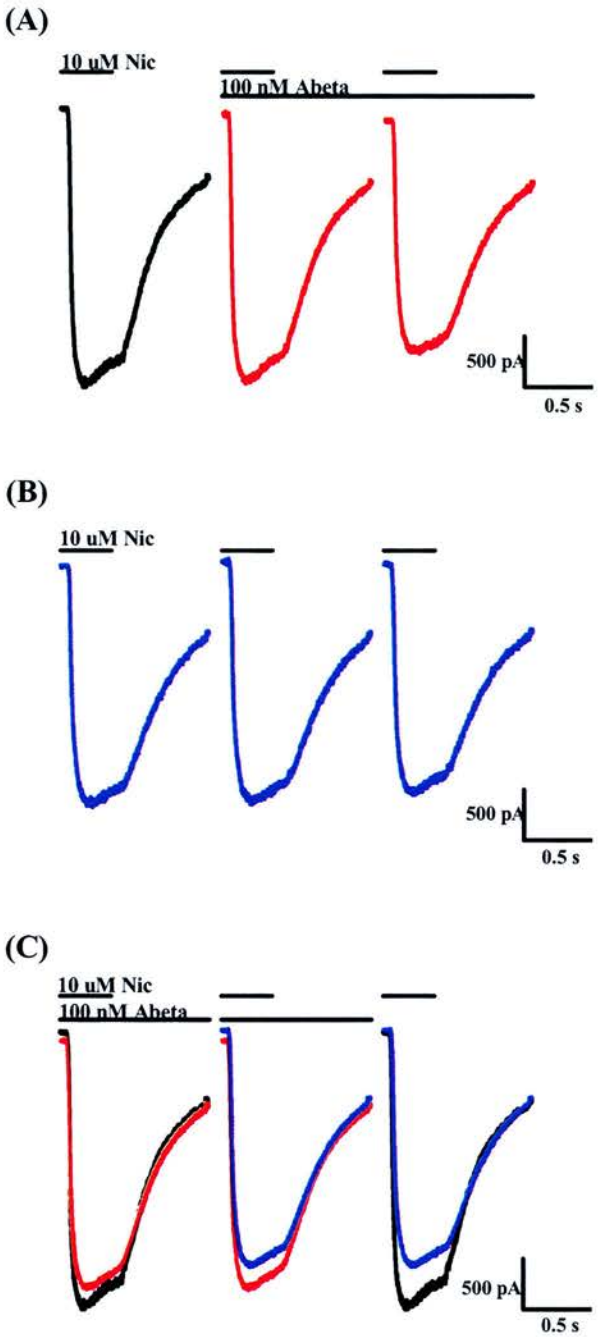

Effect of 100 nM $A\beta_{1-42}$ Resuspended in 5% Acetic Acid on (-)Nicotine Evoked Currents in SH-EP1-h$\alpha_4\beta_2$ Cells. (A) Application of human $A\beta_{1-42}$ produced a significant reduction in the whole cell current induced by (-)nicotine (10 μM) (B) Further characterisation of the current rundown by (-)nicotine application in the SH-EP1-h$\alpha_4\beta_2$ cell line. (C) Representative overlays of the 3 main currents; control (●), human $A\beta_{1-42}$ resuspended in 5 % acetic acid (●) and rundown (●) showing a significant difference between the 3 groups. Traces are from a representative cell.

Figure 5.32

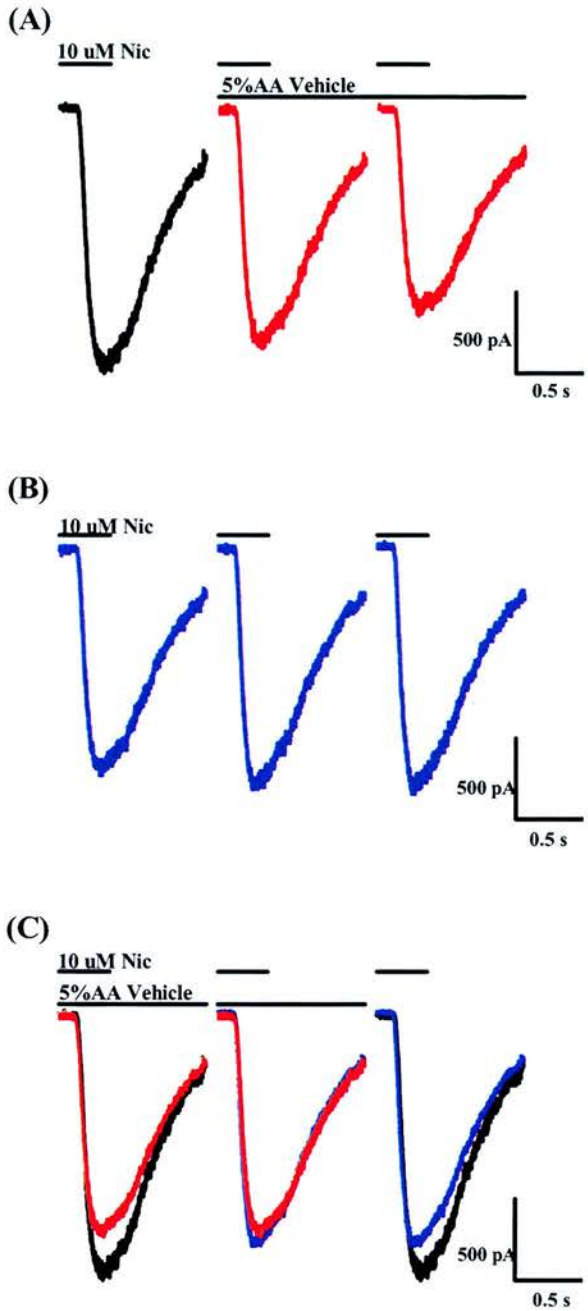

Effect of $A\beta_{1-42}$ 5% Acetic Acid Vehicle on (-)Nicotine Evoked Currents in SH-EP1-h$\alpha_4\beta_2$ Cells. Application of 5 % acetic acid (at a concentration used to dissolve 100 nM $A\beta_{-42}$) induced a significant inhibition in the whole cell current induced by (-)nicotine (10 μM) equivalent to that induced by the 100 nM $A\beta_{1-42}$ solution (B) Further characterisation of the rundown of (-)nicotine induced currents in the SH-EP1-h$\alpha_4\beta_2$ cell line. (C) Representative overlays of the 3 main currents; control (●), 5 % acetic acid vehicle (●) and rundown (●) showing a significant difference between the 3 groups. Traces are from a representative cell.

Figure 5.33

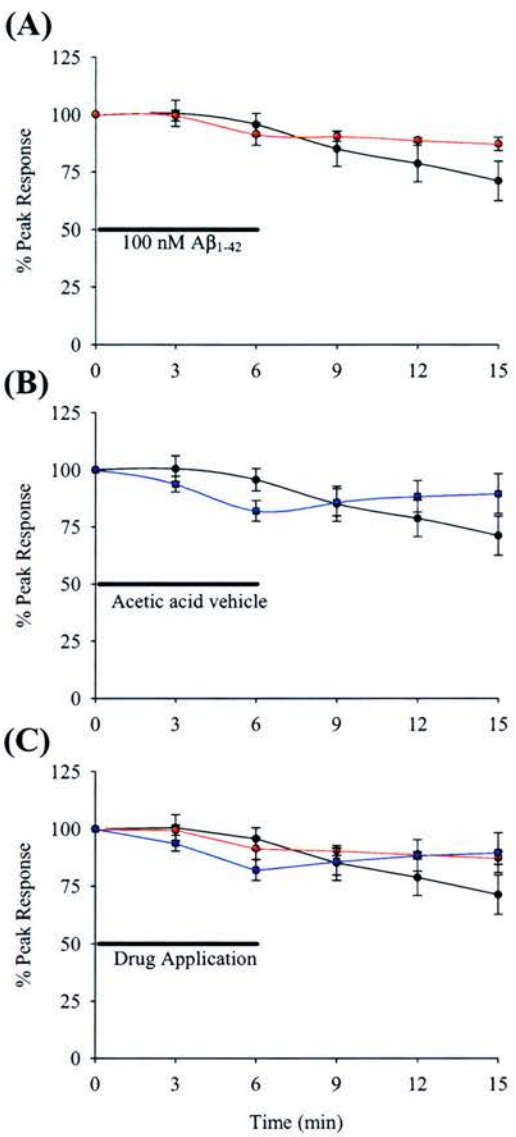

Lack of Inhibition of I_{Nic} in SH-EP1-h$\alpha_4\beta_2$ Cells by Soluble Human Aβ_{1-42} (300 nM) Prepared in 5% Acetic Acid. (-)Nicotine (10 μM) was applied for 375 ms at 3 min intervals. Immediately following the initial 10 μM application of (-)nicotine at time zero, bath solution perfusion was changed to one supplying a continuous perfusate of either Aβ_{1-42} (in 5% acetic acid; ●) or 5 % acetic acid at an equivalent concentration (●). After 2 further applications of (-)nicotine, the Aβ_{1-42}/Vehicle perfusate was stopped (total application time was 6 min) and the bath solution perfusion reinstated. Peak amplitude response for (A) 100 nM Aβ_{1-42} prepared in 5% acetic acid or (B) 5 % acetic acid vehicle was normalised to the peak response produced by the initial application of (-)nicotine. (C) Summary of normalised peak recordings for I_{Nic} in the presence and absence of 100 nM Aβ_{1-42} or 5 % acetic acid vehicle. Recordings were collected from 3 cells and data represent the mean ± S.E.M.

Figure 5.34

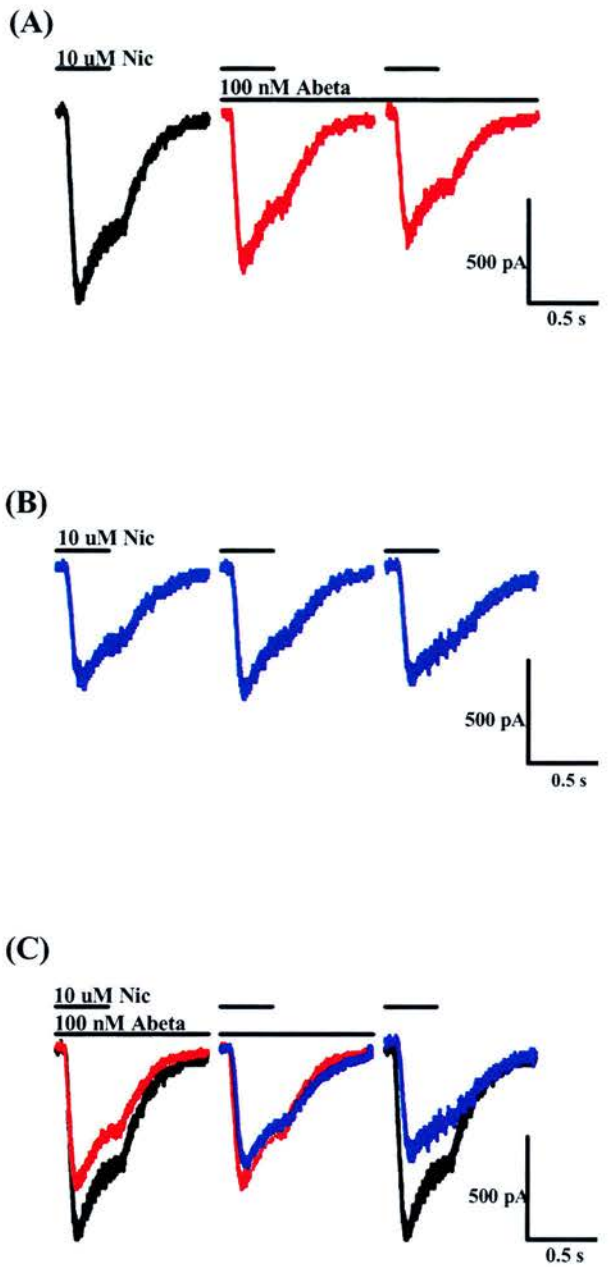

Effect of 100 nM $A\beta_{1-42}$ Resuspended in DMSO/Tris on (-)Nicotine Evoked Currents in SH-EP1-h$\alpha_4\beta_2$ Cells. (A) Application of human $A\beta_{1-42}$ produced a significant reduction in the whole cell current induced by (-)nicotine (10 μM) (B) Further characterisation of the current rundown by (-)nicotine application in the SH-EP1-h$\alpha_4\beta_2$ cell line. (C) Representative overlays of the 3 main currents; control (●), human $A\beta_{1-42}$ resuspended in DMSO/Tris (●) and rundown (●) showing a significant difference between the 3 groups. Traces are from a representative cell.

Figure 5.35

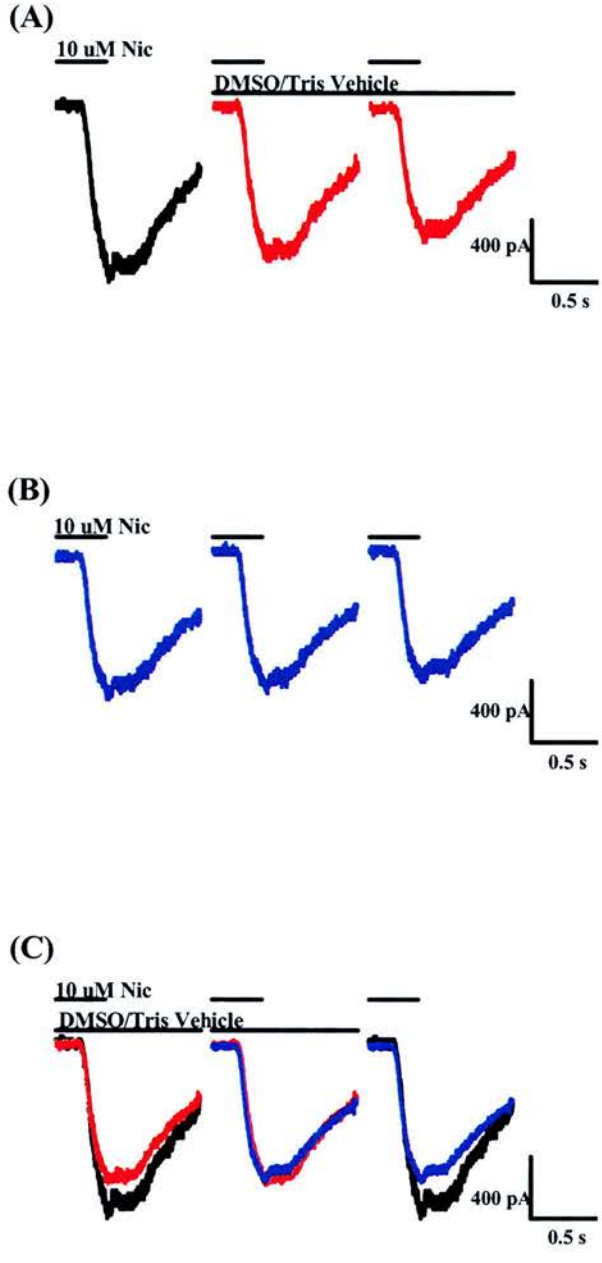

Effect of $A\beta_{1-42}$ DMSO/Tris Vehicle on (-)Nicotine Evoked Currents in SH-EP1-h$\alpha_4\beta_2$ Cells. Application of DMSO/Tris (at a concentration used to dissolve 100 nM $A\beta_{-42}$) induced a significant inhibition in the whole cell current induced by (-)nicotine (10 μM) equivalent to that induced by the 100 nM $A\beta_{1-42}$ solution (B) Further characterisation of the rundown of (-)nicotine induced currents in the SH-EP1-h$\alpha_4\beta_2$ cell line. (C) Representative overlays of the 3 main currents; control (●), DMSO/Tris vehicle (●) and rundown (●) showing a significant difference between the 3 groups. Traces are from a representative cell.

Figure 5.36

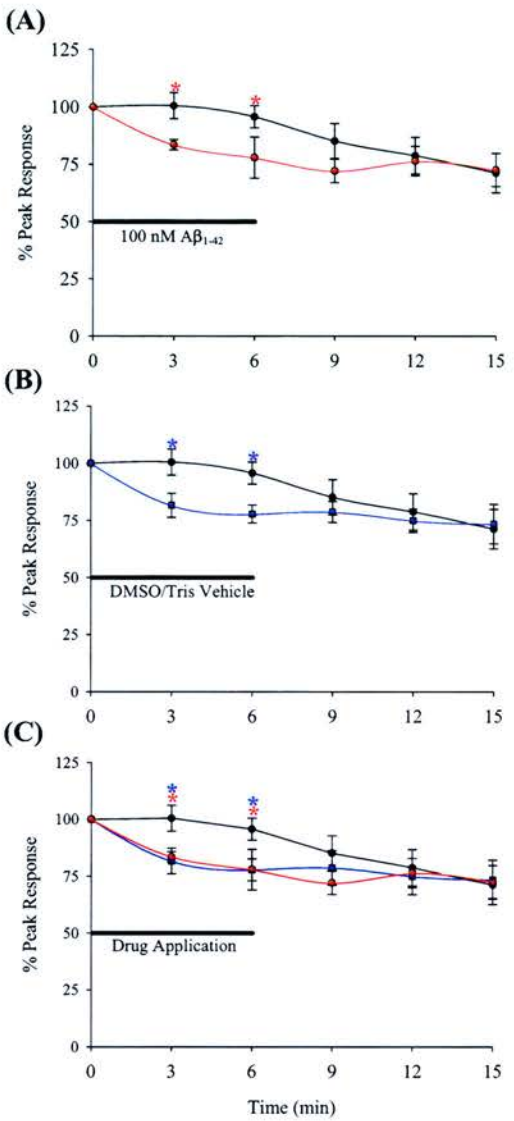

Lack of Inhibition of I_{Nic} in SH-EP1-h$\alpha_4\beta_2$ Cells by Soluble Human Aβ_{1-42} (300 nM) Prepared in DMSO/Tris. (-)Nicotine (10 μM) was applied for 375 ms at 3 min intervals. Immediately following the initial 10 μM application of (-)nicotine at time zero, bath solution perfusion was changed to one supplying a continuous perfusate of either Aβ_{1-42} (in DMSO/Tris; ●) or DMSO/Tris at an equivalent concentration (●). After 2 further applications of (-)nicotine, the Aβ_{1-42}/Vehicle perfusate was stopped (total application time was 6 min) and the bath solution perfusion reinstated. Peak amplitude response for (A) 100 nM Aβ_{1-42} prepared in DMSO/Tris or (B) DMSO/Tris vehicle was normalised to the peak response produced by the initial application of (-)nicotine. (C) Summary of normalised peak recordings for I_{Nic} in the presence and absence of 100 nM Aβ_{1-42} or DMSO/Tris vehicle. Recordings were collected from 3 cells and data represent the mean ± S.E.M.

5.3.3.4 Effect of Rpeptide Human $A\beta_{1-42}$ Acetate salt on (-)Nicotine Evoked Currents in SH-EP1-h$\alpha_4\beta_2$ Cells

During the course of my studies, Wu and colleagues (2004) published a paper showing the Rpeptide $A\beta_{1-42}$ (100 nM) inhibited human $\alpha_4\beta_2$ nAChRs expressed in SH-EP1 cells. Therefore, the final human $A\beta_{1-42}$ solution utilised was a newly available $A\beta_{1-42}$ acetate salt (Rpeptide Ltd., USA) that was water soluble, potentially eliminating the confounding vehicle effects. Representative traces from single cells exposed to either 100 or 300 nM $A\beta_{1-42}$ are shown in Figures 5.37 and 5.38. To ensure no inhibitory effect of vehicle, an acetate salt solution equivalent to that used to dissolve 300 nM Rpeptide $A\beta_{1-42}$ was examined. Vehicle alone had no inhibitory inhibitory effect on I_{Nic} in SH-EP1-h$\alpha_4\beta_2$ cells (Figure 5.39). The effect of both Rpeptide human $A\beta_{1-42}$ (100 and 300 nM) and the equivalent high concentration acetate vehicle are summarised in Figure 5.40, where you can clearly see that neither concentration of $A\beta_{1-42}$ had any effect on (-)nicotine evoked currents in human $\alpha_4\beta_2$ nAChRs that was distinct from vehicle.

Figure 5.37

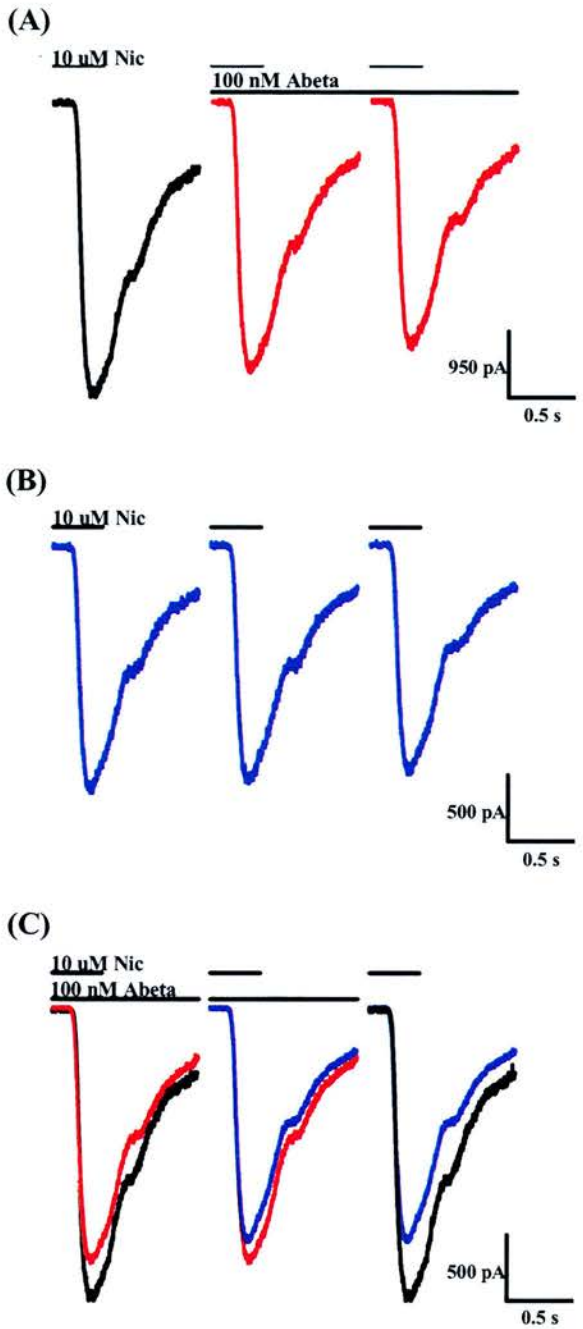

Effect of Rpeptide Human $A\beta_{1-42}$ Acetate Salt (100 nM) on (-)Nicotine Evoked Currents in SH-EP1-h$\alpha_4\beta_2$ Cells. (A) Application of human $A\beta_{1-42}$ produced a significant reduction in the whole cell current induced by (-)nicotine (10 μM) (B) Further characterisation of the current rundown by (-)nicotine application in the SH-EP1-h$\alpha_4\beta_2$ cell line. (C) Representative overlays of the 3 main currents; control (●), Rpeptide human $A\beta_{1-42}$ (●) and rundown (●) showing a significant difference between the 3 groups. Traces are from a representative cell.

Figure 5.38

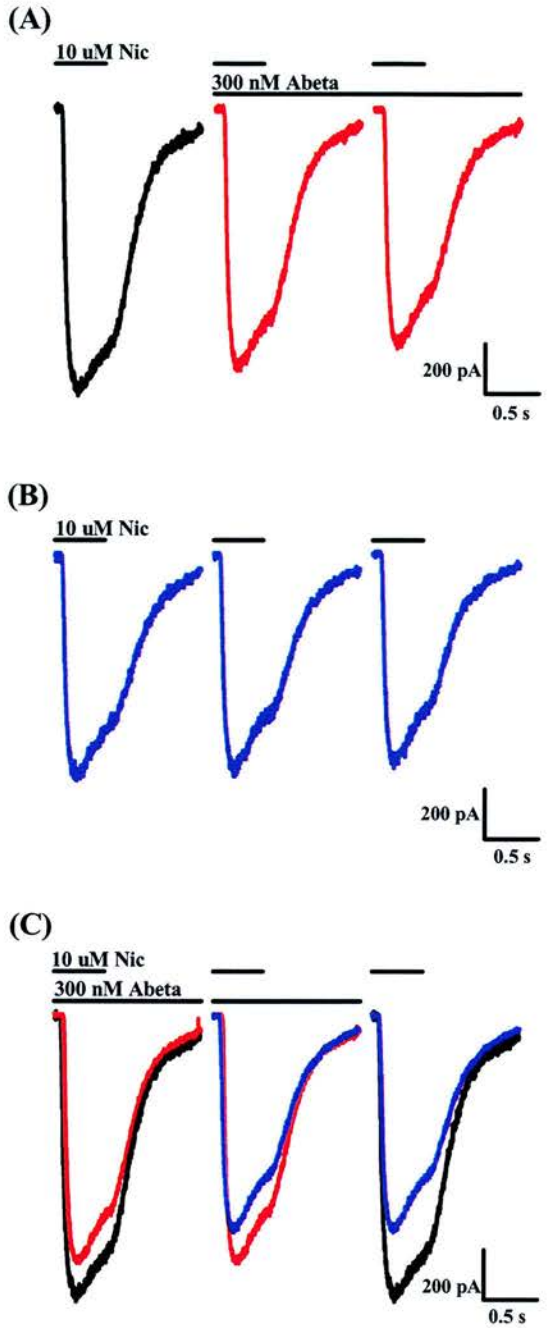

Effect of Rpeptide Human $A\beta_{1-42}$ Acetate Salt (300 nM) on (-)Nicotine Evoked Currents in SH-EP1-h$\alpha_4\beta_2$ Cells. (A) Application of human $A\beta_{1-42}$ produced a significant reduction in the whole cell current induced by (-)nicotine (10 μM) (B) Further characterisation of the current rundown by (-)nicotine application in the SH-EP1-h$\alpha_4\beta_2$ cell line. (C) Representative overlays of the 3 main currents; control (●), Rpeptide human $A\beta_{1-42}$ (●) and rundown (●) showing a significant difference between the 3 groups. Traces are from a representative cell.

Figure 5.39

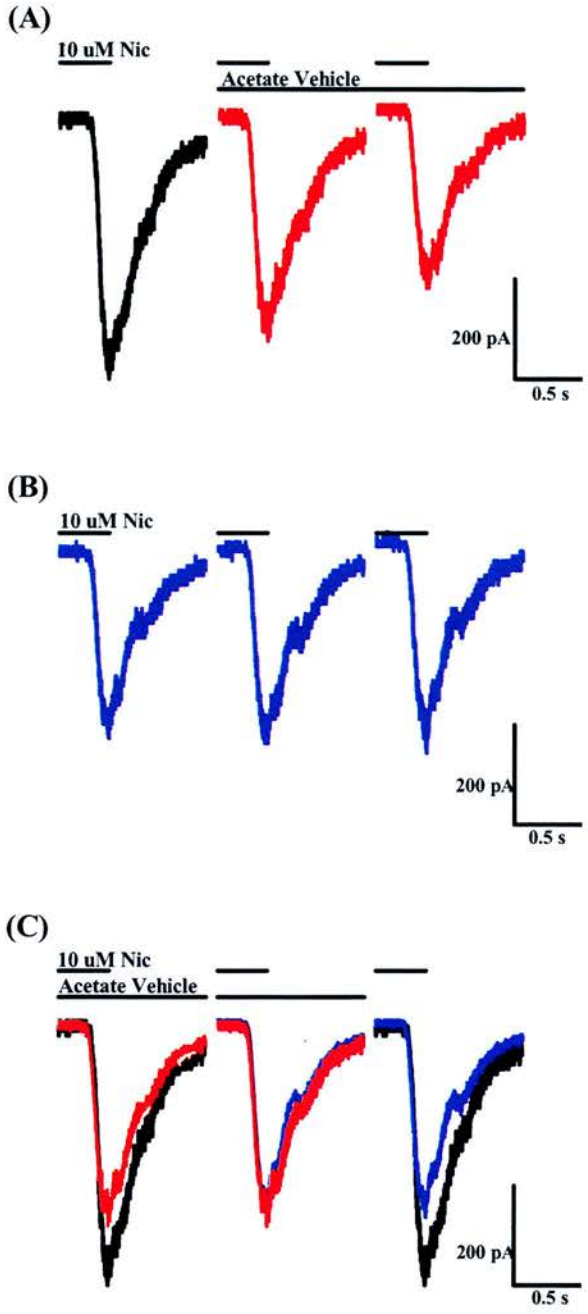

Effect of $A\beta_{1-42}$ Acetate Vehicle on (-)Nicotine Evoked Currents in SH-EP1-h$\alpha_4\beta_2$ Cells. Application of acetate vehicle (at a concentration used to dissolve 300 nM $A\beta_{-42}$) induced a significant inhibition in the whole cell current induced by (-)nicotine (10 μM) equivalent to that induced by the 100 nM $A\beta_{1-42}$ solution (B) Further characterisation of the rundown of (-)nicotine induced currents in the SH-EP1-h$\alpha_4\beta_2$ cell line. (C) Representative overlays of the 3 main currents; control (●), DMSO/Tris vehicle (●) and rundown (●) showing a significant difference between the 3 groups. Traces are from a representative cell.

Figure 5.40

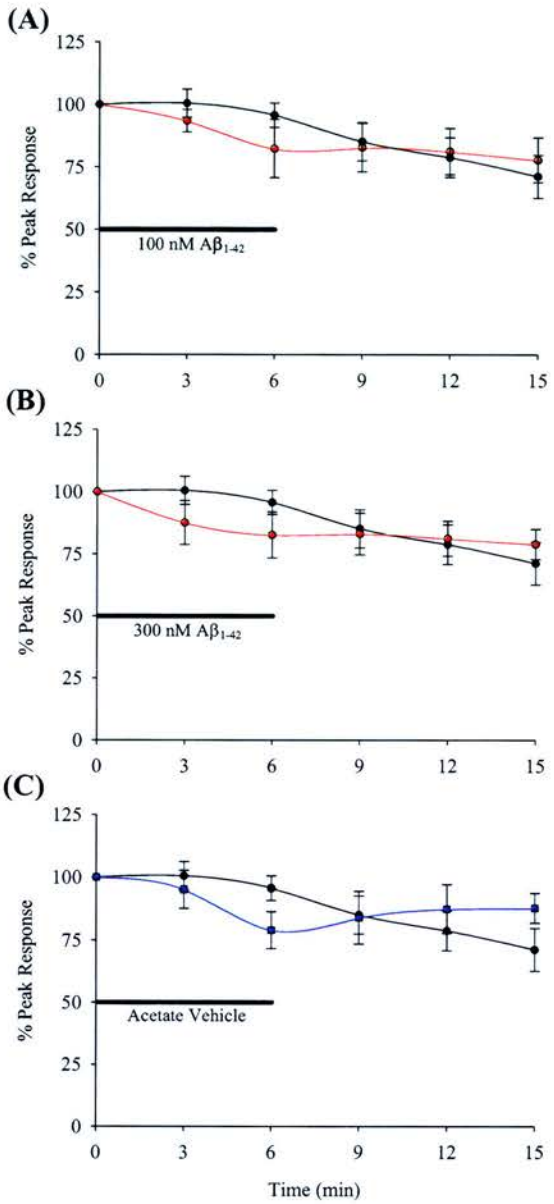

Lack of Inhibition of I_{Nic} in SH-EP1-h$\alpha_4\beta_2$ Cells by $A\beta_{1-42}$ Rpeptide Acetate Salt. (-)Nicotine (10 μM) was applied for 375 ms at 3 min intervals. Immediately following the initial 10 μM application of (-)nicotine at time zero, bath solution perfusion was changed to one supplying a continuous perfusate of either (A) $A\beta_{1-42}$ (100 nM) or (B) $A\beta_{1-42}$ (300 nM) or (C) acetate vehicle at an equivalent concentration (●). After 2 further applications of (-)nicotine, the $A\beta_{1-42}$/Vehicle perfusate was stopped (total application time was 6 min) and the bath solution perfusion reinstated. Peak amplitude responses were normalised to the peak response produced by the initial application of (-)nicotine. Recordings were collected from 3 cells and data represent the mean ± S.E.M.

5.4 Examination of Human α_7 nAChR Electrophysiology

The inability to detect changes in intracellular calcium and membrane potential of SH-EP1-hα_7 cells (detailed in the Section 5.2.3) may simply result from assay insensitivity for these cells. As such, whole cell current recording was used to characterise the pharmacology of the human α_7 nAChR. As discussed above, electrophysiological analysis of single cells allows more detailed investigation of the functional viability of receptors.

5.4.1 Characterisation of the Pharmacological Properties of the Human α_7 nAChR Using Whole Cell Patch Clamp Studies in SH-EP1-hα_7 Cells

Electrophysiology experiments were performed using whole cell recording in a voltage clamp mode at a holding potential (V_H) of -60 mV. Although nominally a stable cell line, application of (-)nicotine to SH-EP1-hα_7 cells resulted in the absence of or low peak current amplitudes of only a few picoamperes. Indeed, the majority of cells failed to exhibit functional responses despite using both K^+-free and K^+-containing electrodes as discussed in Section 5.3.1 (pg 189) for the human $\alpha_4\beta_2$ nAChRs. To encourage functional surface expression of the human α_7 nAChR, Molinari and colleagues (1998) treated HEK293 cells with nicotinic agonists and antagonists. Pre-treatment of the SH-EP1-hα_7 cells with α_7 nAChR-specific antagonist MLA did not result in consistent, or indeed, increased functional responses in these cells. However, treatment with MLA did allow completion of a full (-)nicotine dose-response curve from which an EC_{50} of 43 μM was measured (Figure 5.41A & C).

5.4.2 Characterisation of the Pharmacological Properties of the Human α_7 nAChR Using Other Cell Lines

The lack of consistent functional responses obtainable from the SH-EP1-hα_7 cell line led me to look to other cell lines from which I might determine functional α_7 nAChR pharmacology. The rat pituitary cell line, GH4C1, in which the human α_7 nAChR was over-expressed, was obtained from the European Collection of Cell Cultures (ECACC) and maintained in our laboratories (Section 2.2.2). Like the SH-EP1 cell line, GH4C1 cells do not express any native α_7 nAChRs and has been used by other groups to investigate α_7 nAChR pharmacology (Quik *et al.*, 1996; Sweileh *et al.*, 2000). Unfortunately, peak current responses in GH4C1 cells were also low and inconsistent, again reflecting the difficult of expressing functional α_7 nAChRs in neuronal cell lines. However, I did obtain a full (-

)nicotine dose response profile with a (-)nicotine EC_{50} value of 53 μM, consistent with that obtained from the SH-EP1-hα_7 cells (Figure 5.41B & C).

Finally, I conducted both electrophysiological and [^{3}H]-MLA binding studies to assess the potential of IMR32 cells for functional studies. Like SH-EP1 cells, IMR32 cells are a neuroblastoma derived cell line but have been shown to express native α_7 nAChRs (Gotti *et al.*, 1995). Only a small level of [^{3}H]-MLA binding was observed in GH4C1 cells. Consistent with the lack of [^{3}H]-MLA binding in this cell line (Figure 5.4.2), no functional responses were obtained from the IMR32 cells.

Figure 5.41

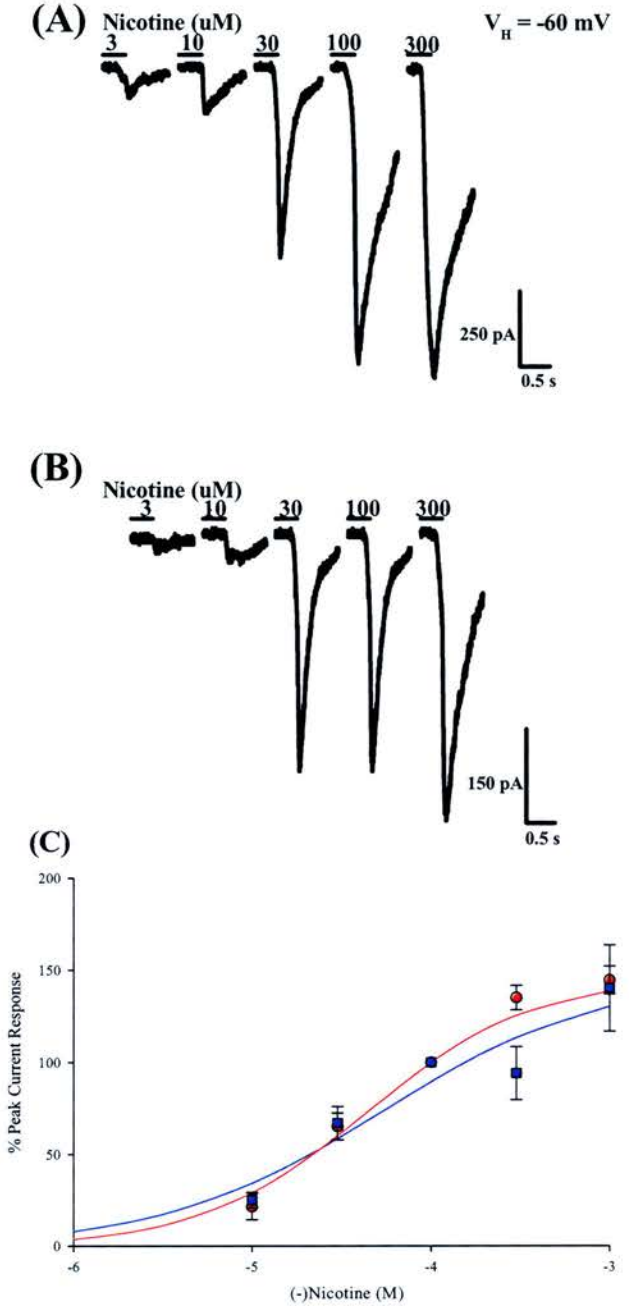

(-)Nicotine Evoked-Currents in SH-EP1 and GH4C1 Cells in Which the Human α_7 nAChR was Over-Expressed. Representative traces of a single cell in response to (-)nicotine in (A) SH-EP1-hα_7 or (B) GH4C1 cells. (C) The concentration-response relationship of (-)nicotine with normalised peak current amplitude (ordinate; percentage of response in same cell to 1 mM (-)nicotine as a function of dose (abscissa in molar untils, log scale) of (-)nicotine in the SH-EP1-hα_7 (●, EC_{50} = 43 μM, n = 9) or GH4C1 (■, EC_{50} = 53 μM; n =4) cells.

Figure 5.42

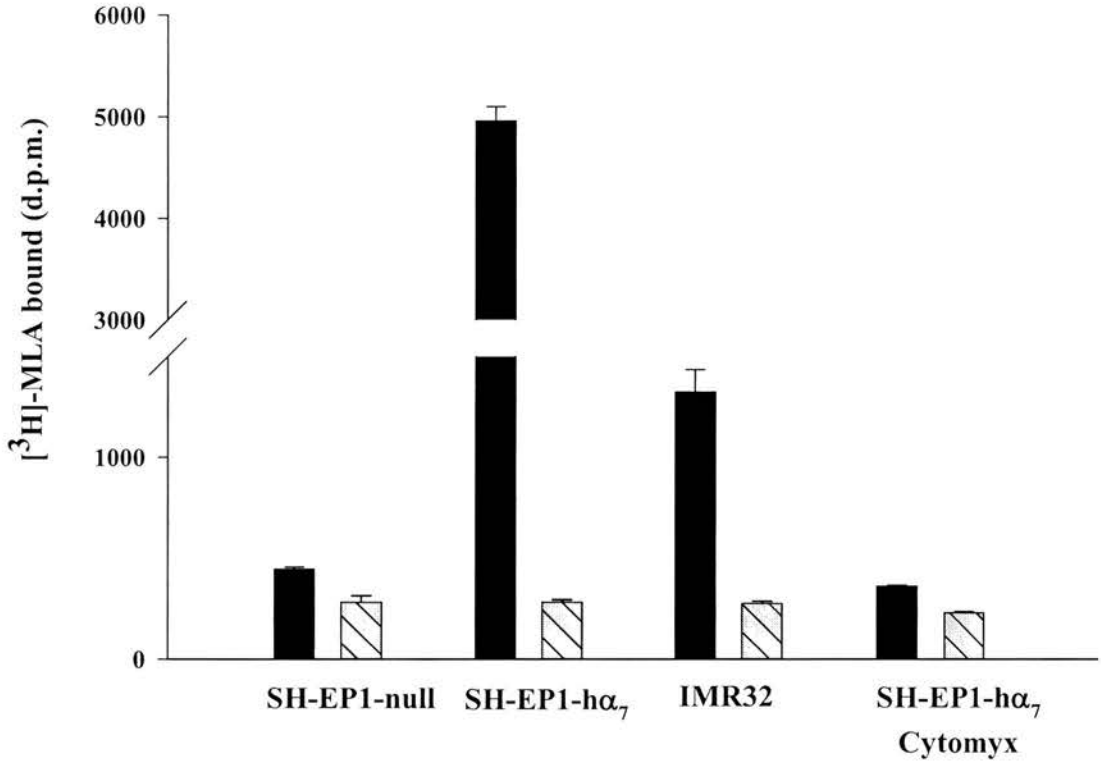

Proportions of [^{3}H]-MLA Binding in Various Cell Membrane Preparations. Membranes (~60 μg) prepared from SH-EP1-Null (SH-EP-host), SH-EP1-hα_7, IMR32, and SH-EP1 cells transiently transfected with the human α_7 nAChR (SH-EP1-hα_7) were incubated with [^{3}H]-MLA (2.5 nM) in a total assay volume of 250 μl for 60 min at 22°C. ■ Total Binding whilst non-specific binding (▩) was determined in the presence of 10 μM *d*-tubocurarine.

5.5.1 Co-Immunoprecipitation Analysis of Human $\alpha_4\beta_2$ or α_7 nAChRs with Human $A\beta_{1-42}$

At the outset of my Ph.D, Wang and colleagues (2000a), presented some exciting data showing the co-localisation and co-immunoprecipitation of human $A\beta_{1-42}$ with the human α_7 nAChR. To confirm and extend these finding I examined whether human $A\beta_{1-42}$ could co-immunoprecipitate with either the human $\alpha_4\beta_2$ or the α_7 nAChRs. SH-EP1 cells stably expressing either the human $\alpha_4\beta_2$ or α_7 nAChR were used in these studies and were incubated with human $A\beta_{1-42}$ for 30 min, probed with the appropriate IP antibody and finally analysed using western analysis. Initial experiments determined the ability of anti-α_4, anti-α_7, or anti-$A\beta_{1-42}$ antibodies to detect the presence of the α_4, α_7, or human $A\beta_{1-42}$, respectively, on a Western blot. Finally, prior to their use in co-immunoprecipitation studies, the ability of the anti-α_4, anti-α_7, and anti-$A\beta_{1-42}$ antibodies to detect immunoprecipitation of their target was assessed.

5.5.1.1 Western Blot Analysis of the Human α_4 nAChR Subunit

Lysates were prepared (see Methods Section 2.7.1) from SH-EP1-h$\alpha_4\beta_2$ cells and then subjected to Western blot analysis with a rat monoclonal anti-α_4 nAChR antibody (mAb299). No band was detected in lysates prepared from SH-EP1 cells indicating there was no detectable native α_4 nAChR subunits in the host cell line (Figure 5.43). In contrast, a clear band at a molecular weight of 60 kDa was identified, consistent with the molecular weight predicted from the amino acid sequence of the human α_4 nAChR subunit (Figure 5.43; Elliott *et al.*, 1996).

5.5.1.1A Immunoprecipitation Analysis of the Human α_4 nAChR Subunit

Lysates prepared from SH-EP1-h$\alpha_4\beta_2$ cells were immunoprecipitated with the anti-α_4 nAChR subunit antibody H133 (rabbit polyclonal). Following precipitation of the antigen-H133 complex using Protein G agarose, the complex was eluted and successfully analysed by Western blot analysis using the anti-α_4 nAChR subunit monoclonal antibody mAb299 (mouse; Figure 5.44). Clear bands were observed at 60 kDa in both the control lysate and in the sample which had been subjected to immunoprecipitation (Figure 5.44).

Figure 5.43

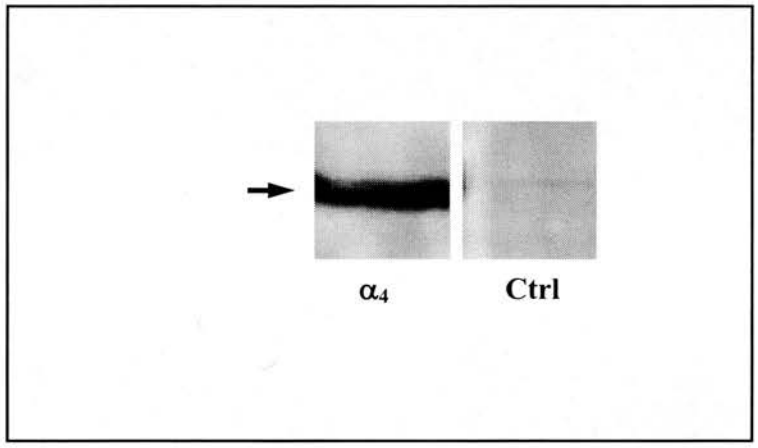

Western Blot Analysis of SH-EP1-hα$_4$β$_2$ Cell Lysates with an Anti-α$_4$ nAChR Subunit Antibody. Solubilised SH-EP1-hα$_4$β$_2$ cells (30 μg) and SH-EP1-Host cells (Ctrl, 30 μg) were subjected to SDS-PAGE separation on NuPAGE® 4-12 % Bis-Tris Gels (Invitrogen, UK) before transferring to nitrocellulose membranes for Western blot analysis. Membranes were blocked by a PBS buffer containing 5 % skim milk powder and incubated overnight (4°C) with the anti-α$_4$ nAChR subunit antibody 299 (rat monoclonal, 1:1,000, Sigma). Following three 5 min washes in PBS buffer containing 0.05 % Tween20 (PBS_T), horseradish peroxidase conjugated goat anti-rat conjugated IgG secondary antibody (Santa Cruz Biotechnology, 1:1,000) was added to the reaction medium. After 1 h membranes were washed (3 x 5 min) in PSB_T and visualised using ECL^+ chemiluminescence kit (Amersham Biosciences, UK). A clear band at 60 kDa can be observed in the α$_4$ nAChR sample.

Figure 5.44

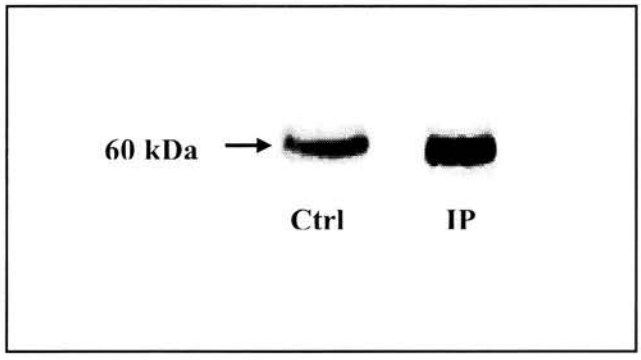

Immunoprecipitation of the Anti-α_4 nAChR Subunit Antibodies in SH-EP1-h$\alpha_4\beta_2$ cell lysates. Solubilised SH-EP1-h$\alpha_4\beta_2$ cell lysates (1 mg) were incubated overnight (4°C) with the anti-α_4 nAChR subunit antibody H133 (Santa Cruz Biotechnology, 5 μg/ml) and protein G agarose beads (Sigma). The sample was washed three times in NP Buffer (see Methods) and then sample buffer containing β-mercaptoethanol (20 μl/sample) added. Samples were then subjected to electrophoretic separation on NuPAGE® 4-12 % Bis-Tris Gels (Invitrogen, UK) before transfer to nitrocellulose membranes for Western blot analysis. Membranes were blocked in a PBS buffer containing 5 % skimmed milk powder and incubated overnight (4°C) with the rat anti-α_4 nAChR subunit antibody 299 (Sigma, 1:1,000). Following three 5 min washes in PBS buffer containing 0.05 % Tween20 (PBS_T), horseradish peroxidase conjugated goat anti-rat conjugated IgG secondary antibody (Santa Cruz Biotechnology, 1:1,000) was added to the reaction medium. After 1 h membranes were washed (3 x 5 min) in PSB_T and visualised using ECL^+ chemiluminescence kit (Amersham Biosciences, UK). The control sample represents 30 μg of protein prior to addition of antibodies. A clear immunoreactive band at 60 kDa can be observed in both the control (Ctrl; cell lysate) and immunoprecipitation (IP) sample.

5.5.1.2 Development of the Western Blot Analysis of the Human α_7 nAChR subunit

To detect the human α_7 nAChR subunit protein on a Western blot, lysates were prepared from SH-EP1-hα_7 cells and the choice of transfer membrane, blocking solution, and primary antibody sequentially altered in an attempt to enhance the α_7 nAChR protein signal.

5.5.1.3A Transfer of Proteins from the Polyacrylamide Gel to Transfer Membrane

Nitrocellulose and polyvinylidene difluoride (PVDF) membranes constitute two of the most popular transfer membranes. PVDF has a higher protein binding capacity and lower background than nitrocellulose but requires pre-soaking in 100% methanol. This latter step may interfere with the protein of interest causing degradation of sample.

The ability of three different anti-α_7 nAChR subunit antibodies to detect α_7 nAChR protein in Western blots was examined following transfer to either nitrocellulose or PVDF membranes. Lysates were first separated using gel electrophoresis as described before transfer to the membrane of choice. Using nitrocellose membranes, a clear protein band was detected at 55 kDa, consistent with the molecular weight predicted from the amino acid sequence of the human α_7 nAChR (Peng *et al.*, 1994b; Figures 5.45A & 5.45B). Interestingly, this band was only detected using the anti-α_7 nAChR antibodies M220 (mouse monoclonal) and sc-5544 (rabbit polyclonal; Figure 5.45A). Weak or no immunoreactivity was observed when the goat polyclonal anti-α_7nAChR antibody sc-1447 was used (Figure 5.45A). In contrast to the former two antibodies which map to amino acids 380-400 (M220) and 367-502 (sc-5544) of the α_7 nAChR, the sc-1447 epitope maps to the C terminus of the α_7 nAChR and may not be suitable for use with the SH-EP1-hα_7 cell line. When PVDF membranes were used, the immunoreactive signal was weak or absent regardless of antibody employed (Figure 5.45B). In the following Western blot experiments, I attempted to optimise the signal of the anti-α_7 nAChR antibody M220 using the nitrocellulose transfer membrane.

5.5.1.3B Oxidation or Reduction of Samples

The rate-limiting step in Western blot analysis is often the ability of the primary antibody to recognise the antigen epitope within the sample. If the epitope is located within the protein of interest, the protein must be denatured to expose the epitope and enable the antibody to bind. The most common method of protein denaturation is to heat the sample gently (e.g. 95°C for 10 min) before loading it onto the polyacrylamide gel. In addition,

Figure 5.45

(A) Nitrocellulose Membranes

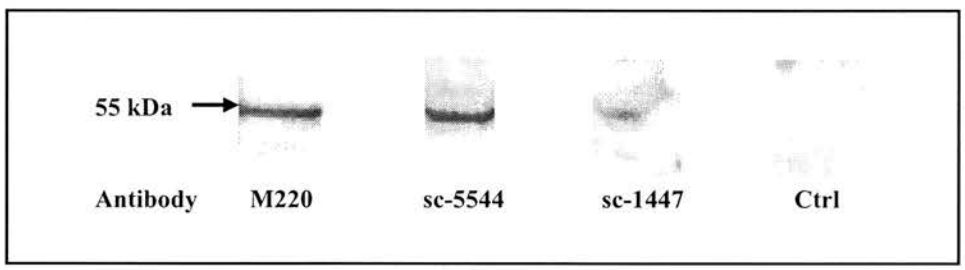

(B) PVDF Membranes

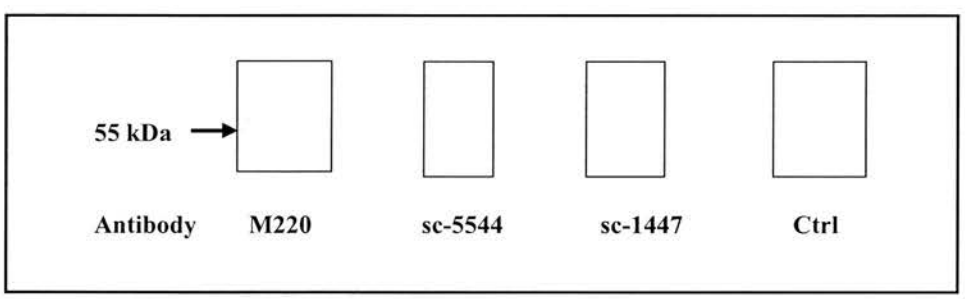

Effect of Transfer Membrane on the Detection of α_7 nAChR Protein in Western Blot Analysis. The ability of anti-α_7 antibodies M220 (mouse monoclonal, Sigma, 1:1,000), sc-5544 (rabbit polyclonal, Santa Cruz Biotechnology, 1:200), and sc-1447 (goat polyclonal, Santa Cruz Bioctechnology, 1:100) to detect the α_7 nAChR subunit was examined using Western blot analysis and (A) nitrocellulose or (B) PVDF membranes for the transfer step (see *Methods*). Lysates were prepared from SH-EP1-hα_7 cells (30 μg) and subjected to Western analysis using the appropriate primary and secondary antibodies (Table 2.1). The control sample (Ctrl) represents a sample (30 μg) prepared from SH-EP1-h$\alpha_4\beta_2$ cell membranes and probed with anti-α_7 antibodies. Clear protein bands were observed when the anti-α_7 nAChR antibodies M220 or sc-5544 were utilised in conjunction with nitrocellulose membranes. The immunoreactive signal using these antibodies and PVDF membranes was weak (M220) or absent (sc-5544). In contrast, weak (A) or no (B) immunoreactive signal was observed using sc-1447 and either nitrocellulose or PVDF membranes. No immunoreactivity was present in control samples.

reducing agents such as dithiothreitol (DTT) or β-mercaptoethanol are often used to break any disulphide bonds present within the protein.

According to the information provided by the supplier (Sigma, M220), the anti-α_7 nAChR M220 only recognises the denatured form of the human α_7 nAChR. As such, all the SH-EP1-hα_7 lysates examined were heated at 95°C for 10 min prior to sample loading on the gel. However, care must also be taken when adding reducing agents to your sample as they can potentially destroy the epitope recognised by the primary antibody. The effect of the reducing agent DTT on the intensity of the α_7 nAChR protein band was examined by preparing samples in the absence or presence of DTT (0.1 M) prior to Western blot analysis. The intensity of the immunoreactive signal did not alter despite inclusion of DTT in the sample buffer (Figure 5.46). Therefore, as a precautionary measure only, DTT continued to be included in the sample buffer.

5.5.1.3C Extraction Buffers

Care must be taken when choosing a detergent to solubilise the membrane preparations used in Western blotting. Detergents work by mimicking the lipid bilayer environment, with the wide range available broadly classified into three categories including ionic, non-ionic, and zwitterionic. Ionic detergents are usually positively (cationic), or negatively (anionic) charged and include sodium dodecyl sulphate (SDS), an anionic detergent which is commonly incorporated into many running buffers. Non-ionic detergents such as Triton X-100 contain uncharged hydrophilic head groups and are generally better suited for breaking lipid-lipid and lipid-protein interactions rather than protein-protein interactions (Bhairi, 2001). In contrast zwitterionic detergents such as 3-[(3-Cholamidopropyl)dimethylammonio]-1-propanesulfonate (CHAPS) exhibit properties of both ionic and non-ionic detergents. These latter detergents lack a net charge, conductivity, and electrophoretic mobility and are efficient at breaking protein-protein interactions (Bhairi, 2001).

The zwitterionic detergent CHAPS and the non-ionic detergent Triton X-100 were used to solubilise membranes from SH-EP1-hα_7 cells, to determine what effect this had on the signal intensity. By maximising the solubilisation process, the protein yield should increase and thereby enhance the 55 kDa immunoreactive signal. A weak protein band was observed at 55 kDa when utilising the CHAPS detergent (Extraction $Buffer_{CHAPS}$, (EB_{CHAPS}) Figure 5.47), whereas a stronger immunoreactive signal was present when using Triton X-100 was employed in the extraction buffer (Extraction $Buffer_{Triton}$, (EB_{Triton}). All subsequent

Figure 5.46

(A) Reducing Conditions

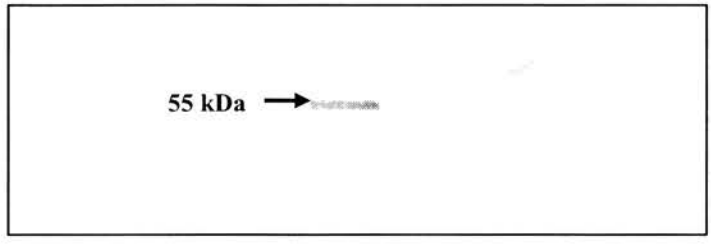

(B) Non-Reducing Conditions

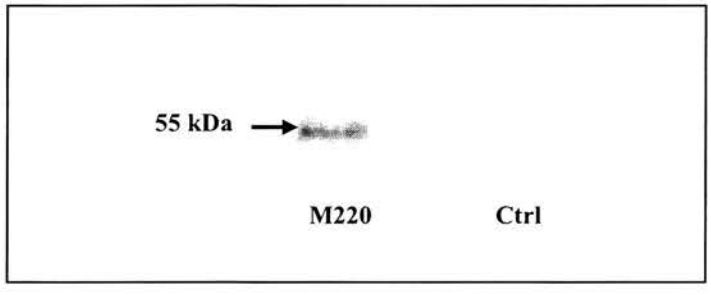

Effect of the Reducing Agent DTT on the Signal Intensity of the α_7 nAChR Protein in Western blots. Lysates (SH-EP1-hα_7 cells) were prepared in sample buffer in the (A) presence or (B) absence of reducing agent dithiothreitol (0.1 M DTT). Following electrophoresis using NuPAGE® Bis-Tris polyacrylamide gels, samples were transferred to nitrocellulose membranes and blocked using PBS buffer containing 5 % semi-skimmed milk. Membranes were probed using the anti-α_7 nAChR subunit antibody M220 (mouse monoclonal, Sigma, 1:1,000) and horseradish peroxidase conjugated rat anti-mouse conjugated IgG secondary antibody (Sigma, 1:10,000) were subsequently visualised using ECL$^+$ chemiluminescence kit (Amersham Biosciences, UK). Clear protein bands at 55 kDa were observed under both (A) reducing and (B) non-reducing conditions. Control (Ctrl) lysates are samples prepared from SH-EP1-h$\alpha_4\beta_2$ cell membranes and probed with anti-α_7 antibody M220.

Figure 5.47

(A) EB_{CHAPS}

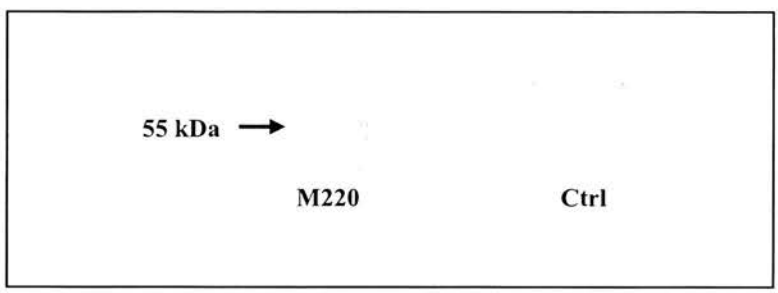

(B) EB_{Triton}

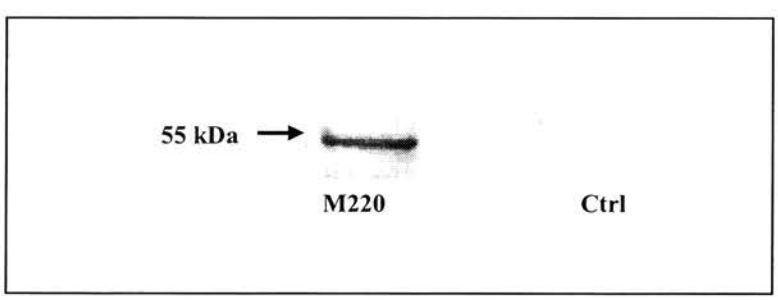

Effect of Detergents on the Signal Intensity of the α_7 nAChR Protein in Western blots. Lysates (SH-EP1-hα_7 cells, 1 mg) were solubilised in extraction buffer containing (A) the zwitterion detergent CHAPS (EB_{CHAPS}) or (B) the non-ionic detergent Triton X-100 (EB_{Triton}), prior to analysis by Western blotting. Membranes probed using the anti-α_7 nAChR subunit antibody M220 (mouse monoclonal, Sigma, 1:1,000) and horseradish peroxidase conjugated rat anti-mouse conjugated IgG secondary antibody (Sigma, 1:10,000) were subsequently visualised using ECL$^+$ chemiluminescence kit (Amersham Biosciences, UK). A clear protein band at 55 kDa was only observed when using EB_{Triton}. Control (Ctrl) lysates are samples prepared from SH-EP1-h$\alpha_4\beta_2$ cell membranes and probed with anti-α_7 antibody M220.

Western blot studies were performed using Triton X-100 as the detergent of choice in the extraction buffer.

5.5.1.3D Summary of Western Blot Analysis of the Human α_7 nAChR Subunit

SH-EP1-hα_7 cells were solubilised in lysate buffer containing the detergent Triton X-100, with the resulting protein then prepared in sample buffer containing the reducing agent DTT and heated (95°C, 10 min) to denature the protein. Following separation on a NuPAGE® 4 – 12 % Bis-Tris polyacrylamide gel, proteins were transferred to a nitrocellulose membrane, prior to incubation (overnight) with the monoclonal mouse anti-α_7 nAChR antibody M220 (primary antibody; 1:1,000), followed by addition of the secondary horse radish peroxidase conjugated goat anti-mouse conjugated IgG (A2004, 1:10,000, Sigma). This protocol resulted in a clear protein band being observed at 55 kDa (Figure 5.48).

5.5.1.3E Immunoprecipitation Analysis of the Human α_7 nAChR subunit

Immunoprecipitation is generally used to concentrate an antigen in situations where it may have been otherwise undetectable using standard Western blotting techniques on a gel. Our target protein (the α_7 nAChR subunit) is detectable as a ~55 kDa protein band which is identical to that of the 55 kDa immunoglobulin (Ig) heavy chain. As a consequence, the choice of IP and primary antibodies is critical as any manifestation of the Ig heavy chain is likely to obscure the presence of the α_7 nAChR band. To avoid this problem and demonstrate that any 55 kDa protein detected represents the α_7 nAChR subunit protein, I utilised antibodies derived from different species. SH-EP1-hα_7 cell lysates were immunoprecipitated with the anti-α_7 nAChR antibody sc-5544 (rabbit polyclonal; 1:200) and, following separation of the antigen-sc-5544 complex with Protein G agarose, the complex was eluted and analysed by Western blot analysis using M220 (mouse monoclonal, 1:1,000) as the primary antibody. Although the human α_7 nAChR subunit protein could be detected in the original lysate, no immunoreactive signal was observed at 55 kDa, indicating the protein has not immunoprecipitated (Figure 5.49A). This experiment was repeated on at least 5 further occasions with the same result on every occasion (data not shown). When the inverse experiment was performed where lysates were immunoprecipitated with M220 (1:500) and probed with sc-5544 (1:1,200), no immunoreactive signal was observed (Figure 5.49B).

Figure 5.48

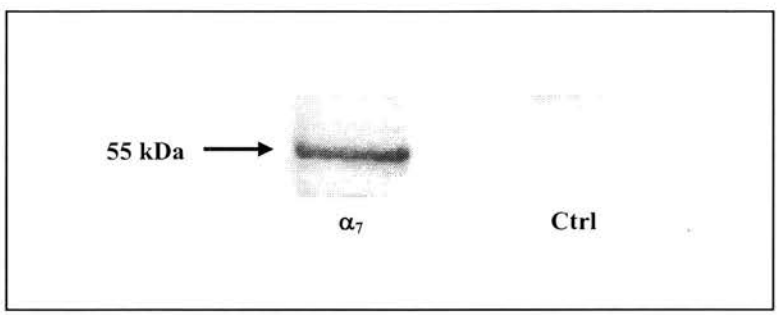

Western Blot Analysis of α_7 nAChR Protein Conducted Under Optimal Conditions Using the Anti-α_7 nAChR Subunit Antibody M220. SH-EP1-hα_7 cells (30 µg) and SH-EP1-h$\alpha_4\beta_2$ cells (Ctrl, 30 µg), solubilised in EB_{Triton} and prepared in sample buffer containing DTT (0.1 M), were subjected to SDS-PAGE separation on NuPAGE® 4-12 % Bis-Tris Gels before transferring to nitrocellulose membranes for Western blot analysis. Membranes were blocked in a PBS buffer containing 5 % skimmed milk powder and incubated overnight (4°C) with the primary anti-α_7 nAChR antibody M220 (mouse monoclonal, Sigma, 1:1,000). Following three 5 min washes in PBS buffer containing 0.05 % Tween 20 (PBS_T), horseradish peroxidase conjugated rat anti-mouse conjugated IgG secondary antibody (Sigma, 1:10,000) was added to the reaction medium. Following incubation (1 h, 22°C), membranes were washed (3 x 5 min) in PSB_T and visualised using ECL^+ chemiluminescence kit (Amersham Biosciences, UK). Although no immunoreactive band was visible in the control SH-EP1-h$\alpha_4\beta_2$ sample, a strong band was detected in the α_7 nAChR sample.

Figure 5.49

(A) IP: sc-5544, WB: M220

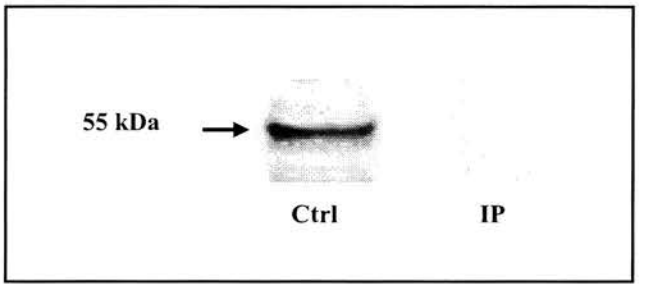

(B) IP: M220, WB: sc-5544

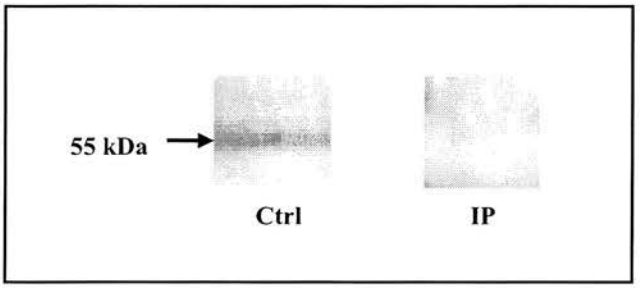

Immunoprecipitation of α_7 nAChR Subunit from SH-EP1-hα_7 Cell Lysates. Lysates were immunoprecipitated (see Methods for full details) with anti-α_7 nAChR antibodies (A) sc-5544 (rabbit) or (B) M220 (mouse) and Western blotted with a second anti-α_7 nAChR antibody (i.e. (A) M220 (B) sc-5544). The control sample represents 30 μg of protein prior to addition of antibodies (positive control). Membranes were visualised using ECL$^+$ chemiluminescence kit (Amersham Biosciences, UK). Although a clear immunoreactive band at 55 kDa can be observed in the control samples, no immunoreactivity was observed in the immunoprecipitated samples.

5.5.1.4 Western Blot Analysis of Human $A\beta_{1-42}$

The ability of the anti-human $A\beta_{1-42}$ antibody 171609 (polyclonal rabbit, Calbiochem® U.K.) and 4G8 (monoclonal mouse, Rpeptide, U.S.A.) to detect $A\beta_{1-42}$ was assessed using Western blotting. A control ("spiked") solution of 10 μg/ml $A\beta_{1-42}$ (Rpeptide) was prepared in sample buffer (containing DTT) and loaded onto a NuPAGE® Bis-Tris polyacrylamide gel. Following transfer to a nitrocellulose membrane, the samples were incubated with primary antibodies 171609 or 4G8, then appropriate secondary antibodies prior to analysis by chemiluminescence. Using the polyclonal antibody 171609, there was a clear protein band observed at 3 kDa (Figure 5.50), consistent with previous studies examining $A\beta_{1-42}$ with molecular weight ranging from 3-10 kDa which are dependent on its fibrillar state (Ida *et al.*, 1996; Roher *et al.*, 1996; Wang *et al.*, 2000a). In addition, lysate samples were prepared from Chinese Hamster Ovary (CHO) cells in which the human amyloid precursor protein (APP) had been over-expressed (Pahlsson & Spitalnik, 1996) and analysed using Western blotting. The anti-human $A\beta_{1-42}$ antibody 171609 again detected a 3 kDa band in CHO-APP cells, consistent with previous the spiked sample (Figure 5.50) and with previous reports (Sun *et al.*, 2002; Arbel *et al.*, 2005). In contrast, no band was seen when the anti-human $A\beta_{1-42}$ 4G8 monoclonal antibody was utilised. All subsequent Western blotting experiments used the anti-$A\beta_{1-42}$ antibody 171609 as the primary antibody.

5.5.1.4A Immunoprecipitation Analysis of Human $A\beta_{1-42}$

A "spiked" solution of $A\beta_{1-42}$ (100 nM, Rpeptide) was immunoprecipitated using the 4G8 anti-$A\beta_{1-42}$ antibody (mouse monoclonal; 1:500) and then analysed by Western blotting with the rabbit polyclonal antibody, 171609 (1:500). Although faint, a distinct 3 kDa band was identified in the original "spiked" sample and in the $A\beta_{1-42}$ immunoprecipitate indicating the procedure has been successful (Figure 5.51).

5.5.1.5 Co-Immunoprecipitation Analysis of the Human α_4 nAChR Subunit and Human $A\beta_{1-42}$

Co-immunoprecipitation is most commonly used to identify a target protein and other molecules that interact with it. To determine whether the human α_4 nAChR subunit and human $A\beta_{1-42}$, co-immunoprecipitate, whole cell lysates from SH-EP1-h$\alpha_4\beta_2$ cells were incubated with 100 nM $A\beta_{1-42}$ for 1 h, prior to solubilisation. The subsequent cell lysate was

Figure 5.50

(A) Anti $A\beta_{1-42}$ Antibody 171609

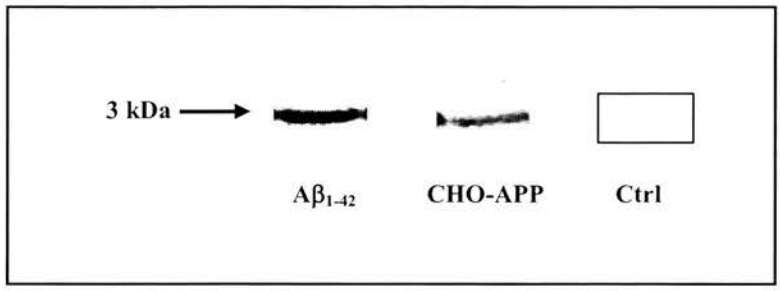

(B) Anti-$A\beta_{1-42}$ Antibody 4G8

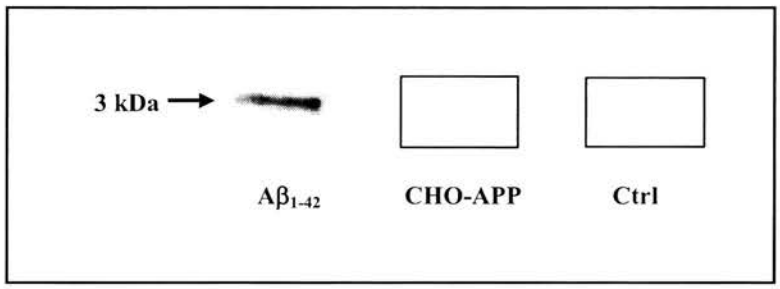

Western Blot Analysis of Human $A\beta_{1-42}$ with Anti-Human $A\beta_{1-42}$ Antibodies 171609 and 4G8. Human $A\beta_{1-42}$ (100 nM in 1 ml EB_{Triton}), CHO-APP cells (30 μg) and SH-EP1-h$\alpha_4\beta_2$ cells (Ctrl, 30 μg) were subjected to SDS-PAGE separation on NuPAGE® 4-12 % Bis-Tris Gels (Invitrogen, UK) before transferring to nitrocellulose membranes for Western analysis. Membranes were blocked in a PBS buffer (see Methods) containing 5 % skimmed milk powder and incubated with either anti-human $A\beta_{1-42}$ antibody (A) 171609 (polyclonal rabbit; Calbiochem; 1:500) or (B) 4G8 (monoclonal mouse, Rpeptide, 1:500) overnight at 4°C. Following three 5 min washes in PBS buffer containing 0.05 % Tween 20 (PBS_T), horseradish peroxidase conjugated goat anti-mouse IgG was added to the 171609 preparation (Sigma, 1:10,000) or horseradish peroxidase conjugated goat anti-rabbit conjugated IgG secondary antibody (Sigma, 1:10,000) to the 4G8 preparation. After incubation at room temperature (1 h), membranes were washed (3 x 5 min) in PSB_T and visualised using ECL^+ chemiluminescence kit (Amersham Biosciences, UK). A clear protein band (3 kDa) was observed in the spiked human $A\beta_{1-42}$ with both antibodies. In contrast, human $A\beta_{1-42}$ (3 kDa) was only detected in CHO-APP cells when anti-human $A\beta_{1-42}$ antibody 171609 was used. Human $A\beta_{1-42}$ was not detected in the control (SH-EP1-h$\alpha_4\beta_2$ cells) samples.

Figure 5.51

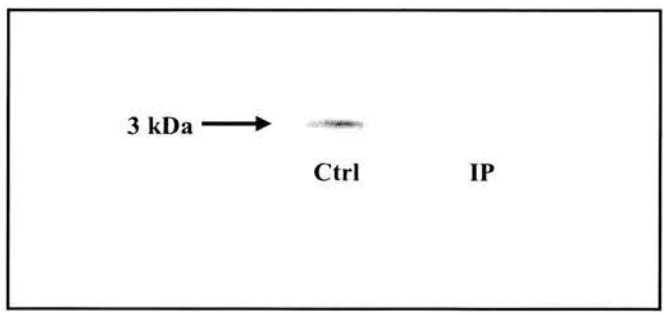

Immunoprecipitation of Human $A\beta_{1-42}$ Using the Anti-Human $A\beta_{1-42}$ Antibodies 4G8 and 171609. $A\beta_{1-42}$ (100 nM final concentration in 1 ml EB_{Triton}) was incubated overnight with anti-human $A\beta_{1-42}$ antibody 4G8 (Rpeptide, 1:500) and protein G agarose beads (Sigma). Samples were then subjected to electrophoretic separation on NuPAGE® 4-12 % Bis-Tris Gels (Invitrogen, UK) before transfer to nitrocellulose membranes for Western blot analysis. Membranes were probed using the anti-human $A\beta_{1-42}$ antibody 171609 (Calbiochem, 1:500) and an anti-mouse horseradish peroxidase conjugated secondary (Sigma, 1:10,000) before visualisation using the ECL^+ chemiluminescence kit (Amersham Biosciences, UK). The control sample (Ctrl) represents 5 µl of the original spiked human $A\beta_{1-42}$ sample solution. A clear immunoreactive band at 3 kDa can be observed in both the control and immunoprecipitation (IP) samples.

immunoprecipitated with the 4G8 anti-human $A\beta_{1-42}$ antibody and samples separated by electrophoresis using NuPAGE® Bis-Tris polyacrylamide gels. Following transfer to nitrocellulose membranes, proteins were stained for α_4 nAChR subunit immunoreactivity using the anti-α_4 antibody mAb299. For the co-immunoprecipitation to be considered successful, a band at 60 kDa must be detected in the immunoprecipitate sample lane. A clear band was detected at 60 kDa (molecular weight of α_4 nAChR subunit) in the original lysate sample, however despite multiple attempts no signal was detected at the same molecular weight in the immunoprecipitated sample (Figure 5.52).

5.5.1.6 Co-Immunoprecipitation Analysis of the Human α_7 nAChR Subunit and Human $A\beta_{1-42}$

Co-immunoprecipitation analysis of the human α_7 nAChR and human $A\beta_{1-42}$ was not carried out as immunoprecipitation of the human α_7 nAChR from the SH-EP1-hα_7 cell lysate was unsuccessful (see 5.5.1.3E, pg 230).

Figure 5.52

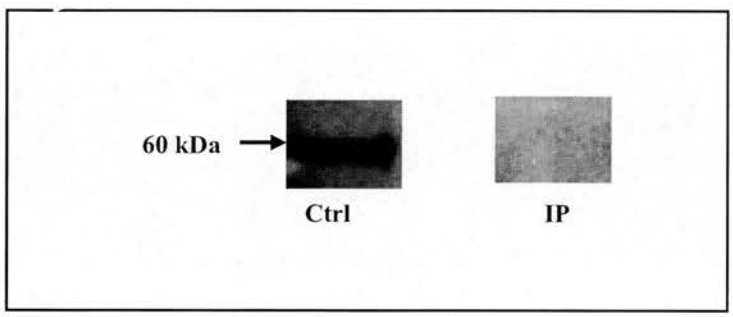

Human $A\beta_{1-42}$ Does Not Co-immunoprecipitate with the Human α_4 nAChR Subunit. Lysate (1 mg solubilised SH-EP1-h$\alpha_4\beta_2$ cell protein) spiked with human $A\beta_{1-42}$ (final concentration 100 nM in 1 ml EB_{Triton}) was incubated overnight with the anti-$A\beta_{1-42}$ antibody 4G8 (Rpeptide, 1:500) and protein G agarose beads (Sigma). Samples were then separated on NuPAGE® Bis-Tris Gels (Invitrogen, UK) before transferring to nitrocellulose membranes for western analysis. Membranes were probed with the anti-α_4 nAChR antibody 299 (rat monoclonal, Sigma, 1:1,000) overnight and horseradish peroxidase conjugated goat anti-rat conjugated IgG secondary antibody (Santa Cruz Biotechnology, 1:1,000). Following a 1 h incubation with the secondary antibody, membranes were washed (3 x 5 min) in PSB buffer containing 0.05 % Tween 20 and visualised using ECL^+ chemiluminescence kit (Amersham Biosciences). The control sample represents 30 μg solubilised SH-EP1-h$\alpha_4\beta_2$ cells spiked with human $A\beta_{1-42}$, prior to addition of any antibodies. Although a clear protein band was observed in the control sample (60 kDa), no such immunoreactivity was observed in the IP sample.

5.6 DISCUSSION

In Chapter 3, Section 3.7.2 (pg 117), radioligand binding assays were used to show the lack of an interaction between soluble and insoluble $A\beta_{1-42}$ with the rodent and human $\alpha_4\beta_2$ and α_7 nAChRs. However, standard radioligand binding assays do not assess how the conformation and the regulation of the channel contribute to the function of the channel. For instance, many receptors require the binding of multiple ligands before channels opening (Chang & Weiss, 1999). Fluorescence based calcium and membrane potential assays and whole-cell patch clamp electrophysiology have been performed to examine the pharmacological and biophysical properties of human $\alpha_4\beta_2$ and α_7 nAChRs expressed in SH-EP1 cells and their interaction with soluble and insoluble human $A\beta_{1-42}$. In addition, any protein-protein interaction have been assessed by examining whether human nAChRs co-immunoprecipitate with human $A\beta_{1-42}$.

5.6.1 Characterisation of Human $\alpha_4\beta_2$ nAChRs Using an Intracellular Calcium Assay

Interest in fluorescence based assays for the assessment of receptors/channels has grown substantially over the past few years (Manning & Sontheimer, 1999; Villarroya *et al.*, 1999; Chavez-Noriega *et al.*, 2000). Furthermore, these assays avoid many of the safety issues associated with assays like the ^{86}Rb efflux assay (Chavez-Noriega *et al.*, 2000). The development of high-throughput screening has led to simpler, less labour-intensive (in comparison to electrophysiology) fluorescence-based assays with enhanced reproducibility (Dooley *et al.*, 1998; Lin *et al.*, 1999; Manning & Sontheimer, 1999; Whiteaker *et al.*, 2001; Baxter *et al.*, 2002; Fitch *et al.*, 2003; Hodder *et al.*, 2004; Whitaker, 2004). The most widely used fluorescent probes for examining the function of nAChRs are the calcium chelating dyes Fluo® and Fura® (Grynkiewicz *et al.*, 1985; Minta *et al.*, 1989; Gee *et al.*, 2000). In the current study the Molecular Devices (U.K.) calcium plus assay kit was utilised. This kit uses a proprietary dye similar in nature to the Fluo-3 and Fluo-4 intensity dyes but also incorporates a secondary dye to mask background fluorescence due to unloaded and extruded dye (Fitch *et al.*, 2003). The masking dye enhances reproducibility by eliminating the need for washing out of extracellular dye, minimising variability due to cell detachment. Alterations in $[Ca^{2+}]_i$ are observed as a change in fluorescence intensity that is captured by the FlexStation fluorometric plate reader (Molecular Devices, U.K.).

It is well documented that nAChR function is modulated by external Ca^{2+} concentration with a number of electrophysiological studies showing maximal potentiation

of nAChR responses when external Ca^{2+} concentrations are between 2 - 20 mM (Mulle *et al.*, 1992; Vernino *et al.*, 1992; Buisson *et al.*, 1996; Sabey *et al.*, 1999; Chavez-Noriega *et al.*, 2000). In agreement with these earlier observations, the $[Ca^{2+}]_i$ response elicited by 10 μM (-)nicotine in SH-EP1-h$\alpha_4\beta_2$ cells was considerably enhanced when the external Ca^{2+} concentration was increased to 20 mM (Mulle *et al.*, 1992; Vernino *et al.*, 1992; Buisson *et al.*, 1996; Chavez-Noriega *et al.*, 2000). However, this concentration of Ca^{2+} is much higher than found physiologically (Benninger *et al.*, 1980; Avoli *et al.*, 1996). Therefore, to keep the external $[Ca^{2+}]$ physiologically relevant as well as comparable with previous studies (Mulle *et al.*, 1992; Vernino *et al.*, 1992; Buisson *et al.*, 1996; Chavez-Noriega *et al.*, 2000), all subsequent experiments were performed with an additional 2.5 mM external Ca^{2+}, which itself increased the (-)nicotine evoked response in $[Ca^{2+}]_i$ by > 300%.

In the $[Ca^{2+}]_i$ assay, EC_{50}/IC_{50} values for nAChR ligands (-)nicotine, cytisine, (±)epibatidine, MLA, and *d*-TC (Figures 5.3 (pg 168) & 5.4 (pg 170)) were consistent with those determined by others using the Molecular Devices calcium assay (Fitch *et al.*, 2003), the ^{86}Rb efflux assay (Marks *et al.*, 1993; Gopalakrishnan *et al.*, 1996; Eaton *et al.*, 2003; Gentry *et al.*, 2003), or a Fluo-3 fluorescence based calcium assay (Chavez-Noriega *et al.*, 2000). Indeed, the (-)nicotine EC_{50} value determined in the current study (22.9 μM) was slightly higher than Chavez-Noriega and colleagues (2000) of 3.5 μM determined using human $\alpha_4\beta_2$ nAChRs expressed in HEK293 cells, but lower than the EC_{50} value of 32 μM determined by Gentry and colleagues (2003) using SH-EP1-h$\alpha_4\beta_2$ cells in a ^{86}Rb efflux assay. Furthermore, the (-)nicotine EC_{50} value of 22.8 nM determined using the calcium assay is not significantly different to that determined using the fluorescence-based membrane potential assay (EC_{50} = 19.5 nM, Chapter 5, Section 5.2). Therefore, high affinity nAChR agonists such as (-)nicotine and (±)epibatidine evoke large alterations in $[Ca^{2+}]_i$, while the α_7 nAChR antagonist MLA exhibits low potency. Together these results indicate that the SH-EP1-h$\alpha_4\beta_2$ cells express $\alpha_4\beta_2$ nAChRs with classic pharmacology.

5.6.2 Human $A\beta_{1-42}$ Does Not Alter (-)Nicotine Evoked $[Ca^{2+}]_i$ Responses in SH-EP1-h$\alpha_4\beta_2$ Cells to (-)Nicotine

To my knowledge, this is the first study to assess whether human $\alpha_4\beta_2$ nAChRs interact with human $A\beta_{1-42}$ using (-)nicotine evoked $[Ca^{2+}]_i$ responses. In agreement with data from $[^3H]$-cytisine binding assays (Chapter 3, Section 3.7.2, pg 117), neither soluble nor insoluble human $A\beta_{1-42}$ inhibited the (-)nicotine evoked $[Ca^{2+}]_i$ responses in SH-EP1-h$\alpha_4\beta_2$ cells (Figures 5.42 - 5.44). Although 10 μM $A\beta_{1-42}$ dissolved in 5 % acetic acid did cause an

inhibition of the (-)nicotine evoked $[Ca^{2+}]_i$ response, an equivalent inhibition was also caused by vehicle alone. Furthermore, a similar observation was made with $A\beta_{1-42}$ dissolved in HEPES, as it appeared to inhibit the cytisine (but not (-)nicotine)-evoked $[Ca^{2+}]_i$ response (Figure 5.5, pg 171). However, again the level of inhibition was not significantly different from that induced by vehicle. Although HEPES, a calcium-buffering solution has been used as a weak ligand in nAChR structure studies (Brejc *et al.*, 2001; Artali *et al.*, 2005) it was surprisingly to find it was such a potent inhibitor of (-)nicotine evoked responses at human $\alpha_4\beta_2$ nAChRs. Yet this finding was not restricted to the $[Ca^{2+}]_i$ assay but was also observed when using other functional techniques discussed below. Therefore, no evidence has been presented to confirm human $A\beta_{1-42}$ inhibits nAChR agonist evoked currents in SH-EP1-h$\alpha_4\beta_2$ cells.

5.6.3 Human $A\beta_{1-42}$ Does Not Alter Membrane Potential of SH-EP1-h$\alpha_4\beta_2$ Cells

Although functional characterisation of nAChR pharmacology using $[Ca^{2+}]_i$ assays is relatively well documented, less characterisation of the use of the fluorescent membrane potential sensitive dyes has been performed. Membrane potential sensitive dyes such as DiBAC(3)(4) have been used for a number of years, however, these have several limitations including a slow onset of response and multistep preparation (de Poorter & Keltjens, 2001; Baxter *et al.*, 2002; Wolff *et al.*, 2003). In a recent publication, Fitch and colleagues (2003) used the new Molecular Devices membrane potential-sensitive dye and suggested the FLIPR® membrane potential assay (Molecular Devices, U.K.) provided a more sensitive measure of nAChR function when compared to the $[Ca^{2+}]_i$ assay. These authors showed that they could detect agonist evoked changes in membrane potential even in those cell lines with little or no demonstrable $[Ca^{2+}]_i$ response (Fitch *et al.*, 2003). Although the establishment of a functional assay (see later discussion) for human α_7 nAChRs proved challenging, the membrane potential assay was established using the SH-EP1-h$\alpha_4\beta_2$ cell line.

In agreement with Fitch and colleagues (2003), using SH-EP1-h$\alpha_4\beta_2$ cells I showed that the membrane potential assay provided comparable data to that obtained in previous $[Ca^{2+}]_i$ (Chavez-Noriega *et al.*, 2000) or in ^{86}Rb efflux assays (Marks *et al.*, 1993; Gopalakrishnan *et al.*, 1996; Eaton *et al.*, 2003; Gentry *et al.*, 2003). In general, agonist affinities were not significantly different than those obtained in the calcium fluorescence assay. However, the EC_{50} value obtained for (±)epibatidine (0.56 ± 0.11 nM) in the membrane potential assay was significantly lower than the EC_{50} of 1.04 ± 0.11 nM detected in the calcium fluorescence assay ($p < 0.01$) whilst the EC_{50} for cytisine was also significantly

lower in the membrane potential assay (EC_{50} = 3.09 ± 0.83 μM, n = 3). These findings may reflect differences in $\alpha_4\beta_2$ nAChR expression in various cell types. For example, in the current study human $\alpha_4\beta_2$ nAChRs were expressed in the SH-EP1 cell line while Fitch and colleagues (2003) used human $\alpha_4\beta_2$ nAChRs expressed in K-177 cells and rat $\alpha_4\beta_2$ nAChRs expressed in KXα4β2R2 cells.

All agonists examined in the human $\alpha_4\beta_2$ nAChR membrane potential assay, with the exception of cytisine (Figure 5.10, pg 178), produced a concentration-dependent increase in fluorescence, with a Hillslope close to unity. Although some researchers (including ourselves) have shown that [^{3}H]-cytisine binds to a single site (Chapter 3, Section 3.4.2, pg 65; Gopalakrishnan *et al.,* 1997; Sabey *et al.*, 1999), two-site binding has been observed for cytisine in electrophysiological experiments (Buisson *et al.*, 1996). The antagonist potency for MLA (415 nM, Figure 5.11, pg 179) determined using the membrane potential assay is slightly lower than that determined using the ^{86}Rb efflux assay (6.6 μM, Chavez-Noriega *et al.,* 2000), electrophysiology (1.5 μM, Buisson *et al.,* 1996), or indeed using the calcium plus assay (875 nM). Furthermore, an additional 2.5 mM external Ca^{2+} decreased depolarisation of SH-EP1-h$\alpha_4\beta_2$ cells in the membrane potential assay (Figure 5.9, pg 177) whereas (-)nicotine evoked changes in $[Ca^{2+}]_i$ response were increased in the presence of higher external Ca^{2+} concentrations (Figure 5.2, pg 167).

In my hands, the membrane potential assay appeared to provide a highly sensitive alterative to measure human $\alpha_4\beta_2$ nAChR functional response with comparable data to calcium assays and ^{86}Rb efflux studies (Marks *et al.*, 1993; Chavez-Noriega *et al.*, 2000; Eaton *et al.*, 2003; Fitch *et al.*, 2003; Gentry *et al.*, 2003). However, in agreement with the calcium assay observations, neither soluble nor insoluble human $A\beta_{1\text{-}42}$ inhibited (-)nicotine evoked changes in membrane potential (Figures 5.13 – 5.15) in SH-EP1-h$\alpha_4\beta_2$ cells.

5.6.4. Whole Cell Patch Clamp Electrophysiological Analysis of Human $\alpha_4\beta_2$ nAChRs

Although the calcium and membrane potential assays proved to be useful tools for assessing the functional interaction of compounds with receptors, electrophysiological analysis of single cells allows more detailed investigation of the functional viability of receptors in cells and tissues and avoid some of the difficulties such as ligand penetration and sensitivity issues surrounding cell-based plate dye assays. Patch clamp electrophysiological recording was first described by Bert Sakmann and Erwin Neher in 1978 for which they subsequently received the Nobel Prize in Medicine or Physiology in 1991. This technique

revolutionised the discipline of physiology, allowing the study of the behaviour of single ion channels or currents in small cells or macro-patches. I have successfully established a protocol to assess the functional viability of human $\alpha_4\beta_2$ nAChRs expressed in SH-EP1 cells using whole cell patch clamp electrophysiology and have subsequently characterised the pharmacological properties of this channel prior to assessing the effects of β-amyloid.

As expected, and in agreement with previous studies using rat and human $\alpha_4\beta_2$ nAChRs (Sudweeks & Yakel, 2000; Wu *et al.*, 2004), an inward current was detected following application of (-)nicotine to the SH-EP1-h$\alpha_4\beta_2$ cells with the agonist log concentration-response profile showing a simple, sigmoidal shape (Figure 5.19, pg 191). The EC_{50} value for (-)nicotine (22 μM) at human $\alpha_4\beta_2$ nAChRs was slightly higher than in other studies using this receptor expressed in SH-EP1 cells (3.2 μM, Wu *et al.,* 2004) or human embryonic kidney cells (HEK293; 1.6 μM, Buisson *et al.*, 1996), perhaps reflecting the presence of rundown in the current study. In addition, the nAChR antagonist *d*-TC inhibited (-)nicotine evoked responses, with 10 μM *d*-TC producing a rightward shift in the (-)nicotine concentration-response curve and a change in (-)nicotine EC_{50} from 22.2 ± 2.2 to 31.4 ± 7.8 μM (Figure 5.19, pg 191).

When (-)nicotine was applied at 3 min intervals to cells in which $\alpha_4\beta_2$ nAChRs have been heterologously expressed, the current underwent "rundown", declining in amplitude with each successive application of agonist (Figure 5.18). This phenomenon is not exclusive to h$\alpha_4\beta_2$ nAChRs with rundown reported for α_7 nAChRs when expressed in SH-EP1 cells (Zhao *et al.*, 2003). Nor is it restricted to the SH-EP1 cell line with rundown reported in P2X receptors expressed in HEK293 cells (Surprenant *et al.*, 2000), voltage-gated Ca^{2+} current responses in dissociated thalamic neurons (Huguenard & Prince, 1994), and $GABA_A$-induced currents in dissociated neurons (Kapur *et al.*, 1999). Attempts were made to minimise rundown in order to avoid compromising an accurate evaluation of ligand concentration-response relationships. Indeed, Zhao and colleagues (2003) showed the use of a K^+-free pipette solution completely abolished rundown of (-)nicotine-induced currents in the SH-EP1-hα_7 cell line. Furthermore Wu and colleagues (2004) working on cells expressing the h$\alpha_4\beta_2$ nAChR, minimised rundown by using the same pipette solutions as that described by Zhao and colleagues (2003). Although the pipette and bath solutions were identical to those described above, no reduction in functional rundown of the (-)nicotine evoked currents in SH-EP1-h$\alpha_4\beta_2$ cells was observed. However, increasing the time between (-)nicotine applications combined with the K^+-free pipette solution reduced rundown to a level where measurements could be taken within the initial 15 minutes of recording. Because

assay conditions were kept as close as possible to those of Wu and colleagues (2004) / Zhao and colleagues (2003) it is difficult to explain the differences in cellular rundown. However, it is possible that the design of our application system resulted in a higher likelihood of cell desensitisation rather than rundown. Indeed, a fundamental difference in the assay procedure used by Zhao and colleagues (2003) and Wu and colleagues (2004) and the present experiments is that the former used a U-tube delivery system and we used an eight-barrel manifold with a single outlet. This could result in a small amount of deadspace between the single outlet tube and therefore, potentially small variations in applied drug concentrations.

I have demonstrated that the SH-EP1-h$\alpha_4\beta_2$ nAChR cell line expresses functional human $\alpha_4\beta_2$ nAChRs with appropriate pharmacology and, as such, demonstrated that it is a viable model to study the potential interaction of human $A\beta_{1-42}$ on human $\alpha_4\beta_2$ nAChR function.

5.6.5. Human $A\beta_{1-42}$ Does Not Inhibit (-)Nicotine Evoked Currents in SH-EP1-h$\alpha_4\beta_2$ Cells

Although several reports have now indicate that Aβ inhibits α_7 nAChRs (Wang *et al.*, 2000a; Wang *et al.*, 2000b; Dineley *et al.*, 2001; Liu *et al.*, 2001; Pettit *et al.*, 2001; Tozaki *et al.*, 2002; Dineley *et al.*, 2002a; Grassi *et al.*, 2003) there is considerably less data on the effects of Aβ on non-α_7 nAChR subtypes (Pettit *et al.*, 2001; Tozaki *et al.*, 2002; Fu & Jhamandas, 2003; Wu *et al.*, 2004). Pettit and colleagues (2001) suggested that $A\beta_{1-42}$ inhibits carbachol-induced currents in rat hippocampal slices, currents that are composed of contributions from the activation of non-α_7 nAChRs and recorded in the presence of atropine to block muscarinic AChR responses. This data was supported by Fu and Jhamandas (2003) who observed that Aβ activated non-α_7 nAChR subtypes in rat basal forebrain membranes, where the predominant nAChR subunit is the α_4 nAChR (Perry *et al.*, 2002). Direct evidence for an interaction between $\alpha_4\beta_2$ nAChR and $A\beta_{1-42}$ specifically was presented by Tozaki and colleagues (2002) who showed $A\beta_{1-42}$ induced inhibition of ACh-induced currents at rat $\alpha_4\beta_2$ nAChRs following expression in *Xenopus* oocytes. Furthermore, Wu and colleagues (2004) recently demonstrated that $A\beta_{1-42}$ inhibited ACh and (-)nicotine-evoked currents in the same SH-EP1 cell line used in the current studies. All of the above mentioned studies used a range of different vehicles to dissolve $A\beta_{1-42}$ and assess its potential interaction with both the rat and human $\alpha_4\beta_2$ nAChRs. In direct contrast to these four studies, I could find no evidence that human $A\beta_{1-42}$ inhibits (-)nicotine evoked currents in SH-EP1-h$\alpha_4\beta_2$ cells. Indeed,

Rpeptide $A\beta_{1-42}$ (100 nM or 300 nM) did not inhibit (-)nicotine evoked currents in SH-EP1-$h\alpha_4\beta_2$ cells despite assay conditions (e.g. pipette and external solutions, cell line, $A\beta_{1-42}$ supplier, etc) being kept identical to those used by Wu and colleagues (2004)(Figures 5.37 & 5.40). β-$Amyloid_{1-42}$ was preincubated with SH-EP1-$h\alpha_4\beta_2$ cells therefore it is unlikely the lack of inhibition in the current study could be explained by $A\beta_{1-42}$ not having adequate time to reach its binding site on the nAChR. Indeed, the time allowed for preincubation (6 min) is consistent with other studies (Tozaki *et al.*, 2002; Wu *et al.*, 2004). Furthermore, it is unlikely that the choice in delivery system (U-tube or eight barrel manifold) would significantly affect the end result as no difference in the slope of the (-)nicotine evoked responses was observed (Chapter 4, Section 5.3.3). As stated in Section 5.6.4, the EC_{50} value for (-)nicotine at the $\alpha_4\beta_2$ nAChR was slightly higher to that obtained in other studies (Buisson *et al.*, 1996; Papke *et al.*, 2000; Wu *et al.*, 2004) possibly reflecting the difficulty of obtaining estimates of EC_{50} in the presence of rundown. However, both this study and that by Wu and colleagues (2004) used EC_{25} to assess the effect of $A\beta_{1-42}$ on (-)nicotine evoked currents in SH-EP1-$h\alpha_4\beta_2$ cells.

It is important to note that only Liu and colleagues (2001) and ourselves present control vehicle data for nAChR and Aβ studies. Vehicle effects with solutions such as 5 % acetic acid and 50/50 DMSO/Tris HCl are not unexpected (Figures 5.32 and 5.35, respectively). However, although HEPES, a calcium-buffering solution has been used as a weak ligand in nAChR structure studies (Artali *et al.*, 2005; Brejc *et al.*, 2002) it was surprisingly to find it was such a potent inhibitor of (-)nicotine evoked responses at human $\alpha_4\beta_2$ nAChRs (Figures 5.23 and 5.29). This finding does not appear to be an artefact of pH as $A\beta_{1-42}$ samples were always adjusted to pH 7.4. The lack of control Aβ vehicle data presented in other studies (Wang *et al.*, 2000a; Wang *et al.*, 2000b; Pettit *et al.*, 2001; Tozaki *et al.*, 2002; Dineley *et al.*, 2002a; Fu & Jhamandas, 2003; Grassi *et al.*, 2003; Wu *et al.*, 2004; Lamb *et al.*, 2005) may simply reflect that these researchers found no evidence of inhibition by their respective vehicles and, as such, chose not to present these results. However, the current study found significant and equivalent inhibition of (-)nicotine evoked currents by $A\beta_{1-42}$ and its vehicle, emphasising the necessity of presenting experimental controls, even when using seemingly innocuous solutions such as HEPES.

5.6.6 The Human α_4 and α_7 nAChR Subunits Do Not Co-Immunoprecipitate with Human $A\beta_{1-42}$

The lack of a direct functional interaction between the nAChR subtypes, $\alpha_4\beta_2$ and α_7 and $A\beta_{1-42}$ does not exclude the possibility of a more indirect interaction between these receptors and the peptide. Indeed, previous studies have reported co-localisation and co-immunoprecipitation of nAChRs and $A\beta_{1-42}$ (Wang *et al.*, 2000a; Nagele *et al.*, 2002). Consequently, studies were performed to determine whether the human $\alpha_4\beta_2$ and α_7 nAChRs co-immunoprecipitate with human $A\beta_{1-42}$.

Western analysis revealed clear protein bands at 60, 55, and 3 kDa using anti-α_4, anti-α_7, and anti-$A\beta_{1-42}$ antibodies, respectively (Figures 5.43, 5.48, & 5.50). Furthermore, successful immunoprecipitation of anti-α_4 and anti-$A\beta_{1-42}$ antibodies (but not anti-α_7 antibodies) has also been demonstrated (Figures 5.44 & 5.51). The α_4 protein band at 60 kDa is consistent with the molecular weight predicted by the amino acid sequence (Elliott *et al.*, 1996) and comparable with previous studies who observed protein bands between 52 kDa (Guan *et al.*, 2000; Wu *et al.*, 2004) and 70 kDa (Elliott *et al.*, 1996; Burghaus *et al.*, 2003). Likewise, the 55 kDa protein band detected is consistent with the predicted amino acid sequence for the α_7 nAChR subunit (Peng *et al.*, 1994b) and comparable with previous studies analyses of α_7 nAChR subunit western blots (Schoepfer *et al.*, 1990; Gotti *et al.*, 1994; Orr-Urtreger *et al.*, 1997; Burghaus *et al.*, 2003; Williams *et al.*, 2005). Finally, β-amyloid$_{1-42}$ ranges in its molecular weight from 3 – 10 kDa depending on the presence of monomers, dimers, and other aggregates (Mak *et al.*, 1994; Wiltfang *et al.*, 1997; Fay *et al.*, 1998; Wang *et al.*, 2000a; Walsh *et al.*, 2002a; Walsh *et al.*, 2002b). As such, the protein band detected at 3 kDa is consistent with a mainly monomeric solution (Wiltfang *et al.*, 1997; Fay *et al.*, 1998; Walsh *et al.*, 2002a).

Regardless of extensive optimisation of α_7 nAChR Western blots, immunoprecipitation of anti-α_7 nAChR antibodies proved unsuccessful and hence, co-immunoprecipitation of the human α_7 nAChR could not be performed. Although both the anti-α_7 nAChR antibodies examined in the immunoprecipitation were successfully used in Western blot experiments, the possibility remains that one or the other is not suitable for immunoprecipitation studies. Indeed, the antigen epitope may not be available to bind the anti-α_7 nAChR immunoprecipitation antibody or the immunoprecipitation antibody itself may bind too weakly to be carried through the immunoprecipitation procedure. Furthermore, although many reports have demonstrated Western analysis of the α_7 nAChR in rodent and

chick brain extracts using monoclonal antibodies from clones 306 and 319 (Schoepfer *et al.*, 1990; Orr-Urtreger *et al.*, 1997; Dineley *et al.*, 2001; Fabian-Fine *et al.*, 2001) many of these reports have used non-commerical antibodies. Reference must also be made to a recent study in which the commercially available anti-α_7 nAChR antibodies used in the current study were shown to recognise multiple protein bands on a Western blot (Herber *et al.*, 2004). As such, care must be taken when choosing the appropriate antibody for both the immunoprecipitation and Western blot analysis. Moreover, the current study may be limited by use of commercially available antibodies only and their questioned specificity for the α_7 nAChR (Herber *et al.*, 2004).

Co-immunoprecipitation is most commonly used to identify a target protein and any other molecules that interact with it. Despite multiple attempts, there is no evidence that the human α_4 nAChR subunit and human $A\beta_{1-42}$ co-immunoprecipitate.

5.6.7 Functional Human α_7 nAChRs are not Stably Expressed in the SH-EP1-hα_7 Cell Line

The failure to demonstrate a functional interaction between the α_7 nAChR and $A\beta_{1-42}$ using fluorescence based assays or whole cell patch clamp, was possibly a result of the lack of consistent expression of functional human α_7 nAChRs in the SH-EP1 cell line. Indeed, α_7 nAChRs are notoriously difficult to express in mammalian cell lines (Cooper & Millar, 1997). Pharmacological, electrophysiological, and biochemical techniques have been utilised by ourselves and others to examine the over-expression of the α_7 nAChR in SH-SY5Y (Puchacz *et al.*, 1994), GH4C1 (Quik *et al.*, 1996; Blumenthal *et al.*, 1997; Cooper & Millar, 1997), PC12 (Blumenthal *et al.*, 1997; Cooper & Millar, 1997; Rangwala *et al.*, 1997), and SH-EP1 cell lines (Peng *et al.*, 1999; Zhao *et al.*, 2003) with varying degrees of success. Certainly, we have successfully characterised [^{3}H]-MLA binding to the human α_7 nAChR (over-expressed in SH-EP1-hα_7 cells or GH4C1) in Chapter 3, Section 3.5 and Chapter 4, Section 5.4, respectively. We have successfully characterised ligand binding to the human α_7 nAChR over-expressed in the SH-EP1-hα_7, GH4C1, and IMR32 cells (Chapter 3, Section 3.5). However, the binding of a radioligand to a receptor does not require it to be fully assembled. Indeed, the α_7 nAChR can exist in various states of assembly including trimers, tetramers, pentamers, as well as aggregates of the subunits (Nicke *et al.*, 2004).

The reasons for inadequate heterologous expression of the α_7 nAChR are poorly understood although it appears that expression is host-cell dependent (Cooper & Millar, 1997; Sweileh *et al.*, 2000). The SH-EP1 cell line stably expressing the human α_7 nAChR was first

reported in the late 1990's (Peng *et al.*, 1999). However, other reports have indicated that the problems associated with α_7 nAChR expression in other cell lines (Puchacz *et al.*, 1994; Quik *et al.*, 1996; Blumenthal *et al.*, 1997; Cooper & Millar, 1997; Rangwala *et al.*, 1997; Rakhilin *et al.*, 1999) are also present in the SH-EP1-hα_7 cell line (Dunckley *et al.*, 2003; Schroeder *et al.*, 2003). Moreover, personal communication with Dr R. J. Lukas, whose laboratory developed the SH-EP1-hα_7 cell line (Peng *et al.*, 1999), suggests not all SH-EP1-hα_7 cells have currents and that surface expression is erratic from passage to passage. Considerable research has focussed on finding methods that increase cell surface expression including altering cell culture conditions (Molinari *et al.*, 1998; Schroeder *et al.*, 2003; Zhao *et al.*, 2003), generation of α_7 nAChR chimeras with the 5-hydroxytryptamine type-3 (5HT3) receptor (Eisele *et al.*, 1993; Papke *et al.*, 2004), and site directed mutagenesis (Chen *et al.*, 1998; Dineley & Patrick, 2000; Dunckley *et al.*, 2003).

To form functional nAChRs at the cell surface, the α_7 nAChR must undergo protein folding and assembly in the endoplasmic reticulum (ER) and gain complex carbohydrates in the Golgi apparatus before subsequent trafficking to the cell surface (Nicke *et al.*, 2004). Recently, the *ric*-3 gene was identified as a requirement for maturation of nAChRs in *Caenorhabditis* elegans (Halevi *et al.*, 2002). Subsequently, identified as a member of a conserved gene family (Halevi *et al.*, 2003), its human equivalent is known as *hric3* (Williams *et al.*, 2005). Although, *ric*-3 was originally thought to be directly involved in α_7 nAChR trafficking (Halevi *et al.*, 2002; Halevi *et al.*, 2003), co-expression of *hric*-3 with the human α_7 nAChR indicates that *ric*-3 facilitates the correct folding and assembly of α_7 nAChR subunits in the ER (Williams *et al.*, 2005). Furthermore, *ric*-3 has been shown to promote trafficking of the 5HT3 receptor perhaps partially explaining the success of the α_7 nAChR-5HT3 chimera (Eisele *et al.*, 1993; Papke *et al.*, 2004; Castillo *et al.*, 2005; Cheng *et al.*, 2005) and has recently been shown to significantly enhance levels of functional $\alpha_4\beta_2$ nAChRs expressed in mammalian cell lines (Lansdell *et al.*, 2005).

Although our laboratory has had intermittent functional expression of human α_7 nAChRs expressed in the SH-EP1 cell line, my studies found no evidence for functional stably expressed human α_7 nAChRs in the SH-EP1-hα_7 cell line, despite the use of calcium and membrane potential fluorescence assays and whole cell patch clamp electrophysiology. Furthermore, although others have shown that pre-treatment of SH-EP1-hα_7 cells with low-concentrations of the α_7 nAChR specific antagonist MLA enhances surface expression (Molinari *et al.*, 1998; Zhao *et al.*, 2003), this finding was not replicated in the current study (Chapter 4, Section 5.4). Studies employing transient transfections or cell lines expressing

native α_7 nAChRs also generally failed to result in high enough receptor numbers to be detected by any of the above functional methods. However, some limited data was obtained from human α_7 nAChRs expressed in the GH4C1 cell line (Chapter 4, Section 5.4).

There are a number of factors associated with low functional expression. These include the presence of mRNA but no protein formation, receptors are simply not surface expressed, or surface expression of an incorrectly folded α_7 nAChR. Experiments performed by our laboratory have determined the presence of both α_7 nAChR mRNA and protein in the SH-EP1-hα_7 cell line and as such replication of these studies has not been performed in the current study. Therefore, the most likely explanation for the discrepancies between our results and the α_7 nAChR-mediated currents detected by the Lukas laboratories (Peng *et al.*, 1999; Schroeder *et al.*, 2003; Zhao *et al.*, 2003; Peng *et al.*, 2005) may be due to fluctuations in *ric-3* and α_7 nAChR expression within the SH-EP1-hα_7 cell line. Further study is required to assess the exact relationship between α_7 nAChRs and *ric*-3 expression in the SH-EP1-hα_7 cell line.

4.7 CONCLUSIONS

In order to pharmacologically characterise the human $\alpha_4\beta_2$ and α_7 nAChRs, I have established 3 separate functional assays; the calcium plus assay, the membrane potential assay, and whole cell electrophysiology of SH-EP1-h$\alpha_4\beta_2$ cells. These assays have verified that SH-EP1-h$\alpha_4\beta_2$ cells are a useful tool to study the function of the human $\alpha_4\beta_2$ nAChR. Furthermore, I have confirmed that the membrane potential assay determines ligand affinities at $\alpha_4\beta_2$ nAChRs that are comparable with or more sensitive than those obtained using the calcium plus assay. Despite the successful development of these assays, I could find no evidence of a direct interaction between the human $\alpha_4\beta_2$ nAChR and human $A\beta_{1\text{-}42}$. Unfortunately, measurement of functional α_7 nAChR responses was hampered by the lack of consistent functional expression of these receptors in the SH-EP1-hα_7 cell line. In addition, the human α_4 subunit did not co-immunoprecipitate with human $A\beta_{1\text{-}42}$ and although a clear α_7 nAChR protein band was detected using Western blot analysis, the protein was not detected by immuno- or co-immunoprecipitated.

6.0 OVERALL CONCLUSIONS

Research into Alzheimer's Disease has focused upon the cholinergic hypothesis (where loss of the cholinergic system precedes that of other neurotransmitter systems) and the Aβ hypothesis (where Aβ is critically responsible for the neurodegeneration observed in AD brains), both of which have been examined separately in many respects. In the last 10 years, some of the research linking the two theories was mainly circumstantial such as (-)nicotine being shown to protect cultured rat cortical neurons against Aβ-induced toxicity (Kihara *et al.*, 1997, 1998). It is six years since two pivotal papers were published by Wang and colleagues (2000a,b) directly linking the cholinergic and amyloid hypotheses by showing that $A\beta_{1-42}$ bound with picomolar affinity to the α_7 nAChR. Subsequent to these studies, a substantial body of literature has appeared indicating a direct and indirect interaction of Aβ with the $\alpha_4\beta_2$ and α_7 nAChRs in AD aetiology (Dineley *et al.*, 2001; 2002a,b; Guan *et al.*, 2001; Liu *et al.*, 2001; Pettit *et al.*, 2001; Shimohama & Kihara, 2001; Apelt *et al.*, 2002; Bednar *et al.*, 2002; Nordberg *et al.*, 2002; Tozaki *et al.*, 2002; Fu & Jhamandas, 2003; Grassi *et al.*, 2003; Klingner *et al.*, 2003; Hellstrom-Lindahl *et al.*, 2004; Martin *et al.*, 2004; Wu *et al.*, 2004; de Fiebre & de Fiebre, 2005; Lamb *et al.*, 2005) although concerns with both of these hypotheses remain. These include whether it is the soluble or insoluble forms of $A\beta_{1-42}$ that is neurotoxic (Walsh *et al.*, 1997, 2002a,b; Teplow *et al.*, 1998; Conway *et al.*, 2000; Bitan *et al.*, 2003; Blanchard *et al.*, 2003; Oddo *et al.*, 2003; Billings *et al.*, 2005; Crowther *et al.*, 2005), and with which nAChR (or indeed both) $A\beta_{1-42}$ may interact. In light of the work by Wang and colleagues (2000a,b), to date, the majority of papers initially published focused on the interaction of (soluble) $A\beta_{1-42}$ and the α_7 nAChR (Dineley *et al.*, 2001, 2002a; Kihara *et al.*, 2001; Liu *et al.*, 2001; Pettit *et al.*, 2001; Tozaki *et al.*, 2002; Grassi *et al.*, 2003). However, it is clear that more studies are now examining the possibility of an interaction between the $\alpha_4\beta_2$ nAChR and $A\beta_{1-42}$ (Kihara *et al.*, 1998; Guan *et al.*, 2001; Liu *et al.*, 2001; Tozaki *et al.*, 2002; Dineley *et al.*, 2002a; Fu & Jhamandas, 2003; Grassi *et al.*, 2003). It is interesting to note that no single study has systematically compared the effects of soluble and insoluble forms of $A\beta_{1-42}$ at either nAChR subtype, choosing instead to examine a single soluble form of $A\beta_{1-42}$ per study.

In the current study, I have attempted to address the type of nAChR involved in any potential interaction with $A\beta_{1-42}$. In addition to examining a variety of different vehicles that promote formation of both soluble and insoluble (aggregated) forms of $A\beta_{1-42}$. To do this, radioligand binding assays ([^{3}H]-epibatidine, [^{3}H]-cytisine, [^{3}H]-MLA, and [^{3}H]-αBgTx binding assays) were established to characterise the pharmacology of rodent and human $\alpha_4\beta_2$

and α_7 nAChRs. Furthermore, the degree of β-sheet aggregation was assessed in a range of vehicles using a thioflavin T assay and the functional interaction between human $\alpha_4\beta_2$ and α_7 nAChRs over-expressed in the SH-EP1 cell line and human $A\beta_{1-42}$ explored using an array of functional assays (intracellular calcium and membrane potential fluorescence assays, and whole-cell patch clamp electrophysiology). The co-localisation of human $A\beta_{1-42}$ with the human $\alpha_4\beta_2$ and α_7 nAChRs using co-immunoprecipitation was also examined.

Using these approaches several conclusions can be drawm. (1) A range of pharmacological ([^{3}H]-epibatidine, [^{3}H]-cytisine, [^{3}H]-MLA, & [^{3}H]αBgTx binding assays) and functional assays (calcium and membrane potential fluorescence assays and whole-cell patch-clamp electrophysiology) with which to study human, rat, and mouse $\alpha_4\beta_2$ and α_7 nAChRs were successfully introduced. (2) Nicotinic agonists were shown to exhibit a higher affinity for human α_7 nAChRs compared to their rat α_7 counterpart. In contrast, no species difference was evident for agonists at rat and human $\alpha_4\beta_2$ nAChRs. (3) The α_7 nAChR antagonists [^{3}H]-αBgTx and [^{3}H]-MLA bind to different number of binding sites on the α_7 nAChR. (4) A thioflavin T assay was established to assess the state of aggregation of $A\beta_{1-42}$ that occurred in a range of vehicles and when serially diluted in three different assay buffers. (5) I have also shown that the human $\alpha_4\beta_2$ nAChR and human $A\beta_{1-42}$ do not co-immunoprecipitate. (6) Furthermore, as part of an on-going collaboration within our group, the [^{3}H]-cytisine and [^{3}H]-MLA binding assays were used to characterise $\alpha_4\beta_2$ and α_7 nAChR pharmacology in α_7 nAChR-transgenic mice. Aspects of this data has been included in a published paper (Young *et al.*, 2004) and in one paper currently accepted for *European Journal of Psychopharmacology.* (7) Finally, despite the successful development of a range of pharmacological and functional assays, no evidence could be presented to show a direct interaction between the human $\alpha_4\beta_2$ or α_7 nAChRs and human $A\beta_{1-42}$. Furthermore, using the radioligand binding assays, no interaction between rat $\alpha_4\beta_2$ and α_7 nAChRs and rat $A\beta_{1-42}$ was observed. Whilst these results have been extensively discussed in previous sections (3.9 and 4.6), I will further discuss the observation that the human nAChRs ($\alpha_4\beta_2$ and α_7), do not interact with human $A\beta_{1-42}$ in the context of on-going literature.

Radioligand binding assays do not assess the overall conformation of the receptor and it is possible that the lack of interaction observed between the human $\alpha_4\beta_2$ and α_7 nAChRs and human $A\beta_{1-42}$ using radioligand binding assays (Section 3.9.4) does not reflect either the binding of $A\beta_{1-42}$ to the receptor or the suitability of the receptor for $A\beta_{1-42}$ binding. However, despite the use of functional assays (calcium and membrane potential

fluorescent assays and the more conventional whole-cell patch clamp electrophysiology), no functional interaction between the nAChRs and $A\beta_{1-42}$ was observed.

This lack of interaction between the $A\beta_{1-42}$ and the nAChRs shown in these studies may simply be because these receptors and $A\beta_{1-42}$ do not interact directly with each other. However, at least two other options exist. There may have been no interaction because (1) $A\beta_{1-42}$ itself may not have been in a form that does not interact with these nAChRs or (2) in the case of the human α_7 nAChR, the expression of this receptor in the SH-EP1 cell line was not stable enough to allow sensitive measurements of functional interaction between this receptor and $A\beta_{1-42}$. As there is less reported evidence to suggest a direct interaction between the $\alpha_4\beta_2$ nAChR and $A\beta_{1-42}$ (Guan *et al.*, 2000; Liu *et al.*, 2001; Tozaki *et al.*, 2002; Dineley *et al.*, 2002a; Fu & Jhamandas, 2003; Grassi *et al.*, 2003), it is perhaps possible that no such interaction actually exists, option one remains a viable reason for the lack of interaction between the $\alpha_4\beta_2$ nAChR and the peptide in the current study. However, in light of the growing body of published work in favour of a direct interaction between the α_7 nAChR and $A\beta_{1-42}$, these latter two theories will be examined in more detail.

6.1 Determination of $A\beta_{1-42}$ β-Sheet Aggregation

As discussed in previous sections (1.3.2.2 and 4.3), there is still no consensus on which form of $A\beta_{1-42}$ is neurotoxic (Walsh *et al.,* 1997; 2002a; Teplow *et al.,* 1998; Conway *et al.,* 2000; Bitan *et al.,* 2003). The examination of $A\beta_{1-42}$ is complicated because it can spontaneously aggregate *in vitro* (Selkoe, 1994; Lendon *et al.*, 1997; Lamb *et al.*, 1999), in addition to the peptide being present in multiple conformations *in vivo* including monomers, oligomers, protofibrils, and mature fibrils (Conroy *et al.,* 1992; Walsh *et al.,* 1997, 2002a; Teplow *et al.,* 1998; Bitan *et al.,* 2003). To address the issue of multiple conformations and therefore potentially different responses, human $A\beta_{1-42}$ was resuspended in a number of different vehicles to produce soluble, non-fibrillar solutions (Calbiochem $A\beta_{1-42}$ in 5 % acetic acid, 50/50 DMSO/Tris, or HEPES buffer, or Rpeptide acetate salt in MilliQ water) and aggregated, fibrillar solutions (Mg^{2+}-free, K^+-free PBS at 37°C for 49 h, Calbiochem $A\beta_{1-42}$). Indeed, to my knowledge, this is the first study to compare the solubility of the $A\beta_{1-42}$ in a range of vehicles and what effect serial dilution had on the composition of the solution. As expected, once resuspended and serially diluted, none of the $A\beta_{1-42}$ solutions used in this study (with the exception of the aggregated $A\beta_{1-42}$) exhibited β-sheet aggregation despite the use of $A\beta_{1-42}$ concentrations ranging from picomolar to millimolar (Section

3.7.1). Futhermore, none of the $A\beta_{1-42}$ solutions examined inhibited [^{3}H]-cytisine or [^{3}H]-MLA binding (Section 3.9.4) or any of the nAChR responses in the functional assay panel (Sections 4.2.1.4, 4.2.3.2, and 4.3.3). It is interesting to note that Grassi and colleagues (2003) suggest that there is batch to batch variation between different lots of $A\beta_{1-42}$. Although a systematic study of $A\beta_{1-42}$ from different lots was performed, in the current study the human (or rat) $A\beta_{1-42}$ used was purchased from Calbiochem for all soluble $A\beta_{1-42}$ solutions, and these $A\beta_{1-42}$ samples did cover a range of lot numbers. Furthermore, in some electrophysiological experiments $A\beta_{1-42}$ from Sigma® (U.K.) was used with the same null result (data not shown) as well as from $A\beta_{1-42}$ from Rpeptide®. Therefore, because I used vehicles used in previous studies (Wang *et al.,* 2000a,b; Liu *et al.,* 2001; Pettit *et al.,* 2001; Grassi *et al.,* 2003), and unless each batch lot of $A\beta_{1-42}$ examined was non-viable, it is unlikely that the observed lack of interaction between the nAChRs and $A\beta_{1-42}$ in the current study is the result of the form of $A\beta_{1-42}$.

6.2 Expression of nAChRs in the SH-EP1 Cell Line

The successful binding of [^{3}H]-cytisine and [^{3}H]-MLA to SH-EP1-h$\alpha_4\beta_2$ and SH-EP1-hα_7 membrane preparations, respectively, does not necessarily prove that the receptors are correctly inserted into the plasma membrane of the SH-EP1 cells. Therefore, it was critical to perform functional studies to assess the interaction of both nicotinic compounds and $A\beta_{1-42}$ with these receptors. In the current study, expression of functional human $\alpha_4\beta_2$ nAChRs was confirmed in the SH-EP1-h$\alpha_4\beta_2$ cell line (Sections 4.2.1.3, 4.2.2.3 and 4.3.2) allowing analysis of any interaction between this receptor subtype and human $A\beta_{1-42}$ to be performed. However, no evidence could be provided to show that $A\beta_{1-42}$ interacted with human $\alpha_4\beta_2$ nAChRs over-expressed in the SH-EP1 cell line (Sections 4.2.1.4, 4.2.3.2, and 4.3). In contrast, functional expression of the human α_7 nAChRs in the SH-EP1-hα_7 cell line was notably intermittently present in some batches of cells and absent in others. Indeed, problems with expression of the α_7 nAChR in neuronal cell lines has already been discussed (Section 4.6.7). Therefore, the inability to perform analysis of any functional interaction between the human α_7 nAChR and human $A\beta_{1-42}$ may have been compromised. As such, until functional expression of the human α_7 in the SH-EP1 cell line has been consistently stabilised, I cannot conclusively state that there is no functional interaction between the human α_7 nAChR and human $A\beta_{1-42}$. Likewise, the lack of functional stability may have affected the co-localisation studies by interfering with the anti-human α_7 nAChR antibodies.

The discovery of the *ric-3* gene and its role in the translocation of correctly folded α_7 nAChRs to the cell surface has implications for any future studies of α_7 nAChR expression in cell lines. Indeed, any future studies of human α_7 nAChRs and human $A\beta_{1-42}$ need to include an examination of *ric-3* levels in the SH-EP1-hα_7 cell line passage to passage and perhaps co-expression of the *ric-3* and α_7 nAChR genes to help promote cell surface expression in the SH-EP1 cell line.

6.3 Recent Publications on the nAChR and $A\beta_{1-42}$ Interaction

In addition to my own research, recent publications analysing the interaction between nAChRs and $A\beta_{1-42}$ only serve to increase the debate. Although Wang and colleagues (2000a,b) showed $A\beta_{1-42}$ inhibited [^{125}I]-αBgTx and [^{3}H]-MLA binding to human α_7 nAChRs with picomolar affinity, this finding was not replicated by de Fiebre and de Fiebre (2005) nor by Dr. R. J. Lukas (personal communication). Furthermore, while Pym and colleagues (2005) expressed a number of different human nAChRs in *Xenopus* oocytes and observed $A\beta_{1-42}$ antagonised responses at α_7 nAChRs, Lamb and colleagues (2005) found $A\beta_{1-42}$ preferentially inhibited non-α_7 nAChRs in rat hippocampal CA1 interneurons. The story has recently become even more complicated following a recent publication by Eric Synder and colleagues (2005). It is well known that N-methyl-D-aspartate glutamate (NMDA) and α_7 nAChRs have potential roles in learning and memory, the disturbance of which is common in many AD patients (Dineley *et al.*, 2001; D'Angelo *et al.*, 2005). Synder and colleagues (2005) have brought these observations together by showing a significant decrease in NMDA1 receptor surface expression on neurons cultured from mice bearing the APP_{swe} gene. Moreover, this decrease could be partially inhibited by pre-treatment with the α_7 nAChR antagonists αBgTx and MLA (Snyder *et al.*, 2005). As such, this paper widens the debate further, implicating an indirect, but critical role for an interaction between $A\beta_{1-42}$ and the α_7 nAChR in learning and memory.

In conclusion, I have successfully developed both pharmacological and functional assays to study rat and human $\alpha_4\beta_2$ and α_7 nAChRs pharmacology whilst some of these assays have also been used to study these receptors in brain membranes from wildtype and α_7 nAChR transgenic mice. Furthermore, I have studied the interaction of the human $\alpha_4\beta_2$ and α_7 nAChRs with $A\beta_{1-42}$, resuspended in several different vehicles to promote or inhibit β-sheet aggregation. However, despite this extensive array of experiments, I could find no

evidence to support the hypothesis that the human $\alpha_4\beta_2$ and α_7 subtypes directly interact with human $A\beta_{1-42}$.

6.4 Future Studies

In order to thoroughly investigate any potential interaction between $A\beta_{1-42}$ and the α_7 nAChRs, it is necessary to have access to a cell line in which the α_7 nAChR is expressed functionally.

It is well documented that the α_7 nAChR is notoriously difficult to express in mammalian cell lines (Cooper & Millar, 1997). Indeed, in the current studies functional expression of the α_7 nAChR in the SH-EP1 cell line was weak or absent, although other groups have reported successful expression (Peng *et al.*, 2005). Recent studies have identified the gene *ric-3* gene to be a requirement for maturation of nAChRs (Halevi *et al.*, 2002) with subsequent studies indicating that this gene facilitates the correct folding and assembly of the α_7 nAChR in the endoplasmic reticulum (Williams *et al.*, 2005). It would be interesting to re-examine the SH-EP1-hα_7 nAChR cell line as a potential tool for functional α_7 nAChR expression, by examining to what extent the *ric-3* gene is present in the cell line whether its expression in the SH-EP1-hα_7 cell line alters through passages. Indeed, it would also be interesting to examine whether co-expression of *ric-3* and the α_7 nAChR would produce a more stable functional cell line.

In addition I would like to examine other models of AD. As mentioned previously, the α_7 nAChR-null mice data presented in this thesis is part of an on-going collaboration within our Institute (Fujisawa Institute of Neuroscience in Edinburgh, now Astellas Centre for Neuroscience in Edinburgh). We are cross-breeding the α_7 nAChR-null mice with mice in which the human APP_{swe} gene has been over-expressed. We hope that this double-transgenic model will allow a full *in vivo* assessment of any nAChR/$A\beta_{1-42}$ interaction. As such, $\alpha_4\beta_2$ and α_7 nAChR pharmacology will be assessed in mice over-expressing the APP_{swe} gene only and in α_7 nAChR-null mice expressing the APP_{swe} gene (double transgenic). A further potential model of interest is *Caenorhabiditis elegans*. Dr Christopher Link (University of Colorado, U.S.A.) has successfully expressed human APP in *C. elegans*, leading to substantial amyloid deposit within the animal (Link, 1995). In contrast to rodent models where amyloid deposition may take many weeks or months, amyloid deposition in *C. elegans* is visible within days of transfection and may be assessed using the β-sheet specific dye thioflavin S and confocal imaging (Link, 1995; Fay *et al.*,

1998; Link *et al.*, 2001). As such, this animal may represent a new and novel method of assessing the effect of nicotinic agonists and antagonists on Aβ deposition.

7.0 Bibliography

ADAMS, C.E., BROIDE, R.S., CHEN, Y., WINZER-SERHAN, U.H., HENDERSON, T.A., LESLIE, F.M. & FREEDMAN, R. (2002). Development of the alpha7 nicotinic cholinergic receptor in rat hippocampal formation. *Brain Res Dev Brain Res*, **139,** 175-87.

ADAMS, C.E., STITZEL, J.A., COLLINS, A.C. & FREEDMAN, R. (2001). Alpha7-nicotinic receptor expression and the anatomical organization of hippocampal interneurons. *Brain Res*, **922,** 180-90.

AGULHON, C., ABITBOL, M., BERTRAND, D. & MALAFOSSE, A. (1999). Localization of mRNA for CHRNA7 in human fetal brain. *Neuroreport*, **10,** 2223-7.

AIYAR, V.N., BENN, M.H., HANNA, T., JACYNO, J., ROTH, S.H. & WILKENS, J.L. (1979). The principal toxin of Delphinium brownii Rydb., and its mode of action. *Experientia*, **35,** 1367-8.

AKABAS, M.H., KAUFMANN, C., ARCHDEACON, P. & KARLIN, A. (1994). Identification of acetylcholine receptor channel-lining residues in the entire M2 segment of the alpha subunit. *Neuron*, **13,** 919-27.

AKIYAMA, H., ARAI, T., KONDO, H., TANNO, E., HAGA, C. & IKEDA, K. (2000a). Cell mediators of inflammation in the Alzheimer disease brain. *Alzheimer Dis Assoc Disord*, **14 Suppl 1,** S47-53.

AKIYAMA, H., BARGER, S., BARNUM, S., BRADT, B., BAUER, J., COLE, G.M., COOPER, N.C., EIKELENBOOM, P., EMMERLING, M., FIEBICH, B.L., FINCH, C.E., FRAUTSCHY, S., GRIFFIN, W.S., HAMPEL, H., HULL, M., LANDRETH, G., LUE, L., MRAK, R., MACKENZIE, I.R. & MCGEER, P.L. (2000b). Inflammation and Alzheimer's disease. *Neurobiol Aging*, **21,** 383-421.

ALBUQUERQUE, E.X., PEREIRA, E.F., BRAGA, M.F., MATSUBAYASHI, H. & ALKONDON, M. (1998). Neuronal nicotinic receptors modulate synaptic function in the hippocampus and are sensitive to blockade by the convulsant strychnine and by the anti-Parkinson drug amantadine. *Toxicol Lett*, **102-103,** 211-8.

ALKONDON, M. & ALBUQUERQUE, E.X. (1993). Diversity of nicotinic acetylcholine receptors in rat hippocampal neurons. I. Pharmacological and functional evidence for distinct structural subtypes. *J Pharmacol Exp Ther*, **265,** 1455-73.

ALKONDON, M., BRAGA, M.F., PEREIRA, E.F., MAELICKE, A. & ALBUQUERQUE, E.X. (2000). alpha7 nicotinic acetylcholine receptors and modulation of gabaergic synaptic transmission in the hippocampus. *Eur J Pharmacol*, **393,** 59-67.

ALKONDON, M., PEREIRA, E.F., CORTES, W.S., MAELICKE, A. & ALBUQUERQUE, E.X. (1997). Choline is a selective agonist of alpha7 nicotinic acetylcholine receptors in the rat brain neurons. *Eur J Neurosci*, **9,** 2734-42.

ALKONDON, M., PEREIRA, E.F., WONNACOTT, S. & ALBUQUERQUE, E.X. (1992). Blockade of nicotinic currents in hippocampal neurons defines methyllycaconitine as a potent and specific receptor antagonist. *Mol Pharmacol*, **41,** 802-8.

ALKONDON, M., RAO, K.S. & ALBUQUERQUE, E.X. (1988). Acetylcholinesterase reactivators modify the functional properties of the nicotinic acetylcholine receptor ion channel. *J Pharmacol Exp Ther*, **245,** 543-56.

ALONSO, A., MEDERLYOVA, A., NOVAK, M., GRUNDKE-IQBAL, I. & IQBAL, K. (2004). Promotion of hyperphosphorylation by frontotemporal dementia tau mutations. *J Biol Chem*, **279,** 34873-81.

ALONSO, A.C., GRUNDKE-IQBAL, I. & IQBAL, K. (1996). Alzheimer's disease hyperphosphorylated tau sequesters normal tau into tangles of filaments and disassembles microtubules. *Nat Med*, **2,** 783-7.

ALONSO, A.C., ZAIDI, T., GRUNDKE-IQBAL, I. & IQBAL, K. (1994). Role of abnormally phosphorylated tau in the breakdown of microtubules in Alzheimer disease. *Proc Natl Acad Sci U S A*, **91,** 5562-6.

ALONSO, A.D., GRUNDKE-IQBAL, I., BARRA, H.S. & IQBAL, K. (1997). Abnormal phosphorylation of tau and the mechanism of Alzheimer neurofibrillary degeneration: sequestration of microtubule-associated proteins 1 and 2 and the disassembly of microtubules by the abnormal tau. *Proc Natl Acad Sci U S A*, **94,** 298-303.

ALZHEIMER, A. (1907). A new disease of the cortex. *Allg. Z. Psychiatr.*, **64,** 146-148.

ANAND, R. & LINDSTROM, J. (1990). Nucleotide sequence of the human nicotinic acetylcholine receptor beta 2 subunit gene. *Nucleic Acids Res*, **18,** 4272.

ANAND, R., PENG, X. & LINDSTROM, J. (1993). Homomeric and native alpha 7 acetylcholine receptors exhibit remarkably similar but non-identical pharmacological properties, suggesting that the native receptor is a heteromeric protein complex. *FEBS Lett*, **327,** 241-6.

ANDERSON, D.J. & ARNERIC, S.P. (1994). Nicotinic receptor binding of [3H]cytisine, [3H]nicotine and [3H]methylcarbamylcholine in rat brain. *Eur J Pharmacol*, **253,** 261-7.

APELT, J., KUMAR, A. & SCHLIEBS, R. (2002). Impairment of cholinergic neurotransmission in adult and aged transgenic Tg2576 mouse brain expressing the Swedish mutation of human beta-amyloid precursor protein. *Brain Res*, **953,** 17-30.

ARBEL, M., YACOBY, I. & SOLOMON, B. (2005). Inhibition of amyloid precursor protein processing by B-secretase through site-directed antibodies. *PNAS*, **103,** 7710-7723.

ARIAS, H.R. (2000). Localization of agonist and competitive antagonist binding sites on nicotinic acetylcholine receptors. *Neurochem Int*, **36,** 595-645.

ARTALI, R., BOMBIERI, G. & MENEGHETTI, F. (2005). Docking of 6-chloropyridazin-3-yl derivatives active on nicotinic acetylcholine receptors into molluscan acetylcholine binding protein (AChBP). *Farmaco*, **60,** 313-20.

ATACK, J.R., PERRY, E.K., BONHAM, J.R., PERRY, R.H., TOMLINSON, B.E., BLESSED, G. & FAIRBAIRN, A. (1983). Molecular forms of acetylcholinesterase in senile dementia of Alzheimer type: selective loss of the intermediate (10S) form. *Neurosci Lett*, **40,** 199-204.

AUSTEN, B.M., FREARS, E.R. & DAVIES, H. (2000). The use of seldi proteinchip arrays to monitor production of Alzheimer's betaamyloid in transfected cells. *J Pept Sci*, **6,** 459-69.

AUSTRALIAN ALZHEIMERS ASSOCIATION (2000). Alzheimer's Disease: About Dementia Help Note.

AVOLI, M., BARBAROSIE, M., LUCKE, A., NAGAO, T., LOPANTSEV, V. & KOHLING, R. (1996). Synchronous GABA-mediated potentials and epileptiform discharges in the rat limbic system in vitro. *J Neurosci*, **16,** 3912-24.

AZAM, L., WINZER-SERHAN, U. & LESLIE, F.M. (2003). Co-expression of alpha7 and beta2 nicotinic acetylcholine receptor subunit mRNAs within rat brain cholinergic neurons. *Neuroscience*, **119,** 965-77.

AZTIRIA, E.M., SOGAYAR, M.C. & BARRANTES, F.J. (2000). Expression of a neuronal nicotinic acetylcholine receptor in insect and mammalian host cell systems. *Neurochem Res*, **25,** 171-80.

BACKMAN, L., JONES, S., BERGER, A.K., LAUKKA, E.J. & SMALL, B.J. (2004). Multiple cognitive deficits during the transition to Alzheimer's disease. *J Intern Med*, **256,** 195-204.

BADIO, B. & DALY, J.W. (1994). Epibatidine, a potent analgetic and nicotinic agonist. *Mol Pharmacol*, **45,** 563-9.

BALASS, M., KATCHALSKI-KATZIR, E. & FUCHS, S. (1997). The alpha-bungarotoxin binding site on the nicotinic acetylcholine receptor: analysis using a phage-epitope library. *Proc Natl Acad Sci U S A*, **94,** 6054-8.

BALES, K.R., VERINA, T., CUMMINS, D.J., DU, Y., DODEL, R.C., SAURA, J., FISHMAN, C.E., DELONG, C.A., PICCARDO, P., PETEGNIEF, V., GHETTI, B. & PAUL, S.M. (1999). Apolipoprotein E is essential for amyloid deposition in the APP(V717F) transgenic mouse model of Alzheimer's disease. *Proc Natl Acad Sci U S A*, **96,** 15233-8.

BANCHER, C., BRUNNER, C., LASSMANN, H., BUDKA, H., JELLINGER, K., WICHE, G., SEITELBERGER, F., GRUNDKE-IQBAL, I., IQBAL, K. & WISNIEWSKI, H.M. (1989). Accumulation of abnormally phosphorylated tau precedes the formation of neurofibrillary tangles in Alzheimer's disease. *Brain Res*, **477,** 90-9.

BANSAL, A., SINGER, J.H., HWANG, B.J., XU, W., BEAUDET, A. & FELLER, M.B. (2000). Mice lacking specific nicotinic acetylcholine receptor subunits exhibit dramatically altered spontaneous activity patterns and reveal a limited role for retinal waves in forming ON and OFF circuits in the inner retina. *J Neurosci*, **20,** 7672-81.

BARTUS, R.T., DEAN, R.L., 3RD, BEER, B. & LIPPA, A.S. (1982). The cholinergic hypothesis of geriatric memory dysfunction. *Science*, **217,** 408-14.

BAXTER, D.F., KIRK, M., GARCIA, A.F., RAIMONDI, A., HOLMQVIST, M.H., FLINT, K.K., BOJANIC, D., DISTEFANO, P.S., CURTIS, R. & XIE, Y. (2002). A novel membrane potential-sensitive fluorescent dye improves cell-based assays for ion channels. *J Biomol Screen*, **7,** 79-85.

BEDNAR, I., PATERSON, D., MARUTLE, A., PHAM, T.M., SVEDBERG, M., HELLSTROM-LINDAHL, E., MOUSAVI, M., COURT, J., MORRIS, C., PERRY, E., MOHAMMED, A., ZHANG, X. & NORDBERG, A. (2002). Selective nicotinic receptor consequences in APP(SWE) transgenic mice. *Mol Cell Neurosci*, **20,** 354-65.

BEHROUZ, N., DEFOSSEZ, A., DELACOURTE, A. & MAZZUCA, M. (1991). The immunohistochemical evidence of amyloid diffuse deposits as a pathological hallmark in Alzheimer's disease. *J Gerontol*, **46,** B209-12.

BENCHERIF, M., LOVETTE, M.E., FOWLER, K.W., ARRINGTON, S., REEVES, L., CALDWELL, W.S. & LIPPIELLO, P.M. (1996). RJR-2403: a nicotinic agonist with CNS selectivity 1. In vitro characterisation. *J Pharmacol Exp Ther*, **279,** 1413-21.

BENNETT, J.P.Y., H.I. (1985). Neurotransmitter, hormone, or drug receptor binding methods. In *Neurotransmitter Receptor Binding*. ed Yamamura, H.I.: Raven Press.

BENNINGER, C., KADIS, J. & PRINCE, D.A. (1980). Extracellular calcium and potassium changes in hippocampal slices. *Brain Res*, **187,** 165-82.

BERNARD, V., NORMAND, E. & BLOCH, B. (1992). Phenotypical characterization of the rat striatal neurons expressing muscarinic receptor genes. *J Neurosci*, **12,** 3591-600.

BERTRAM, L. & TANZI, R.E. (2004). The current status of Alzheimer's disease genetics: what do we tell patients? *Pharmacol Res*, **50,** 385-96.

BERTRAND, D., BUISSON, B., KRAUSE, R.M., HU, H.Y. & BERTRAND, S. (1997). Electrophysiology: a method to investigate the functional properties of ligand-gated channels. *J Recept Signal Transduct Res*, **17,** 227-42.

BERTRAND, D., VALERA, S., BERTRAND, S., BALLIVET, M. & RUNGGER, D. (1991). Steroids inhibit nicotinic acetylcholine receptors. *Neuroreport*, **2,** 277-80.

BHAIRI, S.M. (2001). *Detergents: A guide to the properties and uses of detergents in biological systems*: Calbiochem-Novabiochem.

BILLINGS, L.M., ODDO, S., GREEN, K.N., MCGAUGH, J.L. & LAFERLA, F.M. (2005). Intraneuronal Abeta causes the onset of early Alzheimer's disease-related cognitive deficits in transgenic mice. *Neuron*, **45,** 675-88.

BINDER, L.I., GUILLOZET-BONGAARTS, A.L., GARCIA-SIERRA, F. & BERRY, R.W. (2005). Tau, tangles, and Alzheimer's disease. *Biochim Biophys Acta*, **1739,** 216-23.

BITAN, G., KIRKITADZE, M.D., LOMAKIN, A., VOLLERS, S.S., BENEDEK, G.B. & TEPLOW, D.B. (2003). Amyloid beta -protein (Abeta) assembly: Abeta 40 and Abeta 42 oligomerize through distinct pathways. *Proc Natl Acad Sci U S A*, **100,** 330-5.

BLANCHARD, V., MOUSSAOUI, S., CZECH, C., TOUCHET, N., BONICI, B., PLANCHE, M., CANTON, T., JEDIDI, I., GOHIN, M., WIRTHS, O., BAYER, T.A., LANGUI, D., DUYCKAERTS, C., TREMP, G. & PRADIER, L. (2003). Time sequence of maturation of dystrophic neurites associated with Abeta deposits in APP/PS1 transgenic mice. *Exp Neurol*, **184,** 247-63.

BLOOM, G.S., REN, K. & GLABE, C.G. (2005). Cultured cell and transgenic mouse models for tau pathology linked to beta-amyloid. *Biochim Biophys Acta*, **1739,** 116-24.

BLUMENTHAL, E.M., CONROY, W.G., ROMANO, S.J., KASSNER, P.D. & BERG, D.K. (1997). Detection of functional nicotinic receptors blocked by alpha-bungarotoxin on PC12 cells and dependence of their expression on post-translational events. *J Neurosci*, **17,** 6094-104.

BONCRISTIANO, S., CALHOUN, M.E., KELLY, P.H., PFEIFER, M., BONDOLFI, L., STALDER, M., PHINNEY, A.L., ABRAMOWSKI, D., STURCHLER-PIERRAT, C., ENZ, A., SOMMER, B., STAUFENBIEL, M. & JUCKER, M. (2002). Cholinergic changes in the APP23 transgenic mouse model of cerebral amyloidosis. *J Neurosci*, **22,** 3234-43.

BONNER, T.I., BUCKLEY, N.J., YOUNG, A.C. & BRANN, M.R. (1987). Identification of a family of muscarinic acetylcholine receptor genes. *Science*, **237,** 527-32.

BONNER, T.I., YOUNG, A.C., BRANN, M.R. & BUCKLEY, N.J. (1988). Cloning and expression of the human and rat m5 muscarinic acetylcholine receptor genes. *Neuron*, **1,** 403-10.

BOORMAN, J.P., GROOT-KORMELINK, P.J. & SIVILOTTI, L.G. (2000). Stoichiometry of human recombinant neuronal nicotinic receptors containing the b3 subunit expressed in Xenopus oocytes. *J Physiol*, **529 Pt 3,** 565-77.

BORCHELT, D.R., LEE, M.K., GONZALES, V., SLUNT, H.H., RATOVITSKI, T., JENKINS, N.A., COPELAND, N.G., PRICE, D.L. & SISODIA, S.S. (2002). Accumulation of proteolytic fragments of mutant presenilin 1 and accelerated amyloid deposition are co-regulated in transgenic mice. *Neurobiol Aging*, **23,** 171-7.

BORCHELT, D.R., THINAKARAN, G., ECKMAN, C.B., LEE, M.K., DAVENPORT, F., RATOVITSKY, T., PRADA, C.M., KIM, G., SEEKINS, S., YAGER, D., SLUNT, H.H., WANG, R., SEEGER, M., LEVEY, A.I., GANDY, S.E., COPELAND, N.G., JENKINS, N.A., PRICE, D.L., YOUNKIN, S.G. & SISODIA, S.S. (1996). Familial Alzheimer's disease-linked presenilin 1 variants elevate Abeta1-42/1-40 ratio in vitro and in vivo. *Neuron*, **17,** 1005-13.

BOWEN, D.M., BENTON, J.S., SPILLANE, J.A., SMITH, C.C. & ALLEN, S.J. (1982). Choline acetyltransferase activity and histopathology of frontal neocortex from biopsies of demented patients. *J Neurol Sci*, **57,** 191-202.

BOWEN, D.M. & DAVISON, A.N. (1980). Biochemical changes in the cholinergic system of the ageing brain and in senile dementia. *Psychol Med*, **10,** 315-9.

BOWEN, D.M., SMITH, C.B., WHITE, P. & DAVISON, A.N. (1976). Neurotransmitter-related enzymes and indices of hypoxia in senile dementia and other abiotrophies. *Brain*, **99,** 459-96.

BRAAK, E., BRAAK, H. & MANDELKOW, E.M. (1994). A sequence of cytoskeleton changes related to the formation of neurofibrillary tangles and neuropil threads. *Acta Neuropathol (Berl)*, **87,** 554-67.

BRAAK, H. & BRAAK, E. (1991). Neuropathological stageing of Alzheimer-related changes. *Acta Neuropathol (Berl)*, **82,** 239-59.

BREJC, K., VAN DIJK, W.J., KLAASSEN, R.V., SCHUURMANS, M., VAN DER OOST, J., SMIT, A.B. & SIXMA, T.K. (2001). Crystal structure of an ACh-binding protein reveals the ligand-binding domain of nicotinic receptors. *Nature*, **411,** 269-76.

BROIDE, R.S., ORR-URTREGER, A. & PATRICK, J.W. (2001). Normal apoptosis levels in mice expressing one alpha7 nicotinic receptor null and one L250T mutant allele. *Neuroreport*, **12,** 1643-8.

BUHLER, A.V. & DUNWIDDIE, T.V. (2002). alpha7 nicotinic acetylcholine receptors on GABAergic interneurons evoke dendritic and somatic inhibition of hippocampal neurons. *J Neurophysiol*, **87,** 548-57.

BUISSON, B. & BERTRAND, D. (2001). Chronic exposure to nicotine upregulates the human (alpha)4((beta)2 nicotinic acetylcholine receptor function. *J Neurosci*, **21,** 1819-29.

BUISSON, B., GOPALAKRISHNAN, M., ARNERIC, S.P., SULLIVAN, D. & BERTRAND, D. (1996). Human alpha4beta2 neuronal nicotinic acetylcholine receptor in HEK 293 cells: A patch-clamp study. *J Neurosci*, **16,** 7880-91.

BURGHAUS, L., SCHUTZ, U., KREMPEL, U., LINDSTROM, J. & SCHRODER, H. (2003). Loss of nicotinic acetylcholine receptor subunits alpha4 and alpha7 in the cerebral cortex of Parkinson patients. *Parkinsonism Relat Disord*, **9,** 243-6.

BUSCIGLIO, J., GABUZDA, D.H., MATSUDAIRA, P. & YANKNER, B.A. (1993). Generation of beta-amyloid in the secretory pathway in neuronal and nonneuronal cells. *Proc Natl Acad Sci U S A*, **90,** 2092-6.

BUXBAUM, J.D., GANDY, S.E., CICCHETTI, P., EHRLICH, M.E., CZERNIK, A.J., FRACASSO, R.P., RAMABHADRAN, T.V., UNTERBECK, A.J. & GREENGARD, P. (1990). Processing of Alzheimer beta/A4 amyloid precursor protein: modulation by agents that regulate protein phosphorylation. *Proc Natl Acad Sci U S A*, **87,** 6003-6.

BUXBAUM, J.D., KOO, E.H. & GREENGARD, P. (1993). Protein phosphorylation inhibits production of Alzheimer amyloid beta/A4 peptide. *Proc Natl Acad Sci U S A*, **90,** 9195-8.

BUXBAUM, J.D., LIU, K.N., LUO, Y., SLACK, J.L., STOCKING, K.L., PESCHON, J.J., JOHNSON, R.S., CASTNER, B.J., CERRETTI, D.P. & BLACK, R.A. (1998). Evidence that tumor necrosis factor alpha converting enzyme is involved in regulated alpha-secretase cleavage of the Alzheimer amyloid protein precursor. *J Biol Chem*, **273,** 27765-7.

BUXBAUM, J.D., RUEFLI, A.A., PARKER, C.A., CYPESS, A.M. & GREENGARD, P. (1994). Calcium regulates processing of the Alzheimer amyloid protein precursor in a protein kinase C-independent manner. *Proc Natl Acad Sci U S A*, **91,** 4489-93.

CAI, H., WANG, Y., MCCARTHY, D., WEN, H., BORCHELT, D.R., PRICE, D.L. & WONG, P.C. (2001). BACE1 is the major beta-secretase for generation of Abeta peptides by neurons. *Nat Neurosci*, **4,** 233-4.

CAPORASO, G.L., TAKEI, K., GANDY, S.E., MATTEOLI, M., MUNDIGL, O., GREENGARD, P. & DE CAMILLI, P. (1994). Morphologic and biochemical analysis of the intracellular trafficking of the Alzheimer beta/A4 amyloid precursor protein. *J Neurosci*, **14,** 3122-38.

CARMINE, A.A. & BROGDEN, R.N. (1985). Pirenzepine. A review of its pharmacodynamic and pharmacokinetic properties and therapeutic efficacy in peptic ulcer disease and other allied diseases. *Drugs*, **30,** 85-126.

CASTELLANI, R.J., SMITH, M.A., PERRY, G. & FRIEDLAND, R.P. (2004). Cerebral amyloid angiopathy: major contributor or decorative response to Alzheimer's disease pathogenesis. *Neurobiol Aging*, **25,** 599-602; discussion 603-4.

CASTILLO, M., MULET, J., GUTIERREZ, L.M., ORTIZ, J.A., CASTELAN, F., GERBER, S., SALA, S., SALA, F. & CRIADO, M. (2005). Dual role of the RIC-3 protein in trafficking of serotonin and nicotinic acetylcholine receptors. *J Biol Chem*, **280,** 27062-8.

CHAMPTIAUX, N., GOTTI, C., CORDERO-ERAUSQUIN, M., DAVID, D.J., PRZYBYLSKI, C., LENA, C., CLEMENTI, F., MORETTI, M., ROSSI, F.M., LE NOVERE, N., MCINTOSH, J.M., GARDIER, A.M. & CHANGEUX, J.P. (2003). Subunit composition of functional nicotinic receptors in dopaminergic neurons investigated with knock-out mice. *J Neurosci*, **23,** 7820-9.

CHAMPTIAUX, N., HAN, Z.Y., BESSIS, A., ROSSI, F.M., ZOLI, M., MARUBIO, L., MCINTOSH, J.M. & CHANGEUX, J.P. (2002). Distribution and pharmacology of alpha 6-containing nicotinic acetylcholine receptors analyzed with mutant mice. *J Neurosci*, **22,** 1208-17.

CHANG, W.P., KOELSCH, G., WONG, S., DOWNS, D., DA, H., WEERASENA, V., GORDON, B., DEVASAMUDRAM, T., BILCER, G., GHOSH, A.K. & TANG, J. (2004). In vivo inhibition of Abeta production by memapsin 2 (beta-secretase) inhibitors. *J Neurochem*, **89,** 1409-16.

CHANG, Y. & WEISS, D.S. (1999). Channel opening locks agonist onto the GABAC receptor. *Nat Neurosci*, **2,** 219-25.

CHANGEUX, J.P. & EDELSTEIN, S.J. (1998). Allosteric receptors after 30 years. *Neuron*, **21,** 959-80.

CHARTIER-HARLIN, M.C., CRAWFORD, F., HAMANDI, K., MULLAN, M., GOATE, A., HARDY, J., BACKHOVENS, H., MARTIN, J.J. & BROECKHOVEN, C.V. (1991a). Screening for the beta-amyloid precursor protein mutation (APP717: Val----Ile) in extended pedigrees with early onset Alzheimer's disease. *Neurosci Lett*, **129,** 134-5.

CHARTIER-HARLIN, M.C., CRAWFORD, F., HOULDEN, H., WARREN, A., HUGHES, D., FIDANI, L., GOATE, A., ROSSOR, M., ROQUES, P., HARDY, J. & ET AL. (1991b). Early-onset Alzheimer's disease caused by mutations at codon 717 of the beta-amyloid precursor protein gene. *Nature*, **353,** 844-6.

CHAVEZ-NORIEGA, L.E., CRONA, J.H., WASHBURN, M.S., URRUTIA, A., ELLIOTT, K.J. & JOHNSON, E.C. (1997). Pharmacological characterization of recombinant human neuronal nicotinic acetylcholine receptors h alpha 2 beta 2, h alpha 2 beta 4, h alpha 3 beta 2, h alpha 3 beta 4, h alpha 4 beta 2, h alpha 4 beta 4 and h alpha 7 expressed in Xenopus oocytes. *J Pharmacol Exp Ther*, **280,** 346-56.

CHAVEZ-NORIEGA, L.E., GILLESPIE, A., STAUDERMAN, K.A., CRONA, J.H., CLAEPS, B.O., ELLIOTT, K.J., REID, R.T., RAO, T.S., VELICELEBI, G., HARPOLD, M.M., JOHNSON, E.C. & COREY-NAEVE, J. (2000). Characterization of the recombinant human neuronal nicotinic acetylcholine receptors alpha3beta2 and alpha4beta2 stably expressed in HEK293 cells. *Neuropharmacology*, **39,** 2543-60.

CHEN, D., DANG, H. & PATRICK, J.W. (1998). Contributions of N-linked glycosylation to the expression of a functional alpha 7-nicotinic receptor in Xenopus oocytes. *J Neurochem*, **70,** 349-57.

CHENG, A., MCDONALD, N.A. & CONNOLLY, C.N. (2005). Cell surface expression of 5-hydroxytryptamine type-3 receptors is promoted by RIC-3. *J Biol Chem*, **280,** 22502-7.

CHENG, Y. & PRUSOFF, W.H. (1973). Relationship between the inhibition constant (K1) and the concentration of inhibitor which causes 50 per cent inhibition (I50) of an enzymatic reaction. *Biochem Pharmacol*, **22,** 3099-108.

CHIARA, D.C., DANGOTT, L.J., ECKENHOFF, R.G. & COHEN, J.B. (2003a). Identification of nicotinic acetylcholine receptor amino acids photolabeled by the volatile anesthetic halothane. *Biochemistry*, **42,** 13457-67.

CHIARA, D.C., TRINIDAD, J.C., WANG, D., ZIEBELL, M.R., SULLIVAN, D. & COHEN, J.B. (2003b). Identification of amino acids in the nicotinic acetylcholine receptor agonist binding site and ion channel photolabeled by 4-[(3-trifluoromethyl)-3H-diazirin-3-yl]benzoylcholine, a novel photoaffinity antagonist. *Biochemistry*, **42,** 271-83.

CHYUNG, A.S., GREENBERG, B.D., COOK, D.G., DOMS, R.W. & LEE, V.M. (1997). Novel beta-secretase cleavage of beta-amyloid precursor protein in the endoplasmic reticulum/intermediate compartment of NT2N cells. *J Cell Biol*, **138,** 671-80.

CITRON, M., WESTAWAY, D., XIA, W., CARLSON, G., DIEHL, T., LEVESQUE, G., JOHNSON-WOOD, K., LEE, M., SEUBERT, P., DAVIS, A., KHOLODENKO, D., MOTTER, R., SHERRINGTON, R., PERRY, B., YAO, H., STROME, R., LIEBERBURG, I., ROMMENS, J., KIM, S., SCHENK, D., FRASER, P., ST GEORGE HYSLOP, P. & SELKOE, D.J. (1997). Mutant presenilins of Alzheimer's disease increase production of 42-residue amyloid beta-protein in both transfected cells and transgenic mice. *Nat Med*, **3,** 67-72.

CLARKE, P.B., SCHWARTZ, R.D., PAUL, S.M., PERT, C.B. & PERT, A. (1985). Nicotinic binding in rat brain: autoradiographic comparison of [3H]acetylcholine, [3H]nicotine, and [125I]-alpha-bungarotoxin. *J Neurosci*, **5,** 1307-15.

COLQUHOUN, D. & SAKMANN, B. (1985). Fast events in single-channel currents activated by acetylcholine and its analogues at the frog muscle end-plate. *J Physiol*, **369,** 501-57.

CONNOLLY, J., BOULTER, J. & HEINEMANN, S.F. (1992). Alpha 4-2 beta 2 and other nicotinic acetylcholine receptor subtypes as targets of psychoactive and addictive drugs. *Br J Pharmacol*, **105,** 657-66.

CONROY, W.G., VERNALLIS, A.B. & BERG, D.K. (1992). The alpha 5 gene product assembles with multiple acetylcholine receptor subunits to form distinctive receptor subtypes in brain. *Neuron*, **9,** 679-91.

CONTI-TRONCONI, B.M. & RAFTERY, M.A. (1986). Nicotinic acetylcholine receptor contains multiple binding sites: evidence from binding of alpha-dendrotoxin. *Proc Natl Acad Sci U S A*, **83,** 6646-50.

CONWAY, K.A., LEE, S.J., ROCHET, J.C., DING, T.T., WILLIAMSON, R.E. & LANSBURY, P.T., JR. (2000). Acceleration of oligomerization, not fibrillization, is a shared property of both alpha-synuclein mutations linked to early-onset Parkinson's disease: implications for pathogenesis and therapy. *Proc Natl Acad Sci U S A*, **97,** 571-6.

COOPER, S.T. & MILLAR, N.S. (1997). Host cell-specific folding and assembly of the neuronal nicotinic acetylcholine receptor alpha7 subunit. *J Neurochem*, **68,** 2140-51.

COOPER, S.T. & MILLAR, N.S. (1998). Host cell-specific folding of the neuronal nicotinic receptor alpha8 subunit. *J Neurochem*, **70,** 2585-93.

CORDER, E.H., SAUNDERS, A.M., STRITTMATTER, W.J., SCHMECHEL, D.E., GASKELL, P.C., SMALL, G.W., ROSES, A.D., HAINES, J.L. & PERICAK-VANCE, M.A. (1993). Gene dose of apolipoprotein E type 4 allele and the risk of Alzheimer's disease in late onset families. *Science*, **261,** 921-3.

CORRINGER, P.J., GALZI, J.L., EISELE, J.L., BERTRAND, S., CHANGEUX, J.P. & BERTRAND, D. (1995). Identification of a new component of the agonist binding site of the nicotinic alpha 7 homooligomeric receptor. *J Biol Chem*, **270,** 11749-52.

CORRINGER, P.J., LE NOVERE, N. & CHANGEUX, J.P. (2000). Nicotinic receptors at the amino acid level. *Annu Rev Pharmacol Toxicol*, **40,** 431-58.

COURT, J., MARTIN-RUIZ, C., PIGGOTT, M., SPURDEN, D., GRIFFITHS, M. & PERRY, E. (2001). Nicotinic receptor abnormalities in Alzheimer's disease. *Biol Psychiatry*, **49,** 175-84.

COUTURIER, S., BERTRAND, D., MATTER, J.M., HERNANDEZ, M.C., BERTRAND, S., MILLAR, N., VALERA, S., BARKAS, T. & BALLIVET, M. (1990). A neuronal nicotinic acetylcholine receptor subunit (alpha 7) is developmentally regulated and forms a homo-oligomeric channel blocked by alpha-BTX. *Neuron*, **5,** 847-56.

CRAIG, P.J., BOSE, S., ZWART, R., BEATTIE, R.E., FOLLY, E.A., JOHNSON, L.R., BELL, E., EVANS, N.M., BENEDETTI, G., PEARSON, K.H., MCPHIE, G.I., VOLSEN, S.G., MILLAR, N.S., SHER, E. & BROAD, L.M. (2004). Stable expression and characterisation of a human alpha 7 nicotinic subunit chimera: a tool for functional high-throughput screening. *Eur J Pharmacol*, **502,** 31-40.

CRAWFORD, N., FINLAYSON, K., SHARKEY, J.S. & KELLY, J.S. (2004). Identification of species differences in the pharmacology of the alpha7 nicotinic receptor using the antagonist radioligand [^{3}H]-Methyllycaconitine. In *Cholinergic Mechanisms: Function and Dysfunction*. ed Silman.

CRAWFORD, N., LANG, T.K., KERR, D.S. & DE VRIES, D.J. (1999). High-affinity [3H]kainic acid binding to brain membranes: a re-evaluation of ligand potency and selectivity. *J Pharmacol Toxicol Methods*, **42,** 121-5.

CROWTHER, D.C., KINGHORN, K.J., MIRANDA, E., PAGE, R., CURRY, J.A., DUTHIE, F.A., GUBB, D.C. & LOMAS, D.A. (2005). Intraneuronal Abeta, non-amyloid aggregates and neurodegeneration in a Drosophila model of Alzheimer's disease. *Neuroscience*, **132,** 123-35.

CRUTS, M., HENDRIKS, L. & VAN BROECKHOVEN, C. (1996). The presenilin genes: a new gene family involved in Alzheimer disease pathology. *Hum Mol Genet*, **5 Spec No,** 1449-55.

CUEVAS, J. & BERG, D.K. (1998). Mammalian nicotinic receptors with alpha7 subunits that slowly desensitize and rapidly recover from alpha-bungarotoxin blockade. *J Neurosci*, **18,** 10335-44.

CUEVAS, J., ROTH, A.L. & BERG, D.K. (2000). Two distinct classes of functional 7-containing nicotinic receptor on rat superior cervical ganglion neurons. *J Physiol*, **525 Pt 3,** 735-46.

CUI, C., BOOKER, T.K., ALLEN, R.S., GRADY, S.R., WHITEAKER, P., MARKS, M.J., SALMINEN, O., TRITTO, T., BUTT, C.M., ALLEN, W.R., STITZEL, J.A., MCINTOSH, J.M., BOULTER, J., COLLINS, A.C. & HEINEMANN, S.F. (2003). The beta3 nicotinic receptor subunit: a component of alpha-conotoxin MII-binding nicotinic acetylcholine receptors that modulate dopamine release and related behaviors. *J Neurosci*, **23,** 11045-53.

CUMMING, J.N., ISERLOH, U. & KENNEDY, M.E. (2004). Design and development of BACE-1 inhibitors. *Curr Opin Drug Discov Devel*, **7,** 536-56.

CURTIS, L., BUISSON, B., BERTRAND, S. & BERTRAND, D. (2002). Potentiation of human alpha4beta2 neuronal nicotinic acetylcholine receptor by estradiol. *Mol Pharmacol*, **61,** 127-35.

DAJAS-BAILADOR, F.A., HEIMALA, K. & WONNACOTT, S. (2003). The allosteric potentiation of nicotinic acetylcholine receptors by galantamine is transduced into cellular responses in neurons: Ca2+ signals and neurotransmitter release. *Mol Pharmacol*, **64,** 1217-26.

DALY, J.W., BROWN, G.B., MENSAH-DWUMAH, M. & MYERS, C.W. (1978). Classification of skin alkaloids from neotropical poison-dart frogs (Dendrobatidae). *Toxicon*, **16,** 163-88.

D'ANGELO, E., ROSSI, P., GALL, D., PRESTORI, F., NIEUS, T., MAFFEI, A. & SOLA, E. (2005). Long-term potentiation of synaptic transmission at the mossy fiber-granule cell relay of cerebellum. *Prog Brain Res*, **148,** 69-80.

DANI, J.A. (2001). Overview of nicotinic receptors and their roles in the central nervous system. *Biol Psychiatry*, **49,** 166-74.

DAVIES, A.R., HARDICK, D.J., BLAGBROUGH, I.S., POTTER, B.V., WOLSTENHOLME, A.J. & WONNACOTT, S. (1999). Characterisation of the binding of [3H]methyllycaconitine: a new radioligand for labelling alpha 7-type neuronal nicotinic acetylcholine receptors. *Neuropharmacology*, **38,** 679-90.

DAVIES, P. & MALONEY, A.J. (1976). Selective loss of central cholinergic neurons in Alzheimer's disease. *Lancet*, **2,** 1403.

DAVILA-GARCIA, M.I., HOUGHTLING, R.A., QASBA, S.S. & KELLAR, K.J. (1999). Nicotinic receptor binding sites in rat primary neuronal cells in culture: characterization and their regulation by chronic nicotine. *Brain Res Mol Brain Res*, **66,** 14-23.

DE FIEBRE, N.C. & DE FIEBRE, C.M. (2005). alpha7 Nicotinic acetylcholine receptor knockout selectively enhances ethanol-, but not beta-amyloid-induced neurotoxicity. *Neurosci Lett*, **373,** 42-7.

DE LUCA, V., WANG, H., SQUASSINA, A., WONG, G.W., YEOMANS, J. & KENNEDY, M.E. (2004). Linkage of M5 muscarinic and alpha7-nicotinic receptor genes on 15q13 to schizophrenia. *Neuropsychobiology*, **50,** 124-7.

DE POORTER, L.M. & KELTJENS, J.T. (2001). Convenient fluorescence-based methods to measure membrane potential and intracellular pH in the Archaeon Methanobacterium thermoautotrophicum. *J Microbiol Methods*, **47,** 233-41.

DE STROOPER, B. (2005). Nicastrin: gatekeeper of the gamma-secretase complex. *Cell*, **122,** 318-20.

DE VRIES, D.J., HERALD, C.L., PETTIT, G.R. & BLUMBERG, P.M. (1988). Demonstration of sub-nanomolar affinity of bryostatin 1 for the phorbol ester receptor in rat brain. *Biochem Pharmacol*, **37,** 4069-73.

DECKER, M.W., ANDERSON, D.J., BRIONI, J.D., DONNELLY-ROBERTS, D.L., KANG, C.H., O'NEILL, A.B., PIATTONI-KAPLAN, M., SWANSON, S. & SULLIVAN, J.P. (1995). Erysodine, a competitive antagonist at neuronal nicotinic acetylcholine receptors. *Eur J Pharmacol*, **280,** 79-89.

DEMURO, A., PALMA, E., EUSEBI, F. & MILEDI, R. (2001). Inhibition of nicotinic acetylcholine receptors by bicuculline. *Neuropharmacology*, **41,** 854-61.

DENERIS, E.S., CONNOLLY, J., BOULTER, J., WADA, E., WADA, K., SWANSON, L.W., PATRICK, J. & HEINEMANN, S. (1988). Primary structure and expression of beta 2: a novel subunit of neuronal nicotinic acetylcholine receptors. *Neuron*, **1,** 45-54.

DEUTSCH, S.I., ROSSE, R.B., SCHWARTZ, B.L., WEIZMAN, A., CHILTON, M., ARNOLD, D.S. & MASTROPAOLO, J. (2005). Therapeutic implications of a selective alpha7 nicotinic receptor abnormality in schizophrenia. *Isr J Psychiatry Relat Sci*, **42,** 33-44.

DEVILLERS-THIERY, A., GALZI, J.L., EISELE, J.L., BERTRAND, S., BERTRAND, D. & CHANGEUX, J.P. (1993). Functional architecture of the nicotinic acetylcholine receptor: a prototype of ligand-gated ion channels. *J Membr Biol*, **136,** 97-112.

DEWJI, N.N. (2005). The structure and functions of the presenilins. *Cell Mol Life Sci*, **62,** 1109-19.

DICKSON, D.W. (1997a). Neuropathological diagnosis of Alzheimer's disease: a perspective from longitudinal clinicopathological studies. *Neurobiol Aging*, **18,** S21-6.

DICKSON, D.W. (1997b). The pathogenesis of senile plaques. *J Neuropathol Exp Neurol*, **56,** 321-39.

DICKSON, T.C. & VICKERS, J.C. (2001). The morphological phenotype of beta-amyloid plaques and associated neuritic changes in Alzheimer's disease. *Neuroscience*, **105,** 99-107.

DIDIER, M., BERMAN, S.A., LINDSTROM, J. & BURSZTAJN, S. (1995). Characterization of nicotinic acetylcholine receptors expressed in primary cultures of cerebellar granule cells. *Brain Res Mol Brain Res*, **30,** 17-28.

DINELEY, K.T., BELL, K.A., BUI, D. & SWEATT, J.D. (2002b-a). beta -Amyloid peptide activates alpha 7 nicotinic acetylcholine receptors expressed in Xenopus oocytes. *J Biol Chem*, **277,** 25056-61.

DINELEY, K.T., BELL, K.A., BUI, D. & SWEATT, J.D. (2002a-a). beta -Amyloid peptide activates alpha 7 nicotinic acetylcholine receptors expressed in Xenopus oocytes. *J Biol Chem*, **277,** 25056-61.

DINELEY, K.T. & PATRICK, J.W. (2000). Amino acid determinants of alpha 7 nicotinic acetylcholine receptor surface expression. *J Biol Chem*, **275,** 13974-85.

DINELEY, K.T., WESTERMAN, M., BUI, D., BELL, K., ASHE, K.H. & SWEATT, J.D. (2001). Beta-amyloid activates the mitogen-activated protein kinase cascade via hippocampal alpha7 nicotinic acetylcholine receptors: In vitro and in vivo mechanisms related to Alzheimer's disease. *J Neurosci*, **21,** 4125-33.

DINELEY, K.T., XIA, X., BUI, D., SWEATT, J.D. & ZHENG, H. (2002b-b). Accelerated plaque accumulation, associative learning deficits, and up-regulation of alpha 7 nicotinic receptor protein in transgenic mice co-expressing mutant human presenilin 1 and amyloid precursor proteins. *J Biol Chem*, **277,** 22768-80.

DINELEY, K.T., XIA, X., BUI, D., SWEATT, J.D. & ZHENG, H. (2002a-b). Accelerated plaque accumulation, associative learning deficits, and up-regulation of alpha 7 nicotinic receptor protein in transgenic mice co-expressing mutant human presenilin 1 and amyloid precursor proteins. *J Biol Chem*, **277,** 22768-80.

DODSON, B.A., BRASWELL, L.M. & MILLER, K.W. (1987). Barbiturates bind to an allosteric regulatory site on nicotinic acetylcholine receptor-rich membranes. *Mol Pharmacol*, **32,** 119-26.

DOOLEY, D.J., GEER, J.J., HALEEN, S.J., PROBERT, A.W. & WELCH, K.M. (1998). Assessment of endothelin receptor subtype-mediated increases of [Ca2+]i in distinct rat cell types using fluorimetric imaging. *J Cardiovasc Pharmacol*, **31 Suppl 1,** S192-5.

DRAGO, J., MCCOLL, C.D., HORNE, M.K., FINKELSTEIN, D.I. & ROSS, S.A. (2003). Neuronal nicotinic receptors: insights gained from gene knockout and knockin mutant mice. *Cell Mol Life Sci*, **60,** 1267-80.

DRASDO, A., CAULFIELD, M., BERTRAND, D., BERTRAND, S. & WONNACOTT, S. (1992). Methyllycaconitine: a novel nicotinic antagonist. *Mol. Cell. Neurosci.*, **3,** 237-243.

DRISDEL, R.C. & GREEN, W.N. (2000). Neuronal alpha-bungarotoxin receptors are alpha7 subunit homomers. *J Neurosci*, **20,** 133-9.

DUFF, K. (2001). Transgenic mouse models of Alzheimer's disease: phenotype and mechanisms of pathogenesis. *Biochem Soc Symp*, 195-202.

DUNCKLEY, T., WU, J., ZHAO, L. & LUKAS, R.J. (2003). Mutational analysis of roles for extracellular cysteine residues in the assembly and function of human alpha 7-nicotinic acetylcholine receptors. *Biochemistry*, **42,** 870-6.

EATON, J.B., PENG, J.H., SCHROEDER, K.M., GEORGE, A.A., FRYER, J.D., KRISHNAN, C., BUHLMAN, L., KUO, Y.P., STEINLEIN, O. & LUKAS, R.J. (2003). Characterization of human alpha 4 beta 2-nicotinic acetylcholine receptors stably and heterologously expressed in native nicotinic receptor-null SH-EP1 human epithelial cells. *Mol Pharmacol*, **64,** 1283-94.

EGLEN, R.M., CHOPPIN, A. & WATSON, N. (2001). Therapeutic opportunities from muscarinic receptor research. *Trends Pharmacol Sci*, **22,** 409-14.

EGLEN, R.M., REDDY, H., WATSON, N. & CHALLISS, R.A. (1994). Muscarinic acetylcholine receptor subtypes in smooth muscle. *Trends Pharmacol Sci*, **15,** 114-9.

EILERS, H., SCHAEFFER, E., BICKLER, P.E. & FORSAYETH, J.R. (1997). Functional deactivation of the major neuronal nicotinic receptor caused by nicotine and a protein kinase C-dependent mechanism. *Mol Pharmacol*, **52,** 1105-12.

EISELE, J.L., BERTRAND, S., GALZI, J.L., DEVILLERS-THIERY, A., CHANGEUX, J.P. & BERTRAND, D. (1993). Chimaeric nicotinic-serotonergic receptor combines distinct ligand binding and channel specificities. *Nature*, **366,** 479-83.

ELGOYHEN, A.B., JOHNSON, D.S., BOULTER, J., VETTER, D.E. & HEINEMANN, S. (1994). Alpha 9: an acetylcholine receptor with novel pharmacological properties expressed in rat cochlear hair cells. *Cell*, **79,** 705-15.

ELGOYHEN, A.B., VETTER, D.E., KATZ, E., ROTHLIN, C.V., HEINEMANN, S.F. & BOULTER, J. (2001). alpha10: a determinant of nicotinic cholinergic receptor function in mammalian vestibular and cochlear mechanosensory hair cells. *Proc Natl Acad Sci U S A*, **98,** 3501-6.

ELLIOTT, K.J., ELLIS, S.B., BERCKHAN, K.J., URRUTIA, A., CHAVEZ-NORIEGA, L.E., JOHNSON, E.C., VELICELEBI, G. & HARPOLD, M.M. (1996). Comparative structure of human neuronal alpha 2-alpha 7 and beta 2-beta 4 nicotinic acetylcholine receptor subunits and functional expression of the alpha 2, alpha 3, alpha 4, alpha 7, beta 2, and beta 4 subunits. *J Mol Neurosci*, **7,** 217-28.

ESCH, F.S., KEIM, P.S., BEATTIE, E.C., BLACHER, R.W., CULWELL, A.R., OLTERSDORF, T., MCCLURE, D. & WARD, P.J. (1990). Cleavage of amyloid beta peptide during constitutive processing of its precursor. *Science*, **248,** 1122-4.

ESLER, W.P. & WOLFE, M.S. (2001). A portrait of Alzheimer secretases--new features and familiar faces. *Science*, **293,** 1449-54.

FABIAN-FINE, R., SKEHEL, P., ERRINGTON, M.L., DAVIES, H.A., SHER, E., STEWART, M.G. & FINE, A. (2001). Ultrastructural distribution of the alpha7 nicotinic acetylcholine receptor subunit in rat hippocampus. *J Neurosci*, **21,** 7993-8003.

FALK, L., NORDBERG, A., SEIGER, A., KJAELDGAARD, A. & HELLSTROM-LINDAHL, E. (2003). Higher expression of alpha7 nicotinic acetylcholine receptors in human fetal compared to adult brain. *Brain Res Dev Brain Res*, **142,** 151-60.

FARRER, L.A., CUPPLES, L.A., HAINES, J.L., HYMAN, B., KUKULL, W.A., MAYEUX, R., MYERS, R.H., PERICAK-VANCE, M.A., RISCH, N. & VAN DUIJN, C.M. (1997). Effects of age, sex, and ethnicity on the association between apolipoprotein E genotype and Alzheimer disease. A meta-analysis. APOE and Alzheimer Disease Meta Analysis Consortium. *Jama*, **278,** 1349-56.

FARZAN, M., SCHNITZLER, C.E., VASILIEVA, N., LEUNG, D. & CHOE, H. (2000). BACE2, a beta -secretase homolog, cleaves at the beta site and within the amyloid-beta region of the amyloid-beta precursor protein. *Proc Natl Acad Sci U S A*, **97,** 9712-7.

FAY, D.S., FLUET, A., JOHNSON, C.J. & LINK, C.D. (1998). In vivo aggregation of beta-amyloid peptide variants. *J Neurochem*, **71,** 1616-25.

FAYUK, D. & YAKEL, J.L. (2005). Ca2+ permeability of nicotinic acetylcholine receptors in rat hippocampal CA1 interneurons. *J Physiol*.

FERREIRA, M., EBERT, S.N., PERRY, D.C., YASUDA, R.P., BAKER, C.M., DAVILA-GARCIA, M.I., KELLAR, K.J. & GILLIS, R.A. (2001). Evidence of a functional alpha7-neuronal nicotinic receptor subtype located on motoneurons of the dorsal motor nucleus of the vagus. *J Pharmacol Exp Ther*, **296,** 260-9.

FINLAYSON, K., HODGKISS, J., CRAWFORD, N., MCLUCKIE, J. & SHARKEY, J. (2005). Multiple *in vitro* assays provide no evidence for an interaction between hAB1-42 and the ha4b2 nAChR. In *Cholinergic Mechanisms: Function and Dysfunction*.

FISHER, A. (2000). Therapeutic strategies in Alzheimer's disease: M1 muscarinic agonists. *Jpn J Pharmacol*, **84,** 101-12.

FISHMAN, E.B., SIEK, G.C., MACCALLUM, R.D., BIRD, E.D., VOLICER, L. & MARQUIS, J.K. (1986). Distribution of the molecular forms of acetylcholinesterase in human brain: alterations in dementia of the Alzheimer type. *Ann Neurol*, **19,** 246-52.

FITCH, R.W., XIAO, Y., KELLAR, K.J. & DALY, J.W. (2003). Membrane potential fluorescence: a rapid and highly sensitive assay for nicotinic receptor channel function. *Proc Natl Acad Sci U S A*, **100,** 4909-14.

FLORES, C.M., ROGERS, S.W., PABREZA, L.A., WOLFE, B.B. & KELLAR, K.J. (1992). A subtype of nicotinic cholinergic receptor in rat brain is composed of alpha 4 and beta 2 subunits and is up-regulated by chronic nicotine treatment. *Mol Pharmacol*, **41,** 31-7.

FLYNN, D.D., FERRARI-DILEO, G., MASH, D.C. & LEVEY, A.I. (1995). Differential regulation of molecular subtypes of muscarinic receptors in Alzheimer's disease. *J Neurochem*, **64,** 1888-91.

FLYNN, D.D. & MASH, D.C. (1986). Characterization of L-[3H]nicotine binding in human cerebral cortex: comparison between Alzheimer's disease and the normal. *J Neurochem*, **47,** 1948-54.

FODERO, L.R., MOK, S.S., LOSIC, D., MARTIN, L.L., AGUILAR, M.I., BARROW, C.J., LIVETT, B.G. & SMALL, D.H. (2004). Alpha7-nicotinic acetylcholine receptors mediate an Abeta(1-42)-induced increase in the level of acetylcholinesterase in primary cortical neurones. *J Neurochem*, **88,** 1186-93.

FODERO, L.R., SAEZ-VALERO, J., MCLEAN, C.A., MARTINS, R.N., BEYREUTHER, K., MASTERS, C.L., ROBERTSON, T.A. & SMALL, D.H. (2002). Altered glycosylation of acetylcholinesterase in APP (SW) Tg2576 transgenic mice occurs prior to amyloid plaque deposition. *J Neurochem*, **81,** 441-8.

FOREMAN, J.C.J. (2002). Ligand binding studies of receptors. In *Textbook of Receptor Pharmacology*. ed Foreman, J.C.J. London: CRC Press.

FORGON, M., FARKAS, Z., GULYA, K., PAKASKI, M., PENKE, B. & KASA, P. (1998). Amyloid beta-peptide and its fragments induce acetylcholine release in in vitro basal forebrain tissue slices of rat brain, but do not affect the choline uptake. *Neurobiology (Bp)*, **6,** 359-61.

FRANCESCHINI, D., PAYLOR, R., BROIDE, R., SALAS, R., BASSETTO, L., GOTTI, C. & DE BIASI, M. (2002). Absence of alpha7-containing neuronal nicotinic acetylcholine receptors does not prevent nicotine-induced seizures. *Brain Res Mol Brain Res*, **98,** 29-40.

FRANCIS, P.T., SIMS, N.R., PROCTER, A.W. & BOWEN, D.M. (1993). Cortical pyramidal neurone loss may cause glutamatergic hypoactivity and cognitive impairment in Alzheimer's disease: investigative and therapeutic perspectives. *J Neurochem*, **60,** 1589-604.

FRANCOTTE, P., GRAINDORGE, E., BOVERIE, S., DE TULLIO, P. & PIROTTE, B. (2004). New trends in the design of drugs against Alzheimer's disease. *Curr Med Chem*, **11,** 1757-78.

FREE, R.B., BRYANT, D.L., MCKAY, S.B., KASER, D.J. & MCKAY, D.B. (2002). [3H]Epibatidine binding to bovine adrenal medulla: evidence for alpha3beta4* nicotinic receptors. *Neurosci Lett*, **318,** 98-102.

FU, W. & JHAMANDAS, J.H. (2003). Beta-amyloid peptide activates non-alpha7 nicotinic acetylcholine receptors in rat basal forebrain neurons. *J Neurophysiol*, **90,** 3130-6.

FUCILE, S., PALMA, E., MARTINEZ-TORRES, A., MILEDI, R. & EUSEBI, F. (2002). The single-channel properties of human acetylcholine alpha 7 receptors are altered by fusing alpha 7 to the green fluorescent protein. *Proc Natl Acad Sci U S A*, **99,** 3956-61.

GALZI, J.L. & CHANGEUX, J.P. (1995). Neuronal nicotinic receptors: molecular organization and regulations. *Neuropharmacology*, **34,** 563-82.

GAMES, D., ADAMS, D., ALESSANDRINI, R., BARBOUR, R., BERTHELETTE, P., BLACKWELL, C., CARR, T., CLEMENS, J., DONALDSON, T., GILLESPIE, F. & ET AL. (1995). Alzheimer-type neuropathology in transgenic mice overexpressing V717F beta-amyloid precursor protein. *Nature*, **373,** 523-7.

GARCIA-GUZMAN, M., SALA, F., SALA, S., CAMPOS-CARO, A., STUHMER, W., GUTIERREZ, L.M. & CRIADO, M. (1995). alpha-Bungarotoxin-sensitive nicotinic receptors on bovine chromaffin cells: molecular cloning, functional expression and alternative splicing of the alpha 7 subunit. *Eur J Neurosci*, **7,** 647-55.

GARCIA-SIERRA, F., GHOSHAL, N., QUINN, B., BERRY, R.W. & BINDER, L.I. (2003). Conformational changes and truncation of tau protein during tangle evolution in Alzheimer's disease. *J Alzheimers Dis*, **5,** 65-77.

GAULT, J., ROBINSON, M., BERGER, R., DREBING, C., LOGEL, J., HOPKINS, J., MOORE, T., JACOBS, S., MERIWETHER, J., CHOI, M.J., KIM, E.J., WALTON, K., BUITING, K., DAVIS, A., BREESE, C., FREEDMAN, R. & LEONARD, S. (1998). Genomic organization and partial duplication of the human alpha7 neuronal nicotinic acetylcholine receptor gene (CHRNA7). *Genomics*, **52,** 173-85.

GEE, K.R., BROWN, K.A., CHEN, W.N., BISHOP-STEWART, J., GRAY, D. & JOHNSON, I. (2000). Chemical and physiological characterization of fluo-4 Ca(2+)-indicator dyes. *Cell Calcium*, **27,** 97-106.

GENTRY, C.L., WILKINS, L.H., JR. & LUKAS, R.J. (2003). Effects of prolonged nicotinic ligand exposure on function of heterologously expressed, human alpha4beta2- and alpha4beta4-nicotinic acetylcholine receptors. *J Pharmacol Exp Ther*, **304,** 206-16.

GERMAN, D.C., YAZDANI, U., SPECIALE, S.G., PASBAKHSH, P., GAMES, D. & LIANG, C.L. (2003). Cholinergic neuropathology in a mouse model of Alzheimer's disease. *J Comp Neurol*, **462,** 371-81.

GERZANICH, V., PENG, X., WANG, F., WELLS, G., ANAND, R., FLETCHER, S. & LINDSTROM, J. (1995). Comparative pharmacology of epibatidine: a potent agonist for neuronal nicotinic acetylcholine receptors. *Mol Pharmacol*, **48,** 774-82.

GEULA, C. & MESULAM, M. (1989). Special properties of cholinesterases in the cerebral cortex of Alzheimer's disease. *Brain Res*, **498,** 185-9.

GHOSHAL, N., GARCIA-SIERRA, F., FU, Y., BECKETT, L.A., MUFSON, E.J., KURET, J., BERRY, R.W. & BINDER, L.I. (2001). Tau-66: evidence for a novel tau conformation in Alzheimer's disease. *J Neurochem*, **77,** 1372-85.

GIL, Z., SACK, R.A., KEDMI, M., HARMELIN, A. & ORR-URTREGER, A. (2002). Increased sensitivity to nicotine-induced seizures in mice heterozygous for the L250T mutation in the alpha7 nicotinic acetylcholine receptor. *Neuroreport*, **13,** 191-6.

GILLESPIE, S.L., GOLDE, T.E. & YOUNKIN, S.G. (1992). Secretory processing of the Alzheimer amyloid beta/A4 protein precursor is increased by protein phosphorylation. *Biochem Biophys Res Commun*, **187,** 1285-90.

GIROD, R., CRABTREE, G., ERNSTROM, G., RAMIREZ-LATORRE, J., MCGEHEE, D., TURNER, J. & ROLE, L. (1999). Heteromeric complexes of alpha 5 and/or alpha 7 subunits. Effects of calcium and potential role in nicotine-induced presynaptic facilitation. *Ann N Y Acad Sci*, **868,** 578-90.

GLENNER, G.G. & WONG, C.W. (1984). Alzheimer's disease and Down's syndrome: sharing of a unique cerebrovascular amyloid fibril protein. *Biochem Biophys Res Commun*, **122,** 1131-5.

GNADISCH, D., LONDON, E.D., TERRY, P., HILL, G.R. & MUKHIN, A.G. (1999). High affinity binding of [3H]epibatidine to rat brain membranes. *Neuroreport*, **10,** 1631-6.

GOATE, A., CHARTIER-HARLIN, M.C., MULLAN, M., BROWN, J., CRAWFORD, F., FIDANI, L., GIUFFRA, L., HAYNES, A., IRVING, N., JAMES, L. & ET AL. (1991). Segregation of a missense mutation in the amyloid precursor protein gene with familial Alzheimer's disease. *Nature*, **349,** 704-6.

GOEDERT, M. & JAKES, R. (2005). Mutations causing neurodegenerative tauopathies. *Biochim Biophys Acta*, **1739,** 240-50.

GOEDERT, M., SPILLANTINI, M.G., JAKES, R., RUTHERFORD, D. & CROWTHER, R.A. (1989). Multiple isoforms of human microtubule-associated protein tau: sequences and localization in neurofibrillary tangles of Alzheimer's disease. *Neuron*, **3,** 519-26.

GOLDGABER, D., LERMAN, M.I., MCBRIDE, O.W., SAFFIOTTI, U. & GAJDUSEK, D.C. (1987a). Characterization and chromosomal localization of a cDNA encoding brain amyloid of Alzheimer's disease. *Science*, **235,** 877-80.

GOLDGABER, D., LERMAN, M.I., MCBRIDE, W.O., SAFFIOTTI, U. & GAJDUSEK, D.C. (1987b). Isolation, characterization, and chromosomal localization of human brain cDNA clones coding for the precursor of the amyloid of brain in Alzheimer's disease, Down's syndrome and aging. *J Neural Transm Suppl*, **24,** 23-8.

GOLDMAN, D., DENERIS, E., LUYTEN, W., KOCHHAR, A., PATRICK, J. & HEINEMANN, S. (1987). Members of a nicotinic acetylcholine receptor gene family are expressed in different regions of the mammalian central nervous system. *Cell*, **48,** 965-73.

GOLDSTEIN, A. & BARRETT, R.W. (1987). Ligand dissociation constants from competition binding assays: errors associated with ligand depletion. *Mol Pharmacol*, **31,** 603-9.

GOPALAKRISHNAN, M., BUISSON, B., TOUMA, E., GIORDANO, T., CAMPBELL, J.E., HU, I.C., DONNELLY-ROBERTS, D., ARNERIC, S.P., BERTRAND, D. & SULLIVAN, J.P. (1995). Stable expression and pharmacological properties of the human alpha 7 nicotinic acetylcholine receptor. *Eur J Pharmacol*, **290,** 237-46.

GOPALAKRISHNAN, M., MONTEGGIA, L.M., ANDERSON, D.J., MOLINARI, E.J., PIATTONI-KAPLAN, M., DONNELLY-ROBERTS, D., ARNERIC, S.P. & SULLIVAN, J.P. (1996). Stable expression, pharmacologic properties and regulation of the human neuronal nicotinic acetylcholine alpha 4 beta 2 receptor. *J Pharmacol Exp Ther*, **276,** 289-97.

GORDON, M.N., HOLCOMB, L.A., JANTZEN, P.T., DICARLO, G., WILCOCK, D., BOYETT, K.W., CONNOR, K., MELACHRINO, J., O'CALLAGHAN, J.P. & MORGAN, D. (2002). Time course of the development of Alzheimer-like pathology in the doubly transgenic PS1+APP mouse. *Exp Neurol*, **173,** 183-95.

GORDON, M.N., KING, D.L., DIAMOND, D.M., JANTZEN, P.T., BOYETT, K.V., HOPE, C.E., HATCHER, J.M., DICARLO, G., GOTTSCHALL, W.P., MORGAN, D. & ARENDASH, G.W. (2001). Correlation between cognitive deficits and Abeta deposits in transgenic APP+PS1 mice. *Neurobiol Aging*, **22,** 377-85.

GOTTI, C., BRISCINI, L., VERDERIO, C., OORTGIESEN, M., BALESTRA, B. & CLEMENTI, F. (1995). Native nicotinic acetylcholine receptors in human IMR32 neuroblastoma cells: functional, immunological and pharmacological properties. *Eur J Neurosci*, **7,** 2083-92.

GOTTI, C., HANKE, W., MAURY, K., MORETTI, M., BALLIVET, M., CLEMENTI, F. & BERTRAND, D. (1994). Pharmacology and biophysical properties of alpha 7 and alpha 7-alpha 8 alpha-bungarotoxin receptor subtypes immunopurified from the chick optic lobe. *Eur J Neurosci*, **6,** 1281-91.

GOTZ, J., STREFFER, J.R., DAVID, D., SCHILD, A., HOERNDLI, F., PENNANEN, L., KUROSINSKI, P. & CHEN, F. (2004). Transgenic animal models of Alzheimer's disease and related disorders: histopathology, behavior and therapy. *Mol Psychiatry*, **9,** 664-83.

GOWING, E., ROHER, A.E., WOODS, A.S., COTTER, R.J., CHANEY, M., LITTLE, S.P. & BALL, M.J. (1994). Chemical characterization of A beta 17-42 peptide, a component of diffuse amyloid deposits of Alzheimer disease. *J Biol Chem*, **269,** 10987-90.

GRASSI, F., PALMA, E., TONINI, R., AMICI, M., BALLIVET, M. & EUSEBI, F. (2003). Amyloid beta(1-42) peptide alters the gating of human and mouse alpha-bungarotoxin-sensitive nicotinic receptors. *J Physiol*, **547,** 147-57.

GROOT-KORMELINK, P.J., BOORMAN, J.P. & SIVILOTTI, L.G. (2001). Formation of functional alpha3beta4alpha5 human neuronal nicotinic receptors in Xenopus oocytes: a reporter mutation approach. *Br J Pharmacol*, **134,** 789-96.

GROOT-KORMELINK, P.J., LUYTEN, W.H., COLQUHOUN, D. & SIVILOTTI, L.G. (1998). A reporter mutation approach shows incorporation of the "orphan" subunit beta3 into a functional nicotinic receptor. *J Biol Chem*, **273,** 15317-20.

GRYNKIEWICZ, G., POENIE, M. & TSIEN, R.Y. (1985). A new generation of Ca2+ indicators with greatly improved fluorescence properties. *J Biol Chem*, **260,** 3440-50.

GUAN, Z.Z., MIAO, H., TIAN, J.Y., UNGER, C., NORDBERG, A. & ZHANG, X. (2001). Suppressed expression of nicotinic acetylcholine receptors by nanomolar beta-amyloid peptides in PC12 cells. *J Neural Transm*, **108,** 1417-33.

GUAN, Z.Z., ZHANG, X., BLENNOW, K. & NORDBERG, A. (1999). Decreased protein level of nicotinc receptor alpha7 subunit in the frontal cortex from schizophrenic brain. *Neuroreport*, **10,** 1779-82.

GUAN, Z.Z., ZHANG, X., RAVID, R. & NORDBERG, A. (2000). Decreased protein levels of nicotinic receptor subunits in the hippocampus and temporal cortex of patients with Alzheimer's disease. *J Neurochem*, **74,** 237-43.

GUO, J.Z., TREDWAY, T.L. & CHIAPPINELLI, V.A. (1998). Glutamate and GABA release are enhanced by different subtypes of presynaptic nicotinic receptors in the lateral geniculate nucleus. *J Neurosci*, **18,** 1963-9.

GUO, J.Z., Y., L., SORENSON, E.M. & CHIAPPINELLI, V.A. (2005). Synaptically released and exogenous ACh activates different nicotinic receptors to enhance exoked glutamatergic transmission in the lateral geniculate nucleus. *J Neurophysiol*, **94,** 2549-60.

GUREVICIENE, I., IKONEN, S., GUREVICIUS, K., SARKAKI, A., VAN GROEN, T., PUSSINEN, R., YLINEN, A. & TANILA, H. (2004). Normal induction but accelerated decay of LTP in APP + PS1 transgenic mice. *Neurobiol Dis*, **15,** 188-95.

HAASS, C., HUNG, A.Y., SCHLOSSMACHER, M.G., TEPLOW, D.B. & SELKOE, D.J. (1993). beta-Amyloid peptide and a 3-kDa fragment are derived by distinct cellular mechanisms. *J Biol Chem*, **268,** 3021-4.

HAASS, C., KOO, E.H., MELLON, A., HUNG, A.Y. & SELKOE, D.J. (1992a). Targeting of cell-surface beta-amyloid precursor protein to lysosomes: alternative processing into amyloid-bearing fragments. *Nature*, **357,** 500-3.

HAASS, C., SCHLOSSMACHER, M.G., HUNG, A.Y., VIGO-PELFREY, C., MELLON, A., OSTASZEWSKI, B.L., LIEBERBURG, I., KOO, E.H., SCHENK, D., TEPLOW, D.B. & ET AL. (1992b). Amyloid beta-peptide is produced by cultured cells during normal metabolism. *Nature*, **359,** 322-5.

HAJOS, M., HURST, R.S., HOFFMANN, W.E., KRAUSE, M., WALL, T.M., HIGDON, N.R. & GROPPI, V.E. (2005). The selective alpha7 nicotinic acetylcholine receptor agonist PNU-282987 [N-[(3R)-1-Azabicyclo[2.2.2]oct-3-yl]-4-chlorobenzamide hydrochloride] enhances GABAergic synaptic activity in brain slices and restores auditory gating deficits in anesthetized rats. *J Pharmacol Exp Ther*, **312,** 1213-22.

HALEVI, S., MCKAY, J., PALFREYMAN, M., YASSIN, L., ESHEL, M., JORGENSEN, E. & TREININ, M. (2002). The C. elegans ric-3 gene is required for maturation of nicotinic acetylcholine receptors. *Embo J*, **21,** 1012-20.

HALEVI, S., YASSIN, L., ESHEL, M., SALA, F., SALA, S., CRIADO, M. & TREININ, M. (2003). Conservation within the RIC-3 gene family. Effectors of mammalian nicotinic acetylcholine receptor expression. *J Biol Chem*, **278,** 34411-7.

HALL, M., ZERBE, L., LEONARD, S. & FREEDMAN, R. (1993). Characterization of [3H]cytisine binding to human brain membrane preparations. *Brain Res*, **600,** 127-33.

HANGER, D.P., BETTS, J.C., LOVINY, T.L., BLACKSTOCK, W.P. & ANDERTON, B.H. (1998). New phosphorylation sites identified in hyperphosphorylated tau (paired helical filament-tau) from Alzheimer's disease brain using nanoelectrospray mass spectrometry. *J Neurochem*, **71,** 2465-76.

HARDY, J. & SELKOE, D.J. (2002). The amyloid hypothesis of Alzheimer's disease: progress and problems on the road to therapeutics. *Science*, **297,** 353-6.

HARVEY, S.C. & LUETJE, C.W. (1996). Determinants of competitive antagonist sensitivity on neuronal nicotinic receptor beta subunits. *J Neurosci*, **16,** 3798-806.

HELLSTROM-LINDAHL, E., COURT, J., KEVERNE, J., SVEDBERG, M., LEE, M., MARUTLE, A., THOMAS, A., PERRY, E., BEDNAR, I. & NORDBERG, A. (2004). Nicotine reduces A beta in the brain and cerebral vessels of APPsw mice. *Eur J Neurosci*, **19,** 2703-10.

HERBER, D.L., SEVERANCE, E.G., CUEVAS, J., MORGAN, D. & GORDON, M.N. (2004). Biochemical and histochemical evidence of nonspecific binding of alpha7nAChR antibodies to mouse brain tissue. *J Histochem Cytochem*, **52,** 1367-76.

HERNANDEZ, D., SUGAYA, K., QU, T., MCGOWAN, E., DUFF, K. & MCKINNEY, M. (2001). Survival and plasticity of basal forebrain cholinergic systems in mice transgenic for presenilin-1 and amyloid precursor protein mutant genes. *Neuroreport*, **12,** 1377-84.

HERZIG, M.C., WINKLER, D.T., BURGERMEISTER, P., PFEIFER, M., KOHLER, E., SCHMIDT, S.D., DANNER, S., ABRAMOWSKI, D., STURCHLER-PIERRAT, C., BURKI, K., VAN DUINEN, S.G., MAAT-SCHIEMAN, M.L., STAUFENBIEL, M., MATHEWS, P.M. & JUCKER, M. (2004). Abeta is targeted to the vasculature in a mouse model of hereditary cerebral hemorrhage with amyloidosis. *Nat Neurosci*, **7,** 954-60.

HESS, G.P., UDGAONKAR, J.B. & OLBRICHT, W.L. (1987). Chemical kinetic measurements of transmembrane processes using rapid reaction techniques: acetylcholine receptor. *Annu Rev Biophys Biophys Chem*, **16,** 507-34.

HIBELL, A.D., KIDD, E.J., CHESSELL, I.P., HUMPHREY, P.P. & MICHEL, A.D. (2000). Apparent species differences in the kinetic properties of P2X(7) receptors. *Br J Pharmacol*, **130,** 167-73.

HIMMLER, A., DRECHSEL, D., KIRSCHNER, M.W. & MARTIN, D.W., JR. (1989). Tau consists of a set of proteins with repeated C-terminal microtubule-binding domains and variable N-terminal domains. *Mol Cell Biol*, **9,** 1381-8.

HIRST, C., YEE, I.M. & SADOVNICK, A.D. (1994). Genetic factors that protect against dementia. *Am J Hum Genet*, **55,** 588-9.

HODDER, P., MULL, R., CASSADAY, J., BERRY, K. & STRULOVICI, B. (2004). Miniaturization of intracellular calcium functional assays to 1536-well plate format using a fluorometric imaging plate reader. *J Biomol Screen*, **9,** 417-26.

HOLCOMB, L., GORDON, M.N., MCGOWAN, E., YU, X., BENKOVIC, S., JANTZEN, P., WRIGHT, K., SAAD, I., MUELLER, R., MORGAN, D., SANDERS, S., ZEHR, C., O'CAMPO, K., HARDY, J., PRADA, C.M., ECKMAN, C., YOUNKIN, S., HSIAO, K. & DUFF, K. (1998). Accelerated Alzheimer-type phenotype in transgenic mice carrying both mutant amyloid precursor protein and presenilin 1 transgenes. *Nat Med*, **4,** 97-100.

HORSBURGH, K., MCCARRON, M.O., WHITE, F. & NICOLL, J.A. (2000). The role of apolipoprotein E in Alzheimer's disease, acute brain injury and cerebrovascular disease: evidence of common mechanisms and utility of animal models. *Neurobiol Aging*, **21,** 245-55.

HOUGHTLING, R.A., DAVILA-GARCIA, M.I. & KELLAR, K.J. (1995). Characterization of (+/-)(-)[3H]epibatidine binding to nicotinic cholinergic receptors in rat and human brain. *Mol Pharmacol*, **48,** 280-7.

HSIA, A.Y., MASLIAH, E., MCCONLOGUE, L., YU, G.Q., TATSUNO, G., HU, K., KHOLODENKO, D., MALENKA, R.C., NICOLL, R.A. & MUCKE, L. (1999). Plaque-independent disruption of neural circuits in Alzheimer's disease mouse models. *Proc Natl Acad Sci U S A*, **96,** 3228-33.

HSIAO, K. (1998). Transgenic mice expressing Alzheimer amyloid precursor proteins. *Exp Gerontol*, **33,** 883-9.

HSIAO, K., CHAPMAN, P., NILSEN, S., ECKMAN, C., HARIGAYA, Y., YOUNKIN, S., YANG, F. & COLE, G. (1996). Correlative memory deficits, Abeta elevation, and amyloid plaques in transgenic mice. *Science*, **274,** 99-102.

HSU, Y.N., AMIN, J., WEISS, D.S. & WECKER, L. (1996). Sustained nicotine exposure differentially affects alpha 3 beta 2 and alpha 4 beta 2 neuronal nicotinic receptors expressed in Xenopus oocytes. *J Neurochem*, **66,** 667-75.

HU, L., WONG, T.P., COTE, S.L., BELL, K.F. & CUELLO, A.C. (2003). The impact of Abeta-plaques on cortical cholinergic and non-cholinergic presynaptic boutons in alzheimer's disease-like transgenic mice. *Neuroscience*, **121,** 421-32.

HUGANIR, R.L. & GREENGARD, P. (1990). Regulation of neurotransmitter receptor desensitization by protein phosphorylation. *Neuron*, **5,** 555-67.

HUGUENARD, J.R. & PRINCE, D.A. (1994). Clonazepam suppresses GABAB-mediated inhibition in thalamic relay neurons through effects in nucleus reticularis. *J Neurophysiol*, **71,** 2576-81.

HUSSAIN, I., POWELL, D., HOWLETT, D.R., TEW, D.G., MEEK, T.D., CHAPMAN, C., GLOGER, I.S., MURPHY, K.E., SOUTHAN, C.D., RYAN, D.M., SMITH, T.S., SIMMONS, D.L., WALSH, F.S., DINGWALL, C. & CHRISTIE, G. (1999). Identification of a novel aspartic protease (Asp 2) as beta-secretase. *Mol Cell Neurosci*, **14,** 419-27.

IDA, N., HARTMANN, T., PANTEL, J., SCHRODER, J., ZERFASS, R., FORSTL, H., SANDBRINK, R., MASTERS, C.L. & BEYREUTHER, K. (1996). Analysis of heterogeneous betaA4 peptides in human cerebrospinal fluid and blood by a newly developed sensitive western blot assay. *Journal of Biological Chemistry*, **271,** 22908-22914.

INCE, E., CILIAX, B.J. & LEVEY, A.I. (1997). Differential expression of D1 and D2 dopamine and m4 muscarinic acetylcholine receptor proteins in identified striatonigral neurons. *Synapse*, **27,** 357-66.

INOUE, M. & KURIYAMA, H. (1991). Somatostatin inhibits the nicotinic receptor-activated inward current in guinea pig chromaffin cells. *Biochem Biophys Res Commun*, **174,** 750-7.

IQBAL, K., ALONSO ADEL, C., CHEN, S., CHOHAN, M.O., EL-AKKAD, E., GONG, C.X., KHATOON, S., LI, B., LIU, F., RAHMAN, A., TANIMUKAI, H. & GRUNDKE-IQBAL, I. (2005). Tau pathology in Alzheimer disease and other tauopathies. *Biochim Biophys Acta*, **1739,** 198-210.

IQBAL, K., GRUNDKE-IQBAL, I., ZAIDI, T., MERZ, P.A., WEN, G.Y., SHAIKH, S.S., WISNIEWSKI, H.M., ALAFUZOFF, I. & WINBLAD, B. (1986). Defective brain microtubule assembly in Alzheimer's disease. *Lancet*, **2,** 421-6.

IQBAL, K., ZAIDI, T., BANCHER, C. & GRUNDKE-IQBAL, I. (1994). Alzheimer paired helical filaments. Restoration of the biological activity by dephosphorylation. *FEBS Lett*, **349,** 104-8.

IRIZARRY, M.C., MCNAMARA, M., FEDORCHAK, K., HSIAO, K. & HYMAN, B.T. (1997a). APPSw transgenic mice develop age-related A beta deposits and neuropil abnormalities, but no neuronal loss in CA1. *J Neuropathol Exp Neurol*, **56,** 965-73.

IRIZARRY, M.C., SORIANO, F., MCNAMARA, M., PAGE, K.J., SCHENK, D., GAMES, D. & HYMAN, B.T. (1997b). Abeta deposition is associated with neuropil changes, but not with overt neuronal loss in the human amyloid precursor protein V717F (PDAPP) transgenic mouse. *J Neurosci*, **17,** 7053-9.

ITOH, A., NITTA, A., NADAI, M., NISHIMURA, K., HIROSE, M., HASEGAWA, T. & NABESHIMA, T. (1996). Dysfunction of cholinergic and dopaminergic neuronal systems in beta-amyloid protein--infused rats. *J Neurochem*, **66,** 1113-7.

JOHNSON-WOOD, K., LEE, M., MOTTER, R., HU, K., GORDON, G., BARBOUR, R., KHAN, K., GORDON, M., TAN, H., GAMES, D., LIEBERBURG, I., SCHENK, D., SEUBERT, P. & MCCONLOGUE, L. (1997). Amyloid precursor protein processing and A beta42 deposition in a transgenic mouse model of Alzheimer disease. *Proc Natl Acad Sci U S A*, **94,** 1550-5.

KANG, J., LEMAIRE, H.G., UNTERBECK, A., SALBAUM, J.M., MASTERS, C.L., GRZESCHIK, K.H., MULTHAUP, G., BEYREUTHER, K. & MULLER-HILL, B. (1987). The precursor of Alzheimer's disease amyloid A4 protein resembles a cell-surface receptor. *Nature*, **325,** 733-6.

KAPUR, J., HAAS, K.F. & MACDONALD, R.L. (1999). Physiological properties of GABAA receptors from acutely dissociated rat dentate granule cells. *J Neurophysiol*, **81,** 2464-71.

KATZ, B. & MILEDI, R. (1977). The reversal potential at the desensitized endplate. *Proc R Soc Lond B Biol Sci*, **199,** 329-34.

KATZMAN, R. (1986). Alzheimer's disease. *N Engl J Med*, **314,** 964-73.

KAWAI, H., ZAGO, W. & BERG, D.K. (2002). Nicotinic alpha 7 receptor clusters on hippocampal GABAergic neurons: regulation by synaptic activity and neurotrophins. *J Neurosci*, **22,** 7903-12.

KEEN, M. (1995). The problems and pitfalls of radioligand binding. In *Methods in Molecular Biology: Signal Transduction Protocols*. ed Kendall, D.A.H.T., S.J. N.J.: Humana Press Inc.

KELESHIAN, A.M., EDESON, R.O., LIU, G.J. & MADSEN, B.W. (2000). Evidence for cooperativity between nicotinic acetylcholine receptors in patch clamp records. *Biophys J*, **78,** 1-12.

KELLER, J.J., KELLER, A.B., BOWERS, B.J. & WEHNER, J.M. (2005). Performance of alpha7 nicotinic receptor null mutants is impaired in appetitive learning measured in a signaled nose poke task. *Behav Brain Res*, **162,** 143-52.

KELLY, C.A., HARVEY, R.J. & CAYTON, H. (1997). Drug treatments for Alzheimer's disease. *Bmj*, **314,** 693-4.

KEM, W.R. (2000). The brain alpha7 nicotinic receptor may be an important therapeutic target for the treatment of Alzheimer's disease: studies with DMXBA (GTS-21). *Behav Brain Res*, **113,** 169-81.

KHIROUG, S.S., HARKNESS, P.C., LAMB, P.W., SUDWEEKS, S.N., KHIROUG, L., MILLAR, N.S. & YAKEL, J.L. (2002). Rat nicotinic ACh receptor alpha7 and beta2 subunits co-assemble to form functional heteromeric nicotinic receptor channels. *J Physiol*, **540,** 425-34.

KIHARA, T., SAWADA, H., NAKAMIZO, T., KANKI, R., YAMASHITA, H., MAELICKE, A. & SHIMOHAMA, S. (2004b). Galantamine modulates nicotinic receptor and blocks Abeta-enhanced glutamate toxicity. *Biochem Biophys Res Commun*, **325,** 976-82.

KIHARA, T. & SHIMOHAMA, S. (2004a). Alzheimer's disease and acetylcholine receptors. *Acta Neurobiol Exp (Wars)*, **64,** 99-105.

KIHARA, T., SHIMOHAMA, S., SAWADA, H., HONDA, K., NAKAMIZO, T., SHIBASAKI, H., KUME, T. & AKAIKE, A. (2001). alpha 7 nicotinic receptor transduces signals to phosphatidylinositol 3-kinase to block A beta-amyloid-induced neurotoxicity. *J Biol Chem*, **276,** 13541-6.

KIHARA, T., SHIMOHAMA, S., SAWADA, H., KIMURA, J., KUME, T., KOCHIYAMA, H., MAEDA, T. & AKAIKE, A. (1997). Nicotinic receptor stimulation protects neurons against beta-amyloid toxicity. *Ann Neurol*, **42,** 159-63.

KIHARA, T., SHIMOHAMA, S., URUSHITANI, M., SAWADA, H., KIMURA, J., KUME, T., MAEDA, T. & AKAIKE, A. (1998). Stimulation of alpha4beta2 nicotinic acetylcholine receptors inhibits beta-amyloid toxicity. *Brain Res*, **792,** 331-4.

KLINGNER, M., APELT, J., KUMAR, A., SORGER, D., SABRI, O., STEINBACH, J., SCHEUNEMANN, M. & SCHLIEBS, R. (2003). Alterations in cholinergic and non-cholinergic neurotransmitter receptor densities in transgenic Tg2576 mouse brain with beta-amyloid plaque pathology. *Int J Dev Neurosci*, **21,** 357-69.

KOIKE, H., TOMIOKA, S., SORIMACHI, H., SAIDO, T.C., MARUYAMA, K., OKUYAMA, A., FUJISAWA-SEHARA, A., OHNO, S., SUZUKI, K. & ISHIURA, S. (1999). Membrane-anchored metalloprotease MDC9 has an alpha-secretase activity responsible for processing the amyloid precursor protein. *Biochem J*, **343 Pt 2,** 371-5.

KOPKE, E., TUNG, Y.C., SHAIKH, S., ALONSO, A.C., IQBAL, K. & GRUNDKE-IQBAL, I. (1993). Microtubule-associated protein tau. Abnormal phosphorylation of a non-paired helical filament pool in Alzheimer disease. *J Biol Chem*, **268,** 24374-84.

KUBO, T., FUKUDA, K., MIKAMI, A., MAEDA, A., TAKAHASHI, H., MISHINA, M., HAGA, T., HAGA, K., ICHIYAMA, A., KANGAWA, K. & ET AL. (1986). Cloning, sequencing and expression of complementary DNA encoding the muscarinic acetylcholine receptor. *Nature*, **323,** 411-6.

KUENTZEL, S.L., ALI, S.M., ALTMAN, R.A., GREENBERG, B.D. & RAUB, T.J. (1993). The Alzheimer beta-amyloid protein precursor/protease nexin-II is cleaved by secretase in a trans-Golgi secretory compartment in human neuroglioma cells. *Biochem J*, **295 (Pt 2),** 367-78.

LAEMMLI, U.K. (1970). Cleavage of structural proteins dueing the assembly of the head of bacteriophage T4. *Nature*, **227,** 680-5.

LAMB, B.T., BARDEL, K.A., KULNANE, L.S., ANDERSON, J.J., HOLTZ, G., WAGNER, S.L., SISODIA, S.S. & HOEGER, E.J. (1999). Amyloid production and deposition in mutant amyloid precursor protein and presenilin-1 yeast artificial chromosome transgenic mice. *Nat Neurosci*, **2,** 695-7.

LAMB, P.W., MELTON, M.A. & YAKEL, J.L. (2005). Inhibition of neuronal nicotinic acetylcholine receptor channels expressed in Xenopus oocytes by beta-amyloid1-42 peptide. *J Mol Neurosci*, **27,** 13-22.

LAMMICH, S., KOJRO, E., POSTINA, R., GILBERT, S., PFEIFFER, R., JASIONOWSKI, M., HAASS, C. & FAHRENHOLZ, F. (1999). Constitutive and regulated alpha-secretase cleavage of Alzheimer's amyloid precursor protein by a disintegrin metalloprotease. *Proc Natl Acad Sci U S A*, **96,** 3922-7.

LANSDELL, S.J., GEE, V.J., HARKNESS, P.C., DOWARD, A.I., BAKER, E.R., GIBB, A.J. & MILLAR, N.S. (2005). RIC-3 enhances functional expression of multiple nicotinic acetylcholine receptor subtypes in mammalian cells. *Mol Pharmacol*.

LE NOVERE, N. & CHANGEUX, J.P. (1995). Molecular evolution of the nicotinic acetylcholine receptor: an example of multigene family in excitable cells. *J Mol Evol*, **40,** 155-72.

LEE, R.K., WURTMAN, R.J., COX, A.J. & NITSCH, R.M. (1995). Amyloid precursor protein processing is stimulated by metabotropic glutamate receptors. *Proc Natl Acad Sci U S A*, **92,** 8083-7.

LEMERE, C.A., BLUSZTAJN, J.K., YAMAGUCHI, H., WISNIEWSKI, T., SAIDO, T.C. & SELKOE, D.J. (1996). Sequence of deposition of heterogeneous amyloid beta-peptides and APO E in Down syndrome: implications for initial events in amyloid plaque formation. *Neurobiol Dis*, **3,** 16-32.

LENA, C. & CHANGEUX, J.P. (1993). Allosteric modulations of the nicotinic acetylcholine receptor. *Trends Neurosci*, **16,** 181-6.

LENDON, C.L., ASHALL, F. & GOATE, A.M. (1997). Exploring the etiology of Alzheimer disease using molecular genetics. *Jama*, **277,** 825-31.

LEONARD, R.J., LABARCA, C.G., CHARNET, P., DAVIDSON, N. & LESTER, H.A. (1988). Evidence that the M2 membrane-spanning region lines the ion channel pore of the nicotinic receptor. *Science*, **242,** 1578-81.

LESTER, H.A., FONCK, C., TAPPER, A.R., MCKINNEY, S., DAMAJ, M.I., BALOGH, S., OWENS, J., WEHNER, J.M., COLLINS, A.C. & LABARCA, C. (2003). Hypersensitive knockin mouse strains identify receptors and pathways for nicotine action. *Curr Opin Drug Discov Devel*, **6,** 633-9.

LEUNG, G.M., YEUNG, R.Y., CHI, I. & CHU, L.W. (2003). The economics of Alzheimer disease. *Dement Geriatr Cogn Disord*, **15,** 34-43.

LEVEY, A.I. (1993). Immunological localization of m1-m5 muscarinic acetylcholine receptors in peripheral tissues and brain. *Life Sci*, **52,** 441-8.

LEVEY, A.I., KITT, C.A., SIMONDS, W.F., PRICE, D.L. & BRANN, M.R. (1991). Identification and localization of muscarinic acetylcholine receptor proteins in brain with subtype-specific antibodies. *J Neurosci*, **11,** 3218-26.

LEVIN, E.D., BETTEGOWDA, C., BLOSSER, J. & GORDON, J. (1999). AR-R17779, an alpha7 nicotinic agonist, improves learning and memory in rats. *Behav Pharmacol*, **10,** 675-80.

LEVIN, E.D., BRADLEY, A., ADDY, N. & SIGURANI, N. (2002). Hippocampal alpha 7 and alpha 4 beta 2 nicotinic receptors and working memory. *Neuroscience*, **109,** 757-65.

LEVIN, E.D. & SIMON, B.B. (1998). Nicotinic acetylcholine involvement in cognitive function in animals. *Psychopharmacology (Berl)*, **138,** 217-30.

LEVINE, H., 3RD (1993). Thioflavine T interaction with synthetic Alzheimer's disease beta-amyloid peptides: detection of amyloid aggregation in solution. *Protein Sci*, **2,** 404-10.

LEVY, E., CARMAN, M.D., FERNANDEZ-MADRID, I.J., POWER, M.D., LIEBERBURG, I., VAN DUINEN, S.G., BOTS, G.T., LUYENDIJK, W. & FRANGIONE, B. (1990). Mutation of the Alzheimer's disease amyloid gene in hereditary cerebral hemorrhage, Dutch type. *Science*, **248,** 1124-6.

LEVY-LAHAD, E., LAHAD, A., WIJSMAN, E.M., BIRD, T.D. & SCHELLENBERG, G.D. (1995a). Apolipoprotein E genotypes and age of onset in early-onset familial Alzheimer's disease. *Ann Neurol*, **38,** 678-80.

LEVY-LAHAD, E., WASCO, W., POORKAJ, P., ROMANO, D.M., OSHIMA, J., PETTINGELL, W.H., YU, C.E., JONDRO, P.D., SCHMIDT, S.D., WANG, K. & ET AL. (1995b). Candidate gene for the chromosome 1 familial Alzheimer's disease locus. *Science*, **269,** 973-7.

LEVY-LAHAD, E., WIJSMAN, E.M., NEMENS, E., ANDERSON, L., GODDARD, K.A., WEBER, J.L., BIRD, T.D. & SCHELLENBERG, G.D. (1995c). A familial Alzheimer's disease locus on chromosome 1. *Science*, **269,** 970-3.

LEWIS, J., DICKSON, D.W., LIN, W.L., CHISHOLM, L., CORRAL, A., JONES, G., YEN, S.H., SAHARA, N., SKIPPER, L., YAGER, D., ECKMAN, C., HARDY, J., HUTTON, M. & MCGOWAN, E. (2001). Enhanced neurofibrillary degeneration in transgenic mice expressing mutant tau and APP. *Science*, **293,** 1487-91.

LIN, K., SADEE, W. & QUILLAN, J.M. (1999). Rapid measurements of intracellular calcium using a fluorescence plate reader. *Biotechniques*, **26,** 318-22, 324-6.

LIN, X., KOELSCH, G., WU, S., DOWNS, D., DASHTI, A. & TANG, J. (2000). Human aspartic protease memapsin 2 cleaves the beta-secretase site of beta-amyloid precursor protein. *Proc Natl Acad Sci U S A*, **97,** 1456-60.

LIND, R.J., HARDICK, D.J., BLAGBROUGH, I.S., POTTER, B.V., WOLSTENHOLME, A.J., DAVIES, A.R., CLOUGH, M.S., EARLEY, F.G., REYNOLDS, S.E. & WONNACOTT, S. (2001). [3H]-Methyllycaconitine: a high affinity radioligand that labels invertebrate nicotinic acetylcholine receptors. *Insect Biochem Mol Biol*, **31,** 533-42.

LINDWALL, G. & COLE, R.D. (1984). Phosphorylation affects the ability of tau protein to promote microtubule assembly. *J Biol Chem*, **259,** 5301-5.

LING, Y., MORGAN, K. & KALSHEKER, N. (2003). Amyloid precursor protein (APP) and the biology of proteolytic processing: relevance to Alzheimer's disease. *Int J Biochem Cell Biol*, **35,** 1505-35.

LIU, Q., KAWAI, H. & BERG, D.K. (2001). beta -Amyloid peptide blocks the response of alpha 7-containing nicotinic receptors on hippocampal neurons. *Proc Natl Acad Sci U S A*, **98,** 4734-9.

LOPEZ, M.G., FONTERIZ, R.I., GANDIA, L., DE LA FUENTE, M., VILLARROYA, M., GARCIA-SANCHO, J. & GARCIA, A.G. (1993). The nicotinic acetylcholine receptor of the bovine chromaffin cell, a new target for dihydropyridines. *Eur J Pharmacol*, **247,** 199-207.

LOWE, S.L., BOWEN, D.M., FRANCIS, P.T. & NEARY, D. (1990). Ante mortem cerebral amino acid concentrations indicate selective degeneration of glutamate-enriched neurons in Alzheimer's disease. *Neuroscience*, **38,** 571-7.

LUE, L.F., KUO, Y.M., ROHER, A.E., BRACHOVA, L., SHEN, Y., SUE, L., BEACH, T., KURTH, J.H., RYDEL, R.E. & ROGERS, J. (1999). Soluble amyloid beta peptide concentration as a predictor of synaptic change in Alzheimer's disease. *Am J Pathol*, **155,** 853-62.

LUKAS, R.J. & CULLEN, M.J. (1988). An isotopic rubidium ion efflux assay for the functional characterization of nicotinic acetylcholine receptors on clonal cell lines. *Anal Biochem*, **175,** 212-8.

LUKAS, R.J., MORIMOTO, H., HANLEY, M.R. & BENNETT, E.L. (1981). Radiolabeled alpha-bungarotoxin derivatives: kinetic interaction with nicotinic acetylcholine receptors. *Biochemistry*, **20,** 7373-8.

LUO, Y., BOLON, B., KAHN, S., BENNETT, B.D., BABU-KHAN, S., DENIS, P., FAN, W., KHA, H., ZHANG, J., GONG, Y., MARTIN, L., LOUIS, J.C., YAN, Q., RICHARDS, W.G., CITRON, M. & VASSAR, R. (2001). Mice deficient in BACE1, the Alzheimer's beta-secretase, have normal phenotype and abolished beta-amyloid generation. *Nat Neurosci*, **4,** 231-2.

LUTH, H.J., APELT, J., IHUNWO, A.O., ARENDT, T. & SCHLIEBS, R. (2003). Degeneration of beta-amyloid-associated cholinergic structures in transgenic APP SW mice. *Brain Res*, **977,** 16-22.

MACALLAN, D.R., LUNT, G.G., WONNACOTT, S., SWANSON, K.L., RAPOPORT, H. & ALBUQUERQUE, E.X. (1988). Methyllycaconitine and (+)-anatoxin-a differentiate between nicotinic receptors in vertebrate and invertebrate nervous systems. *FEBS Lett*, **226,** 357-63.

MACDONALD, R.L. & TWYMAN, R.E. (1992). Kinetic properties and regulation of GABAA receptor channels. *Ion Channels*, **3,** 315-43.

MAELICKE, A., SCHRATTENHOLZ, A., SAMOCHOCKI, M., RADINA, M. & ALBUQUERQUE, E.X. (2000). Allosterically potentiating ligands of nicotinic receptors as a treatment strategy for Alzheimer's disease. *Behav Brain Res*, **113,** 199-206.

MAK, K., YANG, F., VINTERS, H.V., FRAUTSCHY, S.A. & COLE, G.M. (1994). Polyclonals to beta-amyloid(1-42) identify most plaque and vascular deposits in Alzheimer cortex, but not striatum. *Brain Res*, **667,** 138-42.

MANN, D.M., YATES, P.O., MARCYNIUK, B. & RAVINDRA, C.R. (1986). The topography of plaques and tangles in Down's syndrome patients of different ages. *Neuropathol Appl Neurobiol*, **12,** 447-57.

MANNING, T.J., JR. & SONTHEIMER, H. (1999). Recording of intracellular Ca2+, Cl-, pH and membrane potential in cultured astrocytes using a fluorescence plate reader. *J Neurosci Methods*, **91,** 73-81.

MARKS, M.J. & COLLINS, A.C. (1982). Characterization of nicotine binding in mouse brain and comparison with the binding of alpha-bungarotoxin and quinuclidinyl benzilate. *Mol Pharmacol*, **22,** 554-64.

MARKS, M.J., FARNHAM, D.A., GRADY, S.R. & COLLINS, A.C. (1993). Nicotinic receptor function determined by stimulation of rubidium efflux from mouse brain synaptosomes. *J Pharmacol Exp Ther*, **264,** 542-52.

MARKS, M.J., SMITH, K.W. & COLLINS, A.C. (1998). Differential agonist inhibition identifies multiple epibatidine binding sites in mouse brain. *J Pharmacol Exp Ther*, **285,** 377-86.

MARTIN, S.E., DE FIEBRE, N.E. & DE FIEBRE, C.M. (2004). The alpha7 nicotinic acetylcholine receptor-selective antagonist, methyllycaconitine, partially protects against beta-amyloid(1-42) toxicity in primary neuron-enriched cultures. *Brain Res*, **1022,** 254-6.

MARTIN-RUIZ, C.M., COURT, J.A., MOLNAR, E., LEE, M., GOTTI, C., MAMALAKI, A., TSOULOUFIS, T., TZARTOS, S., BALLARD, C., PERRY, R.H. & PERRY, E.K. (1999). Alpha4 but not alpha3 and alpha7 nicotinic acetylcholine receptor subunits are lost from the temporal cortex in Alzheimer's disease. *J Neurochem*, **73,** 1635-40.

MARUTLE, A., WARPMAN, U., BOGDANOVIC, N., LANNFELT, L. & NORDBERG, A. (1999). Neuronal nicotinic receptor deficits in Alzheimer patients with the Swedish amyloid precursor protein 670/671 mutation. *J Neurochem*, **72,** 1161-9.

MASTERS, C.L., SIMMS, G., WEINMAN, N.A., MULTHAUP, G., MCDONALD, B.L. & BEYREUTHER, K. (1985). Amyloid plaque core protein in Alzheimer disease and Down syndrome. *Proc Natl Acad Sci U S A*, **82,** 4245-9.

MATTSON, M.P. (1994). Calcium and neuronal injury in Alzheimer's disease. Contributions of beta-amyloid precursor protein mismetabolism, free radicals, and metabolic compromise. *Ann N Y Acad Sci*, **747,** 50-76.

MATTSON, M.P. (1997). Cellular actions of beta-amyloid precursor protein and its soluble and fibrillogenic derivatives. *Physiol Rev*, **77,** 1081-132.

MAYEUX, R., STERN, Y. & SPANTON, S. (1985). Heterogeneity in dementia of the Alzheimer type: evidence of subgroups. *Neurology*, **35,** 453-61.

MESULAM, M.M., MUFSON, E.J., LEVEY, A.I. & WAINER, B.H. (1983). Cholinergic innervation of cortex by the basal forebrain: cytochemistry and cortical connections of the septal area, diagonal band nuclei, nucleus basalis (substantia innominata), and hypothalamus in the rhesus monkey. *J Comp Neurol*, **214,** 170-97.

MESULAM, M.M. & VAN HOESEN, G.W. (1976). Acetylcholinesterase-rich projections from the basal forebrain of the rhesus monkey to neocortex. *Brain Res*, **109,** 152-7.

MESULAM, M.M., VOLICER, L., MARQUIS, J.K., MUFSON, E.J. & GREEN, R.C. (1986). Systematic regional differences in the cholinergic innervation of the primate cerebral cortex: distribution of enzyme activities and some behavioral implications. *Ann Neurol*, **19,** 144-51.

MILLS, J. & REINER, P.B. (1999). Regulation of amyloid precursor protein cleavage. *J Neurochem*, **72,** 443-60.

MINTA, A., KAO, J.P. & TSIEN, R.Y. (1989). Fluorescent indicators for cytosolic calcium based on rhodamine and fluorescein chromophores. *J Biol Chem*, **264,** 8171-8.

MINTER, L.M., TURLEY, D.M., DAS, P., SHIN, H.M., JOSHI, I., LAWLOR, R.G., CHO, O.H., PALAGA, T., GOTTIPATI, S., TELFER, J.C., KOSTURA, L., FAUQ, A.H., SIMPSON, K., SUCH, K.A., MIELE, L., GOLDE, T.E., MILLER, S.D. & OSBORNE, B.A. (2005). Inhibitors of gamma-secretase block in vivo and in vitro T helper type 1 polarisation by preventing Notch upregulation of Tbx21. *Nat Immunol*, **6,** 680-8.

MOECHARS, D., DEWACHTER, I., LORENT, K., REVERSE, D., BAEKELANDT, V., NAIDU, A., TESSEUR, I., SPITTAELS, K., HAUTE, C.V., CHECLER, F., GODAUX, E., CORDELL, B. & VAN LEUVEN, F. (1999). Early phenotypic changes in transgenic mice that overexpress different mutants of amyloid precursor protein in brain. *J Biol Chem*, **274,** 6483-92.

MOLINARI, E.J., DELBONO, O., MESSI, M.L., RENGANATHAN, M., ARNERIC, S.P., SULLIVAN, J.P. & GOPALAKRISHNAN, M. (1998). Up-regulation of human alpha7 nicotinic receptors by chronic treatment with activator and antagonist ligands. *Eur J Pharmacol*, **347,** 131-9.

MONTEGGIA, L.M., GOPALAKRISHNAN, M., TOUMA, E., IDLER, K.B., NASH, N., ARNERIC, S.P., SULLIVAN, J.P. & GIORDANO, T. (1995). Cloning and transient expression of genes encoding the human alpha 4 and beta 2 neuronal nicotinic acetylcholine receptor (nAChR) subunits. *Gene*, **155,** 189-93.

MOORE, S., DAVIES, Y. & GIBSON, G. (2000). Do inhibitors of beta-amyloid aggregation also inhibit the aggregation of other amyloid-forming peptides? *Neurobiol Aging*, **21,** S54.

MORLEY, B.J. & RODRIGUEZ-SIERRA, J.F. (2004). A phenotype for the alpha 7 nicotinic acetylcholine receptor null mutant. *Brain Res*, **1023,** 41-7.

MORRIS, J.C. & RUBIN, E.H. (1991). Clinical diagnosis and course of Alzheimer's disease. *Psychiatr Clin North Am*, **14,** 223-36.

MUGNAINI, M., TESSARI, M., TARTER, G., MERLO PICH, E., CHIAMULERA, C. & BUNNEMANN, B. (2002). Upregulation of [3H]methyllycaconitine binding sites following continuous infusion of nicotine, without changes of alpha7 or alpha6 subunit mRNA: an autoradiography and in situ hybridization study in rat brain. *Eur J Neurosci*, **16,** 1633-46.

MULLAN, M., CRAWFORD, F., AXELMAN, K., HOULDEN, H., LILIUS, L., WINBLAD, B. & LANNFELT, L. (1992). A pathogenic mutation for probable Alzheimer's disease in the APP gene at the N-terminus of beta-amyloid. *Nat Genet*, **1,** 345-7.

MULLE, C., LENA, C. & CHANGEUX, J.P. (1992). Potentiation of nicotinic receptor response by external calcium in rat central neurons. *Neuron*, **8,** 937-45.

MULLEN, G., NAPIER, J., BALESTRA, M., DECORY, T., HALE, G., MACOR, J., MACK, R., LOCH, J., 3RD, WU, E., KOVER, A., VERHOEST, P., SAMPOGNARO, A., PHILLIPS, E., ZHU, Y., MURRAY, R., GRIFFITH, R., BLOSSER, J., GURLEY, D., MACHULSKIS, A. & ZONARONE, J. (2000). (-)Spiro[1-azabicyclo[2.2.2]octane-3,5'-oxazolidin-2'-one], a conformationally restricted analogue of acetylcholine, is a highly selective full agonist at the alpha 7 nicotinic acetylcholine receptor. *J Med Chem*, **43,** 4045-50.

NAGELE, R.G., D'ANDREA, M.R., ANDERSON, W.J. & WANG, H.Y. (2002). Intracellular accumulation of beta-amyloid(1-42) in neurons is facilitated by the alpha 7 nicotinic acetylcholine receptor in Alzheimer's disease. *Neuroscience*, **110,** 199-211.

NASLUND, J., HAROUTUNIAN, V., MOHS, R., DAVIS, K.L., DAVIES, P., GREENGARD, P. & BUXBAUM, J.D. (2000). Correlation between elevated levels of amyloid beta-peptide in the brain and cognitive decline. *Jama*, **283,** 1571-7.

NAVARRO, H.A., XU, H., ZHONG, D., ABRAHAM, P. & CARROLL, F.I. (2002). In vitro and in vivo characterization of [125I]iodomethyllycaconitine in the rat. *Synapse*, **44,** 117-23.

NEF, P., ONEYSER, C., ALLIOD, C., COUTURIER, S. & BALLIVET, M. (1988). Genes expressed in the brain define three distinct neuronal nicotinic acetylcholine receptors. *Embo J*, **7,** 595-601.

NELSON, M.E., KURYATOV, A., CHOI, C.H., ZHOU, Y. & LINDSTROM, J. (2003). Alternate stoichiometries of alpha4beta2 nicotinic acetylcholine receptors. *Mol Pharmacol*, **63,** 332-41.

NICKE, A., THURAU, H., SADTLER, S., RETTINGER, J. & SCHMALZING, G. (2004). Assembly of nicotinic a7 subunits in *Xenopus* oocytes is partially blocked at the tetramer level. *FEBS Lett*, **575,** 52-58.

NITSCH, R.M., SLACK, B.E., WURTMAN, R.J. & GROWDON, J.H. (1992). Release of Alzheimer amyloid precursor derivatives stimulated by activation of muscarinic acetylcholine receptors. *Science*, **258,** 304-7.

NORDBERG, A., ADEM, A., HARDY, J. & WINBLAD, B. (1988). Change in nicotinic receptor subtypes in temporal cortex of Alzheimer brains. *Neurosci Lett*, **86,** 317-21.

NORDBERG, A., HARTVIG, P., LILJA, A., VIITANEN, M., AMBERLA, K., LUNDQVIST, H., ANDERSSON, Y., ULIN, J., WINBLAD, B. & LANGSTROM, B. (1990). Decreased uptake and binding of 11C-nicotine in brain of Alzheimer patients as visualized by positron emission tomography. *J Neural Transm Park Dis Dement Sect*, **2,** 215-24.

NORDBERG, A., HELLSTROM-LINDAHL, E., LEE, M., JOHNSON, M., MOUSAVI, M., HALL, R., PERRY, E., BEDNAR, I. & COURT, J. (2002). Chronic nicotine treatment reduces beta-amyloidosis in the brain of a mouse model of Alzheimer's disease (APPsw). *J Neurochem*, **81,** 655-8.

NORDBERG, A., LUNDQVIST, H., HARTVIG, P., ANDERSSON, J., JOHANSSON, M., HELLSTROM-LINDAHI, E. & LANGSTROM, B. (1997). Imaging of nicotinic and muscarinic receptors in Alzheimer's disease: effect of tacrine treatment. *Dement Geriatr Cogn Disord*, **8,** 78-84.

NORDBERG, A., LUNDQVIST, H., HARTVIG, P., LILJA, A. & LANGSTROM, B. (1995). Kinetic analysis of regional (S)(-)11C-nicotine binding in normal and Alzheimer brains--in vivo assessment using positron emission tomography. *Alzheimer Dis Assoc Disord*, **9,** 21-7.

NORDBERG, A. & WINBLAD, B. (1986). Reduced number of [3H]nicotine and [3H]acetylcholine binding sites in the frontal cortex of Alzheimer brains. *Neurosci Lett*, **72,** 115-9.

NUUTINEN, S., AHTEE, L. & TUOMINEN, R.K. (2005). Time and brain region specific up-regulation of low affinity neuronal nicotinic receptors during chronic nicotine administration in mice. *Eur J Pharmacol*, **515,** 83-9.

ODDO, S., BILLINGS, L., KESSLAK, J.P., CRIBBS, D.H. & LAFERLA, F.M. (2004). Abeta immunotherapy leads to clearance of early, but not late, hyperphosphorylated tau aggregates via the proteasome. *Neuron*, **43,** 321-32.

ODDO, S., CACCAMO, A., GREEN, K.N., LIANG, K., TRAN, L., CHEN, Y., LESLIE, F.M. & LAFERLA, F.M. (2005). Chronic nicotine administration exacerbates tau pathology in a transgenic model of Alzheimer's disease. *PNAS*, **102,** 3046-51.

ODDO, S., CACCAMO, A., KITAZAWA, M., TSENG, B.P. & LAFERLA, F.M. (2003). Amyloid deposition precedes tangle formation in a triple transgenic model of Alzheimer's disease. *Neurobiol Aging*, **24,** 1063-70.

OLALE, F., GERZANICH, V., KURYATOV, A., WANG, F. & LINDSTROM, J. (1997). Chronic nicotine exposure differentially affects the function of human alpha3, alpha4, and alpha7 neuronal nicotinic receptor subtypes. *J Pharmacol Exp Ther*, **283,** 675-83.

OLSON, M.I. & SHAW, C.M. (1969). Presenile dementia and Alzheimer's disease in mongolism. *Brain*, **92,** 147-56.

O'NEILL, M.J., MURRAY, T.K., LAKICS, V., VISANJI, N.P. & DUTY, S. (2002). The role of neuronal nicotinic acetylcholine receptors in acute and chronic neurodegeneration. *Curr Drug Targets CNS Neurol Disord*, **1,** 399-411.

ONO, K., HASEGAWA, K., YAMADA, M. & NAIKI, H. (2002). Nicotine breaks down preformed Alzheimer's beta-amyloid fibrils in vitro. *Biol Psychiatry*, **52,** 880-6.

ORB, S., WIEACKER, J., LABARCA, C., FONCK, C., LESTER, H.A. & SCHWARZ, J. (2004). Knockin mice with Leu9'Ser alpha4-nicotinic receptors: substantia nigra dopaminergic neurons are hypersensitive to agonist and lost postnatally. *Physiol Genomics*, **18,** 299-307.

ORR-URTREGER, A., BROIDE, R.S., KASTEN, M.R., DANG, H., DANI, J.A., BEAUDET, A.L. & PATRICK, J.W. (2000). Mice homozygous for the L250T mutation in the alpha7 nicotinic acetylcholine receptor show increased neuronal apoptosis and die within 1 day of birth. *J Neurochem*, **74,** 2154-66.

ORR-URTREGER, A., GOLDNER, F.M., SAEKI, M., LORENZO, I., GOLDBERG, L., DE BIASI, M., DANI, J.A., PATRICK, J.W. & BEAUDET, A.L. (1997). Mice deficient in the alpha7 neuronal nicotinic acetylcholine receptor lack alpha-bungarotoxin binding sites and hippocampal fast nicotinic currents. *J Neurosci*, **17,** 9165-71.

PABREZA, L.A., DHAWAN, S. & KELLAR, K.J. (1991). [3H]cytisine binding to nicotinic cholinergic receptors in brain. *Mol Pharmacol*, **39,** 9-12.

PACHECO, M.A., PASTOOR, T.E., LUKAS, R.J. & WECKER, L. (2001). Characterisation of human alpha4beta2 neuronal nicotinic receptors stably expressed in SH-EP1 cells. *Neurochem Res*, **62,** 283-93.

PAHLSSON, P. & SPITALNIK, S.L. (1996). The role of glycosylation in synthesis and secretion of beta-amyloid precursor protein by Chinese hamster ovary cells. *Arch Biochem Biophys*, **331,** 177-86.

PALMA, E., BERTRAND, S., BINZONI, T. & BERTRAND, D. (1996). Neuronal nicotinic alpha 7 receptor expressed in Xenopus oocytes presents five putative binding sites for methyllycaconitine. *J Physiol*, **491 (Pt 1),** 151-61.

PALMA, E., MAGGI, L., BARABINO, B., EUSEBI, F. & BALLIVET, M. (1999). Nicotinic acetylcholine receptors assembled from the alpha7 and beta3 subunits. *J Biol Chem*, **274,** 18335-40.

PALMA, E., MILEO, A.M., MARTINEZ-TORRES, A., EUSEBI, F. & MILEDI, R. (2002). Some properties of human neuronal alpha 7 nicotinic acetylcholine receptors fused to the green fluorescent protein. *Proc Natl Acad Sci U S A*, **99,** 3950-5.

PALMER, A.M. (2003). Cholinergic therapies for Alzheimer's disease: progress and prospects. *Curr Opin Investig Drugs*, **4,** 820-5.

PAPKE, R.L. & HEINEMANN, S.F. (1994). Partial agonist properties of cytisine on neuronal nicotinic receptors containing the beta 2 subunit. *Mol Pharmacol*, **45,** 142-9.

PAPKE, R.L., PORTER PAPKE, J.K. & ROSE, G.M. (2004). Activity of alpha 7-sensitive agonists at nicotinic and serotonin 5HT3 receptors expressed in Xenopus oocytes. *Bioorg Med Chem Lett*, **14,** 1849-53.

PAPKE, R.L., WEBSTER, J.C., LIPPIELLO, P.M., BENCHERIF, M. & FRANCIS, M.M. (2000). The activation and inhibition of human nicotinic acetylcholine receptor by RJR-2403 indicate a selectivity for the alpha4beta2 receptor subtype. *J Neurochem*, **75,** 204-16.

PARADISO, K., ZHANG, J. & STEINBACH, J.H. (2001). The C terminus of the human nicotinic alpha4beta2 receptor forms a binding site required for the potentiation by an estrogenic steroid. *J Neurosci*, **21,** 6561-6568.

PASCUZZO, G.J., AKAIKE, A., MALEQUE, M.A., SHAW, K.P., ARONSTAM, R.S., RICKETT, D.L. & ALBUQUERQUE, E.X. (1984). The nature of the interactions of pyridostigmine with the nicotinic acetylcholine receptor-ionic channel complex. I. Agonist, desensitizing, and binding properties. *Mol Pharmacol*, **25,** 92-101.

PATERSON, D. & NORDBERG, A. (2000). Neuronal nicotinic receptors in the human brain. *Prog Neurobiol*, **61,** 75-111.

PAYLOR, R., NGUYEN, M., CRAWLEY, J.N., PATRICK, J., BEAUDET, A. & ORR-URTREGER, A. (1998). Alpha7 nicotinic receptor subunits are not necessary for hippocampal-dependent learning or sensorimotor gating: a behavioral characterization of Acra7-deficient mice. *Learn Mem*, **5,** 302-16.

PENG, J.H., FRYER, J.D., HURST, R.S., SCHROEDER, K.M., GEORGE, A.A., MORRISSY, S., GROPPI, V.E., LEONARD, S.S. & LUKAS, R.J. (2005). High-affinity epibatidine binding of functional, human alpha7-nicotinic acetylcholine receptors stably and heterologously expressed de novo in human SH-EP1 cells. *J Pharmacol Exp Ther*, **313,** 24-35.

PENG, J.H., LUCERO, L., FRYER, J., HERL, J., LEONARD, S.S. & LUKAS, R.J. (1999). Inducible, heterologous expression of human alpha7-nicotinic acetylcholine receptors in a native nicotinic receptor-null human clonal line. *Brain Res*, **825,** 172-9.

PENG, X., GERZANICH, V., ANAND, R., WHITING, P.J. & LINDSTROM, J. (1994a). Nicotine-induced increase in neuronal nicotinic receptors results from a decrease in the rate of receptor turnover. *Mol Pharmacol*, **46,** 523-30.

PENG, X., KATZ, M., GERZANICH, V., ANAND, R. & LINDSTROM, J. (1994b). Human alpha 7 acetylcholine receptor: cloning of the alpha 7 subunit from the SH-SY5Y cell line and determination of pharmacological properties of native receptors and functional alpha 7 homomers expressed in Xenopus oocytes. *Mol Pharmacol*, **45,** 546-54.

PERALTA, E.G., WINSLOW, J.W., PETERSON, G.L., SMITH, D.H., ASHKENAZI, A., RAMACHANDRAN, J., SCHIMERLIK, M.I. & CAPON, D.J. (1987). Primary structure and biochemical properties of an M2 muscarinic receptor. *Science*, **236,** 600-5.

PEREIRA, E.F., REINHARDT-MAELICKE, S., SCHRATTENHOLZ, A., MAELICKE, A. & ALBUQUERQUE, E.X. (1993). Identification and functional characterization of a new agonist site on nicotinic acetylcholine receptors of cultured hippocampal neurons. *J Pharmacol Exp Ther*, **265,** 1474-91.

PERRY, D.C., XIAO, Y., NGUYEN, H.N., MUSACHIO, J.L., DAVILA-GARCIA, M.I. & KELLAR, K.J. (2002). Measuring nicotinic receptors with characteristics of alpha4beta2, alpha3beta2 and alpha3beta4 in rat tissues by autoradiography. *J Neurochem*, **82,** 468-81.

PERRY, E., WALKER, M., GRACE, J. & PERRY, R. (1999). Acetylcholine in mind: a neurotransmitter correlate of consciousness? *Trends Neurosci*, **22,** 273-80.

PERRY, E.K., GIBSON, P.H., BLESSED, G., PERRY, R.H. & TOMLINSON, B.E. (1977). Neurotransmitter enzyme abnormalities in senile dementia. Choline acetyltransferase and glutamic acid decarboxylase activities in necropsy brain tissue. *J Neurol Sci*, **34,** 247-65.

PERRY, E.K., MORRIS, C.M., COURT, J.A., CHENG, A., FAIRBAIRN, A.F., MCKEITH, I.G., IRVING, D., BROWN, A. & PERRY, R.H. (1995). Alteration in nicotine binding sites in Parkinson's disease, Lewy body dementia and Alzheimer's disease: possible index of early neuropathology. *Neuroscience*, **64,** 385-95.

PERRY, E.K., PERRY, R.H., BLESSED, G. & TOMLINSON, B.E. (1978a). Changes in brain cholinesterases in senile dementia of Alzheimer type. *Neuropathol Appl Neurobiol*, **4,** 273-7.

PERRY, E.K., SMITH, C.J., COURT, J.A. & PERRY, R.H. (1990). Cholinergic nicotinic and muscarinic receptors in dementia of Alzheimer, Parkinson and Lewy body types. *J Neural Transm Park Dis Dement Sect*, **2,** 149-58.

PERRY, E.K., TOMLINSON, B.E., BLESSED, G., BERGMANN, K., GIBSON, P.H. & PERRY, R.H. (1978b). Correlation of cholinergic abnormalities with senile plaques and mental test scores in senile dementia. *Br Med J*, **2,** 1457-9.

PETRYNIAK, M.A., WURTMAN, R.J. & SLACK, B.E. (1996). Elevated intracellular calcium concentration increases secretory processing of the amyloid precursor protein by a tyrosine phosphorylation-dependent mechanism. *Biochem J*, **320 (Pt 3),** 957-63.

PETTIT, D.L., SHAO, Z. & YAKEL, J.L. (2001). beta-Amyloid(1-42) peptide directly modulates nicotinic receptors in the rat hippocampal slice. *J Neurosci*, **21,** RC120.

PIETILA, K., LAHDE, T., ATTILA, M., AHTEE, L. & NORDBERG, A. (1998). Regulation of nicotinic receptors in the brain of mice withdrawn from chronic oral nicotine treatment. *Naunyn Schmiedebergs Arch Pharmacol*, **357,** 176-82.

POIRIER, J. (2005). Apolipoprotein E, cholesterol transport and synthesis in sporadic Alzheimer's disease. *Neurobiol Aging*, **26,** 355-61.

POLLACK, S.J. & LEWIS, H. (2005). Secretase inhibitors for Alzheimer's diseases: challenges of a promiscuous protease. *Curr Opin Investig Drugs*, **6,** 35-47.

PONTE, P., GONZALEZ-DEWHITT, P., SCHILLING, J., MILLER, J., HSU, D., GREENBERG, B., DAVIS, K., WALLACE, W., LIEBERBURG, I. & FULLER, F. (1988). A new A4 amyloid mRNA contains a domain homologous to serine proteinase inhibitors. *Nature*, **331,** 525-7.

PRADO, M.A., REIS, R.A., PRADO, V.F., DE MELLO, M.C., GOMEZ, M.V. & DE MELLO, F.G. (2002). Regulation of acetylcholine synthesis and storage. *Neurochem Int*, **41,** 291-9.

PRICE, G.W., ROBERTS, C., WATSON, J., BURTON, M., MULHOLLAND, K., MIDDLEMISS, D.N. & JONES, B.J. (1996). Species difference in 5-HT autoreceptors. *Behav Brain Res*, **73,** 79-82.

PROKOP, S., SHIROTANI, K., EDBAUER, D., HAASS, C. & STEINER, H. (2004). Requirement of PEN-2 for stabilisation of the presenilin N-/C-terminal fragment heterodimer within the gamma-secretase complex. *J Biol Chem*, **279,** 23255-61.

PUCHACZ, E., BUISSON, B., BERTRAND, D. & LUKAS, R.J. (1994). Functional expression of nicotinic acetylcholine receptors containing rat alpha 7 subunits in human SH-SY5Y neuroblastoma cells. *FEBS Lett*, **354,** 155-9.

PUOLIVALI, J., WANG, J., HEIKKINEN, T., HEIKKILA, M., TAPIOLA, T., VAN GROEN, T. & TANILA, H. (2002). Hippocampal A beta 42 levels correlate with spatial memory deficit in APP and PS1 double transgenic mice. *Neurobiol Dis*, **9,** 339-47.

PYM, L., KEMP, M., RAYMOND-DELPECH, V., BUCKINGHAM, S., BOYD, C.A. & SATTELLE, D. (2005). Subtype-specific actions of beta-amyloid peptides on recombinant human neuronal nicotinic acetylcholine receptors (alpha7, alpha4beta2, alpha3beta4) expressed in Xenopus laevis oocytes. *Br J Pharmacol*.

QUIK, M., CHOREMIS, J., KOMOURIAN, J., LUKAS, R.J. & PUCHACZ, E. (1996). Similarity between rat brain nicotinic alpha-bungarotoxin receptors and stably expressed alpha-bungarotoxin binding sites. *J Neurochem*, **67,** 145-54.

RAFTERY, M.A., HUNKAPILLER, M.W., STRADER, C.D. & HOOD, L.E. (1980). Acetylcholine receptor: complex of homologous subunits. *Science*, **208,** 1454-6.

RAKHILIN, S., DRISDEL, R.C., SAGHER, D., MCGEHEE, D.S., VALLEJO, Y. & GREEN, W.N. (1999). alpha-bungarotoxin receptors contain alpha7 subunits in two different disulfide-bonded conformations. *J Cell Biol*, **146,** 203-18.

RAMIREZ-LATORRE, J., YU, C.R., QU, X., PERIN, F., KARLIN, A. & ROLE, L. (1996). Functional contributions of alpha5 subunit to neuronal acetylcholine receptor channels. *Nature*, **380,** 347-51.

RANGWALA, F., DRISDEL, R.C., RAKHILIN, S., KO, E., ATLURI, P., HARKINS, A.B., FOX, A.P., SALMAN, S.S. & GREEN, W.N. (1997). Neuronal alpha-bungarotoxin receptors differ structurally from other nicotinic acetycholine receptors. *J Neurosci*, **17,** 8201-12.

RAY, W.J., ASHALL, F. & GOATE, A.M. (1998). Molecular pathogenesis of sporadic and familial forms of Alzheimer's disease. *Mol Med Today*, **4,** 151-7.

REES, T., HAMMOND, P.I., SOREQ, H., YOUNKIN, S. & BRIMIJOIN, S. (2003). Acetylcholinesterase promotes beta-amyloid plaques in cerebral cortex. *Neurobiol Aging*, **24,** 777-87.

RICHARDSON, J.C., KENDAL, C.E., ANDERSON, R., PRIEST, F., GOWER, E., SODEN, P., GRAY, R., TOPPS, S., HOWLETT, D.R., LAVENDER, D., CLARKE, N.J., BARNES, J.C., HAWORTH, R., STEWART, M.G. & RUPNIAK, H.T. (2003). Ultrastructural and behavioural changes precede amyloid deposition in a transgenic model of Alzheimer's disease. *Neuroscience*, **122,** 213-28.

RINNE, J.O., MYLLYKYLA, T., LONNBERG, P. & MARJAMAKI, P. (1991). A postmortem study of brain nicotinic receptors in Parkinson's and Alzheimer's disease. *Brain Res*, **547,** 167-70.

ROBAKIS, N.K., WISNIEWSKI, H.M., JENKINS, E.C., DEVINE-GAGE, E.A., HOUCK, G.E., YAO, X.L., RAMAKRISHNA, N., WOLFE, G., SILVERMAN, W.P. & BROWN, W.T. (1987). Chromosome 21q21 sublocalisation of gene encoding beta-amyloid peptide in cerebral vessels and neuritic (senile) plaques of people with Alzheimer disease and Down syndrome. *Lancet*, **1,** 384-5.

ROGAEV, E.I., SHERRINGTON, R., ROGAEVA, E.A., LEVESQUE, G., IKEDA, M., LIANG, Y., CHI, H., LIN, C., HOLMAN, K., TSUDA, T. & ET AL. (1995). Familial Alzheimer's disease in kindreds with missense mutations in a gene on chromosome 1 related to the Alzheimer's disease type 3 gene. *Nature*, **376,** 775-8.

ROHER, A.E., CHANEY, M.O., KUO, Y.M., WEBSTER, S.D., STINE, W.B., HAVERKAMP, L.J., WOODS, A.S., COTTER, R.J., TUOHY, J.M., KRAFFT, G.A., BONNELL, B.S. & EMMERLING, M.R. (1996). Morphology and toxicity of Abeta-(1-42) dimer derived from neuritic and vascular amyloid deposits of Alzheimer's disease. *Journal of Biological Chemistry*, **271,** 20631-20635.

ROLE, L.W. & BERG, D.K. (1996). Nicotinic receptors in the development and modulation of CNS synapses. *Neuron*, **16,** 1077-85.

ROMANELLI, M.F., MORRIS, J.C., ASHKIN, K. & COBEN, L.A. (1990). Advanced Alzheimer's disease is a risk factor for late-onset seizures. *Arch Neurol*, **47,** 847-50.

ROSS, R.A., SPENGLER, B.A. & BIEDLER, J.L. (1983). Coordinate morphological and biochemical interconversion of human neuroblastoma cells. *J Natl Cancer Inst*, **71,** 741-7.

ROSS, S.A., WONG, J.Y., CLIFFORD, J.J., KINSELLA, A., MASSALAS, J.S., HORNE, M.K., SCHEFFER, I.E., KOLA, I., WADDINGTON, J.L., BERKOVIC, S.F. & DRAGO, J. (2000). Phenotypic characterization of an alpha 4 neuronal nicotinic acetylcholine receptor subunit knock-out mouse. *J Neurosci*, **20,** 6431-41.

ROSSOR, M.N., FOX, N.C., FREEBOROUGH, P.A. & HARVEY, R.J. (1996). Clinical features of sporadic and familial Alzheimer's disease. *Neurodegeneration*, **5,** 393-7.

ROSSOR, M.N., GARRETT, N.J., JOHNSON, A.L., MOUNTJOY, C.Q., ROTH, M. & IVERSEN, L.L. (1982). A post-mortem study of the cholinergic and GABA systems in senile dementia. *Brain*, **105,** 313-30.

RYLETT, R.J., BALL, M.J. & COLHOUN, E.H. (1983). Evidence for high affinity choline transport in synaptosomes prepared from hippocampus and neocortex of patients with Alzheimer's disease. *Brain Res*, **289,** 169-75.

SABBAGH, M.N., REID, R.T., HANSEN, L.A., ALFORD, M. & THAL, L.J. (2001). Correlation of nicotinic receptor binding with clinical and neuropathological changes in Alzheimer's disease and dementia with Lewy bodies. *J Neural Transm*, **108,** 1149-57.

SABEY, K., PARADISO, K., ZHANG, J. & STEINBACH, J.H. (1999). Ligand binding and activation of rat nicotinic alpha4beta2 receptors stably expressed in HEK293 cells. *Mol Pharmacol*, **55,** 58-66.

SADIK, K. & WILCOCK, G. (2003). The increasing burden of Alzheimer disease. *Alzheimer Dis Assoc Disord*, **17 Suppl 3,** S75-9.

SALAS, R., PIERI, F. & DE BIASI, M. (2004). Decreased signs of nicotine withdrawal in mice null for the beta4 nicotinic acetylcholine receptor subunit. *J Neurosci*, **24,** 10035-9.

SALOMON, A.R., MARCINOWSKI, K.J., FRIEDLAND, R.P. & ZAGORSKI, M.G. (1996). Nicotine inhibits amyloid formation by the beta-peptide. *Biochemistry*, **35,** 13568-78.

SAMOCHOCKI, M., ZERLIN, M., JOSTOCK, R., GROOT KORMELINK, P.J., LUYTEN, W.H., ALBUQUERQUE, E.X. & MAELICKE, A. (2000). Galantamine is an allosterically potentiating ligand of the human alpha4/beta2 nAChR. *Acta Neurol Scand Suppl*, **176,** 68-73.

SANSOM, M.S., ADCOCK, C. & SMITH, G.R. (1998). Modelling and simulation of ion channels: applications to the nicotinic acetylcholine receptor. *J Struct Biol*, **121,** 246-62.

SARAGOZA, P.A., MODIR, J.G., GOEL, N., FRENCH, K.L., LI, L., NOWAK, M.W. & STITZEL, J.A. (2003). Identification of an alternatively processed nicotinic receptor alpha7 subunit RNA in mouse brain. *Brain Res Mol Brain Res*, **117,** 15-26.

SAUNDERS, A.M., STRITTMATTER, W.J., SCHMECHEL, D., GEORGE-HYSLOP, P.H., PERICAK-VANCE, M.A., JOO, S.H., ROSI, B.L., GUSELLA, J.F., CRAPPER-MACLACHLAN, D.R., ALBERTS, M.J. & ET AL. (1993). Association of apolipoprotein E allele epsilon 4 with late-onset familial and sporadic Alzheimer's disease. *Neurology*, **43,** 1467-72.

SAVONENKO, A., XU, G.M., MELNIKOVA, T., MORTON, J.L., GONZALES, V., WONG, M.P., PRICE, D.L., TANG, F., MARKOWSKA, A.L. & BORCHELT, D.R. (2005). Episodic-like memory deficits in the APPswe/PS1dE9 mouse model of Alzheimer's disease: relationships to beta-amyloid deposition and neurotransmitter abnormalities. *Neurobiol Dis*, **18,** 602-17.

SCHELLENBERG, G.D. (1995a). Genetic dissection of Alzheimer disease, a heterogeneous disorder. *Proc Natl Acad Sci U S A*, **92,** 8552-9.

SCHELLENBERG, G.D. (1995b). Molecular genetics of familial Alzheimer's disease. *Arzneimittelforschung*, **45,** 418-24.

SCHELLENBERG, G.D. (1995c). Progress in Alzheimer's disease genetics. *Curr Opin Neurol*, **8,** 262-7.

SCHELLENBERG, G.D., BIRD, T.D., WIJSMAN, E.M., ORR, H.T., ANDERSON, L., NEMENS, E., WHITE, J.A., BONNYCASTLE, L., WEBER, J.L., ALONSO, M.E. & ET AL. (1992). Genetic linkage evidence for a familial Alzheimer's disease locus on chromosome 14. *Science*, **258,** 668-71.

SCHEUNER, D., ECKMAN, C., JENSEN, M., SONG, X., CITRON, M., SUZUKI, N., BIRD, T.D., HARDY, J., HUTTON, M., KUKULL, W., LARSON, E., LEVY-LAHAD, E., VIITANEN, M., PESKIND, E., POORKAJ, P., SCHELLENBERG, G., TANZI, R., WASCO, W., LANNFELT, L., SELKOE, D. & YOUNKIN, S. (1996). Secreted amyloid beta-protein similar to that in the senile plaques of Alzheimer's disease is increased in vivo by the presenilin 1 and 2 and APP mutations linked to familial Alzheimer's disease. *Nat Med*, **2,** 864-70.

SCHMITT, B., BERNHARDT, T., MOELLER, H.J., HEUSER, I. & FROLICH, L. (2004). Combination therapy in Alzheimer's disease: a review of current evidence. *CNS Drugs*, **18,** 827-44.

SCHOEPFER, R., CONROY, W.G., WHITING, P., GORE, M. & LINDSTROM, J. (1990). Brain alpha-bungarotoxin binding protein cDNAs and MAbs reveal subtypes of this branch of the ligand-gated ion channel gene superfamily. *Neuron*, **5,** 35-48.

SCHOEPFER, R., WHITING, P., ESCH, F., BLACHER, R., SHIMASAKI, S. & LINDSTROM, J. (1988). cDNA clones coding for the structural subunit of a chicken brain nicotinic acetylcholine receptor. *Neuron*, **1,** 241-8.

SCHRODER, H., GIACOBINI, E., STRUBLE, R.G., ZILLES, K., MAELICKE, A., LUITEN, P.G. & STROSBERG, A.D. (1991). Cellular distribution and expression of cortical acetylcholine receptors in aging and Alzheimer's disease. *Ann N Y Acad Sci*, **640,** 189-92.

SCHROEDER, K.M., WU, J., ZHAO, L. & LUKAS, R.J. (2003). Regulation by cycloheximide and lowered temperature of cell-surface alpha7-nicotinic acetylcholine receptor expression on transfected SH-EP1 cells. *J Neurochem*, **85,** 581-91.

SCOTT, L.J. & GOA, K.L. (2000). Galantamine: a review of its use in Alzheimer's disease. *Drugs*, **60,** 1095-122.

SEGUELA, P., WADICHE, J., DINELEY-MILLER, K., DANI, J.A. & PATRICK, J.W. (1993). Molecular cloning, functional properties, and distribution of rat brain alpha 7: a nicotinic cation channel highly permeable to calcium. *J Neurosci*, **13,** 596-604.

SELKOE, D.J. (1991a). Alzheimer's disease. In the beginning. *Nature*, **354,** 432-3.

SELKOE, D.J. (1994). Alzheimer's disease: a central role for amyloid. *J Neuropathol Exp Neurol*, **53,** 438-47.

SELKOE, D.J. (1991b). Amyloid protein and Alzheimer's disease. *Sci Am*, **265,** 68-71, 74-6, 78.

SELKOE, D.J. (1990). Deciphering Alzheimer's disease: the amyloid precursor protein yields new clues. *Science*, **248,** 1058-60.

SELKOE, D.J. (1991c). The molecular pathology of Alzheimer's disease. *Neuron*, **6,** 487-98.

SELKOE, D.J. (1993). Physiological production of the beta-amyloid protein and the mechanism of Alzheimer's disease. *Trends Neurosci*, **16,** 403-9.

SENGUPTA, A., KABAT, J., NOVAK, M., WU, Q., GRUNDKE-IQBAL, I. & IQBAL, K. (1998). Phosphorylation of tau at both Thr 231 and Ser 262 is required for maximal inhibition of its binding to microtubules. *Arch Biochem Biophys*, **357,** 299-309.

SEUBERT, P., VIGO-PELFREY, C., ESCH, F., LEE, M., DOVEY, H., DAVIS, D., SINHA, S., SCHLOSSMACHER, M., WHALEY, J., SWINDLEHURST, C. & ET AL. (1992). Isolation and quantification of soluble Alzheimer's beta-peptide from biological fluids. *Nature*, **359,** 325-7.

SEVERANCE, E.G., ZHANG, H., CRUZ, Y., PAKHLEVANIANTS, S., HADLEY, S.H., AMIN, J., WECKER, L., REED, C. & CUEVAS, J. (2004). The alpha7 nicotinic acetylcholine receptor subunit exists in two isoforms that contribute to functional ligand-gated ion channels. *Mol Pharmacol*, **66,** 420-9.

SHAO, Z. & YAKEL, J.L. (2000). Single channel properties of neuronal nicotinic ACh receptors in stratum radiatum interneurons of rat hippocampal slices. *J Physiol*, **527 Pt 3,** 507-13.

SHARPLES, C.G.V. & WONNACOTT, S. (2004). Neuronal Nicotinic Receptors. In www.tocris.com.

SHERRINGTON, R., ROGAEV, E.I., LIANG, Y., ROGAEVA, E.A., LEVESQUE, G., IKEDA, M., CHI, H., LIN, C., LI, G., HOLMAN, K. & ET AL. (1995). Cloning of a gene bearing missense mutations in early-onset familial Alzheimer's disease. *Nature*, **375,** 754-60.

SHIMOHAMA, S. & KIHARA, T. (2001). Nicotinic receptor-mediated protection against beta-amyloid neurotoxicity. *Biol Psychiatry*, **49,** 233-9.

SHIROTANI, K., EDBAUER, D., KOSTKA, M., STEINER, H. & HAASS, C. (2004). Immature nicastrin stabilises APH-1 independent of PEN-2 and presenilin: identification of nicastrin mutants that selectively interact with APH-1. *J Neurochem*, **89,** 1520-7.

SHOJI, M., GOLDE, T.E., GHISO, J., CHEUNG, T.T., ESTUS, S., SHAFFER, L.M., CAI, X.D., MCKAY, D.M., TINTNER, R., FRANGIONE, B. & ET AL. (1992). Production of the Alzheimer amyloid beta protein by normal proteolytic processing. *Science*, **258,** 126-9.

SHUTE, C.C. & LEWIS, P.R. (1967). The ascending cholinergic reticular system: neocortical, olfactory and subcortical projections. *Brain*, **90,** 497-520.

SHYTLE, R.D., SILVER, A.A., WILKINSON, B.J. & SANBERG, P.R. (2002). A pilot controlled trial of transdermal nicotine in the treatment of attention deficit hyperactivity disorder. *World J Biol Psychiatry*, **3,** 150-5.

SIHVER, W., GILLBERG, P.G. & NORDBERG, A. (1998). Laminar distribution of nicotinic receptor subtypes in human cerebral cortex as determined by [3H](-)nicotine, [3H]cytisine and [3H]epibatidine in vitro autoradiography. *Neuroscience*, **85,** 1121-33.

SIHVER, W., GILLBERG, P.G., SVENSSON, A.L. & NORDBERG, A. (1999). Autoradiographic comparison of [3H](-)nicotine, [3H]cytisine and [3H]epibatidine binding in relation to vesicular acetylcholine transport sites in the temporal cortex in Alzheimer's disease. *Neuroscience*, **94,** 685-96.

SIMS, N.R., BOWEN, D.M., ALLEN, S.J., SMITH, C.C., NEARY, D., THOMAS, D.J. & DAVISON, A.N. (1983). Presynaptic cholinergic dysfunction in patients with dementia. *J Neurochem*, **40,** 503-9.

SINGER, S., ROSSI, S., VERZOSA, S., HASHIM, A., LONOW, R., COOPER, T., SERSHEN, H. & LAJTHA, A. (2004). Nicotine-induced changes in neurotransmitter levels in brain areas associated with cognitive function. *Neurochem Res*, **29,** 1779-92.

SINHA, S., ANDERSON, J.P., BARBOUR, R., BASI, G.S., CACCAVELLO, R., DAVIS, D., DOAN, M., DOVEY, H.F., FRIGON, N., HONG, J., JACOBSON-CROAK, K., JEWETT, N., KEIM, P., KNOPS, J., LIEBERBURG, I., POWER, M., TAN, H., TATSUNO, G., TUNG, J., SCHENK, D., SEUBERT, P., SUOMENSAARI, S.M., WANG, S., WALKER, D., JOHN, V. & ET AL. (1999). Purification and cloning of amyloid precursor protein beta-secretase from human brain. *Nature*, **402,** 537-40.

SINHA, S. & LIEBERBURG, I. (1999). Cellular mechanisms of beta-amyloid production and secretion. *Proc Natl Acad Sci U S A*, **96,** 11049-53.

SISODIA, S.S. (1992). Beta-amyloid precursor protein cleavage by a membrane-bound protease. *Proc Natl Acad Sci U S A*, **89,** 6075-9.

SISODIA, S.S., KOO, E.H., BEYREUTHER, K., UNTERBECK, A. & PRICE, D.L. (1990). Evidence that beta-amyloid protein in Alzheimer's disease is not derived by normal processing. *Science*, **248,** 492-5.

SLOANE, P.D., ZIMMERMAN, S., SUCHINDRAN, C., REED, P., WANG, L., BOUSTANI, M. & SUDHA, S. (2002). The public health impact of Alzheimer's disease, 2000-2050: potential implication of treatment advances. *Annu Rev Public Health*, **23,** 213-31.

SMITH, M.J., KWOK, J.B., MCLEAN, C.A., KRIL, J.J., BROE, G.A., NICHOLSON, G.A., CAPPAI, R., HALLUPP, M., COTTON, R.G., MASTERS, C.L., SCHOFIELD, P.R. & BROOKS, W.S. (2001). Variable phenotype of Alzheimer's disease with spastic paraparesis. *Ann Neurol*, **49,** 125-9.

SNYDER, E.M., NONG, Y., ALMEIDA, C.G., PAUL, S., MORAN, T., CHOI, E.Y., NAIRN, A.C., SALTER, M.W., LOMBROSO, P.J., GOURAS, G.K. & GREENGARD, P. (2005). Regulation of NMDA receptor trafficking by amyloid-beta. *Nat Neurosci*, **8,** 1051-8.

SOBRIO, F., DEBRUYNE, D., DHILLY, M., CHAZALVIEL, L., CAMSONNE, R., KAKIUCHI, T., TSUKADA, H. & BARRE, L. (2005). Evaluation in rats and primates of [11C]-mecamylamine, a potential nicotinic acetylcholine receptor radioligand for positron emission tomography. *Neurochem Int*, **46,** 479-88.

SOLANO, D.C., SIRONI, M., BONFINI, C., SOLERTE, S.B., GOVONI, S. & RACCHI, M. (2000). Insulin regulates soluble amyloid precursor protein release via phosphatidyl inositol 3 kinase-dependent pathway. *Faseb J*, **14,** 1015-22.

SONKUSARE, S.K., KAUL, C.L. & RAMARAO, P. (2005). Dementia of Alzheimer's disease and other neurodegenerative disorders--memantine, a new hope. *Pharmacol Res*, **51,** 1-17.

STOLERMAN, I.P., MIRZA, N.R., HAHN, B. & SHOAIB, M. (2000). Nicotine in an animal model of attention. *Eur J Pharmacol*, **393,** 147-54.

STORCH, A., SCHRATTENHOLZ, A., COOPER, J.C., ABDEL GHANI, E.M., GUTBROD, O., WEBER, K.H., REINHARDT, S., LOBRON, C., HERMSEN, B., SOSKIC, V. & ET AL. (1995). Physostigmine, galanthamine and codeine act as 'noncompetitive nicotinic receptor agonists' on clonal rat pheochromocytoma cells. *Eur J Pharmacol*, **290,** 207-19.

STRITTMATTER, W.J. & ROSES, A.D. (1996). Apolipoprotein E and Alzheimer's disease. *Annu Rev Neurosci*, **19,** 53-77.

STRUHL, G. & ADACHI, A. (2000). Requirements for presenilin-dependent cleavage of notch and other transmembrane proteins. *Mol Cell*, **6,** 625-36.

STURCHLER-PIERRAT, C., ABRAMOWSKI, D., DUKE, M., WIEDERHOLD, K.H., MISTL, C., ROTHACHER, S., LEDERMANN, B., BURKI, K., FREY, P., PAGANETTI, P.A., WARIDEL, C., CALHOUN, M.E., JUCKER, M., PROBST, A., STAUFENBIEL, M. & SOMMER, B. (1997). Two amyloid precursor protein transgenic mouse models with Alzheimer disease-like pathology. *Proc Natl Acad Sci U S A*, **94,** 13287-92.

STURCHLER-PIERRAT, C. & STAUFENBIEL, M. (2000). Pathogenic mechanisms of Alzheimer's disease analyzed in the APP23 transgenic mouse model. *Ann N Y Acad Sci*, **920,** 134-9.

SUDWEEKS, S.N. & YAKEL, J.L. (2000). Functional and molecular characterization of neuronal nicotinic ACh receptors in rat CA1 hippocampal neurons. *J Physiol*, **527 Pt 3,** 515-28.

SUGAYA, K., GIACOBINI, E. & CHIAPPINELLI, V.A. (1990). Nicotinic acetylcholine receptor subtypes in human frontal cortex: changes in Alzheimer's disease. *J Neurosci Res*, **27,** 349-59.

SULLIVAN, D., CHIARA, D.C. & COHEN, J.B. (2002). Mapping the agonist binding site of the nicotinic acetylcholine receptor by cysteine scanning mutagenesis: antagonist footprint and secondary structure prediction. *Mol Pharmacol*, **61,** 463-72.

SULLIVAN, D.A. & COHEN, J.B. (2000). Mapping the agonist binding site of the nicotinic acetylcholine receptor. Orientation requirements for activation by covalent agonist. *J Biol Chem*, **275,** 12651-60.

SUN, X., COLE, G.M., CHU, T., XIA, W., GALASKO, D., YAMAGUCHI, H., TANEMURA, K., FRAUTSCHY, S.A. & TAKASHIMAN, A. (2002). Intracellular AB is increased by okadaic acid exposure in transfected neuronal and non-neuronal cell lines. *Neurobiol Aging*, **23,** 195-203.

SURPRENANT, A., SCHNEIDER, D.A., WILSON, H.L., GALLIGAN, J.J. & NORTH, R.A. (2000). Functional properties of heteromeric P2X(1/5) receptors expressed in HEK cells and excitatory junction potentials in guinea-pig submucosal arterioles. *J Auton Nerv Syst*, **81,** 249-63.

SWEILEH, W., WENBERG, K., XU, J., FORSAYETH, J., HARDY, S. & LORING, R.H. (2000). Multistep expression and assembly of neuronal nicotinic receptors is both host-cell- and receptor-subtype-dependent. *Brain Res Mol Brain Res*, **75,** 293-302.

TANZI, R.E., GUSELLA, J.F., WATKINS, P.C., BRUNS, G.A., ST GEORGE-HYSLOP, P., VAN KEUREN, M.L., PATTERSON, D., PAGAN, S., KURNIT, D.M. & NEVE, R.L. (1987). Amyloid beta protein gene: cDNA, mRNA distribution, and genetic linkage near the Alzheimer locus. *Science*, **235,** 880-4.

TAYLOR, B.M., SARVER, R.W., FICI, G., POORMAN, R.A., LUTZKE, B.S., MOLINARI, A., KAWABE, T., KAPPENMAN, K., BUHL, A.E. & EPPS, D.E. (2003). Spontaneous aggregation and cytotoxicity of the beta-amyloid Abeta1-40: a kinetic model. *J Protein Chem*, **22,** 31-40.

TAYLOR, P., RADIC, Z., KREIENKAMP, H.J., MAEDA, R., LUO, Z., FUENTES, M.E., VELLOM, D. & PICKERING, N. (1994). Expression and ligand specificity of acetylcholinesterase and the nicotinic receptor: a tale of two cholinergic sites. *Biochem Soc Trans*, **22,** 740-5.

TEPLOW, D.B. (1998). Structural and kinetic features of amyloid beta-protein fibrillogenesis. *Amyloid*, **5,** 121-42.

THUNECKE, M., LOBBIA, A., KOSCIESSA, U., DYRKS, T., OAKLEY, A.E., TURNER, J., SAENGER, W. & GEORGALIS, Y. (1998). Aggregation of A beta Alzheimer's disease-related peptide studied by dynamic light scattering. *J Pept Res*, **52,** 509-17.

TIAN, L., PRIOR, C., DEMPSTER, J. & MARSHALL, I.G. (1997). Hexamethonium- and methyllycaconitine-induced changes in acetylcholine release from rat motor nerve terminals. *Br J Pharmacol*, **122,** 1025-34.

TOMITA, T. & IWATSUBO, T. (2004). The inhibition of gamma-secretase as a therapeutic approach to Alzheimer's disease. *Drug News Perspect*, **17,** 321-5.

TOZAKI, H., MATSUMOTO, A., KANNO, T., NAGAI, K., NAGATA, T., YAMAMOTO, S. & NISHIZAKI, T. (2002). The inhibitory and facilitatory actions of amyloid-beta peptides on nicotinic ACh receptors and AMPA receptors. *Biochem Biophys Res Commun*, **294,** 42-5.

TSUNEKI, H., SALAS, R. & DANI, J.A. (2003). Mouse muscle denervation increases expression of an alpha7 nicotinic receptor with unusual pharmacology. *J Physiol*, **547,** 169-79.

TUCKER, H.M., KIHIKO-EHMANN, M. & ESTUS, S. (2002). Urokinase-type plasminogen activator inhibits amyloid-beta neurotoxicity and fibrillogenesis via plasminogen. *J Neurosci Res*, **70,** 249-55.

TULVING, E. & SCHACTER, D.L. (1990). Priming and human memory systems. *Science*, **247,** 301-6.

UDGAONKAR, J.B. & HESS, G.P. (1987a). Acetylcholine receptor: channel-opening kinetics evaluated by rapid chemical kinetic and single-channel current measurements. *Biophys J*, **52,** 873-83.

UDGAONKAR, J.B. & HESS, G.P. (1987b). Chemical kinetic measurements of a mammalian acetylcholine receptor by a fast-reaction technique. *Proc Natl Acad Sci U S A*, **84,** 8758-62.

VALENZUELA, C.F., DOWDING, A.J., ARIAS, H.R. & JOHNSON, D.A. (1994). Antibody-induced conformational changes in the Torpedo nicotinic acetylcholine receptor: a fluorescence study. *Biochemistry*, **33,** 6586-94.

VAN BROECKHOVEN, C., HAAN, J., BAKKER, E., HARDY, J.A., VAN HUL, W., WEHNERT, A., VEGTER-VAN DER VLIS, M. & ROOS, R.A. (1990). Amyloid beta protein precursor gene and hereditary cerebral hemorrhage with amyloidosis (Dutch). *Science*, **248,** 1120-2.

VAN DEN BEUKEL, I., VAN KLEEF, R.G. & OORTGIESEN, M. (1998). Differential effects of physostigmine and organophosphates on nicotinic receptors in neuronal cells of different species. *Neurotoxicology*, **19,** 777-87.

VAN HOESEN, G.W. & SOLODKIN, A. (1994). Cellular and system neuroanatomical changes in Alzheimer's disease. *Ann N Y Acad Sci*, **747,** 12-35.

VASSAR, P.S. & CULLING, C.F. (1959). Fluorescent stains, with special reference to amyloid and connective tissues. *Arch Pathol*, **68,** 487-98.

VASSAR, R., BENNETT, B.D., BABU-KHAN, S., KAHN, S., MENDIAZ, E.A., DENIS, P., TEPLOW, D.B., ROSS, S., AMARANTE, P., LOELOFF, R., LUO, Y., FISHER, S., FULLER, J., EDENSON, S., LILE, J., JAROSINSKI, M.A., BIERE, A.L., CURRAN, E., BURGESS, T., LOUIS, J.C., COLLINS, F., TREANOR, J., ROGERS, G. & CITRON, M. (1999). Beta-secretase cleavage of Alzheimer's amyloid precursor protein by the transmembrane aspartic protease BACE. *Science*, **286,** 735-41.

VELEZ-PARDO, C., JIMENEZ DEL RIO, M. & LOPERA, F. (1998). Familial Alzheimer's disease: oxidative stress, beta-amyloid, presenilins, and cell death. *Gen Pharmacol*, **31,** 675-81.

VELICELEBI, G., STAUDERMAN, K.A., VARNEY, M.A., AKONG, M., HESS, S.D. & JOHNSON, E.C. (1999). Fluorescence techniques for measuring ion channel activity. *Methods Enzymol*, **294,** 20-47.

VERNINO, S., AMADOR, M., LUETJE, C.W., PATRICK, J. & DANI, J.A. (1992). Calcium modulation and high calcium permeability of neuronal nicotinic acetylcholine receptors. *Neuron*, **8,** 127-34.

VILARO, M.T., PALACIOS, J.M. & MENGOD, G. (1990). Localization of m5 muscarinic receptor mRNA in rat brain examined by in situ hybridization histochemistry. *Neurosci Lett*, **114,** 154-9.

VILLARROYA, M., LOPEZ, M.G., CANO-ABAD, M.F. & GARCIA, A.G. (1999). Measurement of Ca2+ entry using 45Ca2+. *Methods Mol Biol*, **114,** 137-47.

VILLIGER, Y., SZANTO, I., JACONI, S., BLANCHET, C., BUISSON, B., KRAUSE, K.H., BERTRAND, D. & ROMAND, J.A. (2002). Expression of an alpha7 duplicate nicotinic acetylcholine receptor-related protein in human leukocytes. *J Neuroimmunol*, **126,** 86-98.

VOLPICELLI, L.A. & LEVEY, A.I. (2004). Muscarinic acetylcholine receptor subtypes in cerebral cortex and hippocampus. *Prog Brain Res*, **145,** 59-66.

WALKER, J.W., LUKAS, R.J. & MCNAMEE, M.G. (1981). Effects of thio-group modifications on the ion permeability control and ligand binding properties of Torpedo californica acetylcholine receptor. *Biochemistry*, **20,** 2191-9.

WALSH, D.M., KLYUBIN, I., FADEEVA, J.V., CULLEN, W.K., ANWYL, R., WOLFE, M.S., ROWAN, M.J. & SELKOE, D.J. (2002a). Naturally secreted oligomers of amyloid beta protein potently inhibit hippocampal long-term potentiation in vivo. *Nature*, **416,** 535-9.

WALSH, D.M., KLYUBIN, I., FADEEVA, J.V., ROWAN, M.J. & SELKOE, D.J. (2002b). Amyloid-beta oliomers: their production, toxicity and therapeutic inhibition. *Biochem Soc Trans*, **30,** 552-7.

WALSH, D.M., LOMAKIN, A., BENEDEK, G.B., CONDRON, M.M. & TEPLOW, D.B. (1997). Amyloid beta-protein fibrillogenesis. Detection of a protofibrillar intermediate. *J Biol Chem*, **272,** 22364-72.

WALSH, D.M., TOWNSEND, M., PODLISNY, M.B., SHANKAR, G.M., FADEEVA, J.V., AGNAF, O.E., HARTLEY, D.M. & SELKOE, D.J. (2005). Certain inhibitors of synthetic amyloid beta-peptide (Abeta) fibrillogenesis block oligomerization of natural Abeta and thereby rescue long-term potentiation. *J Neurosci*, **25,** 2455-62.

WANG, F., GERZANICH, V., WELLS, G.B., ANAND, R., PENG, X., KEYSER, K. & LINDSTROM, J. (1996). Assembly of human neuronal nicotinic receptor alpha5 subunits with alpha3, beta2, and beta4 subunits. *J Biol Chem*, **271,** 17656-65.

WANG, H., YU, M., OCHANI, M., AMELLA, C.A., TANOVIC, M., SUSARLA, S., LI, J.H., WANG, H., YANG, H., ULLOA, L., AL-ABED, Y., CZURA, C.J. & TRACEY, K.J. (2003). Nicotinic acetylcholine receptor alpha7 subunit is an essential regulator of inflammation. *Nature*, **421,** 384-8.

WANG, H.Y., D'ANDREA, M.R. & NAGELE, R.G. (2002a). Cerebellar diffuse amyloid plaques are derived from dendritic Abeta42 accumulations in Purkinje cells. *Neurobiol Aging*, **23,** 213-23.

WANG, H.Y., LEE, D.H., D'ANDREA, M.R., PETERSON, P.A., SHANK, R.P. & REITZ, A.B. (2000a). beta-Amyloid(1-42) binds to alpha7 nicotinic acetylcholine receptor with high affinity. Implications for Alzheimer's disease pathology. *J Biol Chem*, **275,** 5626-32.

WANG, H.Y., LEE, D.H., DAVIS, C.B. & SHANK, R.P. (2000b). Amyloid peptide Abeta(1-42) binds selectively and with picomolar affinity to alpha7 nicotinic acetylcholine receptors. *J Neurochem*, **75,** 1155-61.

WANG, J., DICKSON, D.W., TROJANOWSKI, J.Q. & LEE, V.M. (1999). The levels of soluble versus insoluble brain Abeta distinguish Alzheimer's disease from normal and pathologic aging. *Exp Neurol*, **158,** 328-37.

WANG, J.Z., GONG, C.X., ZAIDI, T., GRUNDKE-IQBAL, I. & IQBAL, K. (1995). Dephosphorylation of Alzheimer paired helical filaments by protein phosphatase-2A and -2B. *J Biol Chem*, **270,** 4854-60.

WANG, N., ORR-URTREGER, A., CHAPMAN, J., RABINOWITZ, R., NACHMAN, R. & KORCZYN, A.D. (2002b). Autonomic function in mice lacking alpha5 neuronal nicotinic acetylcholine receptor subunit. *J Physiol*, **542,** 347-54.

WARD, J.M., COCKCROFT, V.B., LUNT, G.G., SMILLIE, F.S. & WONNACOTT, S. (1990). Methyllycaconitine: a selective probe for neuronal alpha-bungarotoxin binding sites. *FEBS Lett*, **270,** 45-8.

WEIDEMANN, A., KONIG, G., BUNKE, D., FISCHER, P., SALBAUM, J.M., MASTERS, C.L. & BEYREUTHER, K. (1989). Identification, biogenesis, and localization of precursors of Alzheimer's disease A4 amyloid protein. *Cell*, **57,** 115-26.

WEINER, D.M., LEVEY, A.I. & BRANN, M.R. (1990). Expression of muscarinic acetylcholine and dopamine receptor mRNAs in rat basal ganglia. *Proc Natl Acad Sci U S A*, **87,** 7050-4.

WEINGARTEN, M.D., LOCKWOOD, A.H., HWO, S.Y. & KIRSCHNER, M.W. (1975). A protein factor essential for microtubule assembly. *Proc Natl Acad Sci U S A*, **72,** 1858-62.

WENGENACK, T.M., WHELAN, S., CURRAN, G.L., DUFF, K.E. & PODUSLO, J.F. (2000). Quantitative histological analysis of amyloid deposition in Alzheimer's double transgenic mouse brain. *Neuroscience*, **101,** 939-44.

WENK, H., BIGL, V. & MEYER, U. (1980). Cholinergic projections from magnocellular nuclei of the basal forebrain to cortical areas in rats. *Brain Res*, **2,** 295-316.

WESS, J. (1993). Molecular basis of muscarinic acetylcholine receptor function. *Trends Pharmacol Sci*, **14,** 308-13.

WHITAKER, M. (2004). Calcium imaging. *Methods Cell Biol*, **74,** 443-68.

WHITE, H.K. & LEVIN, E.D. (1999). Four-week nicotine skin patch treatment effects on cognitive performance in Alzheimer's disease. *Psychopharmacology (Berl)*, **143,** 158-65.

WHITEAKER, K.L., GOPALAKRISHNAN, S.M., GROEBE, D., SHIEH, C.C., WARRIOR, U., BURNS, D.J., COGHLAN, M.J., SCOTT, V.E. & GOPALAKRISHNAN, M. (2001). Validation of FLIPR membrane potential dye for high throughput screening of potassium channel modulators. *J Biomol Screen*, **6,** 305-12.

WHITEAKER, P., DAVIES, A.R., MARKS, M.J., BLAGBROUGH, I.S., POTTER, B.V., WOLSTENHOLME, A.J., COLLINS, A.C. & WONNACOTT, S. (1999). An autoradiographic study of the distribution of binding sites for the novel alpha7-selective nicotinic radioligand [3H]-methyllycaconitine in the mouse brain. *Eur J Neurosci*, **11,** 2689-96.

WHITEAKER, P., PETERSON, C.G., XU, W., MCINTOSH, J.M., PAYLOR, R., BEAUDET, A.L., COLLINS, A.C. & MARKS, M.J. (2002). Involvement of the alpha3 subunit in central nicotinic binding populations. *J Neurosci*, **22,** 2522-9.

WHITEAKER, P., SHARPLES, C.G. & WONNACOTT, S. (1998). Agonist-induced up-regulation of alpha4beta2 nicotinic acetylcholine receptors in M10 cells: pharmacological and spatial definition. *Mol Pharmacol*, **53,** 950-62.

WHITEHOUSE, P.J. (1993). Cholinergic therapy in dementia. *Acta Neurol Scand Suppl*, **149,** 42-5.

WHITEHOUSE, P.J., MARTINO, A.M., ANTUONO, P.G., LOWENSTEIN, P.R., COYLE, J.T., PRICE, D.L. & KELLAR, K.J. (1986). Nicotinic acetylcholine binding sites in Alzheimer's disease. *Brain Res*, **371,** 146-51.

WHITEHOUSE, P.J., PRICE, D.L., CLARK, A.W., COYLE, J.T. & DELONG, M.R. (1981). Alzheimer disease: evidence for selective loss of cholinergic neurons in the nucleus basalis. *Ann Neurol*, **10,** 122-6.

WHITEHOUSE, P.J., PRICE, D.L., STRUBLE, R.G., CLARK, A.W., COYLE, J.T. & DELON, M.R. (1982). Alzheimer's disease and senile dementia: loss of neurons in the basal forebrain. *Science*, **215,** 1237-9.

WHITING, P., SCHOEPFER, R., LINDSTROM, J. & PRIESTLEY, T. (1991). Structural and pharmacological characterization of the major brain nicotinic acetylcholine receptor subtype stably expressed in mouse fibroblasts. *Mol Pharmacol*, **40,** 463-72.

WILCOCK, G.K., ESIRI, M.M., BOWEN, D.M. & SMITH, C.C. (1982). Alzheimer's disease. Correlation of cortical choline acetyltransferase activity with the severity of dementia and histological abnormalities. *J Neurol Sci*, **57,** 407-17.

WILLIAMS, M.E., BURTON, B., URRUTIA, A., SHCHERBATKO, A., CHAVEZ-NORIEGA, L.E., COHEN, C.J. & AIYAR, J. (2005). Ric-3 promotes functional expression of the nicotinic acetylcholine receptor alpha7 subunit in mammalian cells. *J Biol Chem*, **280,** 1257-63.

WILSON, G. & KARLIN, A. (2001). Acetylcholine receptor channel structure in the resting, open, and desensitized states probed with the substituted-cysteine-accessibility method. *Proc Natl Acad Sci U S A*, **98,** 1241-8.

WILTFANG, J., SMIRNOV, A., SCHNIERSTEIN, B., KELEMAN, G., MATTHIES, U., KLAFKI, H.W., STAUFENBIEL, M., HUTHER, G., HUTHER, E. & KORNHUBER, J. (1997). Improved electrophoretic separation and immunoblotting of beta-amyloid (A-beat) peptides 1-40, 1-42, and 1-43. *Electrophoresis*, **18,** 527-32.

WIMO, A., WINBALD, B., AGUERO-TORRES, H. & VON STRAUSS, E. (2003). The magnitude of dementia occurrence in the world. *Alzheimer Dis Assoc Disord*, **17,** 63-67.

WINKLER, D.T., BONDOLFI, L., HERZIG, M.C., JANN, L., CALHOUN, M.E., WIEDERHOLD, K.H., TOLNAY, M., STAUFENBIEL, M. & JUCKER, M. (2001). Spontaneous hemorrhagic stroke in a mouse model of cerebral amyloid angiopathy. *J Neurosci*, **21,** 1619-27.

WIRTHS, O., MULTHAUP, G. & BAYER, T.A. (2004). A modified beta-amyloid hypothesis: intraneuronal accumulation of the beta-amyloid peptide--the first step of a fatal cascade. *J Neurochem*, **91,** 513-20.

WOLF, O.T., KUDIELKA, B.M., HELLHAMMER, D.H., HELLHAMMER, J. & KIRSCHBAUM, C. (1998). Opposing effects of DHEA replacement in elderly subjects on declarative memory and attention after exposure to a laboratory stressor. *Psychoneuroendocrinology*, **23,** 617-629.

WOLFF, C., FUKS, B. & CHATELAIN, P. (2003). Comparative study of membrane potential-sensitive fluorescent probes and their use in ion channel screening assays. *J Biomol Screen*, **8,** 533-43.

WONG, T.P., DEBEIR, T., DUFF, K. & CUELLO, A.C. (1999). Reorganization of cholinergic terminals in the cerebral cortex and hippocampus in transgenic mice carrying mutated presenilin-1 and amyloid precursor protein transgenes. *J Neurosci*, **19,** 2706-16.

WONNACOTT, S., ALBUQUERQUE, E.X. & BERTRAND, D. (1993). Methyllycaconitine: a new probe that discriminates between nicotinic acetylcholine receptor subclasses. *Methods Neurosci.*, **12,** 263-275.

WU, J., KUO, Y.P., GEORGE, A.A., XU, L., HU, J. & LUKAS, R.J. (2004). beta-Amyloid directly inhibits human alpha4beta2-nicotinic acetylcholine receptors heterologously expressed in human SH-EP1 cells. *J Biol Chem*, **279,** 37842-51.

XIAO, Y. & KELLAR, K.J. (2004). The comparative pharmacology and up-regulation of rat neuronal nicotinic receptor subtype binding sites stably expressed in transfected mammalian cells. *J Pharmacol Exp Ther*, **310,** 98-107.

XU, W., GELBER, S., ORR-URTREGER, A., ARMSTRONG, D., LEWIS, R.A., OU, C.N., PATRICK, J., ROLE, L., DE BIASI, M. & BEAUDET, A.L. (1999a). Megacystis, mydriasis, and ion channel defect in mice lacking the alpha3 neuronal nicotinic acetylcholine receptor. *Proc Natl Acad Sci U S A*, **96,** 5746-51.

XU, W., ORR-URTREGER, A., NIGRO, F., GELBER, S., SUTCLIFFE, C.B., ARMSTRONG, D., PATRICK, J.W., ROLE, L.W., BEAUDET, A.L. & DE BIASI, M. (1999b). Multiorgan autonomic dysfunction in mice lacking the beta2 and the beta4 subunits of neuronal nicotinic acetylcholine receptors. *J Neurosci*, **19,** 9298-305.

YAMADA, K. & TOSHITAKA, N. (2002). Therapeutic approaches to the treatment of Alzheimer's disease. *Drugs Today (Barc)*, **38,** 631-7.

YAN, R., BIENKOWSKI, M.J., SHUCK, M.E., MIAO, H., TORY, M.C., PAULEY, A.M., BRASHIER, J.R., STRATMAN, N.C., MATHEWS, W.R., BUHL, A.E., CARTER, D.B., TOMASSELLI, A.G., PARODI, L.A., HEINRIKSON, R.L. & GURNEY, M.E. (1999). Membrane-anchored aspartyl protease with Alzheimer's disease beta-secretase activity. *Nature*, **402,** 533-7.

YANG, Y.K., NELSON, L., KAMARAJU, L., WILSON, W. & MCEVOY, J.P. (2002). Nicotine decreases bradykinesia-rigidity in haloperidol-treated patients with schizophrenia. *Neuropsychopharmacology*, **27,** 684-6.

YASSIN, L., SAMSON, A.O., HALEVI, S., ESHEL, M. & TREININ, M. (2002). Mutations in the extracellular domain and in the membrane-spanning domains interfere with nicotinic acetylcholine receptor maturation. *Biochemistry*, **41,** 12329-35.

YASUDA, R.P., CIESLA, W., FLORES, L.R., WALL, S.J., LI, M., SATKUS, S.A., WEISSTEIN, J.S., SPAGNOLA, B.V. & WOLFE, B.B. (1993). Development of antisera selective for m4 and m5 muscarinic cholinergic receptors: distribution of m4 and m5 receptors in rat brain. *Mol Pharmacol*, **43,** 149-57.

YATES, S.L., BENCHERIF, M., FLUHLER, E.N. & LIPPIELLO, P.M. (1995). Up-regulation of nicotinic acetylcholine receptors following chronic exposure of rats to mainstream cigarette smoke or alpha 4 beta 2 receptors to nicotine. *Biochem Pharmacol*, **50,** 2001-8.

YOSHIIKE, Y., CHUI, D.H., AKAGI, T., TANAKA, N. & TAKASHIMA, A. (2003). Specific compositions of amyloid-beta peptides as the determinant of toxic beta-aggregation. *J Biol Chem*, **278,** 23648-55.

YOST, C.S. & DODSON, B.A. (1993). Inhibition of the nicotinic acetylcholine receptor by barbiturates and by procaine: do they act at different sites? *Cell Mol Neurobiol*, **13,** 159-72.

YOUNG, J.W., FINLAYSON, K., CRAWFORD, N., MARSTON, H.M., KELLY, J.S. & SHARKEY, J. (2005). Impaired sustained attention in mice is associated with a reduced alpha 7 nicotinic receptor density. *Pyschopharmacology, submitted.*

YOUNG, J.W., FINLAYSON, K., SPRATT, C., MARSTON, H.M., CRAWFORD, N., KELLY, J.S. & SHARKEY, J. (2004). Nicotine improves sustained attention in mice: evidence for involvement of the alpha7 nicotinic acetylcholine receptor. *Neuropsychopharmacology*, **29,** 891-900.

YU, C.R. & ROLE, L.W. (1998a). Functional contribution of the alpha5 subunit to neuronal nicotinic channels expressed by chick sympathetic ganglion neurones. *J Physiol*, **509 (Pt 3),** 667-81.

YU, C.R. & ROLE, L.W. (1998b). Functional contribution of the alpha7 subunit to multiple subtypes of nicotinic receptors in embryonic chick sympathetic neurones. *J Physiol*, **509 (Pt 3),** 651-65.

YU, W.F., GUAN, Z.Z., BOGDANOVIC, N. & NORDBERG, A. (2005). High selective expression of alpha7 nicotinic receptors on astrocytes in the brains of patients with sporadic Alzheimer's disease and patients carrying Swedish APP 670/671 mutation: a possible association with neuritic plaques. *Exp Neurol*, **192,** 215-25.

YUM, L., WOLF, K.M. & CHIAPPINELLI, V.A. (1996). Nicotinic acetylcholine receptors in separate brain regions exhibit different affinities for methyllycaconitine. *Neuroscience*, **72,** 545-55.

ZAMANI, M.R., ALLEN, Y.S., OWEN, G.P. & GRAY, J.A. (1997). Nicotine modulates the neurotoxic effect of beta-amyloid protein(25-35)) in hippocampal cultures. *Neuroreport*, **8,** 513-7.

ZAREI, M.M., RADCLIFFE, K.A., CHEN, D., PATRICK, J.W. & DANI, J.A. (1999). Distributions of nicotinic acetycholine receptor alpha7 and beta2 subunits on cultured hippocampal neurons. *Neuroscience*, **88,** 755-64.

ZHANG, J. & STEINBACH, J.H. (2003). Cytisine binds with similar affinity to nicotinic alpha4beta2 receptors on the cell surface and in homogenates. *Brain Res*, **959,** 98-102.

ZHAO, L., KUO, Y.P., GEORGE, A.A., PENG, J.H., PURANDARE, M.S., SCHROEDER, K.M., LUKAS, R.J. & WU, J. (2003). Functional properties of homomeric, human alpha 7-nicotinic acetylcholine receptors heterologously expressed in the SH-EP1 human epithelial cell line. *J Pharmacol Exp Ther*, **305,** 1132-41.

ZOLI, M., LENA, C., PICCIOTTO, M.R. & CHANGEUX, J.P. (1998). Identification of four classes of brain nicotinic receptors using beta2 mutant mice. *J Neurosci*, **18,** 4461-72.

ZWART, R., VAN KLEEF, R.G., GOTTI, C., SMULDERS, C.J. & VIJVERBERG, H.P. (2000). Competitive potentiation of acetylcholine effects on neuronal nicotinic receptors by acetylcholinesterase-inhibiting drugs. *J Neurochem*, **75,** 2492-500.

ZWART, R. & VIJVERBERG, H.P. (1997). Potentiation and inhibition of neuronal nicotinic receptors by atropine: competitive and noncompetitive effects. *Mol Pharmacol*, **52,** 886-95.